A New Aminoglycoside Antibiotic Effective Against NpmA-Expressing Escherichia coli

HARVARD UNIVERSITY
Graduate School of Arts and Sciences

DISSERTATION ACCEPTANCE CERTIFICATE

The undersigned, appointed by the

Department of Chemistry & Chemical Biology

have examined a dissertation entitled:

A New Aminoglycoside Antibiotic Effective Against NpmA-Expressing *Escherichia coli*.

presented by: Matthew T. Peszko

candidate for the degree of Doctor of Philosophy and hereby certify that it is worthy of acceptance.

Signature _____
Typed name: Professor Andrew G. Myers

Signature _____
Typed name: Professor Emily P. Balskus

Signature _____
Typed name: Professor Brian B. Liau

Date: 18 January 2024

A New Aminoglycoside Antibiotic Effective Against NpmA-Expressing *Escherichia coli*

A dissertation presented

by

Matthew T. Peszko

to

The Department of Chemistry and Chemical Biology

in partial fulfillment of the requirements

for the degree of

Doctor of Philosophy

in the subject of Chemistry

Harvard University

Cambridge, Massachusetts

January 2024

Dissertation Advisor: Professor Andrew G. Myers Matthew T. Peszko

A New Aminoglycoside Antibiotic Effective Against NpmA-Expressing *Escherichia coli*

Abstract

Aminoglycoside antibiotics (AGAs) are pseudo-oligosaccharide natural products that have provided effective treatments for life-threatening bacterial infections for over seventy years. Decades of clinical use has resulted in the widespread proliferation of aminoglycoside resistance genes which, when coupled with longstanding toxicity challenges, limits the utility of aminoglycosides in a clinical setting. While the most common mechanism of resistance to AGAs comes in the form of aminoglycoside modifying enzymes (AMEs), ribosomal RNA methyltransferases (RMTs) that directly modify the AGA binding site are increasingly concerning as they frequently coincide on mobile genetic elements containing resistance genes to other antibiotic classes. In 2003, a novel plasmid-mediated aminoglycoside resistance methyltransferase (NpmA) was identified in a clinical isolate of *Escherichia coli* that provides extensive resistance to the entire class of AGAs. As of starting this research, no AGA is reported to overcome this resistance mechanism. This dissertation presents synthetic advancements and exploratory studies

towards next-generation aminoglycoside antibiotics seeking to overcome RMT mechanisms of resistance.

In chapter 1, I discuss AGAs as a natural product class and their history. I review mechanisms of action, the basis for antibacterial activity, as well as the biosynthetic origins. I additionally discuss the basis for mammalian toxicity to AGAs and for bacterial resistance, and modern strategies for circumventing both.

In chapter 2, I provide a history of semisynthetic modifications to aminoglycosides. With particular focus on modifications that have translated to clinical efficacy and overcoming resistance, I review the most promising changes to the aminoglycoside scaffold in designing next-generation AGA therapeutics.

In chapter 3, I present my efforts to prepare fully synthetic 2-deoxystreptamine (2-DOS) as a protected component for an improved synthesis of next-generation AGAs. I describe a key design strategy hinging on intramolecular aldol reaction to establish contiguous equatorial stereocenters during the cyclohexane annulation. Several approaches were examined to access the desired aldolization intermediate to no avail: a tandem addition to a γ,δ-epoxyenone, a stereoselective union between a functionalized organometallic nucleophile and an optically active cyanohydrin, and a linear approach utilizing Vince's lactam as a readily differentiated chiral pool building block. Previous syntheses are also discussed.

In chapter 4, I describe the design and synthesis of C5'-modified AGAs to counter NpmA resistance. Two synthetic strategies are explored: a partially synthetic strategy featuring the union of a synthetic ring I glycosyl donor with a semisynthetic ring II-IV acceptor, and a semisynthetic strategy providing access to a diversifiable C6'-carboxylic acid. Key transformations include a diastereoselective Corey-Bakshi-Shibata reduction of a glutamate-derived aryl ketone to directly

yield a C5-aryl lactol, the glycosylation between a C5-phenyl deoxyglycoside donor and pseudotrisaccharide glycosyl acceptors, and the decarboxylative elimination of an aminoglycoside β-hydroxy acid to yield a 4'-deoxypentenoside. Synthetic pitfalls are simultaneously discussed as potential avenues for future AGA semisynthesis endeavors. With this chemistry, novel AGAs were prepared and evaluated against NpmA-expressing bacteria.

For chapter 5, as part of an unrelated research project, I present the mechanism proposed for the transformation of cyclopentanone to a dienoic acid and reveal it to be in error. I show that carbon 11 derives not from dimethylsulfoxide as proposed, but from dichloromethane present in the "quenching" solution. The intermediacy of an α-chloromethyl ketone and its subsequent fragmentation in the presence of hydroxide ion is supported by additional experiments, and by extensive literature precedent.

Table of Contents

To my family and friends

for their boundless love and support

and for always seeing the best version of myself

Acknowledgements

I would first and foremost like to thank Professor Andrew G. Myers for his mentorship and guidance. For over five years since beginning at Harvard, Andy's tenacity with the lab's research endeavors has strengthened the scientific development of not just myself, but of every colleague I have had the pleasure to know during my time in the department. His pursuit of elegance and practicality has emboldened me to pursue worthwhile research efforts and to always be thinking creatively about how to tackle problems. He has always encouraged me to move forward with proper focus and has consistently helped me adapt in times of struggle. Andy will undoubtedly be an inspiration for the rest of my career, and it has been an unparalleled honor to have his counsel as I have approached my doctoral research challenges.

I would similarly like to thank Professor Brian B. Liau for his amazing support as a member of my thesis committee. I faced a significant number of personal challenges during my doctoral research and throughout these experiences Brian has been continuously encouraging and focused with his guidance. I am extremely grateful for having served as a teaching fellow for Chemistry 110 for multiple years and have benefitted greatly from the exposure to his own scientific endeavors, research interests, and expertise. I can only express gratitude for his influence on my development as a scientist and I hope to have his continued guidance in the years to come.

I additionally want to acknowledge the third member of my committee, Professor Emily P. Balskus. I could tell upon our first meeting during the recruitment process that she would be incredibly insightful as a mentor, and her extensive experience across the fields of both organic chemistry and chemical biology are an inspiration for myself to become a well-rounded scientist.

Her support as I have looked to start my career has been especially poignant for me and has assured me of my future goals.

To my committee, I can only express extreme gratitude for your guidance and counsel; I regret not utilizing it more during my doctoral research. I sincerely hope to have your continued support throughout the rest of my career.

During my five years with the Myers group, I have had the incomparable joy of knowing outstanding scientists that have been both friends and colleagues. On my project I first came to know Dr. Sven Hildebrant, for who I am incredibly thankful that he recognized my abilities and allowed me to get hands-on with our chemistry right away. At the time, his preparation for both a newborn and job search of his own made his mentorship especially valuable and I am thankful to have his friendship today still. I would later be joined by Dr. Kelly Craft who amazed me with her diligence and attention to detail. I am extremely thankful for her time on my project, her patience while collaborating with a less experienced version of myself, and our shared sense of humor; I credit her as someone I aspire to as a carbohydrate chemist with unparalleled thoroughness. For the aminoglycoside group, I would last like to thank Dr. Fan Liu. I had the wonderful chance to meet her at the 2019 International Course on Antibiotics and Resistance, and as the former lead for the aminoglycoside project she has been an ever-present voice of encouragement. Her continued presence and our multiple meetings since have been a great avenue of support in navigating my thesis.

Beyond my team members, many Myers lab colleagues have been incomparable resources socially and academically. I want to thank Dr. Dan Terwilliger, my bay mate as I started in the Myers group, for the unmatched positivity in the day-to-day scientific challenges I faced. His friendship and joyous attitude towards science was always motivating and I cannot thank him

enough for his influence on me as a person. I would next like to thank Dr. Jason Anesini, the first cohort member I came to know well, for his friendship and for serving as a member of my wedding party. I will eternally reminisce of the days (and weekends) in lab discussing music, politics, and current events, and I will always aspire to have a comparable determination with my career. Next, I would like to thank Anna Renner, another cohort member who joined the Myers lab at the same time as I. She was inspiring both as a thorough scientist and endless source of positivity. I would next like to thank Kelvin Wu, who has been a wonderful friend and amazingly talented scientist. To Dr. Ethan Magno, I am thankful to have had as an insightful and compassionate friend. To Dr. Jeremy Mason, I hope you remain as inspiring a chemist as during my early years in the group. I will be eternally grateful for everyone here and the rest of the Myers group for their continuous camaraderie and encouragement.

Outside the Harvard community, I am extremely grateful for the affection of many scientists, friends, and family members. To my undergraduate research advisor Professor Christian Melander, I am most sincerely thankful for his enabling of my first research experiences and for providing me a space to develop the skills promoting my early years of success at Harvard. I will forever be thankful for his assistance with choosing a graduate school and for his uplifting tutelage in chemistry. Another professor of profound influence on my career is Professor Jeremiah Feducia. From his time serving as my undergraduate curriculum advisor to now he has provided immeasurable support with editing documents and life advice. Without him I would unquestionably be in a worse position than I am today. I would like to sincerely thank two friends from my time at NC State: Nicholas Hahn and Alexandra Hahn, who have been continuous friends despite the extreme distance put between us by my decision to come here for graduate school. I am thankful to have had the support of Eleni Doerr, whose love, friendship, and dedication during

my time in graduate school could never be replaced. And lastly, I want to thank my parents, James Peszko and Lisa Peszko, for allowing me to flourish as an individual and always believing in my capabilities. Without their support I would not have had the freedom to pursue my studies as thoroughly as I have been able to.

To all my friends, family, and colleagues, I hope this thesis represents a fraction of the gratitude I have for all of you.

List of Abbreviations

A	adenosine
Å	angstrom
A. baumannii	*Acinetobacter baumannii*
AAC	aminoglycoside N-acetyltransferase
Ac	acetyl
Acetyl-CoA	acetyl coenzyme A
Alloc	allyloxycarbonyl
AME	aminoglycoside modifying enzyme
ANT	aminoglycoside O-nucleotidyltransferase
APH	aminoglycoside O-phosphotransferase
Ar	argon
armA	aminoglycoside resistance methylase, gene *armA*
ATCC	American type culture collection
ATP	adenosine triphosphate
BAIB	bis-acetoxy iodobenzene
BDA	butane-diacetal
Bn	benzyl
Boc	tert-butoxycarbonyl
Bu	butyl
Bz	benzoyl

C	cytosine
Calcd	calculated
CAM	ceric ammonium molybdate
cErm	constitutive erythromycin ribosome methylase
D	dextrorotary
DCC	N,N’-dicyclohexylcarbodiimide
DIBAL-H	diisobutylaluminum hydride
DIC	N,N’-diisopropylcarbodiimide
DMAP	4-dimethylaminopyridine
DMF	dimethylformamide
DMFDNA	dimethylformamide dineopentyl acetal
DMP	Dess–Martin periodinane
DMSO	dimethylsulfoxide
DNA	deoxyribonucleic acid
DOS	deoxystreptamine
dr	diastereomeric ratio
E. coli	*Escherichia coli*
E. faecalis	*Enterococcus faecalis*
EDC	1-ethyl-3-(3-dimethylaminopropyl)carbodiimide
EDPI	energy dependent phase I
EDPII	energy dependent phase II
ee	enantiomeric excess
EIP	energy independent phase

equiv	equivalent
ESI	electrospray ionization
Et	ethyl
FDA	food and drug administration
FT-IR	Fourier transform infrared
g	gram
G	guanosine
h	hour
H. influenzae	*Haemophilus influenzae*
HABA	(*S*)-4-amino-2-hydroxybutanoyl
HCN	hydrogen cyanide
HPLC	high performance liquid chromatography
HRMS	high resolution mass spectrometry
Hz	hertz
J	coupling constant
K. pneumoniae	*Klebsiella pneumoniae*
L	levorotary
LDA	lithium diisopropylamide
M	molar
mA1408	methylated adenosine 1408
mCPBA	*meta*-chloroperbenzoic acid
Me	methyl
MFP	membrane fusion protein

mg	milligram
MHz	megahertz
MIC	minimum inhibitory concentration
min	minutes
mL	milliliter
mmol	millimole
mol	mole
MOM	methoxymethyl
mRNA	messenger ribonucleic acid
MRSA	methicillin-resistant *Staphylococcus aureus*
Ms	methanesulfonyl
N_3	azide
NADH	nicotinamide adenine dinucleotide
NAG	*N*-acetyl-β-glucosaminidase
NDM-1	New Delhi metallo-β-lactamase 1
NIS	N-iodosuccinimide
NMR	nuclear magnetic resonance
nOe	nuclear Overhauser effect
ºC	degree Celsius
OMF	outer-membrane factor
P. aeruginosa	*Pseudomonas aeruginosa*
PMB	*para*-methoxybenzyl
PDB	protein data bank

pH	hydrogen ion concentration
Ph	phenyl
ppm	parts per million
Pr	propyl
R	rectus (Cahn–Ingold–Prelog system)
rac	racemate
R_f	retention factor
rt	room temperature
RMT	ribosome methyltransferase
RNA	ribonucleic acid
RND	resistance-nodulation-division
rRNA	ribosomal ribonucleic acid
S	sinister (Cahn–Ingold–Prelog system)
S. aureus	*Staphylococcus aureus*
S. pneumoniae	*Streptococcus pneumoniae*
T	thymidine
TBS	tert-butyldimethylsilyl
TBSOTf	tert-butyldimethylsilyl trifluoromethanesulfonate
Tf	trifluoromethanesulfonyl
Tf_2O	trifluoromethanesulfonic anhydride
TFA	trifluoroacetic acid
TFE	trifluoroethanol
TfN3	trifluoromethanesulfonyl azide

THF	tetrahydrofuran
TIPS	triisopropylsilyl
TLC	thin layer chromatography
TMS	trimethylsilyl
tRNA	transfer ribonucleic acid
U	uridine
UDP	uridine diphosphate
UV	ultraviolet
µ	micro
µL	microliter
µmol	micromole
δ	chemical shift

Chapter 1. Introduction to Aminoglycoside Antibiotics: Structure, Mechanism of Action, and Biological Properties

1.1. Discovery of Aminoglycoside Antibiotics – Isolation History

Aminoglycoside antibiotics (AGAs) have been in continuous clinical use for over seven decades.[1] The premier member of the family, Streptomycin, was isolated by Professor Albert Schatz in 1943 while he was pursuing graduate studies under Professor Selman Waksman (Figure 1.1).[2] Streptomycin proved effective against mycobacteria, making it the first treatment option for tuberculosis,[3] and further established microorganisms as viable sources for antimicrobial agents and chemotherapies. Streptomycin additionally proved effective in treating gram-negative bacterial infections, including those caused by *Pseudomonas aeruginosa*, as well as gram-positive infections resistant to penicillin. Output of streptomycin grew globally over the three years after isolation to support both clinical studies and the advancement of early semisynthetic derivatives .[4]

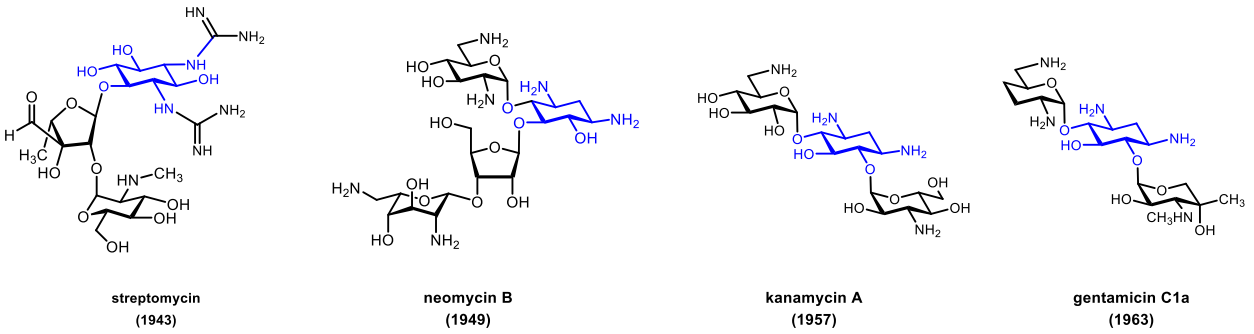

Figure 1.1. Representative aminoglycoside antibiotics and their isolation year.

While streptomycin was isolated from *Streptomyces griseus*, other aminoglycoside antibiotics were later identified from various species of soil bacteria (Figure 1.1). Select examples include neomycin (1949),[5] Paromomycin (1956),[6] Kanamycin A (1957),[7] gentamicin (1963),[8]

tobramycin (1967),[9] and sisomicin (1970).[10] Many of these compounds displayed efficacy against bacterial infections but clinical usage has varied over time. Toxicity was one consideration: despite neomycin exhibiting efficacy against streptomycin-resistant bacteria, its usage was limited due to dangerous toxicity.[11,12] At present, gentamicin is the most prescribed aminoglycoside, and is produced as a complex mixture of many components (the majority components are gentamicin C_1, C_{1a}, and C_2, Figure 1.2).[13-15] Aminoglycosides are generally useful for emergency and life-threatening infections due to the lack of allergic response and broad-spectrum antimicrobial activity. Aminoglycosides are also applicable as inhalant drugs for the treatment of cystic fibrosis patients,[16] and they additionally remain part of some drug cocktails used in the treatment of tuberculosis.[17]

1.2. Aminoglycoside Nomenclature and Structure

Since the isolation of streptomycin, a large variety of aminoglycosides have been developed both from natural sources and semisynthesis campaigns. The naming conventions that differentiate members within the class are with respect to the producing organism: compounds isolated from *Streptomyces* species are allocated the suffix '-mycin' while those isolated from *Micromonospora* and *Bacillus* are given the suffixes '-micin' and '-osin', respectively.

All aminoglycosides share a common aminocyclitol motif (Figures 1.1 and 1.2, shown in blue) that is by itself *meso* until additional carbohydrate units are appended.[18] This highly substituted cyclohexane ring, dubbed streptamine with respect to the parent compound,[19] has its numbering convention denoted in Figure 1.2C. A disaccharide unit attached at the C4 hydroxyl of streptamine constitutes the remainder of the streptomycin structure. However, streptomycin is unique among aminoglycosides as most members of the family contain 2-deoxystreptamine as the

core scaffold (Figure 1.2A–B). These aminoglycosides can be further categorized by the glycosylation pattern of the 2-deoxystreptamine core: 4,5-subsubstituted aminoglycosides (Figure 1.2A) and 4,6-disubstituted aminoglycosides (Figure 1.2B). In all cases, and glucosyl ring with varying degrees of hydroxylation is attached to the C4-hydroxyl. More complex attachments at the 4-position are tolerated as seen with apramycin (Figure 1.2C). Additional structural variety is observed when the remaining glycosyl subunits are added. In the 4,5-disubstituted subfamily, members such as neomycin have a paromobiosyl moiety attached to the C5-hydroxyl group, whereas butirosin has only a ribose. For the 4,6-disubstituted subfamily, they may broadly be categorized as kanamycins or gentamicins, with sisomicin as an outlier in structure featuring an unsaturated sugar linked at the C4'-hydroxyl. These structures differ at the C6- carbohydrate component, both 3-aminosugars; in gentamicin a tertiary alcohol is a noteworthy structural element. Those that do not fall within those subfamilies may be classified as "atypical" aminoglycosides such as apramycin, which features a unique dialdose (octose) sugar linkage to the C4-hydroxyl that is additionally coupled to a 4-aminoglucose.

Aminoglycoside rings are numbered using longstanding conventions in aminoglycoside literature (Figure 1.2). Typically, the glucosamine-type carbohydrate linked though the C4-hydroxyl is referred to as ring I followed by the aminocyclitol as ring II. Thereafter, additional carbohydrates can be numbered by counting away from the 2-deoxystreptamine ring. Carbon and position numbering for the carbohydrates is consistent with standards in carbohydrate chemistry. The aminocyclitol unit, usually 2-deoxystrepamine, is counted without priming and takes priority.

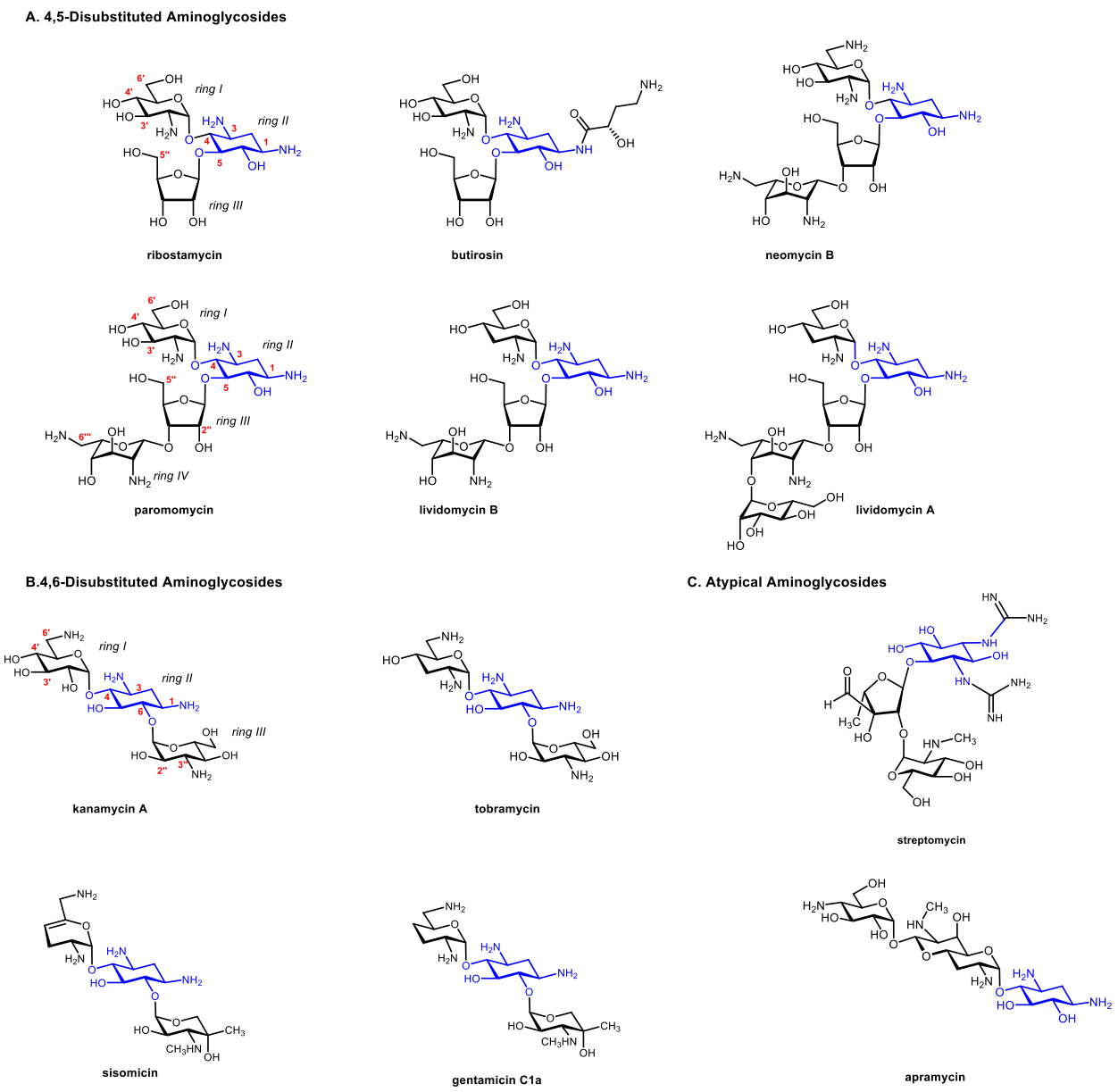

Figure 1.2. (A) Aminoglycoside antibiotics bearing additional glycosides linked through the C4 and C5 hydroxyls. (B) Aminoglycoside antibiotics bearing additional glycosides linked through the C4 and C6 hydroxyls. (C) Aminoglycoside antibiotics which are monosubstituted on 2-deoxystreptamine.

The glucose-type sugar linked at C4 then takes single-primed numbering for its carbons, and additional carbohydrate units are given additional primes as necessary (e.g. 2'', 3''', etc…).

1.3. Aminoglycoside Biosynthesis

Most aminoglycoside carbohydrate units are biosynthetically derived from building blocks such as glucose, xylose, and ribose.[20] The aminocyclitol 2-deoxystreptamine originates from glucose 6-phosphate that undergoes oxidation and elimination to yield a vinyl ketone (Figure 1.3). Hydridic 1,2-reduction of the ketone and type II Ferrier rearrangement forms the cyclohexane structure, which after sequential transamination reactions forms 2-deoxystreptamine. Glucose 6-phosphate also serves as the precursor to *myo*-inositol upstream in the streptamine biosynthetic pathway. Oxidation, transamination, and guanidinylation occurring twice in sequence affords the bis-guanidinylated structure.[21]

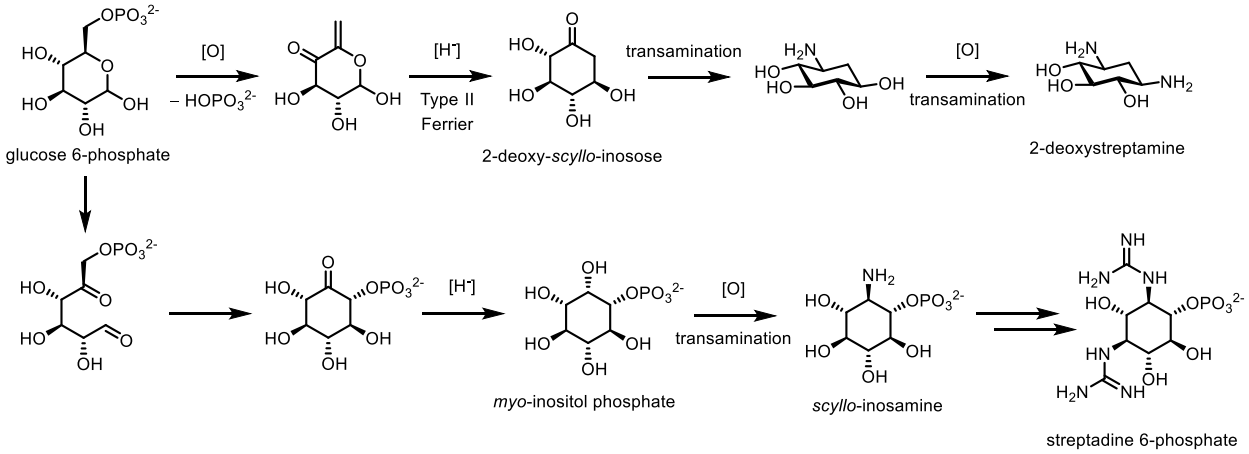

Figure 1.3. The biosynthetic conversion of glucose 6-phosphate to 2-deoxystreptamine and bis-guanidinylated streptamine phosphate.

The disaccharide portion of paromomycin is constructed by glycosylation between UDP-glucosamine, from glucose 6-phosphate, and 2-deoxystreptamine (Figure 1.4).[22] An additional

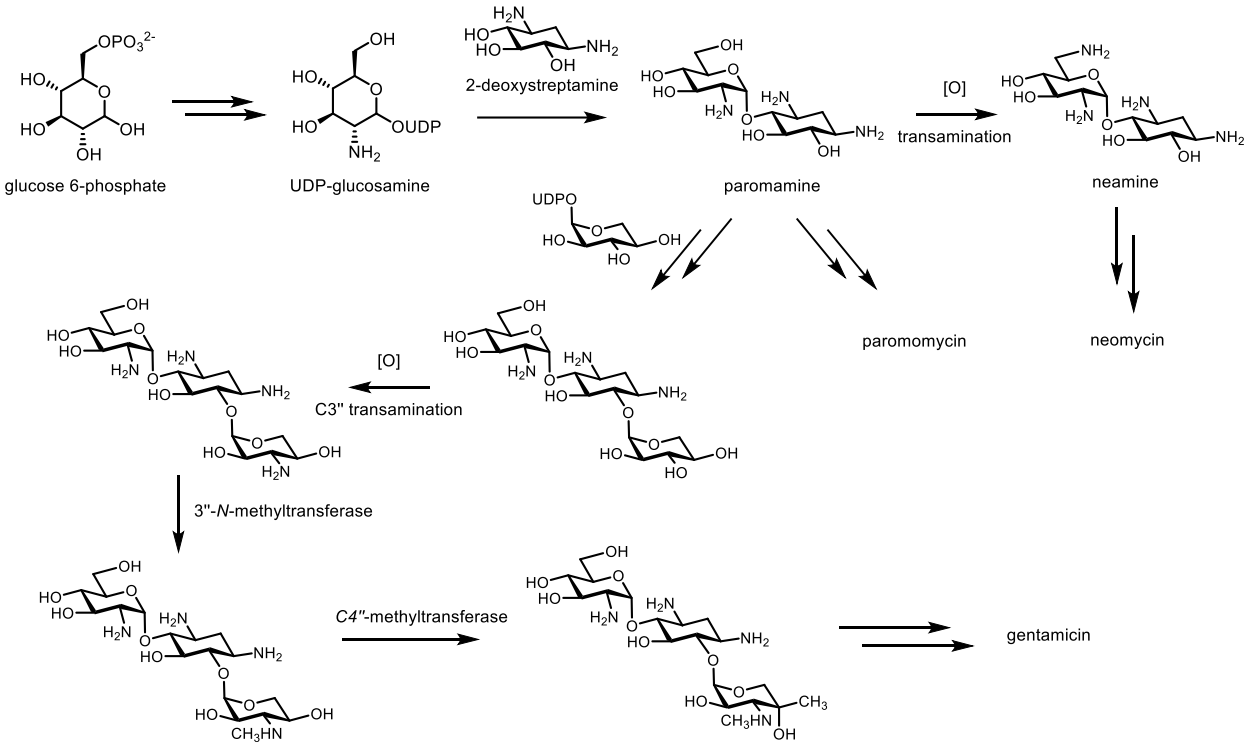

Figure 1.4. Biosynthetic construction of 2-deoxystreptamine family antibiotics.

transamination converts this structure to neamine, the disaccharide parent to neomycin. Glucose 6-phosphate similarly serves as the precursor to ring IV of neomycin and to ring III of kanamycin[23] by comparable transformations. Ring III of 4,5-disubstituted aminoglycosides is an unmodified ribose glycosylated at C3, while ring III of gentamicin and sisomicin is constructed using a unique radical *S*-adenosyl methionine methyltransferase.[24,25] Apramycin, an atypical aminoglycoside, bears a structurally unique ring II bicyclic dialdose moiety.[26] The biosynthetic pathway for the octose construction proceeds via aldolization between an *N*-acetylated enolate, generated from either *N*-acetyl glucosamine or galactosamine, and a 6'-oxolividamine electrophile (Figure 1.5). The subsequent acetal formation yields aprosamine from lividamine (3'-deoxyparomamine).

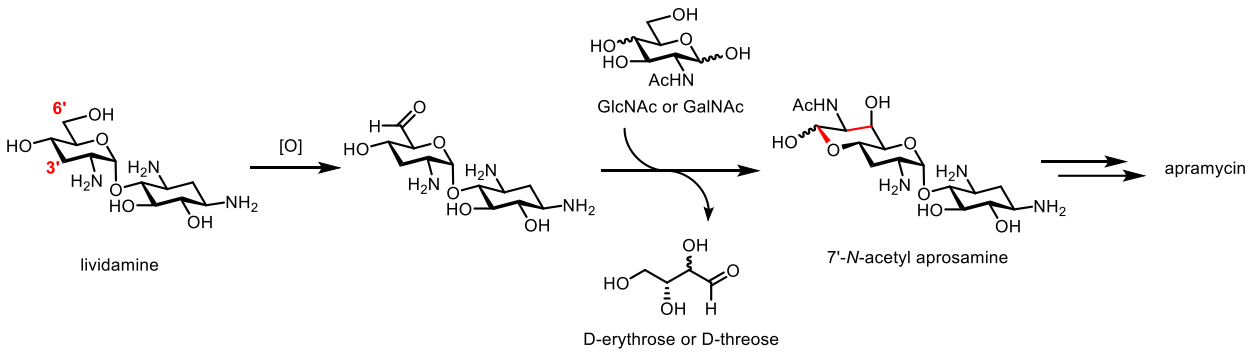

Figure 1.5. Biosynthesis of the aprosamine dialdose core from lividamine. Bonds constructed in the [6+2] coupling reaction are shown in red.

1.4. Mechanism of Action

Critical to bacterial life is the construction of proteins from genetic information in the form of RNA, the process of translation that occurs in the ribosome. The bacterial ribosome is composed of two subunits,[27] a large 50S subunit and a small 30S subunit; these subunits are each constructed from both ribosomal RNA (rRNA) and ribosomal proteins, which together match incoming messenger RNA (mRNA) strands with aminoacyl transfer RNA (tRNA) to translate a developing peptide chain. Recognition of tRNA occurs at the interface of the two subunits, wherein the tRNA must bind the A site, be recognized as correct by the ribosome and undergo peptide bond formation to extend the developing peptide in the P site, and ultimately translocate to the E site for ejection from the ribosome.

Ribosomal translation can be broken down into four distinct phases: initiation, elongation, termination, and recycling (Figure 1.6).[28,29] Aminoglycosides bearing 2-deoxystreptamine as their

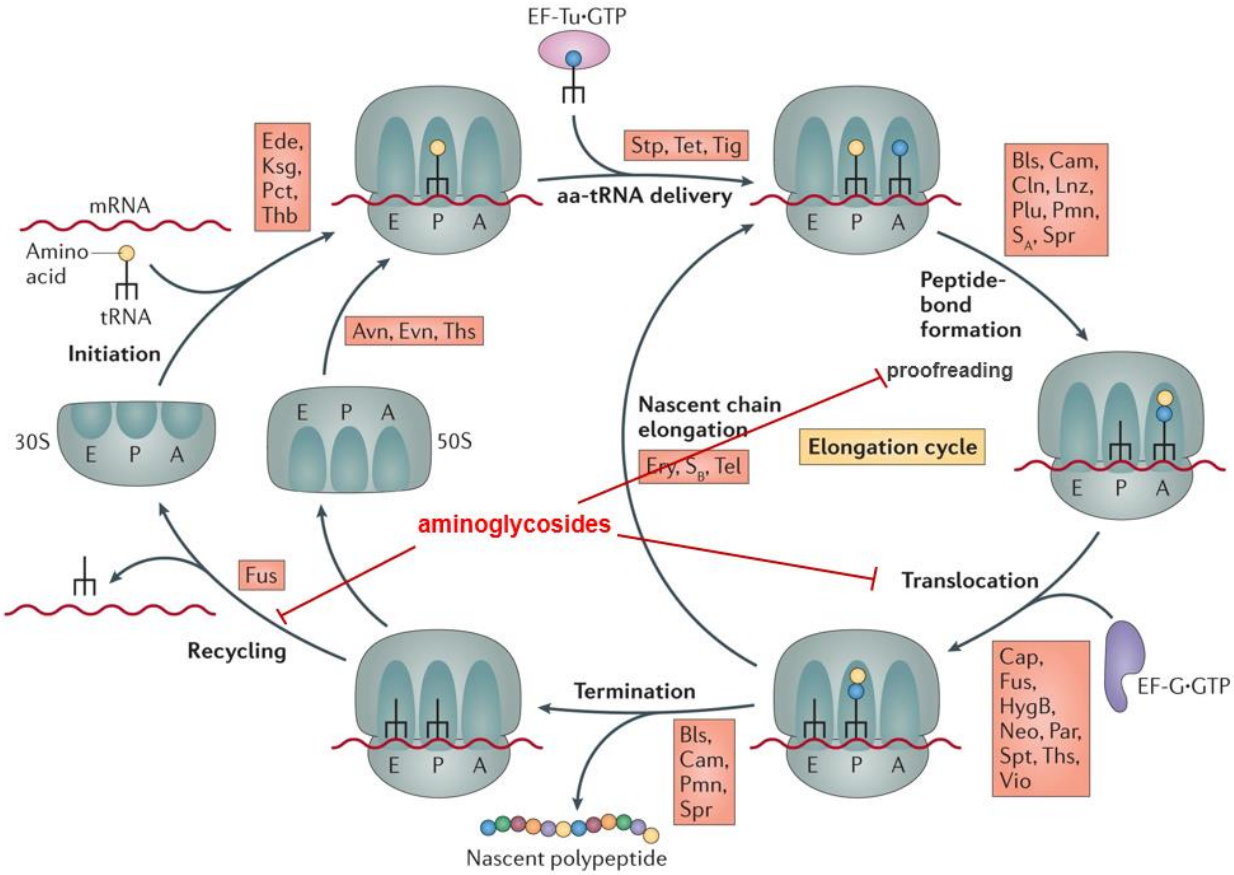

Figure 1.6. Aminoglycoside antibiotics bind the bacterial ribosome and interfere with multiple stages of translation. Figure adapted from reference 29.

core derive their bactericidal activity by interfering with multiple stages of protein translation.[30–34] Primarily, 2-deoxystreptamine antibiotics bind in the decoding region near helix 44 of the 30S subunit, where translational fidelity is reduced and continuous tRNA readthrough is promoted (Figure 1.7).[35] Similarly, ribosomal translocation and recycling is inhibited by binding interactions with helix 69 in the large subunit.[36,37] Streptomycin has a distinct but nearby binding site to typical aminoglycosides and is thought to interfere with translation by increasing the rate at which structurally similar tRNAs are incorporated.

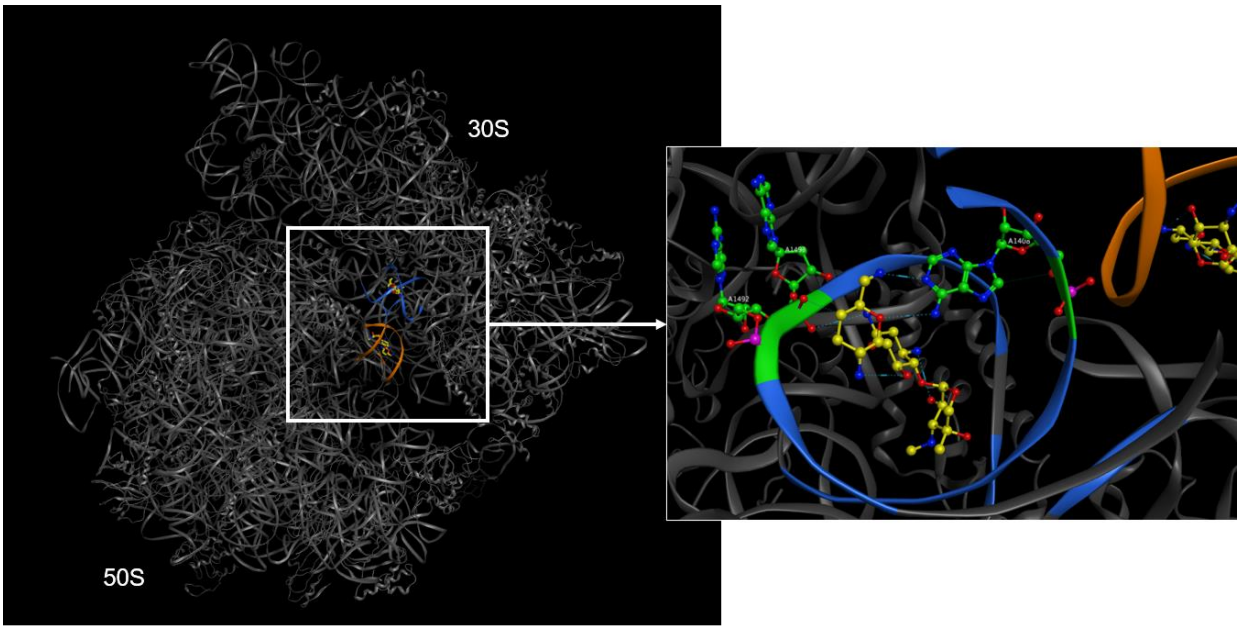

Figure 1.7. Aminoglycosides bind in the 30S subunit within helix 44 (Blue) of the ribosomal RNA; a nearby binding site in helix 69 (orange) is also known. Bases A1408, A1492, and A1493 are shown in green. (PDB: 4V53). Figure adapted from reference 36.

Codon-anticodon helix formation between aminoacyl tRNA and mRNA at the ribosomal A site is responsible for the accuracy of translation, which has an error frequency of less than one per thousand.[35,38] However, energetic differences between mRNA and near-cognate tRNA helix formation do not account for the high level of accuracy,[39] which supports the critical role of the ribosome in improving the correctness of translation. Two critical residues in helix 44, A1492 and A1493, alongside G530 in the rRNA are crucial to ribosomal recognition of tRNA correctness in the A site.[35] Binding of tRNA induces a conformational shift in the dynamic ribosome structure, wherein A1492 and A1493 rotate into an extra-helical conformation and form stabilizing contacts within the codon-anticodon helix. With incorrect tRNA in the A-site, insufficient stabilizing interactions are generated which allows disassociation of near-cognate tRNA away from the ribosome.

All 2-deoxystreptamine class aminoglycosides share overlapping binding sites within the bacterial ribosome, regardless of 4,5-disubstitution or 4,6-disubstitution; apramycin also binds in an identical region despite being 4-monosubstituted. Both NMR[40] and crystallographic studies display how binding of 2-deoxystreptamine antibiotics interferes with the hydrogen bonding network in helix 44, causing displacement of A1492 and A1493 identical to translational readthrough (Figure 1.8).[35,38.41] A dense network of hydrogen bonds between aminoglycosides and the rRNA as well as electrostatic contacts by the protonated amines with the RNA phosphates assist in stabilizing the flipped-out conformation. By stabilizing the extra-helical conformation of A1492 and A1493, continuous readthrough of non-cognate tRNA is promoted, which results in the

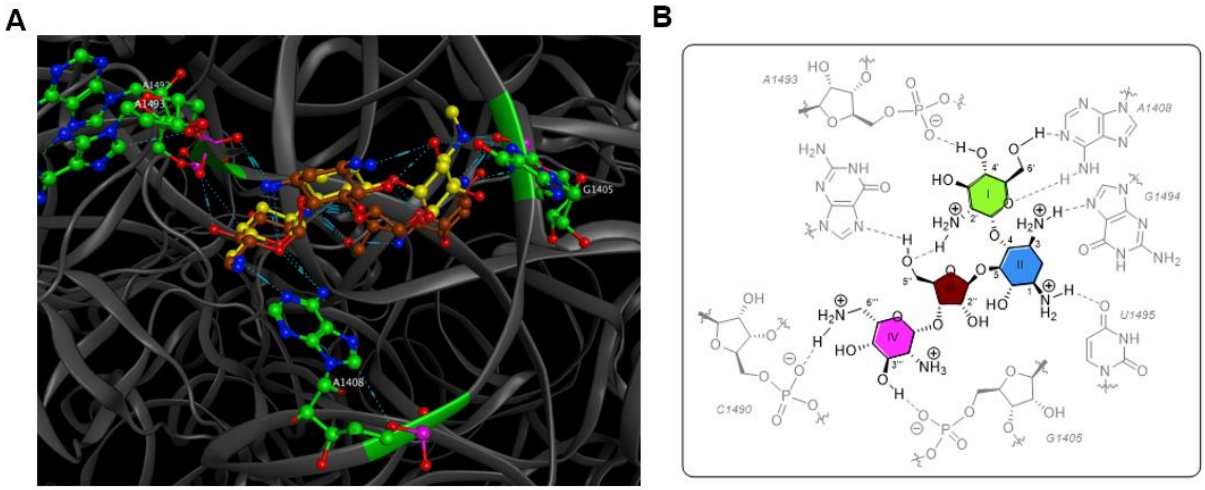

Figure 1.9. (A) Gentamicin (yellow) and neomycin (orange) share a binding site within helix 44 of the decoding region (PDB:4V52 and 4V53). (B) Cartoon depiction of aminoglycoside hydrogen-bonding interactions for 4,5-disubstituted members with the bacterial ribosome. Figure adapted from reference 41.

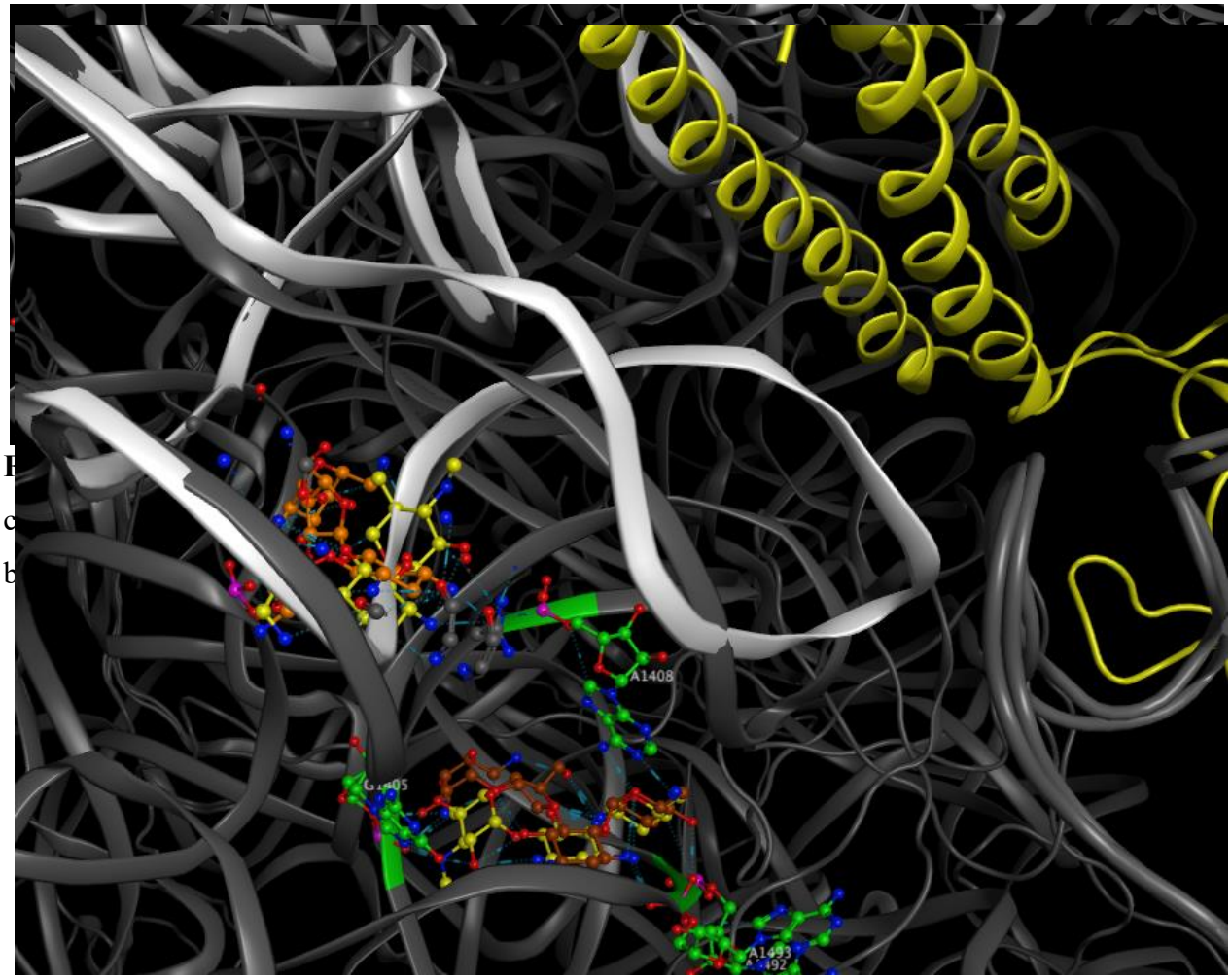

Figure 1.10. Both gentamicin (yellow) and neomycin (orange) bind in the helix 69 region (dark grey, PDB: 4V52 + 4V53). In the absence of aminoglycosides, the bacterial ribosome helix 69 (white) adopts a conformation allowing interaction with the ribosome recycling factor (yellow, PDB: 4V54).

synthesis of nonsense proteins by misreading of mRNA. This binding mode is shared among all 2-deoxystreptamine aminoglycosides (Figure 1.9).

X-ray crystallographic insight also displays 2-deoxystreptamine aminoglycosides bind in the helix 69 large subunit rRNA, where they inhibit translocation of complete peptides and restrict ribosomal recycling.[42-46] By restricting the movement of the large subunit and inhibiting the ability

of the ribosome recycling factor to displace helix 69, the inter-subunit flexibility that allows for translocation is restricted (Figure 1.10).

1.5. Aminoglycoside Uptake and Bactericidal Activity

Contrary to most ribosome-targeting antibiotics, streptomycin and 2-deoxystreptamine aminoglycosides are not bacteriostatic, but bactericidal.[30] While we understand the structural nature of aminoglycoside binding and mechanism of action, a direct correlation between translational fidelity and the downstream bactericidal activity has not been established.[47] One hypothesis is that misfolded proteins resulting from disrupted translation insert themselves into bacterial membranes, activating stress- and redox-response systems as well as causing membrane depolarization.[48] Ultimately, this is thought to result in the presence of periplasmic proteases and the generation of reactive oxygen species.[49] Alternatively, introduction of mistranslation by mutating ribosomal proteins S4 or S5 does not result in loss of bacterial cell viability.[50] Thus, there is no mechanism known by which mistranslation causes activation of these stress response pathways.

Mechanistic support is still needed for the entry of aminoglycosides into bacterial cells. No transporters are known, and there is no uptake system displaying substrate specificity.[51] Uptake overall is non-saturable and proposed to occur over three phases.[52] In the first, electrostatic interactions between the positively charged amines and outer membrane anions, lipopolysaccharides in Gram-negative bacteria or teichoic acids in Gram-positive bacteria, promote an energy-independent association. Some mobility through membrane porins is thought to occur. The energy-dependent phase I (EDPI) requires a transmembrane potential and follows the energy-independent phase. Aminoglycosides will slowly accumulate during this second phase,

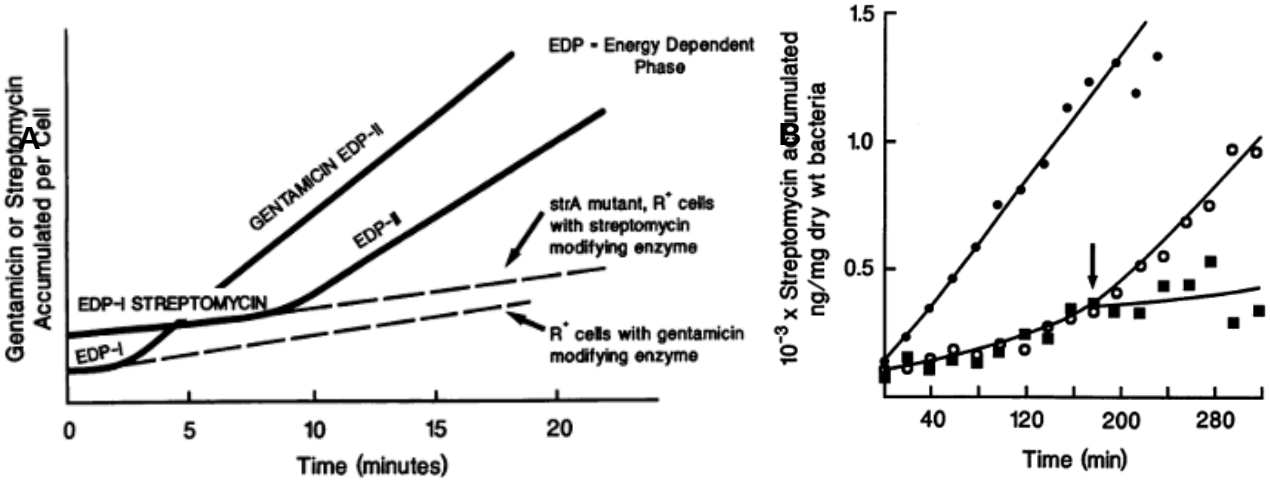

Figure 1.11. (A) Uptake of both gentamicin and streptomycin is split between slow accumulation (EDPI) and rapid uptake (EDPII). Strains with AME resistance display drastically impeded accumulation. (B) Uptake of streptomycin changes based on growth conditions: (●) cells are grown under aerobic conditions. (○) cells are grown under anerobic conditions. (■) cells have been poisoned at the time indicated by an arrow and have reduced energy consumption. Figures are taken from reference 54.

and an initial antibiotic response induces mistranslation that ultimately lowers membrane integrity following the insertion of misfolded proteins into the membrane.[53] Lastly, the corruption of the membrane results in significantly increased aminoglycoside uptake in the energy-dependent phase II (EDPII). During EDPII, aminoglycoside entry into the cell is greatly accelerated as evidenced by increased ATP hydrolysis. The highly increased aminoglycoside entry saturates ribosomes, ultimately leading to greatly restricted protein synthesis. In summary, the initially slow ionic interaction phase is followed by EDPI, which leads to rapid uptake in EDPII and cell death (Figure 1.11A).

Reliance on the electron transport chain for aminoglycoside uptake is further demonstrated by anaerobic organisms having intrinsic resistance to aminoglycosides (Figure 1.11B).[54] Naturally,

active translation is also necessary for aminoglycosides to exhibit their activity, as well as subsequently drive the self-promoted uptake of EDPII.[50] Despite having a recognizable three-phase uptake process, definitive machinery that assists in their self-promoted uptake remains unidentified.

1.6. Bacterial Resistance to Aminoglycosides

As with many classes of antibiotics, aminoglycosides have become decreasingly utilized due to the dissemination of antimicrobial resistance genes.[31] Aminoglycoside resistance spread is driven in part by antibiotic misuse worldwide as well as a general decline in antibiotic discovery campaigns over the last several decades.[55] Multi-drug resistant pathogens, especially those within the ESKAPE list (*Enterobacteria*, *Staphylococcus aureus*, *Klebsiella pneumonia*, *Acinetobacter baumannii*, *Pseudomonas aeruginosa*, and *Enterococcus faecium*), make up the bulk of nosocomial infections (Table 1.1) which carry resistance to many classes of antibiotics.

Aminoglycoside resistance can be broadly divided into three categories: covalent modification of the aminoglycoside scaffold by modifying enzymes, enzymatic modification of the ribosomal binding site, and changes to membrane permeability as well as expression of efflux systems. These will be discussed individually and in further detail below.[57]

1.6.1. Aminoglycoside Modifying Enzymes

Cofactor-dependent modification of the drug scaffold is the most common mechanism of resistance to aminoglycosides, and this is achieved by aminoglycoside modifying enzymes (AMEs).[31] These can be present in both Gram-positive and Gram-negative pathogens and can be expressed concurrently with one another to provide higher levels of resistance; these enzymes

frequently have multiple substrates upon which they act. Many of these enzymes are easily spread due to their occurrence on mobile genetic elements such as plasmids, transposons, and integrons.[57]

AMEs themselves can be divided into three sub-categories: aminoglycoside *N*-acetyltransferase (AAC), aminoglycoside *O*-phosphotransferase (APH), or aminoglycoside *O*-nucleotidyltransferase (ANT). The convention for nomenclature[58] places a number in parenthesis following the enzyme type to designate the position modified by the enzyme; this number is followed by a Roman numeral and letter to indicate the resistance profile and gene, respectively.

Table 1.1. Occurrence of gentamicin resistance in several regions between 1998–2007.[56]

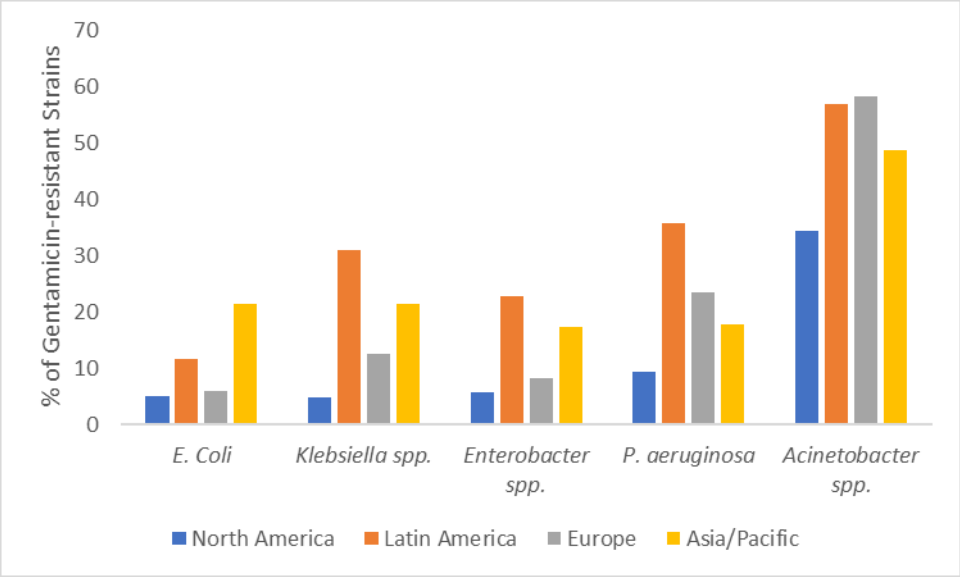

To demonstrate, both APH(3')-I and APH(3')-IIIa phosphorylate the 3'-hydroxyl of aminoglycosides, but they are different genes and enzymes with different resistance profiles.

The 2-deoxystreptamine substitution pattern of additional carbohydrates determines the individual aminoglycoside susceptibility to AMEs (Figure 1.12). AMEs are most effective at lower aminoglycoside concentrations,[57] where they inactivate the drugs in the energy independent and

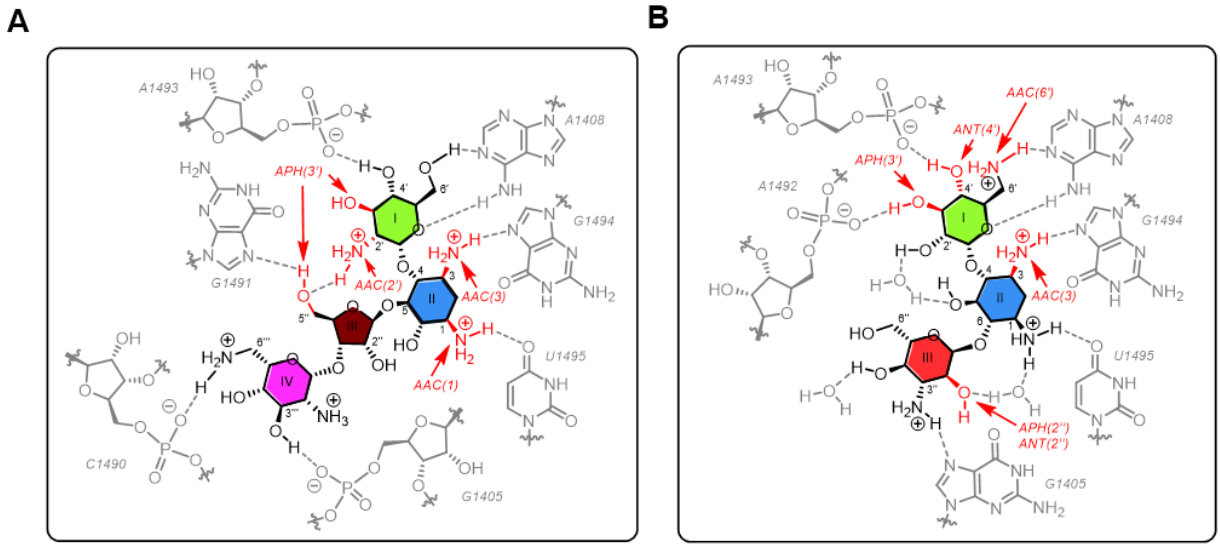

Figure 1.12. (A) Susceptibility of 4,5-disubstituted aminoglycosides to modifying enzymes. (B) Susceptibility of 4,6-disubstituted aminoglycosides to modifying enzymes.

EDPI phases of aminoglycoside uptake and preclude the later self-promoted accumulation of aminoglycosides within the bacterial cell.[51]

1.6.1.1. Aminoglycoside Acetyltransferase (AAC)

The acetyl-CoA cofactor-dependent enzymes that acetylate the multiple amine functional groups on aminoglycosides are the aminoglycoside acetyltransferases (AAC). The ring I and ring II amines of aminoglycosides are extremely critical for ribosome binding, and acetylation of the amines reduces the electrostatic interaction by removing charge and additionally introduces steric clashing in the binding site.[11a]

Being a widely conserved structural motif, the 6'-amine becomes acetylated by the most widely disseminated acetyltransferase, AAC(6').[31] In Gram-negative bacteria, the AAC(6')-I isoform is most commonly found, while in *Pseudomonas* only AAC(6')-II is observed.[58] A bifunctional enzyme AAC(6')/APH(2'') contains the isoform AAC(6')-Ie and is commonly observed in *Staphylococcus* and *Enterococcus* species. A chromosomal copy of an *aac(6')* gene

can be found in *E. faecium* and *Acinetobacter* spp. that contributes to their intrinsic aminoglycoside resistance, while most *aac(6')* genes are encoded non-chromosomally.[56,59] AAC(6') enzymes have highly promiscuous active sites and structural homology to the *N-acetyltransferase* superfamily, as supported by X-ray crystallography of this AME bound to aminoglycosides (Figure 1.13).[60–62]

AAC(3) enzymes are exclusively found in Gram-negative bacteria, including a large percentage of *Acinetobacter* and *Pseudomonas* isolates.[31] This class of enzymes unfortunately targets the most clinically relevant 4,6-disubstituted aminoglycosides, with lesser activity against the 4,5-disubstituted family members. The AAC(3)-IV isoform is uniquely active against the atypical aminoglycoside apramycin,[63] an investigational 4-monosubstitued family member that is not modified by the majority of AMEs.

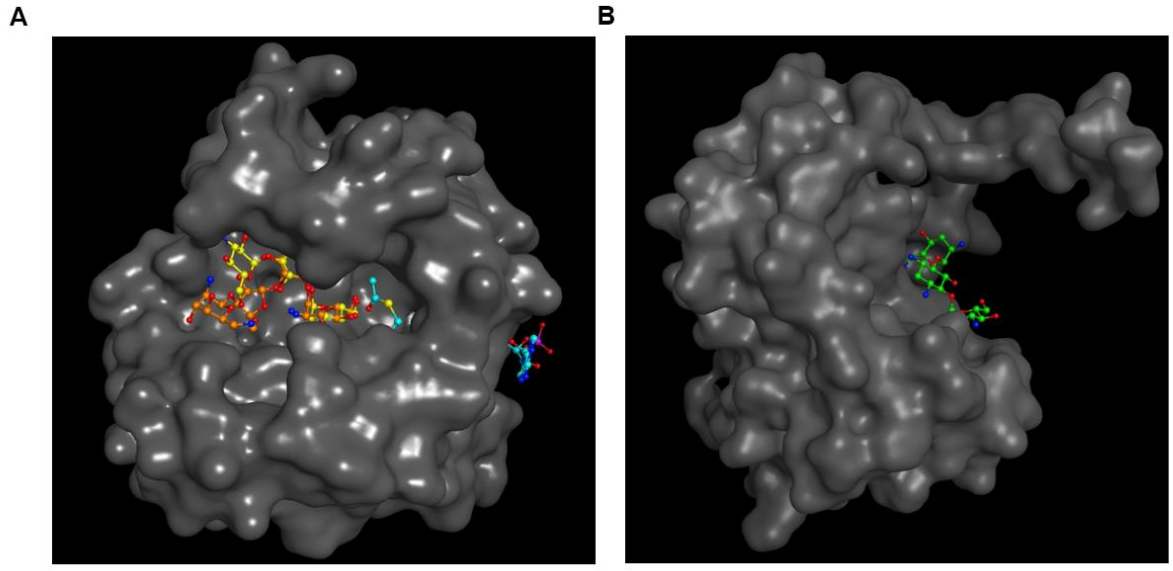

Figure 1.13. (A) Binding of kanamycin C (yellow, PDB: 1V0C) and paromomycin (orange, PDB: 2VQY) with acetyl-CoA (teal) in the AAC(6'-Ib binding site.[61] (B) Tobramycin (green) bound to the *Acinetobacter* spp. AAC(6')-Ig (PDB: 4EVY).[62]

AAC(2') is not commonly detected and generally unique to *Providencia* strains and to a lesser extent *Mycobacteria*.[64] A chromosomal *aac(2')-Ia* gene is found within *P. stuartii* in nosocomial settings that provides resistance to both 4,5- and 4,6-disubstituted aminoglycosides.[57] Clinical isolates of *E. coli* transformed with AAC(2') isoforms become highly resistant to the 4,5-disubstitued aminoglycosides neomycin and paromomycin.[65]

The AAC(1) gene is extremely rare in clinical contexts and has less detrimental effects on antibiotic activity. The most recently developed aminoglycosides for clinical use all possess the *N1*-(*S*)-4-amino-2-hydroxybutyramide side chain which lowers the relevance of this enzyme.

1.6.1.2. Aminoglycoside Phosphotransferase (APH)

Aminoglycoside phosphotransferase (APH) kinase enzymes phosphorylate the multitude of hydroxyls that decorate the aminoglycoside scaffold in an ATP or GTP-dependent manner.[11a] By phosphorylating the hydroxyls and introducing a negative charge, the ionic binding affinity for the ribosomal binding site is greatly reduced.[31]

The most prevalent aminoglycoside phosphotransferase in both dissemination and number of isoforms is the APH(3') enzymes. In Gram-negative bacteria, APH(3')-I is frequently found[58] and provides resistance to 4,5-disubstituted aminoglycosides as well as some 4,6-disubstituted family members (e.g. kanamycin). A chromosomal *aph(3")-II* gene can be found in *Pseudomonas aeruginosa* that confers resistance to any aminoglycoside with a 3'-hydroxyl group. In Gram-positive pathogens, the APH(3')-IIIa isoform provides widespread resistance to 4,5- and 4,6-disubstituted aminoglycosides; in the 4,5-disubstituted subfamily, this enzyme additionally acts as a bifunctional APH(5'') enzyme which can additionally phosphorylate the 5''-hydroxyl of ring III. This can be punishing even for aminoglycosides such as lividomycin, which lack a 3'-hydroxyl

but are still modified by this enzyme at the 5''-position.[66] The promiscuous phosphorylation activity can be attributed to the open binding site observed by its X-ray crystallography data (Figure 1.14).[67] *Acinetobacter* spp. gain considerable resistance to critically important aminoglycosides due to the frequency of APH(3')-VI resistance.

As part of the bifunctional AAC(6')/APH(2'') family of enzymes, APH(2'') enzymes provide high levels of gentamicin resistance; these enzymes are not typically found as enzymes isolated from the acetyltransferase domain, although some isolated phosphotransferases are known.[69] The phosphotransferase of *E. faecium*, APH(2'')-IIa has reported X-ray crystallographic structures, which similarly displays an open binding site for promiscuous aminoglycoside activity.[68]

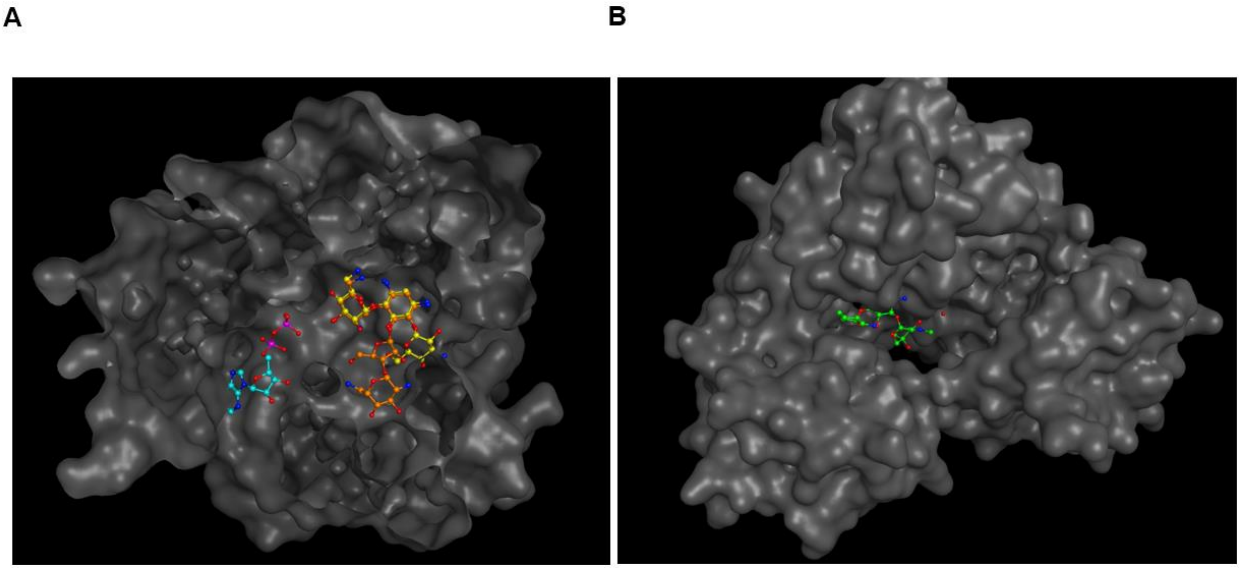

Figure 1.14. (A) Binding of neomycin (orange, PDB: 1L8T) and kanamycin A (orange, PDB: 2B0Q) to APH(3')-IIIa and a nonhydrolyzable nucleotide (teal).[67] (B) Gentamicin (green) bound to the *E. faecium* APH(2'')-IIa (PDB: 3HAM).[68]

APH(6) is less clinically relevant as it only effects streptomycin. Furthermore, APH(4) and APH(9) provide resistance to the non-canonical aminoglycosides hygromycin and spectinomycin but these are not common in the clinic.[31]

1.6.1.3. Aminoglycoside Nucleotidyltransferase (ANT)

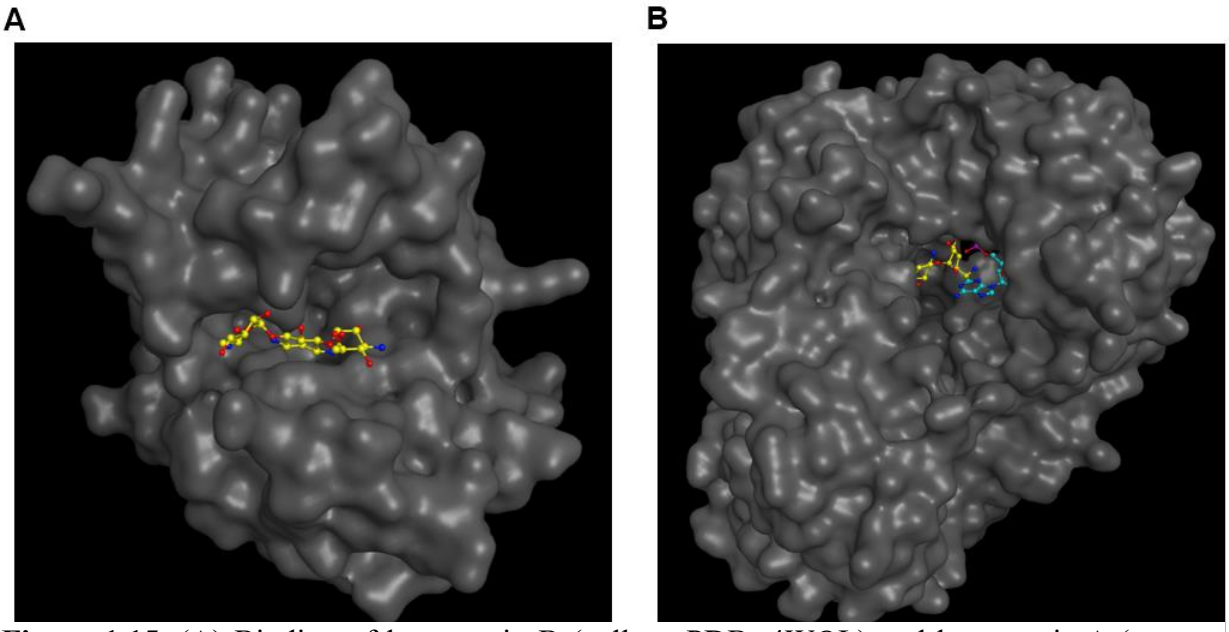

Figure 1.15. (A) Binding of kanamycin B (yellow, PDB: 4WQL) and kanamycin A (orange, PDB: 2B0Q) to ANT(2'') . (B) Kanamycin A (yellow) bound to dimeric ANT(4')-Ia and cocrystallized with nonhydroylyzable nucleotide substrate (PDB: 1KYN).[71]

The aminoglycoside nucleotidyltransferase (ANT) family of enzymes utilize ATP as a cofactor to form a covalent linkage between adenosine monophosphate and a hydroxyl on the aminoglycoside scaffold.[33] The most clinically significant enzyme, ANT(2'')-I, is common among Gram-negative species such as *Pseudomonas aeruginosa* and *Acinetobacter baumannii*; this isoform provides high-level gentamicin resistance (Figure 1.15A).[70] An enzyme only found in Gram-positive bacteria is the isoform ANT(4')-I that can phosphorylate either the 4'- or 4''-hydroxyl groups of aminoglycosides (Figure 1.15B).[71] This enzyme is found in over 30% of

Staphylococcus strains, and contributes to the multi-drug resistance of methicillin resistant *Staphylococcus aureus* (MRSA). ANT(4')-II was first seen in *Pseudomonas aeruginosa* but has since been detected in other Gram-negative pathogens.[72] Streptomycin is susceptible to action by ANT(3'') and ANT(6) enzymes, while ANT(9) nucleotidylates spectinomycin.[31]

1.6.2. Modification of the Ribosomal Target

The highly conserved nature of the ribosome makes point mutations in the 16S rRNA a rare occurrence. However, the point mutation A1408G provides complete resistance to 2-deoxystreptamine aminoglycosides due to the loss of stabilizing interactions with helix 44.[73] Most pathogens carry multiple copies of rRNA genes,[74] making single point mutations clinically irrelevant for antibiotic resistance; these single mutations are a more significant form of resistance in mycobacteria which only carry single copies of rRNA genes.[75]

Ribosomal methyltransferases (RMTs)[76] originate in aminoglycoside-producing actinomycetes and encompass another mechanism of resistance by which the bacterial ribosome undergoes modification. Producing organisms, among them actinomycetes and later the gentamicin producing *Micromonospora purpurea*, host enzymes that provide self-sustainability in the presence of their antimicrobial metabolites.[77,78] In 2003, RMTs ArmA as well as the RmtA–D family were discovered from plasmids in *P. aeruginosa*[79] and *K. pneumoniae*.[80] Since this discovery, ArmA and related RMTs that methylate N7 of G1405 have become globally disseminated.[81] By methylating this position, all 4,6-disubstituted aminoglycosides lose activity as the introduced methyl group at N7 both electrostatically clashes with the 3''-amine and creates steric bulk to disfavor aminoglycoside binding; this RMT family does not provide resistance to 4,5-disubstituted aminoglycosides such as neomycin (Figure 1.16).

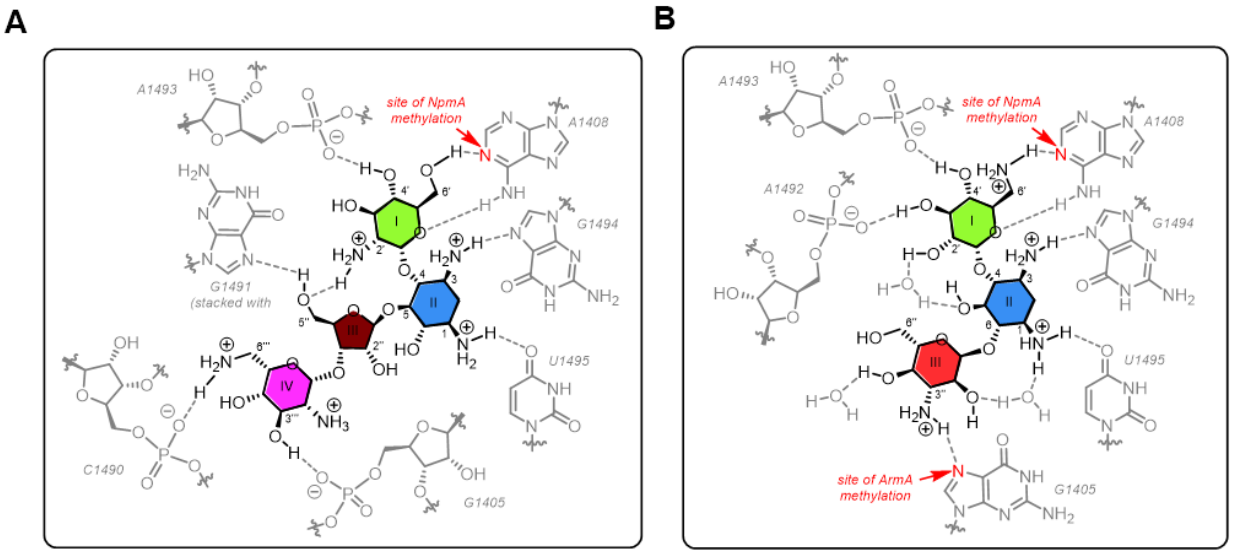

Figure 1.16. (A) RMT resistance to 4,5-disubstituted aminoglycosides arises from *N1*-methylation of base A1408 by NpmA. (B) 4,6-disubstituted aminoglycosides are susceptible to both NpmA methylation of A1408 and also ArmA methylation at G1405.

A second family of RMTs methylates N1 of base A1408 in the aminoglycoside binding site.[82] These *S*-adenosyl-methionine cofactor-utilizing enzymes, NpmA or KamB, confer complete resistance to all 2-deoxystreptamine aminoglycosides, 4,5- or 4,6-disubstituted as well as the atypical aminoglycoside apramycin.

While still less common than AMEs as a mechanism of resistance, RMTs pose a challenging threat of mobile genetic elements that provide high levels of resistance to the majority of aminoglycosides seen in the clinic. Especially concerning, these genes[83,84] frequently coincide with resistance elements to other classes of antibiotics. For example, the N7-G1405 methyltransferase ArmA is known to coincide on the same plasmid as New Delhi metallo-β-lactamase 1 (NDM-1), which itself provides high levels of β-lactam resistance; the spread of aminoglycoside RMT resistance will undoubtedly lead to surges in multi-drug resistant pathogens.

1.6.3. Efflux Flux and Membrane Susceptibility Changes

Membrane permeability changes are one mechanism by which *P. aeruginosa* exhibits aminoglycoside resistance.[85] The two-component regulatory system PhoP-PhoQ confers structural changes to the outer membrane lipopolysaccharide layer in response to polyamines[86] or Mg^{2+} starvation,[87] leading to aminoglycoside resistance. In addition, the EDPI phase of aminoglycoside uptake is restricted in response to electron-transport chain mutations[88] as well as the repression of respiratory pathways by nitric oxide production,[89] which altogether slows aminoglycoside threshold buildup leading to self-promoted uptake on the route to cell death.

Efflux is a significant contributor to aminoglycoside resistance that acts synergistically with changes in outer membrane permeability, particularly with Gram-negative pathogens like *Pseudomonas aeruginosa*.[90] The resistance nodulation division (RND) family of transmembrane

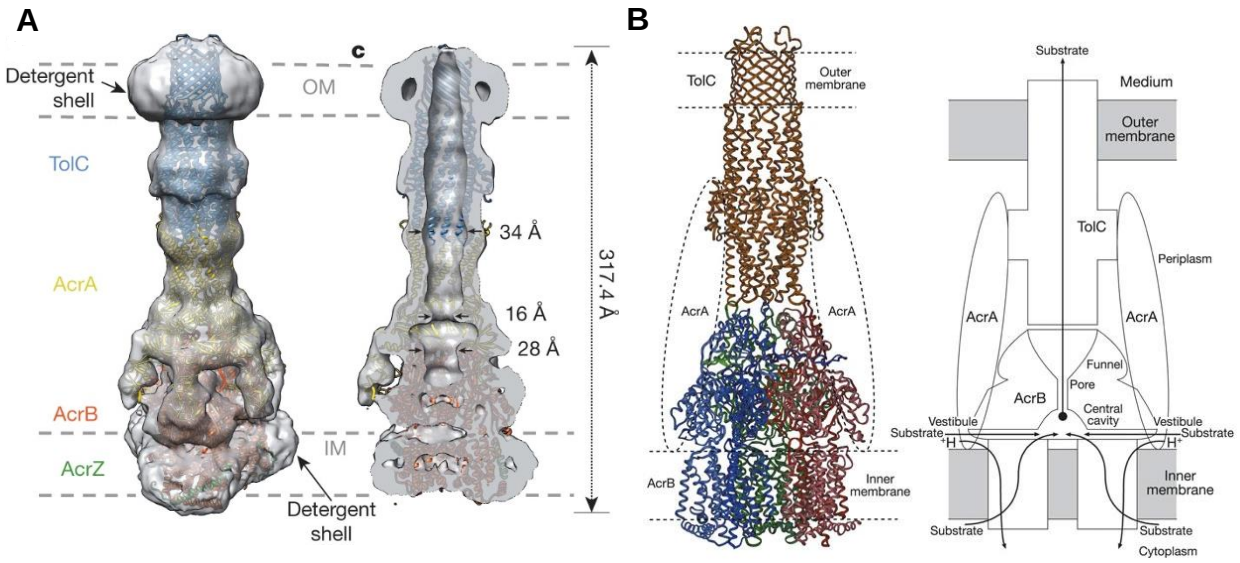

Figure 1.17. (A) Cryo-EM model and cross-section of the RND multidrug efflux system of *E. coli*, AcrAB-TolC. (B) A schematic mechanism and outline for the AcrAB-TolC efflux system (figures taken from reference 93).

efflux enzymes are exclusively found in Gram-negative bacteria and have three components: the RND membrane pump, a periplasmic membrane fusion protein (MFP), and an outer-membrane factor (OMF).[91,92] The extensive size of the pump allows transport of aminoglycosides from inside the cell directly to the extracellular space (Figure 1.17).[93] RND pumps in aminoglycoside efflux are distinct from those that export other antibiotics in which their binding pockets are far more hydrophilic; the hydrophobic binding sites used to efflux other classes make aminoglycosides poor substrates for these systems. Aminoglycoside efflux systems are named MexXY-OprM in *Pseudomonas aeruginosa*, AcrAD-TolC in *Escherichia coli*, and AdeAB-AdeC in *Acinetobacter baumannii*. These pumps become overexpressed in response to aminoglycoside treatment[94] and are a common occurrence in multi-drug resistant pathogens.[90]

1.6.4. Resistance Conclusions

Geographical location correlates with the expression and detection of many different resistance phenotypes, and these mechanisms can occur together or in isolation.[95] A summary of the most common resistance genes for the ESKAPE pathogens is shown below (Table 1.2). The most recently approved aminoglycoside, plazomicin (2018), was designed to overcome numerous modes of AME resistance. However, future aminoglycoside development must overcome the widely disseminated RMT mechanisms of resistance such as ArmA; plazomicin remains susceptible to both N7-G1405 and N1-A1408 RMT resistance.

Table 1.2. The most frequently occurring resistance phenotypes among ESKAPE pathogens.

Pathogen	**Most common resistance determinants**
Enterococci[96]	APH(3'')-IIIa, AAC(6')/APH(2'')
S. Aureus[97]	AAC(6')-Ie/APH(2''), ANT(4')-Ia, APH(3')-IIIa
K. pneumoniae[98]	AAC(6')-Ib, ANT(3'')-Ia, ANT(2'')-Ia
Acinetobacter spp.[99,100]	Efflux upregulation, AAC(3)-I, APH(3')-VI, AAC(6')-I, ANT(2'')-I, AAC(3)-II, ArmA
P. aeruginosa[99,101]	Efflux upregulation, AAC(6')-II, ANT(2'')-I, chromosomal APH(3')-II, AAC(6')-I, AAC(3)-I, ArmA
Enterobacteriaceae[99]	AAC(3)-II, AAC(6')-I, ANT(2'')-I, ArmA, AAC(3)-I

1.7. Toxicity of Aminoglycosides

From its early clinical development in the 1940s, streptomycin has readily observed nephrotoxic and ototoxic events at higher doses.[102] These adverse effects are observed with aminoglycosides of both natural and semisynthetic origin. Structure-toxicity relationships have correlated lower amine basicity[103,104] and a lower number of amine groups[105] as indicators of improved safety profiles. Due to natural similarity in the bacterial ribosomal with the human counterparts, the toxicity of aminoglycosides can be attributed to off-target toxicity by inhibiting mammalian cytosolic and mitochondrial ribosomes. Work by Prof. Erik C. Böttger has identified the atypical aminoglycoside apramycin as having an improved safety profile on account of its higher selectivity in bacterial ribosome binding.[106] Semisynthetic analogs that have benefited aminoglycoside selectivity and correlates with observed toxicity will be discussed further in Chapter 2. While mechanisms of aminoglycoside toxicity are not fully characterized, the primary side effects and relevant biochemical pathways for their nephrotoxicity[107–109] and ototoxicity[110,111] will be discussed in the sections to follow.

1.7.1. Aminoglycoside Nephrotoxicity

No metabolic transformations are performed on aminoglycosides; they are instead processed by glomerular filtration through the urine.[112] Driven by the polycationic interaction of aminoglycosides well extracellular phospholipids,[113] up to 5% of administered antibiotic is absorbed by epithelial cells.[107] Myeloid bodies occur at the same time as lysosomal accumulation of aminoglycosides and results in swelling.[114] The rupture of the lysosome releases both aminoglycosides and hydrolase enzymes which disrupt cellular structure and downstream results in apotosis.[107] Definitive targets leading to tubular necrosis are unknown, but this symptom at high doses is the prerequisite for renal shutdown.

The ability of an aminoglycoside to disrupt membrane function is correlated with their nephrotoxicity.[1] In general, 4,5-disubstituted aminoglycosides display the highest levels of nephrotoxicity while 4,6-disubtituted members and streptomycin are more tolerated.[112]

Perhaps the most significant breakthrough in aminoglycoside-induced nephrotoxicity was advances in pharmacokinetic understanding for aminoglycosides. At clinically relevant concentrations of aminoglycoside antimicrobial activity, kidney tubular cells displayed saturable kinetics for aminoglycoside uptake.[115] The antimicrobial activity was additionally correlated with peak serum level, or "C_{max} driven" efficacy, as opposed to length of high concentration exposure. Additional animal models[116] and human pharmacokinetic studies indicated that gentamicin, when administered once daily, had measurably lower kidney cell concentrations when distributed in multiple doses or continuous infusions.[117] Once-daily dosing is now the accepted standard for aminoglycoside treatment as it maintains serum drug levels lower than that required for binding to tissue receptors.[118,119]

1.7.2. Aminoglycoside Ototoxicity

Ototoxic events during aminoglycoside therapy are irreversible, unlike their nephrotoxic counterparts; in some reports a permanent 30% loss of hearing has been described following antibiotic treatment.[110] Aminoglycoside ototoxicity generally occurs in two forms: cochlear hair cell damage within the ear that results in hearing loss (Figure 1.18),[111] or vestibular impairment that is associated with dizziness.[112] Cochlear toxicity damages hearing across frequency ranges but may not be detected early due to initial onset of hearing loss falling outside ranges generally tested. New semisynthetic derivatives seek to circumvent the ototoxic effect of aminoglycosides be improving the selectivity for the bacterial ribosome, and these will be discussed further in Chapter 2.

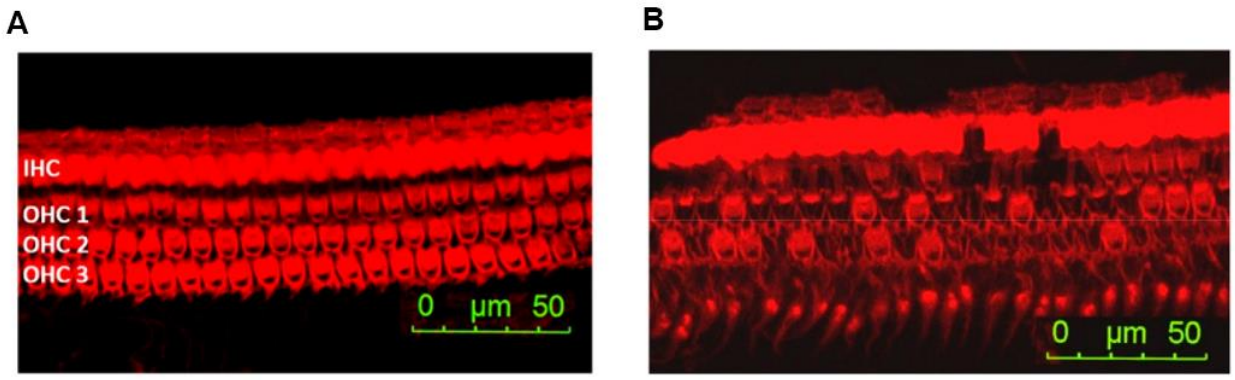

Figure 1.18. (A) Microscopic examination of guinea pig inner hair cells (IHC) and outer hair cells (OHC) layers following saline treatment for 14 days. The hair cells remain undamaged. (B) Treatment of guinea pigs with gentamicin over 14 days reveals extensive damage to the IHC and OHC layers. Figure taken from reference 127.

Aminoglycoside entry into the inner ear cells occurs minutes after administration.[120] The half-life of aminoglycosides in the inner ear cells can exceed 30 days, far longer than the 3–5 hour half-life serum concentrations.[121] Therefore, the effects of aminoglycoside damage can continue

long past clearance from the bloodstream. The cochlear hair cells are the primary target of aminoglycosides which become damaged upon treatment.[110] These cells are responsible for auditory signal transmission as well as balance; these cells cannot be regenerated if damaged which explains the irreversibility of aminoglycoside-induced hearing loss. Accumulation in the cochlear hair cells is thought to result from aminoglycoside uptake through cation-sensitive mechanotransducer channels.

Side effects are observed in up to 20% of patients following aminoglycoside treatment. Ototoxic events are of far greater likelihood when patients have point mutations in the mitochondrial 12S rRNA, specifically nucleotide 1555 (A1555G) or the less common C1494U mutant.[122,123] The change in the mammalian ribosome brings more structural similarity to the bacterial ribosome, resulting in promoted aminoglycoside binding. Inhibition of mammalian ribosomes is thought to result in aminoglycoside-associated ototoxicity. However, the mechanism of hair cell death is not fully characterized. Aminoglycoside chelation with transition metals is a known phenomenon and is also associated with increased free radical formation. The reactions of aminoglycosides in cells are also thought to result in reactive oxygen species[124]; these effects are consistently reduced in a guinea pig model[125] wherein chelating iron is concurrently dosed at the same time as aminoglycosides. Gentamicin is known to promote the formation of radicals in the presence of transition metals. Aminoglycoside dosing has been demonstrated to result in redox-response pathways stimulating superoxide radical generation by NADPH oxidase.[126] Both the inhibition of mitochondrial ribosomes and the interference with redox function are likely related and important precursors in aminoglycoside ototoxicity pathways.

1.8. References

1. Begg, E. J.; Barclay, M. L. *Br. J. Clin. Pharmacol.* **1995**, *39*, 597.

2. (a) Jones, D.; Metzger, H. J.; Schatz, A.; Waksman, S. A. *Science* **1944**, *100*, 103; (b) Schatz, A.; Bugle, E.; Waksman, S. A. *Proc. Soc. Exp. Biol. Med.* **1944**, *55*, 66.

3. Schatz, A.; Waksman, S. A. *Proc. Soc. Exp. Biol. Med.* **1944**, *57*, 244.

4. Waksman, S. A. Nobel Lecture: Streptomycin: Background, Isolation, Properties, and Utilization. http://www.nobelprize.org/nobel_prizes/medicine/laureates/1952/waksmanlecture.html (accessed Jan 16).

5. (a) Waksman, S. A.; Lechevalier, H. A. Science 1949, 109, 305; (b) Waksman, S. A.; Lechevalier, H. A.; Harris, D. A. *J. Clin. Invest.* **1949**, *28*, 934.

6. (a) Parke, Davis & Company. Belgian Patent 547,976, October 12, 1956; (b) Haskell, T. H.; French, J. C.; Bartz, Q. R. *J. Am. Chem. Soc.* **1959**, *81*, 3480.

7. Umezawa, H.; Ueda, M.; Maeda, K.; Yagishita, K.; Kondo, S.; Okami, Y.; Utahara, R.; Osato, Y.; Nitta, K.; Takeuchi, T. *J. Antibiot.* **1957**, *10*, 181.

8. (a) Weinstein, M. J.; Luedemann, G. M.; Oden, E. M.; Wagman, G. H. *Antimicrob. Agents Chemother.* **1963**, *161*, 1; (b) Black, J.; Calesnick, B.; Williams, D.; Weinstein, M. J. *Antimicrob. Agents Chemother.* **1963**, *161*, 138; (c) Weinstein, M. J.; Luedemann, G. M.; Oden, E. M.; Wagman, G. H.; Rosselet, J. P.; Marquez, J. A.; Coniglio, C. T.; Charney, W.; Herzog, H. L.; Black, J. *J. Med. Chem.* **1963**, *6*, 463.

9. Higgins, C. E.; Kastner, R. E. *Antimicrob. Agents Chemother.* **1967**, *7*, 324.

10. Weinstein, M. J.; Marquez, J. A.; Testa, R. T.; Wagman, G. H.; Oden, E. M.; Waitz, J. A. *J. Antibiot.* 1970, 23, 551.

11. (a) *Aminoglycoside Antibiotics: From Chemical Biology to Drug Discovery*. 1 ed.; John Wiley & Sons: 2007; (b) Lechevalier, H. A. *CRC Crit. Rev. Microbiol.* **1975**, *3*, 359.

12. A Price, K. E. *Antimicrob. Agents Chemother.* **1986**, *29*, 543.

13. Daniels, P. J. L.; Rane, D. F.; McCombie, S. W.; Testa, R. T.; Wright, J. J.; Nagabhushan, T. L., Chemical and Biological Modification of Antibiotics of the Gentamicin Group. In *Aminocyclitol Antibiotics*, American Chemical Society: 1980; Vol. 125, pp 371.

14. Avent, M. L.; Rogers, B. A.; Cheng, A. C.; Paterson, D. L. *Intern. Med.* **2011**, *41*, 441.

15. Jana, S.; Rajasekaran, P.; Haldimann, K.; Vasella, A.; Böttger, E.C.; Hobbie, S.N.; Crich, D. *ACS Infect. Dis.* **2023**, *9*, 1622.

16. Tan, K. H.-V.; Mulheran, M.; Knox, A. J.; Smyth, A. R. *Am. J. Respir. Crit. Care Med.* **2003**, *167*, 819.

17. Millard, J.; Ugarte-Gil, C.; Moore, D. A. J. *BMJ* **2015**, *350*.

18. Busscher, G. F.; Rutjes, F. P. J. T.; van Delft, F. L. *Chem. Rev.* **2005**, *105*, 775.

19. Carter, H. E.; Clark, R. K.; Dickman, S. R.; Loo, Y. H.; Meek, J. S.; Skell, P. S.; Strong, W. A.; Alberi, J. T.; Bartz, Q. R.; Binkley, S. B.; Crooks, H. M.; Hooper, I. R.; Rebstock, M. C. *Science* **1946**, *103*, 53.

20. Flatt, P. M.; Mahmud, T. *Nat. Prod. Rep.* **2007**, *24*, 358.

21. Dewick, P. M., Carbohydrates. In *Medicinal Natural Products*, John Wiley & Sons, Ltd: 2009; pp 485.

22. Huang, F.; Spiteller, D.; Koorbanally, N. A.; Li, Y.; Llewellyn, N. M.; Spencer, J. B. *ChemBioChem* **2007**, *8*, 283.

23. Park, J. W.; Park, S. R.; Nepal, K. K.; Han, A. R.; Ban, Y. H.; Yoo, Y. J.; Kim, E. J.; Kim, E. M.; Kim, D.; Sohng, J. K.; Yoon, Y. J. *Nat. Chem. Biol.* **2011**, *7*, 843.

24. Park, J. W.; Hong, J. S. J.; Parajuli, N.; Jung, W. S.; Park, S. R.; Lim, S.-K.; Sohng, J. K.; Yoon, Y. J. *Proc. Natl. Acad. Sci. USA* **2008**, *105*, 8399.

25. Huang, C.; Huang, F.; Moison, E.; Guo, J.; Jian, X.; Duan, X.; Deng, Z.; Leadlay, Peter F.; Sun, Y. *Chem. Biol.* **2015**, *22*, 251.

26. Fan, P.-H.; Sato, S.; Yeh, Y.-C.; Liu, H. *J. Am. Chem. Soc.* **2023**, *145*, 21361.

27. (a) Steitz, T. A. *Nat. Rev. Mol. Cell Biol.* **2008**, *9*, 242; (b) Alberts, B., Johnson, A., Lewis, J., Raff, M., Roberts, K., and Walter, P, *Molecular biology of the cell*. 4th ed.; Garland Science: New York, 2002.

28. Marshall, R. A.; Aitken, C. E.; Dorywalska, M.; Puglisi, J. D. *Annu. Rev. Biochem* **2008**, *77*, 177.

29. Wilson, D. N. *Nat. Rev. Microbiol.* **2014**, *12*, 35.

30. Wilson, D. N. *Crit. Rev. Biochem. Mol. Biol.* **2009**, *44*, 393.

31. Becker, B.; Cooper, M. A. *ACS Chem. Biol.* **2013**, *8*, 105.

32. Fosso, M. Y.; Li, Y.; Garneau-Tsodikova, S. *Med, Chem. Comm.* **2014**, *5*, 1075.

33. Houghton, J. L.; Green, K. D.; Chen, W.; GarneauTsodikova, S. *ChemBioChem* **2010**, *11*, 880.

34. Ogle, J. M.; Brodersen, D. E.; Clemons, W. M.; Tarry, M. J.; Carter, A. P.; Ramakrishnan, V. *Science* **2001**, *292*, 897.

35. Borovinskaya, M. A.; Pai, R. D.; Zhang, W.; Schuwirth, B. S.; Holton, J. M.; Hirokawa, G.; Kaji, H.; Kaji, A.; Cate, J. H. D. *Nat. Struct. Mol. Biol.* **2007**, *14*, 727.

36. Wang, L.; Pulk, A.; Wasserman, M. R.; Feldman, M. B.; Altman, R. B.; Cate, J. H. D.; Blanchard, S. C. *Nat. Struct. Mol. Biol.* **2012**, *19*, 957.

37. Ibba, M.; Söll; Dieter *Science* **1999**, *286*, 1893.

38. Johansson, M.; Lovmar, M.; Ehrenberg, M. *Curr. Opin. Microbiol.* **2008**, *11*, 141.

39. (a) Fourmy, D.; Recht, M. I.; Blanchard, S. C.; Puglisi, J. D. Science 1996, 274, 1367; (b) Fourmy, D.; Recht, M. I.; Puglisi, J. D. J. Mol. Biol. 1998, 277, 347; (c) Fourmy, D.; Yoshizawa, S.; Puglisi, J. D. *J. Mol. Biol.* **1998**, *277*, 333.

40. Carter, A. P.; Clemons, W. M.; Brodersen, D. E.; Morgan-Warren, R. J.; Wimberly, B. T.; Ramakrishnan, V. *Nature* **2000**, *407*, 340.

41. Scheunemann, A. E.; Graham, W. D.; Vendeix, F. A. P.; Agris, P. F. *Nucleic Acids Res.* **2010**, *38*, 3094.

42. Schuwirth, B. S.; Borovinskaya, M. A.; Hau, C. W.; Zhang, W.; Vila-Sanjurjo, A.; Holton, J. M.; Cate, J. H. D. *Science* **2005**, *310*, 827.

43. (a) Dorner, S.; Brunelle, J. L.; Sharma, D.; Green, R. *Nat. Struct. Mol. Biol.* **2006**, *13*, 234; (b) Munro, J. B.; Wasserman, M. R.; Altman, R. B.; Wang, L.; Blanchard, S. C. *Nat. Struct. Mol. Biol.* **2010**, *17*, 1470.

44. (a) Jesús Cabañas, M.; Vázquez, D.; Modolell, J. *Biochem. Biophys. Res. Commun.* **1978**, *83*, 991; (b) Misumi, M.; Nishimura, T.; Komai, T.; Tanaka, N. *Biochem. Biophys. Res. Commun.* **1978**, *84*, 358.

45. Shoji, S.; Walker, S. E.; Fredrick, K. *Mol. Cell* **2006**, *24*, 931.

46. (a) Ogle, J. M.; Murphy, F. V.; Tarry, M. J.; Ramakrishnan, V. Cell 2002, 111, 721; (b) Gromadski, K. B.; Rodnina, M. V. *Nat. Struct. Mol. Biol.* **2004**, *11*, 316.

47. Davis, B. D. *Microbiol. Rev.* **1987**, *51*, 341.

48. Kohanski, M. A.; Dwyer, D. J.; Wierzbowski, J.; Cottarel, G.; Collins, J. J. *Cell* **2008**, *135*, 679.

49. Kohanski, M. A.; Dwyer, D. J.; Hayete, B.; Lawrence, C. A.; Collins, J. J. *Cell* **2007**, *130*, 797.

50. Zimmermann, R. A.; Garvin, R. T.; Gorini, L. *Proc. Natl. Acad. Sci. USA* **1971**, *68*, 2263.

51. Taber, H. W.; Mueller, J. P.; Miller, P. F.; Arrow, A. S. *Microbiol. Rev.* **1987**, *51*, 439.

52. Vakulenko, S. B.; Mobashery, S. *Clin. Microbiol. Rev.* **2003**, *16*, 430.

53. Magnet, S.; Blanchard, J. S. *Chem. Rev.* **2005**, *105*, 477.

54. Schlessinger, D. *Clin. Microbiol. Rev.* **1988**, *1*, 54.

55. Boucher, H. W.; Talbot, G. H.; Benjamin, J. D. K.; Bradley, J.; Guidos, R. J.; Jones, R. N.; Murray, B. E.; Bonomo, R. A.; Gilbert, D. *Clin. Infect. Dis.* **2013**, *56*, 1685.

56. Biedenbach, D.; Jones, R.; Miller, G.; Armstrong, E. Ten-year trend in aminoglycoside resistance from a worldwide collection of Gram-negative pathogens (1998-2007), In 19th European Congress of Clinical Microbiology and Infectious Diseases, Helsinki, Finland, 2009. http://www.achaogen.com/media-all/2009/7/21/ten-year-trend-in-aminoglycoside-resistancefrom-a-worldwide-collection-of-gram-negative-pathogens-1998-2007.

57. Davies, J.; Wright, G. D. *Trends Microbiol.* **1997**, *5*, 234.

58. Shaw, K.; Rather, P.; Hare, R.; Miller, G. *Microbiol. Rev.* **1993**, *57*, 138.

59. Costa, Y.; Galimand, M.; Leclercq, R.; Duval, J.; Courvalin, P. *Antimicrob. Agents Chemother.* **1993**, *37*, 1896.

60. Vetting, M. W.; Park, C. H.; Hegde, S. S.; Jacoby, G. A.; Hooper, D. C.; Blanchard, J. S. *Biochemistry* **2008**, *47*, 9825.

61. Stogios, P. J.; Kuhn, M. L.; Evdokimova, E.; Law, M.; Courvalin, P.; Savchenko, A. *ACS Infect. Dis.* **2017**, *3*, 132.

62. Vetting, M. W.; de Carvalho, L. P. S.; Yu, M.; Hegde, S. S.; Magnet, S.; Roderick, S. L.; Blanchard, J. S. *Arch. Biochem. Biophys.* **2005**, *433*, 212.

63. Quirke, J.C.K.; Rajasekaran, P.; Sarpe, V.A.; Sonousi, A.; Osinnii, I.; Gysin, M.; Haldimann, K.; Fang, Q.-J.; Shcherbakov, D.; Hobbie, S.N.; Sha, S.-H.; Schacht, J.; Vasella, A.; Böttger, E.C.; Crich, D. *J. Am. Chem. Soc.* **2020**, *142*, 530.

64. Vetting, M. W.; Hegde, S. S.; Javid-Majd, F.; Blanchard, J. S.; Roderick, S. L. *Nat. Struct. Mol. Biol.* **2002**, *9*, 653.

65. Cox, G.; Ejim, L.; Stogios, P.J.; Koteva, K.; Bordeleau, E.; Evdokimova, E.; Sieron, A.O.; Savchenko, A.; Serio, A.W.; Krause, K.M.; Wright, G.D. *ACS Infect. Dis.* **2018**, *4*, 980.

66. Kondo, S.; Yamamoto, H.; Naganawa, H.; Umezawa, H.; Mitsuhashi, S. *J. Antibiot.* **1972**, *25*, 483.

67. Fong, D. H.; Berghuis, A. M. *EMBO J.* **2002**, *21*, 2323.

68. Young, P. G.; Walanj, R.; Lakshmi, V.; Byrnes, L. J.; Metcalf, P.; Baker, E. N.; Vakulenko, S. B.; Smith, C. A. *J. Bacteriol.* **2009**, 191, 4133.

69. Toth, M.; Chow, J. W.; Mobashery, S.; Vakulenko, S. B. *J. Biol. Chem.* **2009**, *284*, 6690.

70. Cox, G.; Stogios, P. J.; Savchenko, A.; Wright, G. D. *mBio* **2015**, *6*.

71. Pedersen, L. C.; Benning, M. M.; Holden, H. M. *Biochemistry* **1995**, *34*, 13305.

72. Jacoby, G. A.; Blaser, M.; Santanam, P.; Hächler, H.; Kayser, F.; Hare, R.; Miller, G. *Antimicrob. Agents Chemother.* **1990**, *34*, 2381.

73. (a) De Stasio, E. A.; Moazed, D.; Noller, H. F.; Dahlberg, A. E. *EMBO J.* **1989**, *8*, 1213; (b) Springer, B.; Kidan, Y. G.; Prammananan, T.; Ellrott, K.; Böttger, E. C.; Sander, P. *Antimicrob. Agents Chemother.* **2001**, *45*, 2877.

74. Maianti, J. P. Semisynthetic Aminoglycoside Antibiotics – Toward Biomimetic Synthesis, Evasion of Bacterial Resistance and Reduced Toxicity. M.Sc. thesis, University of Montreal, Montreal, Canada, 2010.

75. (a) Prammananan, T.; Sander, P.; Brown, B. A.; Frischkorn, K.; Onyi, G. O.; Zhang, Y.; Böttger, E. C.; Wallace, J. R. J. *J. Infect. Dis.* **1998**, *177*, 1573; (b) Shcherbakov, D.; Akbergenov, R.; Matt, T.; Sander, P.; Andersson, D. I.; Böttger, E. C. *Mol. Microbiol.* **2010**, *77*, 830.

76. Doi, Y.; Arakawa, Y. *Clin. Infect. Dis.* **2007**, *45*, 88.

77. Cundliffe, E. Annu. Rev. *Microbiol*. **1989**, *43*, 207.

78. Thompson, J.; Skeggs, P. A.; Cundliffe, E. *Mol. Gen. Genet.* **1985**, *201*, 168.

79. Yokoyama, K.; Doi, Y.; Yamane, K.; Kurokawa, H.; Shibata, N.; Shibayama, K.; Yagi, T.; Kato, H.; Arakawa, Y. *Lancet* **2003**, *362*, 1888.

80. Galimand, M.; Courvalin, P.; Lambert, T. *Antimicrob. Agents Chemother.* **2003**, *47*, 2565.

81. Karthikeyan, K.; Thirunarayan, M.; Krishnan, P. *J. Antimicrob. Chemother.* **2010**, *65*, 2253.

82. Wachino, J.; Shibayama, K.; Kurokawa, H.; Kimura, K.; Yamane, K.; Suzuki, S.; Shibata, N.; Ike, Y.; Arakawa, Y. *Antimicrob. Agents Chemother.* **2007**, *51*, 4401.

83. Aggen, J. B.; Armstrong, E. S.; Goldblum, A. A.; Dozzo, P.; Linsell, M. S.; Gliedt, M. J.; Hildebrandt, D. J.; Feeney, L. A.; Kubo, A.; Matias, R. D. *Antimicrob. Agents Chemother.* **2010**, *54*, 4636.

84. Fritsche, T. R.; Castanheira, M.; Miller, G. H.; Jones, R. N.; Armstrong, E. S. *Antimicrob. Agents Chemother.* **2008**, *52*, 1843.

85. Bryan, L.; O'hara, K.; Wong, S. *Antimicrob. Agents Chemother.* **1984**, *26*, 250.

86. Kwon, D. H.; Lu, C.-D. *Antimicrob. Agents Chemother.* **2006**, *50*, 1615.

87. Macfarlane, E. L. A.; Kwasnicka, A.; Hancock, R. E. W. *Microbiology* **2000**, *146*, 2543.

88. Muir, M. E.; Hanwell, D. R.; Wallace, B. J. *BBA-Bioenergetics* **1981**, *638*, 234.

89. (a) Gusarov, I.; Shatalin, K.; Starodubtseva, M.; Nudler, E. Science 2009, 325, 1380; (b) McCollister, B. D.; Hoffman, M.; Husain, M.; Vázquez-Torres, A. *Antimicrob. Agents Chemother.* **2011**, *55*, 2189.

90. Li, X.-Z.; Plésiat, P.; Nikaido, H. *Clin. Microbiol. Rev.* **2015**, *28*, 337.

91. Nikaido, H.; Pagès, J.-M. *FEMS Microbiol. Rev.* **2012**, *36*, 340.

92. Kumar, A.; Schweizer, H. P. *Adv. Drug Deliv. Rev.* **2005**, *57*, 1486.

93. (a) Nakashima, R.; Sakurai, K.; Yamasaki, S.; Hayashi, K.; Nagata, C.; Hoshino, K.; Onodera, Y.; Nishino, K.; Yamaguchi, A. *Nature* **2013**, *500*, 102; (b) Murakami, S.; Nakashima, R.; Yamashita, E.; Yamaguchi, A. *Nature* **2002**, *419*, 587; (c) Murakami, S.; Nakashima, R.; Yamashita, E.; Matsumoto, T.; Yamaguchi, A. *Nature* **2006**, *443*, 173; (d) Du, D.; Wang, Z.; James, N. R.; Voss, J. E.; Klimont, E.; Ohene-Agyei, T.; Venter, H.; Chiu, W.; Luisi, B. F. *Nature* **2014**, *509*, 512.

94. Masuda, N.; Sakagawa, E.; Ohya, S.; Gotoh, N.; Tsujimoto, H.; Nishino, T. *Antimicrob. Agents Chemother.* **2000**, *44*, 2242.

95. (a) Miller, G. H.; Sabatelli, F. J.; Hare, R. S.; Glupczynski, Y.; Mackey, P.; Shlaes, D.; Shimizu, K.; Shaw, K. J. *Clin. Infect. Dis.* **1997**, *24*, S46; (b) Över, U.; Gür, D.; Ünal, S.; Miller, G. H. *Clin. Microbiol. Infect.* **2001**, *7*, 470.

96. Kobayashi, N.; Alam, M. M.; Nishimoto, Y.; Urasawa, S.; Uehara, N.; Watanabe, N. *Epidemiol. Infect.* **2001**, *126*, 197.

97. Schmitz, F.-J.; Fluit, A. C.; Gondolf, M.; Beyrau, R.; Lindenlauf, E.; Verhoef, J.; Heinz, H.-P.; Jones, M. E. *J. Antimicrob. Chemother*. **1999**, *43*, 253.

98. Endimiani, A.; Hujer, K. M.; Hujer, A. M.; Armstrong, E. S.; Choudhary, Y.; Aggen, J. B.; Bonomo, R. A. *Antimicrob. Agents Chemother.* **2009**, *53*, 4504.

99. Armstrong, E. S.; Miller, G. H. *Curr. Opin. Microbiol.* **2010**, *13*, 565.

100. Hujer, K. M.; Hujer, A. M.; Hulten, E. A.; Bajaksouzian, S.; Adams, J. M.; Donskey, C. J.; Ecker, D. J.; Massire, C.; Eshoo, M. W.; Sampath, R. *Antimicrob. Agents Chemother.* **2006**, *50*, 4114.

101. Poole, K. *Antimicrob. Agents Chemother.* **2005**, *49*, 479.

102. (a) Hinshaw, H. C.; Feldman, W. H. *Proc. Mayo Clin.* **1945**, *20*, 313; (b) Kahlmeter, G.; Dahlager, J. I. *J. Antimicrob. Chemother.* **1984**, *13*, 9.

103. Shitara, T.; Kobayashi, Y.; Tsuchiya, T.; Umezawa, S. *Carbohydr. Res.* **1992**, *232*, 273.

104. Chen, L.; Hainrichson, M.; Bourdetsky, D.; Mor, A.; Yaron, S.; Baasov, T. *Bioorg. Med. Chem.* **2008**, *16*, 8940.

105. Fujisawa, K.; Hoshiya, T.; Kawaguchi, H. *J. Antibiot.* **1974**, 27, 677.

106. Tanja, M.; Ng, C.L.; Lang, K.; Sha, S.-H.; Akbergenov, R.; Shcherbakov, D.; Meyer, M.; Duscha, S.; Xie, J.; Dubbaka, S.R.; Perez-Fernandez, D.; Vasella, A.; Ramakrishnan, V.; Schacht, J.; Böttger, E. C. *Proc. Natl. Acad. Sci. USA*, **2012**, *109*, 10984.

107. Mingeot-Leclercq, M.-P.; Tulkens, P. M. *Antimicrob. Agents Chemother.* **1999**, *43*, 1003.

108. Nagai, J.; Takano, M. *Drug Metab. Pharmacokinet.* **2004**, *19*, 159.

109. Servais, H.; Ortiz, A.; Devuyst, O.; Denamur, S.; Tulkens, P.; Mingeot-Leclercq, M.-P. *Apoptosis* **2008**, *13*, 11.

110. Guthrie, O. n. W. *Toxicology* **2008**, *249*, 91.

111. Huth, M.; Ricci, A.; Cheng, A. *Int. J. Pediatr. Otorhinolaryngol*. **2011**, *2011*.

112. Koeda, T.; Umemura, K.; Yokota, M., Toxicology and Pharmacology of Aminoglycoside Antibiotics. In *Aminoglycoside Antibiotics*, Umezawa, H.; Hooper, I. R., Eds. Springer Berlin Heidelberg: Berlin, Heidelberg, 1982; pp 293.

113. Laurent, G.; Kishore, B. K.; Tulkens, P. M. *Biochem. Pharmacol.* **1990**, *40*, 2383.

114. Jao, W.; Manaligod, J. R.; Gerardo, L. T.; Castillo, M. M. *J. Pathology* **1983**, *139*, 33.

115. Giuliano, R. A.; Verpooten, G. A.; Verbist, L.; Wedeen, R. P.; De Broe, M. E. *J. Pharmacol. Exp. Ther.* **1986**, *236*, 470.

116. Reiner, N. E.; Bloxham, D. D.; Thompson, W. L. *J. Antimicrob. Chemother.* **1978**, *4*, 85.

117. Freeman, C. D.; Nicolau, D. P.; Belliveau, P.; Nightingale, C. *J. Antimicrob. Chemother.* **1997**, *39*, 677.

118. Conly, J. M.; Gold, W.; Shafran, S. D. *Can. J. Infect. Dis.* **1994**, *5*, 205.

119. Eliopoulos, G. M.; Drusano, G. L.; Ambrose, P. G.; Bhavnani, S. M.; Bertino, J. S.; Nafziger, A. N.; Louie, A. *Clin. Infect. Dis.* **2007**, *45*, 753.

120. Tran Ba Huy, P.; Bernard, P.; Schacht, J. *J. Clin. Invest.* **1986**, *77*, 1492.

121. Henley, C. M.; Schacht, J. *Audiology* **1988**, *27*, 137.

122. Prezant, T. R.; Agapian, J. V.; Bohlman, M. C.; Bu, X.; Öztas, S.; Qiu, W.-Q.; Arnos, K. S.; Cortopassi, G. A.; Jaber, L.; Rotter, J. I. *Nature Genet.* **1993**, *4*, 289.

123. (a) Hamasaki, K.; Rando, R. R. *Biochemistry* **1997**, *36*, 12323; (b) Hobbie, S. N.; Akshay, S.; Kalapala, S. K.; Bruell, C. M.; Shcherbakov, D.; Böttger, E. C. *Proc. Natl. Acad. Sci. USA* **2008**, *105*, 20888.

124. Priuska, E. M.; Schacht, J. *Biochem. Pharmacol.* **1995**, *50*, 1749.

125. Song, B.-B.; Schacht, J. *Hearing research* **1996**, *94*, 87.

126. Jiang, H.; Sha, S.-H.; Schacht, J. *J. Neurosci. Res.* **2006**, *83*, 1544.

127. Matsushita, T.; Sati, G.; Kondasinghe, N.; Pirrone, M.; Kato, T.; Waduge, P.; Kumar, H.; Sanchon, A.; Dobosz-Bartoszek, M.; Shcherbakov, D.; Juhas, M.; Hobbie, S. N.; Schrepfer, T.; Chow, C. S.; Polikanov, Y.; Schacht, J.; Vasella, A.; Böttger, E. C.; Crich, D. *J. Am. Chem. Soc.* **2019**, *141*, 5051.

Chapter 2. Overview of Aminoglycoside Semisynthesis: Semisynthetic Achievements and Site-Selective Modifications

2.1 Semisynthesis of Aminoglycoside antibiotics – Historic Examples

Billions of years of evolutionary pressure have molded aminoglycoside antibiotics as chemical weapons in an inter-species struggle for survival. Naturally, the properties that have made these molecules effective within their microbial communities do not necessarily make them suitable for use in humans to treat infection. Medicinal chemists have utilized these secondary metabolites as starting materials in semisynthesis, the chemical modification of natural products to create non-natural derivatives.[1] In this section, the semisynthesis of several aminoglycosides approved for use in humans will be discussed as examples of success with the practice. In addition, targeted modifications to different positions on the drug scaffold will be presented as strategies for new aminoglycoside discovery. Comprehensive reviews of site-selective aminoglycoside modification and related patents have been published previously,[2,3] and this chapter will seek to cover molecules that have achieved clinical success or provide early hints at the direction of next-generation aminoglycoside development.

The first semisynthetic modification of aminoglycosides occurred just three years after the isolation of streptomycin, where a platinum-catalyzed hydrogenation afforded dihydrostreptomycin[4] that bared comparable antimicrobial activity while having improved chemical stability (Figure 2.1); this drug was later found to have a different toxicological profile.[5] Both streptomycin and dihydrostreptomycin continue to find clinical use or maintain utility in veterinary medicine.

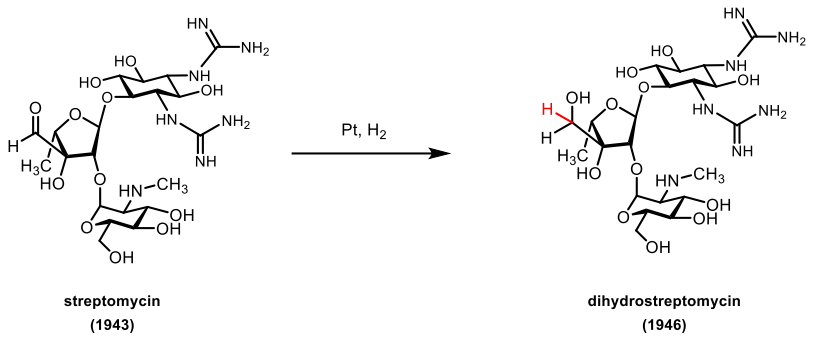

Figure 2.1. Hydrogenation of streptomycin provided access to dihydrostreptomycin, an aminoglycoside of improved chemical stability.

The dissemination of aminoglycoside modifying enzymes (AMEs, Chapter 1, section 1.6.1) led to interest in semisynthetic modification to remove the liabilities for covalent drug inactivation.[6] Meiji-Seika of Japan developed dibekacin semisynthetically from kanamycin B (Figure 2.2).[7] By deoxygenating at C3' and C4', the susceptibility to APH(3') and ANT(4') as the

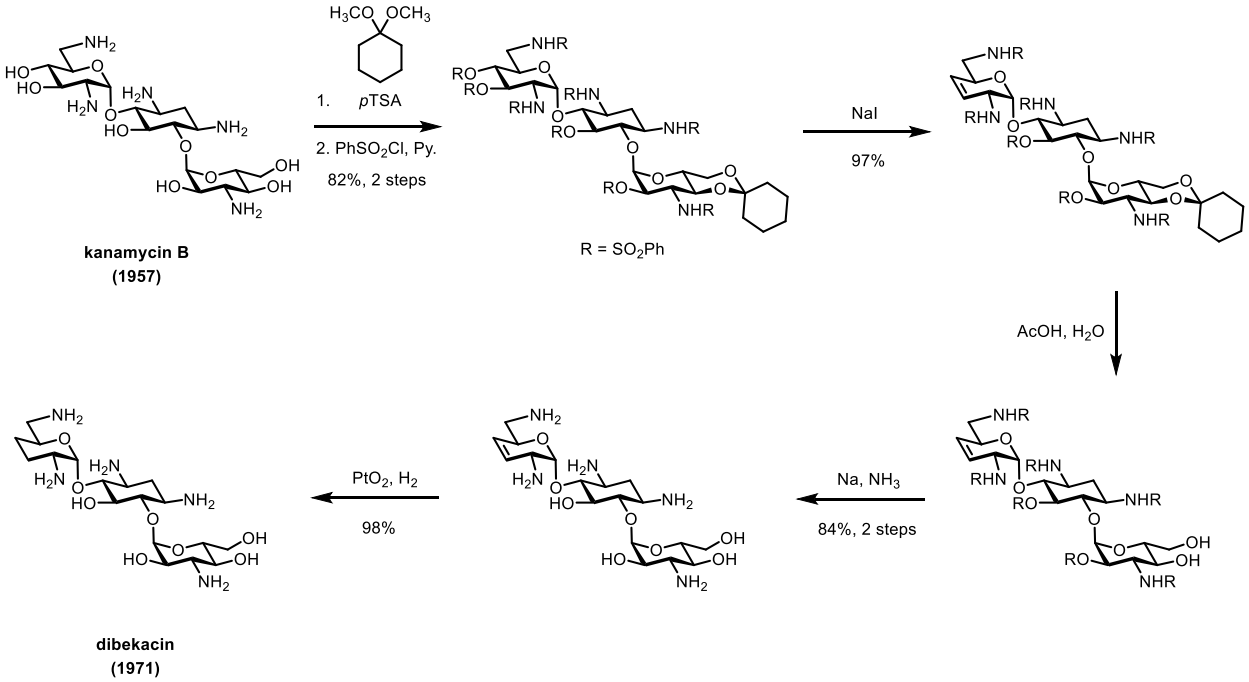

Figure 2.2. Semisynthesis of dibekacin from kanamycin B.

most common AMEs was removed, at the cost of worsened toxicity.[8] Displaying activity against *Staphylocci* and *Pseudomonas*, dibekacin launched worldwide except for the United States in 1975.[9]

Perhaps the most impactful semisynthetic discovery came with the isolation of butirosin, which carries the (*S*)-4-amino-2-hydroxybutyryl (HABA) side chain.[10] In comparison to ribostamycin, which lacks the HABA chain, butirosin displays activity against *Pseudomonas* and other strains which are resistant to ribostamycin and kanamycin.[11] Scientists at Bristol-Myers developed amikacin from kanamycin A in 1972 by appending this side chain over three steps

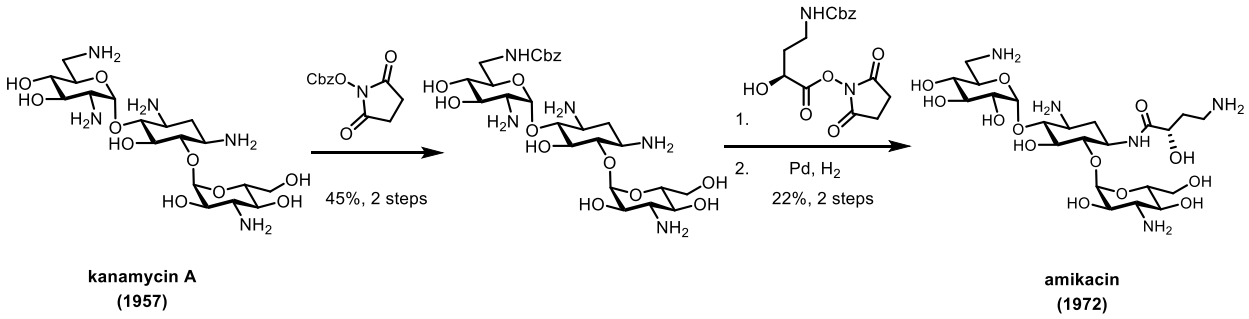

Figure 2.3. Semisynthesis of amikacin from kanamycin A.

(Figure 2.3). Attachment of the HABA chain to amikacin provides protection from the C2''-hydroxyl by steric shielding and similarly reduces susceptibility to the APH(3') and AAC(3) resistance phenotypes.[12,13] This structural change with amikacin was also associated with an alleviated nephrotoxicity relative to kanamycin.[14,15] Process routes for aminoglycoside development typically have similarly low yields and low step counts; the syntheses will typically utilize regioselective strategies in amine functionalization that provide poor yields of desired intermediates. X-ray crystallography displays the binding of the HABA chain in comparison to other aminoglycosides provides two additional hydrogen bond contacts within the bacterial ribosome, suggestive of an improved affinity (Figure 2.4).[16]

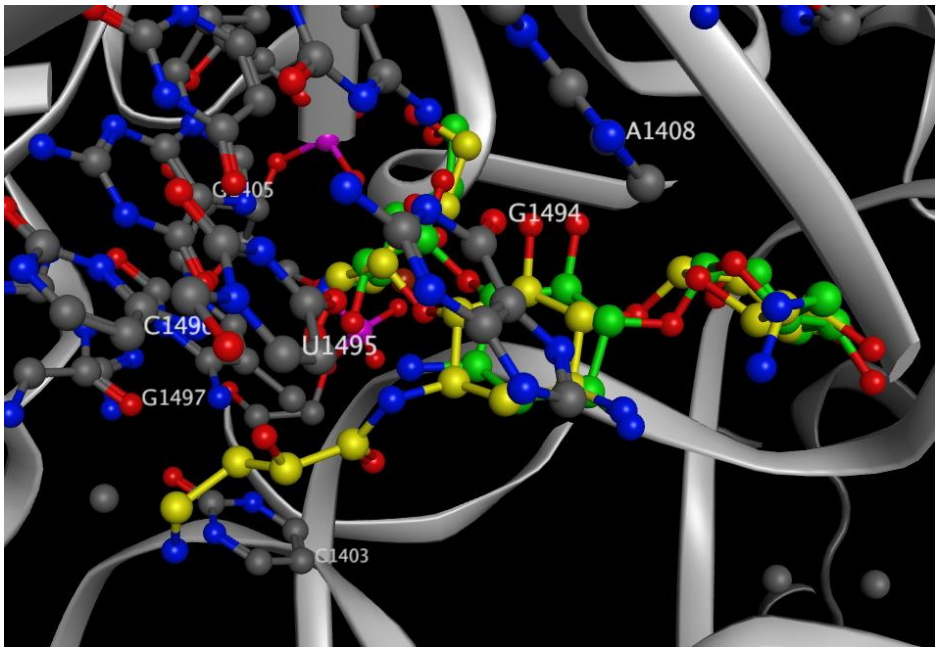

Figure 2.4. Crystal structures of amikacin (yellow, PDB: 8EV6) and kanamycin A (green, PDB: 8EV7). The HABA chain of amikacin reaches deeper into the helix 44 pocket and can gain additional hydrogen bonding interactions.[16]

The success of amikacin led to the development of arbekacin as a second-generation semisynthetic aminoglycoside.[17] Developed in 1973 as an acylated derivative of dibekacin, the synthesis of arbekacin occurs in five steps and utilizes a unique chelating agent to restrict the reactivity of several amine groups (Figure 2.5).[18–20] Arbekacin is comparably toxic to dibekacin[8] and retains activity against Gram-positive species that express APH(3'), ANT(4'), ANT(4''), and the bifunctional AAC(6')/APH(2'') enzymes. Since its approval in Japan in 1990, arbekacin has seen extensive use for the treatment of MRSA infections.[6]

Acylated aminoglycosides were continuously explored as seen with the advancement of isepamicin as a semisynthetic analog of gentamicin B (Figure 2.6).[20] Proceeding in four steps, the semisynthesis also suffers from low yields due to acylation regioselectivity issues. Introduction of a propionic aminoalcohol side chain with isepamicin improved its activity against ANT(2'')-

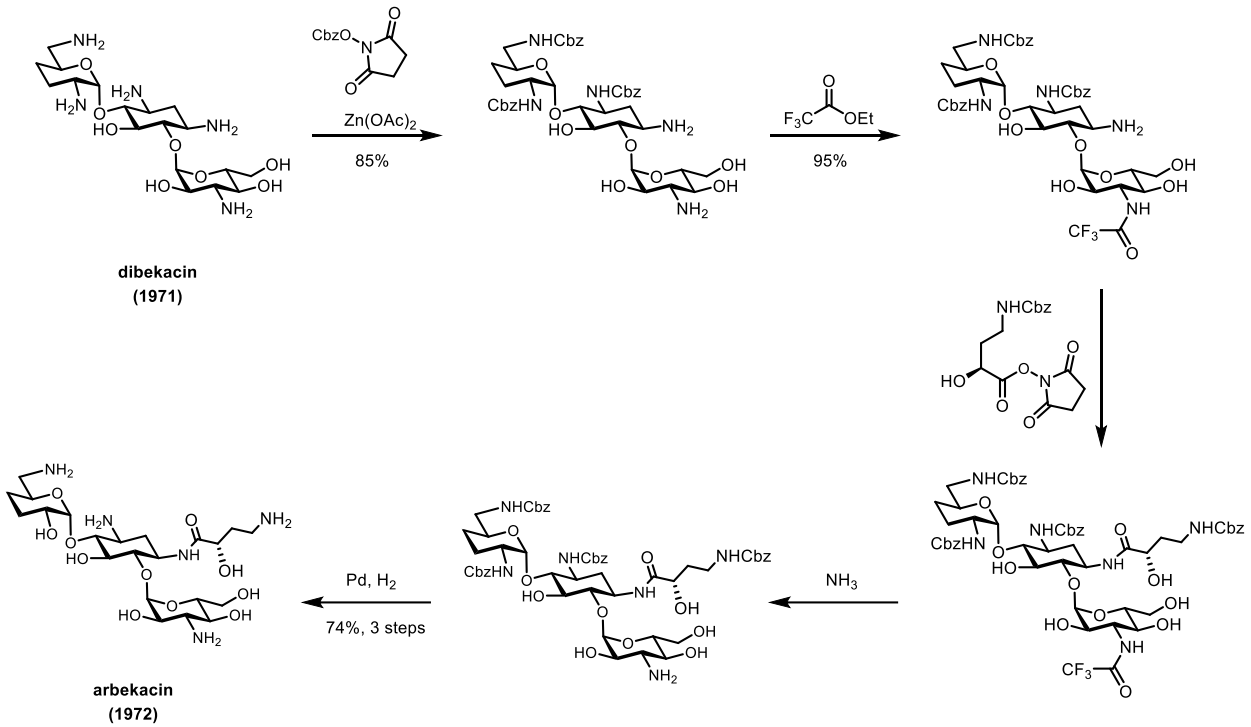

Figure 2.5. The semisynthetic aminoglycoside dibekacin, derived from kanamycin B, is used as starting material in the 5-step synthesis of arbekacin.

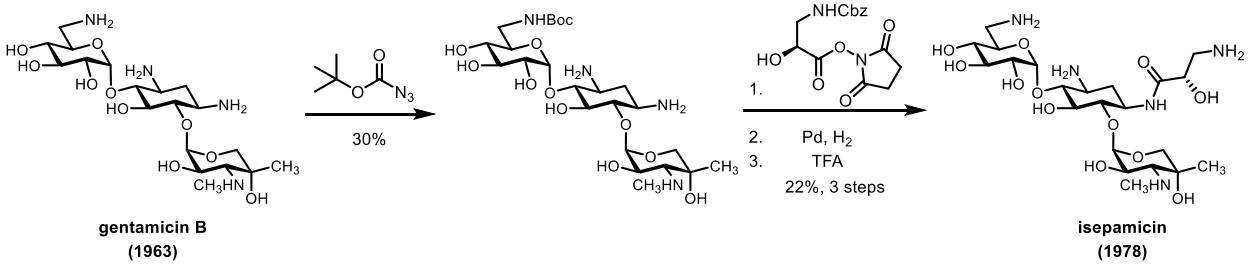

Figure 2.6. The first semisynthetic derivative of gentamicin, isepamicin, was prepared by a 4-step sequence in 1978.

expressing strains, although isepamicin is not as effective as gentamicin complex against *Pseudomonas*.[20] With lower observed toxicity than gentamicin complex, isepamicin gained Japanese approval in 1988.[21]

In 1976, alkylation of sisomicin by reductive amination yielded netilmicin, which later became approved globally in 1985 (Figure 2.7).[6] In an optimized procedure making use of

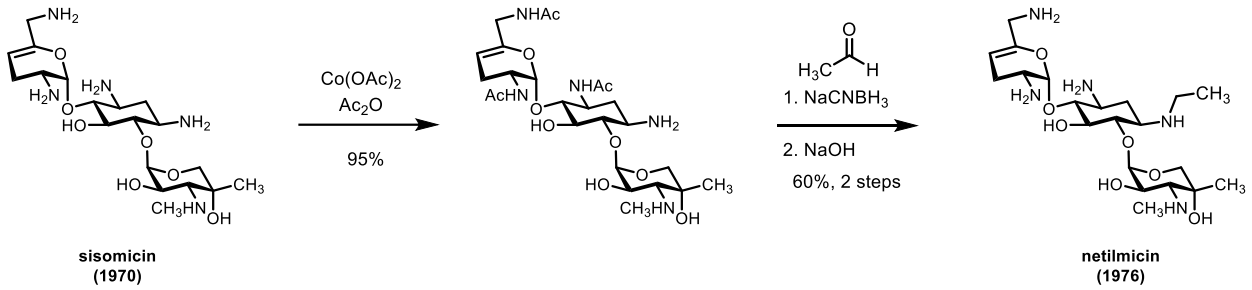

Figure 2.7. The synthesis of netilmicin from sisomicin proceeds via a selective 3-step synthesis in 57% yield. A direct reductive amination at the C1-amine provides netilmicin but only in a reduced 25% yield.

chelation chemistry to selectively acetylate three of the five amines, the synthesis of netilmicin from sisomicin proceeds in three steps and 57% yield.[22–24] Despite early indications in animal models of reduced toxicity, later studies in humans display comparable toxicity profiles to past aminoglycoside antibiotics.[8]

The most recently approved member of the aminoglycoside class would not arrive for three more decades until the approval on plazomicin in 2018 (Figure 2.8). Plazomicin was developed by Achaogen to combat widespread resistance to fluoroquinolone and carbapenem antibiotics in Gram-negative bacteria; resistance to amikacin developed within ten years of its introduction which furthered the need for Gram-negative active compounds.[25] Plazomicin is synthesized in 7 steps from sisomicin in 0.16% overall yield due to costly HPLC purifications and regioselection challenges.[26,27] The critical advancement for plazomicin is the introduction of the hydroxyethyl group at the C6'-amine by reductive amination. Alkylation at the C6'-amine protects against the AAC(6') and AAC(6')/APH(2'') resistance phenotypes which would normally cripple many 4,6-disubstituted aminoglycosides.[26] Coupled with the HABA side chain, plazomicin retains activity

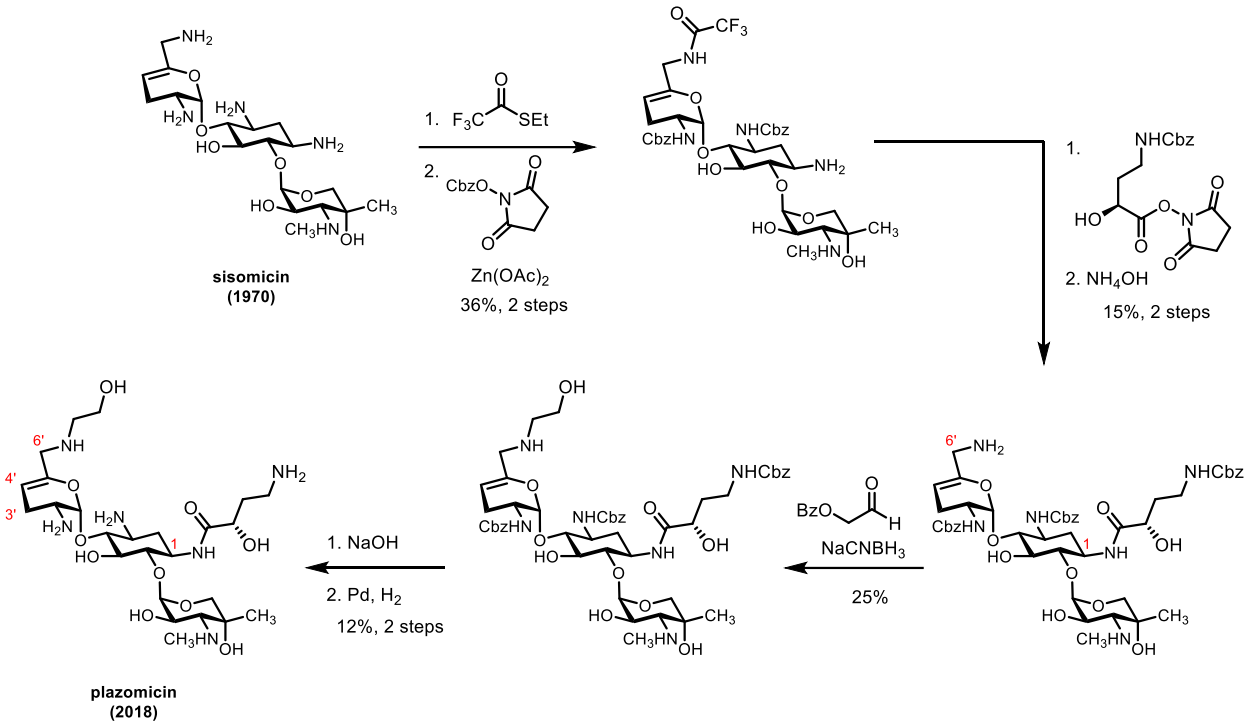

Figure 2.8. Plazomicin is prepared from sisomicin in 7 steps and 0.16% overall yield. Plazomicin was approved for cUTI and other systemic infections lacking other treatment options in 2018.

against the majority of aminoglycoside modifying enzymes, with the notable exception in the uncommon AAC(2') phenotype; this enzyme is normally found chromosomally encoded in *P. stuartii*.[28,29] Plazomicin displays a superior spectrum of activity when compared against all other approved aminoglycosides. However, like all 4,6-disubstituted aminoglycosides, plazomicin succumbs to expression of G1405 ribosomal methyltransferases such as ArmA; it also does not overcome the N1-A1408 methylation caused by NpmA.[27,28,30] Promising toxicity studies[31] led to plazomicin's FDA approval in 2018 for complicated urinary tract infections or infections with few available treatment options.

The work of Prof. David Crich has elucidated the individual activities of gentamicin components via semisynthesis (Figure 2.9).[32–34] While gentamicin complex is typically depicted

as its primary component, gentamicin C1a, commercial gentamicin is a mixture of several aminoglycoside natural products not adequately resolved in the production process. Starting from sisomicin, they accessed multiple gentamicin congeners that display various methylation patterns on ring I and determined the individual antiribosomal and antimicrobial activities. Unsurprisingly, gentamicin C1a was the most active congener but was unique in its low ototoxicity risk as

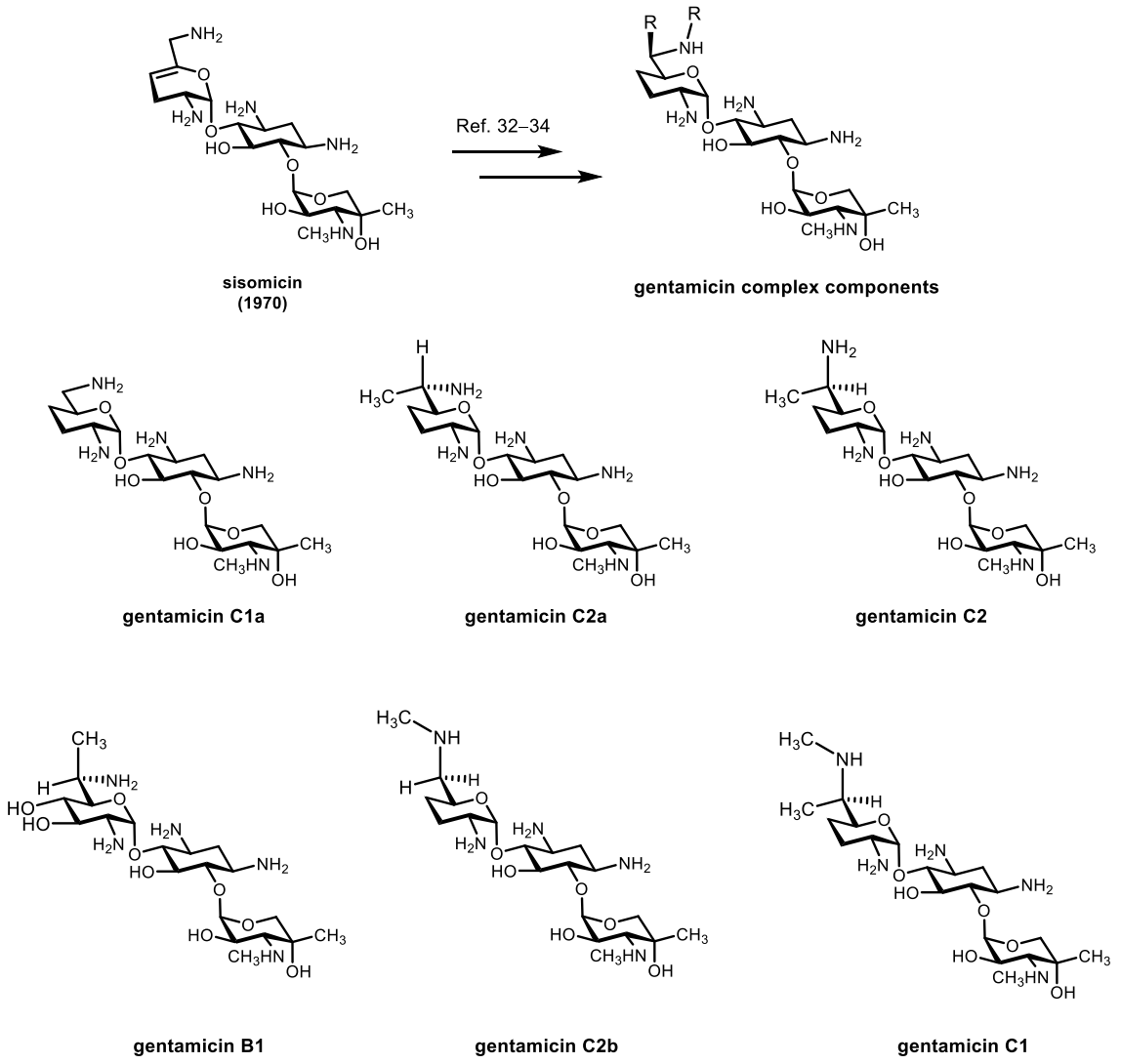

Figure 2.9. Gentamicin components may be individually prepared from sisomicin by semisynthesis. Gentamicin X2 was also accessed but is not depicted on account of its comparably poor antiribosomal activity.

determined by mitochondrial ribosome inhibition. The individual components also displayed different susceptibility to AAC(6') phenotypes and all lost activity against AAC(3). When coupled with the minor differences in activity and humanized ribosome inhibition, they determined that there was little need for improved resolution of gentamicin components and the mixtures currently obtained by fermentation would remain acceptable dosage forms.

2.2 Ring I Modification

The glucosamine or purpurosamine unit that constitutes ring I of most 2-deoxystreptamine aminoglycosides has been heavily explored by semisynthesis in pursuit of new antibiotics. The exploration is driven in part by the wide array of AMEs that target ring I by acetylation of the C6'- and C2'-amines or by modification of the C3'- and C4'-hydroxyls. Clinically, the major advancements of semisynthesis have been seen in the dideoxygenation of the glucosamine residue in the production of dibekacin which overcame APH(3') and ANT(4') resistance. The advancement of plazomicin highlights the potential in C6'-amine alkylation to circumvent AAC(6') resistance.

Crich and co. believed ribosomal target selectivity would be a guiding factor in the development of next-generation aminoglycoside antibiotics without ototoxic side effects. To better understand aminoglycoside ribosome selectivity, the collaboration developed humanized hybrid ribosomes for *E. coli* to mimic the mammalian cytosolic, mitochondrial, and deafness-sensitivity mutant mitochondrial (A1555G) ribosomes.[35] Semisynthetic access to 4',6'-acetals as well as 4'-*O*-ethers of paromomycin revealed markedly improved bacterial ribosome selectivity (Figure 2.10A). The 4'-*O*-ethyl derivative showed promising activity with little inhibitory activity for human-type ribosomes and indicated C4' as an exciting avenue for aminoglycoside development.

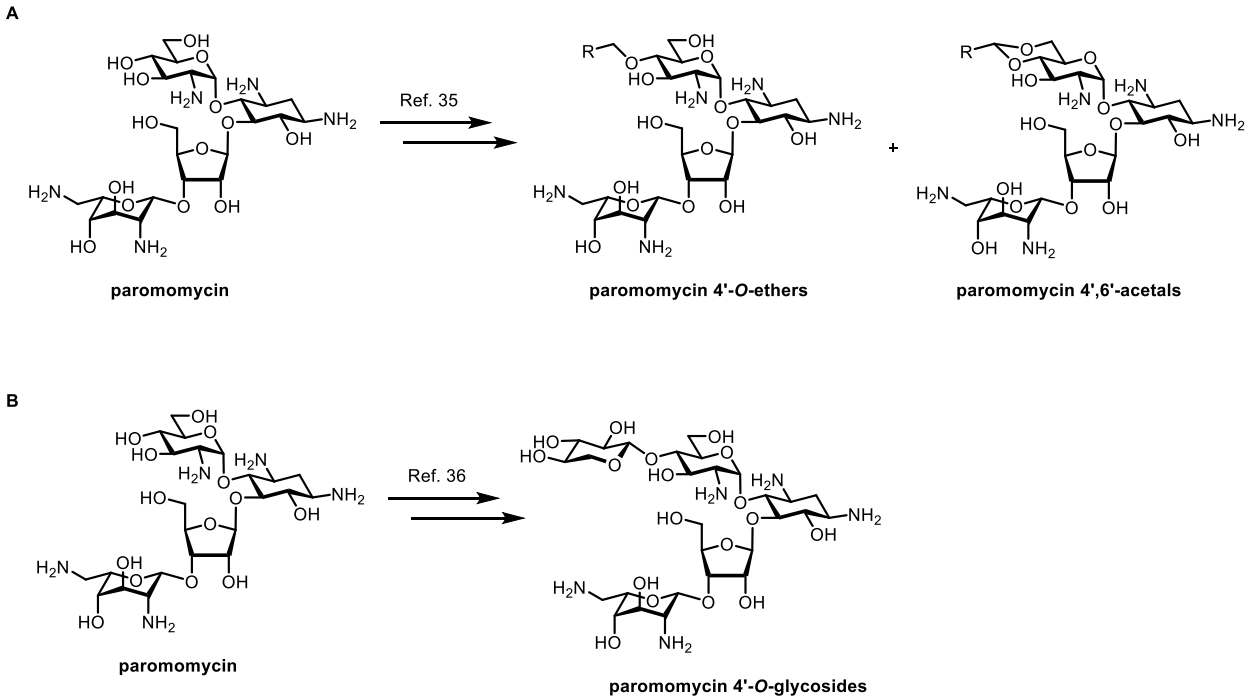

Figure 2.10. (A) Paromomycin ethers and acetals were prepared by Crich and evaluated for ribosomal inhibitory activity. (B) Later studies showed 4'-glycosylation of the paromomycin scaffold to also provide improved ribosomal selectivity.

The utility of hybridized ribosomes to assess aminoglycoside selectivity paved the way for the synthesis of paromomycin 4'-*O*-glycoside products.[36] Regioselective reduction of the perbenzylated-perazidated acetal of paromomycin to unveil to C4'-hydroxyl facilitated an exhausted survey of glycosylated products (Figure 2.10B). These pseudopentasaccharides displayed modest activity against ESKAPE pathogens, and the ribosomal inhibition data established strong links between inhibitory activity with *in vitro* MIC data. Aminoglycoside 4'-*O*-glycosylation prevented action by the ANT(4') resistance determinant in MRSA and *E. coli*, but this modification did not rescue against APH(3') resistance.

Extension of the 4'-*O*-alkylation strategy to overcome aminoglycoside ribosomal selectivity was performed by Crich and co. for both the 4,5- and 4,6-disubstituted aminoglycoside

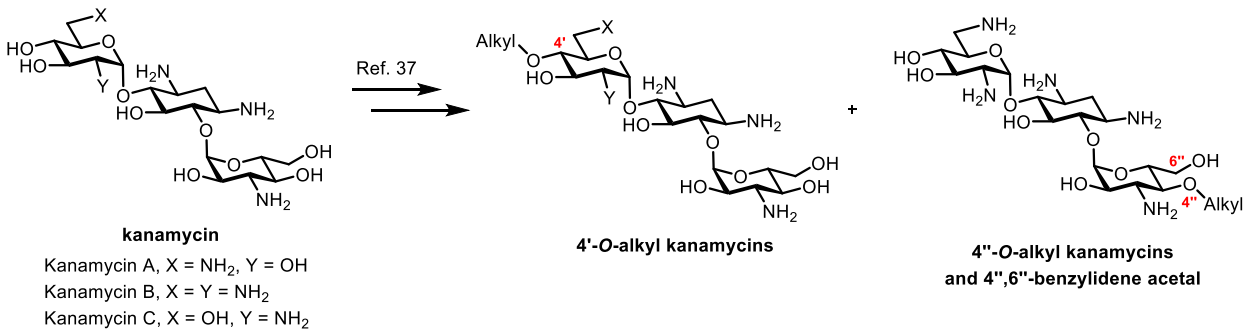

Figure 2.11. Kanamycin 4'-*O*-ethers were prepared and evaluated for ribosomal selectivity and antibacterial activity.[37]

families. In the kanamycin family, alkylation at the C4'-hydroxyl resulted in significant losses in antimicrobial activity, except in the case of kanamycin B having two amines on ring I at C2' and C6' (Figure 2.11).[37] For kanamycin B, C4'-alkylation resulted in only minor losses in activity for the bacterial ribosome, and all analogs lost some potency in MIC assays against *E. coli* when compared to the parent natural product. Benzylidene acetal formation resulted in significant declines in activity for the kanamycin family. Kanamycin B 4'-*O*-alkylation did not result in improved selectivity for the bacterial ribosome and these analogs were not pursued further; however, these modifications rescued the scaffold from AMEs that target the C4'-hydroxyl.

In the neomycin series, 4'-*O*-alkylation provided protection against the widespread AMEs that covalently modify this position and rescues neomycin from their activity (Figure 2.12).[38] This series did not overcome modifications to the APH(3') resistance phenotype, while the 4,5-disubstituted aminoglycosides from this work remained active against strains carrying AAC(3) and AAC(2') resistance. While di-functionalizations between the C6'-amine and other positions were

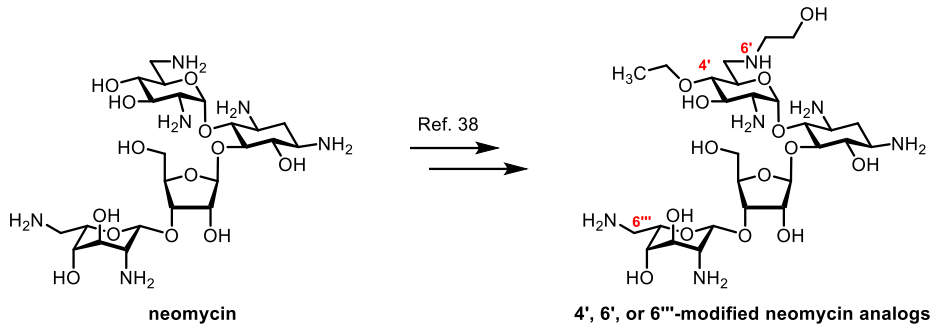

Figure 2.12. Neomycin 4'- and 6'-modifications can improve selectivity without compromising antibacterial efficacy. *N6'''*-alkyklation is largely irrelevant.[38]

deleterious to antibacterial potency, 6'-*N*-hydroxyethyl modified neomycins were rescued from AAC(6') resistance phenotypes. Additionally, this modification provided noticeable increases in selectivity for bacterial over mammalian ribosomes, suggestive of a reduced toxicity risk.

Crich and Böttger expanded their work on 4'-*O*-alkylated 4,5-disubstituted aminoglycosides to the synthesis of bicyclic ring I analogs mimicking the structure of apramycin,[39] an atypical aminoglycoside with uniquely selective bacterial ribosome binding (Figure 2.13). Gratifyingly, a bicyclic paromomycin analog displayed comparable activity to its parent against

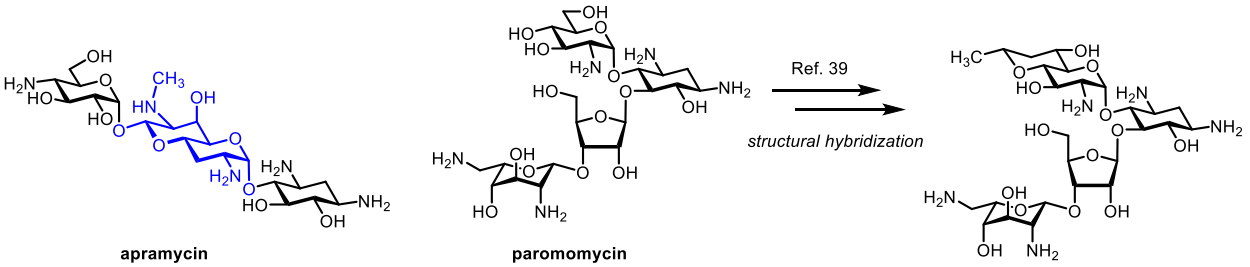

Figure 2.13. Inspired by the bicyclic ring II of apramycin (blue), Crich prepared bicyclic paromomycin analogs with improved bacterial ribosome selectivity.[39]

MRSA and *E. coli* while retaining activity against the ANT(4'), APH(3'), and AAC(6') resistance determinants. The enhanced rigidity imparted to the structure in the bicycle favors the native ribosomal interaction to improve antiribosomal activity. Additionally, these modifications

increased selectivity for the bacterial ribosome as compared to eukaryotic mitochondrial and cytosolic ribosomes and was expected to have a greater therapeutic index. Bicyclized analogs were later shown to be sensitive to ring size when imparting conformational rigidity.[40]

Alkylation of the 2'-amine has previously been investigated as a strategy to overcome ribosomal selectivity limitations and improve activity against aminoglycoside modifying enzymes in 4,5-disubstituted aminoglycosides (Figure 2.14).[41] While in neomycin, several manipulations of both *N*-alkylation or deletion were tolerated, paromomycin and ribostamycin analogs suffered in their antiribosomal activity due to loss of a critical basic amine and disruption of the hydrogen bond network with ring III. Conformationally restricted analogs that had been described similarly suffered in their activity.[42] While the 2'-*N*-alkylation is tolerated with more than five basic primary

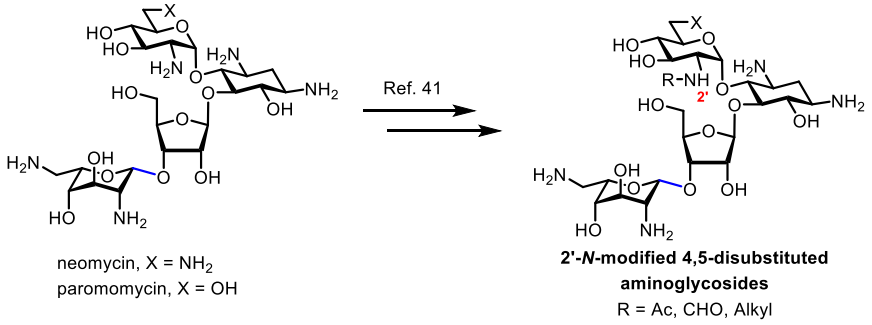

Figure 2.14. 2'-*N*-alkylated aminoglycosides reduced the activity of AAC(2') against the 4,5-disubstituted scaffold. However, this modification was only useful when a requisite number of amines elsewhere in the structure provided tolerable binding affinity changes with 2'-modification.[41]

amines in the parent structure, these modifications are highly deleterious to activity in the absence of the five suitably oriented primary amines elsewhere in the structure. This modification provided modest increases in selectivity, indicating the neomycin functionalization at the C2'-amine may provide a definitive strategy to overcome AAC(2') resistance while simultaneously reducing the

toxicological risk. One rationalization for the observed increase in ribosomal selectivity is attributed to the subtle increase in binding through the C4'-C-H stacking interaction with the ribonucleobase at position 1491 in a CH-π interaction.

Ricci and colleagues evaluated the *N1*-methanesulfonylated sisomicin (N1MS) analog for antimicrobial activity and ototoxic potential (Figure 2.15).[43] Sulfonylation at this position significantly reduced the total charge of this 4,6-disubstiuted aminoglycoside and resulted in a

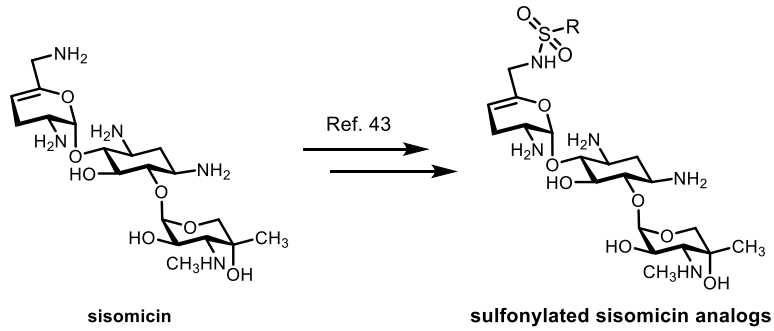

Figure 2.15. Sulfonylation of sisomicin provides analogs with significantly reduced ototoxic potential.

rescue of cochlear hair cells *in vivo*. This modification was additionally associated with minimal loss of antibiotic activity. Larger sulfonyl groups and bis-sulfonylation were less tolerated, although all modifications reduced the ototoxic potential. N1MS was as much as 17-fold less toxic than sisomicin and thought to lower absorption through cochlear mechanoelectrical transducer channels due to the increased molecular size and reduced charge.

A significant development in the 4,5-disubstituted aminoglycosides was made with the synthesis of propylamycin by Crich (Figure 2.16).[44] Replacement of the C4'-hydroxyl with a propyl or ethylthio moiety reduced the susceptibility to ANT(4') and APH(3') resistance while retaining antimicrobial activity. These modifications furthermore rescued cochlear hair cells in an *in vivo* guinea pig model and displayed lowered ototoxicity risk when compared to gentamicin.

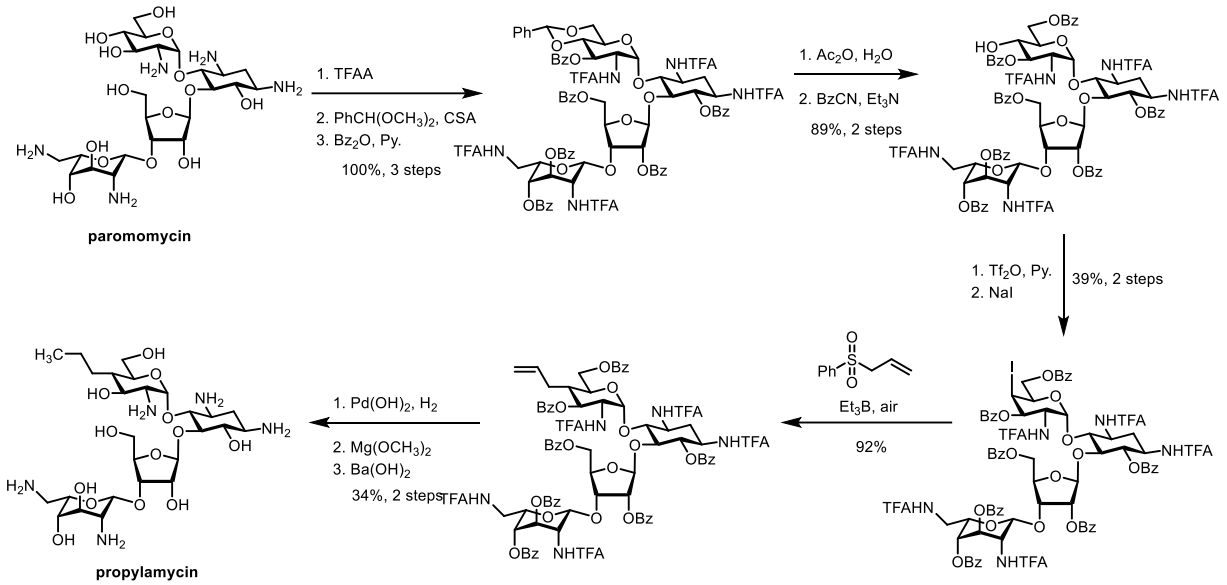

Figure 2.16. The semisynthetic aminoglycoside propylamycin was prepared from paromomycin and has reduced ototoxicity *in vivo*.[44]

The synthesis of propylamycin proceeded in 10 steps and 11% overall yield on a 100-gram scale. Additional analogs derivatized at the C5''-hydroxyl were later explored to overcome APH(3') modification of the ribosyl 5''-hydroxyl but displayed a worsened ribosomal selectivity.[45] Deoxygenation of propylamycin at the 3'-position showed no improvement relative to propylamycin and thus 4'-propylation was sufficient for inhibiting the action of AMEs targeting C3'.

A collection of work by Hanessian demonstrated the ability to selectively deoxygenate ring I at C3' in 4,5-disubstituted aminoglycosides under palladium catalysis.[46–48] By functionally creating a neomycin-sisomicin hybrid (Figure 2.17),[48] the new analog displayed >32-fold improvement in activity against *Pseudomonas* with a chromosomal *aph(3')* gene and *Staphylococcus aureus* expressing ANT(4') as compared to neomycin. The analogous

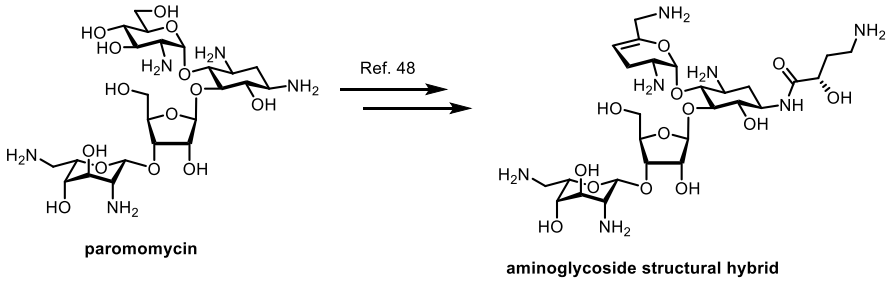

Figure 2.17. Hanessian and co. describe the evolution of paromomycin to a structurally hybridized analog across several publications.[48]

transformation to yield a paromomycin (C6'-hydroxyl) variant suffered in its baseline activity against *E. coli* and *K. pneumoniae*.

2.3 Ring II Modification

The core motif that is present in aminoglycosides, 2-deoxystreptamine, is generally glycosylated at C4 and either C5 or C6 to yield the current arsenal of natural products with clinical relevance.[49] Given the dense functionalization about this cyclohexane, little effort has been made to further functionalize this ring; The chemistry that has been explored has been fruitless except N1 acylation (e.g. HABA chain) shielding against AAC(3) isoforms. Conversely, direct modification of the C3-amine is known to cause significant decreases in activity due to the loss of critical binding contacts in the bacterial ribosome.[50]

Hanessian provided a survey of modified HABA chains appended to neomycin when trying to reduce toxicity (Figure 2.18).[51] Introduction of β,β-difluorination to the HABA chain resulted in a marked decrease in liver toxicity.[52] When combined with the concurrent modifications through the synthesis to dideoxygenation both ring I and ring IV, these analogs retained activity against multiple resistance enzymes and present a new potential for semisynthetic aminoglycoside development. Difluorination of the HABA chain is hypothesized to reduce the basicity and charge

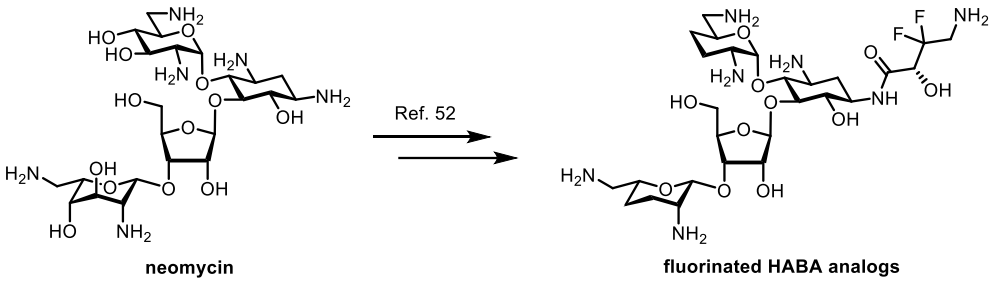

Figure 2.18. Hanessian and co. prepare neomycin derivatives with fluorinated HABA chains. The difluorinated analog shown displayed significantly reduced kidney toxicity *in vitro*.[52]

of structural amines, a factor that is correlated with toxicological risk as seen with the improved toxicity of N1MS.

Aside from HABA introduction, the non-glycosylated hydroxyls have been explored for both inversion, fluorination, and deletion as possible aminoglycoside analogs. The discovery team at Meiji-Seika developed access to 5-epi-arbekacin and the 6'-*N*-methylated analog.[53–55] In combination with the HABA chain, these modifications enabled the arbekacin scaffold to overcome MRSA expressing ANT(4') and the bifunctional AAC(6')-APH(2'')-Ib enzymes.

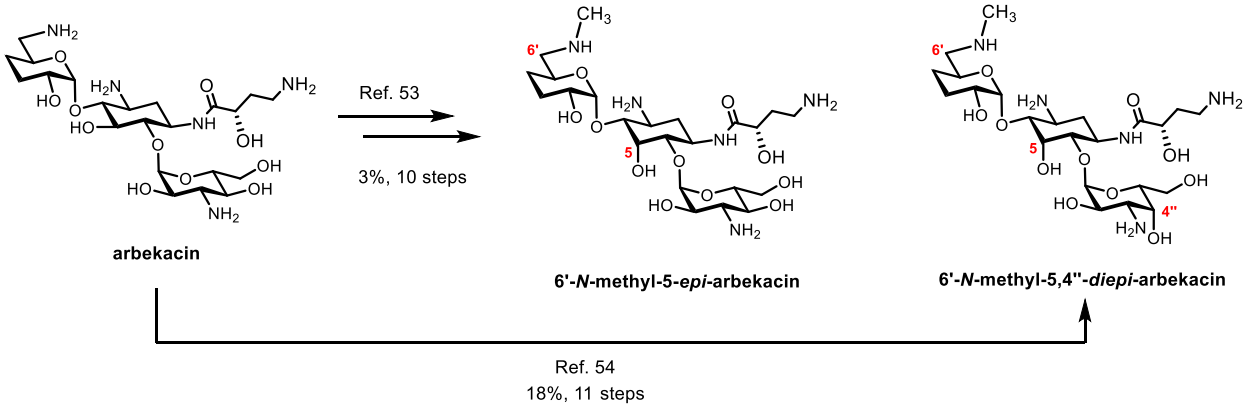

Figure 2.19. The team of Ikeda at Meiji Seika prepared 6'-*N*-methyl-5-*epi*-arbekacin by a 10-step semisynthesis from arbekacin. Later studies would lead to the discovery of diepimeric analogs such as TS2307 (not depicted) and its 6'-*N*-methylated congener.[53,54]

Importantly, 6'-amine methylation was necessary to overcome the AAC(6') phenotype analogous to the gentamicin or plazomicin scaffold, and displayed improved activity against *Pseudomonas* relative to arbekacin. While analog chemistry for accessing the 5-epi-arbekacin analogs allowed invertive halogenation to occur, the 5-epi-halo derivatives possessed lowered antimicrobial activity.

2.4 Ring III & IV modification

Changes to ring III for the kanamycin family of 4,6-disubstituted aminoglycosides resulted in significant losses of antiribosomal activity for ring III benzylidene acetal products (see Figure 2.11).[37] Alternatively, 4''-*O*-ethers of kanamycin B showed few losses in their ability to inhibit translation, as well as minimal losses in antimicrobial activity; however, these were associated with negligible changes to ribosomal selectivity. Unlike C4'-modified analogs, modification to ring III by benzylidene acetalization or alkylation at C4'' did not rescue kanamycin B from AME resistance. Comparable observations that C4''-modification may yield improved aminoglycosides were noted by the Chang laboratory using a glycodiversification approach.[56] The replacement of ring III in 4,6-disubstituted aminoglycosides with alkylamine chains is known to serve as acceptable surrogates based on the antimicrobial activity of these products.[57]

The work of Ikeda on novel arbekacin derivatives led to investigation of doubly epimeric analogs to overcome the remaining AMEs AAC(6')-APH(2'') and ANT(4').[54] In previously showing that 5-epi-arbekacin derivatives displayed increased stability towards these phenotypes, they prepared 5,4''-diepi-arbekacin as well as 6'-*N*-methylated analogs and found they displayed enhanced activity towards these resistance phenotypes (Figure 2.19). Both the diepi- and diepi-6'-*N*-methylated analogs showed comparable activity to arbekacin against *S.aureus*, *E. coli*, and *P. aeruginosa*. Both analogs displayed improved MICs when compared to arbekacin against MRSA

expressing ANT(4') and the bifunctional AAC(6')-APH(2'') enzyme. Additionally, the *N*-methylated derivative gained substantial activity against *Pseudomonas* expressing the AAC(6')-Ib isoform; together these results indicate doubly-epimeric aminoglycosides, including an epimerized stereocenter on ring III, as viable strategies to overcome AME resistance phenotypes. The culmination of these studies was found in the Meiji-Seika compound TS2037 that was evaluated *in vivo*.[55] In a MRSA infection model, TS2037 proved more effective by ED_{50} than those of arbekacin, gentamicin, vancomycin, or linezolid. In both susceptible and resistance *P. aeruginosa* infection models, TS2037 displayed greater efficacy than tobramycin, arbekacin, or gentamicin. In a *N*-acetyl-β-glucosaminidase (NAG) assay for kidney tubular cell stability, TS2037 led to increased release of NAG suggesting greater nephrotoxicity risk that may be offset by an adjustment in dosing consistent with its improved spectrum of activity. As of now TS2037 remains investigational.

In the 4,5-disubstituted aminoglycosides, the analogous modifications to ring IV as the C6'-amine functionalization described earlier (see Figure 2.12) provided modest changes to ribosomal selectivity patterns; ring IV modifications to neomycin and paromomycin are consistent with the hypothesis that ring IV serves primarily as a cationic anchor in the bacterial ribosome.[38]

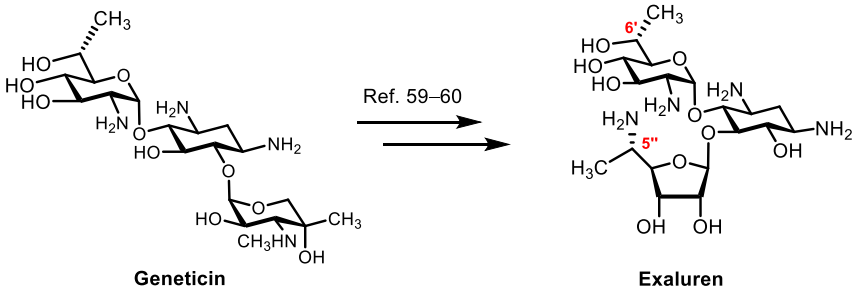

Figure 2.20. The natural product geneticin was converted into the experimental stop codon-readthrough therapeutic Exaluren and is designed to target mammalian cytosolic ribosomes.

This has been further established in prior work from Chi-Huey Wong, wherein replacement of the neomycin ring IV with alkyl diamine chains results in reduced ribosomal binding while retaining antibiotic efficacy.[58] Modifications to ring III in this series have significant implications for ribosomal selectivity. ELX-02 (Exaluren) is a specifically engineered aminoglycoside designed to selectively target mammalian cytosolic ribosomes (Figure 2.20).[59,60] The chiral secondary alcohol positioned at C6' on ring I alongside a 5''-amine moiety enhances the mammalian ribosome codon readthrough with implications for treating premature stop codon diseases such as cystic fibrosis. The other position of interest in the ring III subunit of 4,5-disubstituted aminoglycosides, C2'', which was selectively probed by Hanessian through an arsenal of C2''-*O*-ether paromomycin analogs.[61] The alkylated ring III ethers displayed comparable MIC values to paromomycin against *E. coli* and *S. aureus*. These compounds additionally displayed an alternative ring III binding mode based on X-ray crystallography.

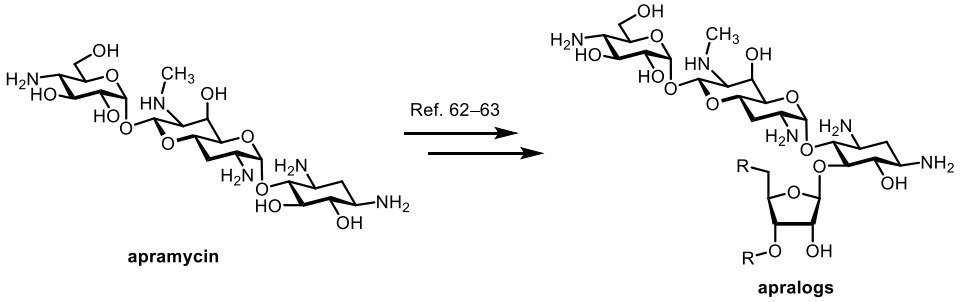

Figure 2.21. Multiple groups have targeted the apramycin scaffold for modification to overcome both aminoglycoside resistance and ototoxicity.

Research from both Crich and Fridman shows that ribosylation can improve activity and ribosomal target selectivity for apramycin derivatives (Figure 2.21).[62,63] Prior work from Fridman provided proof of concept that ribosylation of the C5-hydroxyl of neamine derivatives improves the preference for prokaryotic ribosome inhibition, while the 4,6-disubstituted aminoglycosides

suffered from additional glycosylations at C5.[64] The "apralogs" developed by Crich specifically gained some resistance to action by the AAC(3)-IV resistance determinant, one of the only AME isoforms problematic for the apramycin parent scaffold. Lead compounds from this study were advanced to *in vivo* studies that demonstrated superior activity compared to the parent in a mice thigh infection model; *ex vivo* studies with mouse cochlear explants revealed a reduced risk of ototoxicity as predicted by ribosomal target selectivity.

Due to the improved toxicological profile of the atypical aminoglycoside apramycin, another synthetic campaign focused on this subfamily for semisynthetic discovery campaigns. Otsuka and colleagues described the modification of aprosamine from which several analogs showed improved activity compared to apramycin against carbapenem-resistant *Enterobacteriacea*, MRSA, and vancomycin-resistant *enterococci*.[65] The most promising members within this series featured deoxygenation at C5 of 2-deoxystreptamine or further appending of the HABA chain to ring I to shield against AAC(3) resistance.

2.5 Summary

A majority of aminoglycoside semisynthetic modifications have involved the removal or shielding of groups functionalized by AMEs on the neamine core; this is accomplished by dideoxygenation of 3',4'-diol, 6'-*N*-methylation, and *N1*-acylation. In light of the semisynthetic accomplishments of plazomicin, recent research programs have shifted focus towards new aminoglycosides that both overcome multiple resistance determinants, especially G1405 methyltransferase phenotypes, and simultaneously display reduced ototoxic potential. Despite these semisynthetic precedents, no new clinical candidate has advanced that overcomes NpmA resistance.

2.6 References

1. Wright, P. M.; Seiple, I. B.; Myers, A. G. *Angew. Chem. Int. Ed.* **2014**, *53*, 8840.

2. Chandrika, N.T.; Garneau-Tsodikova, S. *Chem Soc. Rev.* **2018**, *47*, 1189.

3. Chandrika, N.T.; Garneau-Tsodikova, S. *Med. Chem. Commun.* **2016**, *7*, 50.

4. (a) Peck, R. L.; Hoffhine, C. E.; Folkers, K. *J. Am. Chem. Soc.* **1946**, *68*, 1390; (b) Bartz, Q. R.; Controulis, J.; Crooks, H. M.; Rebstock, M. C. *J. Am. Chem. Soc.* **1946**, *68*, 2163.

5. Blakley, B. W. *Am. J. Otol.* **1997**, *18*, 520.

6. Kondo, S.; Hotta, K. *J. Infect. Chemother.* **1999**, *5*, 1.

7. (a) Umezawa, H.; Umezawa, S.; Tsuchiya, T.; Okazaki, Y. *J. Antibiot.* **1971**, *24*, 485; (b) Matsuno, T.; Yoneta, T.; Fukatsu, S.; Umemura, E. *Carbohydr. Res.* **1982**, *109*, 271.

8. Price, K. E. *Antimicrob. Agents Chemother.* **1986**, *29*, 543.

9. Price, K. E. *Am. J. Med.* **1986**, *80*, 182.

10. Kawaguchi, H.; Naito, T.; Nakagawa, S.; Fujisawa, K.-I. *J. Antibiot.* **1972**, *25*, 695.

11. Woo, P. W. K.; Dion, H. W.; Bartz, Q. R. *Tetrahedron Lett.* **1971**, *12*, 2617.

12. Price, K.; Ghisholm, D.; Misiek, M.; Leitner, F.; Tsai, Y. *J. Antibiot.* **1972**, *25*, 709.

13. Aminoglycoside Antibiotics: From Chemical Biology to Drug Discovery. 1 ed.; John Wiley & Sons: 2007.

14. De Broe, M. E.; Paulus, G. J.; Verpooten, G. A.; Roels, F.; Buyssens, N.; Wedeen, R.; Van Hoof, F.; Tulkens, P. M. *Kidney Int.* **1984**, *25*, 643.

15. Carlier, M.-B.; Rollman, B.; Van Hoof, F. i.; Tulkens, P. *Biochem. Pharmacol.* **1982**, *31*, 3861.

16. Kondo, J.; François, B.; Russell, R. J.; Murray, J. B.; Westhof, E. *Biochimie* **2006**, *88*, 1027.

17. Kondo, S.; Iinuma, K.; Yamamoto, H.; Maeda, K.; Umezawa, H. *J. Antibiot.* **1973**, *26*, 412.

18. Tsuchiya, T.; Takagi, Y.; Umezawa, S. *Tetrahedron Lett.* **1979**, *20*, 4951.

19. (a) Iinuma, K.; Murai, Y. *J. Synth. Org. Chem Jpn.* **1999**, *57*, 368; (b) Kobayashi, Y.; Uchida, H.; Kawakami, Y. *International Journal of Antimicrobial Agents* **1995**, *5*, 227.

20. Nagabhushan, T.; Cooper, A.; Tsai, H.; Daniels, P.; Miller, G. *J. Antibiot.* **1978**, *31*, 681.

21. Miller, G. H.; Chiu, P. J.; Waitz, J. A. *J. Antibiot.* **1978**, *31*, 688.

22. Wright, J. J. *J. Chem. Soc., Chem. Commun.* **1976**, *206*.

23. Nagabhushan, T. L.; Cooper, A. B.; Turner, W. N.; Tsai, H.; McCombie, S.; Mallams, A. K.; Rane, D.; Wright, J. J.; Reichert, P. *J. Am. Chem. Soc.* **1978**, *100*, 5253.

24. Daniels, P. J. L.; Rane, D. F.; McCombie, S. W.; Testa, R. T.; Wright, J. J.; Nagabhushan, T. L., Chemical and Biological Modification of Antibiotics of the Gentamicin Group. In *Aminocyclitol Antibiotics*, American Chemical Society: 1980; Vol. 125, pp 371.

25. Miller, G. H.; Sabatelli, F. J.; Hare, R. S.; Glupczynski, Y.; Mackey, P.; Shlaes, D.; Shimizu, K.; Shaw, K. J. *Clin. Infect. Dis.* **1997**, *24*, S46.

26. Armstrong, E. S.; Miller, G. H. *Curr. Opin. Microbiol.* **2010**, *13*, 565.

27. Zhanel, G. G.; Lawson, C. D.; Zelenitsky, S.; Findlay, B.; Schweizer, F.; Adam, H.; Walkty, A.; Rubinstein, E.; Gin, A. S.; Hoban, D. J. *Expert Rev. Anti Infect. Ther.* **2012**, *10*, 459.

28. Aggen, J. B.; Armstrong, E. S.; Goldblum, A. A.; Dozzo, P.; Linsell, M. S.; Gliedt, M. J.; Hildebrandt, D. J.; Feeney, L. A.; Kubo, A.; Matias, R. D. *Antimicrob. Agents Chemother.* **2010**, *54*, 4636.

29. Endimiani, A.; Hujer, K. M.; Hujer, A. M.; Armstrong, E. S.; Choudhary, Y.; Aggen, J. B.; Bonomo, R. A. *Antimicrob. Agents Chemother.* **2009**, *53*, 4504.

30. (a) Galani, I.; Souli, M.; Daikos, G. L.; Chrysouli, Z.; Poulakou, G.; Psichogiou, M.; Panagea, T.; Argyropoulou, A.; Stefanou, I.; Plakias, G.; Giamarellou, H.; Petrikkos, G. J. Chemother. 2012, 24, 191; (b) Jones, R. N.; Armstrong, E. S.; Aggen, J. B.; Biedenbach, D. J.; Miller, G. H. Antimicrobial Activity of ACHN-490, a Neoglycoside, Tested Against a Contemporary Collection of Clinical Isolates Including Problematic Antimicrobial-Resistant Phenotypes, In 49th Interscience Conference on Antimicrobial Agents and Chemotherapy, San Francisco, CA, 2009. ; (c) Castanheira, M.; Mendes, R. E.; Streit, J. M.; Flamm, R. K. Activity of Plazomicin and Comparator Agents Tested against Gram-Negative and -Positive Clinical Isolates Collected in USA Hospitals During 2015, In IDWeek, New Orleans, LA, 2016. http://www.achaogen.com/media-all/2016/10/28/activity-of-plazomicin-and-comparator-agentstested-against-gram-negative-and-positive-clinical-isolates-collected-in-usa-hospitals-during2015.

31. Cass, R. T.; Brooks, C. D.; Havrilla, N. A.; Tack, K. J.; Borin, M. T.; Young, D.; Bruss, J. B. *Antimicrob. Agents Chemother.* **2011**, *55*, 5874.

32. Rajasekaran, P.; Crich, D. *Org. Lett.* **2020**, *22*, 3850.

33. Jana, S.; Crich, D. *Org. Let.* **2022**, *24*, 8564.

34. Jana, S.; Rajasekaran, P.; Haldimann, K.; Vasella, A.; Böttger, E.C.; Hobbie, S.N.; Crich, D. *ACS Infect. Dis.* **2023**, *9*, 1622.

35. Perez-Fernandez, D.; Shcherbakov, D.; Matt, T.; Leong, N. C.; Kudyba, I.; Duscha, S.; Boukari, H.; Patak, R.; Dubbaka, S. R.; Lang, K.; Meyer, M.; Akbergenov, R.; Freihofer, P.; Vaddi, S.; Thommes, P.; Ramakrishnan, V.; Vasella, A.; Böttger, E. C. *Nat. Commun.* **2014**, *5*, 1.

36. Matsushita, T.; Chen, W.; Juskeviciene, R.; Teo, Y.; Shcherbakov, D.; Vasella, A.; Böttger, E. C.; Crich, D. *J. Am. Chem. Soc.* **2015**, *137*, 7706.

37. Kato, T.; Yang, G.; Teo, Y.; Juskeviciene, R.; Perez-Fernandez, D.; Shinde, H. M.; Salian, S.; Bernet, B.; Vasella, A.; Böttger, E. C.; Crich, D. *ACS Infect. Dis.* **2016***, 1*, 479.

38. Sati, G. C.; Shcherbakov, D.; Hobbie, S. N.; Vasella, A.; Böttger, E. C.; Crich, D. *ACS Infect. Dis.* **2017**, *3*, 368.

39. Mandhapati, A. R.; Yang, G.; Kato, T.; Shcherbakov, D.; Hobbie, S. N.; Vasella, A.; Böttger, E. C.; Crich, D. *J. Am. Chem. Soc.* **2017**, *139*, 14611.

40. Pirrone, M.G.; Hobbie, S.N.; Vasella, A.; Böttger, E. C.; Crich, D. *RSC Med. Chem.* **2021**, *12*, 1585.

41. Sati, G. C.; Sarpe, V. A.; Furukawa, T.; Mondal, S.; Mantovani, M.; Hobbie, S. N.; Vasella, A.; Bo, E. C.; Crich, D. *ACS Infect. Dis.* **2019**, *5*, 1718.

42. Bastida, A.; Hidalgo, A.; Chiara, J.L.; Torrado, M.; Corzana, F.; Pérez-Cañadillas, J.M.; Groves, P.; Garcia-Junceda, E.; Gonzalez, C.; Jimenez-Barbero, J.; Asensio, J.L. *J. Am. Chem. Soc.* **2006**, *128*, 100.

43. Huth, M. E.; Han, K.; Sotoudeh, K.; Hsieh, Y.; Effertz, T.; Vu, A. A.; Verhoeven, S.; Hsieh, M. H.; Greenhouse, R.; Cheng, A. G.; Ricci, A. J. *J. Clin. Invest.* **2015**, *125*, 583.

44. Matsushita, T.; Sati, G.; Kondasinghe, N.; Pirrone, M.; Kato, T.; Waduge, P.; Kumar, H.; Sanchon, A.; Dobosz-Bartoszek, M.; Shcherbakov, D.; Juhas, M.; Hobbie, S. N.; Schrepfer, T.; Chow, C. S.; Polikanov, Y.; Schacht, J.; Vasella, A.; Böttger, E. C.; Crich, D. *J. Am. Chem. Soc.* **2019**, *141*, 5051.

45. Lubriks, D.; Zogota, R.; Sarpe, V.A.; Matsushita, T.; Sati, G.C.; Haldimann, K.; Gysin, M.; Böttger, E. C, Vasella, A.; Suna, E.; Hobbie, S.N.; Crich, D. *ACS Infect. Dis.* **2021**, *7*, 2413.

46. Hanessian, S.; Giguère, A.; Grzyb, J.; Maianti, J.P.; Saavedra, O.M.; Aggen, J.B.; Linsell, M.S.; Goldblum, A.A.; Hildebrandt, D.J.; Kane, T.R.; Dozzo, P.; Gliedt, M.J.; Matias, R.D.; Feeney, L.A.; Armstrong, E.S. *ACS Med. Chem. Lett.* **2011**, *2*, 924.

47. Hanessian, S.; Maianti, J.P.; Matias, R.D.; Feeney, L.A.; Armstrong, E.S. *Org. Lett.* **2011**, *13*, 6476.

48. Maianti, J.P.; Hanessian, S. *Med. Chem. Commun.* **2016**, *7*, 170.

49. Busscher, G. F.; Rutjes, F. P. J. T.; van Delft, F. L. *Chem. Rev.* **2005**, *105*, 775.

50. Daniels, P. J. L.; Rane, D. F.; McCombie, S. W.; Testa, R. T.; Wright, J. J.; Nagabhushan, T.L., Chemical and Biological Modification of Antibiotics of the Gentamicin Group. In *Aminocyclitol Antibiotics*, American Chemical Society: 1980; Vol. 125, pp 371.

51. Hanessian, S.; Kornienko, A.; Swayze, E.E. *Tetrahedron*, **2003**, *59*, 995.

52. Maianti, J. P.; Kanazawa, H.; Dozzo, P.; Matias, R. D.; Feeney, L. A.; Armstrong, E. S.; Hildebrandt, D. J.; Kane, T. R.; Gliedt, M. J.; Goldblum, A. A.; Linsell, M. S.; Aggen, J. B.; Kondo, J.; Hanessian, S. *ACS Chem. Biol.* **2014**, *9*, 2067.

53. Hiraiwa, Y.; Usui, T.; Akiyama, Y.; Maebashi, K.; Minowa, N.; Ikeda, D. *Bioorg. Med. Chem. Lett.* **2007**, *17*, 3540.

54. Hiraiwa, Y.; Minowa, N.; Usui, T.; Akiyama, Y.; Maebashi, K.; Ikeda, D. *Bioorg. Med. Chem. Lett.* **2007**, *17*, 6369.

55. Hirai, Y.; Maebashi, K.; Fushimi, H.; Hiraiwa, Y.; Murakami, S.; Usui, T.; Akiyama, Y.; Minowa, N.; Ikeda, D. *J. Antibiot.***2018**, *71*, 363.

56. Li, J.; Wang, J.; Czyryca, P.G.; Chang, H.; Orsak, T.W.; Evanson, R.; Chang, C.-W.T. *Org. Lett.* **2004**, *6*, 1381.

57. Greenberg, W. A.; Priestley, E. S.; Sears, P. S.; Alper, P. B.; Rosenbohm, C.; Hendrix, M.; Hung, S.-C.; Wong, C.-H. *J. Am. Chem. Soc.* **1999**, *121*, 6527.

58. Alper, P.B.; Hendrix, M.; Sears, P.; Wong, C.-H. *J. Am. Chem. Soc.* **1998**, *120*, 1965.

59. Kandasamy, J.; Atia-Glikin, D.; Shulman, E.; Shapira, K.; Shavit, M.; Belakhov, V.; Baasov, T. *J. Med. Chem.* **2012**, *55*, 10630.

60. Shulman, E.; Belakhov, V.; Wei, G.; Kendall, A.; Meyron-Holtz, E.G.; Ben-Shachar, D.; Schacht, J.; Baasov, T. *J. Biol. Chem.* **2014**, *289*, 2318.

61. Hanessian, S.; Szychowski, J.; Adhikari, S.S.; Vasquez, G.; Kandasamy, P.; Swayze, E.E.; Migawa, M.T.; Ranken, R.; François, B.; Wirmer-Bartoschek, J.; Kondo, J.; Westhof, E. *J. Med. Chem.* **2007**, *50*, 2352.

62. Zada, S.L.; Baruch, B.B.; Simhaev, L.; Engel, H.; Fridman, M. *J. Am. Chem. Soc.* **2020**, *142*, 3077.

63. Quirke, J. C. K.; Rajasekaran, P.; Sarpe, V. A.; Sonousi, A.; Osinnii, I.; Gysin, M.; Haldimann, K.; Fang, Q.; Shcherbakov, D.; Hobbie, S. N.; Sha, S.; Schacht, J.; Vasella, A.; Bottger, E. C.; Crich, D. *J. Am. Chem. Soc. 2020*, **142**, 530.

64. Herzog, I.M.; Zada, S.L.; Fridman, M. *J. Med. Chem.* **2016**, *59*, 8008.

65. Otsuka, Y.; Umemura, E.; Takamiya, Y.; Ishibashi, T.; Hayashi, C.; Yamada, K.; Igarashi, M.; Shibasaki, M.; Takahashi, Y. *ACS Infect. Dis.* **2023**, *9*, 886.

Chapter 3. Fully Synthetic 2-Deoxystreptamine: Historic Syntheses and Efforts Towards a Next-Generation Route

3.1 Introduction

At the core of all aminoglycoside antibiotics is an aminocyclitol subunit, usually 2-deoxystreptamine, which is appended with glycosides to form the antibiotic structure (Figure 3.1, blue).[1,2] The conservation of 2-deoxystreptamine across aminoglycoside subfamilies is indicative of its role in affinity for the bacterial ribosome; minor changes to 2-deoxystreptamine can have significant impact on both the toxicology and activity of analogs. Perhaps the most critical semisynthetic discovery was the introduction of the (*S*)-4-amino-2-hydroxybutyramide (HABA) side chain at the C1 amine of 2-deoxystreptamine; attachment of the HABA chain to the C1 amine of kanamycin A results in the superior clinical agent amikacin. The HABA side chain was also introduced in the development of arbekacin and the most recently approved member of the aminoglycoside class, plazomicin. While several other modifications to 2-deoxystreptamine have been explored, none have been as fruitful as the HABA chain for activity and protection again modifying enzymes. An ideal synthesis of 2-deoxystreptamine would necessarily permit selective incorporation of the HABA chain so as to provide resistance to activity of AAC(3) isoforms.[3,4] Modifications at the C3 amine have historically been detrimental to activity and have thus not been explored for overcoming AAC(3) resistance.[5]

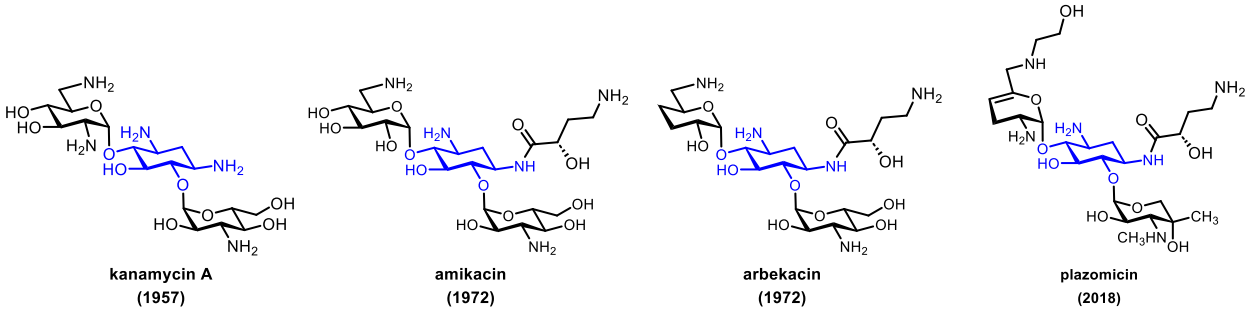

Figure 3.1. AGAs with 2-deoxystreptamine (blue) and some clinically relevant antibiotics with the C1 amine HABA side chain.

3.2 Syntheses of 2-deoxystreptamine

Derived biosynthetically from glucose-6-phosphate, 2-deoxystreptamine is *meso* in its native form, which brings forward the synthetic question of strategy for inducing asymmetry. Because of this, 2-deoxystreptamine for biological and synthetic studies typically originates from semisynthetic degradation of aminoglycoside natural products. Select examples exist to prepare 2-deoxystreptamine by *de novo* methods that do not originate from carbohydrates and will be discussed, including a total synthesis developed within the Myers laboratory.

3.2.1 Methods for resolution of meso 2-deoxystreptamine

Degradation of natural products has been a ubiquitous source of the individual carbohydrate and 2-deoxystreptamine subunits in the discovery of new aminoglycoside antibiotics. As 2-deoxystreptamine is itself *meso* when not conjugated to additional carbohydrates, several strategies for the resolution of 2-deoxystreptamine in protected form have been explored previously (Figure 3.2).

Prolific in the aminoglycoside research area, the group of Professor Chi-Huey Wong disclosed two separate enzymatic methods for resolution of *meso* 2-deoxystreptamine.[6,7] In the first, 2-deoxystreptamine was selectively alloc protected at the C3-amine by action of the protease subtilisin BPN', giving triol **1** in 76% yield and 99% *ee* (Figure 3.2A). The second utilized the diazido-triacetate of 2-deoxystreptamine **2** in a regioselective hydrolysis by the *Candida antarctica* lipase, providing alcohol **3** in 71% yield (Figure 3.2B). Prinzbach described the reaction of the *E. coli* penicillin amidase promoting hydrolysis of amide **4**; following global acetylation the acetamide **5** was obtained in 76% yield over two steps with 97% *ee*.[8] The Wong group also disclosed a chemical method for resolving 2-deoxystreptamine derivative **6**.[9] A chiral dipyran

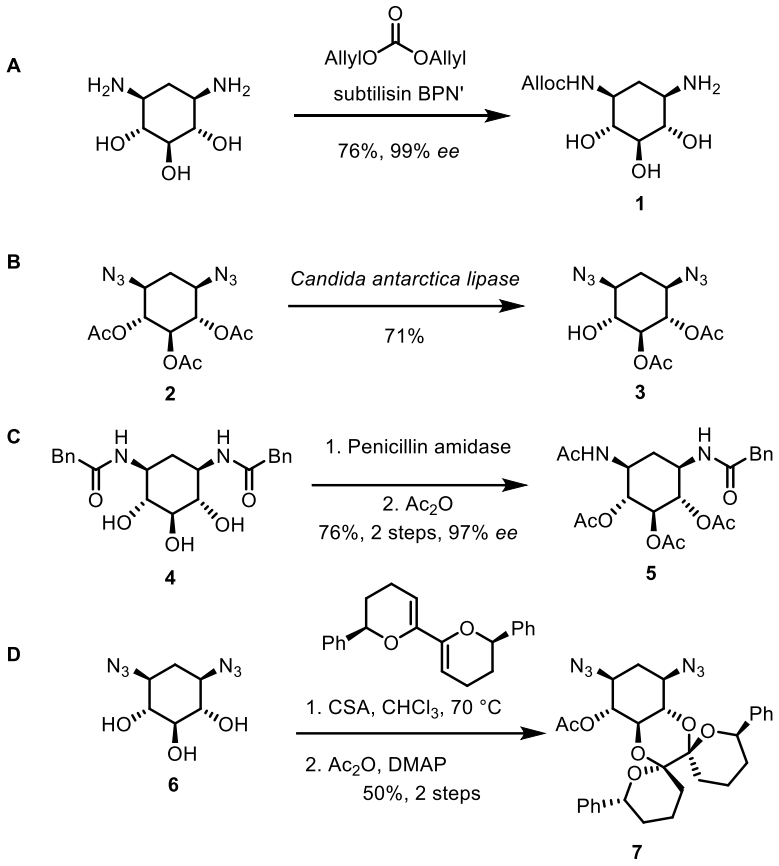

Figure 3.2. Select examples for resolution of meso 2-deoxystreptamine. (A) Aminotriol **1** can be accessed from 2-deoxystreptamine by the protease subtilisin BPN'. (B) The *Candida antarctica* lipase selectively hydrolyzes triacetate **2** to give **3**. (C) Penicillin amidase can differentiate the two amides of **4**. (D) Triol **6** can be resolved following protection as the bis-spiroketal **7**.

would selectively protect the C5 and C6 hydroxyl as spiroketals in the presence of camphorsulfonic acid, giving **7** in 50% yield following an acetylation. These methods demonstrate that resolution of 2-deoxystreptamine has been a rich resource for the preparation of new aminoglycoside antibiotics, despite the inability to conveniently modify the cyclohexane scaffold.[10]

3.2.2 Racemic and asymmetric syntheses of protected 2-deoxystreptamine

The unique aminocyclitol motif 2-deoxystreptamine has been an inspiration for synthetic chemists since its structure was elucidated.[11] While most syntheses (many outlined in reference 1) begin with carbohydrate[12] or highly oxygenated cyclohexanes[13] such as *myo*-inositol, a handful of syntheses prepare 2-deoxystreptamine via *de novo* synthetic design. Two groundbreaking syntheses are described in Figure 3.3; Dijkstra reported in 1968 that dinitroarene **8** could be fully hydrogenated to give all-*cis* 1,3-diamino-4,5,6-trihydroxycyclohexane (Figure 3.3A).[14] Acetylation produced diacetamide **9** in 39% over the 2 steps. Subsequent oxidations mediated by

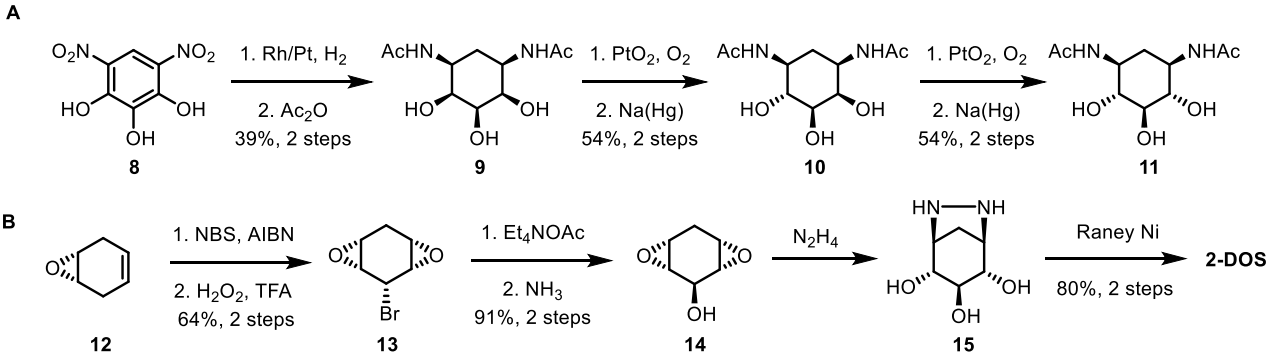

Figure 3.3. Two approaches to synthetic 2-deoxystreptamine. (A) Dijkstra approach featuring global hydrogenation of dinitropyrogallol **8**. (B) Prinzbach approach demonstrating a double epoxide opening of **14**.

platinum (IV) oxide and oxygen followed by a sodium amalgam reduction inverted one of the hydroxyl stereocenters, giving **10**. Repeating this sequence inverted the hydroxyl opposite on the ring, providing **11**.

An intuitive disconnection for 2-deoxystreptamine can be made from sequential additions to epoxides by amines to set the relative *trans* relationships with the adjacent hydroxyls. This was the approach of Prinzbach in 1975 where the epoxide **12** from 1,4-cyclohexadiene was first converted to an allylic bromide and oxidized once more to give bisepoxide **13** (Figure 3.3B).[15] A

substitution reaction by tetraethylammonium acetate followed by aminolysis of the intermediate acetate ester yielded alcohol **14** in 91% for the two step sequence. Finally, the epoxide additions were realized in tandem via the addition of hydrazine, forming an intermediate bicycle **15** that was reduced with Raney nickel to give 2-deoxystreptamine.

Van Delft and colleagues have disclosed two separate syntheses of 2-deoxystreptamine which utilized non-carbohydrate building blocks.[16,17] The first of which was a racemic approach that began with the Diels-Alder adduct of cyclopentadiene and *p*-benzoquinone **16** (Figure 3.4).[18] Two sequential reductions furnished intermediate **17**, first reported by Takano and Ogasawara.[19,20] Nucleophilic epoxidation and Luche reduction provided alcohol **18**, which then underwent retro-

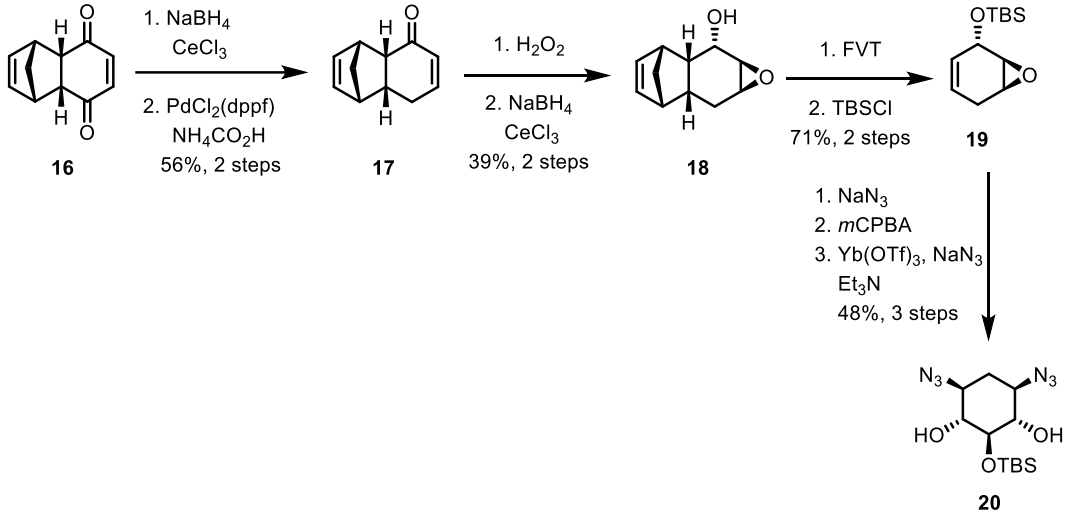

Figure 3.4. Racemic van Delft synthesis of *meso* diazide **20**.

Diels-Alder by flash vacuum thermolysis and hydroxyl silylation to afford alkene **19**. A three-step sequence furnished *meso* 2-deoxystreptamine analog **20**: azide opening of the epoxide, epoxidation using *meta*-chloroperbenzoic acid, and finally a lewis-acid promoted addition of sodium azide. Overall, this synthesis proceeded in nine steps and 7% yield of **20** from **16**.

A second, asymmetric synthesis was later disclosed which utilized allylglycine derivative **21** (Figure 3.5).[17] Addition of 2-lithiothiazole followed by diastereoselective reduction with

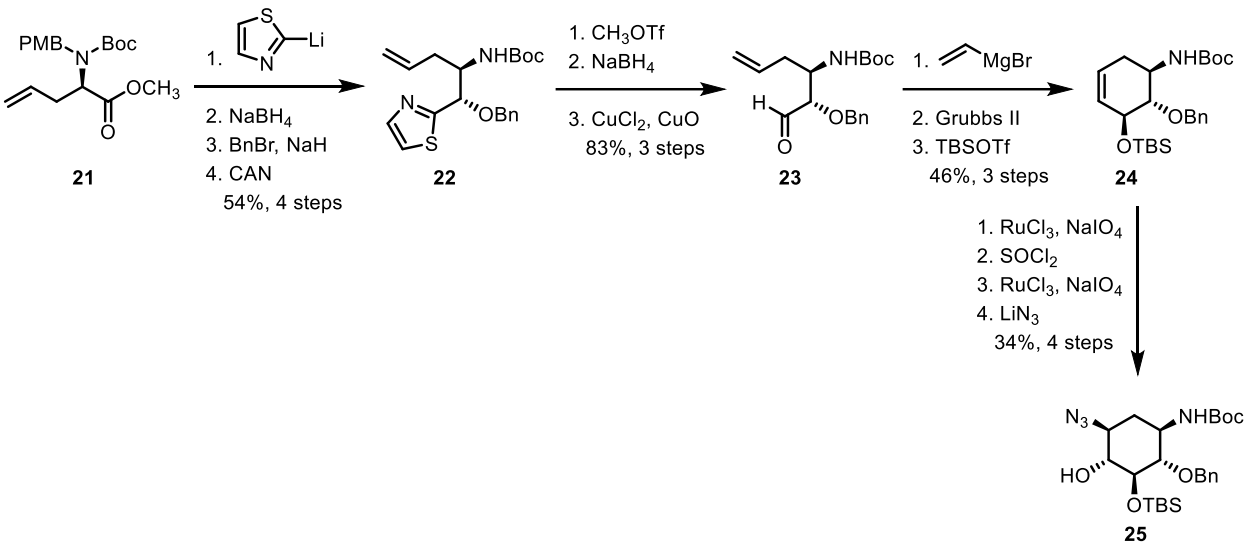

Figure 3.5. Asymmteric van Delft synthesis of 2-deoxystreptamine building block **25** from allylglycine derivative **21**.

sodium borohydride provided an intermediate benzylic alcohol. Benzyl ether formation and *p*-methoxybenzyl amine deprotection by ceric ammonium nitrate provided carbamate **22** in 54% yield over the 4 steps. Activation of the thiazole with methyl trifluoromethanesulfonate generated an imidazolium that was then reduced to provide aldehyde **23** in 83% yield over 3 steps. Grignard addition and ring-closing metathesis by Grubbs II gave a cyclohexene, whose silylation with TBSCl gave silyl ether **24**. To complete the synthesis of **25**, dihydroxylation of **24** followed by the treatment with thionyl chloride and an additional oxidation generated a cyclic sulfate intermediate. Cyclic sulfates are proposed to have better selectivity in the final step, azidation by treatment with lithium azide, ultimately giving **25** in 7% yield over 14 steps from **21**.

As part of a synthetic program to develop fully synthetic aminoglycoside antibiotics, Dr. Fan Liu developed a first-generation synthesis of orthogonally protected 2-deoxystreptamine suitable to use in the preparation of gentamicin derivatives for her thesis project in the Myers group (Figure 3.6).[21] Critical to the success of this synthesis was the development of an intramolecular

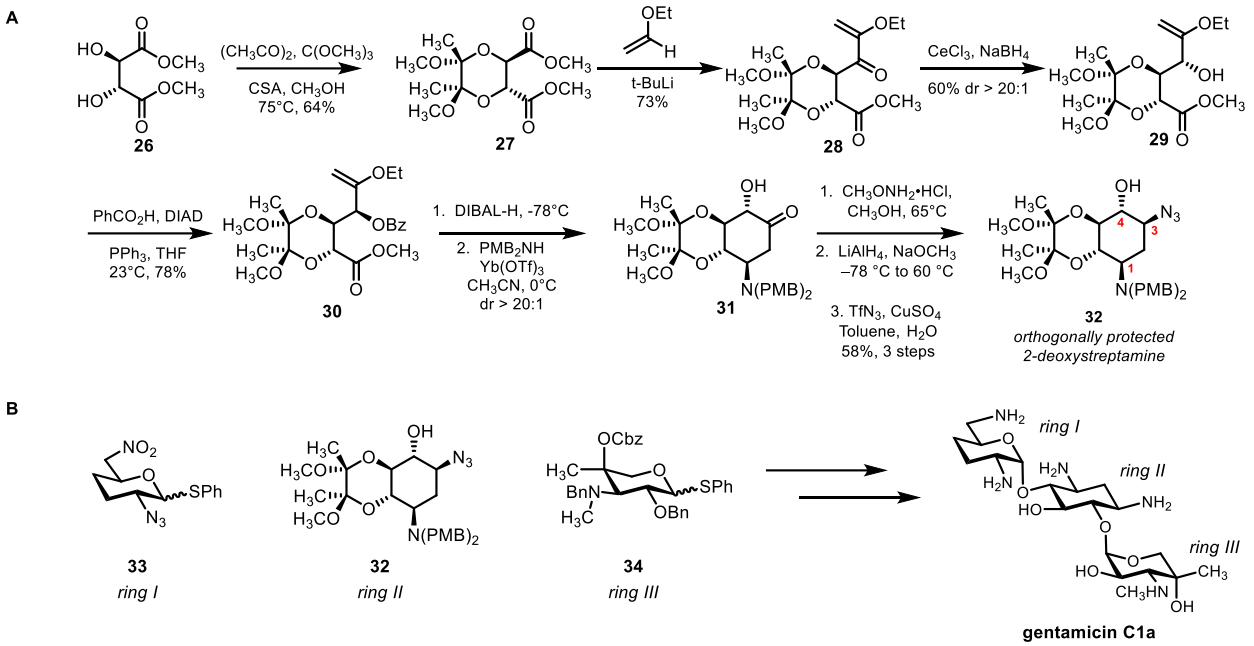

Figure 3.6. (A) Dr. Fan Liu's synthesis of 2-deoxystreptamine and the preparation of fully synthetic gentamicin C1a. (B) Components used in the synthesis of gentamicin C1a.

Mannich reaction which proceeded with high diastereoselectivity (>20:1), attributable to the fusion to the butanediacetal (BDA) protecting group. Fan's synthesis began with the BDA protection of (+)-dimethyl tartate **26** to give diketal **27**. Mono-addition of lithiated ethyl vinyl ether produced an a-alkoxy enone **28**, which was diastereoselectively reduced under Luche conditions to provide allylic alcohol **29**. However, the so obtained incorrect diastereomer necessitated a Mitsunobu inversion with benzoic acid to generate diester **30**. The diester **30** was then reduced with DIBAL-H, and intramolecular Mannich reaction was achieved with a combination of bis-*para*-methoxybenzyl amine and ytterbium (III) triflate, providing b-amino ketone **31** in 40% yield for the two steps. A three-step sequence consisting of oxime formation, directed reduction with lithium aluminum hydride, and diazotransfer from trifluoromethanesulfonic azide afforded protected 2-deoxystreptamine with a hydroxyl at C4 primed for coupling to ring I glycosyl donors. She simultaneously developed syntheses of purpurosamine and garosamine thioglycosyl donors **33**-**34**

that were coupled to **32** in sequence. Deprotection then completed the total synthesis of gentamicin C1a. Some noteworthy aspects of this synthesis are the orthogonality in the C1 and C3 amine protecting groups and the preparation of each aminoglycoside ring with non-carbohydrate building blocks. Unfortunately, despite access to the 4,6-disubstituted family of aminoglycosides with the ability to incorporate the HABA chain, no antibiotics developed from this chemistry were able to circumvent ribosomal methyltransferase resistance mechanisms.

While pursuing my graduate studies, the Sarlah group disclosed an asymmetric synthesis of 2-deoxystreptamine *en route* to the 4,5-disubstituted aminoglycoside ribostamycin (Figure 3.7).[22] Many methods for dearomative animation have been developed within their laboratory, and here the synthesis began by the enantioselective cycloaddition between *N*-methyl-1,2,4-triazoline-3,5-dione **35** and benzene with concurrent copper-mediated allylic reduction; this formally provides the 1,2-hydroamination product **36** in 92% *ee*, 65% yield on gram scale. Boc-protection of the resulting urazole facilitated anti-selective epoxidation to **37** and, following Boc-deprotection, enabled the 5-exo-tet cyclization to establish the C1 and C3 amine stereocenters in masked form. Benzylation of the resulting allylic alcohol yielded **38**, which was followed by bromohydrin formation and epoxide reversion under basic conditions to establish the C5 hydroxyl stereochemistry in **39**. This simultaneously allowed the C4-hydroxyl stereocenter to be introduced by anti-addition to the epoxide with lithiated acetophenone oxime, providing **40**. With the stereochemistry of 2-deoxystreptamine established, the ribose fragment **41** was installed by concurrent thiolation and activation with silver perchlorate, coupling the ribose donor with complete b-selectivity to afford **42**. Reduction of the oxime mediated by an acetic acid solution of zinc metal unmasked the C4-hydroxyl, allowing glycosylation between azidated neosamine donor

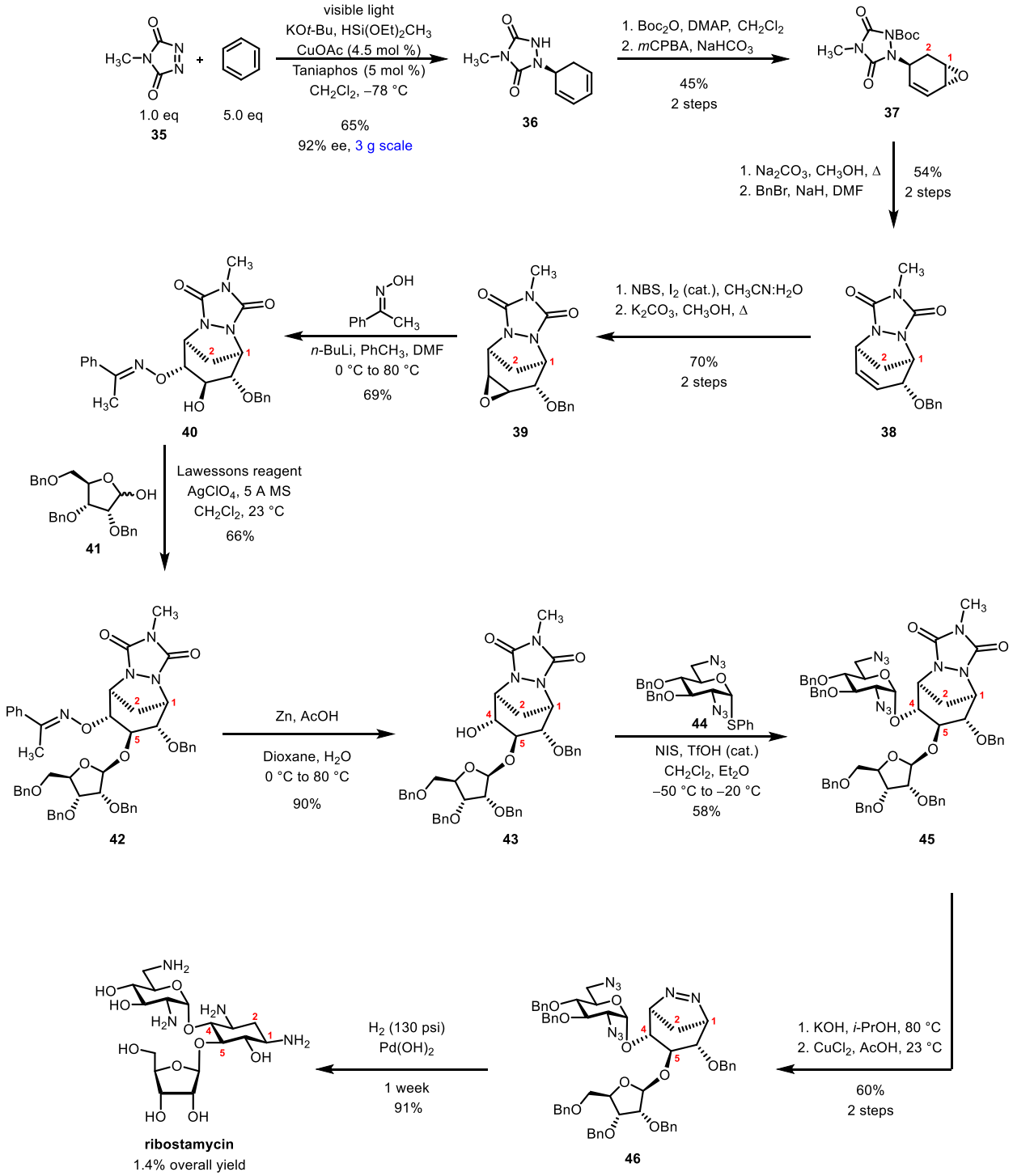

Figure 3.7. Sarlah group synthesis of ribostamycin. 2-DOS numbering is denoted in red.

44 and acceptor **43** to yield a protected ribostamycin **45**. Conversion of the urazole to a cyclic diazene was achieved under basic conditions, and a final hydrogenolysis of the azides and benzyl groups revealed ribostamycin; this synthesis was achieved in 14 steps with 1.4% overall yield.

3.3 Intramolecular Aldolization strategy to 2-deoxystreptamine

Several factors contributed to routes used while pursuing protected 2-deoxystreptamine. First, we desired a highly convergent and diastereoselective coupling between two stereochemically rich components, ideally setting multiple stereocenters for 2-DOS in one transformation. Even in the absence of such a transform, we recognized the importance of orthogonality in the C1 and C3 amine protecting groups analogous to Fan's first-generation synthesis,[21] thereby allowing incorporation of HABA-like side chains and the potential for C3 modification. Differing from the first-generation strategy was a focus on accessing 4,5-disubstituted aminoglycosides as opposed to their 4,6-subfamily members, thereby intrinsically gaining activity in the presence of highly disseminated G1405 methyltransferases such as *armA*.[23] We furthermore recognized that glycosylation at C5 could occur prior to that at C4, as the inverse synthesis might hinder the reactivity at the C5-hydroxyl in the presence of a C4 glycoside.[24] With these factors in mind, we proposed a retrosynthesis as outlined in Figure 3.8. Upon accessing my desired aldol reaction, I intended to utilize the C4 hydroxyl to set the C3 amine stereochemistry of **47** by a directed reduction from an intermediate such as **48** (Figure 3.8A). The protection of **48** would arise from aldol product **49**, itself generated from ketoaldehyde **50**. The disconnection to **50** would provide multiple disconnections to access such an intermediate from oxidation of a hydroxyketone, such as **51**, or olefins **52** and **53** (Figure 3.8B). Hydroxyketone **51** would be

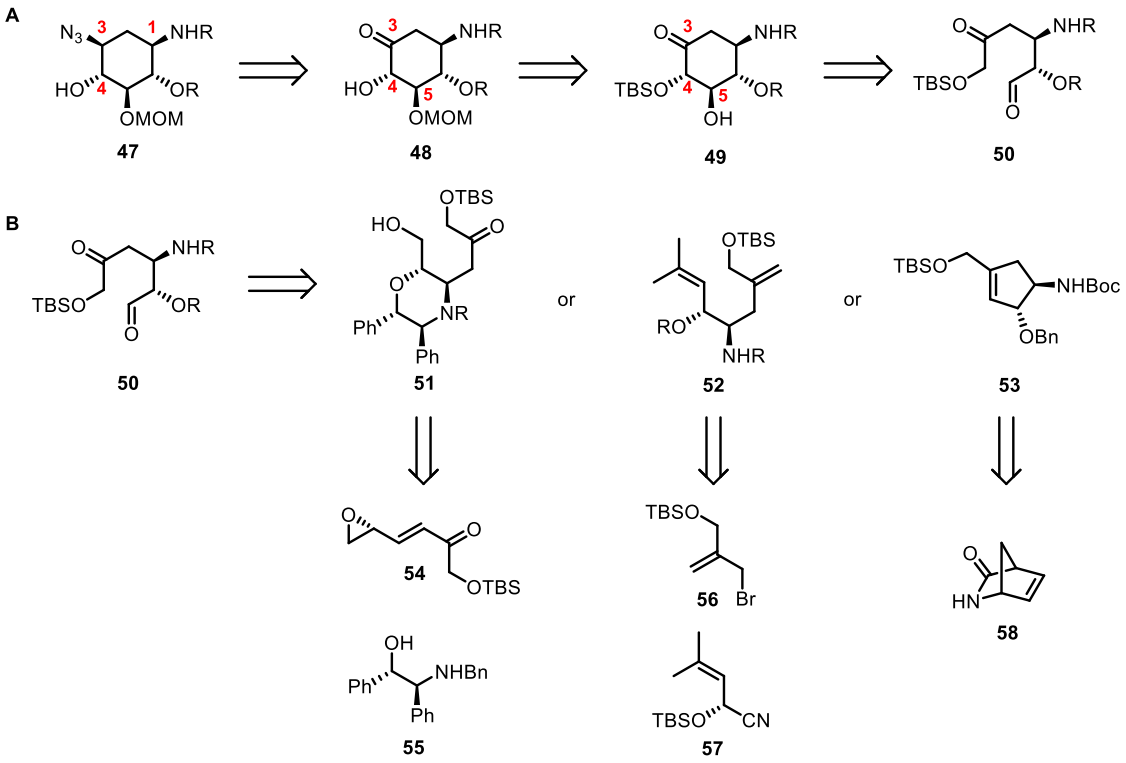

Figure 3.8. (A) Retrosynthesis from 2-deoxystreptamine acceptor **47** to ketoaldehyde aldol precursor **50** with generic protecting groups for the C1 amine and C6 hydroxyl. (B) Potential disconnections to **50** from hydroxyketone **51** or alkenes **52** and **53** and their respective components.

traceable to stereodefined g,d-epoxyenone **54** which we intended to join with aminoalcohols such as **55**;[25] the diphenyl backbone would be removed in the final aminoglycoside hydrogenolysis. Alternatively, diolefin **52** could be accessed via stereoselective reduction of a metalated imine formed from **56**[26] undergoing coupling with optically active cyanohydrin **57**. Lastly, olefin **53** could serve as a precursor to **50** via ozonolysis and would be accessed from commercially available and optically pure Vince's lactam **58**.[27]

3.3.1 Preparation and reactivity of a γ,δ-epoxyenone

I first desired to explore the reactivity of epoxyenone **54** and its potential "snap" together with aminoalcohol **55**. Precedent for such a transform was limited, and the reaction of amines with such an epoxyketone might be liable to reversibility in the aza-Michael addition and funnel material towards epoxide alkylation products.[28]

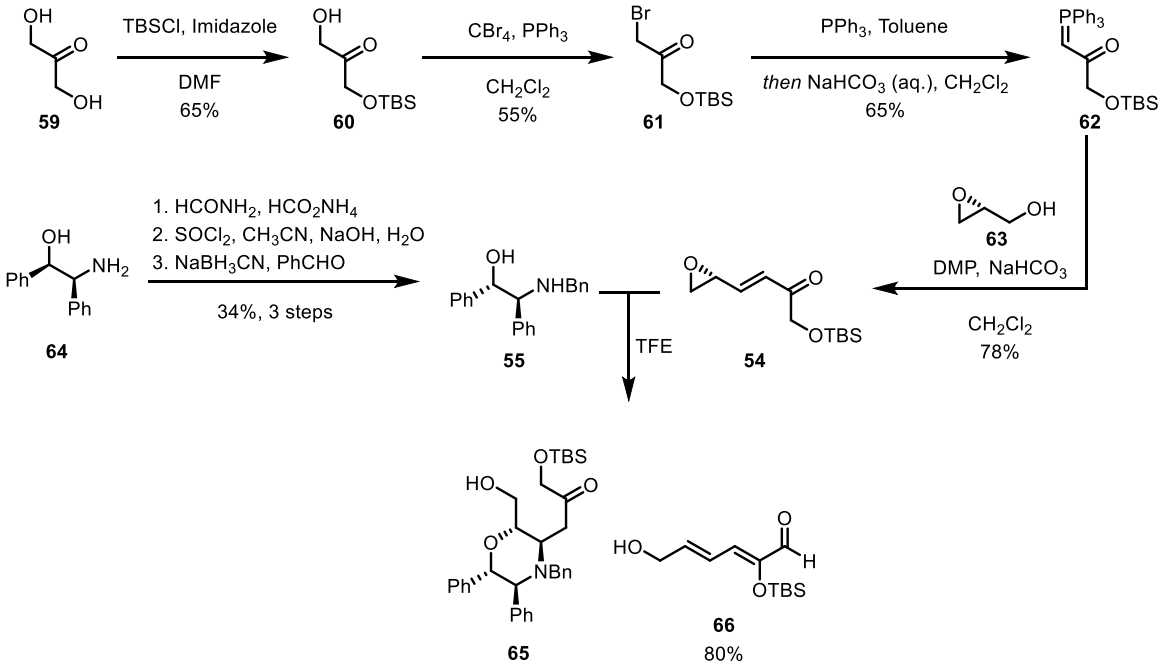

Figure 3.9. Synthesis of components epoxyenone **54** and aminoalcohol **55** that failed to merge, instead promoting silyl migration.

Starting from dihydroxy acetone **59**, monosilylation was achieved with TBSCl giving silyl ether **60** in 65% yield (Figure 3.9). Appel reaction[26] of the remaining alcohol with carbon tetrabromide and triphenylphosphine generated a-bromoketone **61** in 55% yield. Haloketone **61** was transformed into olefination reagent **62** by treatment with triphenylphosphine and a subsequent basification to generate the phosphorane in 65% yield over two steps. To establish the epoxide stereochemistry, commercially available (*R*)-glycidol **63** was oxidized with Dess-Martin

periodinane,[29] and in the same flask the addition of phosphorane **62** resulted in olefination with high *E*-selectivity due to the stabilization of the phosphorane by the vicinal ketone. To prepare **55**, diphenyl-aminoalcohol **54** used in the preparation of pseudoephenamine[25] served as a valuable precursor. The inversion of the alcohol stereochemistry to yield our desired (*1S*,*2S*)-diphenylaminoethanol has been demonstrated on multi-kilogram scale. Reductive amination then provided **55** in 34% yield over the three steps.

With the desired components in hand, initial experimentation inspired the use of trifluoroethanol as solvent to promote aza-Michael reaction due to the increased acidity relative to other protic solvents. However, substituted morpholine **65** could never be identified in the crude mixtures, even with consumption of **54**. Instead, conjugated enal **66** could be obtained as the sole

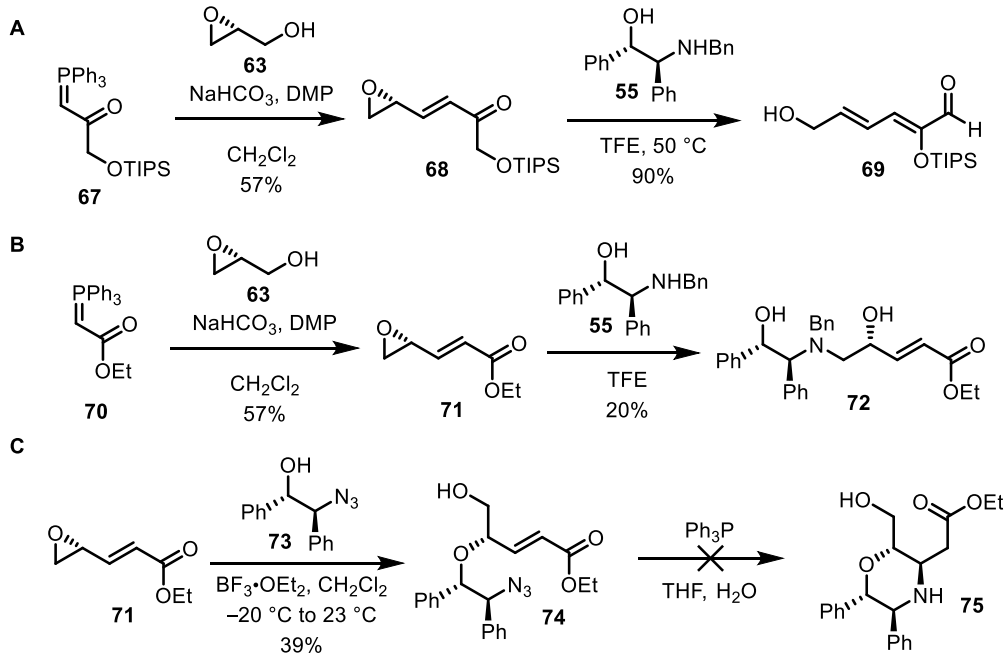

Figure 3.10. (A) Synthesis of alternative epoxyenone **68** that also undergoes silyl migration to **69**. (B) An unsaturated ester **71** reacts with aminoalcohol **55** by epoxide addition and not Michael reaction. (C) Azidoalcohol **73** may add to epoxide **71**, but amine deprotection does not result in access to morpholine **75**.

product in 80% yield, the result of a silyl group transfer following deprotonation by **55**. I explored numerous strategies to circumvent this mode of reactivity (Figure 3.10). I first prepared TIPS-protected enone **68** by olefination of phosphorane **67** (obtained by analogous synthesis of **54** in Figure 3.9, not depicted) with glycidaldehyde in 57% yield; I expected that a bulkier silyl protecting group would suppress the migration reactivity (Figure 3.10A).[30] However, upon treatment of this epoxyenone with **55** in trifluoroethanol no reaction occurred until the mixture was heated, then yielding extended enal **69** in 90% yield. Commercially available phosphorane **70** was used to generate unsaturated ester **71** to investigate aminoalcohol addition in the absence of any migratory group. Unfortunately, reaction with **55** occurs by alkylation at the epoxide terminus and not via aza-Michael addition, producing **72** in 20% after HPLC purification. Use of a less substituted amine component similarly results in epoxide alkylation, with small amounts of internal epoxide alkylation (~5%) observed. Lastly, I generated azidoalcohol **73** by diazotransfer with triflic azide. Coupling of **71** and **73** promoted by boron trifluoride diethyl etherate afforded ether **74** in 39% yield. Despite this initial coupling, azide deprotection of **74** failed to produce the desired morpholine scaffold **75**; careful study of the crude NMR suggested that the incorrect stereochemistry for the amine was obtained as the major product.

3.3.2 Preparation and attempted union with an optically active cyanohydrin

With discouraging results from a proposed epoxyenone addition, I explored the chemistry of an optically active cyanohydrin coupling with organometallic and reducing agents in tandem.[31] Starting from commercial phosphonate ester **76**, a one-pot aldolization and olefination yielded allylic alcohol **77** in 61% following distillation (Figure 3.11). Protection of the alcohol as the TBS ether gave **78**, and DIBAL-H reduction of the unsaturated ester gave **79** in 89% yield over two

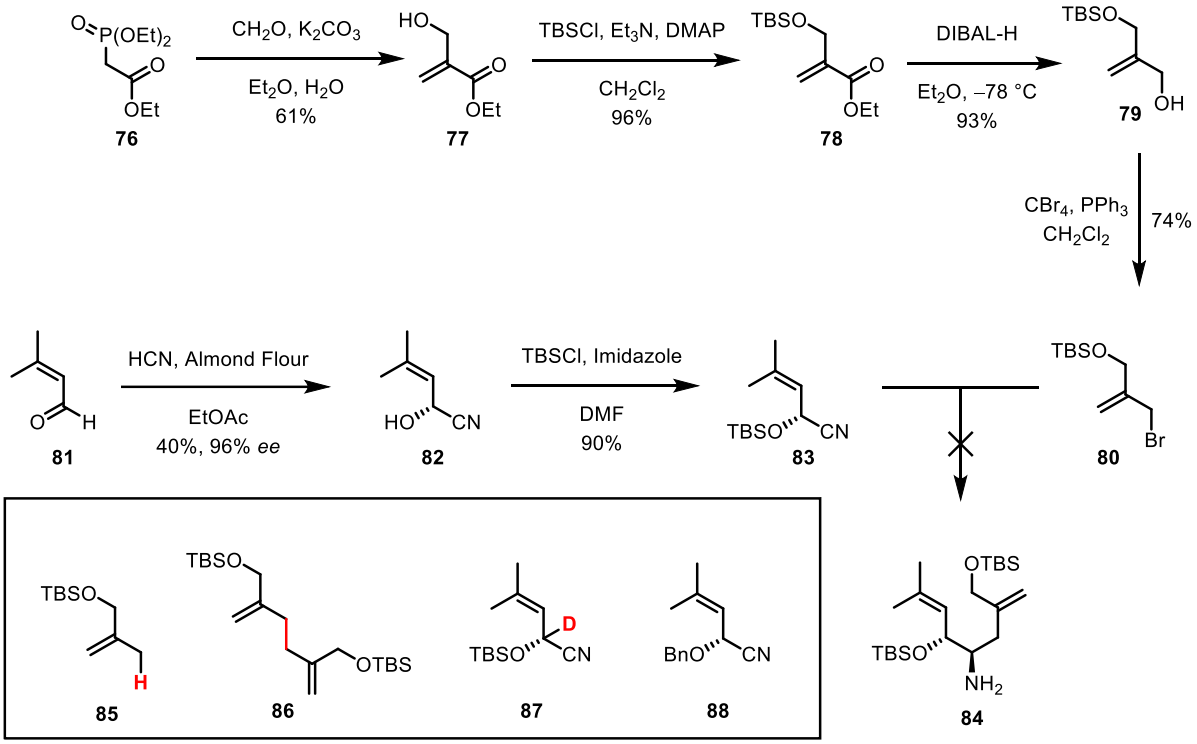

Figure 3.11. Preparation of component halide **80** and optically active cyanohydrin **83**, as well as noteworthy byproducts.

steps. Halogenation was achieved with triphenylphosphine and carbon tetrabromide to provide allylic halide **80** in 74% yield.[26] To generate the cyanohydrin, a small body of literature pointed to the oxynitrilase enzyme from almonds as a convenient source for enantioselective cyanation of aldehydes.[32] Among these substrates, prenal **81** was compatible with the (*R*)-oxynitrilase of almond flour and was successfully transformed into cyanohydrin **82** with 96% *ee* in 40% yield. Protection as the TBS ether proceeded in 90% yield, but unfortunately product **83** could not be successfully coupled with **80** under a variety of metalation or reduction conditions. A common source of non-productive reactivity lay with the allylic halide **80**. This reagent was especially prone to proto-dehalogenation and homocoupling, affording **85** and **86** as major byproducts, respectively. Alternatively, in the event of successful organometallic preparations, the high acidity of the

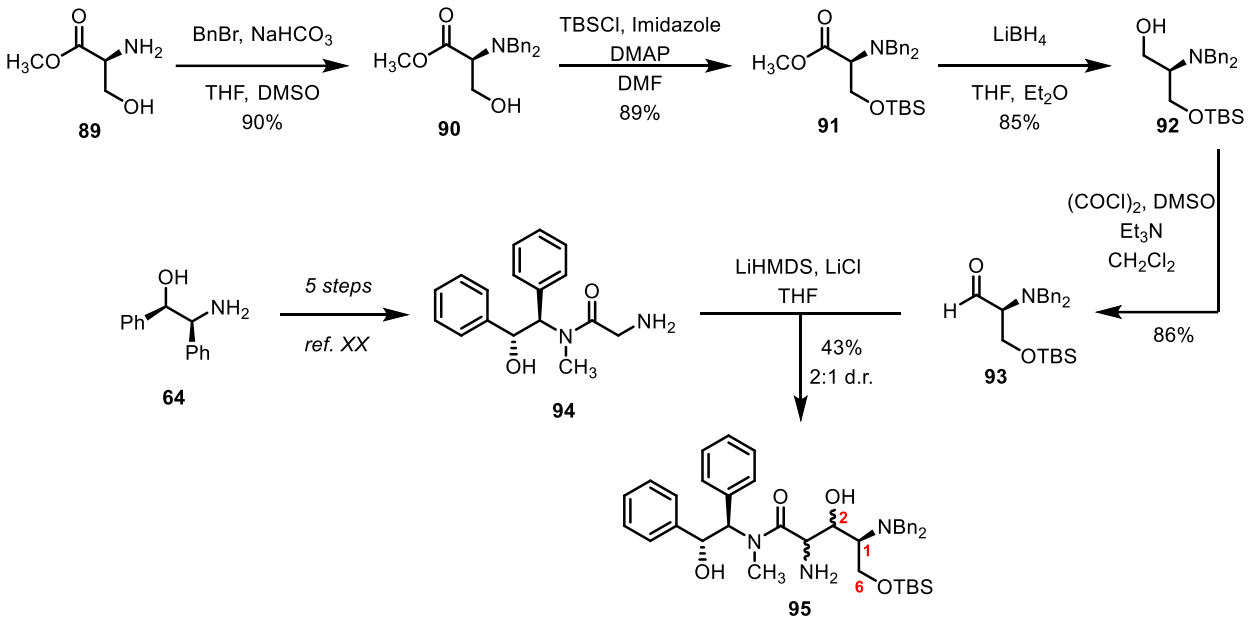

Figure 3.12. Synthesis of Reetz aldehyde **93** and aldolization with pseudoephenamine glycinamide **94**.

cyanohydrin proton was prone to exchange, as identified from experimental quenches with deuterated media to generate **87**. Lastly, benzylation of **82** could be achieved, affording **88**; but this substrate was similarly recalcitrant to organometallic coupling or reduction, and with these results we shifted our focus to alternative approaches.

3.3.3 Aldolization of pseudoephenamine glycinamide with a Reetz aldehyde

We briefly considered the aldolization reaction between *N,N*-dibenzylaminoaldehydes that were developed by Manfred Reetz[33] and known to be slow to epimerize relative to other a-heteroatom aldehydes. This route appealed to us due to the potential in having oxygenation at C2 of the streptamine ring. Alternatively, the serine building block of choice may be modified to facilitate alkylation as opposed to aldol reaction, giving canonical 2-deoxystreptamine at the end of the synthesis. Starting from serine methyl ester **89**, benzylation of the amine with excess benzyl

bromide provided *N,N*-dibenzylated **90** in 90% yield (Figure 3.12). TBS protection of the side chain alcohol proceeded in 89% yield, affording **91**. Lithium borohydride allowed the reduction of the C-terminal ester, providing aminoalcohol **92** in 85% yield. Lastly, Swern oxidation provided aldehyde **93** in 86% yield and reasonable purity without the need for chromatography. Pseudoephenamine glycinamide **94**, developed for stereoselective aldol reactions in the Myers group as a modern counterpart to pseudoephedrine, was prepared via literature procedures from commercial **64**.[34] However, upon aldolization, diamine **95** was generated in poor yields with low diastereoselection (43%, 2:1 d.r. and not determined). With this result and recognizing the likely difficulty of introducing the C5 component, we quickly pivoted from this strategy and pursued other sources for 2-deoxystreptamine.

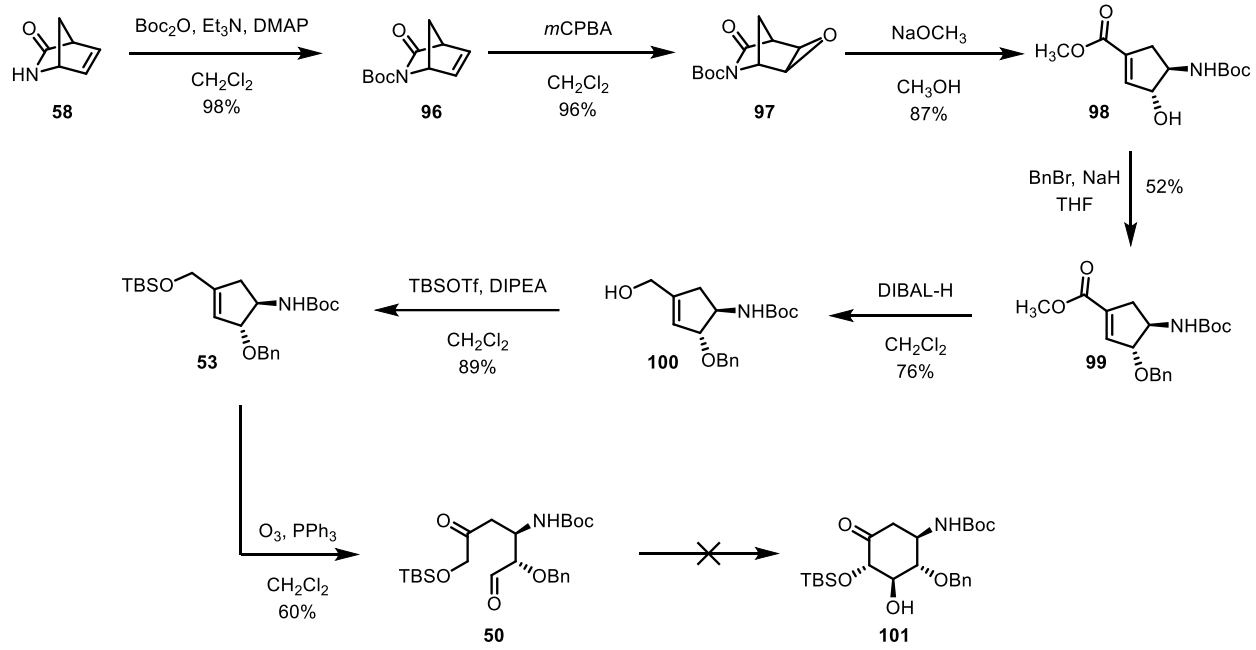

Figure 3.13. A linear synthesis from Vince's lactam **58** provided access to differentiated cyclopentene **53**, ultimately allowed exploration of the aldol reaction of **50**.

3.3.4 A differentiated cyclopentene prepared from Vince's lactam

I identified cyclopentene **53** as a potential precursor to ketoaldehyde **50**. A differentially protected cyclopentene could likely be prepared from commercially available Vince's lactam **58** following epoxidation and opening lactam by solvolysis (Figure 3.13).[27] In the forward sense, **58** was first protected as the *tert*-butylcarbamate **96** in 98% yield. Subsequent exposure to *m*CPBA for four days generated the *exo* epoxide **97** exclusively in 96% yield. With activation by the carbamate, methanolysis of the lactam by sodium methoxide and subsequent elimination of the epoxide formed allylic alcohol **98** in 87% yield for a single transformation. Benzylation of the resulting alcohol **98** to give **99**, and DIBAL-H reduction of the ester product provided **100** in 40% yield over two steps. Silylation of the primary alcohol gave access to **53** in 89% yield. With differentiated cyclopentene **53** in hand, ozonolytic cleavage of the alkene and reduction by triphenylphosphine cleanly yielded ketoaldehyde **50** following chromatography. An array of conditions was explored to induce aldolization, all of which led to decomposition or b-elimination byproducts that were non-productive to accessing hydroxyketone **101**.

3.4 Semisynthetic 2-deoxystreptamine from neomycin B

With the aldolization reaction explored, we turned to semisynthetic access to 2-deoxystreptmaine derivatives. Strong precedent existed from the work of van Delft, as well as prior optimizations within the Myers laboratory (Figure 3.14).[21,35] Starting from neomycin B, acidic methanolysis led to fragmentation of the ring II – ring III glycosidic linkage to yield crude neamine, which could be globally azidated using trifluoromethanesulfonic azide to give tetraazide **102** in 70% yield after both steps. Careful monitoring of the acetylation of **102** could selectively

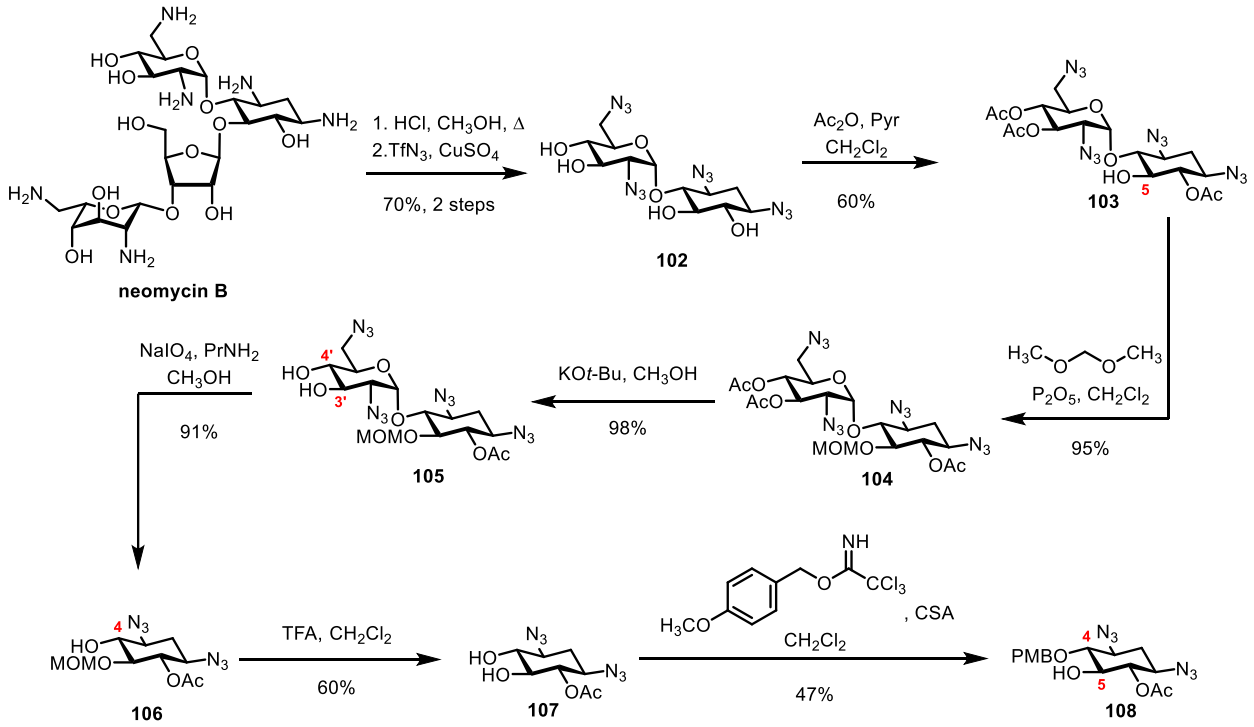

Figure 3.14. Degradation of neomycin B led to semisynthetic 2-deoxystreptamine acceptors **106**, **107**, and **108**.

acylate the 3',4'-diol, as well as the more reactive C6-hydroxyl of ring I to yield triacetate **103** in 60% yield. Treatment of C5-hydroxyl **103** with dimethoxy methane and phosphorous pentoxide generated the MOM-protected triacetate **104** in 95% yield. The more accessible C3' and C4' acetates were selectively solvolyzed with methanolic potassium *tert*-butoxide to give diol **105** in 98% yield. Lastly, periodate-mediated cleavage of the diol, followed by alkyl amine condensation on the dialdehyde intermediate eliminated the glycosidic bond between rings I and II, providing 2-deoxystreptamine acceptor **106** in 91% yield; this synthesis gave **106** in 37% overall yield from neomycin B on decagram scale. This acceptor has notable features in the orthogonal protection between the C5 and C6 hydroxyls and has some slight differentiation of the azides due to the vicinal acetate at C6. In expecting the MOM group to potentially be cumbersome late stage, as

well as desiring a ring II-IV glycosyl acceptor for paromomycin derivatives, I prepared diol **107** by treatment of **106** with trifluoroacetic acid in dichloromethane. Subsequent *para*-methoxybenzylation via the trichloroacetimidate reagent occurred preferentially at the more electron-rich C4 hydroxyl, giving PMB-protected **108** in 47% yield. These 2-deoxystreptamine acceptors could serve as coupling partners to ring I glycosyl donors in the pursuit of antibiotics overcoming NpmA resistance.

3.5 Summary

In summary, I have proposed and explored the synthesis of protected 2-deoxystreptamine via four notable routes. These strategies relied on an intramolecular aldolization of an intermediate keto-aldehyde, which was ultimately accessed from Vince's lactam in 17% yield over 7 steps. However, the desired cyclohexane annulation failed to be realized, necessitating the preparation of 2-deoxystreptamine derivatives semisynthetically from neomycin B. This semisynthesis provided access to 2-deoxystreptamine analog **106** in 37% over 6 steps from neomycin B, alongside diol **107** and *para*-methoxybenzylated derivative **108**.

3.6 References

1. Busscher, G. F.; Rutjes, F. P. J. T.; van Delft, F. L. *Chem. Rev.* **2005**, *105*, 775.

2. *Aminoglycoside Antibiotics*: From Chemical Biology to Drug Discovery. 1 ed.; John Wiley & Sons: 2007.

3. Shaw, K.; Rather, P.; Hare, R.; Miller, G. *Microbiol. Rev.* **1993**, *57*, 138.

4. Aggen, J. B.; Armstrong, E. S.; Goldblum, A. A.; Dozzo, P.; Linsell, M. S.; Gliedt, M. J.; Hildebrandt, D. J.; Feeney, L. A.; Kubo, A.; Matias, R. D. *Antimicrob. Agents Chemother.* **2010**, *54*, 4636.

5. Daniels, P. J. L.; Rane, D. F.; McCombie, S. W.; Testa, R. T.; Wright, J. J.; Nagabhushan, T. L., Chemical and Biological Modification of Antibiotics of the Gentamicin Group. In *Aminocyclitol Antibiotics*, American Chemical Society: 1980; Vol. 125, pp 371.

6. Greenberg, W. A.; Priestley, E. S.; Sears, P. S.; Alper, P. B.; Rosenbohm, C.; Hendrix, M.; Hung, S.-C.; Wong, C.-H. *J. Am. Chem. Soc.* **1999**, *121*, 6527.

7. Orsat, B.; Alper, P. B.; Moree, W.; Mak, C.-P.; Wong, C.-H. *J. Am. Chem. Soc.* **1996**, *118*, 712.

8. Grabowski, S.; Armbruster, J.; Prinzbach, H. *Tetrahedron Lett.* **1997**, *38*, 5485.

9. (a) Downham, R.; Edwards, P. J.; Entwistle, D. A.; Hughes, A. B.; Kim, K. S.; Ley, S. V. *Tetrahedron: Asymmetry* **1995**, *6*, 2403; (b) Ley, S. V.; Polara, A. *J. Org. Chem.* **2007**, *72*, 5943.

10. Tan, C.-H.; Rando, R. R. *Bioorg. Med. Chem. Lett.* **2003**, *13*, 901.

11. Kuehl, F. A.; Bishop, M. N.; Folkers, K. *J. Am. Chem. Soc.* **1951**, *73*, 881.

12. (a) Nakajima, M.; Hasegawa, A.; Kurihara, N. *Tetrahedron Lett.* **1964**, 5, 967; (b) Canas-Rodriguez, A.; Galan Ruiz-Poveda, S.; Gomez-Sanchez, A.; Blanco Gonzalez, E. *Carbohydr. Res.* **1977**, *59*, 240; (c) Suami, T.; Ogawa, S.; Tanno, N.; Suguro, M.; Rinehart, K. L. *J. Am. Chem. Soc.* **1973**, *95*, 8734; (d) Tona, R.; Bertolini, R.; Hunziker, J. *Org. Lett.* **2000**, *2*, 1693; (e) Baer, H. H.; Arai, I.; Radatus, B.; Rodwell, J.; Chinh, N. *Can. J. Chem.* **1987**, *65*, 1443; (f) da Silva, E. T.; Hyaric, M. L.; Machado, A. S.; de Almeida, M. V. *Tetrahedron Lett.* **1998**, *39*, 6659; (g) Yoshikawa, M.; Ikeda, Y.; Kayakiri, H.; Kitagawa, I. *Chemischer Informationsdienst* **1982**, *13*.

13. (a) Ogawa, S.; Ueda, T.; Funaki, Y.; Hongo, Y.; Kasuga, A.; Suami, T. *J. Org. Chem.* **1977**, *42*, 3083; (b) Suami, T.; Ogawa, S.; Sano, H. *Tetrahedron Lett.* **1967**, *8*, 2671.

14. Dijkstra, D. *Recl. Trav. Chim. Pays-Bas* **1968**, *87*, 161.

15. Prinzbach, H.; Keller, R.; Schwesinger, R. *Angew. Chem.* **1975**, *87*, 626.

16. Busscher, G. F.; Groothuys, S.; de Gelder, R.; Rutjes, F. P. J. T.; van Delft, F. L. *J. Org. Chem.* **2004**, *69*, 4477.

17. Busscher, G. F.; Rutjes, F. P. J. T.; van Delft, F. L. *Tetrahedron Lett.* **2004**, *45*, 3629.

18. Oda, M.; Kawase, T.; O'ada, T.; Enomoto, T. *Org. Synth.* **1996**, *73*, 253.

19. (a) Takano, S.; Higashi, Y.; Kamikubo, T.; Moriya, M.; Ogasawara, K. *Synthesis* **1993**, *1993*, 948; (b) Takano, S.; Moriya, M.; Kamikubo, T.; Hiroya, K.; Ogasawara, K. *Tetrahedron Lett.* **1993**, *34*, 8485.

20. Marchand, A. P.; LaRoe, W. D.; Sharma, G. V. M.; Suri, S. C.; Reddy, D. S. *J. Org. Chem.* **1986**, *51*, 1622.

21. Liu, F. Development of a Component-Based Synthesis for the Discovery of New Aminoglycoside Antibiotics, and Diastereoselective Michael-Claisen Cyclizations En Route to 5-Oxatetracyclines. Ph.D. thesis, Harvard University, Cambridge, MA United States, 2017.

22. Ungarean, C.N.; Galer, P.; Zhang, Y.; Lee, K.S.; Ngai, J.M.; Lee, S.; Liu, P.; Sarlah, D. *Nat. Synth.* **2022**, *1*, 542.

23. Matsushita, T.; Sati, G.; Kondasinghe, N.; Pirrone, M.; Kato, T.; Waduge, P.; Kumar, H.; Sanchon, A.; Dobosz-Bartoszek, M.; Shcherbakov, D.; Juhas, M.; Hobbie, S. N.; Schrepfer, T.; Chow, C. S.; Polikanov, Y.; Schacht, J.; Vasella, A.; Böttger, E. C.; Crich, D. *J. Am. Chem. Soc.* **2019**, *141*, 5051.

24. Chou, C.-H.; Wu, C.-S.; Chen, C.-H.; Kulkarni, S.S.; Wong, C.-H.; Hung, S.-C. *Org. Lett.* **2004**, *6*, 585.

25. Mellem, K.T.; Myers, A.G. *Org. Lett.* **2013**, *15*, 5594.

26. Brass, S.; Gerber, H.-D.; Dörr, S.; Diederich, W.E. *Tetrahedron*, **2006**, *62*, 1777.

27. Singh, R.; Vince, R. *Chem. Rev.* **2012**, *112*, 4642.

28. Miyazawa, M.; Ishibashi, N.; Ohnuma, S.; Miyashita, M. *Tetrahedron Lett.* **1997**, *38*, 3419.

29. Dess, D.B.; Martin, J.C. *J. Am. Chem. Soc.* **1991**, *113*, 7277.

30. Strand, D. Norrby, P.-O.; Rein, T. *J. Org. Chem.* **2006**, *71*, 1879.

31. Pohland, A.; Sullivan, H.R. *J. Am. Chem. Soc.* **1953**, *75*, 5898.

32. Zandbergen, P.; van der Linden, J.; Brussee, J.; van der Gen, A. *Synth. Commun.* **1991**, *21*, 1387.

33. Reetz, M.T. *Chem. Rev.* **1999**, *99*, 1121.

34. Seiple, I. B.; Mercer, J. A.; Sussman, R. J.; Zhang, Z.; Myers, A. G. *Angew. Chem. Int. Ed.* **2014**, *53*, 4642.

35. van den Broek, S. A. M. W.; Gruijters, B. W. T.; Rutjes, F. P. J. T.; van Delft, F. L.; Blaauw, R. H. *J. Org. Chem.* **2007**, *72*, 3577.

36. Still, W.C.; Khan, M.; Mitra, A. *J. Org. Chem.* **1978**, *43*, 2923.

3.7 Experimental Section

General Experimental Procedures. All reactions were performed in flame-dried round-bottom flasks fitted with rubber septa under positive argon pressure, unless otherwise noted. Air- and moisture-sensitive liquids were transferred via syringe. Organic solutions were concentrated by rotary evaporation (house vacuum, ca. 25-40 Torr) at ≤40 °C, unless otherwise noted. Analytical thin-layer chromatography (TLC) was performed using glass plates precoated with silica gel (0.25 mm, 60 Å pore-size, 230-400 mesh, Merck KGA) impregnated with a fluorescent indicator (254 nm). TLC plates were visualized by exposure to ultraviolet light, then stained with an aqueous potassium permanganate ($KMnO_4$), aqueous Ceric Ammonium Molybdate (CAM), ethanolic ninhydrin, or ethanolic bromocresol green stain and briefly heated using a heat gun; visualization of deprotected aminoglycosides was also achieved by exposing the plate to 20% sulfuric acid in ethanol and charring with a heat gun. Flash-column chromatography was performed as described by Still et al.,[36] employing silica gel (60 Å, 15-40 μM, EMD Millipore Corp.). All temperature measurements of reaction mixtures refer to the temperature of the heating/cooling bath unless otherwise specified. Structural assignments were made with additional information from gCOSY, gHSQC, and gHMBC experiments.

Materials. Commercial solvents and reagents were used as received.

Instrumentation. Proton magnetic resonance (^{1}H NMR) spectra were recorded on Bruker 400 (400 MHz) or 500 (500 MHz) NMR spectrometers at 23 °C. Proton chemical shifts are expressed in parts per million (ppm, δ scale) and are referenced to residual protium in the NMR solvent ($CHCl_3$, δ 7.26, CD_3OD, δ 3.45, C_6D_6, δ 7.16, D_2O δ 4.79). Data are represented as follows: chemical shift, multiplicity (s = singlet, d = doublet, t = triplet, q = quartet, p = quintet, m = multiplet and/or multiple resonances, br = broad), coupling constant (*J*) in Hertz (Hz) and

integration. Carbon nuclear magnetic resonance spectra (^{13}C NMR) were recorded on Bruker 400 (100 MHz) NMR spectrometers at 23 °C. Carbon chemical shifts are expressed in parts per million (ppm, δ scale) and are referenced to the carbon resonances of the NMR solvent ($CDCl_3$, δ 77.16, CD_3OD, δ 49.03 and C_6D_6, δ 128.06). Infrared (IR) spectra were obtained using a Bruker ALPHA FT-IR spectrometer. Data are represented as follows: frequency of absorption (cm^{-1}), intensity of absorption (s = strong, m = medium, w = weak, br = broad). High resolution mass spectra were obtained at the Harvard University Mass Spectrometry Facility using the Thermo Q Exactive Plus Orbitrap mass spectrometer via Electrospray Ionization (ESI).

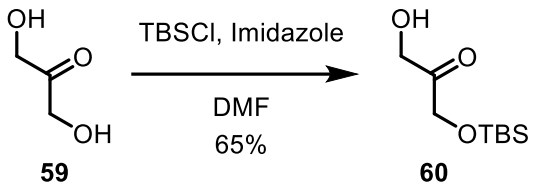

59 **60**

1-((*tert*-butyldimethylsilyl)oxy)-3-hydroxypropan-2-one (60)

To a flame-dried flask charged with a magnetic stir bar under Ar atmosphere was added dihydroxyacetone **59** (10.81 g, 120 mmol, 3 equiv) followed by anhydrous DMF (80 mL) and imidazole (3.54 g, 52 mmol, 3 equiv). At room temperature, TBSCl (6.03 g, 40 mmol, 1 equiv) was added in three portions over 5 minutes, and the reaction stirred overnight. The reaction was quenched by addition of water (100 mL) and the aqueous phase extracted with diethyl ether (4 x 100 mL). Drying of the combined organic phases with sodium sulfate, filtration, and concentration under rotary evaporation provided the crude material, which was further purified by flash chromatography on silica gel, eluting with a gradient from 5–20% ethyl acetate in hexanes to provide product **60** upon concentration as a clear oil (5.3 g, 25.9 mmol, 65%). *The product tended to dimerize upon storage and could be cracked by distillation under high vacuum and temperature*.

R_f: (20% ethyl acetate in hexanes, $KMnO_4$): 0.20

^1H NMR (500 MHz, $CDCl_3$): δ 4.50 (d, J = 4.8 Hz, 2H), 4.31 (s, 2H), 2.98 (t, J = 4.9 Hz, 1H), 0.92 (s, 9H), 0.10 (s, 6H).

FTIR (neat), cm^{-1}: 3468 (br), 2954 (m), 2930 (m), 1729 (s)

HRMS (ESI-TOF) m/z: $[M+H]^+$ Calcd for $C_9H_{21}O_3Si$ 203.1109; Found 203.1103.

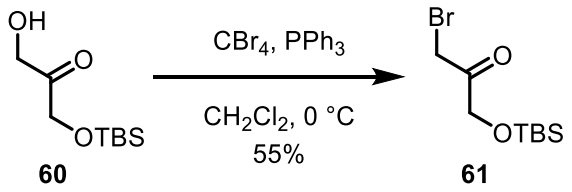

1-bromo-3-((*tert*-butyldimethylsilyl)oxy)propan-2-one (61)

To a flame-dried flask charged with a stir bar under Ar atmosphere was added hydroxy ketone **60** (3.76 g, 18.4 mmol, 1 equiv) followed by anhydrous dichloromethane (70 mL) and the solution cooled to 0 °C by ice water bath. Triphenylphosphine (5.31 g, 20.2 mmol, 1.1 equiv) and carbon tetrabromide (6.71 g, 20.2 mmol, 1.1 equiv) were added in sequence, and the reaction stirred for 2 hours at 0 °C. The reaction was quenched by addition of saturated aqueous sodium bicarbonate solution (70 mL) and the layers allowed to separate. The aqueous layer was washed with dichloromethane (1 x 70 mL) and the combined dichloromethane portions dried over sodium sulfate, filtered, and concentrated to give the crude material. Purification by flash chromatography on silica gel, eluting with a gradient from 0–15% ethyl acetate in hexanes, provided **61** as a colorless oil (2.7 g, 10.1 mmol, 55%).

R_f: (20% ethyl acetate in hexanes, $KMnO_4$): 0.60

^1H NMR (500 MHz, $CDCl_3$): δ 4.38 (s, 2H), 4.14 (s, 2H), 0.95 (s, 9H), 0.13 (s, 6H).

FTIR (neat), cm^{-1}: 2954 (m), 2930 (s), 2858 (m), 1729 (s).

HRMS (ESI-TOF) m/z: $[M-Br]^+$ Calcd for $C_9H_{19}BrO_2Si$ 187.1149; Found 187.1079

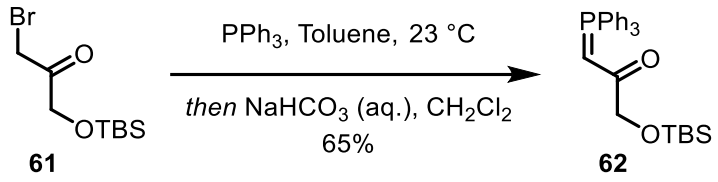

1-((*tert*-butyldimethylsilyl)oxy)-3-(triphenyl-| ^{5}-phosphaneylidene)propan-2-one (62)

To a flask containing a stir bar and a solution of bromoketone **61** (2.7 g, 10.1 mmol, 1 equiv) in toluene was added triphenylphosphine (2.65 g, 10.1 mmol, 1 equiv). A white precipitate began to form and while stirring at ambient temperature for 30 minutes thickened into a slurry. The white suspension was then cooled to 0 °C and the solids collected by filtration. The crude solids were dissolved in dichloromethane and water (5:1, 25 mL) and solid sodium bicarbonate (1.70 g, 20.2 mmol, 2 equiv) were added, and the suspension stirred vigorously for 5 minutes at ambient temperature. The mixture was diluted with dichloromethane (80 mL), the layers separated, and the organic phase dried on sodium sulfate. Filtration and concentration under vacuum provided the phosphorous ylide **62** as a yellow solid (2.95 g, 6.58 mmol, 65%).

^{1}H NMR (600 MHz, $CDCl_3$): δ 7.72 – 7.38 (m, 15H), 4.29 (d, J = 26.1 Hz, 1H), 4.10 (s, 2H), 0.93 (s, 9H), 0.11 (s, 6H).

FTIR (neat), cm^{-1}: 3056 (w), 2593 (m), 2927 (m), 2854 (m), 1569 (s).

HRMS (ESI-TOF) m/z: $[M+H]^+$ Calcd for $C_{27}H_{34}O_2PSi$ 449.2060; Found 449.2061.

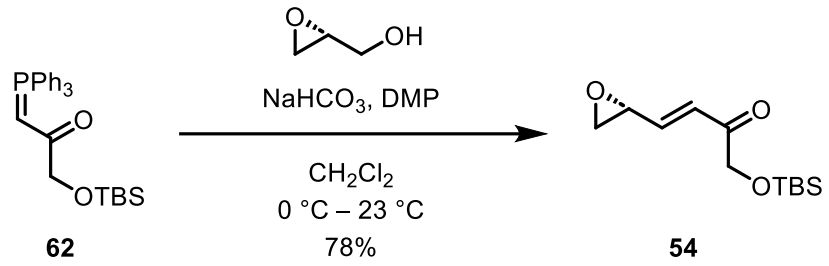

(*R,E*)-1-((*tert*-butyldimethylsilyl)oxy)-4-(oxiran-2-yl)but-3-en-2-one (54)

To a solution of *(R)*-glycidol (200 mL, 3.01 mmol, 1 equiv) in dichloromethane (16.7 mL) was added solid sodium bicarbonate (2.53 g, 30.1 mmol, 10 equiv) and the solution cooled to 0 °C. Dess-Martin periodinane (1.53 g, 3.61 mmol, 1.2 equiv) was added, the ice bath removed, and the solution stirred for 4 hours at ambient temperature. The solution was then diluted with an additional portion of dichloromethane (5.6 mL) and phosphorane **62** (1.76 g, 3.91 mmol, 1.3 equiv) was added, and the solution then stirred overnight. The solution was then cooled to 0 °C and a 1:1 mixture of saturated aqueous sodium thiosulfate:saturated aqueous sodium bicarbonate (totaling 50 mL) was added, and the solution then allowed to warm to room temperature over 30 minutes with stirring. The mixture was poured into a separatory funnel containing dichloromethane (100 mL), followed by vigorous extraction of the mixture into the dichloromethane portion. The separated aqueous phase was washed with an additional portion of dichloromethane (50 mL) and the combined organic layers washed with water (100 mL) and brine (100 mL). The organic phase was dried on sodium sulfate, filtered, and concentrated under vacuum to give crude material which was further purified by flash chromatography on silica gel grading from hexanes to 30% ethyl acetate in hexanes, affording epoxyenone **54** as a yellow oil (570 mg, 2.35 mmol, 78%).

R_f: (50% ethyl acetate in hexanes, $KMnO_4$): 0.66

^{1}H NMR (500 MHz, $CDCl_3$): δ 6.75 (d, J = 15.9 Hz, 1H), 6.62 (dd, J = 15.9, 7.2 Hz, 1H), 4.32 (s, 2H), 3.47 (ddd, J = 6.9, 4.1, 2.5 Hz, 1H), 3.07 (dd, J = 5.5, 4.2 Hz, 1H), 2.72 (dd, J = 5.6, 2.5 Hz, 1H), 0.92 (s, 9H), 0.09 (s, 6H).

$^{13}C\{^{1}H\}$ NMR (125 MHz, $CDCl_3$): δ 197.9, 143.8, 127.2, 68.9, 50.8, 49.6, 25.9, 18.5, -5.3.

HRMS (ESI-TOF) m/z: $[M+H]^+$ Calcd for $C_{12}H_{23}O_3Si$ 243.1411; Found 243.1412.

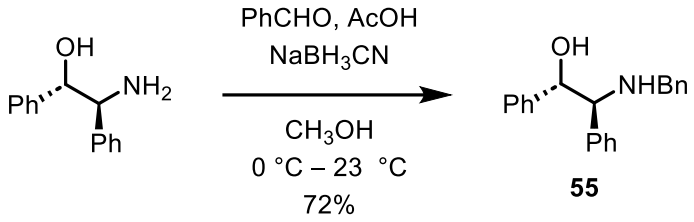

(*1S,2S*)-2-(benzylamino)-1,2-diphenylethan-1-ol (55)

To an oven-dried flask charged with a stir bar under Ar atmosphere was added (*1S,2S*)-2-amino-1,2-diphenylethan-1-ol (450 mg, 2.11 mmol, 1 equiv) and anhydrous methanol (23 mL). The solution was cooled to 0 °C, and acetic acid (5 drops), benzaldehyde (240 mL, 2.32 mmol, 1.1 equiv), and sodium cyanoborohydride (146 mg, 2.32 mmol, 1.1 equiv) were added in sequence. The mixture was allowed to warm to room temperature while stirring overnight. After 20 hours, LCMS indicated complete consumption of starting material and the solution was quenched with saturated aqueous sodium carbonate (50 mL). The mixture was extracted into ethyl acetate (200 mL), and the organic layer washed with saturated aqueous sodium carbonate (200 mL) and brine (200 mL). The organic layer was dried on sodium sulfate, filtered, and concentrated to provide the crude material, which was purified by flash chromatography on silica gel, grading from 5% – 10% methanol + 0.1% triethylamine in dichloromethane. The concentrated product fractions provided *N*-benzylated aminoalcohol **55** (458 mg, 2.11 mmol, 72%).

R_f: (10% methanol + 0.1% triethylamine in dichloromethane, $KMnO_4$): 0.50

^1H NMR (600 MHz, $CDCl_3$): δ 7.40 – 7.36 (m, 1H), 7.35 – 7.30 (m, 2H), 7.29 – 7.20 (m, 5H), 7.18 – 7.13 (m, 3H), 7.05 (m, 4H), 4.70 (s, 1H), 4.61 (d, J = 8.5 Hz, 1H), 3.73 (d, J = 13.0 Hz, 1H), 3.67 (d, J = 8.6 Hz, 1H), 3.58 (d, J = 13.0 Hz, 1H).

$^{13}C\{^1H\}$ NMR (125MHz, $CDCl_3$): δ 141.2, 139.8, 128.7, 128.6, 128.5, 128.4, 128.0, 127.9, 127.8, 127.7, 127.6, 127.3, 127.1, 127.0, 77.9, 69.8, 51.4.

HRMS (ESI-TOF) m/z: $[M+H]^+$ Calcd for $C_{21}H_{22}NO$ 304.1696; Found 304.1694.

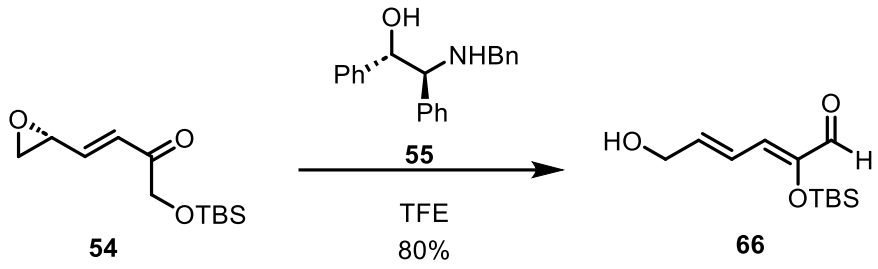

(2Z,4E)-2-((tert-butyldimethylsilyl)oxy)-6-hydroxyhexa-2,4-dienal (66)

A solution of epoxyenone **54** (5.00 mg, 21.0 µmol, 1 equiv) in trifluoroethanol (20 µL) was treated with a 1 M solution of **55** (12.4 mg, 41 µmol in 40 µL TFE, 2 equiv) at room temperature. The mixture was allowed to stir overnight and then concentrated. Purification by reverse phase HPLC, eluting from 5-95% acetonitrile in water over 40 minutes, gave aldehyde **66** (4.00 mg, 16.8 µmol, 80%).

^{1}H NMR (600 MHz, $CDCl_3$): δ 9.17 (s, 1H), 6.82 (ddt, J = 15.5, 11.0, 1.7 Hz, 1H), 6.24 – 6.15 (m, 2H), 4.30 (dd, J = 5.4, 1.7 Hz, 2H), 0.97 (s, 9H), 0.19 (s, 6H).

^{13}C{^{1}H} NMR (151MHz, $CDCl_3$): δ 188.80, 149.99, 138.50, 130.75, 123.95, 63.42, 25.97, 25.93, 18.80, -3.95.

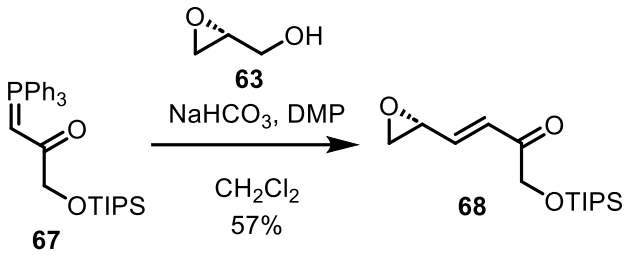

(*R*,*E*)-4-(oxiran-2-yl)-1-((triisopropylsilyl)oxy)but-3-en-2-one (68)

To a solution of (*R*)-glycidol **63** (10.0 mg, 0.135 mmol, 1 equiv) in DCM (750 µL) was added DMP (68.7 mg, 0.162 mmol, 1.2 equiv) at room temperature. The solution stirred vigorously for 1.5 hours and phosphorane **67** (prepared analogously to **62** from **60**, 70.0 mg, 0.143 mmol, 1.06 equiv) was added as a DCM (1.00 mL) solution. This mixture was stirred overnight at ambient conditions and quenched by addition of 50% saturated sodium bicarbonate solution/50% saturated sodium thiosulfate solution. After stirring for 10 minutes, the phases were separated and the aqueous washed with dichloromethane (3 x 7 mL). The combined organic layers were washed with saturated aqueous sodium bicarbonate (5 mL) and brine (5 mL), dried on sodium sulfate, filtered, and concentrated to give crude material. Purification by flash chromatography on silica gel, eluting with 5% ethyl acetate in hexanes, gave epoxy enone **68** as a yellow oil (22 mg, 0.077 mmol, 57%).

^{1}H NMR (600 MHz, $CDCl_3$): δ 6.89 (d, J = 15.8 Hz, 1H), 6.65 (ddd, J = 15.8, 7.4, 1.4 Hz, 1H), 4.36 (s, 2H), 3.54 – 3.36 (m, 1H), 3.08 (ddd, J = 5.6, 4.1, 1.3 Hz, 1H), 2.73 (dt, J = 5.5, 1.9 Hz, 1H), 1.19 – 1.11 (m, 3H), 1.07 (d, J = 7.3 Hz, 18H).

^{13}C{^{1}H} NMR (151MHz, $CDCl_3$): δ 198.3, 144.0, 127.1, 69.3, 50.9, 49.6, 18.0, 12.0.

FTIR (neat), cm^{-1}: 2943 (m), 2865 (m), 1698 (m), 1630 (m).

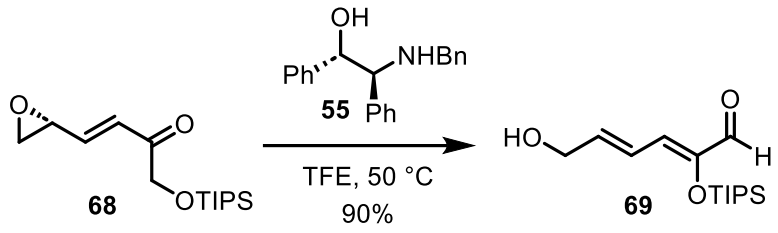

(*2Z,4E*)-6-hydroxy-2-((triisopropylsilyl)oxy)hexa-2,4-dienal (69)

A solution of **68** (10.0 mg, 0.035 mmol, 1 equiv) in trifluoroethanol (200 µL) was treated with **55** (10.7 mg, 0.035 mmol, 1 equiv) at room temperature. The mixture was allowed to stir overnight, and LC/MS monitoring indicated formation of a new product. The temperature was raised to 50 °C and stirring continued for another 18 hours (40 hours total). The reaction was halted by cooling, diluting with DCM (3 mL), and concentrated under reduced pressure. Purification by flash chromatography, grading from 0- 50% ethyl acetate in hexanes gave dienal **69** (9.00 mg, 0.032 mmol, 90%).

^{1}H NMR (400 MHz, $CDCl_3$): δ 9.19 (s, 1H), 6.98 – 6.75 (m, 1H), 6.30 – 6.06 (m, 2H), 4.35 – 4.26 (m, 2H), 1.34 – 1.23 (m, 3H), 1.07 (d, J = 7.5 Hz, 18H).

^{13}C{^{1}H} NMR (101MHz, $CDCl_3$): δ 188.7, 150.6, 138.1, 129.8, 124.2, 63.6, 29.9, 18.2, 13.8.

FTIR (neat), cm^{-1}: 3358 (br), 2923 (s), 2862 (s), 1685 (s), 1634 (m).

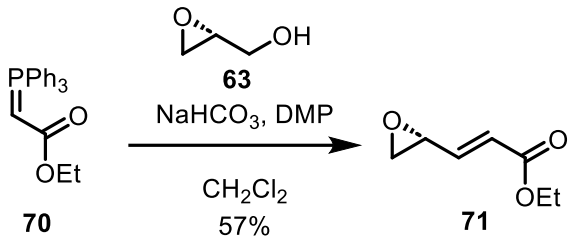

Ethyl (*R*,*E*)-3-(oxiran-2-yl)acrylate (71)

A solution of (*R*)-glycidol **63** (100.0 mg, 1.35 mmol, 1 equiv) and solid sodium bicarbonate (1.13 g, 13.5 mmol, 10 equiv) in DCM (7.5 mL) was treated with DMP (687 mg, 1.62 mmol, 1.2 equiv) at room temperature. The solution stirred vigorously for 2 hours and phosphorane **70** (611 mg, 1.76 mmol, 1.3 equiv) was added as a solid followed by additional DCM (2 mL). The solution stirred vigorously overnight and was quenched by addition of 50% saturated aqueous sodium bicarbonate/50% saturated aqueous sodium thiosulfate (20 mL). The mixture was stirred for 10 minutes, and the phases separated and diluted with additional DCM (25 mL). The aqueous layer was washed with an additional portion of DCM (25 mL) and the combined organic layers washed with saturated aqueous sodium bicarbonate (50 mL) and brine (50 mL). The organic phase was dried on sodium sulfate, filtered, and concentrated to give crude; purification was achieved by flash chromatography on silica gel, eluting with 5% ethyl acetate in hexanes to give **71** (109 mg, 0.769 mmol, 57%).

^{1}H NMR (500 MHz, $CDCl_3$): δ 6.62 (dd, J = 15.7, 7.4 Hz, 1H), 6.18 (d, J = 15.7 Hz, 1H), 4.20 (q, J = 7.1 Hz, 2H), 3.52 – 3.42 (m, 1H), 3.19 – 3.00 (m, 1H), 2.72 (dd, J = 5.5, 2.5 Hz, 1H), 1.29 (t, J = 7.1 Hz, 3H).

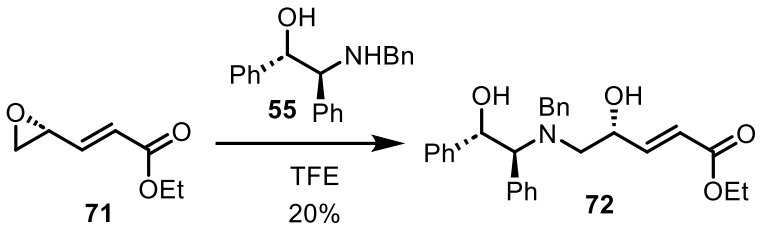

ethyl (*R,E*)-5-(benzyl((*1S,2S*)-2-hydroxy-1,2-diphenylethyl)amino)-4-hydroxypent-2-enoate (72)

A solution of epoxide **71** (20.0 mg, 0.141 mmol, 1 equiv) in trifluoroethanol (280 μL) at room temperature was treated with aminoalcohol **55** (42.7 mg, 0.141 mmol, 1 equiv) and the mixture stirred overnight at 50 °C. The solvent was removed under reduced pressure and the crude mixture was purified by HPLC, eluting from 5% to 95% acetonitrile in water (+0.1% formic acid) over 40 minutes, to yield tertiary amine **72** (13 mg, 0.029 mmol, 20%).

^{1}H NMR (400 MHz, $CDCl_3$): δ 7.51 – 7.29 (m, 5H), 7.24 – 6.99 (m, 10H), 6.83 (dd, J = 15.6, 4.8 Hz, 1H), 6.06 (dd, J = 15.7, 1.7 Hz, 1H), 5.15 (d, J = 10.3 Hz, 1H), 4.24 – 4.09 (m, 4H), 3.95 (d, J = 10.3 Hz, 1H), 3.26 (dd, J = 13.3, 1.6 Hz, 1H), 3.03 – 2.88 (m, 1H), 2.66 (dd, J = 13.9, 6.9 Hz, 1H), 1.47 – 0.86 (m, 3H).

^{13}C{^{1}H} NMR (101MHz, $CDCl_3$): δ 166.4, 148.1, 141.2, 138.9, 129.9, 129.2, 128.9, 128.3, 128.2, 128.0, 127.5, 121.5, 73.2, 72.6, 70.8, 60.6, 56.7, 55.8, 14.4.

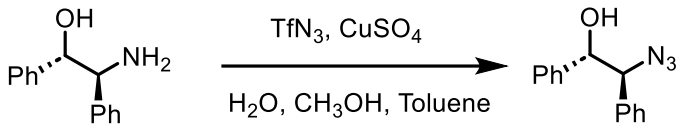

73

(*1S,2S*)-2-azido-1,2-diphenylethan-1-ol (73)

Preparation of TfN_3 (caution: triflic azide is explosive when neat. Readers are advised to only handle triflic azide as a solution in dichloromethane or preferably, toluene):

Sodium azide (1.341 g, 20.63 mmol, 4.4 equiv) was dissolved in water (3.4 mL) and stirred vigorously, then toluene (3.4 mL) was added, and the mixture cooled to 0 °C. Tf_2O (1.743 mL, 10.32 mmol, 2.2 equiv) was added dropwise to the biphasic mixture and stirred for 0.5 hours. After 0.5 hours, the reaction was warmed to room temperature and stirred for an additional 1.5 hours. The reaction was quenched with 2 mL of saturated aqueous $NaHCO_3$ solution, and the two phases were allowed to separate. The aqueous phase was extracted twice with toluene (3 mL) and the organic phases were all combined. The organic solution was adjusted to a final volume of 10.3 mL to yield a 1 M solution of triflic azide, which was used immediately without storage.

Diazo transfer:

(*1S,2S*)-2-amino-1,2-diphenylethan-1-ol (1.00 g, 4.69 mmol, 1 equiv) was added to water (6 mL) and cooled to 0 °C. Copper (II) sulfate pentahydrate (59 mg, 0.234 mmol, 0.05 equiv) and sodium bicarbonate (1.576 g, 18.75 mmol, 4 eq) were added. The mixture was then diluted with methanol (41 mL) and the prepared triflic azide solution (1 M in toluene, 10.3 mL, 10.32 mmol, 2.2 eq) was added. The mixture was allowed to warm to room temperature and stirred for 2.5 hours. The solution was then filtered and saturated NH_4Cl solution was added (5 mL); the volatiles were then evaporated. The remaining aqueous solution was extracted with diethyl ether (3x20 mL), washed with saturated Na_2CO_3 (2x 20 mL), brine (20 mL) and dried over Na_2SO_4. To concentrated crude

material was further purified by flash chromatography, grading from hexanes to 50% ethyl acetate in hexanes to give azido alcohol **73** as an oil (1.041 g, 4.35 mmol, 93%).

^{1}H NMR (400 MHz, $CDCl_3$): δ 7.28 – 7.23 (m, 3H), 7.21 (m, 3H), 7.09 (m, 4H), 4.75 (d, J = 7.9 Hz, 1H), 4.62 (d, J = 7.9 Hz, 1H), 2.74 (s, 1H).

$^{13}C\{^{1}H\}$ NMR (101MHz, $CDCl_3$): δ 139.36, 136.14, 128.66, 128.32, 128.29, 127.97, 127.01, 78.14, 73.08.

FTIR (neat), cm^{-1}: 3412 (br), 3066 (w), 3032 (m), 2103 (s).

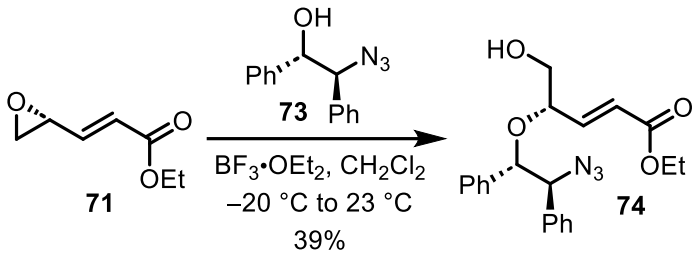

ethyl (*S,E*)-4-((*1S,2S*)-2-azido-1,2-diphenylethoxy)-5-hydroxypent-2-enoate (74)

A solution of epoxide **71** (20.0 mg, 0.141 mmol, 1 equiv) and azidoalcohol **73** (101 mg, 0.422 mmol, 3 equiv) in DCM (280 µL) was cooled to - 20 °C with a salt+ice bath and boron trifluoride diethyl etherate (36 µL, 0.281 mmol, 2 equiv). The ice bath was removed, and after warming to room temperature and stirring for an additional hour the reaction was quenched with addition of water. The aqueous was washed with ethyl acetate (5 mL), and the combined organics washed with sat. aq. sodium bicarbonate solution (5 mL) and brine (5 mL), dried on sodium sulfate, filtered, and concentrated to give crude material. Purification by flash chromatography on silica gel, grading from hexanes to 50% ethyl acetate in hexanes gave **74** (21 mg, 0.055 mmol, 39%).

^{1}H NMR (400 MHz, $CDCl_3$): δ 7.24 – 7.13 (m, 6H), 7.03 (m, 4H), 6.68 (dd, J = 15.7, 5.1 Hz, 1H), 5.97 (dd, J = 15.7, 1.8 Hz, 1H), 4.74 (d, J = 8.6 Hz, 1H), 4.58 (d, J = 8.5 Hz, 1H), 4.20 – 4.06 (m, 3H), 3.82 (d, J = 11.3 Hz, 1H), 3.67 (d, J = 11.7 Hz, 1H), 2.79 (s, 1H), 1.30 – 1.20 (m, 3H).

^{13}C{^{1}H} NMR (101MHz, $CDCl_3$): δ 166.02, 144.37, 137.48, 135.75, 128.63, 128.57, 128.34, 127.94, 127.71, 122.88, 85.94, 79.01, 71.73, 64.31, 60.58, 14.37, 14.31.

FTIR (neat), cm^{-1}: 3468 (br), 3063 (w), 3033 (w), 2982 (m), 2929 (m), 2102 (s), 1711 (s), 1657 (m).

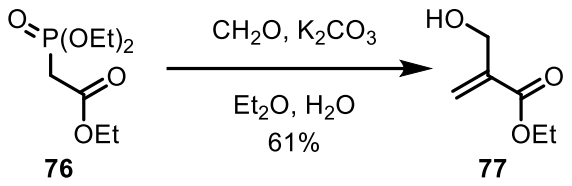

76 **77**

Ethyl 2-(hydroxymethyl)acrylate (77)

To a three-necked round bottom flask fitted with a condenser and thermometer was added paraformaldehyde (9.93 g, 331 mmol, 4.12 equiv), water (23.0 mL), and 1 N phosphoric acid (0.83 mL). The cloudy solution was heated to 90 °C and stirred vigorously for 2.5 hours to form a clear solution. The solution was cooled to room temperature and triethyl phosphonoacetate **76** (18.0 g, 80.0 mmol, 1 equiv) was added. An aqueous solution of potassium carbonate (12.54 g, 91 mmol, 1.13 equiv in 12.4 mL water) was added dropwise by syringe pump over 1 hour. During this time, the reaction temperature remained between 30–40 °C. Following complete addition of the potassium carbonate solution, the reaction was stirred for 5 minutes between 35–40 °C, cooled to 0 °C by ice bath, and then diethyl ether (40 mL) and brine (30 mL) were added. The aqueous layer was extracted with diethyl ether (3 x 20 mL) and the combined organics were washed with brine (2 x 20 mL), dried on magnesium sulfate, filtered, and concentrated to provide a clear liquid. The residue was distilled (150 °C at 10 torr) to afford **77** as a clear liquid (6.35 g, 48.8 mmol, 61%).

R_f: (33% ethyl acetate in hexanes, $KMnO_4$): 0.30

^1H NMR (400 MHz, $CDCl_3$): δ 6.25 (d, J = 0.9 Hz, 1H), 5.82 (d, J = 1.4 Hz, 1H), 4.32 (dd, J = 1.4, 0.8 Hz, 2H), 4.24 (q, J = 7.2 Hz, 2H), 2.29 (s, 1H), 1.31 (t, J = 7.1 Hz, 3H).

$^{13}C\{^1H\}$ NMR (101 MHz, $CDCl_3$): δ 166.50, 139.67, 125.73, 62.72, 61.02, 14.29.

FTIR (neat), cm^{-1}: 3434 (br), 2984 (m), 2909 (w), 2869 (w), 1707 (s), 1637 (m).

HRMS (ESI-TOF) m/z: $[M+H]^+$ Calcd for $C_6H_{11}O_3$ 131.0703; Found 131.0703.

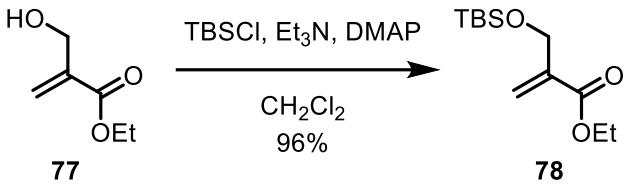

Ethyl 2-(((*tert*-butyldimethylsilyl)oxy)methyl)acrylate (78)

To a solution of **77** (1.63 g, 12.52 mmol, 1 equiv) in anhydrous dichloromethane (25.1 mL) under Ar atmosphere at 0 °C was sequentially added TBSCl (2.26 g, 15.03 mmol, 1.4 equiv), triethylamine (5.24 mL, 37.6 mmol, 3 equiv), and DMAP (153 mg, 1.25 mmol, 0.1 equiv). Solution was stirred at 0 °C for 40 minutes then allowed to stir at room temperature for 4 hours before an additional TBSCl portion (380 mg, 2.52 mmol, 0.2 equiv) was added. The solution was stirred overnight at ambient conditions and diluted then dichloromethane (30 mL). The organic layer was washed with 1 N hydrochloric acid (20 mL), saturated aqueous sodium bicarbonate (20 mL), and brine (20 mL). The organic layer was dried on magnesium sulfate, filtered, and concentrated to give a yellow liquid, which was further purified by flash chromatography on silica gel, eluting with a gradient from hexanes to 1% ethyl acetate in hexanes. Product containing fractions were combined and concentrated to give silyl ether **78** as a clear oil (2.94 g, 12.0 mmol, 96%).

R_f: (10% Ethyl acetate in hexanes, CAM): 0.78

^{1}H NMR (400 MHz, $CDCl_3$): δ 6.25 (q, J = 2.0 Hz, 1H), 5.90 (q, J = 2.1 Hz, 1H), 4.37 (t, J = 2.1 Hz, 2H), 4.21 (q, J = 7.1 Hz, 2H), 1.30 (t, J = 7.1 Hz, 3H), 0.92 (s, 9H), 0.09 (s, 6H).

^{13}C{^{1}H} NMR (101 MHz, $CDCl_3$): δ 165.98, 139.92, 123.57, 61.51, 60.51, 25.88, 18.35, 14.22, -5.43.

FTIR (neat), cm^{-1}: 2956 (m), 2930 (m), 2886 (w), 2858 (m), 1714 (s).

HRMS (ESI-TOF) m/z: $[M+H]^+$ Calcd for $C_{12}H_{25}O_3Si$ 245.1567; Found 245.1571.

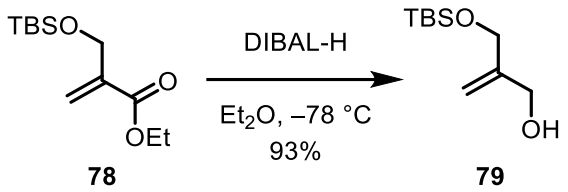

78 79

2-(((*tert*-butyldimethylsilyl)oxy)methyl)prop-2-en-1-ol (79)

In a flame-dried flask charged with a stir bar under Ar atmosphere, a solution of **78** (376 mg, 1.54 mmol, 1 equiv) in diethyl ether (10.3 mL) was cooled to -78 °C and diisobutyl aluminum hydride solution (25% w/w in toluene, 3.33 mL, 4.62 mmol, 3 equiv) was added dropwise over 10 minutes. The reaction was stirred for 2 hours at this temperature then quenched by the addition of Rochelle's salt solution (10 mL) and further diluted with ethyl acetate (8 mL). The quenched mixture stirred vigorously at room temperature until two distinct layers formed, after which the organic layer was separated and the aqueous extracted further with ethyl acetate (2 x 3 mL). The combined organic layers were washed with brine (8 mL), dried on magnesium sulfate, filtered, and concentrated to yield allylic alcohol **79** as a clear liquid, sufficiently pure without the need for chromatography (290 mg, 1.44 mmol, 93%).

R_f: (20% ethyl acetate in hexanes, $KMnO_4$): 0.40

^1H NMR (400 MHz, $CDCl_3$): δ 5.16 – 4.85 (m, 2H), 4.23 (s, 2H), 4.16 (d, J = 1.2 Hz, 2H), 2.12 (s, 1H), 0.91 (s, 9H), 0.08 (s, 6H).

$^{13}C\{^1H\}$ NMR (101 MHz, $CDCl_3$): δ 147.59, 111.20, 65.21, 64.75, 25.99, 18.42, -5.30.

FTIR (neat), cm^{-1}: 3344 (br), 2954 (m), 2929 (m), 2857 (m), 1658 (w).

HRMS (ESI-TOF) m/z: $[M+H]^+$ Calcd for $C_{10}H_{23}O_2Si$ 203.1462; Found 203.1464.

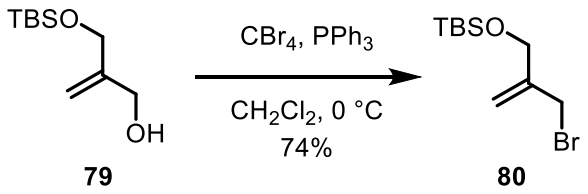

79 **80**

((2-(bromomethyl)allyl)oxy)(*tert*-butyl)dimethylsilane (80)

To a solution of alcohol **79** (994 mg, 4.91 mmol, 1 equiv) in anhydrous dichloromethane (16.4 mL) at 0 °C was added carbon tetrabromide (2.44 g, 7.37 mmol, 1.5 equiv) and triphenylphosphine (1.55 g, 5.89 mmol, 1.2 equiv), sequentially. The reaction was stirred at 0 °C for 40 minutes then quenched by the slow addition of saturated aqueous sodium bicarbonate solution (6 mL) and warmed to room temperature. The phases were separated and the aqueous washed with ethyl acetate (3 x 6 mL). The combined organic layers were washed with brine (10 mL), dried on magnesium sulfate, filtered, and concentrated. The concentrated crude residue was further purified by flash chromatography on silica gel, grading from hexanes to 1% ethyl acetate in hexanes to provide allylic bromide **80** as a clear oil (960 mg, 3.62 mmol, 74%).

R_f: (10% ethyl acetate in hexanes, $KMnO_4$): 0.93

^1H NMR (400 MHz, $CDCl_3$): δ 5.25 (q, J = 1.0 Hz, 1H), 5.24 (q, J = 1.5 Hz, 1H), 4.27 (t, J = 1.3 Hz, 2H), 4.01 (d, J = 0.7 Hz, 2H), 0.92 (s, 9H), 0.10 (s, 6H).

$^{13}C\{^1H\}$ NMR (101 MHz, $CDCl_3$): δ 144.98, 114.97, 63.63, 32.96, 26.03, 18.50, -5.25.

FTIR (neat), cm^{-1}: 2954 (m), 2929 (m), 2884 (w), 2857 (m), 1715 (w).

HRMS (ESI-TOF) m/z: $[M+H]^+$ Calcd for $C_{10}H_{22}BrOSi$ 265.0618; Found 265.0622.

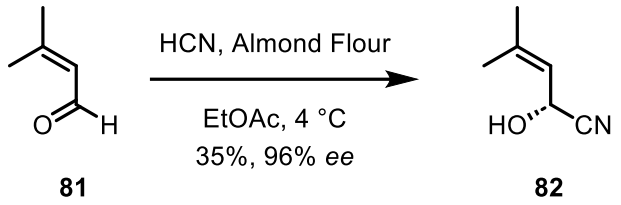

81 **82**

(*R*)-2-hydroxy-4-methylpent-3-enenitrile (82)

Preparation of HCN solution: A solution of sodium cyanide (8.74 g, 178 mmol, 1.5 equiv) in water (300 mL) was treated with acetic acid dropwise until a pH of 5.5 was reached (pH paper). The aqueous solution of hydrogen cyanide was extracted into ethyl acetate (400 mL), and this solution added directly to the swollen flour mixture containing aldehyde as described below.

Flour preparation and cyanation: Commercial almond flour (Whole Foods' Bob's Red Mill, 30 g) was defatted by washing on a paper filter with ethyl acetate until a dripping volume of 500 mL filtrate had been reached. The flour was air dried in the fume hood for 4 hours, then transferred to a round-bottomed flask containing a stir bar (Note: at this stage the mass of almond flour was now reduced to 17 g from defatting). A solution of pH 5.5 citrate buffer (0.02 M) was added, and the flour allowed to swell for 20 minutes at room temperature. To this mixture, 3-methyl-but-2-enal **81** (10.0 g, 119 mmol, 1 equiv) was added, followed by the previously prepared HCN solution, and the reaction transferred to a cold room at 4 °C where it stirred for 3 days. The solution was then filtered through a pad of Celite®, dried on sodium sulfate, filtered once more, and concentrated to yield crude residue. The crude material was purified by flash chromatography on silica, grading from 10% ethyl acetate to 50% ethyl acetate in hexanes to provide cyanohydrin **82** as a yellow oil (4.6 g, 41.4 mmol, 35%, 96% *ee* by Mosher's ester)

R_f: (25% Ethyl acetate in hexanes, $KMnO_4$): 0.43

^{1}H NMR (400 MHz, $CDCl_3$): δ 5.39 (dtd, J = 8.6, 2.8, 1.5 Hz, 1H), 5.11 (dd, J = 8.7, 2.0 Hz, 1H), 1.80 (t, J = 1.9 Hz, 3H), 1.75 (dd, J = 2.8, 1.5 Hz, 3H).

$^{13}C\{^{1}H\}$ NMR (101 MHz, $CDCl_3$): δ 142.04, 119.55, 119.52, 58.01, 25.67, 18.49.

FTIR (neat), cm^{-1}: 3415 (br), 2978 (m), 2918 (m), 1675 (m).

HRMS (ESI-TOF) m/z: $[M+H]^+$ Calcd for $C_6H_{10}NO$ 112.0757; Found 112.0755.

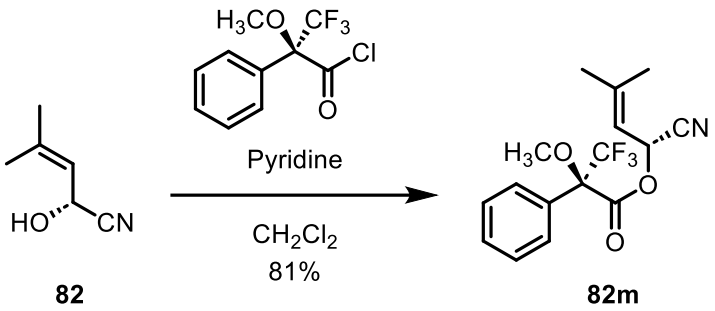

(*R*)-1-cyano-3-methylbut-2-en-1-yl (*R*)-3,3,3-trifluoro-2-methoxy-2-phenylpropanoate (82m)

To a flame-dried flask charged with a stir bar under Ar atmosphere was transferred a solution of cyanohydrin **82** (10 mg, 0.09 mmol, 1 equiv) in dichloromethane (800 mL). Sequentially, pyridine (22 mL, 0.27 mmol, 3 equiv) and (*S*)-Mosher's acid chloride (32 mL, 0.17 mmol, 1.9 equiv) and the reaction allowed to stir at ambient temperature while monitoring by TLC. After 2 hours, the reaction was partitioned between diethyl ether and water (5 mL), the aqueous layer extracted with additional ether (3 x 3 mL), and the combined organic phases dried on sodium sulfate. Filtration, concentration under vacuum, and purification of the resulting residue by flash chromatography on silica, eluting with 10% ethyl acetate in hexanes, yielded mosher ester **82m** as a clear oil (24 mg, 0.073 mmol, 81%). Analysis of the ^{19}F NMR determined the *ee* of the starting material to be 96%. ^{1}H NMR (400 MHz, $CDCl_3$): δ 7.47 (m, 2H), 7.44 – 7.39 (m, 3H), 6.16 (d, J = 9.1 Hz, 1H), 5.47 – 5.24 (m, 1H), 3.58 (s, 3H), 1.80 (d, J = 1.5 Hz, 3H), 1.77 (d, J = 1.4 Hz, 3H).

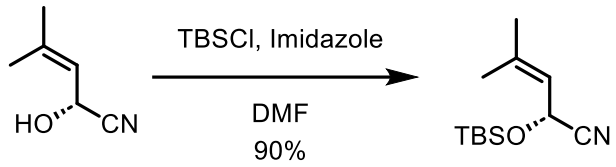

82 **83**

(*R*)-2-((*tert*-butyldimethylsilyl)oxy)-4-methylpent-3-enenitrile (83)

A solution of cyanohydrin **82** (205 mg, 1.84 mmol, 1 equiv) in anhydrous DMF (6.00 mL) was transferred to a flame-dried flask charged with a stir bar under Ar atmosphere. Imidazole (377 mg, 5.53 mmol, 3 equiv) and TBSCl (361 mg, 2.40 mmol, 1.3 equiv) were added sequentially, and the solution stirred overnight at ambient temperature. The reaction was quenched by the addition of water, stirred for 15 minutes, and then poured onto diethyl ether (10 mL). The separated aqueous layer was washed with additional ether (2 x 5 mL) and the combined ether layers washed with 10% w/w aqueous lithium chloride solution (3 x 10 mL), water (10 mL), and lastly brine (10 mL). The organic phase was dried on sodium sulfate, filtered, and concentrated; purification by flash chromatography on silica, grading from hexanes to 10% ethyl acetate in hexanes, provided the silylated cyanohydrin **83** as a clear oil (374 mg, 1.66 mmol, 90%). *Product may be volatile, use caution when drying under high vacuum*.

R_f: (25% Ethyl acetate in hexanes, $KMnO_4$): 0.86

^{1}H NMR (400 MHz, $CDCl_3$): δ 5.33 (dq, J = 8.4, 1.4 Hz, 1H), 5.08 (d, J = 8.4 Hz, 1H), 1.77 (s, 3H), 1.72 (t, J = 1.1 Hz, 3H), 0.90 (d, J = 1.0 Hz, 9H), 0.16 (s, 3H), 0.13 (s, 3H).

^{13}C{^{1}H} NMR (101 MHz, $CDCl_3$): δ 139.12, 121.31, 119.64, 59.12, 25.67, 18.51, 18.22, -4.80, -4.83.

FTIR (neat), cm^{-1}: 2955 (m), 2930 (m), 2858 (m), 1673 (w).

HRMS (ESI-TOF) m/z: $[M+H]^+$ Calcd for $C_{12}H_{24}NOSi$ 226.1622; Found 226.1619.

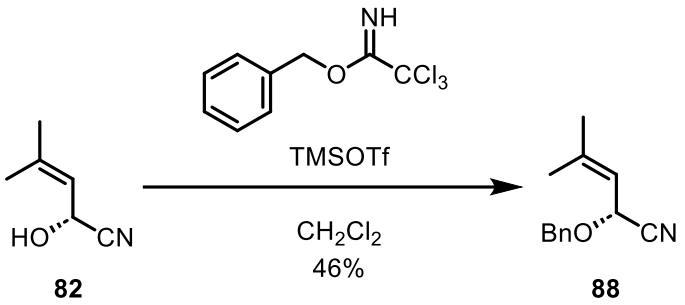

82 **88**

(*R*)-2-(benzyloxy)-4-methylpent-3-enenitrile (88)

To a flame-dried flask charged with a stir bar under Ar atmosphere was added cyanohydrin **82** (205 mg, 1.84 mmol, 1 equiv), benzyl trichloroacetimidate (685 mL, 3.69 mmol, 2 equiv) and anhydrous dichloromethane (18 mL). The solution was cooled to 0 °C, and trimethylsilyl trifluoromethanesulfonate (67 mL, 0.37 mmol, 0.2 equiv) was added dropwise. The ice bath was removed, allowing the reaction to warm to room temperature, and stirred overnight. The reaction was quenched after 20 hours by addition of water (18 mL). The mixture was poured onto 50% saturated aqueous sodium bicarbonate solution (100 mL) and following vigorous shaking the organic layer separated. The aqueous layer was extracted with dichloromethane (3 x 50 mL), and the combined organic layers dried on magnesium sulfate, filtered, and concentrated. Purification by flash chromatography on silica, eluting with 2.5% ethyl acetate in hexanes, afforded benzylated cyanohydrin **83** as an oil (170 mg, 0.845 mmol, 46%).

R_f: (25% Ethyl acetate in hexanes, $KMnO_4$): 0.74

^1H NMR (400 MHz, $CDCl_3$): δ 7.30 – 7.22 (m, 6H), 5.29 (ddt, J = 7.2, 3.0, 1.5 Hz, 1H), 4.71 – 4.65 (m, 2H), 4.49 – 4.44 (m, 2H), 1.69 (d, J = 1.5 Hz, 3H), 1.53 (d, J = 1.4 Hz, 3H).

$^{13}C\{^1H\}$ NMR (101 MHz, $CDCl_3$): δ 142.57, 136.12, 128.81, 128.60, 128.55, 128.48, 127.93, 117.76, 71.42, 64.04, 25.76, 18.59.

FTIR (neat), cm^{-1}: 3022 (w), 2916 (m), 1766 (m).

HRMS (ESI-TOF) m/z: $[M+H]^+$ Calcd for $C_{13}H_{16}NO$ 202.1226; Found 202.1223.

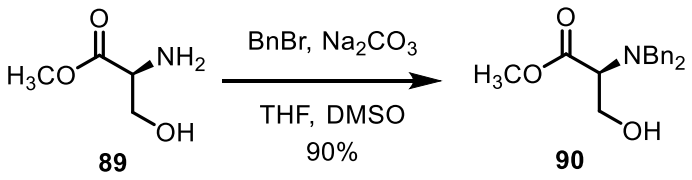

Methyl dibenzyl-*L*-serinate (90)

To a suspension of **89** (100 mg, 0.642 mmol, 1 equiv) in THF (1.60 mL) and DMSO (400 µL) was added benzyl bromide (230 µL, 1.93 mmol, 3 equiv) and sodium carbonate (273 mg, 2.57 mmol, 4 equiv) in sequence. The mixture was stirred vigorously and brought to 60 °C and maintained at this temperature for 24 hours. After cooling, the mixture was diluted with water (20 mL), the aqueous separated and further washed with diethyl ether (3 x 10 mL). The combined organics were washed with brine (12 mL), dried over magnesium sulfate, filtered, and concentrated to give the crude material. Purification by flash chromatography, eluting with 15% ethyl acetate in hexanes, gave **90** as a colorless oil (173 mg, 0.578 mmol, 90%).

^{1}H NMR (400 MHz, $CDCl_3$): δ 7.31 – 7.26 (m, 4H), 7.25 – 7.17 (m, 6H), 3.86 (d, J = 13.5 Hz, 2H), 3.74 (s, 3H), 3.70 (dd, J = 7.5, 2.7 Hz, 2H), 3.63 (d, J = 13.4 Hz, 2H), 3.51 (dd, J = 8.0, 7.0 Hz, 1H).

^{13}C{^{1}H} NMR (101 MHz, $CDCl_3$): δ 171.85, 138.78, 129.10, 128.65, 128.62, 127.54, 127.04, 65.36, 61.90, 59.46, 54.93, 51.56.

FTIR (neat), cm^{-1}: 3436 (br), 3028 (m), 2950 (m), 1728 (s).

HRMS (ESI-TOF) m/z: $[M+H]^+$ Calcd for $C_{18}H_{22}NO_3$ 300.1594; Found 300.1600.

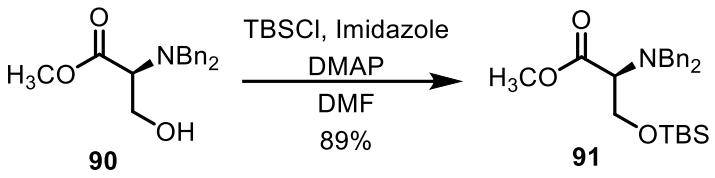

methyl *N,N*-dibenzyl-O-(*tert*-butyldimethylsilyl)-*L*-serinate (91)

A solution of alcohol **90** (1.74 g, 5.81 mmol, 1 equiv) in DMF (19.4 mL) was treated with TBSCl (1.14 g, 7.56 mmol, 1.30 equiv), imidazole (0.594 g, 8.72 mmol, 1.50 equiv), and DMAP (0.071 g, 0.581 mmol, 0.10 equiv) at room temperature sequentially. The reaction was stirred for 19 hours and diluted with ethyl acetate (60 mL). The solution was washed with 1 N HCl (3 x 20 mL) and brine (20 mL), then dried on magnesium sulfate. Filtration, concentration, and purification via flash chromatography on silica gel, eluting with 3% ethyl acetate in hexanes, gave **91** as a colorless oil (2.14 g, 5.17 mmol, 89%).

^{1}H NMR (400 MHz, $CDCl_3$): δ 7.42 – 7.37 (m, 4H), 7.34 – 7.27 (m, 4H), 7.25 – 7.19 (m, 2H), 3.99 (dd, J = 10.2, 6.5 Hz, 1H), 3.94 (d, J = 14.3 Hz, 2H), 3.88 (dd, J = 10.1, 6.0 Hz, 1H), 3.75 (s, 3H), 3.68 (d, J = 14.1 Hz, 2H), 3.55 (t, J = 6.1 Hz, 1H), 0.85 (s, 9H), -0.01 (s, 6H).

^{13}C{^{1}H} NMR (101 MHz, $CDCl_3$): δ 172.18, 140.02, 128.84, 128.33, 127.04, 63.14, 62.84, 55.59, 51.22, 25.91, 18.28, -5.45, -5.50.

FTIR (neat), cm^{-1}: 3028 (w), 2951 (m), 2942 (m), 2855 (m), 1734 (s).

HRMS (ESI-TOF) m/z: $[M+H]^+$ Calcd for $C_{24}H_{36}NO_3Si$ 414.2459; Found 414.2462.

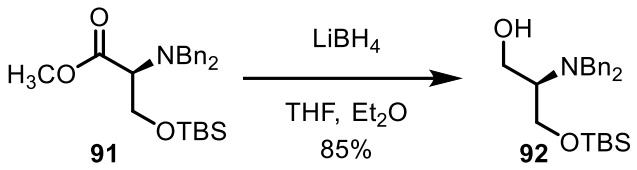

(*R*)-3-((*tert*-butyldimethylsilyl)oxy)-2-(dibenzylamino)propan-1-ol (92)

A solution of **91** (1.077 g, 2.60 mmol, 1 equiv) in diethyl ether (17.4 mL) was cooled to 0 °C and treated with lithium borohydride (252 mg, 10.42 mmol, 4 equiv) and methanol (420 µL) sequentially. After 10 minutes, the ice bath was removed, and the solution stirred at ambient conditions for 3 hours. The reaction was quenched by the addition of saturated aqueous ammonium chloride (15 mL), and the aqueous layer extracted with ethyl acetate (3 x 5 mL). The combined organic phases were washed with brine (10 mL), dried on magnesium sulfate, filtered, and concentrated. The crude material was purified by flash chromatography on silica gel, grading from hexanes to 5% ethyl acetate in hexanes, to give **92** as a clear oil (0.850 mg, 2.20 mmol, 85%).

^{1}H NMR (400 MHz, $CDCl_3$): δ 7.35 – 7.27 (m, 8H), 7.25 – 7.22 (m, 2H), 3.90 (d, J = 13.4 Hz, 2H), 3.86 (dd, J = 10.6, 6.1 Hz, 1H), 3.74 (dd, J = 10.6, 5.8 Hz, 1H), 3.66 (d, J = 13.4 Hz, 2H), 3.61 – 3.51 (m, 2H), 3.01 (dq, J = 9.0, 5.8 Hz, 1H), 2.90 (s, 9H), 0.09 (s, 3H), 0.09 (s, 3H).

^{13}C{^{1}H} NMR (101 MHz, $CDCl_3$): δ 139.77, 129.10, 128.57, 127.28, 61.05, 59.93, 59.73, 54.24, 26.03, 18.29, -5.38, -5.42.

FTIR (neat), cm^{-1}: 3449 (br), 3028 (w), 2952 (m), 2927 (m), 2855 (m).

HRMS (ESI-TOF) m/z: $[M+H]^+$ Calcd for $C_{23}H_{36}NO_2Si$ 386.2510; Found 386.2512.

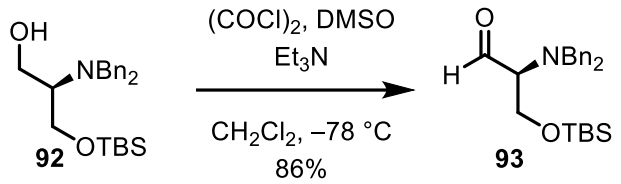

(*S*)-3-((*tert*-butyldimethylsilyl)oxy)-2-(dibenzylamino)propanal (93)

A solution of oxalyl chloride (2.0 M in DCM, 260 µL, 0.519 mmol, 2 equiv) in dichloromethane (1.0 mL) was cooled to - 78 °C and DMSO (81 µL, 1.14 mmol, 4.4 equiv) was added dropwise. This solution was stirred for 10 minutes, and alcohol **92** (100 mg, 0.259 mmol, 1 equiv) as a DCM solution (1.4 mL) was added dropwise over 2 minutes. After stirring an additional 18 minutes, triethylamine (325 µL, 2.33 mmol, 9 equiv) was added. The resulting solution was stirred 25 minutes, removed from the cooling bath, and diluted with water (5 mL). The organic layer was separated and the aqueous washed with dichloromethane (3 x 2 mL). The combined organic layers were washed with dilute aqueous HCl solution (3 mL), water (3 mL), saturated aqueous sodium bicarbonate (3 mL), and brine (2 x 3 mL). The organics were dried on magnesium sulfate, filtered, and concentrated to give a crude film, which was diluted in hexanes and minimal ethyl acetate and then passed through a plug of cotton to give aldehyde **93** after concentration as a yellow oil (85.6 mg, 0.223 mmol, 86%).

^{1}H NMR (400 MHz, $CDCl_3$): δ 9.73 (s, 1H), 7.40 (d, J = 6.9 Hz, 4H), 7.36 – 7.29 (m, 4H), 7.27 – 7.21 (m, 2H), 4.05 (dd, J = 5.7, 1.3 Hz, 2H), 3.89 (d, J = 3.1 Hz, 4H), 3.39 (t, J = 5.7 Hz, 1H), 0.91 (s, 9H), 0.09 (s, 3H), 0.08 (s, 3H).

FTIR (neat), cm^{-1}: 3028 (w), 2927 (m), 2855 (m), 1720 (m).

HRMS (ESI-TOF) m/z: $[M+H]^+$ Calcd for $C_{23}H_{34}NO_2Si$ 384.2353; Found 384.2356.

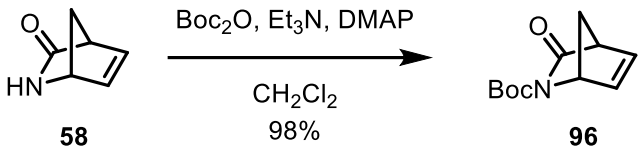

***tert*-butyl (*1R,4S*)-3-oxo-2-azabicyclo[2.2.1]hept-5-ene-2-carboxylate (96)**

In a flame-dried flask charged with a stir bar under an Ar atmosphere (*1R,4S*)-2-azabicyclo[2.2.1]hept-5-en-3-one **58** (500 mg, 4.58 mmol, 1 equiv) was combined with triethylamine (702 mL, 5.04 mmol, 1.1 equiv), DMAP (5.6 mg, 0.046 mmol, 0.01 equiv), and dichloromethane (4.6 mL). The solution was cooled to 0 °C, and solid Boc-anhydride (1.10 g, 5.04 mmol, 1.1 equiv) was added in portions. The cooling bath was removed, and the solution stirred at ambient temperature for 24 hours, then poured onto water (20 mL). The aqueous layer was washed with dichloromethane (3 x 15 mL) and the combined organic phases dried on magnesium sulfate, filtered, and concentrated to produce crude material. Purification by flash chromatography on silica, grading from hexanes to 15% ethyl acetate in hexanes, provided *N*-Boc Vince's lactam **96** as a white solid (935 mg, 4.47 mmol, 98%).

R_f: (25% Ethyl acetate in hexanes, $KMnO_4$): 0.36

^{1}H NMR (400 MHz, $CDCl_3$): δ 6.88 (dd, J = 5.4, 2.2 Hz, 1H), 6.65 (ddd, J = 5.0, 3.2, 1.5 Hz, 1H), 4.94 (d, J = 2.2 Hz, 1H), 3.37 (ddt, J = 3.2, 1.6, 0.8 Hz, 1H), 2.34 (dt, J = 8.5, 1.6 Hz, 1H), 2.14 (dt, J = 8.5, 1.5 Hz, 1H), 1.49 (s, 9H).

$^{13}C\{^1H\}$ NMR (101 MHz, $CDCl_3$): δ 176.36, 150.53, 140.15, 138.34, 82.73, 62.52, 55.05, 54.57, 28.17.

FTIR (neat), cm^{-1}: 2980 (m), 1789 (s), 1758 (s), 1703 (s).

HRMS (ESI-TOF) m/z: $[M+H]^+$ Calcd for $C_{11}H_{16}NO_3$ 210.1125; Found 210.1125.

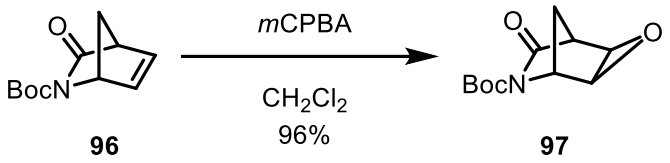

96 **97**

***tert*-butyl (*1S,4S,5R*)-7-oxo-3-oxa-6-azatricyclo[3.2.1.$0^{2,4}$]octane-6-carboxylate (97)**

In a flame-dried flask charged with a stir bar under an Ar atmosphere, a solution of *N*-Boc lactam **96** (311 mg, 1.49 mmol, 1 equiv) in anhydrous dichloromethane (12 mL) was treated with *meta*-chloroperbenzoic acid (75% w/w, 1.10 g, 4.78 mmol, 3.22 equiv) at room temperature. The solution stirred for 4 days and was then concentrated under vacuum, directly loaded onto a silica column, and purified by flash chromatography grading from 5–20% ethyl acetate in hexanes. Product containing fractions yielded a white solid **97** (323 mg, 1.43 mmol, 96%).

R_f: (25% Ethyl acetate in hexanes, $KMnO_4$): 0.37

^1H NMR (400 MHz, $CDCl_3$): δ 4.62 (t, J = 1.6 Hz, 1H), 3.78 (dd, J = 3.6, 1.3 Hz, 1H), 3.62 (dd, J = 3.6, 1.6 Hz, 1H), 3.19 – 2.94 (m, 1H), 1.82 (dt, J = 10.4, 1.7 Hz, 1H), 1.64 (dt, J = 10.4, 1.8 Hz, 1H), 1.53 (s, 9H).

$^{13}C\{^1H\}$ NMR (101 MHz, $CDCl_3$): δ 173.62, 149.89, 83.55, 59.10, 53.28, 50.15, 48.50, 28.20, 27.24.

FTIR (neat), cm^{-1}: 2981 (m), 1786 (s), 1766 (s), 1708 (s).

HRMS (ESI-TOF) m/z: $[M+Na]^+$ Calcd for $C_{11}H_{15}NO_4Na$ 248.0893; Found 248.0892.

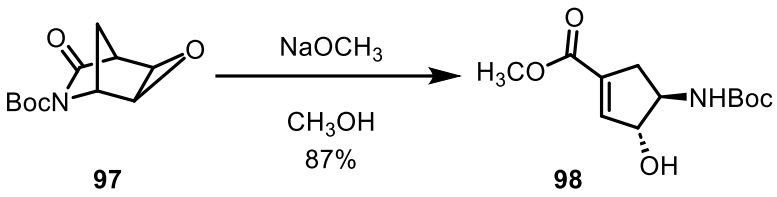

97 98

methyl (*3R,4R*)-4-((*tert*-butoxycarbonyl)amino)-3-hydroxycyclopent-1-ene-1-carboxylate (98)

Sodium methoxide (1 M in anhydrous methanol) was prepared immediately prior to use by transfer of solid sodium to a flame-dried flask under Ar, cooling the flask to 0 °C, and adding anhydrous methanol to create a 1 M solution (based on mass of sodium) after complete sodium dissolution. A solution of epoxy-lactam **97** (323 mg, 1.43 mmol, 1 equiv) in anhydrous methanol (14.3 mL) was treated with the freshly prepared sodium methoxide (1 M in methanol, 143 mL, 0.143 mmol, 0.1 equiv) at 0 °C. The consumption of **97** was monitored by TLC, and after complete consumption (1 hour), the ice bath was removed, and the reaction allowed to stir overnight at ambient temperature (the intermediate TLC spot disappears after stirring overnight and the appearance of the **98** as product on TLC is noted). The reaction was neutralized by addition of Amberlite™ CG50 (Type I) hydrogen form until the pH of solution measured less than 7 (pH paper). The mixture was poured onto a plug of Celite®, eluting with methanol (100 mL), and the concentrated residue purified by flash chromatography on silica gel, grading from hexanes to 20% ethyl acetate in hexanes, to afford hydroxyester **98** (320 mg, 1.24 mmol, 87%).

R_f: (25% Ethyl acetate in hexanes, $KMnO_4$): 0.18

^{1}H NMR (400 MHz, $CDCl_3$): δ 6.65 (q, J = 1.0 Hz, 1H), 4.92 (s, 1H), 4.82 (dq, J = 6.0, 2.1 Hz, 1H), 4.35 (s, 1H), 3.96 (tdd, J = 8.4, 5.8, 4.1 Hz, 1H), 3.76 (s, 3H), 3.05 (dddd, J = 16.0, 8.7, 2.2, 1.2 Hz, 1H), 2.32 (ddt, J = 15.9, 8.3, 2.2 Hz, 1H), 1.46 (s, 9H).

$^{13}C\{^{1}H\}$ NMR (101 MHz, $CDCl_3$): δ 164.92, 157.47, 142.63, 133.74, 83.86, 80.77, 61.22, 51.99, 35.95, 28.46.

FTIR (neat), cm^{-1}: 3366 (br), 2978 (m), 1685 (s), 1524 (m).

HRMS (ESI-TOF) m/z: $[M+Na]^+$ Calcd for $C_{12}H_{19}NO_5Na$ 280.1155; Found 280.1154.

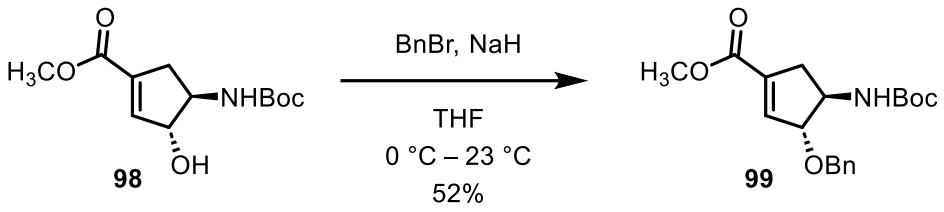

methyl (*3R,4R*)-3-(benzyloxy)-4-((*tert*-butoxycarbonyl)amino)cyclopent-1-ene-1-carboxylate (99)

A solution of alcohol **98** (303 mg, 1.18 mmol, 1 equiv) in anhydrous THF (2.36 mL) was cooled to 0 °C and benzyl bromide (560 mL, 4.71 mmol, 4 equiv) and then sodium hydride (60% w/w dispersion in mineral oil, 51.8 mg, 1.30 mmol, 1.1 equiv) were added in sequence while stirring. The ice bath was removed, the reaction monitored by TLC and quenched after 1 hour by the addition of saturated aqueous ammonium chloride solution at 0 °C. Once bubbling subsided, the mixture was partitioned between water (10 mL) and ethyl acetate (10 mL). The layers were separated, and the aqueous layer washed with ethyl acetate (2 x 10 mL). The combined organic layers were washed with brine (10 mL), dried on magnesium sulfate, filtered, and concentrated to give the crude. Purification was achieved by flash chromatography on silica, grading from hexanes to 15% ethyl acetate in hexanes to give product ether **99** (212 mg, 0.61 mmol, 52%).

R_f: (25% Ethyl acetate in hexanes, $KMnO_4$): 0.42

^1H NMR (400 MHz, $CDCl_3$): δ 7.38 – 7.27 (m, 5H), 6.67 (d, J = 2.0 Hz, 1H), 4.75 – 4.69 (m, 2H), 4.65 (d, J = 11.8 Hz, 1H), 4.51 (dd, J = 4.1, 2.0 Hz, 1H), 4.21 (s, 1H), 3.74 (s, 3H), 3.22 – 2.95 (m, 1H), 2.64 – 2.21 (m, 1H), 1.46 (s, 9H).

$^{13}C\{^1H\}$ NMR (101 MHz, $CDCl_3$): δ 164.93, 155.26, 139.59, 138.08, 137.36, 128.55, 128.04, 127.90, 88.44, 79.78, 71.65, 56.34, 51.90, 37.14, 28.50.

FTIR (neat), cm^{-1}: 2976 (m), 2866 (m), 1702 (s), 1686 (s), 1637 (w).

HRMS (ESI-TOF) m/z: $[M+Na]^+$ Calcd for $C_{19}H_{25}NO_5Na$ 370.1625; Found 370.1625.

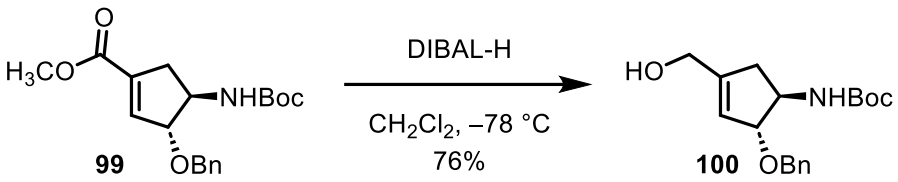

***tert*-butyl ((*1R,2R*)-2-(benzyloxy)-4-(hydroxymethyl)cyclopent-3-en-1-yl)carbamate (100)**

A solution of ester **99** (39.0 mg, 0.112 mmol, 1 equiv) in anhydrous dichloromethane (950 mL) was cooled to - 78 °C and diisobutyl aluminum hydride (25% w/w in toluene, 172 mL, 0.258 mmol, 2.3 equiv) was added dropwise. The solution stirred at this temperature while monitoring by TLC and quenched after 2 hours by the addition of Rochelle's salt solution (5 mL). The stirring mixture was allowed to warm to room temperature while vigorously stirring, and after the appearance of distinct layers, the phases were separated and the aqueous washed with dichloromethane (3 x 5 mL). The combined organic layers were washed with water (10 mL) and brine (10 mL), dried on sodium sulfate, filtered, and concentrated. Purification by flash chromatography on silica, grading from 20–50% ethyl acetate in hexanes to afford alcohol **100** as a white solid (27.4 mg, 0.086 mmol, 76%).

R_f: (50% Ethyl acetate in hexanes, $KMnO_4$): 0.26

^{1}H NMR (400 MHz, $CDCl_3$): δ 7.40 – 7.27 (m, 5H), 5.70 (q, J = 1.9 Hz, 1H), 4.72 (d, J = 11.1 Hz, 2H), 4.61 (d, J = 11.8 Hz, 1H), 4.37 (s, 1H), 4.24 – 4.08 (m, 3H), 2.90 (dd, J = 17.1, 7.6 Hz, 1H), 2.11 (dd, J = 17.1, 3.8 Hz, 1H), 1.83 (s, 9H).

^{13}C{^{1}H} NMR (101 MHz, $CDCl_3$): δ 155.42, 148.17, 138.46, 128.46, 128.12, 127.72, 123.51, 89.31, 79.59, 71.20, 61.64, 55.94, 38.41, 28.53.

FTIR (neat), cm^{-1}: 3325 (br), 2977 (m), 2860 (m), 1685 (s).

HRMS (ESI-TOF) m/z: $[M+H]^+$ Calcd for $C_{18}H_{26}NO_4$ 320.1856; Found 320.1856.

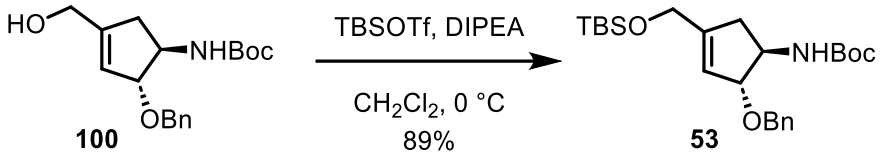

***tert*-butyl ((*1R,2R*)-2-(benzyloxy)-4-(((*tert*-butyldimethylsilyl)oxy)methyl)cyclopent-3-en-1-yl)carbamate (53)**

A solution of Allylic alcohol **100** (130 mg, 0.407 mmol, 1 equiv) in anhydrous dichloromethane (4.07 mL) was cooled to 0 °C and diisopropylethylamine (107 µL, 0.611 mmol, 1.5 equiv) was added. TBSOTf (112 µL, 0.488 mmol, 1.2 equiv) was added dropwise, and the consumption of starting material monitored by TLC. After 2 hours, the reaction was quenched by the addition of saturated aqueous sodium bicarbonate (6 mL), the cold bath removed, and the mixture stirred vigorously for 15 minutes while warming to room temperature. The phases were separated, and the aqueous layer washed with dichloromethane (2 x 6 mL). The combined organic layers were dried on magnesium sulfate, filtered, and concentrated to provide the crude material, which was further purified by flash chromatography on silica gel grading from hexanes to 30% ethyl acetate in hexanes, affording product **53** as a gum (157 mg, 0.362 mmol, 89%).

R_f: (10% Ethyl acetate in hexanes, $KMnO_4$): 0.37

^{1}H NMR (400 MHz, $CDCl_3$): δ 7.39 – 7.24 (m, 5H), 5.66 (d, J = 1.9 Hz, 1H), 4.83 – 4.55 (m, 3H), 4.35 (d, J = 2.4 Hz, 1H), 4.23 – 4.07 (m, 3H), 2.88 (dd, J = 17.6, 7.4 Hz, 1H), 2.18 – 1.96 (m, 1H), 1.46 (s, 9H), 0.90 (s, 9H), 0.06 (s, 6H).

$^{13}C\{^1H\}$ NMR (101 MHz, $CDCl_3$): δ 155.39, 148.08, 138.68, 128.47, 128.11, 127.67, 122.99, 89.47, 79.57, 71.09, 62.14, 55.98, 38.53, 28.56, 26.02, 18.47, -5.23, -5.28.

HRMS (ESI-TOF) m/z: $[M+H]^+$ Calcd for $C_{24}H_{40}NO_4Si$ 434.2722; Found 434.2724.

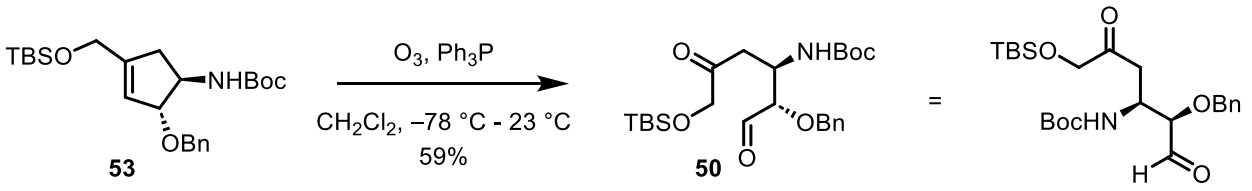

***tert*-butyl ((*2S,3R*)-2-(benzyloxy)-6-((*tert*-butyldimethylsilyl)oxy)-1,5-dioxohexan-3-yl)carbamate (50)**

A solution of silyl ether **53** (30 mg, 69 mmol, 1 equiv) in anhydrous dichloromethane (700 mL) was cooled to - 78 °C, and ozone was bubbled through the solution while stirring until the appearance of a light blue color. Immediately, the flask was relocated and the flask sparged with nitrogen gas to remove the excess ozone, noted by the disappearance of the blue tint of the solution. Thereafter, triphenylphosphine (35 mg, 0.13 mmol, 1.9 equiv) was added in one portion, and the solution stirred overnight while slowly warming to room temperature. After a total of 16 hours the solution was concentrated under vacuum and purification of the crude was performed by flash chromatography on silica gel, grading from 20–40% ethyl acetate in hexanes to give ketoaldehyde **50** (19 mg, 41 mmol, 59%) as a clear oil.

R_f: (25% Ethyl acetate in hexanes, $KMnO_4$): 0.20–0.40 (streaking)

^1H NMR (400 MHz, $CDCl_3$): δ 9.67 (s, 1H), 7.38 – 7.28 (m, 5H), 5.02 (d, J = 9.3 Hz, 1H), 4.80 (d, J = 11.6 Hz, 1H), 4.67 – 4.56 (m, 1H), 4.42 (d, J = 11.6 Hz, 1H), 4.11 (d, J = 2.8 Hz, 1H), 4.03 (s, 2H), 2.96 – 2.70 (m, 2H), 1.39 (s, 9H), 0.92 (s, 9H), 0.08 (s, 3H), 0.07 (s, 3H).

$^{13}C\{^1H\}$ NMR (101 MHz, $CDCl_3$): δ 209.20, 200.64, 155.14, 137.01, 128.73, 128.52, 128.45, 83.42, 80.12, 73.23, 69.34, 46.58, 39.95, 28.53, 28.37, 25.90, 18.37, -5.37, -5.42.

FTIR (neat), cm^{-1}: 2929 (m), 2857 (m), 1711 (s).

HRMS (ESI-TOF) m/z: $[M+H]^+$ Calcd for $C_{24}H_{40}NO_6Si$ 466.2619; Found 466.2612.

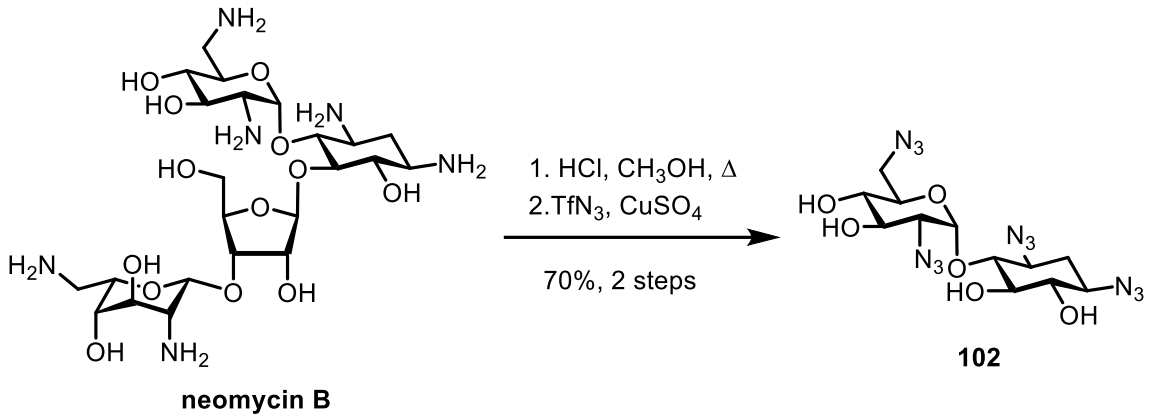

(*2R,3S,4R,5R,6R*)-5-azido-2-(azidomethyl)-6-(((*1R,2R,3S,4R,6S*)-4,6-diazido-2,3-dihydroxycyclohexyl)oxy)tetrahydro-*2H*-pyran-3,4-diol (102)

In a 1 L round-bottom flask, charged with neomycin B trisulfate salt hydrate (26.0 g, 35.1 mmol, 1 equiv) methanol (600 mL) and concentrated hydrochloric acid (55 mL) were added. The flask was fitted with a reflux condenser, and the solution stirred while brought to reflux where it remained overnight. The mixture was allowed to cool to room temperature, after which the solution was partially concentrated under rotary evaporation to approximately half volume. The remaining solution was placed in the refrigerator (- 20 °C) for 30 minutes, and the resulting precipitate was collected by vacuum filtration. Washing of the collected solids with chilled (0 °C) diethyl ether and drying under vacuum provided neamine tetrahydrochloride (13.3 g, 28.4 mmol, 99%), which was used without further purification.

Preparation of Trifluoromethanesulfonyl azide (**CAUTION: This reagent is known to be explosive when neat and should only be handled as a solution in dichloromethane or toluene):** A solution of sodium azide (44.0 g, 677 mmol, 24 equiv) in a 1:1 mixture of water and toluene (330 ml) was cooled to 0 °C and while vigorously stirring, trifluoromethanesulfonic anhydride (57.2 mL, 338 mmol, 12 equiv) was added dropwise by addition funnel. After complete addition,

the ice bath was removed, and the solution stirred for 2 hours at ambient temperature. The reaction was quenched by the addition saturated aqueous sodium bicarbonate until bubbling subsided. The phases were then separated, and the aqueous washed with toluene (165 mL). The combined organic phases furnish a nominally 1 M TfN_3 solution which was used immediately.

Diazotransfer to neamine tetrahydrochloride:

A solution of neamine tetrahydrochloride (13.2 g, 28.2 mmol, 1 equiv) was dissolved in water (300 mL) and methanol (1.00 L) a solution copper (II) sulfate pentahydrate (704 mg, 2.82 mmol, 0.1 equiv) in 4:3:3 triethylamine:water:methanol (100 mL) was added. Lastly the freshly prepared TfN_3 solution was added dropwise while vigorously stirring. The solution became a dark blue color, and over 4 hours while stirring at room temperature assumed a green tint. Solid sodium bicarbonate (13.0 g) was added, and the solution stirred for an additional 10 minutes. The volatiles were removed under vacuum, and the remaining aqueous residue was washed with ethyl acetate (3 x 200 mL). The combined organic phases were washed with saturated aqueous sodium carbonate (2 x 300 mL). The concentrated crude material was purified by flash chromatography on silica gel, grading from 30–85% to afford tetraazidoneamine **102** as a white solid (8.50 g, 19.9 mmol, 71%, 70% over 2 steps).

R_f: (66% Ethyl acetate in hexanes, $KMnO_4$): 0.56

^{1}H NMR (400 MHz, CD_3OD): δ 5.65 (d, J = 3.8 Hz, 1H), 4.18 (ddd, J = 9.9, 5.5, 2.4 Hz, 1H), 3.88 (dd, J = 10.5, 8.8 Hz, 1H), 3.55 – 3.34 (m, 6H), 3.31 – 3.24 (m, 2H), 3.13 (dd, J = 10.5, 3.8 Hz, 1H), 2.26 (dt, J = 12.9, 4.2 Hz, 1H), 1.43 (q, J = 12.3 Hz, 1H)

[x]HRMS (ESI-TOF) m/z: $[M+Na]^+$ Calcd for $C_{12}H_{18}N_{12}O_6Na$ 449.1370; Found 449.1376.

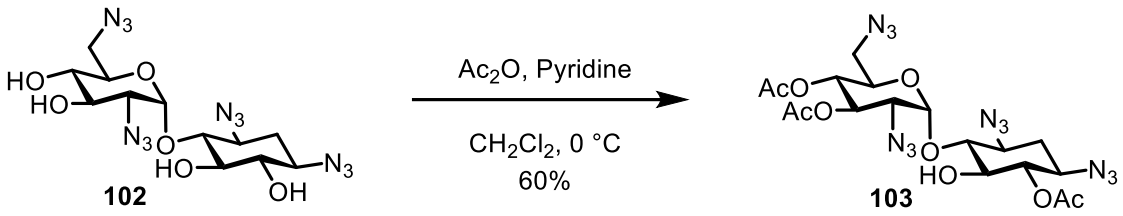

(*2R,3R,4R,5R,6R*)-6-(((*1R,2S,3S,4R,6S*)-3-acetoxy-4,6-diazido-2-hydroxycyclohexyl)oxy)-5-azido-2-(azidomethyl)tetrahydro-*2H*-pyran-3,4-diyl diacetate (103)

In a 500 mL round-bottom flask, a solution of tetraazidoneamine **102** (8.3 g, 19.5 mmol, 1 equiv) in 1:1 dichloromethane:pyridine (147 mL) was cooled to 0 °C and acetic anhydride (147 mL, 1560 mmol, 67 equiv) was added. The cooling bath was removed, and the solution allowed to warm to 23 °C and stirred for 1.5 hours. The solution was then further diluted with dichloromethane (140 mL) and poured onto chilled (0 °C), stirring saturated aqueous sodium bicarbonate solution (500 mL). After bubbling subsided, the layers were separated and the organic layer washed with water (2 x 65 mL). The volatiles were removed under vacuum and the remaining residue was suspended in ethyl acetate (130 mL), washed with saturated ammonium chloride solution (2 x 130 mL) and brine (130 mL). The organic phase was dried on sodium sulfate, filtered, and concentrated, and purification was achieved by flash chromatography on silica gel, grading from 10–70% ethyl acetate in hexanes to afford tetraazidoneamine triacetate **103** as a white solid (6.5 g, 11.8 mmol, 60%). *Major byproduct is the tetra-acetylated derivative which may co-elute if the elution gradient increases quickly.*

R_f: (40% Ethyl acetate in hexanes, $KMnO_4$): 0.48

^{1}H NMR (400 MHz, $CDCl_3$): δ 5.47 (dd, J = 10.4, 9.4 Hz, 1H), 5.35 (d, J = 3.6 Hz, 1H), 5.03 (m, 1H), 4.91 (t, J = 9.8 Hz, 1H), 4.33 (ddd, J = 10.2, 4.9, 2.8 Hz, 1H), 3.68 – 3.63 (m, 2H), 3.53 (ddd,

J = 12.5, 10.0, 4.5 Hz, 1H), 3.44 – 3.29 (m, 4H), 2.39 (dt, J = 13.1, 4.3 Hz, 1H), 2.17 (s, 3H), 2.09 (s, 3H), 2.05 (s, 3H), 1.61 (q, J = 12.7 Hz, 1H).

$^{13}C\{^{1}H\}$ NMR (101 MHz, $CDCl_3$): δ 169.67, 98.81, 78.64, 74.14, 73.54, 69.76, 69.57, 69.37, 60.58, 58.35, 57.62, 50.71, 31.73, 20.64.

FTIR (neat), cm^{-1}: 2926 (m), 2103 (s), 1742 (s).

HRMS (ESI-TOF) m/z: $[M+Na]^+$ Calcd for $C_{18}H_{24}N_{12}O_9Na$ 575.1687; Found 575.1702.

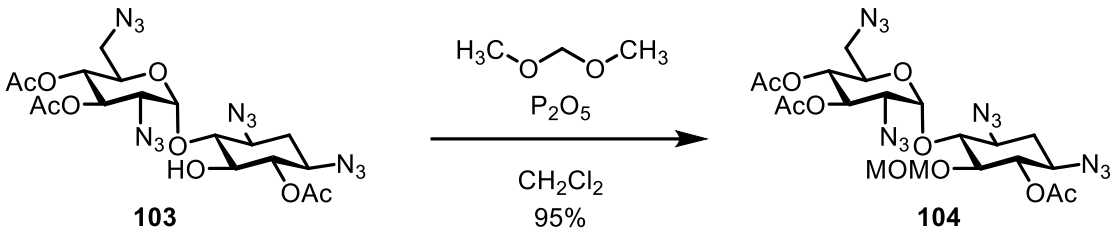

(*2R,3R,4R,5R,6R*)-6-(((*1R,2S,3S,4R,6S*)-3-acetoxy-4,6-diazido-2-(methoxymethoxy)cyclohexyl)oxy)-5-azido-2-(azidomethyl)tetrahydro-*2H*-pyran-3,4-diyl diacetate (104)

A solution of Triacetylated neamine tetraazide **103** (6.50 g, 11.8 mmol, 1 equiv) in dichloromethane (138 mL) was treated while stirring with dimethoxy methane (8.95 mL, 100 mmol, 8.5 equiv) and phosphorous pentoxide (24.7 g, 87 mmol, 7.4 equiv) in sequence. The resulting mixture was stirred for 1 hour at ambient temperature, and then poured onto a mixture of ice and saturated aqueous sodium bicarbonate (300 mL). After the ice completed melting, the phases were separated, and the organic layer washed with water (300 mL) and brine (300 mL). The organic layer was dried over sodium sulfate, filtered, and concentrated to provide the MOM-ether **104** as an off-white solid (6.67 g, 11.2 mmol, 95%).

R_f: (30% Ethyl acetate in hexanes, $KMnO_4$): 0.47

^1H NMR (400 MHz, $CDCl_3$): δ 5.52 (d, J = 3.8 Hz, 1H), 5.47 (dd, J = 10.7, 9.4 Hz, 1H), 5.05 (t, J = 9.7 Hz, 1H), 4.97 (t, J = 9.7 Hz, 1H), 4.82 (d, J = 6.9 Hz, 1H), 4,74 (d, J = 6.9 Hz, 1H), 4.51 (ddd, J = 10.0, 4.9, 2.7 Hz, 1H), 3.62 – 3.56 (m, 2H), 3.50 – 3.43 (m, 2H), 3.39 – 3.28 (m, 6H), 2.39 (dt, J = 13.2, 4.5, 1H), 2.16 (s, 3H), 2.10 (s, 3H), 2.06 (s, 3H), 1.63 (q, J= 12.7 Hz, 1H).

$^{13}C\{^1H\}$ NMR (101 MHz, $CDCl_3$): δ 170.20, 170.16, 169.74, 99.94, 98.09, 84.29, 78.89, 74.60, 70.14, 69.44, 69.36, 60.92, 58.55, 58.22, 56.75, 50.81, 31.60, 21.15, 20.74, 20.71.

FTIR (neat), cm^{-1}: 2961 (w), 2100 (s), 1748 (s).

HRMS (ESI-TOF) m/z: $[M+Na]^+$ Calcd for $C_{20}H_{28}N_{12}O_{10}Na$ 619.1949; Found 619.1973.

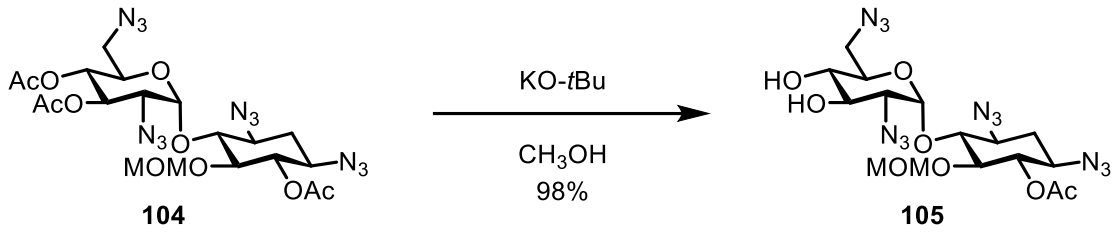

(*1S,2S,3R,4S,6R*)-4,6-diazido-3-(((*2R,3R,4R,5S,6R*)-3-azido-6-(azidomethyl)-4,5-dihydroxytetrahydro-*2H*-pyran-2-yl)oxy)-2-(methoxymethoxy)cyclohexyl acetate (105)

A solution of MOM-ether **104** (6.70 g, 11.2 mmol, 1 equiv) in dry methanol (100 mL) was treated with potassium *tert*-butoxide (1M in THF, 2.25 mL, 2.25 mmol, 0.2 equiv) at ambient conditions. The solution stirred for 1 hours at this temperature, and was then neutralized by the addition of 2 M hydrochloric acid (1.25 mL). The solvents were evaporated, and the remaining residue purified by flash chromatography on silica gel, grading from 30–70% ethyl acetate in hexanes to yield diol **105** (5.64 g, 11.0 mmol, 98%) as a white solid.

R_f: (66% Ethyl acetate in hexanes, $KMnO_4$): 0.68

^1H NMR (400 MHz, $CDCl_3$): δ 5.49 (d, J = 3.8 Hz, 1H), 4.95 (t, J = 9.6 Hz, 1H), 4.82 (d, J = 6.8 Hz, 1H), 4.75 (d, J = 6.8 Hz, 1H), 4.22 (ddd, J = 9.9, 4.3, 2.9 Hz, 1H), 3.98 (t, J = 9.4 Hz, 1H), 3.65 – 3.36 (m, 5H), 3.33 (s, 3H), 3.23 (dd, J = 10.5, 3.8 Hz, 1H), 2.99 (bs, 1H), 2.86 (bs, 1H), 2.35 (dt, J = 13.2, 4.5 Hz, 1H), 2.16 (s, 3H), 1.60 (q, J = 12.7 Hz, 1H).

$^{13}C\{^1H\}$ NMR (101 MHz, $CDCl_3$): δ 170.29, 100.04, 98.26, 84.31, 78.30, 74.74, 71.67, 71.54, 71.29, 62.97, 59.20, 58.39, 56.85, 51.26, 31.97, 21.26.

FTIR (neat), cm^{-1}: 3430 (br), 2938 (m), 2100 (s), 1743 (m).

HRMS (ESI-TOF) m/z: $[M+Na]^+$ Calcd for $C_{16}H_{24}N_{12}O_8Na$ 535.1738; Found 535.1807.

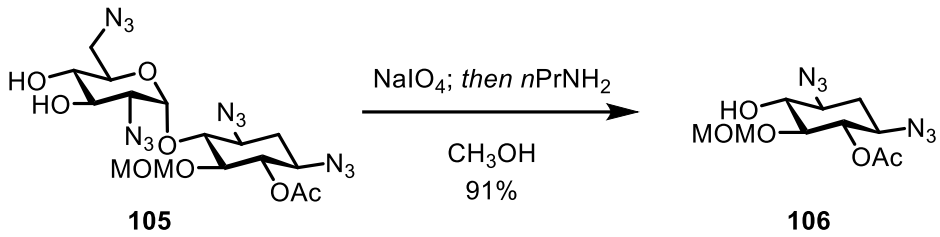

(*1S,2S,3R,4S,6R*)-4,6-diazido-3-hydroxy-2-(methoxymethoxy)cyclohexyl acetate (106)

To a solution of diol **105** (5.76 g, 11.2 mmol, 1 equiv) in methanol (453 mL) was added solid sodium periodate (18.03 g, 84 mmol, 7.5 equiv) and the solution stirred overnight at ambient temperature. A white precipitate had formed, which was removed by filtration, and the filtrate then concentrated, dissolved in ethyl acetate (400 mL), and washed with water (2 x 200 mL) and brine (2 x 200 mL). The organic phase was dried over sodium sulfate, filtered, and the solvents removed under vacuum. The residue was re-dissolved in methanol (470 mL) and *n*-propylamine (2.77 mL, 33.7 mmol, 3 equiv) was added at room temperature. After 1.5 hours of stirring, an additional portion of *n*-propylamine (0.95 mL, 11.6 mmol, 1 equiv) was added and stirring continued for 1 hour. The solvents were then removed under reduced pressure, and the residue purified by flash chromatography on silica gel, grading from 20–40% ethyl acetate in hexanes to afford 2-deoxystreptamine derivative **XX** as an orange solid (3.09 g, 10.3 mmol, 91%).

R_f: (50% Ethyl acetate in hexanes, $KMnO_4$): 0.52

^{1}H NMR (400 MHz, $CDCl_3$): δ 4.96 (t, J = 9.9 Hz, 1H), 4.77 (d, J = 7.0 Hz, 1H), 4.66 (d, J = 7.0 Hz, 1H), 4.30 (d, J = 1.5 Hz, 1H), 3.53 – 3.38 (m, 6H), 2.21 (dt, J = 13.4, 4.5 Hz, 1H), 2.14 (s, 3H), 1.45 (dd, J = 25.9, 12.6 Hz, 1H).

$^{13}C\{^1H\}$ NMR (101 MHz, $CDCl_3$): δ 169.93, 98.47, 84.14, 75.61, 74.13, 59.99, 58.56, 56.37, 31.90, 20.91.

FTIR (neat), cm^{-1}: 3419 (br), 2899 (m), 2096 (s), 1742 (s).

HRMS (ESI-TOF) m/z: $[M+NH_4]^+$ Calcd for $C_{10}H_{20}N_7O_5$ 318.1520; Found 318.1519.

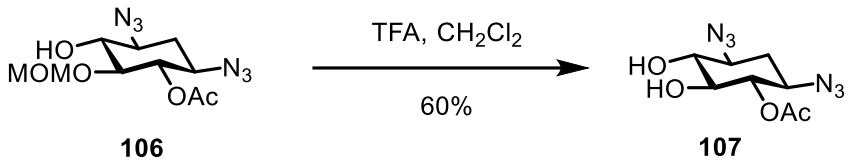

106 **107**

(*1S,2S,3R,4S,6R*)-4,6-diazido-2,3-dihydroxycyclohexyl acetate (107)

A solution of glycosyl acceptor **106** (100 mg, 0.333 mmol, 1 equiv) in anhydrous dichloromethane (2.22 mL) was treated with trifluoroacetic acid (1.11 mL, 14.3 mmol, 43 equiv) and the solution stirred overnight. The solvents were removed under reduced pressure, and the remaining residue purified by flash chromatography on silica gel, grading from 30–50% ethyl acetate in hexanes to provide 2-DOS diol **107** as an off-white solid (51 mg, 0.199 mmol, 60%).

R_f: (50% Ethyl acetate in hexanes, $KMnO_4$): 0.24

^1H NMR (400 MHz, $CDCl_3$): δ 4.79 (s, 2H), 4.74 (t, J = 9.7 Hz, 1H), 3.53 (ddd, J = 12.5, 10.1, 4.5 Hz, 1H), 3.40 – 3.23 (m, 3H), 2.11 (dt, J = 13.2, 4.4 Hz, 1H), 2.05 (s, 3H), 1.31 (q, J = 12.5 Hz, 1H).

$^{13}C\{^1H\}$ NMR (101 MHz, $CDCl_3$): δ 172.07, 77.49, 77.44, 74.79, 61.81, 59.72, 33.02, 20.97.

FTIR (neat), cm^{-1}: 3359 (br), 2924 (w), 2495 (br), 2099 (s), 1734 (s).

HRMS (ESI-TOF) m/z: $[M+H]^+$ Calcd for $C_8H_{13}N_6O_4$ 257.0993; Found 257.0991.

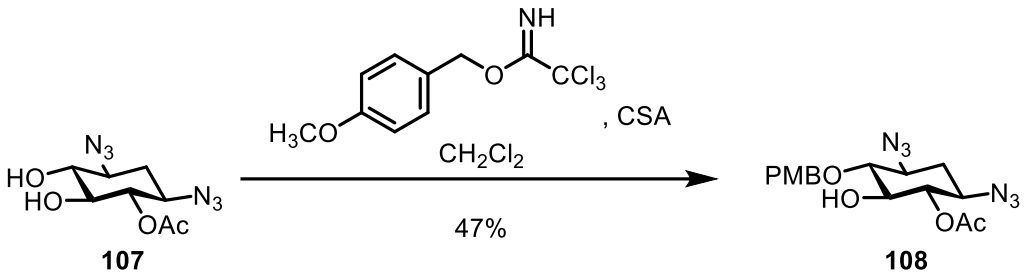

(*1S,2S,3R,4S,6R*)-4,6-diazido-2-hydroxy-3-((4-methoxybenzyl)oxy)cyclohexyl acetate (108)

To a solution of 2-DOS diol **107** (55 mg, 0.22 mmol, 1 equiv) in anhydrous dichloromethane (1.1 mL) was cooled to 0 °C and treated with *p*-methoxybenzyltrichloroacetimidate (56 mL, 0.27 mmol, 1.23 equiv) and camphorsulfonic acid (5 mg, 0.02 mmol, 0.1 equiv) in sequence. The reaction was monitored by TLC, stirring overnight and then quenched by addition of saturated aqueous sodium bicarbonate (5 mL) and extracting with dichloromethane (3 x 5 mL). The combined organic phases were dried on sodium sulfate, filtered, and concentrated to yield the crude. Purifcation by flash chromatography on silica gel, grading from hexanes to 30% ethyl acetate in hexanes afforded PMB-protected 2-DOS **108** as a solid (38 mg, 0.10 mmol, 47%).

R_f: (50% Ethyl acetate in hexanes, CAM): 0.73

^{1}H NMR (400 MHz, $CDCl_3$): δ 7.32 (d, J = 8.6 Hz, 2H), 6.89 (d, J = 8.7 Hz, 2H), 4.92 – 4.82 (m, 2H), 4.72 (d, J = 10.6 Hz, 1H), 3.80 (s, 3H), 3.54 (td, J = 9.5, 2.3 Hz, 1H), 3.44 (dddd, J = 12.4, 9.8, 5.6, 4.5 Hz, 2H), 3.29 (t, J = 9.4 Hz, 1H), 2.46 – 2.38 (m, 1H), 2.23 (dt, J = 13.4, 4.6 Hz, 1H), 2.15 (s, 3H), 1.44 (dt, J = 13.4, 12.5 Hz, 1H).

^{13}C{^{1}H} NMR (101 MHz, $CDCl_3$): δ 170.80, 159.78, 130.19, 129.75, 114.24, 83.85, 75.91, 75.47, 74.25, 60.11, 58.29, 55.42, 32.50, 20.99.

FTIR (neat), cm^{-1}: 3468 (br), 2925 (m), 2095 (s), 1739 (s).

HRMS (ESI-TOF) m/z: $[M+Na]^+$ Calcd for $C_{16}H_{20}N_6O_5Na$ 399.1387; Found 399.1380.

Chapter 4. Design and Synthesis of C5'-modified Aminoglycosides Against NpmA Resistance

4.1 Introduction

Aminoglycoside antibiotics are highly susceptible to microbial resistance enzymes. While aminoglycoside modifying enzymes (AMEs) are the dominant form of proliferated aminoglycoside resistance genes,[1] in recent years ribosomal methyltransferases (RMTs) have become increasingly disseminated.[2] RMTs are of particular concern due to the primary family of aminoglycosides for clinical treatment being within the 4,6-disubstituted subfamily, which are inactive against both N7-G1405 methylation from ArmA or RmtB-G protein family members.

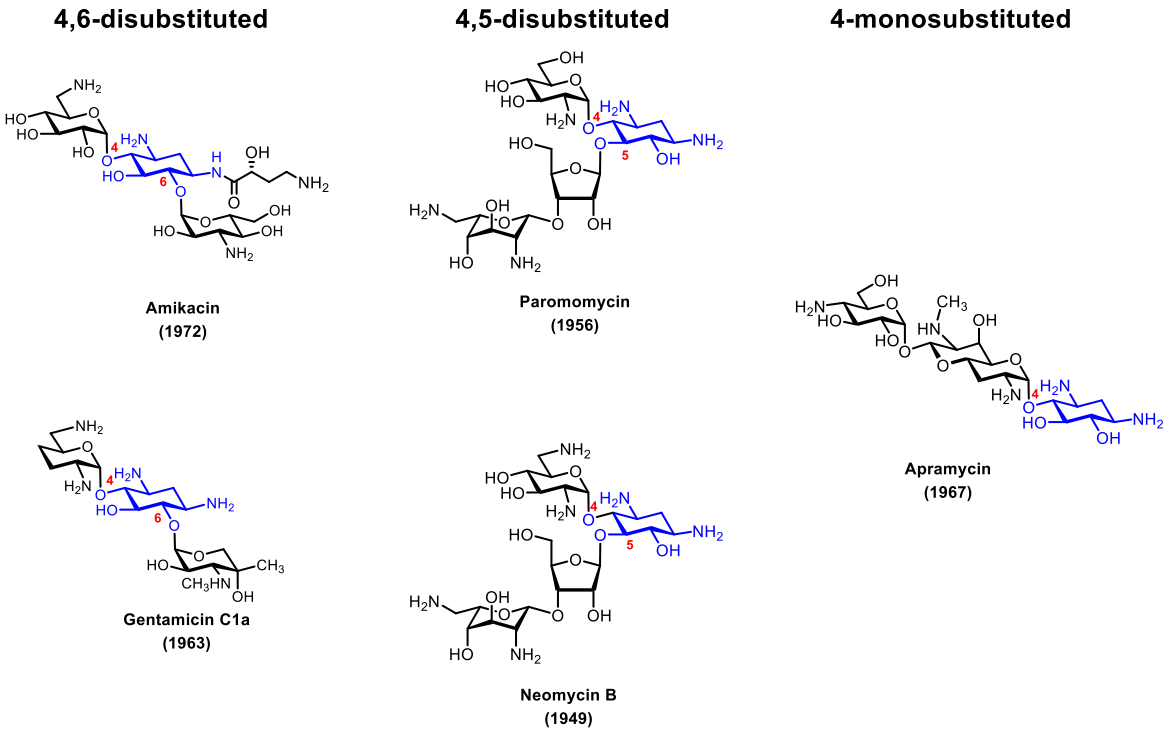

Species	Strain Description	Amikacin	Gentamicin	Paromomycin	Neomycin B	Apramycin
E. coli	CSH-2 - Lab strain, wt	0.13	0.06	0.5	0.13	1
E. coli	*npmA* - plasmid transformant	16	128	4	64	>256
E. coli	*npmA* - Clinical Isolate	256	>256	64	>256	>256

Figure 4.1. A selection of aminoglycoside antibiotics and their activity against NpmA-expressing *E. coli*.[4]

Methyltransferase resistance also frequently coincides on mobile genetic elements harboring genes providing resistance to other classes of antibiotics such as b-lactams.[3] Perhaps even more

concerning, a novel plasmid-mediated aminoglycoside resistance gene (NpmA) was reported in 2007 in a clinical isolate that promotes methylation of N1 of base A1408.[4] The disruption of the critical hydrogen bonding with A1408 responsible for aminoglycoside activity causes complete resistance among this class of antibiotics (Figure 4.1).[5] Even the most recently approved member of the aminoglycoside class, plazomicin (2018), which was designed to overcome numerous AME mechanisms of resistance cannot overcome N7-G1405 or N1-A1408 RMT activity (Figure 4.2).[6]

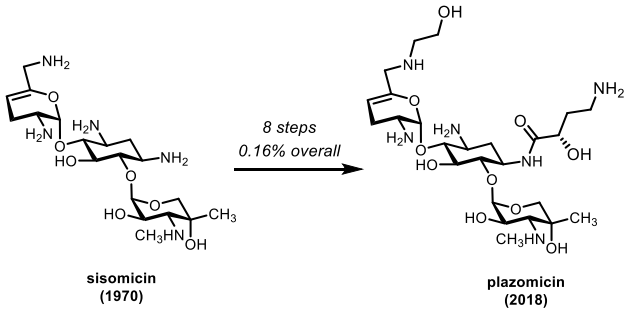

Species	Strain Description	Plazomicin
E. coli	BW25113	2
E. coli	Δ*bamB* Δ*tolC*	1
E. coli	*aac* (3)-IV	2
E. coli	*aac* (6')-Ie-*aph* (2'')-Ia	2
E. coli	*ant* (4')-Ia	2
E. coli	*aph* (3')-IIa	2
E. coli	*aph* (2'')-IVa	8
E. coli	*aac* (2')-Ia	32
E. coli	*armA*	256
E. coli	*rmtB*	>512
E. coli	*npmA*	256
E. coli	*kamB*	256

Figure 4.2. Plazomicin, a semisynthetic derivative of sisomicin, was approved in 2018 and overcomes multiple mechanisms of AME resistance. However, the drug remains susceptible to RMT forms of resistance such as ArmA or NpmA.[6]

As of beginning this dissertation, no aminoglycoside is reported to overcome NpmA resistance, while its detection has been noted in multiple countries. The natural product paromomycin has been shown to lose comparably less activity in the presence of mA1408 due to rotation of the C6'-hydroxyl permitting some interaction with the methylated ribonucleobase.[5] While there is some fitness cost purported by the expression of this resistance gene,[7] NpmA is known to be tolerable across several species of gram-negative bacteria. Considering these reports, we sought to explore new scaffolds for the aminoglycoside class of antibiotics seeking to overcome this resistance mechanism. We first explored 5'-modified neamine scaffolds hoping to avoid electrostatic clashing with methylated A1408 (mA1408) and gain affinity through contacts elsewhere in the binding

domain. Additionally, I utilized a molecular modeling software, Molecular Operating Environment (MOE), to design analogs that might retain affinity in the presence of mA1408 by introducing a cation-p interaction.[8] Finally, en route to analogs that might participate in weak hydrogen bonds with mA1408, a decarboxylative elimination reaction yielded a semisynthetic 4'-deoxypentenoside;[9] the chemistry of this unique motif for aminoglycosides was explored in hopes of providing a pathway to C5'-arylation, but instead provides a strategy for ring I scission from the aminoglycoside scaffold using a variety of methods.

4.2 Design of NpmA Overcoming Analogues

In seeking to overcome NpmA resistance, we considered multiple scaffolds to explore that were synthetically tractable. We first believed that circumventing of NpmA resistance might be achieved by bypassing the introduced steric clash within the binding sight and extending hydrogen bonding contacts elsewhere or to adjacent ribonucleobases (Figure 4.3). This would be accomplished by the development of pseudodisaccharide molecules that would be screened for initial activity and prepared from the coupling of a C5-allyl glycosyl donor and the semisynthetic glycosyl acceptor **106** (Figure 4.4).[10] Globally deprotected neamine derivatives such as **109** (R = NH_2, OH, etc…) could be traced to C5'-allyl pseudodisaccharide **110** by HABA chain coupling

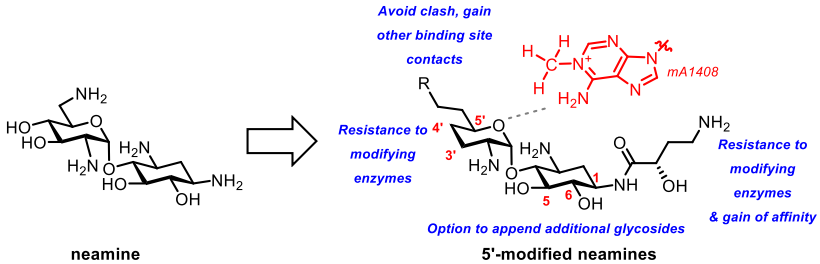

Figure 4.3. Design of C5'-modified neamine scaffold aminoglycosides. The rationale for different features of the scaffold is presented.

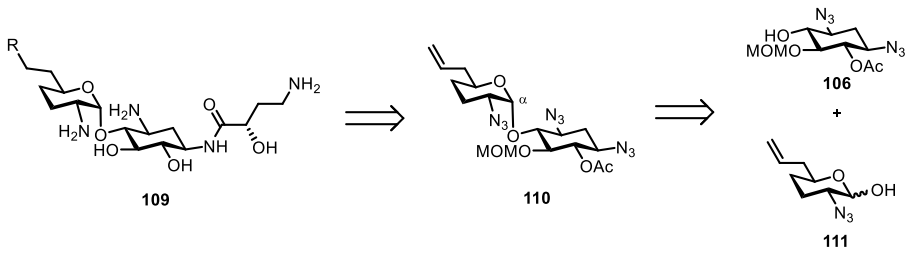

Figure 4.4. Retrosynthesis for the design of C5'-modified neamine derivatives. R = NH_2, OH.

and allyl group modification. Allyl glycoside **110** additionally provides access to further glycosidic coupling by deprotection of the C5-MOM ether or C6-acetate. The intuitive disconnection for pseudodisaccharide **110** would be a glycosylation reaction between a synthetic ring I glycosyl donor **111** and coupling with semisynthetic 2-deoxystreptamine analog **106**. Lactol **111** could be prepared from D-glutamate and would provide access to multiple donors to optimize the glycosylation reaction with **106**.

In the absence of activity from C5'-modified neamine derivatives, I additionally explored the crystal structure of neomycin B bound to the *e. coli* ribosome (MOE, PDB: 4V52). With the

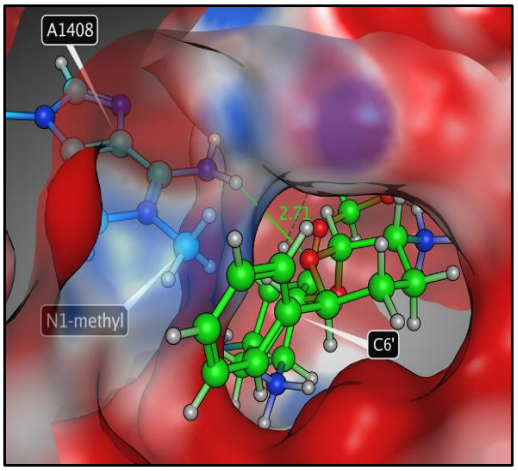

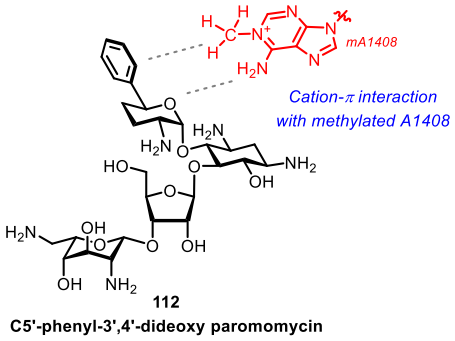

Figure 4.5. (Left) MOE modeling of C5'-phenyl AG **112**, PDB: 4V52. The phenyl group optimally orients to act as a p-donor for the positively charged methyl of mA1408. Hydrogen bond distance is denoted in Å as a green line. (Right) a cartoon depiction of **112** and it's hypothesized interaction with mA1408.

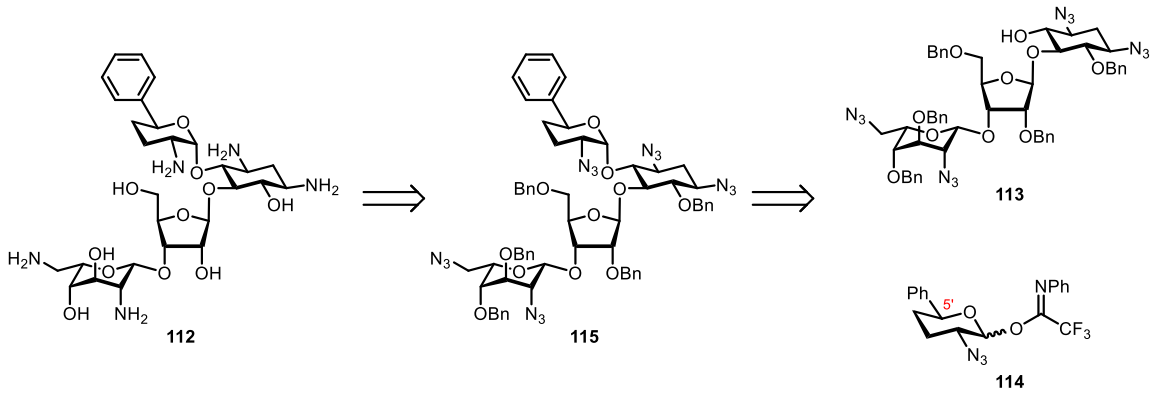

Figure 4.6. Retrosynthesis for the preparation of C5'-arylated aminoglycosides.

knowledge that the ring I binding site can accommodate the larger structures from apramycin or semisynthetic analogs such as propylamycin, I designed C5'-phenyl aminoglycoside **112** (Figure 4.5); minimization within MOE in the presence of mA1408 suggested a proper conformation for a cation-p interaction. To access arylated aminoglycosides at C5', we turned to the recent disclosure of a pseudotrisaccharide acceptor for rings II – IV of aminoglycosides and unprotected at the C4 hydroxyl, **113** (Figure 4.6).[11] Glycosylation between acceptor **113** and synthetic ring I glycosyl donors of type **114** as precursors to **112** following hydrogenolysis of an intermediate such as pseudotetrasaccharide **115**. The hydrogenation of a C5 aryl sugar conjugate has been previously demonstrated, suggesting that the benzylic C5' and pyran ring oxygen bond may be less reductively labile.[12]

Modeling studies suggested that more exotic heterocycles containing N-H bonds would provide additional affinity via hydrogen bonding with the nearby phosphate of A1493. Such C5'-heterocyclic aminoglycosides could hydrogen bond to A1408 in the absence of NpmA expression and potentially retain antibiotic activity against multiple strains of bacteria**.** The benefit of arylation

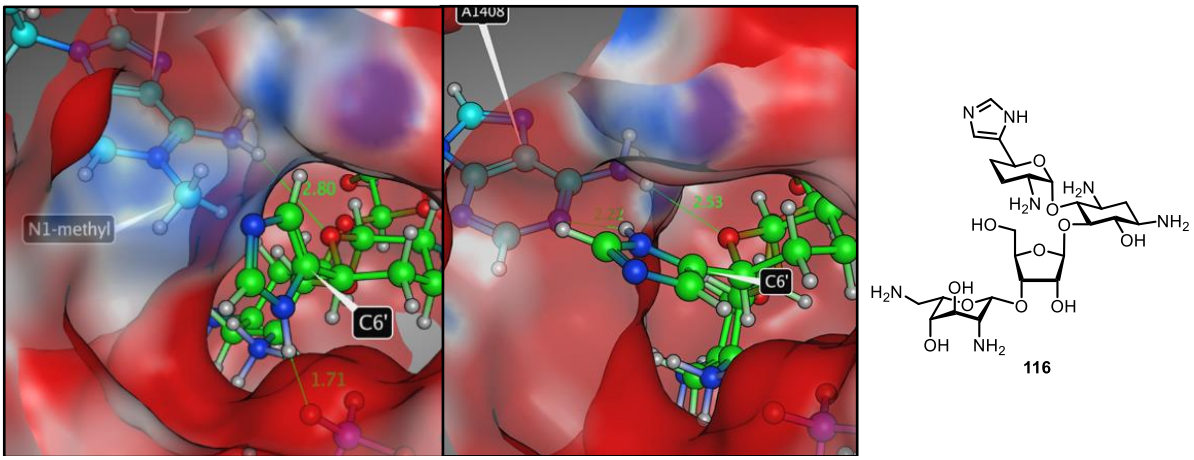

Figure 4.7. MOE modeling of **116** in the AGA binding site. (Left) **116** binding with mA1408 shows a putative cation-p interaction while gaining a hydrogen bond. (Middle) **116** binding with A1408 in the absence of NpmA retains the ring I pseudo-base pairing interaction. (Right) Structure of **116**.

can be further examined with C5'-imidazole aminoglycoside **116** (Figure 4.7). Proper positioning of the N-H within the heterocycle is hypothesized to allow interaction with A1408 and simultaneously allow rotation to serve as p-donor for mA1408, concurrently gaining a hydrogen bond with a nearby phosphate of A1493.

4.3 Synthesis of C5'-allyl lactol donor and preparation of C5'-modified pseudodisaccharides

We initially pursued C5'-homologated pseudodisaccharides to overcome NpmA resistance by bypassing the site of methylation and gaining additional contacts elsewhere in the binding domain. Precedent was established by the existence of complex ring I aminoglycosides such as apramycin and in the hydroxyethyl C6'-amine modification of plazomicin that overcomes AAC(6') resistance. Additionally, differentiation of **110** at the C5 and C6 hydroxyls would facilitate additional glycosylation reactions if an initial scaffold showed promise in minimal inhibitory concentration assays.

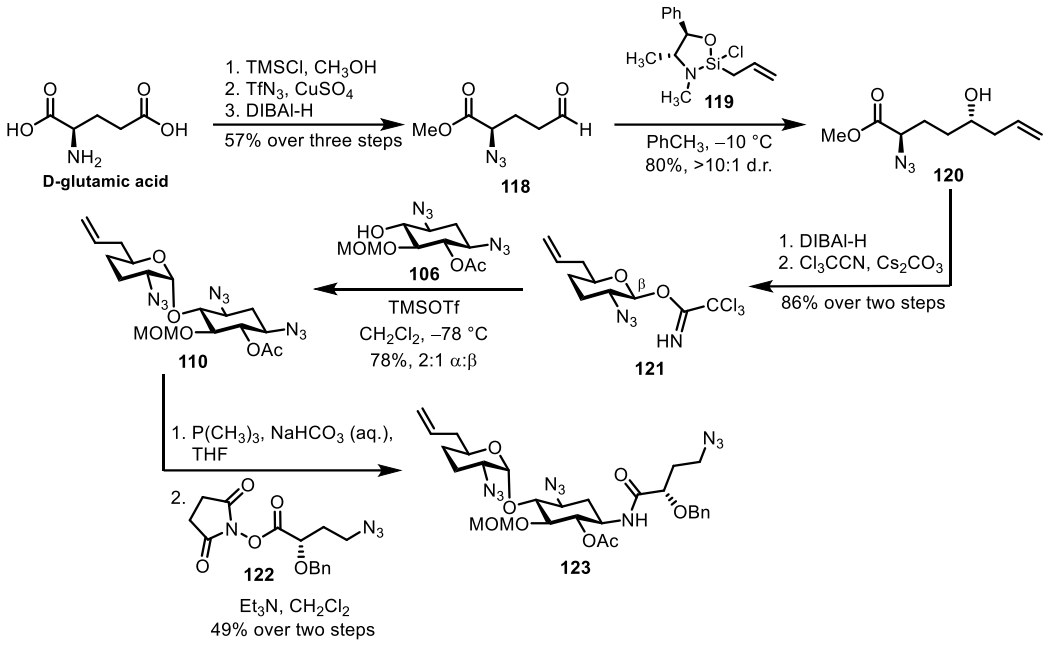

Figure 4.8. Synthesis of diversifiable pseudodisaccharide **110** and regioselective introduction of HABA-side chain yielding protected analog **123**.

We began our pursuit with the synthesis of preparation of lactol **111** from D-glutamic acid (Figure 4.8). Diesterification was achieved with TMSCl in methanol, and subsequent diazotransfer with copper (II) sulfate and triflic azide[13] provides an intermediate azide **117** (not depicted, see experimental section) in 92% yield. Regioselective functionalization of the side chain ester was achieved by reduction with DIBAL-H,[14] favoring the more electron rich ester, to provide aldehyde **118** in 67% yield. Introduction of the allyl chain at C5' was accomplished by treatment of **118** with Leighton reagent **119** in chilled toluene,[15] diastereoselectively forming homoallylic alcohol **120** in 80% yield with greater than 10:1 dr. Treatment of **120** with DIBAL-H provided lactol **111** in 91% yield, bringing to question the choice of glycosylation method. Glycosylations to yield a-anomeric linkages of 2-deoxysugars are notably challenging due to the necessary absence of participating groups.[16] After deliberation, activation of **111** as an imidate donor was achieved with

trichloroacetonitrile and cesium carbonate, giving trichloroacetimidate **121** nearly quantitatively.[17] Trichloroacetimidate donors have wide precedent in glycosylations, and are noteworthy for their ease of preparation, they are readily used without chromatography and can be prepared directly prior to glycosylation, and multiple reagents for activation. In the glycosylation between **121** and **106**, TMSOTf in cold dichloromethane provided pseudodisaccharide **110** in 78% yield on gram scale, slightly favoring the a-anomer 2:1. The poor selectively could not be overcome without severely compromising total yield across a range of reaction temperatures, solvents, and activation methods; a noteworthy result was that the addition of TMSI to the glycosyl acetate congener of **121** in the presence of triphenylphosphine oxide would provide **110** with complete anomeric selectivity, albeit in diminished 36% yield due to instability of the intermediate glycosyl iodide. With **110** in hand, the HABA chain was introduced by regioselective Staudinger reduction of the C1 azide by treatment with trimethylphosphine followed by coupling of N-hydroxysuccimide ester **122** to afford diversifiable intermediate **123**.[18]

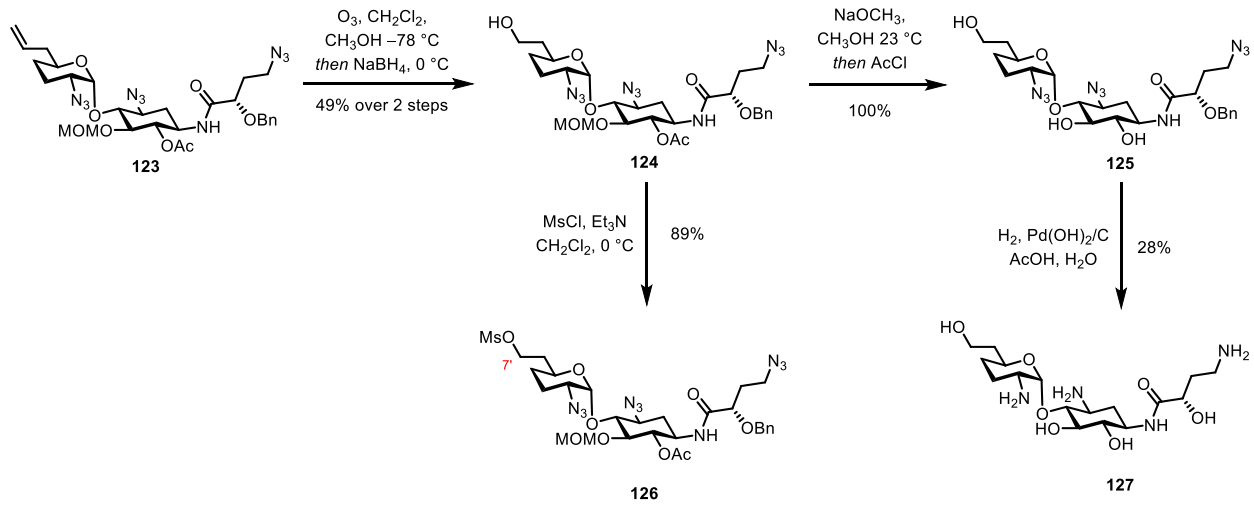

Figure 4.9. Transformation of **123** into diversifiable intermediate **126** and synthetic aminoglycoside **127**.

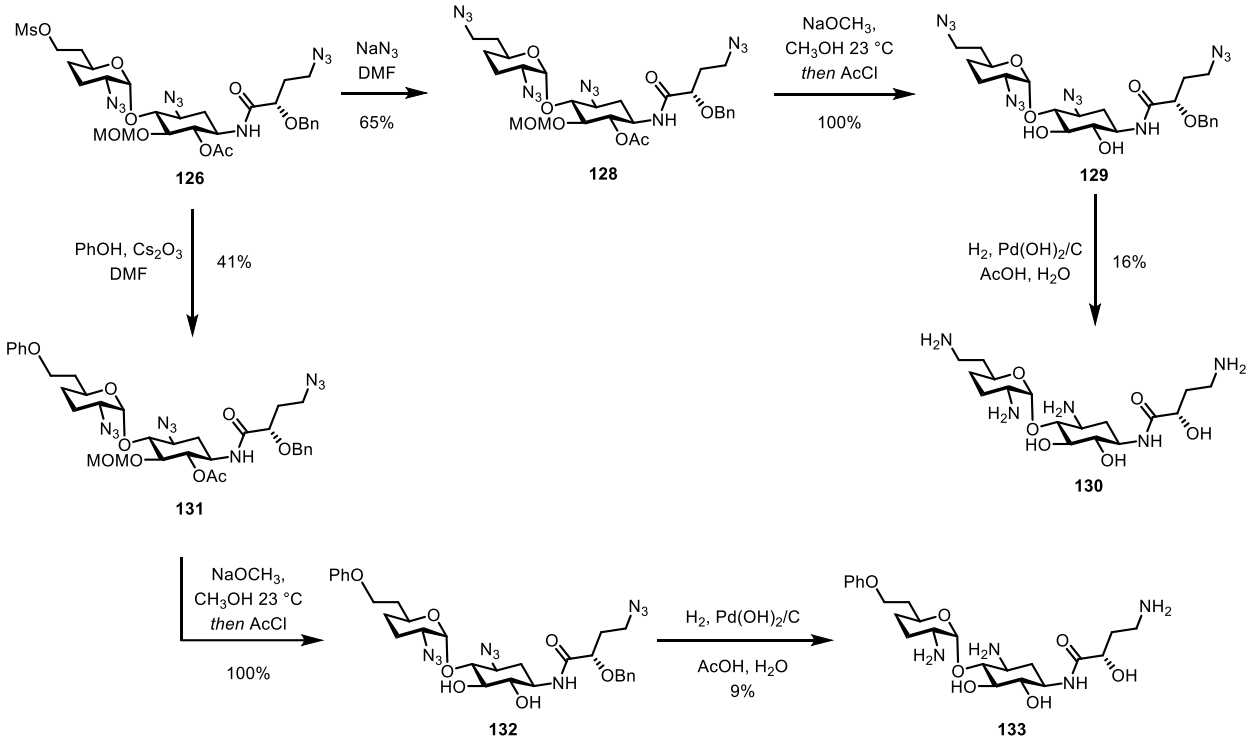

Figure 4.10. Transformation of **126** into synthetic aminoglycosides **130** and **133**.

Pseudodisaccharide **123** served as a valuable precursor to C5'-homologated aminoglycosides. Reductive ozonolysis of the allyl chain yielded **124** in 49% yield, allowing direct deprotection of the 2-deoxystreptamine ring by methanolysis and generation of dry hydrochloric acid (Figure 4.9) to provide triol **125** quantitatively. Alternatively, mesylation of **124** to give **126** in 89% yield provided a C7' modification handle. Deprotection of **125** was achieved by hydrogenation with Pearlman's catalyst,[19] affording 28% of **127** after HPLC purification. Methanesulfonate **126** could be readily converted into azide **128**, whose deprotection to intermediate **129** and subsequent hydrogenation provided **130** in 16% yield (Figure 4.10). Displacement of the sulfonate in **126** with deprotonated phenol afforded phenyl ether **131** in 41% yield. The deprotection sequence repeated as before first provided **132** quantitatively, and later **133** following hydrogenation and HPLC purification in 9% yield.

Antibiotic candidates **127**, **130**, and **133** were evaluated alongside gentamicin C complex (gentamicin) and amikacin against a collection of *E. coli* expressing ribosomal methyltransferase resistance phenotypes ArmA and NpmA (Figure 4.11).[20] All analogs displayed significantly impaired activity against *E. coli* and *S. auereus* laboratory strains, with noteworthy absence of activity against efflux-deficient (ΔtolC) and membrane-compromised (LptD) strains. No compounds displayed activity against methyltransferase expressing strains. Given the pseudodisaccharide neamine shows modest activity against these strains of *E. coli*,[21] these results indicate a loss of interaction with A1408, and subsequently all antimicrobial activity, in C5'-homologated aminoglycosides.

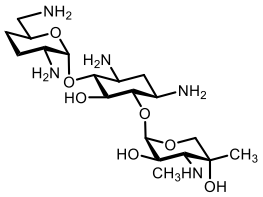

Gentamicin C1a

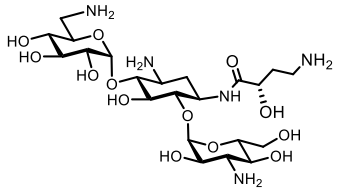

Amikacin

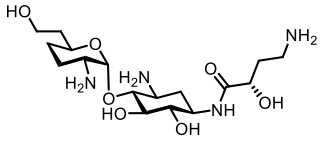

127

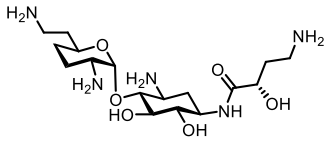

130

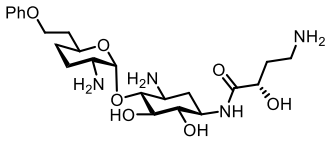

133

Species	Strain Description	Gentamicin	Amikacin	127	130	133
E. coli	ATCC 25922	2	1	>64	>64	>64
E. coli	D*tolC*	1	2	>64	>64	>64
E. coli	*LptD*	0.5	1	>64	>64	>64
E. coli	*MM294+pGB2 WT*	1	4	>64	>64	>64
E. coli	MM294+pGB2 *armA*	>256	>256	>64	>64	>64
E. coli	MM294+pGB2 *npmA*	32	64	>64	>64	>64
S. aureus	ATCC BAA-977 *ermB*	2	4	>64	>64	>64

Figure 4.11. Antibiotic activity of C5'-homologated aminoglycosides **127**, **130**, and **133** as compared to gentamicin and amikacin.

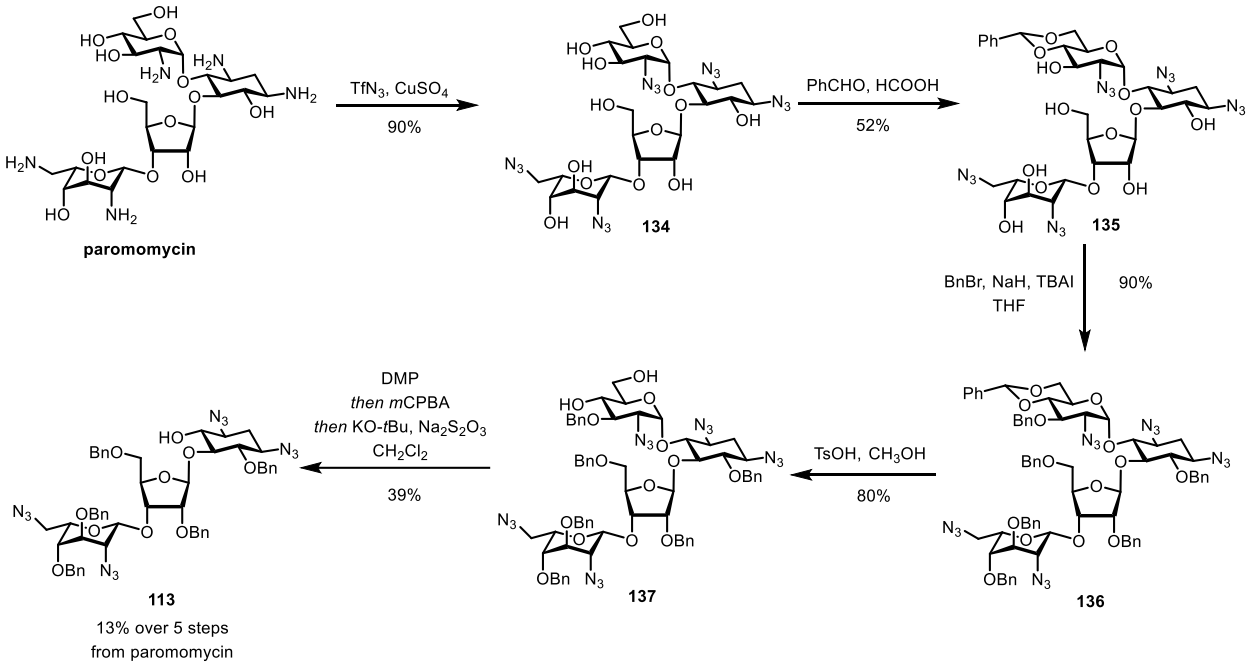

Figure 4.12. Preparation of pseudotrisaccharide acceptor **113** from paromomycin.

4.4 Preparation of C5'-phenyl lactol donor and union with pseudotrisaccharide acceptors

We envisioned that C5'-arylation might introduce bifunctional motifs capable of gaining periphery ribosomal hydrogen bonding contacts while introducing a substrate-receptor cation-π interaction. Targeting **112**, I prepared the recently reported pseudotrisaccharide acceptor **113**[11] and explored the glycosylation with synthetic ring I glycosyl donor **114**. Starting from commercially available paromomycin sulfate, global azidation with triflic azide provided perazidated paromomycin **134** in 90% yield (Figure 4.12). Benzylidene acetal formation was achieved with neat benzaldehyde and formic acid at 4 °C, giving **135** in 52% yield. Global benzylation gave perbenzylated **136**, followed by tosic acid acetal cleavage gave diol **137** in 72% yield for the two steps. Lastly, a one-pot sequence provided **113** following oxidation of the diol, hydroxylation, and ring I glycosidic bond cleavage. The preparation of **113** from paromomycin proceeded in 13% over 5 steps.

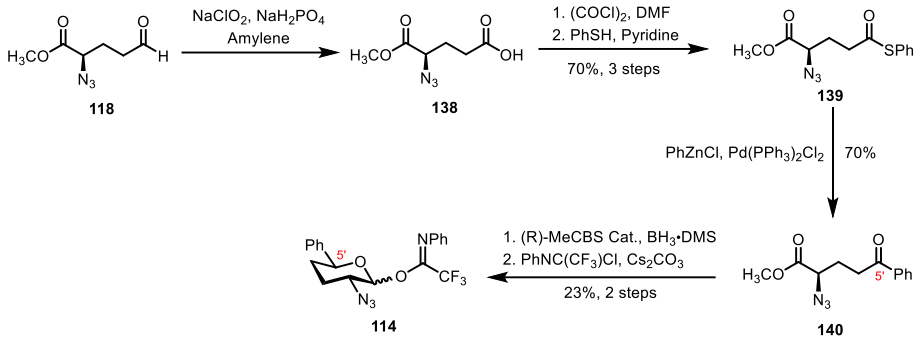

Figure 4.13. Synthesis of trifluoroacetimidate donor **114**.

To prepare C5-arylated glycosyl donors, we turned to regioselectively functionalized glutamate derivative **118** (Figure 4.13). Pinnick oxidation[22] gave mono acid **138**, and acyl halide formation followed by transthioesterification afforded **139** in 70% yield over three steps. Palladium-catalyzed Fukuyama coupling[23] facilitated access to aryl ketone **140**, which was gratifyingly reduced under CBS conditions[24] to directly isolate the lactol donor **142** without the need for an additional ester reduction. During the initial screening of CBS conditions, benzylic alcohol **141** demonstrated lactonization in solution, and thus **142** may be obtained selectively by careful raising of the reaction temperature to minimize overreduction to **143** (Figure 4.14). With

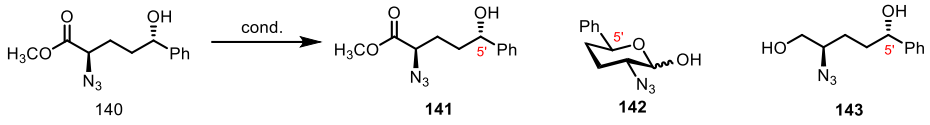

Entry	Catalyst (mol %)	Borane (eq)	Solvent	Temp (°C)	Time (h)	Yield 141	Yield 142	Yield 143
1	10	BH_3•THF (1	THF	-10	4	16%	0%	28%
2	5	BH_3•DMS (1	THF	-15	48	45%	0%	0%
3	5	BH_3•DEA (1	Toluene	23	4	16%	18%	56%
4	5	BH_3•DMS (4	THF	-15	24	78%	0%	0%
5	5	BH_3•DMS (0	THF	23	2	0%	33%	42%
6	5	BH_3•DMS (0	THF	0 to rt	18	0%	46%	30%

Figure 4.14. CBS reduction screening table and yields of products **141**, **142**, and **143**.

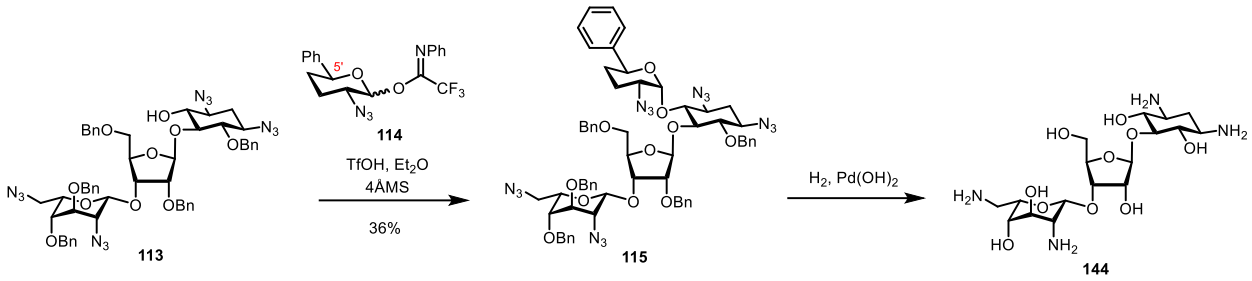

Figure 4.15. Glycosylation between **113** and **114** to yield **115** and subsequently discovered fragmentation of the ring I glycosidic linkage.

acceptor **113** and glycosyl donors in hand, the coupling to prepare **115** was explored. Dehydrative glycosylation methods utilizing **142** as a donor resulted in decomposition.[11] Gratifyingly, the triflic acid promoted glycosylation between **114** and **113** provided **115** with complete anomeric selectivity in 36% yield (Figure 4.15). Unfortunately, all debenzylation methods resulted in fragmentation of the ring I-ring II glycosidic linkage, providing deprotected pseudotrisaccharide **144** as the sole product in lieu of arylated aminoglycoside **112**. Limited examples for C5-aryl sugar deprotections are known, and with these initial results I turned to prepare an alternative acceptor acetylated at the hydroxyl groups.

An alternative glycosyl acceptor for rings II-IV, acetylated except at the C4-hydroxyl, has been previously described[25] but relied on both an enzymatic resolution of a 2-deoxystreptamine triacetate as well as a glycosylation that is not regioselective. I recognized 2-deoxystreptamine analog **108** would serve as a valuable coupling partner to a ring III-ring IV glycosyl donor that may be prepared from neomycin. Starting from neomycin B, global azidation to provide hexaazide **145** followed by acetylation with acetic anhydride in pyridine provided **146** in 56% yield over 2 steps (Figure 4.16A).[26] Cleavage of the ring III-IV glycosidic bond was achieved with boron

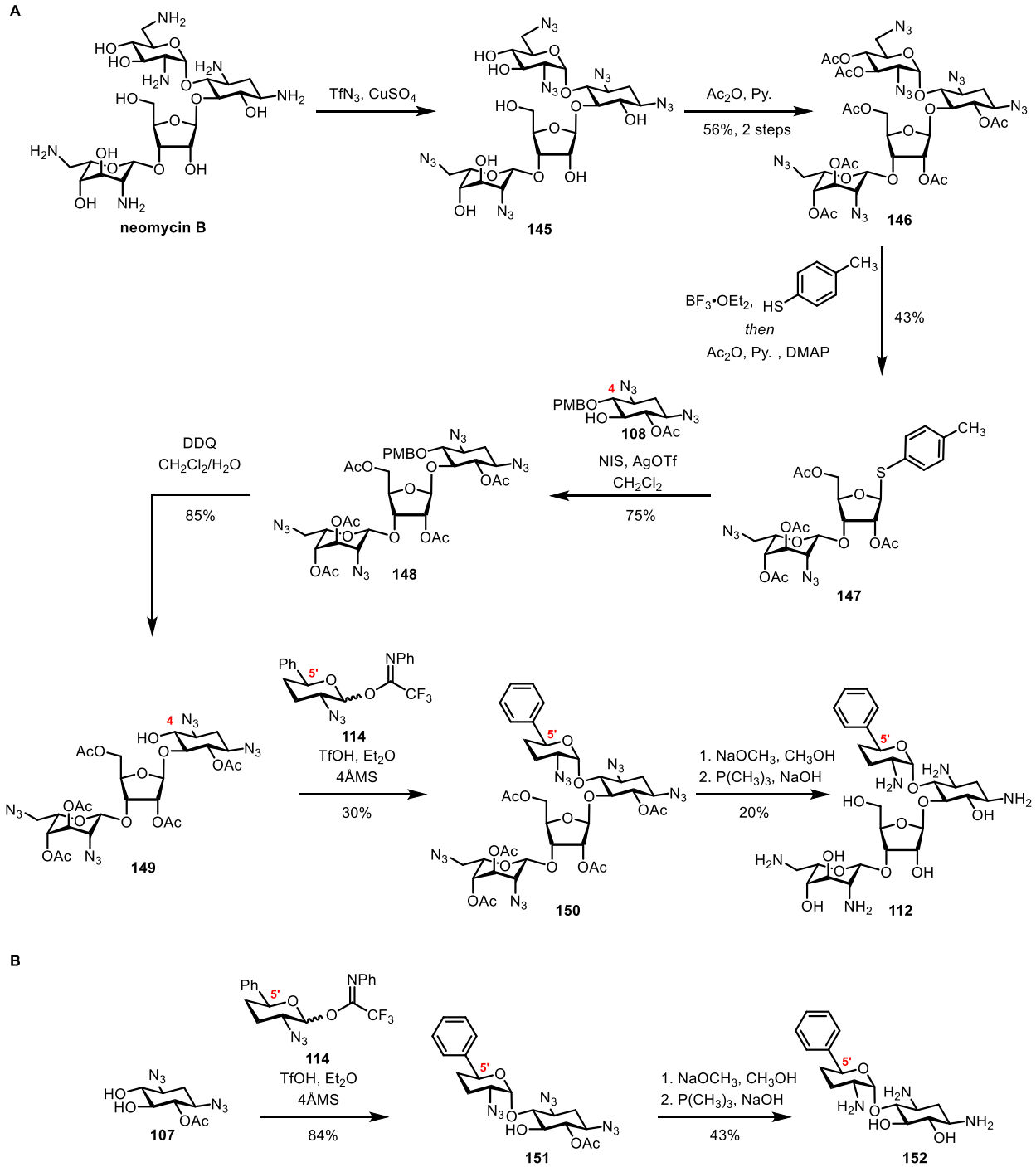

Figure 4.16. (A) Coupling of thioglycoside **147** and acceptor **108** en route to **149**. Glycosylation between **114** and **149** proceeds in poor yield but facilitates access to C5'-phenyl analog **112**. (B) Pseudodisaccharide analog **152** is prepared by coupling of **107** and **114** with subsequent deprotection.

trifluoride etherate, giving access to **147** by trapping the intermediate oxocarbenium with *p*-thiocresol. The byproduct neamine triacetate **103** could be separated following acetylation to isolate **147** in 43% yield. Glycosylation between **108** and **147** was promoted by activation of the thioglycoside with *N*-iodosuccinimide and silver (I) triflate, giving PMB-protected acceptor **148**. Deprotection of the PMB group was accomplished with DDQ, giving **149** in 85% yield. Unfortunately, the glycosylation between newly prepared **149** and glycosyl donor **114** proceeded only in 30% yield, attributable to the reduced nucleophilicity of the disarmed peracetylated acceptor **149**. While deprotection of tetrasaccharide **150** could be achieved by methanolysis of the acetate esters and global azide reduction to give **112**, we determined this strategy would not be suitable for the preparation of structurally diverse C5'-aryl aminoglycosides; this was due both to the poor glycosylation reactivity and the early stage at which diversity of the aryl group was

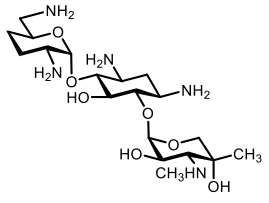

Gentamicin C1a

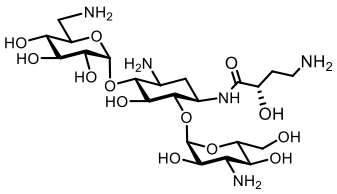

Amikacin

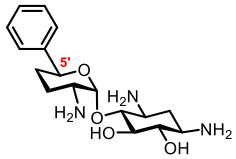

152

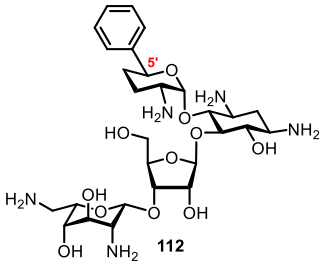

112

Species	Strain Description	Gentamicin	Amikacin	152	112
E. coli	ATCC 25922	2	1	>32	16
E. coli	D*tolC*	1	2	>32	16
E. coli	*LptD*	0.5	1	>32	16
E. coli	*MM294+pGB2 WT*	1	4	>32	>32
E. coli	MM294+pGB2 *armA*	>256	>256	>32	>32
E. coli	MM294+pGB2 *npmA*	32	64	>32	4
S. aureus	ATCC 29213	2	4	>32	32

Figure 4.17. Activity of C5'-phenyl analogs against *E. coli* expressing RMT resistance determinants.

introduced. Coupling of diol **107** with **114** proceeded with high regioselection for the C4-hydroxyl, giving **151** in 84% yield alongside 15% of the C5-glycosylated coproduct. Attempted unions of **147** with **151** gave only succinimide adduct and no glycosylation product. Antibiotic candidates **112** and **152** were prepared and evaluated against *E. coli* harboring *npmA* (Figure 4.17). Gratifyingly, **112** rescues the aminoglycoside structure from NpmA resistance exclusively, and has limited antimicrobial activity in the absence of methylated A1408. These data establish C5'-arylation as a potential avenue of development for AGAs seeking to overcome NpmA resistance.

4.5 Synthesis and reactivity of an aminoglycoside 4'-deoxypentenoside.

Several methods for the functionalization of C6-acids of carbohydrates were explored in the development of an aminoglycoside C5'-arylation reaction. Starting with perazidated paromomycin **134**, benzylidene acetal formation could instead be achieved with catalytic copper

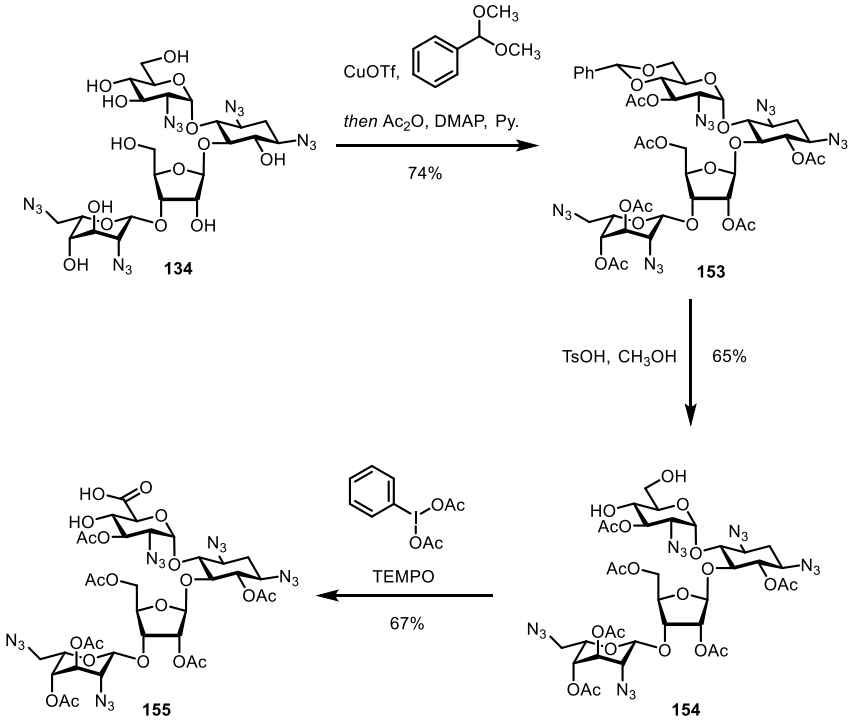

Figure 4.18. Synthesis of 6'-acid **155** from perazidated paromomycin **134**.

(I) triflate and benzaldehyde dimethyl acetal, generating **135** in solution (Figure 4.18).[27] Quenching of the reaction and direct addition of pyridine, acetic anhydride, and DMAP yielded fully protected **153** in 74% yield; copper (I) triflate as acetalization promoter provides significant advantages by removing a tedious workup of formic acid and benzaldehyde as well as removing a chromatographic purification to allow a one-pot acetylation.[28] Tosic acid deprotection of the benzylidene acetal gave **154**, and subsequent primary alcohol oxidation was accomplished with bis-acetoxy iodobenzene (BAIB) and TEMPO to give C6'-acid aminoglycoside **155**. Aminoglycoside 6'-amides were hypothesized to participate in weak hydrogen bonding with

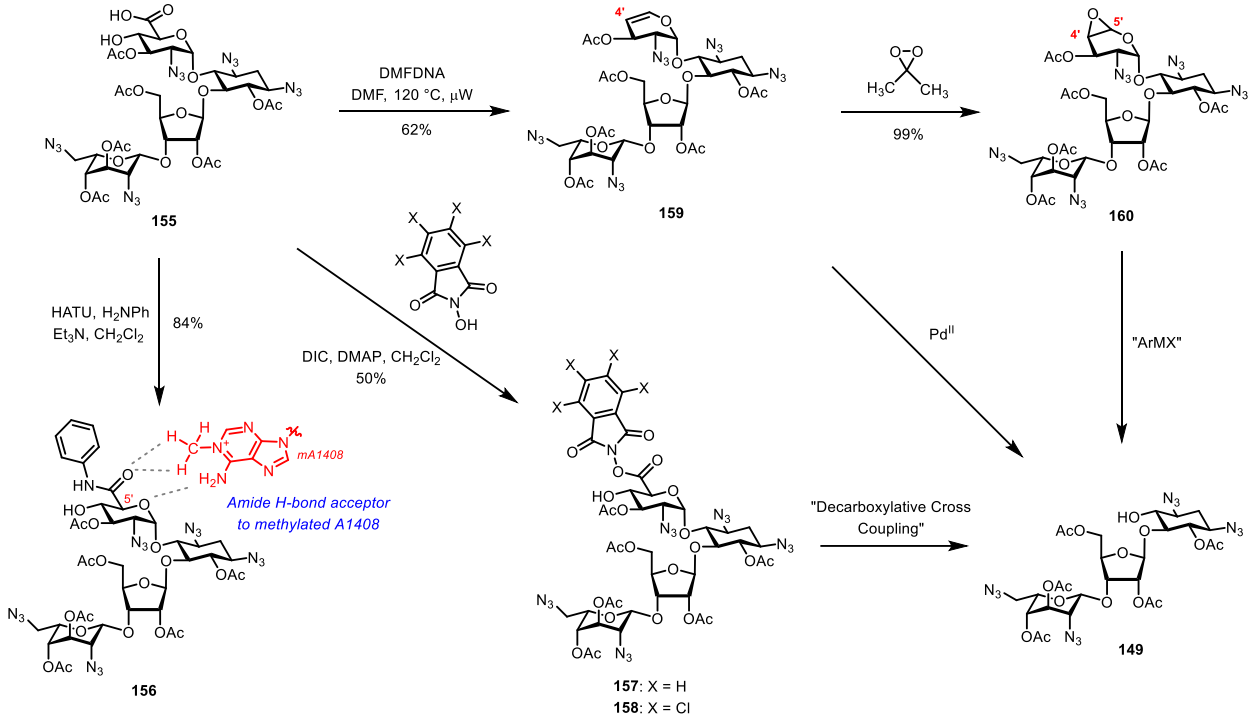

Figure 4.19. Reactivity of 6'-acid **155** primarily results in ring I cleavage.

methylated A1408, and thus HATU mediated coupling of **155** with aniline hydrochloride gave **156** (Figure 4.19). Unfortunately, amide **156** and related products from peptide coupling displayed hydrolytic instability during the deprotection and purification steps. The primary 6'-amide of

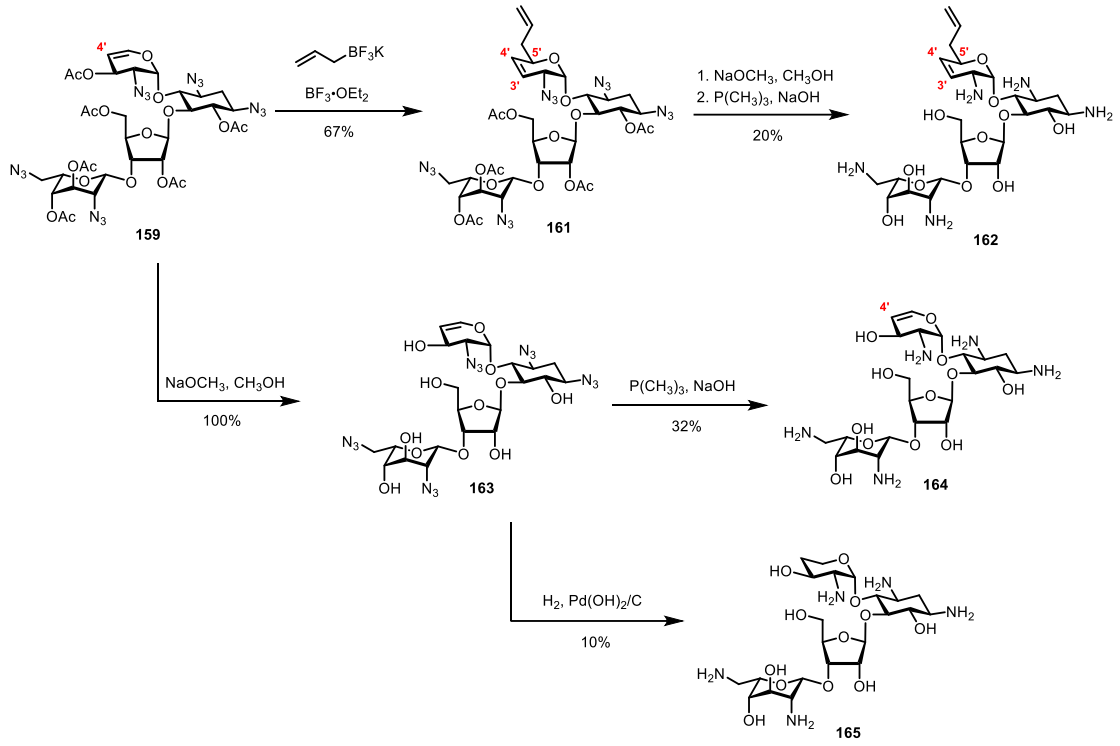

Figure 4.20. Synthesis of analogs **162**, **164**, and **165** from 4'-deoxypentenoside **159**.

neamine has been previously reported[29] and additionally results in a several-hundred fold loss of ribosomal inhibition activity, suggesting that these amide compounds would likely be inactive as antimicrobial candidates. Inspired by recent developments in decarboxylative arylation methodologies,[30] I prepared the phthalimide esters **157** and **158** from **155** by DIC coupling, affording both the tetrahydro and tetrachloro analogs in 50% yield. However, all methods explored for anomeric radical generation returned acid **155** from hydrolysis upon workup, or in some cases pseudotrisaccharide **149** was obtained as the sole product of ring I cleavage. Turning to a collection of literature on the reactivity of 4'-deoxypentenosides from Alexander Wei,[31] I prepared 4'-deoxypentenoside **159** from **155** by inducing decarboxylative elimination with dimethylformamide dineopentyl acetal (DMFDNA). I envisioned the allylic acetate would serve as a suitable leaving group for C5' functionalization. Transition metal-mediated methods for allylic

acetate displacement resulted exclusively in fragmentation between ring I and ring II, returning **149**. Epoxidation of **159** was cleanly achieved with cold solutions of dimethyl dioxirane (DMDO), giving 4'-epoxypentenoside **160** in >95% yields. A broad survey of organometallic reagent couplings revealed that attempts to arylate C5' of the epoxide resulted only in decomposition or ring I loss, again giving **149**.

A serendipitous discovery identified the type I Ferrier reactivity of **159** that could facilitate coupling with trifluoroborate salts (Figure 4.20).[34] The exploratory reaction between **159** and potassium allyltrifluoroborate gratifyingly generated **161** in 67% as a single diastereomer, migrating the olefin with loss of the C3' acetate. Expanding this chemistry to aryl trifluoroborate reagents has resulted in decomposition or regeneration of pseudotrisaccharide **149**. Deprotection by sequential acetate methanolysis and Staudinger reduction[35] provided aminoglycoside **162** following ion-exchange resin chromatography in 20% yield. Deoxypentenoside **159** was quantitatively deacetylated to give polyhydroxylated **163**, whose deprotection via trimethylphosphine or palladium-mediated hydrogenation afforded **164** and **165**, respectively. Antibiotic candidates **162**, **164**, and **165** were evaluated for antimicrobial activity against *E. coli* to determine their activity against ribosomal methyltransferase expressing strains. All compounds from this study exhibited complete loss of activity, including *E. coli* lacking membrane or efflux system integrity (Figure 4.21). Alongside the minimal inhibitory concentrations of **127**, **130**, and **133**, these data display a definitive correlation between loss of A1408 interaction and loss of antibiotic efficacy. The pseudodisaccharide heptopyranosides demonstrate that A1408 methylation cannot be circumvented by homologation of the ring I sugar to gain binding affinity elsewhere in

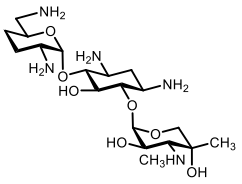

Gentamicin C1a

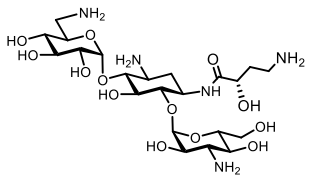

Amikacin

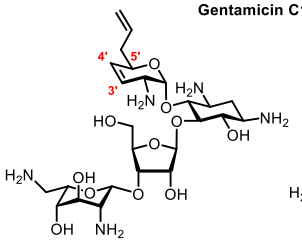

162

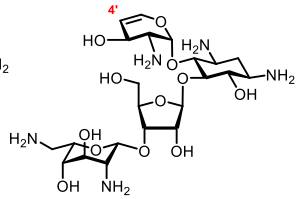

163

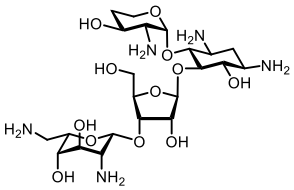

164

Species	Strain Description	Gentamicin	Amikacin	162	164	165
E. coli	ATCC 25922	2	1	>32	>32	>32
E. coli	D*tolC*	1	2	>32	>32	>32
E. coli	*LptD*	0.5	1	>32	>32	>32
E. coli	*MM294+pGB2 WT*	1	4	>32	>32	>32
E. coli	MM294+pGB2 *armA*	>256	>256	>32	>32	>32
E. coli	MM294+pGB2 *npmA*	32	64	>32	>32	>32
S. aureus	ATCC BAA-977 *ermB*	2	4	>32	>32	>32

Fi

str

the ribosome. Likewise, truncation of the sugar to avoid clashing with methylated A1408 fails to retain activity, as mechanistically interaction with A1408 is critical to reduce the fidelity of bacterial translation.

4.5 Summary

I have developed the synthesis of C5-allyl and C5-aryl glycosyl donors for the generation of new aminoglycoside antibiotics and incorporated them into pseudodisaccharide and pseudotetrasaccharide antibiotic candidates, respectively. The syntheses rely on diastereoselective functionalization of aldehyde **118** by Leighton's allylation reagent or the CBS reduction of phenyl ketone **140**. Trihaloacetimidate reagents prepared from the respective lactols facilitated the couplings with cyclohexane acceptors **106**, **107**, **113**, and **149**. New aminoglycoside antibiotics

were assessed against *E. coli* where it was determined the loss of interaction with A1408 on ring I was highly deleterious to antimicrobial activity. Both the C5-allyl derived heptopyranosides and the deoxypentenoside-derived pseudotetrasaccharides failed to overcome methyltransferase resistance, and additionally lacked activity against wild type strains. The C5'-arylation capabilities for aminoglycosides appear limited based on the chemistry explored herein, but initial studies indicate that this motif may be beneficial against NpmA resistance, as determined from the susceptibility of NpmA-expressing *E. coli* to **112**.

Moving forward, we hope that the chemistry described herein paves a path to the discovery of new aminoglycoside antibiotics. With routes to analogs of significant structural diversity, the next-generation aminoglycoside library will hopefully empower our antibiotic arsenal against the highly concerning methyltransferase resistance phenotypes.

4.6 References

1. Ramirez, M. S.; Tolmasky, M. E. *Drug Resist. Updat.* **2010**, *13*, 151.

2. Doi, Y; Wachino, J.-I., Arakawa, Y.; *Infect. Dis. Clin. N. Am.* **2016**, *30*, 523.

3. Galimand, M.; Sabtcheva, S.; Courvalin, P.; Lambert, T. *Antimicrob. Agents Chemother.* **2005**, *49*, 2949.

4. Wachino, J. I.; Shibayama, K.; Kurokawa, H.; Kimura, K.; Yamane, K.; Suzuki, S.; Shibata, N.; Ike, Y.; Arakawa, Y. *Antimicrob. Agents Chemother*. **2007**, *51*, 4401.

5. Kanazawa, H.; Baba, F.; Koganei, M.; Kondo, J. *Nucleic Acids Res.* **2017**, *45*, 12529.

6. Cox, G.; Ejim, L.; Stogios, P.J.; Koteva, K.; Bordeleau, E.; Evdokimova, E.; Sieron, A.O.; Savchenko, A.; Serio, A.W.; Krause, K.M.; Wright, G.D. *ACS Infect. Dis.* **2018**, *4*, 980.

7. Ishizaki, Y.; Shibuya, Y.; Hayashi, C.; Inoue, K.; Kirikae, T.; Tada, T.; Miyoshi-Akiyama, T.; Igarashi, M. *J. Antibiot.* **2018**, *71*, 798.

8. Gallivan, J. P.; Dougherty, D. A. *Proc. Natl. Acad. Sci. U. S. A.* **1999**, *96*, 9459.

9. Philips, K.D.; Zemlicka, J.; Horwitz, J.P. *Carbohydr. Res.* **1973**, *30*, 281.

10. van den Broek, S. A. M. W.; Gruijters, B. W. T.; Rutjes, F. P. J. T.; van Delft, F. L.; Blaauw, R. H. J. Org. Chem. 2007, 72, 3577.

11. Sonousi, A.; Vasella, A.; Crich, D. J. Org. Chem. 2020, 85, 7583.

12. Titz, A.; Marra, A.; Cutting, B.; Smieško, M.; Papandreou, G.; Dondoni, A.; Ernst, B. *Eur. J. Org. Chem.* **2012**, *28*, 5534.

13. Titz, A.; Radic, Z.; Schwardt, O.; Ernst, B. *Tetrahedron Lett.* **2006**, *47*, 2383.

14. Liu, F. Development of a Component-Based Synthesis for the Discovery of New Aminoglycoside Antibiotics, and Diastereoselective Michael-Claisen Cyclizations En Route to 5-Oxatetracyclines. Ph.D. thesis, Harvard University, Cambridge, MA United States, 2017.

15. Kinnaird, J. W. A.; Ng, P. Y.; Kubota, K.; Wang, X.; Leighton, J. L. J. Am. Chem. Soc. 2002, 124, 7920.

16. (a) Bongat, A.F.G.; Demchenko, A.V. *Carbohydr. Res.* **2007**, *342*, 374. (b) Bennett, C.S.; Galan, M.C. *Chem. Rev.* **2018**, *118*, 7931.

17. Das, R.; Mukhopadhyay, B. *ChemistryOpen* **2016**, *5*, 401.

18. Nyffeler, P.T.; Lian, C.-H.; Koeller, K.M.; Wong, C.-H. *J. Am. Chem. Soc.* **2002**, *124*, 10773.
19. Mori, Y.; Seki, M. *J. Org. Chem.* **2003**, *68*, 1571.

20. Lioy, V. S.; Goussard, S.; Guerineau, V.; Yoon, E. J.; Courvalin, P.; Galimand, M.; Grillot-Courvalin, C. *Rna* **2014**, *20*, 382.

21. Minowa, N.; Akiyama, Y.; Hiraiwa, Y.; Maebashi, K.; Usui, T.; Ikeda, D. *Bioorg. Med. Chem. Lett.* **2006**, *16*, 6351.

22. Bal, B.S.; Childers, W.E.; Pinnick, H.W. *Tetrahedron*, **1981**, *37*, 2091.

23. Tang, S.-Q.; Bricard, J.; Schmitt, M.; Bihel, F. *Org. Lett.*, **2019**, *21*, 844.

24. Salunkhe, A.M.; Burkhardt, E.R. *Tetrahedron Lett.* **1997**, *38*, 1523.

25. Hanessian, S.; Adhikari, S.; Szychowski, J.; Pachamuthu, K.; Wang, X.; Migawa, M.T.; Griffey, R.H.; Swayze, E.E. *Tetrahedron* **2007**, *63*, 827.

26. Wu, B.; Yang, J.; He, Y.; Swayze, E.E. *Org. Lett.* **2002**, *4*, 3455.

27. Perez-Fernandez, D.; Shcherbakov, D.; Matt, T.; Leong, N. C.; Kudyba, I.; Duscha, S.; Boukari, H.; Patak, R.; Dubbaka, S. R.; Lang, K.; Meyer, M.; Akbergenov, R.; Freihofer, P.; Vaddi, S.; Thommes, P.; Ramakrishnan, V.; Vasella, A.; Böttger, E. C. *Nat. Commun.* **2014**, *5*, 1.

28. Tran, A.-T.; Jones, R.A.; Pastor, J.; Boisson, J.; Smith, N.; Galan, M.C. *Adv. Synth. Catal.* **2001**, *353*, 2593.

29. Simonsen, K.B.; Ayida, B.K.; Vourloumis, D.; Takahashi, M.; Winters, G.C.; Barluenga, S.; Qamar, S.; Shandrick, S.; Zhao, Q.; Hermann, T. *ChemBioChem* **2002**, *2*, 1223.
30. Laudadio, G.; Palkowitz, M.D.; Ewing, T.E.-H.; Baran, P.S. *ACS Med. Chem. Lett.* **2022**, *13*, 1413.

31. (a) Boulineau, F.P.; Wei, A. *Org. Lett.* **2002**, *4*, 2281 (b) Boulineau, F.P.; Wei, A. *Org. Lett.* **2004**, *6*, 119. (c) Boulineau, F.P.; Wei, A. *J. Org. Chem.* **2004**, *69*, 3391. (d) Cheng, G.; Boulineau, F.P.; Liew, S.-T.; Shi, Q.; Wenthold, P.G.; Wei, A. *Org. Lett.* **2006**, *8*, 4545. (e) Cheng, G.; Fan, R.; Hernández-Torres, J.M.; Boulineau, F.P.; Wei, A. *Org. Lett.* **2007**, *9*, 4849. (f) Alberch, L.; Cheng, G.; Seo, S.-K.; Li, X.; Boulineau, F.P.; Wei, A. *J. Org. Chem.* **2011**, *76*, 2532. (g) Padungros, P.; Fan, R.-H.; Casselman, M.D.; Cheng, G.; Khatri, H.R.; Wei, A. *J. Org. Chem.* **2014**, *79*, 4878.

32. Hara, S.; Taguchi, H.; Yamamoto, H.; Nozaki, H. *Tetrahedron Lett.* **1975**, *19*, 1545.

33. Taber, D.F.; DeMatteo, P.W.; Hassan, R.A. *Org. Synth.* **2013**, *90*, 350.

34. Molander, G.A.; Sandrock, D.L. *Curr. Opin. Drug Discov. Devel.* **2009**, *12*, 811.

35. Quirke, J. C. K.; Rajasekaran, P.; Sarpe, V. A.; Sonousi, A.; Osinnii, I.; Gysin, M.; Haldimann, K.; Fang, Q.; Shcherbakov, D.; Hobbie, S. N.; Sha, S.; Schacht, J.; Vasella, A.; Bottger, E. C.; Crich, D. *J. Am. Chem. Soc.* **2020**, *142*, 530.

36. Still, W.C.; Khan, M.; Mitra, A. *J. Org. Chem.* **1978**, *43*, 2923.

4.7 Experimental Section

General Experimental Procedures. All reactions were performed in flame-dried round-bottom flasks fitted with rubber septa under positive argon pressure, unless otherwise noted. Air- and moisture-sensitive liquids were transferred via syringe. Organic solutions were concentrated by rotary evaporation (house vacuum, ca. 25-40 Torr) at ≤40 °C, unless otherwise noted. Analytical thin-layer chromatography (TLC) was performed using glass plates precoated with silica gel (0.25 mm, 60 Å pore-size, 230-400 mesh, Merck KGA) impregnated with a fluorescent indicator (254 nm). TLC plates were visualized by exposure to ultraviolet light, then stained with an aqueous potassium permanganate ($KMnO_4$), aqueous Ceric Ammonium Molybdate (CAM), ethanolic ninhydrin, or ethanolic bromocresol green stain and briefly heated using a heat gun; visualization of deprotected aminoglycosides was also achieved by exposing the plate to 20% sulfuric acid in ethanol and charring with a heat gun. Flash-column chromatography was performed as described by Still et al.,[36] employing silica gel (60 Å, 15-40 μM, EMD Millipore Corp.). All temperature measurements of reaction mixtures refer to the temperature of the heating/cooling bath unless otherwise specified. Structural assignments were made with additional information from gCOSY, gHSQC, and gHMBC experiments. Sephadex resin chromatography was performed by allowing 10 g of CM Sephadex-C25 to swell overnight in 125 mL DI water at 4 °C and stirred vigorously until homogenous. The mixture was then poured onto a column, and 50 mL 5% aqueous ammonium hydroxide, 50 mL 5% saturated aqueous ammonium chloride, and 250 mL DI water were used in sequence to condition the column. The crude aminoglycoside deprotection was loaded onto the column using a small amount of 10% aqueous acetic acid, and 250 mL of DI was eluted followed by increasing amounts of ammonium hydroxide solution; generally, 20 mL eluent batches were used increasing by 0.1% and grading from 0.1% to 0.7% ammonium hydroxide solution.

Products were detected using a combination of TLC, staining with ninhydrin *and* 20% sulfuric acid in methanol to verify fractions, and mass spectrometry. The combined fractions were acidified using glacial acetic acid (150 μL) and lyophilized to give acetate salts of the products.

Materials. Commercial solvents and reagents were used as received.

Instrumentation. Proton magnetic resonance (^{1}H NMR) spectra were recorded on Bruker 400 (400 MHz) NMR spectrometers at 23 °C. Proton chemical shifts are expressed in parts per million (ppm, δ scale) and are referenced to residual protium in the NMR solvent ($CHCl_3$, δ 7.26, CD_3OD, δ 3.45, C_6D_6, δ 7.16, D_2O δ 4.79). Data are represented as follows: chemical shift, multiplicity (s = singlet, d = doublet, t = triplet, q = quartet, p = quintet, m = multiplet and/or multiple resonances, br = broad), coupling constant (*J*) in Hertz (Hz) and integration. Carbon nuclear magnetic resonance spectra (^{13}C NMR) were recorded on Bruker 400 (100 MHz) NMR spectrometers at 23 °C. Carbon chemical shifts are expressed in parts per million (ppm, δ scale) and are referenced to the carbon resonances of the NMR solvent ($CDCl_3$, δ 77.16, CD_3OD, δ 49.03 and C_6D_6, δ 128.06). Infrared (IR) spectra were obtained using a Bruker ALPHA FT-IR spectrometer. Data are represented as follows: frequency of absorption (cm^{-1}), intensity of absorption (s = strong, m = medium, w = weak, br = broad). High resolution mass spectra were obtained at the Harvard University Mass Spectrometry Facility using the Thermo Q Exactive Plus Orbitrap mass spectrometer via Electrospray Ionization (ESI).

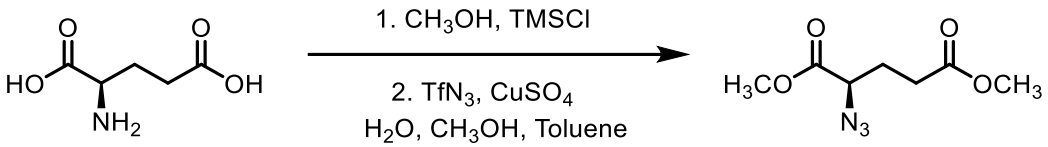

D-glutamatic acid **117**

dimethyl (*R*)-2-azidopentanedioate (117)

Diesterification of D-glutamate:

A solution of D-glutamate (5.00 g, 34.0 mmol, 1 equiv) was cooled to 0 °C and trimethylsilyl chloride (19 mL, 150 mmol, 4.4 equiv) was added dropwise over 10 minutes. The cooling bath was removed, the solution stirred for 18 hours, and the solvents then removed under vacuum. The crude dimethyl-glutamate was dried under high vacuum for 2 hours.

Preparation of TfN_3:

Sodium azide (9.72 g, 149 mmol, 4.4 equiv) in a 1:1 mixture of water and toluene (50 mL total) was stirred vigorously and cooled to 0 °C. Trifluoromethane sulfonic anhydride (12.6 mL, 74.7 mmol, 2.2 equiv) was added dropwise and the solution stirred for 30 minutes at 0 °C. The cooling bath was removed, and the solution stirred at room temperature for 1 hour. The reaction was quenched by addition of saturated aqueous sodium bicarbonate (12 mL) and the phases separated. The aqueous was washed with toluene (2 x 20 mL) and the combined organic phases (totaling 75 mL) produce a ~1 M solution of TfN_3.

Diazotransfer to dimethyl D-glu:

Crude dimethyl glutamate as a solution in water (44 mL) was cooled to 0 °C and copper (II) sulfate pentahydrate (424 mg, 1.70 mmol, 0.05 equiv) and sodium bicarbonate (11.41 g, 136 mmol, 4 equiv) were added in sequence. The stirring mixture was diluted with methanol (295 mL), and the solution of TfN_3 in toluene was added dropwise. The mixture was allowed to warm to room

temperature and stirred for an additional 2.5 hours. The solution was then filtered through a fritted funnel and saturated aqueous ammonium chloride solution (30 mL) was added. The volatile solvents were removed by rotary evaporation and the remaining aqueous residue extracted with diethyl ether (3 x 50 mL). The combined organic layers were washed with saturated aqueous sodium carbonate (2 x 50 mL) and brine (50 mL), then dried over sodium sulfate. The filtered and concentrated crude material was further purified by flash chromatography on silica, grading from hexanes to 30% ethyl acetate in hexanes, giving the product azide **117** as a clear oil (6.23 g, 31.2 mmol, 92%).

R_f: (25% Ethyl acetate in hexanes, $KMnO_4$): 0.28

^1H NMR (400 MHz, $CDCl_3$): δ 4.00 (dd, J = 8.7, 5.1 Hz, 1H), 3.79 (s, 3H), 3.68 (s, 3H), 2.56 – 2.37 (m, 2H), 2.18 (dtd, J = 14.2, 7.5, 5.1 Hz, 1H), 2.00 (dddd, J = 14.1, 8.7, 7.5, 6.5 Hz, 1H).

$^{13}C\{^1H\}$ NMR (101 MHz, $CDCl_3$): δ 172.77, 170.54, 61.12, 52.84, 51.94, 29.91, 26.58.

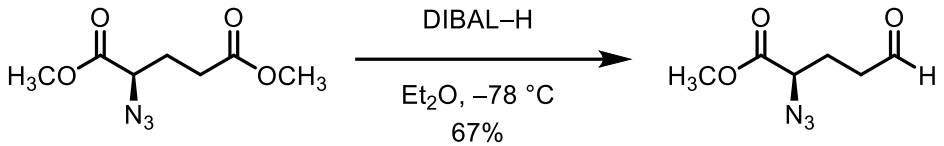

117 **118**

methyl (*R*)-2-azido-5-oxopentanoate (118)

A solution of diester **117** (2.00 g, 9.94 mmol, 1 equiv) in diethyl ether (100 mL) was cooled to - 78 °C and diisobutylaluminum hydride (25% in toluene, 8.02 mL, 11.9 mmol, 1.2 equiv) was added dropwise over 6 minutes. The solution was stirred at this temperature for 2.5 hours; water (34 mL) was added at - 78 °C and the resulting suspension allowed to warm slowly to room temperature with stirring. The opaque gel that formed was filtered through Celite®, eluting with additional ether (250 mL), and the concentrated residue purified by flash chromatography on silica, grading from 20–60% diethyl ether in hexanes to yield aldehyde **118** (1.14 g, 6.65 mmol, 67%). *Caution: aldehyde **118** is volatile and the usage of ether for purification is advised to avoid the need for extending drying on a vacuum pump.*

R_f: (25% Ethyl acetate in hexanes, $KMnO_4$): 0.44

^1H NMR (400 MHz, $CDCl_3$): δ 9.78 (s, 1H), 4.01 (dd, J = 8.4, 5.2 Hz, 1H), 3.80 (s, 3H), 2.62 (ddt, J = 7.3, 6.5, 1.0 Hz, 2H), 2.19 (dtd, J = 14.5, 7.3, 5.2 Hz, 1H), 2.01 (dddd, J = 14.5, 8.4, 7.3, 6.5 Hz, 1H).

$^{13}C\{^1H\}$ NMR (101 MHz, $CDCl_3$): δ 200.33, 170.50, 61.06, 52.91, 39.68, 23.91.

HRMS (ESI-TOF) m/z: $[M+NH_4]^+$ Calcd for $C_6H_{13}N_4O_3$ 189.0982; Found 189.0983.

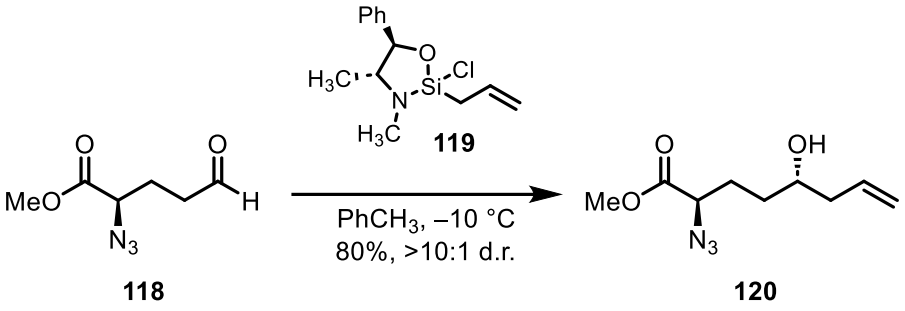

methyl (*2R,5S*)-2-azido-5-hydroxyoct-7-enoate (120)

A solution of silane reagent **119** (1.90 g, 7.10 mmol, 1.5 equiv) in toluene (18 mL) was cooled to - 10 °C and aldehyde **118** (810 mg, 4.73 mmol, 1 equiv) as a toluene solution (6 mL) was added dropwise over 3 minutes. The solution stirred at - 10 °C for 2.5 hours, and 10% (w/w) citric acid (19 mL) and ethyl acetate (19 mL) were added. The biphasic mixture was vigorously stirred for 15 minutes, and the phases separated. The aqueous was washed with additional ethyl acetate (2 x 25 mL) and the combined organic phases were dried on magnesium sulfate, filtered, and concentrated. Purification by flash chromatography on silica gel, grading from 15–50% ethyl acetate in hexanes provided the product **120** as a yellow oil (790 mg, 3.70 mmol, 78%, >10:1 dr).

R_f: (50% Ethyl acetate in hexanes, $KMnO_4$): 0.49

^1H NMR (400 MHz, $CDCl_3$): δ 5.80 (dddd, J = 16.5, 11.2, 7.9, 6.6 Hz, 1H), 5.18 – 5.11 (m, 2H), 3.92 (dd, J = 8.6, 5.0 Hz, 1H), 3.79 (s, 3H), 3.72 – 3.60 (m, 1H), 2.37 – 2.25 (m, 1H), 2.23 – 2.14 (m, 1H), 2.13 – 2.01 (m, 1H), 1.87 – 1.76 (m, 1H), 1.72 (brd, J = 3.0 Hz, 1H), 1.64 (ddd, J = 19.3, 9.8, 4.6 Hz, 1H), 1.58 – 1.48 (m, 1H).

$^{13}C\{^1H\}$ NMR (101 MHz, $CDCl_3$): δ 171.1, 134.3, 118.8, 70.3, 62.3, 52.7, 42.3, 32.8, 28.1.

FTIR (neat), cm^{-1}: 3412 (br), 2930 (w), 2102 (s), 1740 (s), 1437 (w), 1203 (m), 1076 (m).

HRMS (ESI-TOF) m/z: $[M+H]^+$ Calcd for $C_9H_{16}N_3O_3Na$ 214.1186; Found 214.1187.

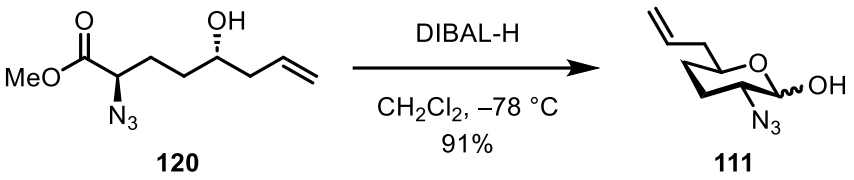

(*3R,6S*)-6-allyl-3-azidotetrahydro-*2H*-pyran-2-ol (111)

A solution of hydroxyester **120** (790 mg, 3.70 mmol, 1 equiv) in anhydrous dichloromethane (37 mL) was cooled to - 78 °C and DIBAL-H (25% weight in toluene, 6.23 mL, 9.26 mmol, 2.5 equiv) was added dropwise. The reaction was stirred for 1.25 hours, then quenched by the addition of propionaldehyde (430 mL, 1.5 eq) and 1 N hydrochloric acid (11 mL). The mixture was allowed to warm to room temperature and diluted with water (20 mL) and brine (5 mL). The separated dichloromethane layer was washed with brine (100 mL), and the combined aqueous phases were washed with ethyl acetate (3 x 50 mL). The combined ethyl acetate layers were washed with brine (100 mL), and the organic phases were all combined, dried on sodium sulfate, filtered, and concentrated. Purification by flash chromatography on silica gel, grading from hexanes to 20% ethyl acetate in hexanes provided lactol **111** as a white solid (618 mg, 3.37 mmol, 91%, 1:1 a:b).

R_f: (50% Ethyl acetate in hexanes, $KMnO_4$): 0.63

^{1}H NMR (400 MHz, $CDCl_3$): δ 5.87 – 5.72 (m, 2H, H7'α,β), 5.24 (d, J = 3.1 Hz, 1H, H1'α), 5.17 – 4.98(m, 4H, H8'α,β), 4.56 (dd, J = 7.5, 5.1 Hz, 1H, H1'β), 4.09 – 3.98 (m, 1H, H5'α), 3.62 (d, J = 5.0 Hz, 1H, OHβ), 3.57 – 3.43 (m, 1H, H5'β), 3.20 (ddd, J = 12.9, 9.2, 5.2 Hz, 2H, H2'α,β), 3.06 (d, J = 3.0 Hz, 1H, OHα), 2.44 – 2.14 (m, 4H, H6'α,β), 1.94 – 1.76 (m, 2H), 1.74 – 1.64 (m, 2H), 1.51 – 1.20 (m, 4H).

$^{13}C\{^{1}H\}$ NMR (101 MHz, $CDCl_3$): δ 134.5 (C7'α), 134.1 (C7'β), 117.7 (C8'β), 117.4 (C8'α), 98.4 (C1'β), 92.2 (C1'α), 75.8 (C5'β), 67.7 (C5'α), 62.1 (C2'β), 58.6 (C2'α), 39.8 (C6'α,β), 30.0 (α), 29.7 (β), 28.1 (β), 22.1 (α).

FTIR (neat), cm^{-1}: 3383 (br), 2932 (w), 2102 (s), 1740 (s), 1299 (w), 1065 (w).

HRMS (ESI-TOF) m/z: $[M+Na]^+$ Calcd for $C_8H_{13}N_3O_2Na$ 206.0900; Found 206.0900.

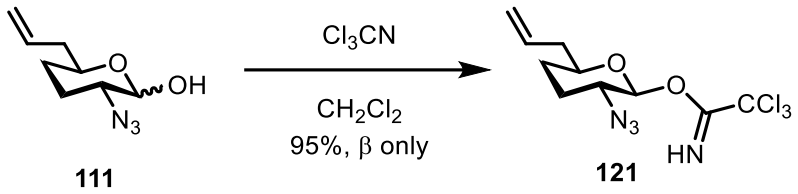

(*2S,3R,6S*)-6-allyl-3-azidotetrahydro-*2H*-pyran-2-yl 2,2,2-trichloroacetimidate (121)

A solution of lactol **111** (15 mg, 0.082 mmol, 1 equiv) in dichloromethane (4.5 mL) was treated with trichloroacetonitrile (82 mL, 0.82 mmol, 10 equiv)) and cesium carbonate (5.3 mg, 0.016 mmol, 0.2 equiv). The solution was stirred for 1 hour and filtered through a cotton plug. The resulting trichloroacetimidate product **121** (25.5 mg, 0.078 mmol, 95%) was suitably pure and used in glycosylation reactions without purification. *Note: trichloroacetimidates are known to decompose on silica, affording the trichloroacetamide.*

R_f (20 % ethyl acetate-hexanes, $KMnO_4$): 0.44

^{1}H NMR (400 MHz, C_6D_6): δ 8.61 (s, 1H, NH), 5.71 (d, J = 8.3 Hz, 1H, H1'), 5.77 – 5.60 (m, 1H, H7'), 5.09 – 4.86 (m, 2H, H8'), 3.10 (dddd, J = 13.3, 11.5, 7.2, 3.6 Hz, 2H, H2', H5'), 2.25 – 2.11 (m, 1H, H6'), 2.05 – 1.93 (m, 1H, H6'), 1.56 – 1.42 (m, 1H), 1.41 – 1.13 (m, 1H), 1.08 – 0.77 (m, 2H).

^{13}C NMR (100 MHz, C_6D_6): δ 161.7 (C=N), 134.5 (C7', 117.6 (C8'), 100.0 (C1'), 76.4 (C5'), 60.5 (C2'), 40.0 (C6'), 29.4, 28.5. (-CCl3 not observed)

FTIR (neat), cm^{-1}: 3341 (w), 2929 (w), 2103 (s), 1674 (s), 1294 (m), 1046 (s).

HRMS (ESI-TOF) m/z: $[M+Na]^+$ $C_{10}H_{13}Cl_3N_4O_2Na$ 350.9967; Found: 350.9964.

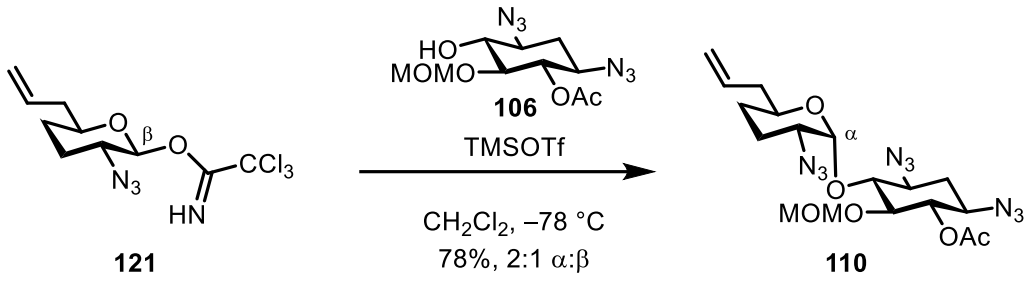

(*1S,2S,3R,4S,6R*)-3-(((*2R,3R,6S*)-6-allyl-3-azidotetrahydro-*2H*-pyran-2-yl)oxy)-4,6-diazido-2-(methoxymethoxy)cyclohexyl acetate (110)

Glycosyl donor **121** (1.09 g, 3.33 mmol, 2 equiv) and 2-DOS acceptor **106** (500 mg, 1.67 mmol, 1 equiv) were combined with a stir bar in a flame-dried flask and concentrated from toluene 3x, then dried under high vacuum for an additional 0.5 hours. The mixture was dissolved in anhydrous dichloromethane (17 mL) and cooled to - 78 °C under Ar atmosphere. TMSOTf (60 mL, 0.333 mmol, 0.2 equiv) was then added dropwise and the reaction stirred for 1.5 hours. Quenching with triethylamine (0.5 mL), warming to room temperature, filtering through Celite®, and concentrating provided the crude material. Purification was achieved by flash chromatography on silica gel, grading from hexanes to 50% ethyl acetate in hexanes, to provide product as a mixture of anomers **110** (483 mg, 1.04 mmol, 62%, 2:1 a:b). *Reactions tended to perform with higher yields on smaller scale. The addition of mol. sieves can help with dryness on a smaller scale.*

R_f (50 % ethyl acetate-hexanes, CAM): 0.70

^{1}H NMR (500 MHz, $CDCl_3$): δ 5.86 – 5.75 (m, 2H, H7'α,β), 5.40 (d, J = 3.5 Hz, 1H, H1'α), 5.13 – 5.03(m, 4H, H8'α,β), 4.99 – 4.89 (m, 3H, H6α,β, MOM-CH2 β), 4.82 (d, J = 6.8 Hz, 1H, MOM-CH2 α), 4.73 (d, J = 6.9 Hz, 1H, MOM-CH2 α), 4.61 (d, J = 7.9 Hz, 1H, H1'β), 4.59 (d, J = 7.2 Hz, 1H, MOM-CH2 β), 4.12 (dtd, J = 8.5, 6.3, 2.3 Hz, 1H, H5'α), 3.71 – 3.63 (m, 1H, H4α), 3.60 – 3.52 (m, 3H, H5α,β, H4β), 3.43 (dddd, J = 29.8, 12.5, 10.0, 4.5 Hz, 5H, H1α,β, H3α,β, H5'β),

3.33 (s, 3H, MOM-CH3 β), 3.31 (s, 3H, MOM-CH3α), 3.22 – 3.14 (m, 1H, H2'β), 3.09 (ddd, J = 12.7, 4.3, 3.8 Hz, 1H, H2'α), 2.36 – 2.25 (m, 4H, H6'α,β, H2α,β), 2.21 (ddd, J = 14.1, 6.8, 2.7 Hz, 2H, H6'α,β), 2.16 (s, 3H, COCH3 β), 2.15 (s, 3H, COCH3 α), 2.08 (ddd, J = 25.4, 12.7, 3.8 Hz, 2H, H3'α,β), 1.96 – 1.80 (m, 3H, H3'α,β, H4'α), 1.69 – 1.63 (m, 1H, H4'β), 1.56 (q, J = 12.7 Hz, 2H, H2α,β), 1.49 – 1.37 (m, 1H, H4'α), 1.36 – 1.25 (m, 1H, H4'β).

^{13}C NMR (125 MHz, $CDCl_3$): δ 170.3 (C=O α), 170.1 (C=O β), 134.4 (7'α), 134.1 (7'β), 117.6 (8'β), 117.3 (8'α), 104.3 (1'β), 99.9 (MOM-CH2 α), 98.5 (MOM-CH2 β), 98.1 (1'α), 84.6 (5α), 81.6 (5β), 77.9 (4β), 77.4 (4α), 75.5 (5'β), 74.8 (6α), 74.6 (6β), 68.1 (5'α), 61.1 (1a,β/3α,β), 61.1 (2'β), 59.8 (1a,β/3α,β), 58.5 (1a,β/3α,β), 58.5 (1a,β/3α,β), 58.1 (2'α), 56.8 (MOM-CH3 β), 56.0 (MOM-CH3 α), 39.9 (6'α), 39.9 (6'β), 32.3 (2α), 32.2 (2β), 29.9 (4'α), 29.7 (4'β), 28.3 (3'β), 22.3 (3'α), 21.3 (COCH3 α), 21.2 (COCH3 β).

FTIR (neat), cm^{-1}: 2947 (w), 2101 (s), 1748 (m), 1373 (m), 1226 (m), 1036 (m).

HRMS (ESI-TOF) m/z: $[M+Na]^+$ $C_{18}H_{27}N_9O_6Na$ 488.1977; Found: 488.1977.

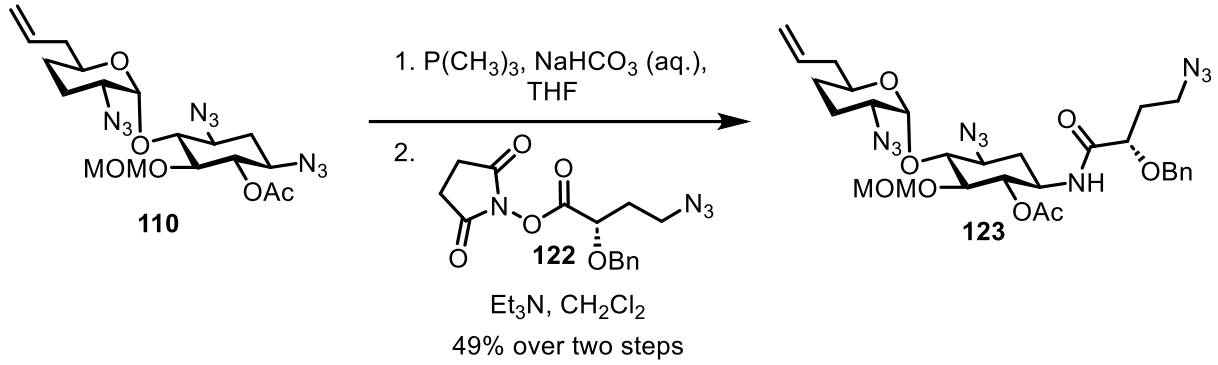

(*1S,2S,3R,4S,6R*)-3-(((*2R,3R,6S*)-6-allyl-3-azidotetrahydro-*2H*-pyran-2-yl)oxy)-4-azido-6-((*S*)-4-azido-2-(benzyloxy)butanamido)-2-(methoxymethoxy)cyclohexyl acetate (123)

A solution of allyl glycoside **110** (77 mg, 0.17 mmol, 1 equiv) in THF (0.7 mL) was treated with saturated aqueous sodium bicarbonate (0.1 mL) and trimethylphosphine solution (1 M in THF, 182 mL, 0.182 mmol, 1.1 equiv) in sequence at room temperature. The reaction stirred for 2.5 hours, then was quenched by the addition of diethyl ether (3 mL), saturated aqueous sodium carbonate (0.2 mL), and brine (0.5 mL). The layers were separated, and the aqueous washed with additional ether (2 x 3 mL). The combined organic layers were dried on sodium sulfate, filtered, and concentrated to give crude intermediate *N1*-amine (not depicted).

The crude amine was dissolved in anhydrous dichloromethane (1 mL) alongside HABA chain **122** (66 mg, 0.20 mmol, 1.2 equiv) and DIPEA was added (87 mL, 0.50 mmol, 3 equiv) at room temperature. The solution stirred overnight, and was quenched by the addition of ethyl acetate (3 mL) and 10% w/w citric acid solution (1 mL). The separated aqueous layer was washed with ethyl acetate (2 x 3 mL), and the combined organics dried on sodium sulfate, filtered, and concentrated to give the crude material. Purification by flash chromatography provided *N1*-amide **123** (53 mg, 0.081 mmol, 49%). *Minor impurities from HABA chain starting material*.

^{1}H NMR (500 MHz, $CDCl_3$): δ 7.43 – 7.31 (m, 5H, -OCH2Ph), 6.70 (d, J = 8.5 Hz, 1H, NH), 5.82 (ddt, J = 17.2, 10.2, 7.0 Hz, 1H, H7'), 5.40 (d, J = 3.4 Hz, 1H, H1'), 5.14 – 5.03 (m, 2H, H8'), 4.82 (d, J = 6.7 Hz, 1H, MOM-CH2), 4.85 – 4.75 (m, 1H, H6), 4.74 (d, J = 6.7 Hz, 1H, MOM-CH2), 4.58 (d, J = 11.9 Hz, 1H, -OCH2Ph), 4.52 (d, J = 11.8 Hz, 1H, -OCH2Ph) 4.20 – 4.11 (m, 1H, H5'), 4.02 – 3.95 (m, 1H, H1), 3.93 (dd, J = 8.0, 4.2 Hz, 1H, H2''), 3.69 – 3.57 (m, 2H, H4, H5), 3.47 – 3.41 (m, 1H, H3), 3.34 (dd, J = 7.3, 6.4 Hz, 1H, H4''), 3.30 (s, 3H, MOM-CH3) 3.11 – 3.05 (m, 1H, H2'), 2.30 (dt, J = 13.3, 6.6 Hz, 1H, H6'), 2.22 (ddd, J = 12.9, 8.5, 4.3 Hz, 1H, H6', H2), 2.14 – 2.04 (m, 1H, H3'), 2.07 (s, 3H, COCH3), 2.02 – 1.94 (m, 1H, H3''), 1.92 – 1.81 (m, 3H, H3'', H3', H4'), 1.42 (ddd, J = 16.9, 13.0, 3.4 Hz, 1H, H4'), 1.28 (dd, J = 25.2, 12.4 Hz, 1H, H2). ^{13}C NMR (100 MHz, $CDCl_3$): δ 172.0(C=O), 171.7 (C=O), 136.8 (OCH2Ph), 134.5 (7'), 129.0 (OCH2Ph), 128.7 (OCH2Ph), 128.3 (OCH2Ph), 117.2 (8'), 99.3 (MOM-CH2), 98.3 (1'), 83.9 (5), 77.8 (4), 77.4 (2''), 74.5 (6), 73.6 (OCH2Ph), 68.1 (5'), 59.8 (3), 58.1 (2'), 56.5 (MOM-CH3), 47.6 (1), 47.4 (4''), 40.0 (6'), 33.0 (2), 32.2 (3''), 29.9 (4'), 22.4 (3'), 21.2 (COCH3). FTIR (neat), cm^{-1}: 3351 (br), 2944 (w), 2101 (s), 1733 (w), 1663 (w), 1531 (w), 1247 (m), 1029 (m).

HRMS (ESI-TOF) m/z: $[M+H]^+$ $C_{29}H_{41}N_{10}O_8$ 657.3103; Found: 657.3104.

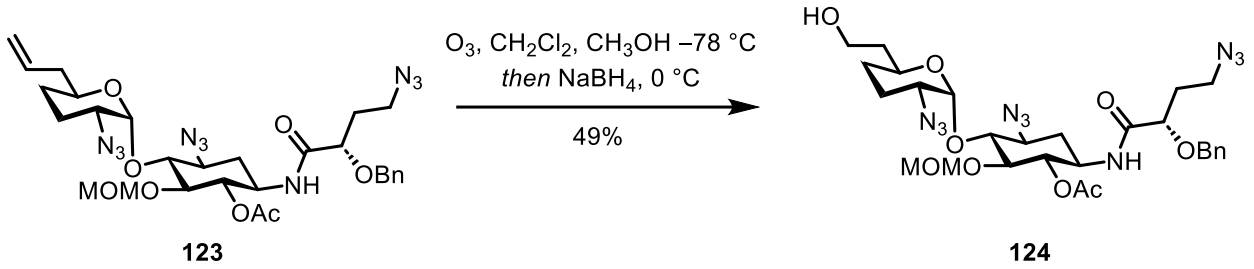

(*1S,2S,3R,4S,6R*)-4-azido-6-((*S*)-4-azido-2-(benzyloxy)butanamido)-3-(((*2R,3R,6S*)-3-azido-6-(2-hydroxyethyl)tetrahydro-*2H*-pyran-2-yl)oxy)-2-(methoxymethoxy)cyclohexyl acetate (124)

A stream of ozone was passed through a solution of pseudodisaccharide **123** (53.0 mg, 0.081 mmol, 1 equiv) in dichloromethane (1.0 mL) and methanol (1.0 mL) at - 78 °C until the solution took a light blue color. Stirring continued for 5 minutes and the residual ozone was then removed by bubbling nitrogen through the solution. The solution was warmed to 0 °C and sodium borohydride (15.3 mg, 0.404 mmol, 5 equiv) was added in two portions over 1 hour. The solution was then poured onto saturated aqueous ammonium chloride solution (1.0 mL) and the mixture washed with ethyl acetate (5 mL). The aqueous was washed with additional ethyl acetate (3 x 5 mL), and the combined organic layers dried on sodium sulfate, filtered, and concentrated. The crude material was purified by flash chromatography on silica gel, grading from 30–70% ethyl acetate in hexanes to provide alcohol **124** (26.0 mg, 0.039 mmol, 49%) as a colorless oil.

R_f: (100% Ethyl acetate in hexanes, $KMnO_4$): 0.61

^{1}H NMR (400 MHz, $CDCl_3$): δ 7.43 – 7.30 (m, 5H), 6.71 (d, J = 8.5 Hz, 1H), 5.43 (d, J = 3.4 Hz, 1H), 4.84 – 4.78 (m, 2H), 4.74 (d, J = 6.7 Hz, 1H), 4.54 (q, J = 11.8 Hz, 2H), 4.31 – 4.22 (m, 1H), 4.03 – 3.95 (m, 1H), 3.92 (dd, J = 8.0, 4.1 Hz, 1H), 3.81 (ddd, J = 11.4, 7.4, 4.1 Hz, 1H), 3.73 (ddd, J = 11.0, 6.3, 4.4 Hz, 1H), 3.66 (t, J = 8.7 Hz, 1H), 3.57 (t, J = 9.1 Hz, 1H), 3.54 – 3.46 (m, 1H),

3.38 – 3.32 (m, 2H), 3.31 (s, 3H), 3.09 (dt, J = 12.7, 4.2 Hz, 1H), 2.23 (dt, J = 12.9, 4.3 Hz, 1H), 2.18 – 2.08 (m, 1H), 2.07 (s, 3H), 1.95 (dddd, J = 25.1, 17.4, 7.8, 4.0 Hz, 2H), 1.83 (ddd, J = 14.0, 7.9, 5.1 Hz, 2H), 1.79 – 1.63 (m, 2H), 1.51 (ddd, J = 25.3, 13.2, 3.7 Hz, 1H), 1.29 (dd, J = 23.0, 10.6 Hz, 1H).

$^{13}C\{^{1}H\}$ NMR (101 MHz, $CDCl_3$): δ 172.0, 171.6, 136.7, 129.0, 128.7, 128.3, 99.4, 97.7, 84.0, 77.7, 77.3, 74.5, 73.6, 67.2, 60.1, 57.9, 56.6, 47.6, 47.4, 38.0, 33.1, 32.1, 30.8, 22.3, 21.1.

FTIR (neat), cm^{-1}: 3344 (br). 2944 (w), 2098 (s), 1732 (m), 1663 (m), 1527 (m), 1240 (s), 1027 (s).

HRMS (ESI-TOF) m/z: $[M+H]^+$ Calcd for $C_{28}H_{41}N_{10}O_9$ 661.3052; Found 661.3054.

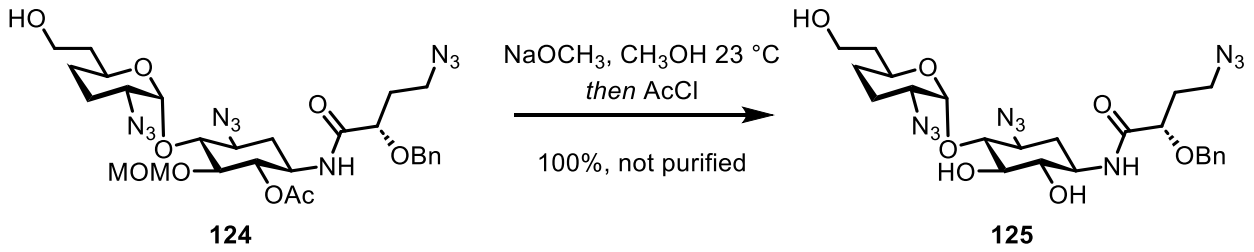

124 **125**

(*S*)-4-azido-N-((*1R,2S,3R,4R,5S*)-5-azido-4-(((*2R,3R,6S*)-3-azido-6-(2-hydroxyethyl)tetrahydro-*2H*-pyran-2-yl)oxy)-2,3-dihydroxycyclohexyl)-2-(benzyloxy)butanamide (125)

A solution of alcohol **124** (14.0 mg, 0.021 mmol, 1 equiv) in methanol (0.3 mL) was treated with sodium methoxide solution (0.5 M in methanol, 212 mL, 0.106 mmol, 5.00 equiv) at 23 °C. Stirring proceeded for 2 hours at ambient conditions, and the mixture was then cooled to 0 °C while acetyl chloride (23 mL, 0.318 mmol, 15.00 equiv) was added. The mixture was allowed to warm to room temperature and stirred for an additional 2 hours before being poured onto a mixture of ethyl acetate (5.0 mL) and saturated aqueous sodium bicarbonate solution (0.5 mL). The layers were separated and the aqueous washed with ethyl acetate (2 x 5.0 mL). The combined organic phases were dried on sodium sulfate, filtered, and concentrated to provide crude triol **125** (quantitative) which was used without further purification.

^{1}H NMR (500 MHz, $CDCl_3$): δ 7.44 – 7.30 (m, 5H), 6.68 (d, J = 7.9 Hz, 1H), 5.31 (d, J = 3.3 Hz, 1H), 4.62 (d, J = 11.6 Hz, 1H), 4.53 (d, J = 11.6 Hz, 1H), 4.21 (ddd, J = 11.4, 7.5, 3.6 Hz, 1H), 4.01 (dd, J = 6.7, 4.7 Hz, 1H), 3.97 (brs, 1H), 3.91 – 3.70 (m, 3H), 3.56 (dd, J = 12.8, 5.5 Hz, 1H), 3.51 – 3.33 (m, 6H), 3.29 (t, J = 9.7 Hz, 1H), 2.63 (brs, 1H), 2.23 (dt, J = 12.9, 4.4 Hz, 1H), 2.14 – 1.99 (m, 3H), 1.97 – 1.87 (m, 1H), 1.87 – 1.79 (m, 1H), 1.77 – 1.65 (m, 2H), 1.51 (ddd, J = 25.4, 13.5, 3.9 Hz, 1H), 1.36 (dd, J = 25.1, 12.5 Hz, 1H).

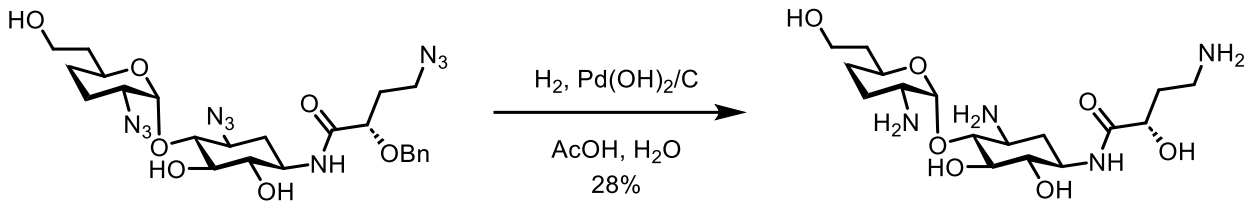

125 **127**

(*S*)-4-amino-N-((*1R,2S,3R,4R,5S*)-5-amino-4-(((*2R,3R,6S*)-3-amino-6-(2-hydroxyethyl)tetrahydro-*2H*-pyran-2-yl)oxy)-2,3-dihydroxycyclohexyl)-2-hydroxybutanamide (127)

To a solution of triol **125** (12.2 mg, 0.021 mmol, 1.00 equiv) in 4:1 acetic acid:water (1.0 mL total) was added palladium hydroxide on carbon (20% w/w, 30.0 mg, 0.043 mmol, 2.00 equiv) at 23 °C. The atmosphere was exchanged by briefly evacuating the flask, and backfilling with hydrogen and then flushing with hydrogen for 5 minutes. The heterogenous mixture stirred for 7 hours and was then filtered through a Celite® plug, washing with water (10 mL). The filtrate was concentrated under vacuum and treated with ammonium hydroxide solution (10 mM, 6.0 mL) and concentrated under vacuum. The remaining residue was purified by preparative HPLC on a Waters XBridge BEH C18 column [5 μm, 250 × 10 mm, UV detection at 210 nm, solvent A: 10 mM ammonium hydroxide in water, solvent B: 10 mM ammonium hydroxide in acetonitrile, injection volume: 2.0 mL (10 mM NH3, water), 0 % B for 5 min then gradient elution with 0→20 % B over 15 min, flow rate: 5 mL/min]. The product containing fractions were combined and treated with 2 N HCl (30 mL) and concentrated under vacuum to give **127** as the trihydrochloride salt (3.1 mg, 6.01 mmol , 28%).

^{1}H NMR (500 MHz, D_2O): δ 8.37 (d, J = 8.9 Hz, 1H), 5.51 (d, J = 3.4 Hz, 1H), 4.35 (dd, J = 8.0,

4.0 Hz, 1H), 4.18 – 4.09 (m, 1H), 3.94 (ddd, J = 11.9, 10.4, 4.1 Hz, 1H), 3.86 – 3.80 (m, 1H), 3.77 – 3.70 (m, 2H), 3.66 (t, J = 9.2 Hz, 1H), 3.61 – 3.49 (m, 3H), 3.24 – 3.13 (m, 2H), 2.29 (dt, J = 12.7, 4.1 Hz, 1H), 2.19 (tdd, J = 11.0, 7.4, 4.0 Hz, 1H), 2.08 – 1.97 (m, 3H), 1.93 (dd, J = 13.5, 10.7 Hz, 2H), 1.79 (tt, J = 19.2, 9.5 Hz, 3H), 1.63 – 1.52 (m, 1H).

HRMS (ESI-TOF) m/z: $[M+H]^+$ Calcd for $C_{17}H_{35}N_4O_7$ 407.2500; Found 407.2501.

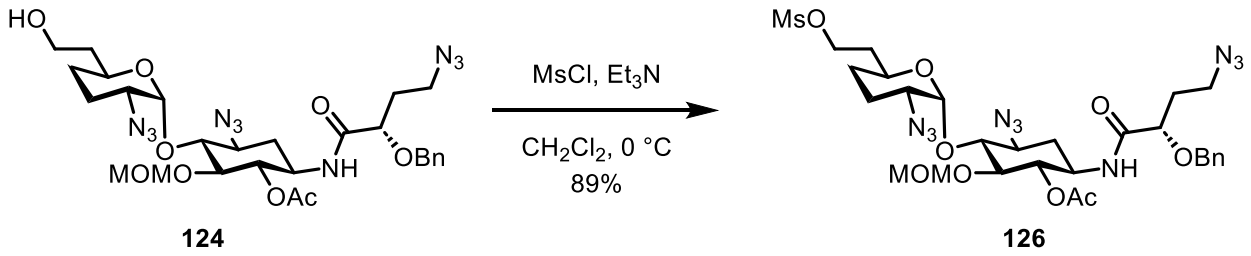

124 **126**

(*1S,2S,3R,4S,6R*)-4-azido-6-((*S*)-4-azido-2-(benzyloxy)butanamido)-3-(((*2R,3R,6S*)-3-azido-6-(2-((methylsulfonyl)oxy)ethyl)tetrahydro-*2H*-pyran-2-yl)oxy)-2-(methoxymethoxy)cyclohexyl acetate (126)

A solution of alcohol **124** (27.0 mg, 0.041 mmol, 1.00 equiv) in dichloromethane (0.8 mL) at 0 °C was treated with triethylamine (11 mL, 0.082 mmol, 2.00 equiv) and methanesulfonyl chloride (4.8 mL, 0.061 mmol, 1.50 equiv) in sequence. After 20 minutes, the solution was poured onto a biphasic mixture of saturated aqueous ammonium chloride (1.0 mL) and ethyl acetate (3.0 mL). The layers were separated and the aqueous extracted with additional ethyl acetate (2 x 5.0 mL). The combined organic layers were dried on sodium sulfate, filtered, and concentrated to provide crude mesylate **126** which was used without additional purification (27.0 mg, 0.037 mmol, 89%).

R_f: (50% Ethyl acetate in hexanes, $KMnO_4$): 0.31

^{1}H NMR (500 MHz, $CDCl_3$): δ 7.43 – 7.30 (m, 5H), 6.71 (d, J = 8.7 Hz, 1H), 5.47 (d, J = 3.3 Hz, 1H), 4.87 – 4.79 (m, 2H), 4.74 (d, J = 6.6 Hz, 1H), 4.53 (s, 2H), 4.43 – 4.37 (m, 1H), 4.36 – 4.30 (m, 1H), 4.22 (dd, J = 11.7, 8.7 Hz, 1H), 3.98 (td, J = 12.8, 4.5 Hz, 1H), 3.91 (dd, J = 8.1, 4.1 Hz, 1H), 3.69 – 3.64 (m, 2H), 3.54 – 3.46 (m, 1H), 3.37 – 3.33 (m, 1H), 3.32 (s, 3H), 3.07 (dt, J = 12.8, 3.8 Hz, 1H), 3.02 (s, 3H), 2.24 – 2.10 (m, 2H), 2.06 (s, 3H), 1.99 – 1.78 (m, 6H), 1.53 – 1.35 (m, 2H).

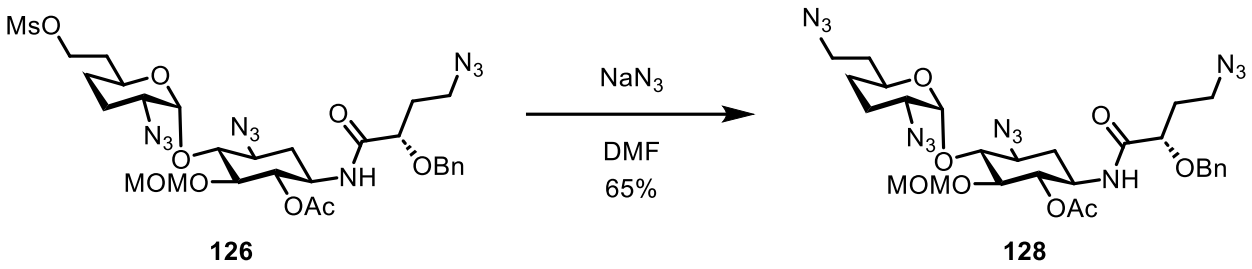

(*1S,2S,3R,4S,6R*)-4-azido-6-((*S*)-4-azido-2-(benzyloxy)butanamido)-3-(((*2R,3R,6S*)-3-azido-6-(2-azidoethyl)tetrahydro-*2H*-pyran-2-yl)oxy)-2-(methoxymethoxy)cyclohexyl acetate (128)

A solution of mesylate **126** (17.0 mg, 0.023 mmol, 1.00 equiv) in DMF (0.2 mL) was treated with sodium azide (6.0 mg, 0.092 mmol, 4.00 equiv) at 23 °C and stirring proceeded for 21 hours. The solution was diluted with ethyl acetate (1.0 mL), filtered, and concentrated to provide crude material. Purification by flash chromatography on silica gel, grading from 20 – 40% ethyl acetate in hexanes provided azide **128** as a white foam (10.2 mg, 0.015 mmol, 65%).

R_f: (50% Ethyl acetate in hexanes, $KMnO_4$): 0.51

^{1}H NMR (500 MHz, $CDCl_3$): δ 7.44 – 7.29 (m, 5H), 6.68 (d, J = 8.5 Hz, 1H), 5.44 (d, J = 3.2 Hz, 1H), 4.88 – 4.78 (m, 2H), 4.74 (dd, J = 6.6, 1.4 Hz, 1H), 4.57 (d, J = 11.8 Hz, 1H), 4.51 (d, J = 11.8 Hz, 1H), 4.25 – 4.12 (m, 1H), 4.04 – 3.95 (m, 1H), 3.93 (dd, J = 8.0, 4.1 Hz, 1H), 3.63 (dt, J = 18.3, 8.8 Hz, 2H), 3.54 – 3.37 (m, 3H), 3.37 – 3.32 (m, 2H), 3.32 (s, 3H), 3.12 – 3.03 (m, 1H), 2.21 (dt, J = 13.2, 4.4 Hz, 1H), 2.16 – 2.08 (m, 1H), 2.07 (s, 3H), 2.03 – 1.78 (m, 5H), 1.73 (dd, J = 13.3, 6.6 Hz, 2H), 1.46 (dd, J = 23.4, 11.5 Hz, 1H), 1.30 (dd, J = 24.6, 12.0 Hz, 2H).

HRMS (ESI-TOF) m/z: $[M+H]^+$ Calcd for $C_{28}H_{40}N_{13}O_8$ 686.3117; Found 686.3116.

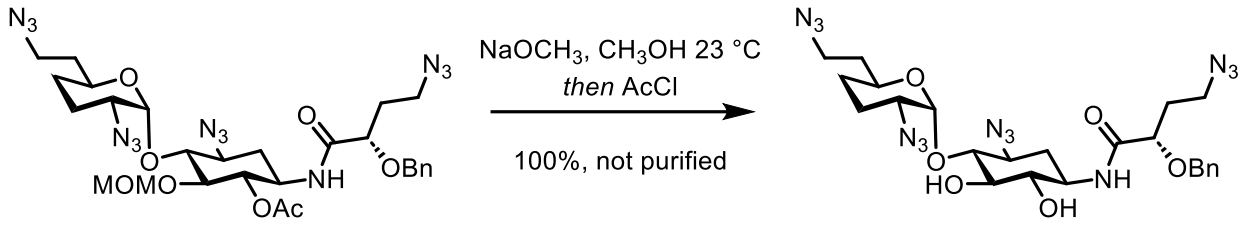

(*S*)-4-azido-N-((*1R,2S,3R,4R,5S*)-5-azido-4-(((*2R,3R,6S*)-3-azido-6-(2-azidoethyl)tetrahydro-*2H*-pyran-2-yl)oxy)-2,3-dihydroxycyclohexyl)-2-(benzyloxy)butanamide (129)

A solution of azide **128** (10.2 mg, 0.015 mmol, 1.00 equiv) in methanol (0.3 mL) was treated with sodium methoxide solution (0.5 M in methanol, 149 mL, 0.074 mmol, 5.00 equiv) at 23 °C. Stirring proceeded for 2 hours at ambient conditions, and the mixture was then cooled to 0 °C while acetyl chloride (16 mL, 0.223 mmol, 15.00 equiv) was added. The mixture was allowed to warm to room temperature and stirred for an additional 2 hours before being poured onto a mixture of ethyl acetate (5.0 mL) and saturated aqueous sodium bicarbonate solution (0.5 mL). The layers were separated and the aqueous washed with ethyl acetate (2 x 5.0 mL). The combined organic phases were dried on sodium sulfate, filtered, and concentrated to provide crude diol **129** (quantitative) which was used without further purification.

^{1}H NMR (500 MHz, $CDCl_3$): δ 7.45 – 7.30 (m, 5H), 6.62 (d, J = 7.7 Hz, 1H), 5.31 (d, J = 3.2 Hz, 1H), 4.64 (d, J = 11.6 Hz, 1H), 4.53 (d, J = 11.6 Hz, 1H), 4.15 – 4.07 (m, 1H), 4.03 (dd, J = 6.5, 4.8 Hz, 1H), 3.90 – 3.81 (m, 1H), 3.71 (d, J = 2.3 Hz, 1H), 3.56 (td, J = 9.0, 2.3 Hz, 1H), 3.51 – 3.35 (m, 7H), 3.29 (td, J = 9.9, 3.0 Hz, 1H), 3.22 (d, J = 3.1 Hz, 1H), 2.23 (dt, J = 13.1, 4.4 Hz, 1H), 2.14 – 2.00 (m, 3H), 1.97 – 1.91 (m, 1H), 1.84 (dd, J = 13.5, 2.7 Hz, 1H), 1.75 (dt, J = 12.1, 4.3 Hz, 2H), 1.46 (ddd, J = 25.3, 13.3, 3.9 Hz, 1H), 1.34 (dd, J = 24.9, 12.4 Hz, 1H).

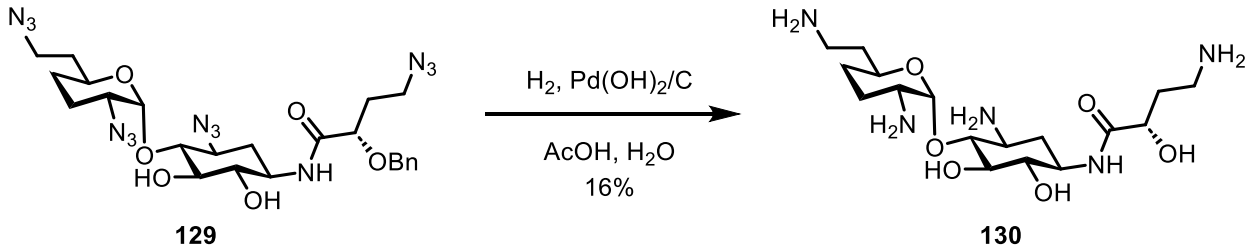

(*S*)-4-amino-N-((*1R,2S,3R,4R,5S*)-5-amino-4-(((*2R,3R,6S*)-3-amino-6-(2-aminoethyl)tetrahydro-*2H*-pyran-2-yl)oxy)-2,3-dihydroxycyclohexyl)-2-hydroxybutanamide (130)

To a solution of diol **129** (8.9 mg, 0.015 mmol, 1.00 equiv) in 4:1 acetic acid:water (1.0 mL total) was added palladium hydroxide on carbon (20% w/w, 20.0 mg, 0.029 mmol, 2.00 equiv) at 23 °C. The atmosphere was exchanged by briefly evacuating the flask, and backfilling with hydrogen and then flushing with hydrogen for 5 minutes. The heterogenous mixture stirred for 7 hours and was then filtered through a Celite® plug, washing with water (10 mL). The filtrate was concentrated under vacuum and treated with ammonium hydroxide solution (10 mM, 6.0 mL) and concentrated under vacuum. The remaining residue was purified by preparative HPLC on a Waters XBridge BEH C18 column [5 μm, 250 × 10 mm, UV detection at 210 nm, solvent A: 10 mM ammonium hydroxide in water, solvent B: 10 mM ammonium hydroxide in acetonitrile, injection volume: 2.0 mL (10 mM NH3, water), 0 % B for 5 min then gradient elution with 0→15 % B over 15 min, flow rate: 5 mL/min]. The product containing fractions were combined and treated with 2 N HCl (30 mL) and concentrated under vacuum to give **130** as the tetrahydrochloride salt (1.3 mg, 2.4 mmol , 16%).

^{1}H NMR (500 MHz, D_2O): δ 5.67 (d, J = 3.3 Hz, 1H), 4.35 (dd, J = 8.1, 4.0 Hz, 1H), 4.15 – 4.06 (m, 1H), 3.98 – 3.91 (m, 1H), 3.90 – 3.82 (m, 1H), 3.67 (t, J = 9.3 Hz, 1H), 3.61 – 3.48 (m, 3H),

3.22 – 3.10 (m, 4H), 2.34 – 2.27 (m, 1H), 2.19 (d, J = 4.7 Hz, 1H), 2.08 – 1.87 (m, 7H), 1.81 (dd, J = 25.2, 12.5 Hz, 2H), 1.63 (dd, J = 19.6, 11.7 Hz, 1H).

HRMS (ESI-TOF) m/z: $[M+H]^+$ Calcd for $C_{17}H_{36}N_5O_6$ 406.2660; Found 406.2659.

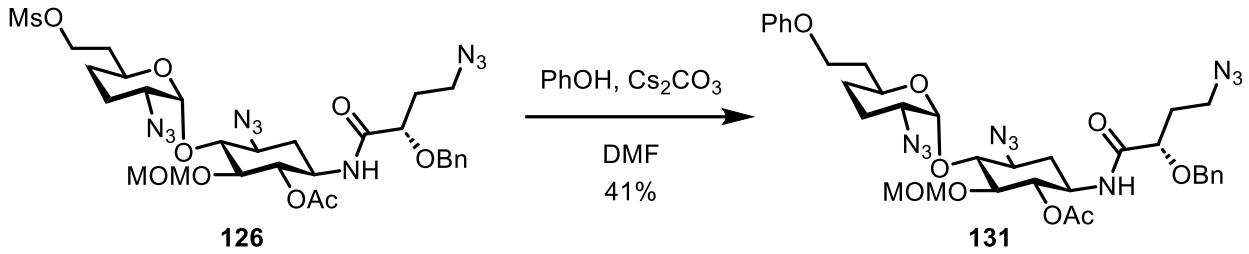

(*1S,2S,3R,4S,6R*)-4-azido-6-((*S*)-4-azido-2-(benzyloxy)butanamido)-3-(((*2R,3R,6S*)-3-azido-6-(2-phenoxyethyl)tetrahydro-*2H*-pyran-2-yl)oxy)-2-(methoxymethoxy)cyclohexyl acetate (131)

A solution of mesylate **126** (16.0 mg, 0.022 mmol, 1.00 equiv) and phenol (6.1 mg, 0.065 mmol, 3.00 equiv) in DMF (0.2 mL) was treated with cesium carbonate (21.2 mg, 0.065 mmol, 3.00 equiv) at 23 °C. The solution was allowed to stir for 23 hours, and then poured onto a mixture of ethyl acetate (1.0 mL) and saturated aqueous sodium bicarbonate (1.0 mL). The layers were separated, and the aqueous layer washed with ethyl acetate (2 x 5.0 mL). The combined organic layers were dried on sodium sulfate, filtered, and concentrated to provide crude material. Purification by flash chromatography on silica gel, grading from 20–40% ethyl acetate in hexanes yielded aryl ether **131** (6.6 mg, 9.0 mmol, 41%).

R_f: (50% Ethyl acetate in hexanes, $KMnO_4$): 0.47

^{1}H NMR (400 MHz, $CDCl_3$): δ 7.45 – 7.31 (m, 5H), 7.30 – 7.22 (m, 2H), 6.92 (dd, J = 7.8, 1.0 Hz, 2H), 6.89 – 6.80 (m, 1H), 6.52 (d, J = 8.8 Hz, 1H), 5.48 (d, J = 3.3 Hz, 1H), 4.83 – 4.77 (m, 1H), 4.73 (d, J = 5.7 Hz, 1H), 4.66 (t, J = 9.7 Hz, 1H), 4.54 (s, 2H), 4.33 (d, J = 11.9 Hz, 1H), 4.18 (dd, J = 15.6, 6.5 Hz, 1H), 4.06 – 3.99 (m, 1H), 3.98 – 3.86 (m, 2H), 3.62 (t, J = 9.3 Hz, 1H), 3.54 (t, J = 8.9 Hz, 1H), 3.46 – 3.38 (m, 1H), 3.37 – 3.33 (m, 1H), 3.32 (s, 3H), 3.11 (d, J = 12.7 Hz, 1H),

2.15 (q, J = 12.1 Hz, 1H), 2.06 (s, 3H), 2.03 – 1.77 (m, 6H), 1.57 – 1.45 (m, 1H), 0.90 (dd, J = 25.3, 12.5 Hz, 1H).

$^{13}C\{^{1}H\}$ NMR (101 MHz, $CDCl_3$): δ 171.9, 171.5, 159.1, 136.8, 129.7, 129.0, 128.7, 128.2, 120.7, 114.7, 99.2, 97.4, 83.6, 77.4, 77.3, 74.6, 73.5, 65.7, 64.1, 60.0, 58.1, 56.6, 47.4, 35.3, 32.9, 32.2, 30.7, 29.9, 22.4, 21.2.

FTIR (neat), cm^{-1}: 3351 (br). 2923 (w), 2100 (s), 1734 (m), 1668 (m), 1527 (m), 1244 (s), 1029 (s).

HRMS (ESI-TOF) m/z: $[M+H]^+$ Calcd for $C_{34}H_{45}N_{10}O_9$ 737.3365; Found 737.3361.

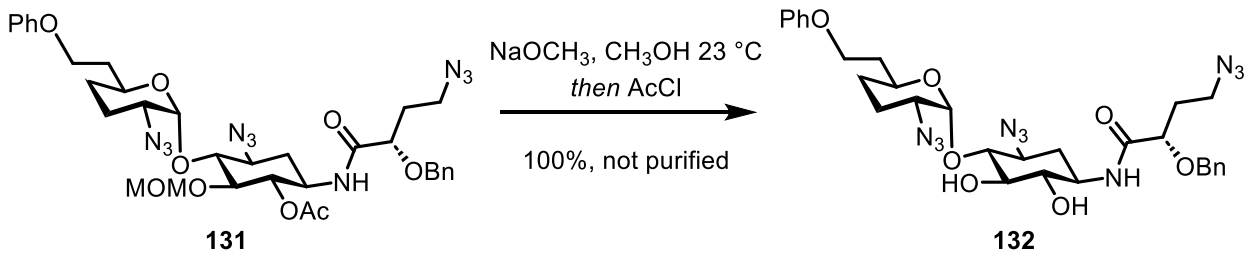

131 **132**

(*S*)-4-azido-N-((*1R,2S,3R,4R,5S*)-5-azido-4-(((*2R,3R,6S*)-3-azido-6-(2-phenoxyethyl)tetrahydro-*2H*-pyran-2-yl)oxy)-2,3-dihydroxycyclohexyl)-2-(benzyloxy)butanamide (132)

A solution of aryl ether **131** (6.6 mg, 0.009 mmol, 1.00 equiv) in methanol (0.3 mL) was treated with sodium methoxide solution (0.5 M in methanol, 90 mL, 0.045 mmol, 5.00 equiv) at 23 °C. Stirring proceeded for 2 hours at ambient conditions, and the mixture was then cooled to 0 °C while acetyl chloride (9.5 mL, 0.134 mmol, 15.00 equiv) was added. The mixture was allowed to warm to room temperature and stirred for an additional 2 hours before being poured onto a mixture of ethyl acetate (5.0 mL) and saturated aqueous sodium bicarbonate solution (0.5 mL). The layers were separated and the aqueous washed with ethyl acetate (2 x 5.0 mL). The combined organic phases were dried on sodium sulfate, filtered, and concentrated to provide crude diol **132** (quantitative) which was used without further purification.

^{1}H NMR (500 MHz, $CDCl_3$): δ 7.38 (dddd, J = 19.5, 8.2, 7.5, 3.0 Hz, 5H), 7.23 (dd, J = 8.6, 7.4 Hz, 2H), 6.90 (dd, J = 8.7, 0.9 Hz, 2H), 6.88 – 6.82 (m, 1H), 6.49 (d, J = 7.7 Hz, 1H), 5.38 (d, J = 3.3 Hz, 1H), 4.64 (d, J = 11.5 Hz, 1H), 4.53 (d, J = 11.5 Hz, 1H), 4.23 (dd, J = 11.8, 5.0 Hz, 1H), 4.15 (ddd, J = 9.4, 7.6, 3.7 Hz, 1H), 4.03 (ddd, J = 11.3, 8.0, 5.2 Hz, 2H), 3.84 – 3.73 (m, 1H), 3.47 – 3.29 (m, 1H), 3.07 (t, J = 9.7 Hz, 6H), 2.20 – 2.00 (m, 5H), 2.00 – 1.87 (m, 5H), 1.52 (ddd, J = 17.1, 13.9, 4.3 Hz, 1H), 1.03 (dd, J = 25.0, 12.5 Hz, 1H).

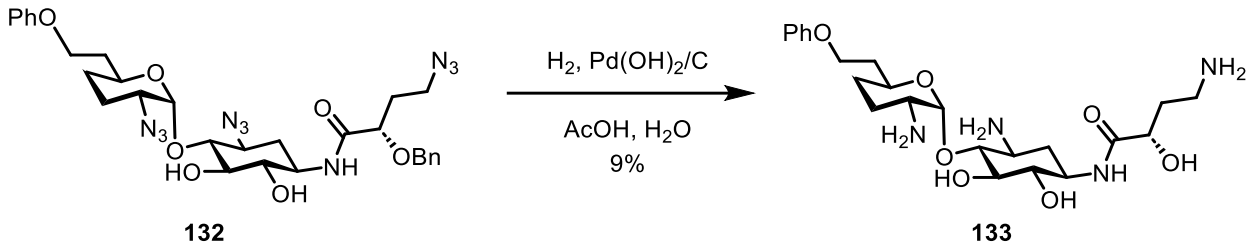

(*S*)-4-amino-N-((*1R,2S,3R,4R,5S*)-5-amino-4-(((*2R,3R,6S*)-3-amino-6-(2-phenoxyethyl)tetrahydro-*2H*-pyran-2-yl)oxy)-2,3-dihydroxycyclohexyl)-2-hydroxybutanamide (133)

To a solution of diol **132** (5.8 mg, 0.009 mmol, 1.00 equiv) in 4:1 acetic acid:water (1.0 mL total) was added palladium hydroxide on carbon (20% w/w, 15.0 mg, 0.0.021 mmol, 2.37 equiv) at 23 °C. The atmosphere was exchanged by briefly evacuating the flask, and backfilling with hydrogen and then flushing with hydrogen for 5 minutes. The heterogenous mixture stirred for 7 hours and was then filtered through a Celite® plug, washing with water (10 mL). The filtrate was concentrated under vacuum and treated with ammonium hydroxide solution (10 mM, 6.0 mL) and concentrated under vacuum. The remaining residue was purified by preparative HPLC on a Waters XBridge BEH C18 column [5 μm, 250 × 10 mm, UV detection at 210 nm, solvent A: 10 mM ammonium hydroxide in water, solvent B: 10 mM ammonium hydroxide in acetonitrile, injection volume: 2.0 mL (10 mM NH_3, water), 0 % B for 5 min then gradient elution with 0→35 % B over 30 min, flow rate: 5 mL/min]. The product containing fractions were combined and treated with 2 N HCl (30 mL) and concentrated under vacuum to give **133** as the trihydrochloride salt (0.5 mg, 0.84 mmol , 9%).

^{1}H NMR (500 MHz, D_2O): δ 7.38 (t, J = 8.0 Hz, 2H), 7.05 (t, J = 7.4 Hz, 1H), 7.02 (d, J = 8.6 Hz, 2H), 5.49 (d, J = 3.3 Hz, 1H), 4.29 (dd, J = 8.0, 4.0 Hz, 1H), 4.27 – 4.19 (m, 2H), 4.17 – 4.09 (m, 1H), 3.90 – 3.83 (m, 1H), 3.76 (t, J = 9.8 Hz, 1H), 3.59 (t, J = 9.4 Hz, 1H), 3.57 – 3.51 (m, 1H),

3.51 – 3.38 (m, 2H), 3.13 (dd, J = 13.4, 6.4 Hz, 2H), 2.21 – 2.10 (m, 2H), 2.09 – 1.87 (m, 6H), 1.61 (dt, J = 22.2, 11.2 Hz, 2H).

HRMS (ESI-TOF) m/z: $[M+H]^+$ Calcd for $C_{23}H_{39}N_4O_7$ 483.2813; Found 483.2816.

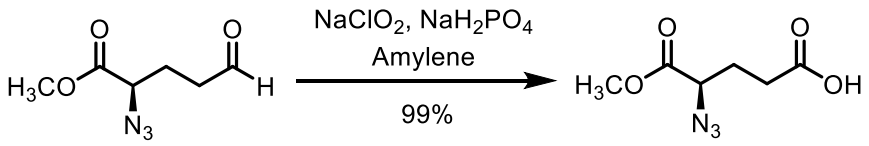

118 138

(*R*)-4-azido-5-methoxy-5-oxopentanoic acid (138)

A solution of aldehyde **118** (657 mg, 3.84 mmol, 1 equiv) in 4:1 THF:H_2O (193 mL) was treated in sequence with sodium dihydrogen phosphate (2.21 g, 18.4 mmol, 4.8 equiv), amylene (24.4 mL, 230 mmol, 60 equiv), and lastly a 1.0 M solution of sodium chlorite (1.666 g, 18.4 mmol, 4.8 equiv) in water (18.4 mL) at ambient temperature. After 20 minutes, the solution was diluted with 100 mL each of water and DCM, and the solution acidified with 6 M HCl until pH was < 3 (pH strip). The phases were separated following vigorous mixing, and the aqueous layer washed with DCM (2 x 100 mL). The combined organic layers were dried on sodium sulfate, filtered, and concentrated to give the crude. Purification by flash chromatography* on silica, eluting from DCM to 5% methanol in DCM gave acid **138** (711 mg, 3.80 mmol, 99%).

*The reaction can be carried through without column chromatography for the purposes of acid halide and thioester preparation.

R_f: (5% methanol in DCM, bromocresol green): 0.28

^{1}H NMR (400 MHz, $CDCl_3$): δ 4.05 (dd, J = 8.7, 5.1 Hz, 1H), 3.82 (s, 3H), 2.64 – 2.48 (m, 2H), 2.28 – 2.14 (m, 1H), 2.08 – 1.96 (m, 1H).

HRMS (ESI-TOF) m/z: $[M+Cl]^-$ Calcd for $C_6H_9N_3O_4Cl$ 222.0287; Found 222.0282.

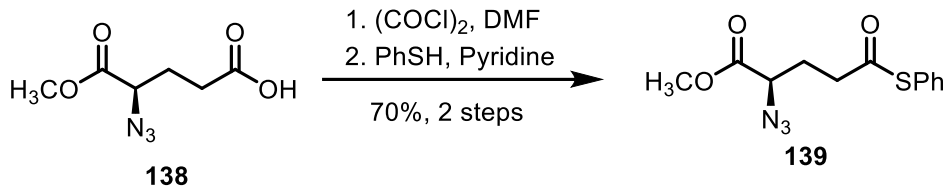

138 **139**

Methyl (*R*)-2-azido-5-oxo-5-(phenylthio)pentanoate (139)

Acid **138** (1.09 g, 5.84 mmol, 1 equiv) in DCM (29.2 mL) was treated at 0 °C with anhydrous DMF (3 drops) and oxalyl chloride (neat, 1.02 mL, 11.7 mmol, 2 equiv) in sequence. *Note large amount of gas evolution*. After bubbling subsided, the ice bath was removed and the solution stirred at ambient temperature while monitoring by TLC for consumption of **138**.* After 2.5 hours the solution was concentrated under vacuum, briefly dried on high vacuum for ~10 minutes, and used immediately in the preparation of thioester **139**.

Quenching of a reaction aliquot with methanol allows for monitoring of the reaction by checking for appearance of methyl ester **117 and consumption of **138**.*

Intermediate acid halide was dissolved in DCM (29.2 mL) and cooled to 0 °C. Pyridine (660 µL, 8.18 mmol, 1.4 equiv) and thiophenol (840 µL, 8.18 mmol, 1.4 equiv) were added. Consumption of acid halide was monitored by TLC (check for consumption of intermediate **117** from methanol quench), and then quenched by addition of 1 N HCl and diethyl ether (20 mL). The separated aqueous layer was washed with additional portions of ether (3 x 20 mL), and the combined organic phases were washed with water (30 mL) and brine (30 mL). The organics were dried on magnesium sulfate, filtered, and concentrated to give crude thioester, which was purified by flash chromatography on silica, grading from hexanes to 5% ethyl acetate in hexanes, to afford **139** as a yellow oil (1.142 g, 4.09 mmol, 70%).

R_f: (10% ethyl acetate in hexanes, $KMnO_4$): 0.27

^{1}H NMR (400 MHz, $CDCl_3$): δ 7.26 (s, 5H), 3.89 (dd, J = 8.7, 5.0 Hz, 1H), 3.65 (s, 3H), 2.76 – 2.56 (m, 2H), 2.15 – 2.04 (m, 1H), 1.90 (dddd, J = 14.1, 8.8, 7.4, 6.3 Hz, 1H).

$^{13}C\{^{1}H\}$ NMR (101 MHz, $CDCl_3$): δ 196.37, 170.40, 134.63, 129.73, 129.41, 127.37, 61.01, 52.94, 39.17, 26.89.

FTIR (neat), cm^{-1}: 2954 (m), 2105 (s), 1741 (s), 1700 (s).

HRMS (ESI-TOF) m/z: $[M+Na]^+$ Calcd for $C_{12}H_{13}N_3O_3SNa$ 302.0570; Found 302.0577

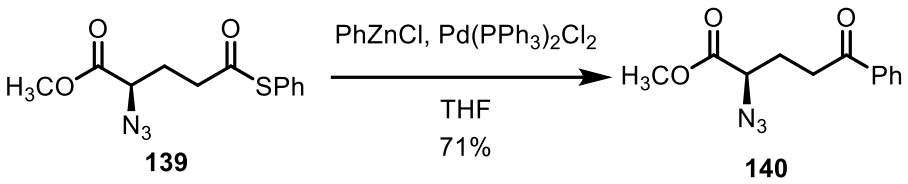

139 **140**

methyl (*R*)-2-azido-5-oxo-5-phenylpentanoate (140)

In a flame dried vial containing a stir bar under Ar was added anhydrous zinc (II) chloride (1.57 g, 11.5 mmol, 3.22 equiv) and the solid dried under high vacuum with application of a heat gun for 5 minutes. Once cooled, the zolid zinc chloride was suspended in anhydrous THF (20 mL), ultrasonicated until the solution became cloudy, and cooled to 0 °C. Phenylmagnesium bromide (1.0 M in THF, 8.23 mL, 8.23 mmol, 2.3 equiv) was added slowly dropwise, and the solution allowed to stir for 3 hours at room temperature.

Separately, a solution of thioester **139** (1.00 g, 3.58 mmol, 1 equiv) in THF (7.5 mL) was treated with bis(triphenylphosphine)palladium (II) chloride (126 mg, 0.179 mmol, 0.05 equiv). The phenylzinc chloride solution was transferred by canula to the stirring combination of **139** and catalyst at room temperature. After 30 minutes, the reaction was quenched by addition of saturated aqueous ammonium chloride (50 mL) and diluted with ethyl acetate (50 mL). The separated aqueous layer was washed with ethyl acetate (3 x 25 mL), and the combined organic layers dried on magnesium sulfate, filtered, and concentrated. Purifcation by flash chromatography on silica gel, grading from hexanes to 5% ethyl acetate in hexanes, gave **140** as yellow oil (630 mg, 2.55 mmol, 71%).

R_f: (10% ethyl acetate in hexanes, $KMnO_4$): 0.25

^{1}H NMR (400 MHz, $CDCl_3$): δ 7.90 – 7.57 (m, 2H), 7.39 – 7.33 (m, 1H), 7.30 – 7.22 (m, 2H), 3.89 (dd, J = 8.5, 5.1 Hz, 1H), 3.60 (s, 3H), 3.03 – 2.77 (m, 2H), 2.23 – 2.06 (m, 1H), 1.93 (dddd, J = 14.4, 8.5, 7.5, 6.0 Hz, 1H).

$^{13}C\{^{1}H\}$ NMR (101 MHz, $CDCl_3$): δ 198.48, 170.83, 136.67, 133.49, 128.83, 128.14, 61.33, 52.87, 34.15, 25.79.

FTIR (neat), cm^{-1}: 2954 (m), 2103 (s), 1741 (s), 1683 (s).

HRMS (ESI-TOF) m/z: $[M+Na]^+$ Calcd for $C_{12}H_{13}N_3O_3Na$ 270.0849; Found 270.0849.

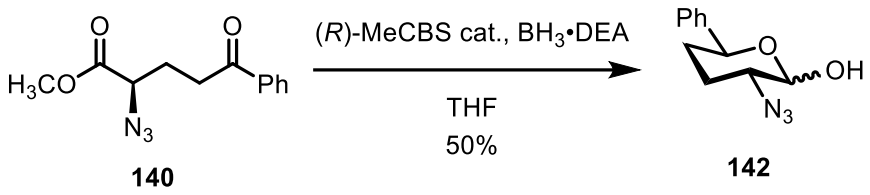

140 **142**

(*3R,6S*)-3-azido-6-phenyltetrahydro-*2H*-pyran-2-ol (142)

A solution of **140** (450 mg, 1.82 mmol, 1 equiv) and (*R*)-MeCBS catalyst (1.0 M in toluene, 182 µL, 0.182 mmol, 0.1 equiv) in THF(3.64 mL) was cooled to - 20 °C and treated with borane-diethylaniline (DEA) complex (230 µL, 1.27 mmol, 0.7 equiv). The solution was allowed to slowly warm to room temperature after 30 minutes and stirred overnight. The reaction was quenched at 0 °C by addition of methanol (1.5 mL) and then 1 N HCl (5 mL) and stirred for 15 minutes at room temperature. The layers were separated and the aqueous washed with ethyl acetate (3 x 10 mL), and the combined organics washed with water (10 mL) and brine (10 mL). Drying on magnesium sulfate, filtration, and concentration provided crude material that was purified by flash chromatography on silica gel, grading from hexanes to 10 % ethyl acetate in hexanes, to give lactol **142** (200 mg, 0.912 mmol, 50%). *Characterization is representative of the 1:1 ratio of anomers.*

R_f: (20% ethyl acetate in hexanes, $KMnO_4$): 0.47

^{1}H NMR (400 MHz, $CDCl_3$): δ 7.40 – 7.27 (m, 10H), 5.41 (t, J = 3.2 Hz, 1H), 5.04 (dd, J = 11.7, 2.4 Hz, 1H), 4.74 (dd, J = 7.8, 4.5 Hz, 1H), 4.50 (dd, J = 11.0, 2.3 Hz, 1H), 3.41 – 3.26 (m, 3H), 2.91 (dd, J = 3.3, 1.6 Hz, 1H), 2.35 – 2.12 (m, 2H), 2.06 – 1.89 (m, 4H), 1.82 – 1.54 (m, 4H).

^{13}C{^{1}H} NMR (101 MHz, $CDCl_3$): δ 141.45, 140.74, 128.64, 128.61, 128.09, 127.92, 126.19, 126.00, 98.81, 92.74, 78.30, 70.38, 61.93, 58.43, 32.84, 32.54, 28.63, 22.65.

HRMS (ESI-TOF) m/z: $[M+Na]^+$ Calcd for $C_{11}H_{13}N_3O_2Na$ 242.0900; Found 242.0892.

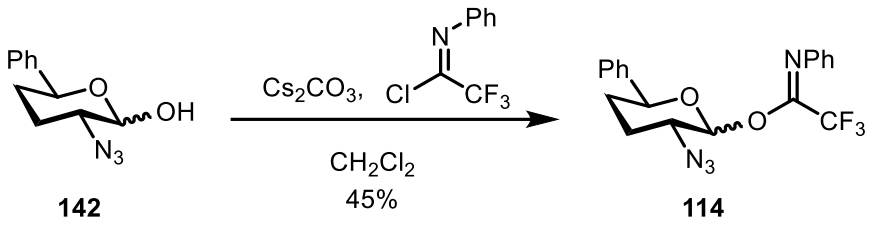

(*3R,6S*)-3-azido-6-phenyltetrahydro-*2H*-pyran-2-yl (*E*)-2,2,2-trifluoro-N-phenylacetimidate (114)

A solution of lactol **142** (50.0 mg, 0.228 mmol, 1 equiv) in DCM (2.28 mL) was treated with 2,2,2-trifluoro-*N*-phenylacetimidoyl chloride (95 mg, 0.456 mmol, 2 equiv) and cesium carbonate (149 mg, 0.456 mmol, 2 equiv) at room temperature. After 4.5 hours, the mixture was filtered through Celite® and concentrated under reduced pressure. Purification by flash chromatography on silica, grading from hexanes to 2% ethyl acetate in hexanes, gave product **114** as a wax (40 mg, 0.10 mmol, 45%).

^{1}H NMR (400 MHz, $CDCl_3$): δ 7.40 – 7.27 (m, 10H), 5.41 (t, J = 3.2 Hz, 1H), 5.04 (dd, J = 11.7, 2.4 Hz, 1H), 4.74 (dd, J = 7.8, 4.5 Hz, 1H), 4.50 (dd, J = 11.0, 2.3 Hz, 1H), 3.41 – 3.26 (m, 3H), 2.91 (dd, J = 3.3, 1.6 Hz, 1H), 2.35 – 2.12 (m, 2H), 2.06 – 1.89 (m, 4H), 1.82 – 1.54 (m, 4H).

^{13}C{^{1}H} NMR (101 MHz, $CDCl_3$): δ 139.98, 129.54, 129.44, 128.73, 128.61, 128.47, 127.99, 125.74, 124.32, 120.43, 119.35, 78.42, 59.64, 31.77, 28.58.

FTIR (neat), cm^{-1}: 3033 (w), 2930 (m), 2103 (s), 1715 (s).

HRMS (ESI-TOF) m/z: $[M+H]^+$ Calcd for $C_{19}H_{18}F_3N_4O_2$ 391.1376; Found 391.1375.

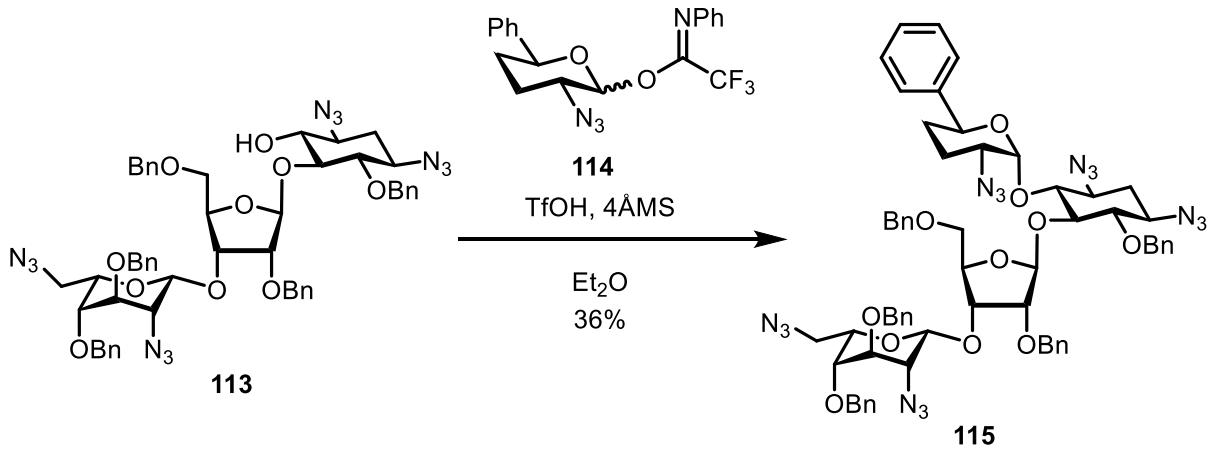

(*2R,3R,4R,5R,6S*)-3-azido-6-(azidomethyl)-4,5-bis(benzyloxy)-2-(((*2R,3R,4R,5S*)-4-(benzyloxy)-2-((benzyloxy)methyl)-5-(((*1R,2R,3S,5R,6S*)-3,5-diazido-2-(((*2R,3R,6S*)-3-azido-6-phenyltetrahydro-*2H*-pyran-2-yl)oxy)-6-(benzyloxy)cyclohexyl)oxy)tetrahydrofuran-3-yl)oxy)tetrahydro-*2H*-pyran (115)

Acceptor **113** was prepared as described previously and the associated spectra are attached in Appendix A. In a flame-dried flask charged with a stir bar, acceptor **113** (80 mg, 0.079 mmol, 1 equiv) and donor **114** (61.9 mg, 0.159 mmol, 2 equiv) were combined and concentrated from benzene three times. The mixture was dissolved in anhydrous ether (1.6 mL) and 4ÅMS were added (150 mg); the solution was stirred for 30 minutes at room temperature. The stirring solution was cooled to - 60 °C and a solution of TfOH (0.1 M in ether*, 79 µ, 7.93 µmol, 0.1 equiv). The reaction was monitored by TLC, slowly warming to - 40 °C after 2 hours, and to - 20 °C after 5 hours. After 6 total hours the reaction was quenched by addition of triethyl amine and filtered through a cotton plug. The concentrated crude material was purified by flash chromatography on silica, grading from 10% ethyl acetate in hexanes to 30% ethyl acetate in hexanes, affording pseudotetrasaccharide **115** as a wax (35 mg, 0.029 mmol, 36%). *The solution of TfOH in ether

was prepared from neat TfOH (stored in a Schlenk flask at - 20 °C) and anhydrous ether at room temperature. The solution was always prepared, used immediately, and never re-used.

^{1}H NMR (400 MHz, $CDCl_3$): δ 7.44 – 7.27 (m, 23H), 7.24 – 7.11 (m, 7H), 6.20 (d, J = 3.4 Hz, 1H), 5.68 (d, J = 5.8 Hz, 1H), 5.03 (dd, J = 11.8, 2.4 Hz, 1H), 4.94 (d, J = 10.7 Hz, 1H), 4.90 (d, J = 1.9 Hz, 1H), 4.65 (dd, J = 17.0, 11.4 Hz, 2H), 4.58 (d, J = 6.8 Hz, 1H), 4.55 (d, J = 6.9 Hz, 1H), 4.47 (d, J = 5.7 Hz, 1H), 4.43 (d, J = 2.2 Hz, 1H), 4.40 (s, 1H), 4.33 – 4.23 (m, 4H), 4.02 – 3.94 (m, 2H), 3.89 (dd, J = 10.3, 2.2 Hz, 1H), 3.83 – 3.75 (m, 3H), 3.66 (dd, J = 12.9, 8.5 Hz, 1H), 3.58 (dd, J = 10.3, 3.2 Hz, 1H), 3.47 (dddd, J = 19.4, 12.5, 9.7, 4.6 Hz, 2H), 3.34 (t, J = 2.4 Hz, 1H), 3.25 (t, J = 9.3 Hz, 1H), 3.11 (d, J = 2.5 Hz, 1H), 2.96 – 2.85 (m, 2H), 2.34 (td, J = 12.7, 3.7 Hz, 1H), 2.24 (dt, J = 13.2, 4.6 Hz, 1H), 2.00 – 1.93 (m, 1H), 1.91 – 1.84 (m, 1H), 1.61 (qd, J = 13.0, 3.4 Hz, 1H), 1.44 – 1.31 (m, 1H).

^{13}C{^{1}H} NMR (101 MHz, $CDCl_3$): δ 142.04, 138.71, 138.16, 137.72, 137.19, 137.12, 128.82, 128.64, 128.57, 128.51, 128.46, 128.36, 128.32, 128.00, 127.97, 127.87, 127.83, 127.51, 127.41, 126.66, 126.27, 105.98, 98.73, 96.32, 84.47, 82.70, 82.23, 81.97, 77.36, 75.66, 75.08, 74.51, 73.48, 73.35, 73.00, 72.48, 71.83, 71.65, 70.66, 70.27, 60.83, 60.58, 57.39, 51.24, 32.82, 29.85, 23.07.

FTIR (neat), cm^{-1}: 3032 (m), 2923 (m), 2097 (s), 1727 (m).

HRMS (ESI-TOF) m/z: $[M+Na]^+$ Calcd for $C_{63}H_{67}N_{15}O_{11}Na$ 1232.5037; Found 1232.5039.

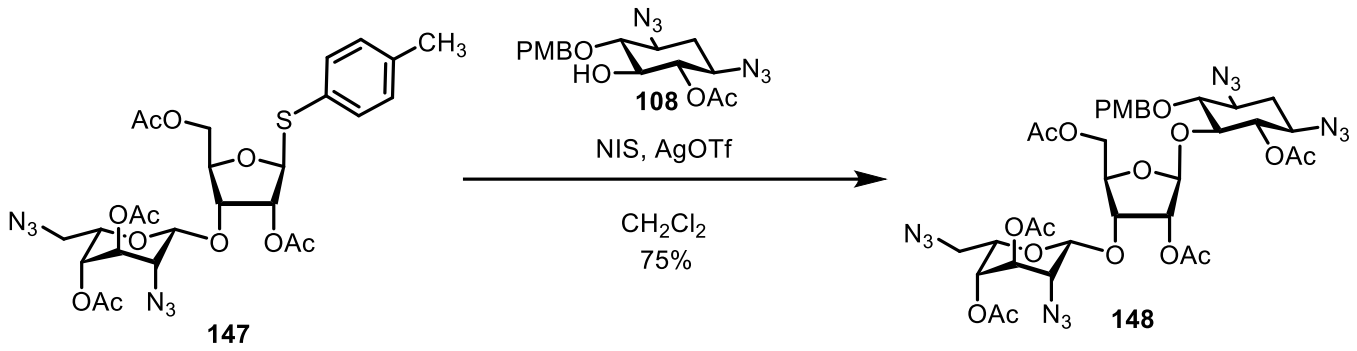

(*2S,3R,4R,5R,6R*)-6-(((*2R,3R,4R,5S*)-4-acetoxy-5-(((*1S,2S,3R,5S,6R*)-2-acetoxy-3,5-diazido-6-((4-methoxybenzyl)oxy)cyclohexyl)oxy)-2-(acetoxymethyl)tetrahydrofuran-3-yl)oxy)-5-azido-2-(azidomethyl)tetrahydro-*2H*-pyran-3,4-diyl diacetate (148)

Thioglycoside **147** has been described elsewhere.[26] Donor **147** (145 mg, 0.228 mmol, 1.1 equiv) and acceptor **108** (78 mg, 0.207 mmol, 1 equiv) were combined and co-evaporated from toluene three times, then suspended in dry DCM (4.2 mL) and dried over 4ÅMS (200 mg) at room temperature for 30 minutes. At the same time, a separate solution of silver triflate (32 mg, 0.124 mmol in 500 µL toluene, 0.6 equiv) was dried over 4ÅMS (40 mg). The solution of donor and acceptor was cooled to - 40 °C, and NIS (51.3 mg, 0.228 mmol, 1.1 equiv) was to the cold solution. The silver triflation solution was then transferred by syringe to the glycosylation flask dropwise, and the glycosylation immediately warmed to - 20 °C to continue stirring. After 4 hours, the reaction was quenched by the addition of triethyl amine (150 µL), stirred for 15 minutes while warming to room temperature, and then filtered through Celite®. Purification by flash chromatography on silica gel, grading from 10 – 40% ethyl acetate in hexanes, gave PMB-acceptor **148** (138 mg, 0.155 mmol, 75%).

R_f: (5% ethyl acetate in hexanes, CAM): 0.55

^{1}H NMR (400 MHz, $CDCl_3$): δ 7.38 (d, J = 8.6 Hz, 2H), 6.86 (d, J = 8.7 Hz, 2H), 5.22 (d, J = 2.1 Hz, 1H), 5.03 (q, J = 2.9 Hz, 2H), 4.91 (m, 4H), 4.86 (d, J = 2.0 Hz, 1H), 4.70 (t, J = 2.3 Hz, 1H), 4.60 (d, J = 10.0 Hz, 1H), 4.45 – 4.37 (m, 2H), 4.36 – 4.27 (m, 2H), 4.21 (dd, J = 12.0, 6.1 Hz, 1H), 4.06 (s, 1H), 3.78 (s, 3H), 3.68 – 3.54 (m, 3H), 3.46 – 3.22 (m, 4H), 2.74 (s, 15H), 2.21 (m, 1H), 1.46 – 1.34 (m, 1H).

^{13}C{^{1}H} NMR (101 MHz, $CDCl_3$): δ 177.64, 171.31, 170.72, 170.42, 169.93, 169.80, 168.67, 159.56, 130.43, 113.86, 107.13, 99.23, 82.23, 81.46, 79.27, 76.19, 75.31, 74.60, 73.52, 68.76, 65.79, 64.32, 60.51, 60.10, 58.48, 56.68, 55.34, 50.64, 32.08, 29.68, 21.15, 21.01, 20.86, 20.82, 20.78, 20.70, 14.29.

FTIR (neat), cm^{-1}: 2940 (w), 2100 (s), 1743 (s), 1709 (s).

HRMS (ESI-TOF) m/z: $[M+NH_4]^+$ Calcd for $C_{35}H_{48}N_{13}O_{16}$ 906.3336; Found 906.3337.

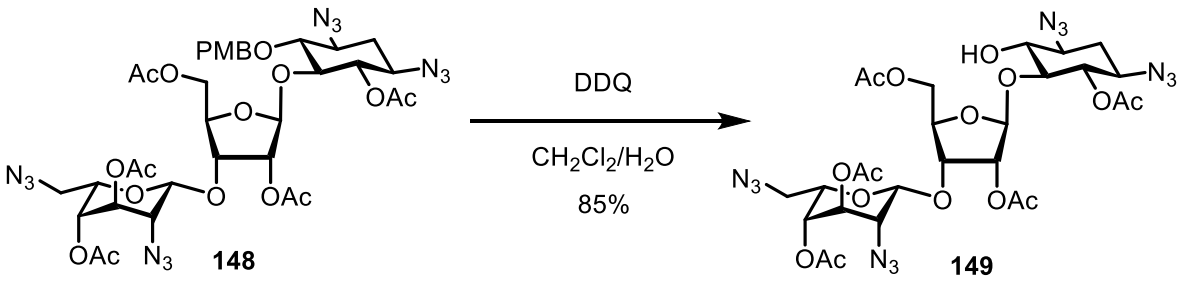

(*2S,3R,4R,5R,6R*)-6-(((*2R,3R,4R,5S*)-4-acetoxy-5-(((*1S,2S,3R,5S,6R*)-2-acetoxy-3,5-diazido-6-hydroxycyclohexyl)oxy)-2-(acetoxymethyl)tetrahydrofuran-3-yl)oxy)-5-azido-2-(azidomethyl)tetrahydro-*2H*-pyran-3,4-diyl diacetate (149)

A solution of **148** (94 mg, 0.11 mmol, 1 equiv) in DCM (2.0 mL) and water (110 μL) at room temperature was treated with DDQ (24 mg, 0.11 mmol, 1 equiv) with vigorous stirring. Each hour, another 1 equiv portion was added and a 450 μL of 8:1 DCM:water was added for dilution. The reaction was stopped after 5 hours (a total of 4 additional equivalents and dilutions occurred) by addition of saturated aqueous sodium thiosulfate solution (10 mL). The mixture was washed with DCM (3 x 10 mL), and the combined organics washed with water (10 mL) and brine (10 mL). The organic layer was dried on magnesium sulfate, filtered, and concentrated. Purification by silica gel chromatography, grading from 20–35% ethyl acetate in hexanes, gave acceptor **149** (69 mg, 0.094 mmol, 85%).

R_f: (50% ethyl acetate in hexanes, CAM): 0.51

^{1}H NMR (400 MHz, $CDCl_3$): δ 5.04 (m, 3H), 4.94 – 4.86 (m, 2H), 4.71 (t, J = 2.4 Hz, 1H), 4.54 (dd, J = 7.7, 4.6 Hz, 1H), 4.44 (dd, J = 13.1, 4.5 Hz, 1H), 4.37 – 4.31 (m, 2H), 4.15 – 4.09 (m, 1H), 3.58 (dd, J = 13.0, 8.1 Hz, 1H), 3.50 – 3.37 (m, 4H), 3.35 (t, J = 2.4 Hz, 1H), 3.31 – 3.20 (m, 1H), 2.20 (t, J = 4.6 Hz, 1H), 2.17 (s, 6H), 2.15 (s, 3H), 2.14 (s, 3H), 2.11 (s, 3H), 1.47 – 1.34 (m, 1H).

$^{13}C\{^{1}H\}$ NMR (101 MHz, $CDCl_3$): δ 170.76, 170.10, 170.07, 169.92, 168.69, 107.10, 98.84, 84.84, 79.39, 75.27, 75.15, 74.59, 74.41, 73.49, 68.74, 65.83, 62.43, 59.41, 58.39, 56.67, 50.73, 32.07, 20.95, 20.85, 20.82, 20.78, 20.72.

FTIR (neat), cm^{-1}: 3515 (br), 2926 (m), 2099 (s), 1742 (s).

HRMS (ESI-TOF) m/z: $[M+Na]^+$ Calcd for $C_{27}H_{36}N_{12}O_{15}Na$ 791.2315; Found 791.2290.

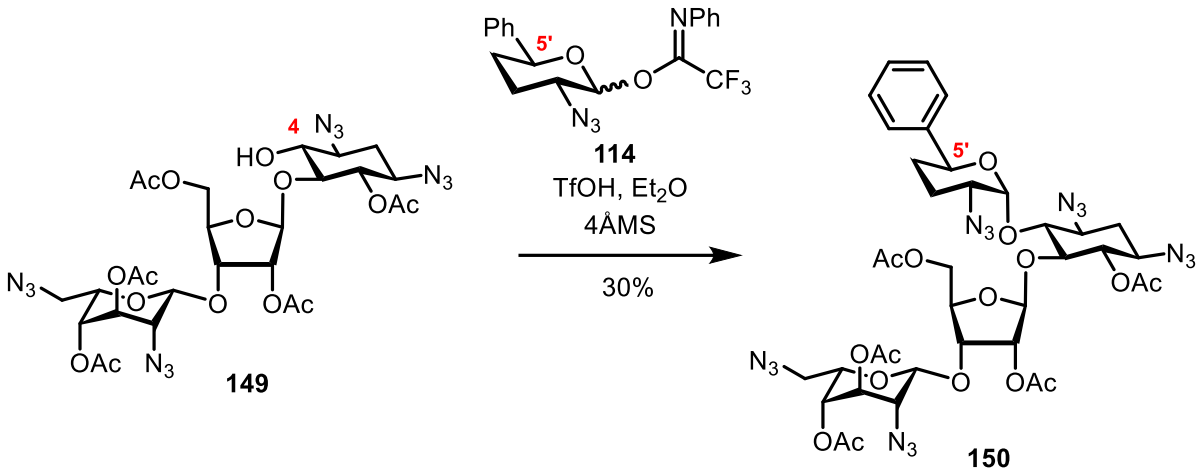

(*2S,3R,4R,5R,6R*)-6-(((*2R,3R,4R,5S*)-4-acetoxy-5-(((*1S,2S,3R,5S,6R*)-2-acetoxy-3,5-diazido-6-(((*2R,3R,6S*)-3-azido-6-phenyltetrahydro-*2H*-pyran-2-yl)oxy)cyclohexyl)oxy)-2-(acetoxymethyl)tetrahydrofuran-3-yl)oxy)-5-azido-2-(azidomethyl)tetrahydro-*2H*-pyran-3,4-diyl diacetate (150)

Donor **114** (30 mg, 0.077 mmol, 2.7 equiv) and acceptor **149** (22 mg, 0.029 mmol, 1 equiv) were combined and concentrated from toluene three times. The residue was dissolved in diethyl ether (290 µL) and dried by addition of 4ÅMS (100 mg) with stirring at room temperature for 30 minutes. The mixture was cooled to - 60 °C and TfOH solution (0.1 molar in ether, 29 µL, 2.9 µmol, 0.1 equiv) was added dropwise. After 2 hours, addition of triethylamine (100 µL) to quench and filtering through celite at room temperature gave the crude, which was further purified by flash chromatography on silica, grading from 15- 25% ethyl acetate in hexanes, to give tetrasaccharide **150** (8 mg, 0.008 mmol, 30%).

R_f: (40% ethyl acetate in hexanes, CAM): 0.37

^{1}H NMR (400 MHz, $CDCl_3$): δ 7.40 – 7.27 (m, 5H), 5.93 (d, J = 3.4 Hz, 1H), 5.37 (d, J = 2.9 Hz, 1H), 5.11 – 4.99 (m, 3H), 4.94 – 4.83 (m, 4H), 4.74 – 4.63 (m, 1H), 4.45 (dd, J = 11.9, 2.4 Hz, 1H), 4.40 – 4.32 (m, 2H), 4.25 (dd, J = 12.0, 5.0 Hz, 1H), 4.09 – 4.04 (m, 1H), 3.91 (t, J = 8.9 Hz,

1H), 3.81 (t, J = 9.1 Hz, 1H), 3.59 (dd, J = 13.0, 8.1 Hz, 1H), 3.56 – 3.49 (m, 1H), 3.47 – 3.35 (m, 2H), 3.32 (t, J = 2.2 Hz, 1H), 3.27 (dd, J = 13.0, 4.5 Hz, 1H), 3.08 (dt, J = 12.5, 4.0 Hz, 1H), 2.32 (ddd, J = 16.0, 10.2, 4.0 Hz, 2H), 2.17 (s, 3H), 2.15 (s, 3H), 2.14 (s, 3H), 2.11 (s, 3H), 2.10 (s, 3H), 1.99 (ddd, J = 12.2, 6.8, 3.5 Hz, 2H), 1.82 – 1.68 (m, 2H), 1.58 – 1.43 (m, 2H).

$^{13}C\{^{1}H\}$ NMR (101 MHz, $CDCl_3$): δ 171.01, 170.24, 169.95, 169.68, 168.71, 141.46, 128.62, 128.00, 126.42, 106.84, 99.46, 96.83, 82.28, 79.57, 76.35, 75.64, 75.19, 75.02, 73.52, 70.59, 68.83, 65.80, 64.09, 60.42, 58.37, 57.41, 56.70, 50.71, 32.58, 32.08, 31.74, 29.86, 29.52, 23.13, 22.81, 21.00, 20.98, 20.94, 20.84, 20.68.

HRMS (ESI-TOF) m/z: $[M+Na]^+$ Calcd for $C_{38}H_{47}N_{15}O_{16}Na$ 992.3217; Found 992.3209.

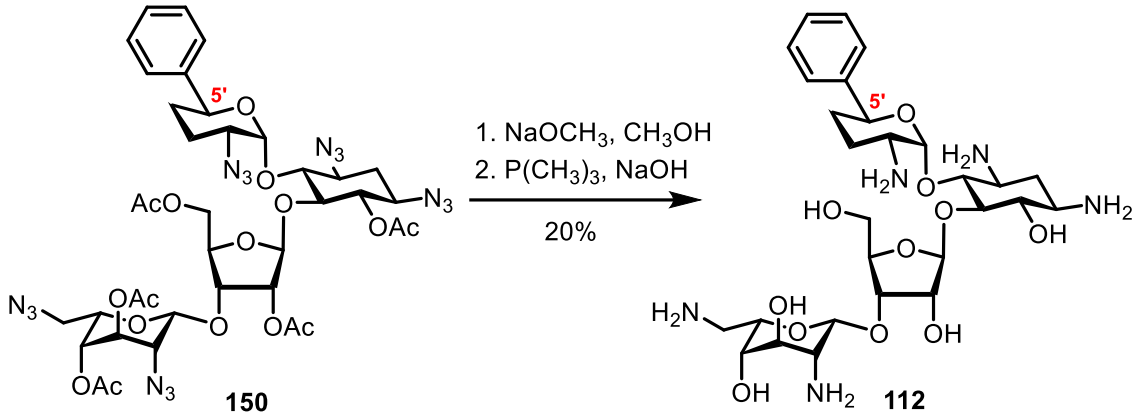

(*2S,3S,4R,5R,6R*)-5-amino-2-(aminomethyl)-6-(((*2R,3S,4R,5S*)-5-(((*1R,2R,3S,5R,6S*)-3,5-diamino-2-(((*2R,3R,6S*)-3-amino-6-phenyltetrahydro-*2H*-pyran-2-yl)oxy)-6-hydroxycyclohexyl)oxy)-4-hydroxy-2-(hydroxymethyl)tetrahydrofuran-3-yl)oxy)tetrahydro-*2H*-pyran-3,4-diol (112)

C5'-phenyl **150** (8.00 mg, 8.25 µmol, 1 equiv) in anhydrous methanol (825 µL) was cooled to 0 °C and treated with freshly prepared sodium methoxide solution (0.1 M in methanol, 99 µL, 9.9 µmol, 1.2 equiv); the solution was allowed to warm to room temperature slowly and stirred overnight. The reaction was quenched by addition of sat. aq. ammonium chloride solution (5 mL) and the mixture washed with ethyl acetate (3 x 5 mL). The combined organic layers were dried on sodium sulfate, filtered, and concentrated to give crude polyalcohol.

The crude poly-alcohol (6.3 mg, 8.3 µmol, 1 equiv) was dissolved in THF (210 µL) and water (210 µL) and sodium hydroxide solution (2.0 M in water, 62 µL, 124 µmol, 15 equiv) were added in sequence. Trimethyl phosphine (1.0 M in THF, 69 µL, 69 µmol, 8.3 equiv) was added the solution immediately brought to 60 °C in an oil bath. Stirring at this temperature was maintained for 4 hours and the reaction then quenched after cooling to room temperature via the addition of glacial acetic acid (100 µL). The solution was washed with diethyl ether (3 x 3 mL), and the separated ether layers discarded. The 10% acetic acid solution of crude **112** was purified by CM Sephadex-C25

chromatography, grading from 0.1% to 0.7% ammonium hydroxide in water. The product-containing fractions (identified by spotting on normal-phase TLC plates and charring in 80:20 ethanol:sulfuric acid) were combined, glacial acetic acid (150 µL) was added, and the product dried by lyophilization to give **112** as the penta-acetate salt* (1.06 mg, 1.68 µmol, 20%).

*the yield is reported on the basis of free-based compound while characterization is reported for the penta-acetate salt.

^{1}H NMR (400 MHz, D_2O): δ 7.46 (s, 5H), 5.72 (d, J = 3.5 Hz, 1H), 5.37 (s, 1H), 5.27 (s, 1H), 5.06 (d, J = 10.2 Hz, 1H), 4.55 – 4.47 (m, 1H), 4.38 (s, 1H), 4.31 (s, 1H), 4.23 (m, 2H), 3.90 (d, J = 10.2 Hz, 1H), 3.82 (m, 2H), 3.75 – 3.65 (m, 3H), 3.64 – 3.54 (m, 2H), 3.44 (dd, J = 13.4, 6.5 Hz, 1H), 3.40 – 3.33 (m, 1H), 3.30 – 3.20 (m, 2H), 2.29 (d, J = 13.1 Hz, 1H), 2.19 – 2.02 (m, 3H), 1.97 (s, 1H), 1.92 (s, 15H), 1.59 (d, J = 12.2 Hz, 1H).

^{13}C{^{1}H} NMR (101 MHz, D_2O): δ 181.30, 139.72, 128.91, 128.61, 126.48, 110.20, 95.31, 85.34, 81.14, 75.37, 73.38, 72.32, 67.83, 67.38, 60.62, 50.94, 50.29, 49.13, 40.41, 23.13, 22.11.

HRMS (ESI-TOF) m/z: $[M+Na]^+$ Calcd for $C_{28}H_{47}N_5O_{11}Na$ 652.3164; Found 652.3165.

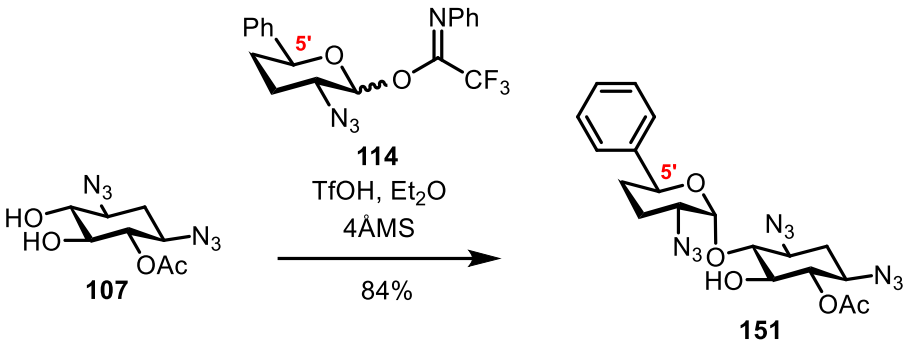

(*1S,2S,3R,4S,6R*)-4,6-diazido-3-(((*2R,3R,6S*)-3-azido-6-phenyltetrahydro-*2H*-pyran-2-yl)oxy)-2-hydroxycyclohexyl acetate (151)

Donor **114** (38 mg, 0.098 mmol, 1 equiv) and acceptor **107** (25 mg, 0.098 mmol, 1 equiv) were combined and concentrated from toluene three times. The residue was dissolved in diethyl ether (1.95 mL) and dried by addition of 4ÅMS (100 mg) with stirring at room temperature for 30 minutes. The mixture was cooled to - 50 °C and TfOH solution* (0.1 molar in ether, 98 µL, 9.8 µmol, 0.1 equiv) was added dropwise. After 1 hour, the reaction was quenched by addition of triethylamine (100 µL) and filtered through celite at room temperature to give the crude, which was further purified by flash chromatography on silica, grading from 10- 25% ethyl acetate in hexanes, to give disaccharide **151** (37.5 mg, 0.082 mmol, 84%) + 15% of C5-regioisomer (separable by column).

R_f: (50% ethyl acetate in hexanes, CAM): 0.88

^{1}H NMR (400 MHz, $CDCl_3$): δ 7.41 – 7.28 (m, 5H), 5.37 (d, J = 3.5 Hz, 1H), 5.09 (dd, J = 11.9, 2.3 Hz, 1H), 4.89 (t, J = 9.9 Hz, 1H), 3.72 – 3.62 (m, 1H), 3.59 (d, J = 3.6 Hz, 1H), 3.56 – 3.46 (m, 2H), 3.40 (ddd, J = 12.2, 9.8, 4.3 Hz, 1H), 2.33 (dt, J = 13.3, 4.5 Hz, 1H), 2.28 – 2.19 (m, 1H), 2.17 (s, 3H), 2.11 – 2.00 (m, 2H), 1.86 – 1.73 (m, 1H), 1.61 – 1.47 (m, 1H).

$^{13}C\{^{1}H\}$ NMR (101 MHz, $CDCl_3$): δ 170.61, 141.29, 128.61, 127.96, 126.22, 99.44, 82.42, 75.32, 75.05, 71.04, 59.24, 58.23, 32.42, 32.38, 23.28, 20.98.

FTIR (neat), cm^{-1}: 3449 (br), 2947 (m), 2095 (s), 1742 (s).

HRMS (ESI-TOF) m/z: $[M+Na]^+$ Calcd for $C_{19}H_{23}N_9O_5Na$ 480.1714; Found 480.1714.

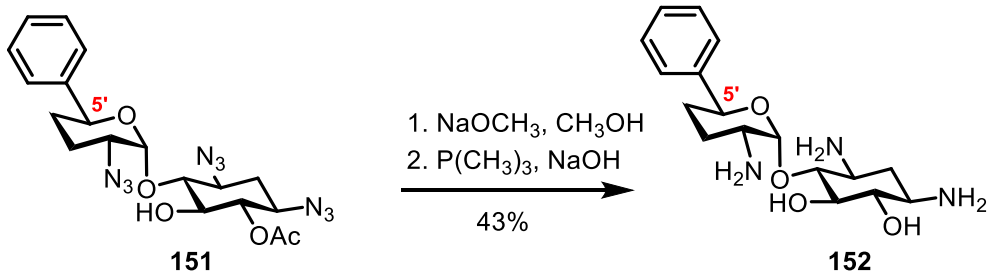

(*1S,2R,3R,4S,6R*)-4,6-diamino-3-(((*2R,3R,6S*)-3-amino-6-phenyltetrahydro-*2H*-pyran-2-yl)oxy)cyclohexane-1,2-diol

C5'-phenyl **151** (16 mg, 35 µmol, 1 equiv) in anhydrous methanol (700 µL) was cooled to 0 °C and treated with freshly prepared sodium methoxide solution (0.1 M in methanol, 350 µL, 35 µmol, 1 equiv); the solution was allowed to warm to room temperature slowly and stirred overnight. The reaction was quenched by the addition of sat. aq. ammonium chloride solution (5 mL) and the mixture washed with ethyl acetate (3 x 5 mL). The combined organic layers were dried on sodium sulfate, filtered, and concentrated to give crude polyalcohol.

The crude polyalcohol (13 mg, 31 µmol, 1 equiv) was dissolved in THF (780 µL) and water (780 µL) and sodium hydroxide solution (2.0 M in water, 195 µL, 391 µmol, 12.5 equiv) were added in sequence. Trimethyl phosphine (1.0 M in THF, 156 µL, 156 µmol, 5 equiv) was added and the solution immediately brought to 60 °C in an oil bath. Stirring at this temperature was maintained for 5 hours and the reaction then quenched after cooling to room temperature via the addition of glacial acetic acid (100 µL). The solution was washed with diethyl ether (3 x 3 mL), and the separated ether layers discarded. The 10% acetic acid solution of crude **152** was purified by CM Sephadex-C25 chromatography, grading from 0.1% to 0.7% ammonium hydroxide in water. The product-containing fractions (identified by spotting on normal-phase TLC plates and charring in

80:20 ethanol:sulfuric acid) were combined, glacial acetic acid (150 µL) was added, and the product dried by lyophilization to give **152** as the triacetate salt* (4.56 mg, 13.5 µmol, 43%).

*the yield is reported on the basis of free-based compound while characterization is reported for the triacetate salt.

^{1}H NMR (400 MHz, D_2O): δ 7.55 – 7.38 (m, 5H), 5.64 (d, J = 3.6 Hz, 1H), 5.04 (dd, J = 11.2, 2.2 Hz, 1H), 3.82 – 3.74 (m, 1H), 3.72 (dq, J = 11.7, 3.8 Hz, 1H), 3.65 (t, J = 9.1 Hz, 1H), 3.55 (dd, J = 10.3, 9.2 Hz, 1H), 3.47 (ddd, J = 12.5, 10.0, 4.2 Hz, 1H), 3.31 (ddd, J = 12.4, 10.2, 4.2 Hz, 1H), 2.45 (dt, J = 12.7, 4.3 Hz, 1H), 2.19 – 2.05 (m, 3H), 2.00 – 1.92 (m, 1H), 1.92 (s, 3H), 1.78 (q, J = 12.5 Hz, 1H).

^{13}C{^{1}H} NMR (101 MHz, D_2O): δ 181.10, 139.82, 128.90, 128.60, 126.31, 96.78, 80.28, 75.07, 72.60, 72.20, 49.85, 49.09, 48.89, 30.35, 28.98, 23.03, 21.99.

HRMS (ESI-TOF) m/z: $[M+H]^+$ Calcd for $C_{17}H_{28}N_3O_4$ 338.2074; Found 338.2078.

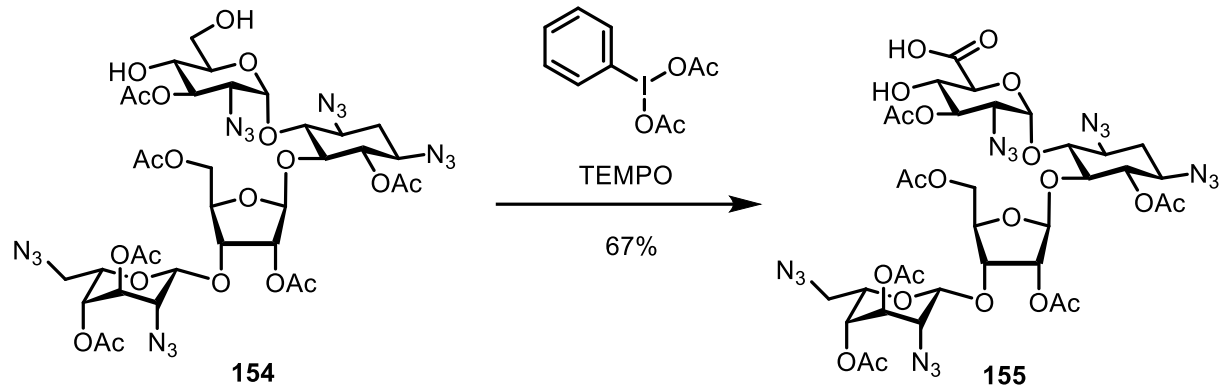

154 155

(*2S,3S,4R,5R,6S*)-4-acetoxy-6-(((*1R,2S,3S,4R,6S*)-3-acetoxy-2-(((*2S,3R,4R,5R*)-3-acetoxy-5-(acetoxymethyl)-4-(((*2R,3R,4R,5R,6S*)-4,5-diacetoxy-3-azido-6-(azidomethyl)tetrahydro-*2H*-pyran-2-yl)oxy)tetrahydrofuran-2-yl)oxy)-4,6-diazidocyclohexyl)oxy)-5-azido-3-hydroxytetrahydro-*2H*-pyran-2-carboxylic acid (155).

A solution of diol **154**[27] (1.95 g, 1.95 mmol, 1equiv) in 2:1 dichloromethane:water (40 mL) was treated with bis(acetoxy)iodobenzene (1.89 g, 5.85 mmol, 3 equiv) and TEMPO (122 mg, 0.780 mmol, 0.4 equiv) were added. After 2 hours of vigorous stirring, the solution was quenched by addition of sat. aq. sodium thiosulfate solution (40 mL) at 0 °C. The solution was acidified with 1 N HCl until pH was < 4 (pH strip), and the aqueous washed with ethyl acetate (3 x 50 mL). The combined organics were dried on sodium sulfate, filtered, and concentrated to give the crude. Purification by flash chromatography on silica, grading from DCM to 5% methanol in DCM gave acid **155** (1.32 g, 1.31 mmol, 67%).

H NMR (400 MHz, $CDCl_3$): δ 5.86 (d, J = 3.6 Hz, 1H), 5.38 (dd, J = 10.5, 8.9 Hz, 1H), 5.32 (d, J = 2.1 Hz, 1H), 5.03 (t, J = 2.8 Hz, 1H), 4.99 – 4.90 (m, 2H), 4.88 (s, 1H), 4.76 (d, J = 9.8 Hz, 1H), 4.71 (t, J = 2.1 Hz, 1H), 4.46 – 4.39 (m, 2H), 4.29 (d, J = 7.8 Hz, 2H), 3.91 – 3.83 (m, 2H), 3.72 (t, J = 8.7 Hz, 1H), 3.61 (dd, J = 13.0, 8.1 Hz, 1H), 3.57 – 3.51 (m, 1H), 3.49 – 3.40 (m, 1H), 3.32

(t, J = 2.3 Hz, 1H), 3.26 (dd, J = 13.0, 4.1 Hz, 1H), 3.20 (dd, J = 10.5, 3.4 Hz, 1H), 2.43 – 2.35 (m, 1H), 2.18 (s, 6H), 2.17 (s, 3H), 2.16 (s, 3H), 2.12 (s, 3H), 2.11 (s, 3H), 1.69 – 1.59 (m, 1H). HRMS (ESI-TOF) m/z: $[M+H]^+$ Calcd for $C_{35}H_{46}N_{15}O_{21}$ 1012.2987; Found 1012.3003.

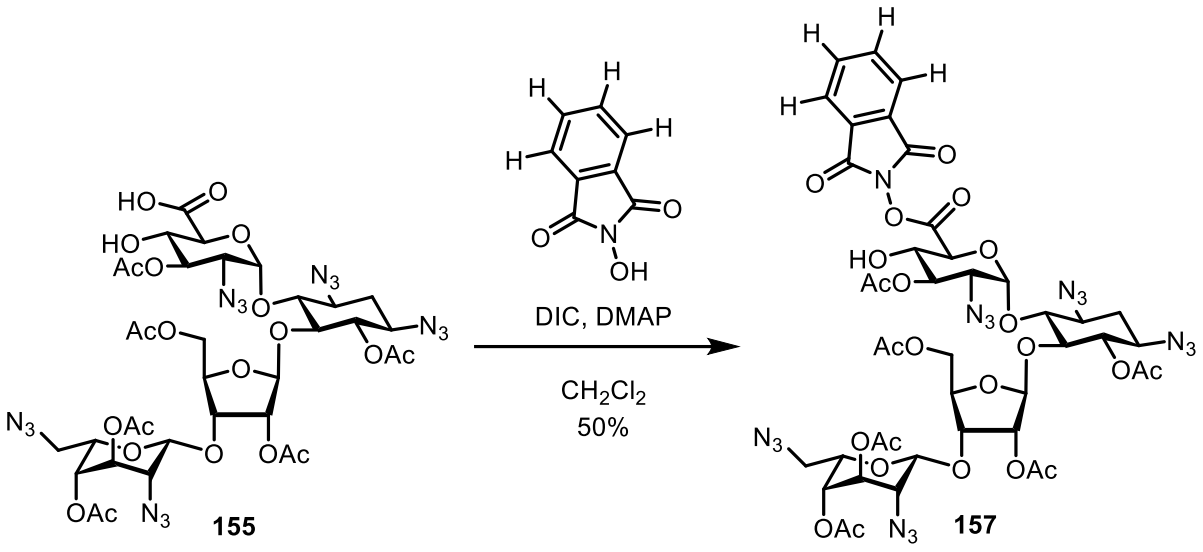

(*2S,3R,4R,5R,6R*)-6-(((*2R,3R,4R,5S*)-4-acetoxy-5-(((*1S,2S,3R,5S,6R*)-2-acetoxy-6-(((*2S,3R,4R,5S,6S*)-4-acetoxy-3-azido-6-(((1,3-dioxoisoindolin-2-yl)oxy)carbonyl)-5-hydroxytetrahydro-*2H*-pyran-2-yl)oxy)-3,5-diazidocyclohexyl)oxy)-2-(acetoxymethyl)tetrahydrofuran-3-yl)oxy)-5-azido-2-(azidomethyl)tetrahydro-*2H*-pyran-3,4-diyl diacetate (157)

Acid **155** (600 mg, 0.593 mmol, 1 equiv) was combined with *N*-hydroxyphthalimide (116 mg, 0.712 mmol, 1.2 equiv) and DMAP (7.2 mg, 0.059 mmol, 0.1 equiv) in DCM (5.93 mL). DIC (102 µL, 0.652 mmol, 1.1 equiv) was added dropwise, and the mixture stirred overnight before being quenched with water and filtered through celite, eluting with ethyl acetate. Flash chromatography on silica, grading from 30- 45% ethyl acetate in hexanes, afford **157** (340 mg, 0.294 mmol, 50%). ^{1}H NMR (400 MHz, $CDCl_3$): δ 7.93 (dd, J = 5.5, 3.1 Hz, 2H), 7.83 (dd, J = 5.5, 3.1 Hz, 2H), 6.48 (d, J = 2.9 Hz, 1H), 6.05 (d, J = 2.7 Hz, 1H), 5.85 (dd, J = 9.4, 2.8 Hz, 1H), 5.32 (s, 1H), 5.06 (t, J = 2.8 Hz, 1H), 4.99 – 4.89 (m, 3H), 4.73 (s, 1H), 4.59 – 4.49 (m, 1H), 4.47 – 4.42 (m, 1H), 4.33 (d, J = 8.8 Hz, 2H), 4.13 (d, J = 7.1 Hz, 1H), 3.67 – 3.54 (m, 1H), 3.49 – 3.37 (m, 1H), 3.37 – 3.25

(m, 1H), 2.38 (d, J = 13.4 Hz, 1H), 2.20 (s, 6H), 2.18 (s, 3H), 2.15 (s, 6H), 1.64 (q, J = 13.5 Hz, 1H).

$^{13}C\{^{1}H\}$ NMR (101 MHz, $CDCl_3$): δ 170.90, 170.24, 161.55, 135.04, 129.00, 124.28, 107.60, 99.37, 98.40, 79.59, 78.11, 75.29, 74.95, 73.52, 65.80, 59.87, 58.23, 56.68, 49.55, 43.19, 32.07, 22.84, 20.84, 20.71.

HRMS (ESI-TOF) m/z: $[M+Na]^+$ Calcd for $C_{43}H_{48}N_{16}O_{23}Na$ 1179.2970; Found 1179.3007

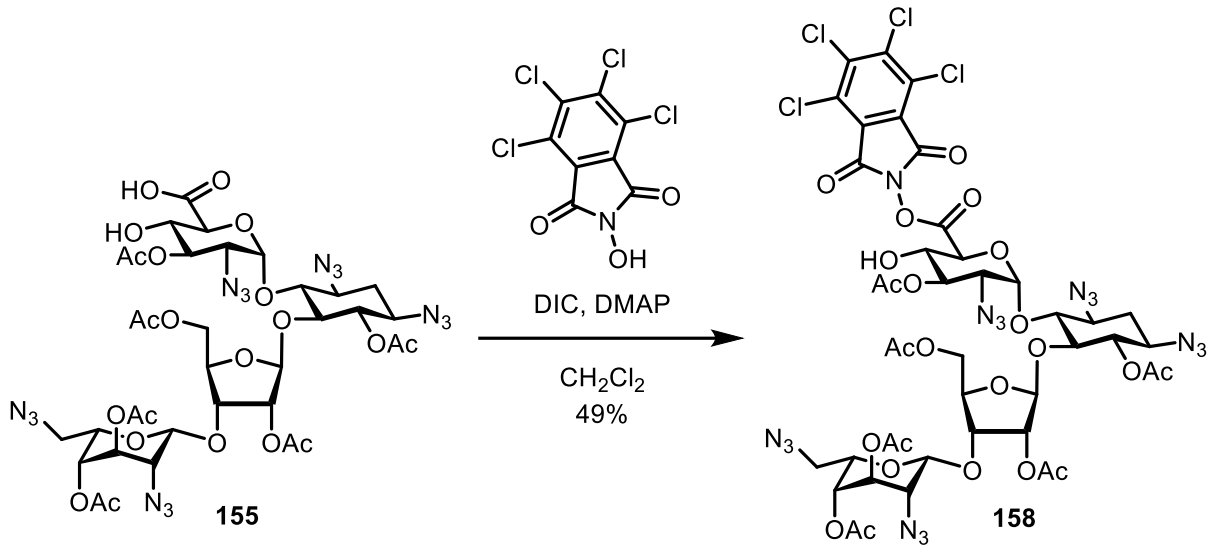

(*2S,3R,4R,5R,6R*)-6-(((*2R,3R,4R,5S*)-4-acetoxy-5-(((*1S,2S,3R,5S,6R*)-2-acetoxy-6-(((*2S,3R,4R,5S,6S*)-4-acetoxy-3-azido-5-hydroxy-6-(((4,5,6,7-tetrachloro-1,3-dioxoisoindolin-2-yl)oxy)carbonyl)tetrahydro-*2H*-pyran-2-yl)oxy)-3,5-diazidocyclohexyl)oxy)-2-(acetoxymethyl)tetrahydrofuran-3-yl)oxy)-5-azido-2-(azidomethyl)tetrahydro-*2H*-pyran-3,4-diyl diacetate (158)

Acid **155** (125 mg, 0.124 mmol, 1 equiv) was combined with tetrachloro-*N*-hydroxyphthalimide (39 mg, 0.130 mmol, 1.05 equiv) and DMAP (1.5 mg, 0.012 mmol, 0.1 equiv) in DCM (1.23 mL). DIC (21 µL, 0.136 mmol, 1.1 equiv) was added dropwise, and the mixture stirred overnight before being quenched with water and filtered through celite, eluting with ethyl acetate. Flash chromatography on silica, grading quickly* from 30- 45% ethyl acetate in hexanes, afford **158** (79 mg, 0.061 mmol, 49%).

*Purification should be performed quickly due to hydrolysis of the product on silica.

^{1}H NMR (400 MHz, $CDCl_3$): δ 6.45 (d, J = 2.9 Hz, 1H), 6.02 (d, J = 2.6 Hz, 1H), 5.81 (dd, J = 9.3, 2.9 Hz, 1H), 5.29 (d, J = 2.4 Hz, 1H), 5.04 (dt, J = 5.7, 2.7 Hz, 3H), 4.96 – 4.84 (m, 4H), 4.76 – 4.67 (m, 2H), 4.58 – 4.49 (m, 1H), 4.45 – 4.37 (m, 1H), 4.36 – 4.23 (m, 2H), 4.19 – 4.07 (m, 1H),

3.82 (dd, J = 6.9, 2.7 Hz, 2H), 3.68 – 3.54 (m, 2H), 3.47 – 3.36 (m, 1H), 3.36 – 3.25 (m, 2H), 2.35 (dt, J = 13.5, 4.5 Hz, 1H), 2.17 (s, 6H), 2.15 (s, 3H), 2.12 (d, J = 1.0 Hz, 6H), 1.60 (q, J = 12.9 Hz, 1H).

$^{13}C\{^{1}H\}$ NMR (101 MHz, $CDCl_3$): δ 170.88, 170.28, 170.20, 169.91, 169.71, 168.66, 157.42, 157.11, 141.32, 138.54, 130.75, 124.75, 113.62, 107.60, 107.11, 99.36, 98.85, 98.42, 84.84, 82.36, 79.61, 78.16, 75.76, 75.25, 74.92, 73.53, 68.81, 65.79, 65.69, 63.22, 58.28, 58.20, 56.67, 50.71, 42.47, 32.00, 21.00, 20.94, 20.91, 20.82, 20.68.

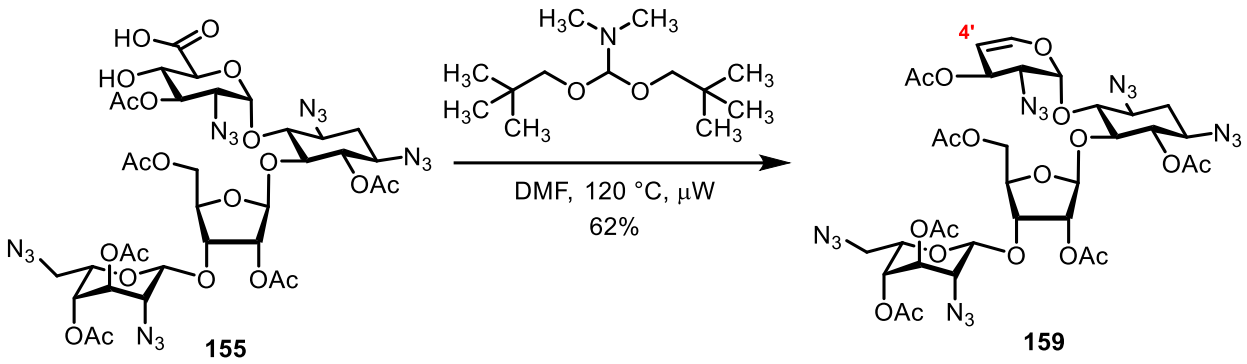

(*2S,3R,4R,5R,6R*)-6-(((2R,3R,4S,5S)-4-acetoxy-5-(((*1S,2R,3R,5S,6S*)-2-acetoxy-6-(((*2R,3R,4S*)-4-acetoxy-3-azido-3,4-dihydro-*2H*-pyran-2-yl)oxy)-3,5-diazidocyclohexyl)methyl)-2-(acetoxymethyl)tetrahydrofuran-3-yl)oxy)-5-azido-2-(azidomethyl)tetrahydro-*2H*-pyran-3,4-diyl diacetate (159)

Crude acid **155** (593 mg, 0.586 mmol, 1 equiv) was dissolved in anhydrous DMF in a microwave vial and degassed for 15 minutes by bubbling argon through the solution. Dimethylformamide dineopentylacetal (DMFDNA, 820 μL, 2.93 mmol, 5 equiv) was added and the vial immediately heated to 120 °C with stirring under microwave irradiation for 20 minutes. The solution was directly concentrated under vacuum to provide the crude, which was purified by flash chromatography on silica gel, grading from 25–30% ethyl acetate in hexanes, to give olefin **159** (345 mg, 0.274 mmol, 62%).

R_f: (50% ethyl acetate in hexanes, CAM): 0.51

^{1}H NMR (400 MHz, $CDCl_3$): δ 6.34 (dd, J = 6.3, 1.4 Hz, 1H), 5.71 (d, J = 2.5 Hz, 1H), 5.52 – 5.44 (m, 1H), 5.28 (d, J = 2.8 Hz, 1H), 5.03 (t, J = 2.8 Hz, 1H), 4.96 – 4.89 (m, 2H), 4.86 (d, J = 2.0 Hz, 1H), 4.84 (d, J = 2.8 Hz, 1H), 4.70 (t, J = 2.3 Hz, 1H), 4.54 – 4.44 (m, 1H), 4.39 (t, J = 5.6 Hz, 1H), 4.32 – 4.23 (m, 2H), 4.10 – 4.04 (m, 1H), 3.78 (dt, J = 26.9, 9.0 Hz, 2H), 3.63 – 3.54 (m, 2H),

3.46 – 3.35 (m, 2H), 3.34 – 3.26 (m, 2H), 2.30 (dt, J = 13.5, 4.6 Hz, 1H), 2.17 (s, 3H), 2.15 (s, 3H), 2.12 (s, 3H), 2.11 (s, 3H), 2.10 (s, 3H), 1.46 (d, J = 13.0 Hz, 1H).

$^{13}C\{^{1}H\}$ NMR (101 MHz, $CDCl_3$): δ 171.31, 170.80, 170.37, 169.92, 169.76, 168.66, 142.75, 107.08, 100.26, 99.47, 97.56, 81.82, 79.60, 78.78, 75.87, 75.26, 74.84, 73.53, 68.83, 66.28, 65.82, 63.43, 60.54, 59.84, 59.02, 58.31, 56.71, 50.74, 32.07, 21.24, 21.02, 20.92, 20.89, 20.82, 20.69.

HRMS (ESI-TOF) m/z: $[M+Na]^+$ Calcd for $C_{34}H_{43}N_{15}O_{18}Na$ 972.2803; Found 972.2792.

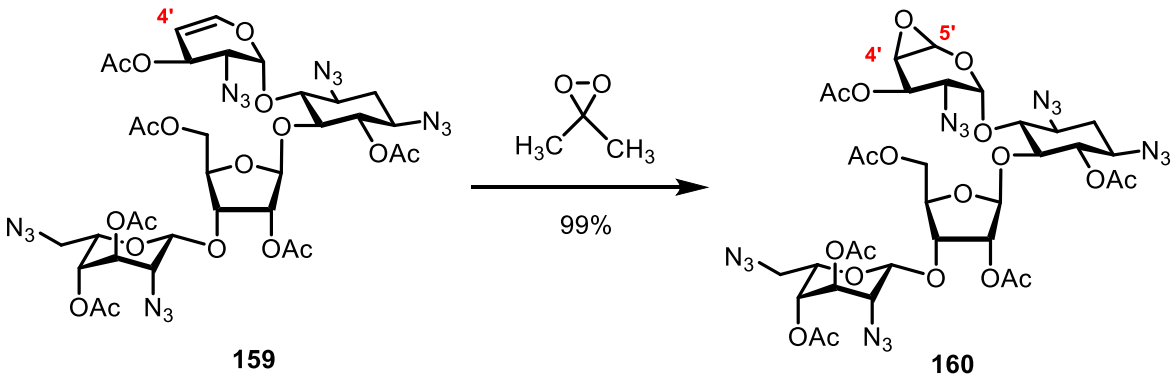

(*2S,3R,4R,5R,6R*)-6-(((*2R,3R,4S,5S*)-4-acetoxy-5-(((*1S,2R,3R,5S,6S*)-2-acetoxy-6-(((*1S,3S,4R,5R,6R*)-5-acetoxy-4-azido-2,7-dioxabicyclo[4.1.0]heptan-3-yl)oxy)-3,5-diazidocyclohexyl)methyl)-2-(acetoxymethyl)tetrahydrofuran-3-yl)oxy)-5-azido-2-(azidomethyl)tetrahydro-*2H*-pyran-3,4-diyl diacetate (160)

4'-deoxypentenoside **159** (30.0 mg, 0.032 mmol, 1 equiv) in DCM (320 µL) was cooled to - 55 °C and pre-cooled DMDO solution (0.05 M in acetone, prepared and titrated according to reference 33, 950 µL, 0.047 mmol, 1.5 equiv) was added dropwise. The reaction was maintained at - 55 °C overnight, and after 20 total hours of stirring the house vacuum was applied to the vessel by needle while the flask remained at - 55 °C for 15 minutes. The flask was then allowed to warm to 0 °C, dried under house vacuum for 30 minutes, and then finally warmed to room temperature and dried an additional 30 minutes. After concentration under vacuum, **160** was obtained as a white foam (30 mg, 0.031 mmol, 99%).

R_f: (50% ethyl acetate in hexanes, $KMnO_4$): 0.51

^1H NMR (400 MHz, $CDCl_3$): δ 5.62 (d, J = 2.4 Hz, 1H), 5.58 (dd, J = 9.8, 2.2 Hz, 1H), 5.27 (d, J = 2.4 Hz, 1H), 5.01 (t, J = 2.9 Hz, 1H), 4.92 (d, J = 2.8 Hz, 1H), 4.91 – 4.85 (m, 2H), 4.69 (t, J = 2.3 Hz, 1H), 4.46 – 4.36 (m, 2H), 4.29 – 4.20 (m, 2H), 4.08 (ddd, J = 8.1, 4.5, 1.9 Hz, 1H), 3.82 – 3.72 (m, 2H), 3.61 – 3.52 (m, 2H), 3.46 – 3.33 (m, 3H), 3.30 (d, J = 2.5 Hz, 1H), 3.27 (dd, J =

13.0, 4.5 Hz, 1H), 2.33 (dt, J = 13.5, 4.5 Hz, 1H), 2.18 (s, 3H), 2.15 (s, 6H), 2.14 (s, 3H), 2.10 (s, 3H), 2.09 (s, 3H), 1.52 (q, J = 12.8 Hz, 1H).

$^{13}C\{^{1}H\}$ NMR (101 MHz, $CDCl_3$): δ 170.80, 170.58, 170.27, 169.93, 169.75, 168.68, 107.44, 99.26, 97.80, 82.20, 79.53, 76.38, 76.00, 75.71, 75.40, 74.94, 73.49, 68.77, 67.00, 65.77, 63.19, 59.83, 58.65, 58.19, 56.62, 53.21, 50.69, 31.92, 21.01, 20.95, 20.88, 20.86, 20.79, 20.66.

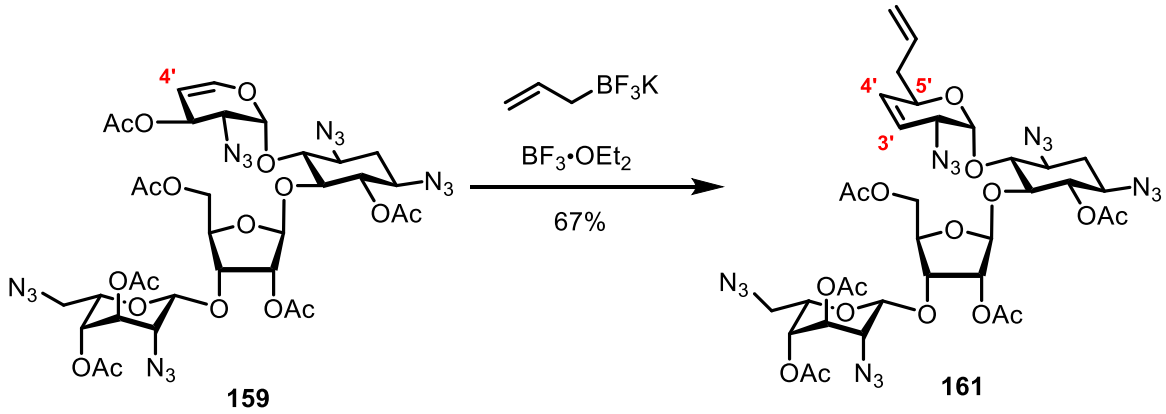

(*2S,3R,4R,5R,6R*)-6-(((*2R,3R,4R,5S*)-4-acetoxy-5-(((*1S,2S,3R,5S,6R*)-2-acetoxy-6-(((*2R,3R,6R*)-6-allyl-3-azido-3,6-dihydro-*2H*-pyran-2-yl)oxy)-3,5-diazidocyclohexyl)oxy)-2-(acetoxymethyl)tetrahydrofuran-3-yl)oxy)-5-azido-2-(azidomethyl)tetrahydro-*2H*-pyran-3,4-diyl diacetate (161)

4'-deoxypentenoside **159** (52.0 mg, 0.055 mmol, 1 equiv) and potassium allyltrifluoroborate (52.7 mg, 0.356 mmol, 6.5 equiv) were combined in a flame-dried vial under Ar and the mixture of solids suspended in acetonitrile (550 µL). The solution was cooled to 0 °C and boron trifluoride etherate (67 µL, 0.547 mmol, 10 equiv) was added dropwise. After 2 hours, the reaction was quenched with sat. aq. sodium bicarbonate (3 mL), extracted with ethyl acetate (3 x 5 mL), and the combined organic phases washed with water (5 mL) and brine (5 mL). The organic layer was dried on magnesium sulfate, filtered, and concentrated. Purification by flash chromatography on silica, grading from 20–30% ethyl acetate in hexanes, gave Ferrier product **161** (34.6 mg, 0.037 mmol, 67%).

R_f: (50% ethyl acetate in hexanes, CAM): 0.54

^{1}H NMR (400 MHz, $CDCl_3$): δ 6.03 (dt, J = 10.3, 2.0 Hz, 1H), 5.83 (ddt, J = 17.1, 10.3, 6.9 Hz, 2H), 5.75 (dt, J = 10.4, 2.8 Hz, 1H), 5.70 (d, J = 3.2 Hz, 1H), 5.27 (d, J = 2.9 Hz, 1H), 5.20 – 5.10 (m, 2H), 5.03 (t, J = 2.9 Hz, 1H), 4.92 (t, J = 9.5 Hz, 1H), 4.87 – 4.83 (m, 2H), 4.72 – 4.66 (m,

1H), 4.60 – 4.51 (m, 1H), 4.41 – 4.33 (m, 2H), 4.29 (td, J = 5.9, 2.2 Hz, 1H), 4.18 (dd, J = 12.0, 5.5 Hz, 1H), 4.09 (ddd, J = 8.1, 4.4, 1.8 Hz, 1H), 3.83 – 3.70 (m, 2H), 3.65 – 3.55 (m, 2H), 3.48 – 3.37 (m, 2H), 3.32 (t, J = 2.2 Hz, 1H), 3.26 (dd, J = 13.0, 4.4 Hz, 1H), 2.37 (dp, J = 21.7, 7.3 Hz, 2H), 2.26 (dt, J = 13.4, 4.6 Hz, 1H), 2.17 (s, 6H), 2.15 (s, 3H), 2.12 (s, 3H), 2.09 (s, 3H), 1.45 (q, J = 12.8 Hz, 1H).

$^{13}C\{^{1}H\}$ NMR (101 MHz, $CDCl_3$): δ 170.74, 170.31, 169.90, 169.73, 168.63, 133.82, 133.26, 120.78, 118.01, 107.20, 99.44, 95.80, 82.62, 79.36, 77.53, 76.12, 75.32, 74.85, 73.61, 70.70, 68.79, 65.78, 64.15, 59.67, 58.45, 56.66, 54.38, 50.70, 38.55, 32.19, 21.01, 20.93, 20.88, 20.79, 20.66.

HRMS (ESI-TOF) m/z: $[M+NH_4]^+$ Calcd for $C_{35}H_{49}N_{16}O_{16}$ 949.3507; Found 949.3507.

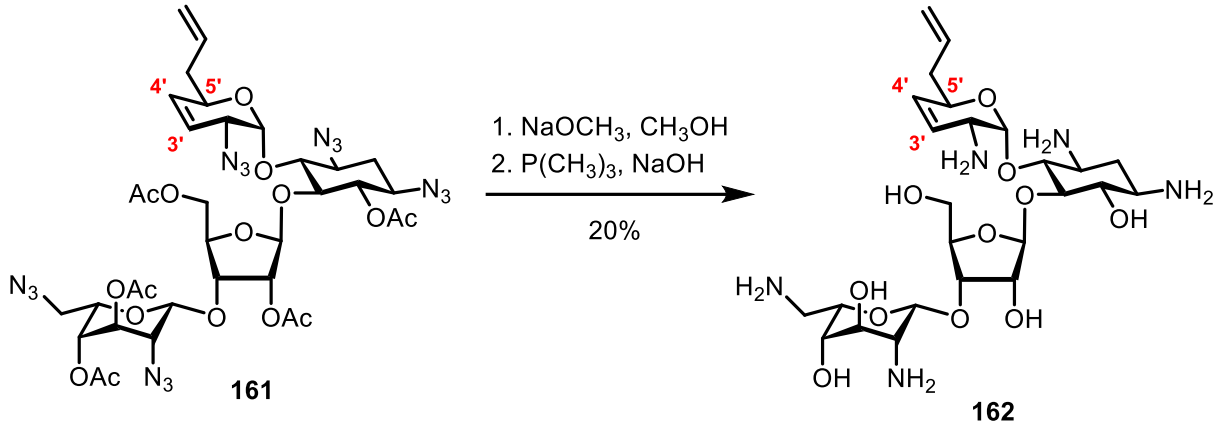

(*2S,3S,4R,5R,6R*)-6-(((*2R,3S,4R,5S*)-5-(((*1R,2R,3S,5R,6S*)-2-(((*2R,3R,6R*)-6-allyl-3-amino-3,6-dihydro-*2H*-pyran-2-yl)oxy)-3,5-diamino-6-hydroxycyclohexyl)oxy)-4-hydroxy-2-(hydroxymethyl)tetrahydrofuran-3-yl)oxy)-5-amino-2-(aminomethyl)tetrahydro-*2H*-pyran-3,4-diol (162)

C5'-allyl **161** (9.8 mg, 10.5 µmol, 1 equiv) in anhydrous methanol (210 µL) was cooled to 0 °C and treated with freshly prepared sodium methoxide solution (0.2 M in methanol, 58 µL, 11.5 µmol, 1.1 equiv); the solution was allowed to warm to room temperature slowly and stirred overnight. The reaction was quenched by addition of sat. aq. ammonium chloride solution (5 mL) and the mixture washed with ethyl acetate (3 x 5 mL). The combined organic layers were dried on sodium sulfate, filtered, and concentrated to give crude polyalcohol.

The crude polyalcohol (7.5 mg, 10.4 µmol, 1 equiv) was dissolved in THF (260 µL) and water (260 µL) and sodium hydroxide solution (1.0 M in water, 130 µL, 130 µmol, 12.5 equiv) were added in sequence. Trimethylphosphine (1.0 M in THF, 80 µL, 80 µmol, 7.7 equiv) was added the solution immediately brought to 60 °C in an oil bath. Stirring at this temperature was maintained for 5 hours and the reaction then quenched after cooling to room temperature via the addition of glacial acetic acid (100 µL). The solution was washed with diethyl ether (3 x 3 mL), and the

separated ether layers discarded. The 10% acetic acid solution of crude **162** was purified by CM Sephadex-C25 chromatography, grading from 0.1% to 0.7% ammonium hydroxide in water. The product-containing fractions (identified by spotting on normal-phase TLC plates and charring in 80:20 ethanol:sulfuric acid) were combined, glacial acetic acid (150 μL) was added, and the product dried by lyophilization to give **112** as the pentaacetate salt* (1 mg, 2 μmol, 20%).

*the yield is reported on the basis of free-based compound while characterization is reported for the pentaacetate salt.

^{1}H NMR (400 MHz, D_2O): δ 6.35 – 6.19 (m, 1H), 6.03 – 5.83 (m, 2H), 5.51 (d, J = 2.6 Hz, 1H), 5.38 – 5.16 (m, 4H), 4.66 (t, J = 7.9 Hz, 1H), 4.49 (t, J = 5.4 Hz, 1H), 4.37 (dd, J = 4.9, 2.6 Hz, 1H), 4.34 – 4.28 (m, 1H), 4.27 – 4.16 (m, 3H), 4.02 (dd, J = 5.4, 2.4 Hz, 1H), 3.87 – 3.76 (m, 3H), 3.76 – 3.66 (m, 2H), 3.58 – 3.48 (m, 2H), 3.46 – 3.32 (m, 2H), 3.31 – 3.14 (m, 2H), 2.51 (t, J = 7.1 Hz, 2H), 2.36 (dq, J = 13.1, 4.5 Hz, 1H), 1.92 (s, 15H), 1.62 (t, J = 12.6 Hz, 1H).

^{13}C{^{1}H} NMR (101 MHz, D_2O): δ 181.39, 136.16, 134.51, 118.22, 110.24, 96.01, 92.58, 84.34, 81.41, 76.32, 73.73, 73.29, 70.25, 68.01, 67.50, 61.51, 51.04, 49.95, 48.80, 45.17, 40.45, 37.06, 23.19.

HRMS (ESI-TOF) m/z: $[M+H]^+$ Calcd for $C_{25}H_{46}N_5O_{11}$ 592.3188; Found 592.3198.

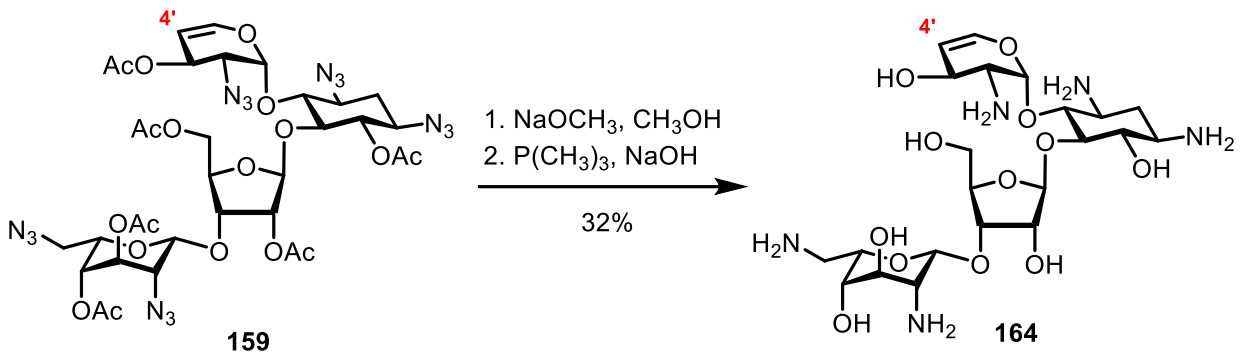

(*2S,3S,4R,5R,6R*)-5-amino-2-(aminomethyl)-6-(((*2R,3S,4S,5S*)-5-(((*1R,2S,3S,5R,6R*)-3,5-diamino-2-(((*2R,3R,4S*)-3-amino-4-hydroxy-3,4-dihydro-*2H*-pyran-2-yl)oxy)-6-hydroxycyclohexyl)methyl)-4-hydroxy-2-(hydroxymethyl)tetrahydrofuran-3-yl)oxy)tetrahydro-*2H*-pyran-3,4-diol (164)

4'-deoxypentenoside **159** (40 mg, 42 µmol, 1 equiv) in anhydrous methanol (840 µL) was cooled to 0 °C and treated with freshly prepared sodium methoxide solution (1 M in methanol, 42 µL, 42 µmol, 1 equiv); the solution was allowed to warm to room temperature slowly and stirred overnight. The reaction was quenched by the addition of sat. aq. ammonium chloride solution (5 mL) and the mixture washed with ethyl acetate (3 x 5 mL). The combined organic layers were dried on sodium sulfate, filtered, and concentrated to give crude polyalcohol.

The crude polyalcohol (25 mg, 8.3 µmol, 1 equiv) was dissolved in THF (900 µL) and water (900 µL) and sodium hydroxide solution (1.0 M in water, 450 µL, 450 µmol, 12.5 equiv) were added in sequence. Trimethylphosphine (1.0 M in THF, 233 µL, 233 µmol, 6.5 equiv) was added the solution immediately brought to 60 °C in an oil bath. Stirring at this temperature was maintained for 5 hours and the reaction then quenched after cooling to room temperature via the addition of glacial acetic acid (100 µL). The solution was washed with diethyl ether (3 x 3 mL), and the separated ether layers discarded. The 10% acetic acid solution of crude **164** was purified by CM

Sephadex-C25 chromatography, grading from 0.1% to 0.7% ammonium hydroxide in water. The product-containing fractions (identified by spotting on normal-phase TLC plates and charring in 80:20 ethanol:sulfuric acid) were combined, glacial acetic acid (150 μL) was added, and the product dried by lyophilization to give **164** as the pentaacetate salt* (10 mg, 12 μmol, 32%).

*the yield is reported on the basis of free-based compound while characterization is reported for the pentaacetate salt.

^{1}H NMR (400 MHz, D_2O): δ 6.53 (d, J = 6.2 Hz, 1H), 5.53 (d, J = 2.1 Hz, 1H), 5.38 – 5.22 (m, 2H), 5.24 – 5.11 (m, 1H), 4.51 (t, J = 5.7 Hz, 1H), 4.36 (dd, J = 4.8, 2.9 Hz, 2H), 4.31 (t, J = 5.3 Hz, 1H), 4.24 (t, J = 3.1 Hz, 1H), 4.20 – 4.14 (m, 1H), 4.07 (t, J = 9.8 Hz, 1H), 3.89 (dd, J = 12.3, 3.5 Hz, 1H), 3.85 – 3.73 (m, 4H), 3.69 (t, J = 9.8 Hz, 1H), 3.60 – 3.56 (m, 1H), 3.55 – 3.29 (m, 4H), 2.49 (dt, J = 12.4, 4.3 Hz, 1H), 1.94 (s, 15H), 1.83 (q, J = 12.2 Hz, 1H).

^{13}C{^{1}H} NMR (101 MHz, D_2O): δ 180.89, 142.77, 109.88, 102.10, 95.53, 95.27, 83.03, 81.36, 78.58, 75.94, 73.32, 72.01, 70.24, 67.67, 67.24, 61.94, 60.88, 51.95, 50.86, 49.81, 48.38, 40.43, 28.12, 22.93.

HRMS (ESI-TOF) m/z: $[M+Na]^+$ Calcd for $C_{22}H_{41}N_5O_{12}Na$ 590.2644; Found 590.2643.

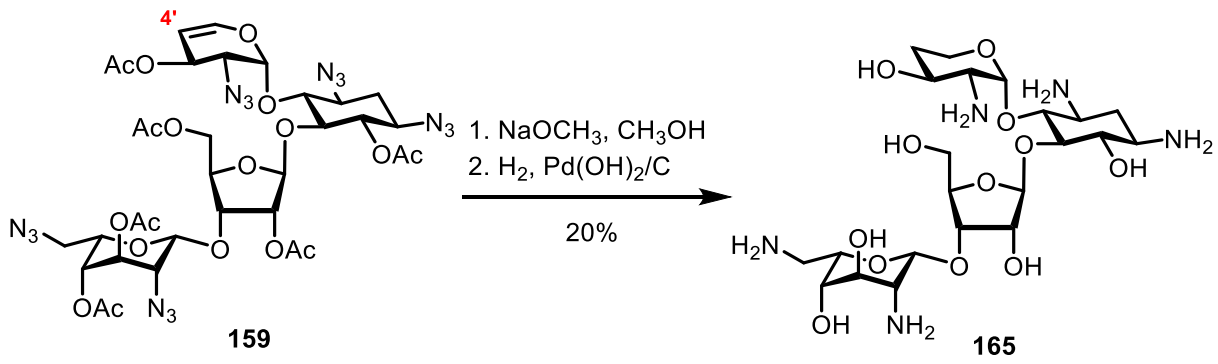

(*2S,3S,4R,5R,6R*)-5-amino-2-(aminomethyl)-6-(((*2R,3S,4R,5S*)-5-(((*1R,2R,3S,5R,6S*)-3,5-diamino-2-(((*2R,3R,4S*)-3-amino-4-hydroxytetrahydro-*2H*-pyran-2-yl)oxy)-6-hydroxycyclohexyl)oxy)-4-hydroxy-2-(hydroxymethyl)tetrahydrofuran-3-yl)oxy)tetrahydro-*2H*-pyran-3,4-diol (165)

4'-deoxypentenoside **159** (26.0 mg, 27.4 μmol, 1 equiv) in anhydrous methanol (550 μL) was cooled to 0 °C and treated with freshly prepared sodium methoxide solution (0.2 M in methanol, 150 μL, 30.0 μmol, 1.1 equiv); the solution was allowed to warm to room temperature slowly and stirred overnight. The reaction was quenched by the addition of sat. aq. ammonium chloride solution (5 mL) and the mixture washed with ethyl acetate (3 x 5 mL). The combined organic layers were dried on sodium sulfate, filtered, and concentrated to give crude polyalcohol.

The crude polyalcohol (19 mg, 8.3 μmol, 1 equiv) was dissolved in equal parts water, methanol, ethyl acetate, and acetic acid (totaling 560 μL). Palladium (II) hydroxide on carbon (20% w/w, 38 mg, 54 μmol, 2 equiv) was added and the atmosphere exchanged for nitrogen three times on a Schlenk manifold, and then instead backfilled with hydrogen gas three times. The hydrogen balloon bubbled gas through the solution (venting with a needle) for 10 minutes while stirring, and then the needle removed and the hydrogenation stirred overnight. The reaction was halted by passing the solution through a pad of celite, eluting with water. Acetic acid was added to make a

~10% aqueous solution of **165** which was purified by CM Sephadex-C25 chromatography, grading from 0.1% to 0.7% ammonium hydroxide in water. The product-containing fractions (identified by spotting on normal-phase TLC plates and charring in 80:20 ethanol:sulfuric acid) were combined, glacial acetic acid (150 µL) was added, and the product dried by lyophilization to give **165** as the pentaacetate salt* (2 mg, 4 µmol, 10%).

*the yield is reported on the basis of free-based compound while characterization is reported for the pentaacetate salt.

^{1}H NMR (400 MHz, D_2O): δ 5.50 (d, J = 2.9 Hz, 1H), 5.30 (d, J = 2.0 Hz, 2H), 4.54 (dd, J = 6.7, 4.8 Hz, 1H), 4.39 (dd, J = 4.8, 2.1 Hz, 1H), 4.32 (ddd, J = 6.8, 3.9, 1.5 Hz, 1H), 4.24 (t, J = 3.1 Hz, 1H), 4.20 (ddd, J = 7.7, 5.6, 3.8 Hz, 2H), 3.96 – 3.74 (m, 7H), 3.65 – 3.61 (m, 1H), 3.60 – 3.56 (m, 1H), 3.47 (dt, J = 6.8, 2.8 Hz, 1H), 3.43 (d, J = 6.8 Hz, 1H), 3.38 (dd, J = 13.8, 3.9 Hz, 1H), 3.38 – 3.23 (m, 3H), 2.41 (dt, J = 12.5, 4.1 Hz, 1H), 2.04 (dq, J = 10.6, 3.6 Hz, 1H), 1.81 – 1.64 (m, 2H).

^{13}C{^{1}H} NMR (101 MHz, D_2O): δ 181.28, 110.23, 96.47, 95.48, 84.14, 81.18, 78.67, 75.50, 73.27, 72.54, 70.25, 67.74, 67.28, 64.52, 60.56, 60.46, 53.36, 50.88, 49.94, 48.67, 40.41, 29.46, 29.20, 23.13.

HRMS (ESI-TOF) m/z: $[M+H]^+$ Calcd for $C_{22}H_{44}N_5O_{12}$ 570.2981; Found 570.2983.

Chapter 5. Self-Condensation of Cyclopentanone to Form a Dienoic Acid: Resolution of a Mechanistic Puzzle of Long Duration

5.1 Transformation Background and Original Mechanistic Proposal

In 1973, Comer and Temple described the self-condensation of cyclopentanone and its subsequent fragmentation to an 11-carbon dienoic **166** in 59% yield after treatment with dimsyl

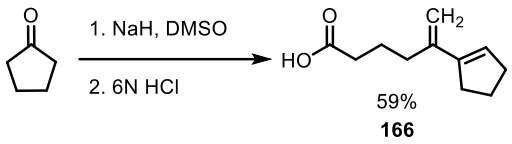

Figure 5.1. The self-condesnation of cyclopentanone to give **166** as described by Comer and Temple.

sodium (Figure 5.1).[1] The published transformation formed the basis of a contemporaneous patent application[2] by the same authors, wherein it was stated "Dienoic acid δ-methylene-1-cyclopentene-1-pentanoic acid is obtained by reacting [sic] cyclopentanone with one chemical equivalent of methylsulfinylmethide alkali metal salt in dimethyl sulfoxide." Concurrent with the disclosure of this transformation, they supplied mechanistic studies in proposition of the mechanism outlined in Figure 5.2. Critical to the unique mechanism outlined below was the sigmatropic rearrangement

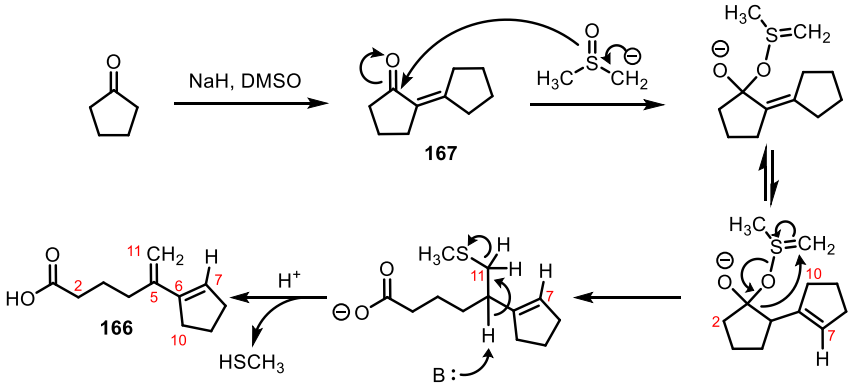

Figure 5.2. Proposed mechanism for the formation of dienoic acid **1**. Adapted from ref 1. Copyright 1973 American Chemical Society.

of an *O*-acyloxy sulfoxonium ylide, facilitating the C-1 and C-5 bond fragmentation. Following this shift, elimination of methanethiol would yield **166** after protonation.

In 1974 Professor Stuart L. Schreiber (S.L.S., then a graduate student) replicated these surprising results, and had on occasion the opportunity to discuss this mechanistic proposal with Prof. R.B. Woodward. Following a detailed analysis of a full set of spectroscopic data it was determined the structural assignment of **166** had been correct, further verified by Prof. Woodward upon his own analysis. The issue of mechanism, a focal point of their discussion, was never satisfactorily resolved despite lengthy and skeptical consideration, and the problem was set aside when a different thesis project, not involving compound **166**, was prioritized for study. The problem resurfaced during reminiscences of graduate school and the question was posed anew: what is the operative mechanism for the formation of **166**? In this chapter, additional mechanistic studies alongside substantial literature precedent provide support for an alternative mechanistic proposal that we believe satisfactorily resolves a puzzle of roughly five decades in duration.

To support their original mechanistic proposal, Comer and Temple cited the results of two mechanistic experiments that they had conducted. In the first of these they showed that the proposed intermediate α-cyclopentylidenecyclopentanone, **167**, was indeed transformed into dienoic acid **166** under conditions replicating those of Figure 5.1, albeit in a reduced yield (26%,

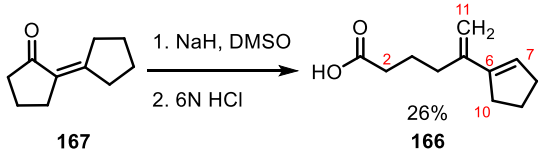

Figure 5.3. Comer and Temple fragmentation of proposed intermediate **167** to **166**.

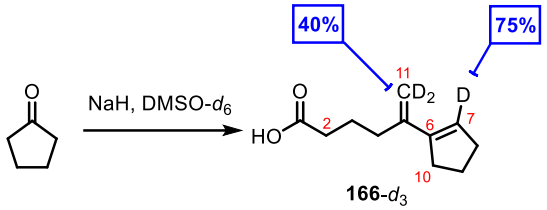

Figure 5.4. Reported deuteration studies of product **166** when conducting the reaction in DMSO-d_6.[1]

Figure 5.3). In the second, they showed that when the transformation of Figure 5.1 was conducted in DMSO-d_6 (99.5%) in lieu of DMSO as the solvent, product **166** was obtained (yield not specified, Figure 5.4) "partially deuterated at the methylene group (40%) and the ring vinyl proton (75%)".

5.2 Replication and new mechanistic evidence.

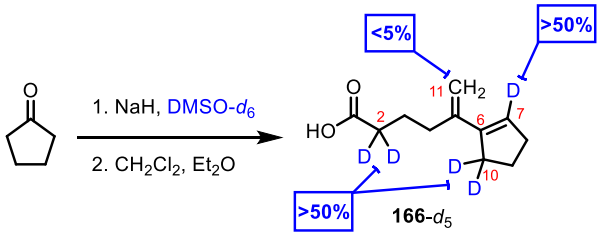

Figure 5.5. Replicated deuteration with assignments supported by NMR experiments.

When we replicated this experiment, our NMR analysis of the product **166** revealed that deuteration had occurred at C-2, C-7, and C-10 (>50%, Figure 5.5) but not C-11 (<5%) (Figure 5.5). Considering it more likely that C-11 originated from the dichloromethane present in the

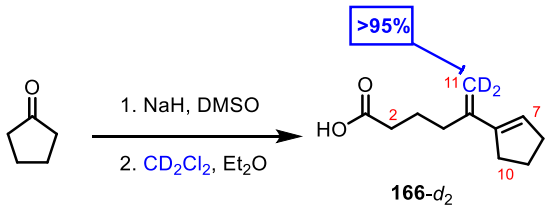

Figure 5.6. Incorporation of deuterated methylene following quench with CD_2Cl_2.

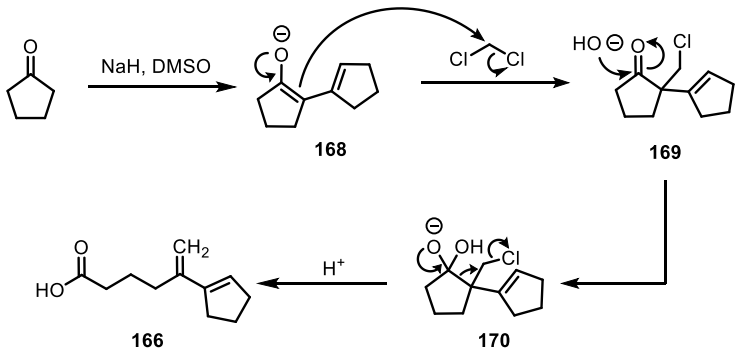

Figure 5.7. New mechanistic proposal utilizing dichloromethane as electrophile.

quenching solution rather than DMSO as originally, we conducted the transformation depicted in Figure 5.6 using dichloromethane-d_2 (99.9%) in lieu of CH_2Cl_2 in the quenching solution and obtained dienoic acid **166** (23% yield) with >95% deuteration at C-11. This result is consistent with the alternative mechanistic proposal depicted in Figure 5.7. In this proposal, self-condensation of cyclopentanone in the presence of dimsyl sodium (1 equiv) in DMSO forms the dienolate intermediate **168**. During the quench, which takes place over an extended period (as specified in the original protocol) we propose that alkylation of the dienolate **168** with dichloromethane as electrophile forms the α-chloromethyl ketone **169** as an intermediate. Subsequent attack by hydroxide then leads to fragmention of **169** to form **166** in its carboxylate form. As further support for the revised mechanisms of Figure 5.7, I dependently prepared the proposed intermediate **169** in 91% yield by alkylation of the potassium enolate of **167** with iodochloromethane at 0 °C (Figure 5.8). When **169** was subsequently exposed to potassium hydroxide in DMSO and ether, fragmentation occurred, and product **166** was obtained in 89% yield following an acidic workup.

5.3 Existing precedent for fragmentation of ketones to enoic acids.

The transformation of α-chloromethyl ketone **169** to dienoic acid **166** has considerable close precedent (Figure 5.9).[3-7] For example, Eschenmoser and Fray reported in 1952 that sulfonate ester

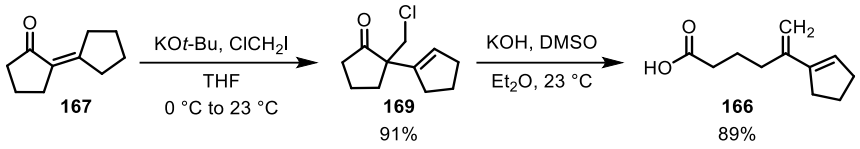

Figure 5.8. Synthesis of α-chloromethyl ketone **169** and its stepwise fragmentation to **166**.

171 undergoes fragmentation to form carboxylic acid **172** in 82% yield upon exposure to aqueous potassium hydroxide (Figure 5.9A.). Wenkert et. Al. disclosed a similar transformation arising from treatment of α-dichloromethylketone **173** with potassium tert-butoxide (Figure 5.9B).[4] Similarly, dibrominated camphor derivative **176** was shown to undergo fragmentation to exocyclic olefin **177** in high yields after treatment with sodium methoxide (Figure 5.9C).[6] An even larger array of nucleophiles was demonstrated by Hierold et, Al. to be competent in the fragmentation of α-halomethyl-β-ketoesters. In addition to solvolysis products, the formation of amides or terminal alcohols was achieved when utilizing amine or hydride nucleophiles, respectively.

5.4 Summary

Considering the studies reported herein and precedent cited, we believe the question of mechanism for the transformation of Figure 5.1 to be resolved. Substantial precedent combined with the stepwise fragmentation of an α-disubstituted halomethyl cyclopentanone provide support for a correction to the originally proposed mechanism. NMR evidence also directly indicates dichloromethane as the C-11 precursor in product **166**. Deuterium incorporation from dichloromethane-d_2 in the quenching solution negates DMSO as a deuterium donor, and the absence of product formed when quenching the reaction with aqueous hydrochloric acid demonstrates the necessity of dichloromethane for product formation.

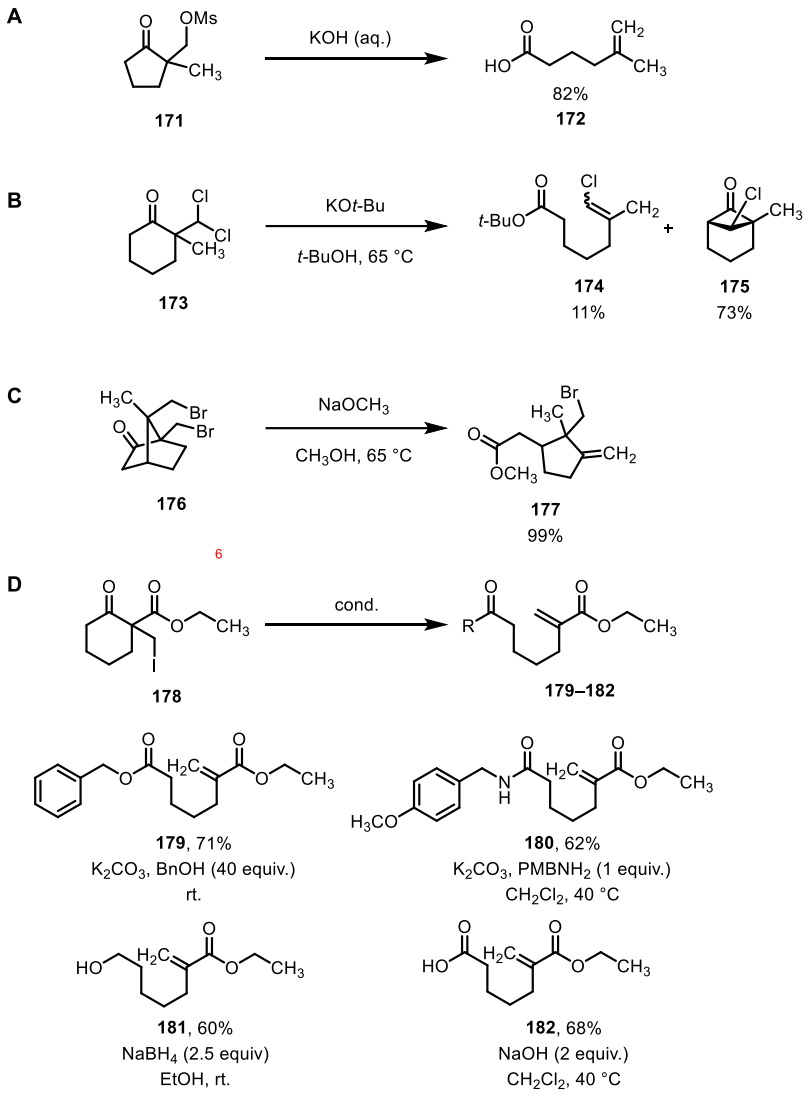

Figure 5.9. Selected examples of α-disubstituted ketone fragmentation. (A). Eschenmoser and Fray reporting solvolysis of methanesulfonate **171**. (B) A dichloromethylketone solvent addition byproduct. (C) Methanolysis of camphor-derived **176**. (D) Various nucleophiles add to and fragment α-iodomethyl-β-ketoesters.

5.5 References

1. Comer, W.T.; Temple, D.L. The reaction of Cyclopentanones with Methylsulfinyl Carbanion. *Journal of Organic Chemistry*, **1973**, *38* (12), 2121–2125.

2. Comer, W.T.; Rayburn, J.W.; Temple, D.L. d-methylene-1-cyclopentene-1-pentanoic acid. U.S. Patent WO 3853949, December 10, 1974.

3. Eschenmoser, A.; Frey, A. Über die Spaltung des Mesylesters von 2-Methyl-2-oxymethyl-cyclopentanon mit Basen. *Helvetica Chimica Acta*. **1952**, *35*, 1660–1666.

4. Wenkert, E.; Bakuzis, P.; Baumgarten, R.J.; Doddrell, D.; Jeffs, P.W.; Leicht, C.L.; Mueller, R.A.; Yoshikoshi, A. 1-Methylbicyclo[3.1.1]heptan-6-one and Related Substances. *J. Am. Chem. Soc.* **1970**, *92* (6), 1617–1624.

5. Wenkert, E.; Bakuzis, P.; Baumgarten, R.J.; Leicht, C.L.; Schenk, H.P. Homo-Favorskii Rearrangement. *J. Am. Chem. Soc.* **1970**, *93* (13), 3208–3216.

6. Clase, J.A.; Money, T.; Enantiospecific Synthesis of a Chiral Intermediate in Steroid Synthesis. *Synthesis*, **1989**, *1989* (12), 934–936.

7. Hierold, J.; Hsia, T.; Lupton, D.W. The Grob/Eschenmoser fragmentation of cycloalkanones bearing β-electron withdrawing groups: a general strategy to acyclic synthetic intermediates. *Organic and Biomolecular Chemistry*, **2011**, *9*, 783–792.

8. Still, W.C.; Khan, M.; Mitra, A. *J. Org. Chem.* **1978**, *43*, 2923.

9. Sharma, L.K.; Kim, K.B.; Elliott, G.I. *Green Chem.* **2011**, *13*, 1546.

5.6 Experimental Section

General Experimental Procedures. All reactions were performed in flame-dried round-bottom flasks fitted with rubber septa under positive argon pressure, unless otherwise noted. Air- and moisture-sensitive liquids were transferred via syringe. Organic solutions were concentrated by rotary evaporation (house vacuum, ca. 25-40 Torr) at ≤40 °C, unless otherwise noted. Analytical thin-layer chromatography (TLC) was performed using glass plates precoated with silica gel (0.25 mm, 60 Å pore-size, 230-400 mesh, Merck KGA) impregnated with a fluorescent indicator (254 nm). TLC plates were visualized by exposure to ultraviolet light, then stained with an aqueous potassium permanganate ($KMnO_4$) stain and briefly heated using a heat gun. Flash-column chromatography was performed as described by Still et al.,[8] employing silica gel (60 Å, 15-40 μM, EMD Millipore Corp.). All temperature measurements of reaction mixtures refer to the temperature of the heating/cooling bath unless otherwise specified. Structural assignments were made with additional information from gCOSY, gHSQC, and gHMBC experiments.

Materials. Commercial solvents and reagents were used as received. Cyclopentylidene cyclopentanone (**2**) was prepared as described by Sharma et al.,[9] and the associated procedure is described below.

Instrumentation. Proton magnetic resonance (^{1}H NMR) spectra were recorded on Bruker 400 (400 MHz) NMR spectrometers at 23 °C. Proton chemical shifts are expressed in parts per million (ppm, δ scale) and are referenced to residual protium in the NMR solvent ($CHCl_3$, δ 7.26, and C_6D_6, δ 7.16). Data are represented as follows: chemical shift, multiplicity (s = singlet, d = doublet, t = triplet, q = quartet, p = quintet, m = multiplet and/or multiple resonances, br = broad), coupling constant (*J*) in Hertz (Hz) and integration. Carbon nuclear magnetic resonance spectra (^{13}C NMR)

were recorded on Bruker 400 (100 MHz) NMR spectrometers at 23 °C. Carbon chemical shifts are expressed in parts per million (ppm, δ scale) and are referenced to the carbon resonances of the NMR solvent ($CDCl_3$, δ 77.16, and C_6D_6, δ 128.06). Infrared (IR) spectra were obtained using a Bruker ALPHA FT-IR spectrometer. Data are represented as follows: frequency of absorption (cm^{-1}), intensity of absorption (s = strong, m = medium, w = weak, br = broad). High resolution mass spectra were obtained at the Harvard University Mass Spectrometry Facility using the Thermo Q Exactive Plus Orbitrap mass spectrometer via Electrospray Ionization (ESI).

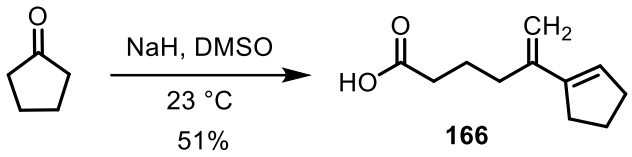

166

5-(cyclopent-1-en-1-yl)hex-5-enoic acid (166)

Sodium hydride (60% w/w suspension in mineral oil, 514 mg, 12.8 mmol, 1.08 eq) was added to vigorously stirring DMSO* (2.38 mL) at room temperature, and the stirred suspension brought to 70 °C by oil bath. Stirring continued at this temperature until gas evolution subsided (1 hour). The cloudy-grey mixture was then cooled by a room temperature water bath, and cyclopentanone (1.00 g, 11.9 mmol, 1 eq) was added dropwise (*notable exotherm and gas evolution, slow addition advised*). The reaction was maintained at 20 °C using an external water bath for 30 minutes, then the bath removed, and the mixture stirred for 5 hours at ambient temperature. The solution was poured onto a chilled (0 °C) solution of 1:1 ether:dichloromethane* (10 mL) and refrigerated (-20 °C) overnight. The precipitate was collected by vacuum filtration through a fritted funnel, and the solids washed with 9:1 ether:dichloromethane (20 mL). The solid salts were redissolved in water (15 mL) and acidified using 6 M HCl (1 mL) such that the pH was < 4 (pH paper) and the aqueous phase extracted into ether (15 mL). The organic phase was dried with $MgSO_4$, filtered, and evaporated to yield **1** (546 mg, 3.03 mmol, 51%) as an orange oil.† Additional purification can be achieved with flash chromatography on silica gel, eluting with a gradient from 20% Et_2O in hexanes to 50% Et_2O in hexanes to provide **166** as an off-white/orange solid (428 mg, 2.38 mmol, 40%). Note: Our yields never met or exceeded that reported by Comer and Temple (59% prior to an additional acidic precipitation)[2], hence the discrepancy in the yield reported here with that depicted in figure 1 within this chapter. *Readers are additionally advised of the explosion hazard associated with generating dimsyl sodium*.

R_f: (50% ethyl acetate in hexanes, $KMnO_4$): 0.34

^{1}H NMR (400 MHz, $CDCl_3$): δ 5.80 (t, J = 2.0 Hz, 1H), 4.93 (s, 1H), 4.91 (s, 1H), 2.51 – 2.42 (m, 4H), 2.42 – 2.29 (m, 4H), 1.88 (m, 4H).

$^{13}C\{^{1}H\}$ NMR (101 MHz, $CDCl_3$): δ 179.1, 143.3, 143.1, 127.3, 112.0, 33.5, 33.39, 33.36, 32.7, 23.8, 23.1.

^{1}H NMR (400 MHz, C_6D_6): δ 5.65 (td, J = 2.6, 1.2 Hz, 1H), 4.93 (s, 1H), 4.86 (s, 1H), 2.38 (tq, J = 7.9, 2.1 Hz, 2H), 2.33 – 2.25 (m, 2H), 2.19 (td, J = 7.6, 1.1 Hz, 2H), 2.11 (t, J = 7.3 Hz, 2H), 1.81 – 1.66 (m, 4H).

$^{13}C\{^{1}H\}$ NMR (101 MHz, C_6D_6): δ 180.1, 143.4, 143.1, 126.9, 111.9, 33.32, 33.25, 32.6, 23.8, 23.1.

FTIR (neat), cm^{-1}: 3087 (br), 2953 (m), 2847 (m), 2255 (w), 1707 (s), 1626 (w), 1593 (w), 1411 (m), 1242 (s).

HRMS (ESI-TOF) m/z: $[M+H]^+$ Calcd for $C_{11}H_{17}O_2$ 181.1223; Found 181.1224.

*Yields of **166**-d_2, when utilizing CD_2Cl_2 in quenching media, and **166**-d_x (mixtures from d_1 to d_5), when utilizing DMSO-d_6 as solvent, were 23% and 16%, respectively.

† A small aliquot (100 μL) from the reaction mixture was instead quenched with 1M aq. HCl (as opposed to dichloromethane-containing solutions) and extracted into diethyl ether (1 mL). The organic layer was dried on magnesium sulfate, filtered, and concentrated to provide crude material, which was identified as a mixture of **167** and its β,γ-unsaturated isomer (section 4.3).

Utilizing CD_2Cl_2 in the quenching solution affords **166** of mass: HRMS (ESI-TOF) m/z: $[M+H]^+$ Calcd for $C_{11}H_{15}D_2O_2$ 183.1349; Found 183.1349.

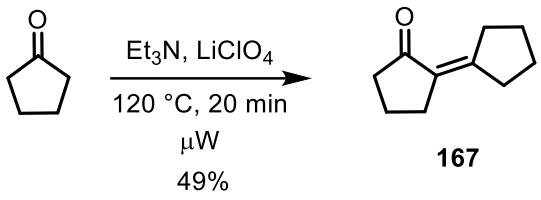

[1,1'-bi(cyclopentylidene)]-2-one (167)

Compound **167** was prepared according to literature precedent.[3] Cyclopentanone (10.00 g, 119 mmol, 1 eq) was combined with anhydrous triethylamine (6.63 mL, 47.6 mmol, 40 mol %) in a sealed tube containing anhydrous lithium perchlorate (5.06 g, 47.6 mmol, 40 mol %, dried by vacuum oven) and the mixture sonicated for 10 minutes. The tube was then heated by microwave irradiation to 120 °C for 20 minutes, and after cooling was poured onto saturated aqueous ammonium chloride solution (400 mL). The aqueous was extracted with ethyl acetate (3 x 200 mL), and the combined organics dried with magnesium sulfate, filtered, and concentrated to provide crude orange material. Vacuum distillation (external oil bath at 140 °C, 10 torr, distillate collected at 95 °C) of the crude material afforded **167** (4.4 g, 59.5 mmol, 49%) as a clear oil.

R_f (10% ethyl acetate in hexanes, $KMnO_4$): 0.40

^1H NMR (400 MHz, $CDCl_3$) δ 2.78 (tt, J = 7.3, 2.8 Hz, 2H), 2.53 (tp, J = 7.6, 2.6 Hz, 2H), 2.29 (m, 4H), 1.91 (p, J = 7.6 Hz, 2H), 1.70 (tdd, J = 11.3, 9.4, 5.9 Hz, 4H).

$^{13}C\{^1H\}$ NMR (101 MHz, $CDCl_3$) δ 207.4, 158.6, 127.9, 39.8, 34.3, 32.6, 29.5, 26.9, 25.2, 20.1.

FTIR (neat), cm^{-1}: 2956 (m), 2871 (m), 1710 (s), 1636 (s), 1413 (m), 1251 (s), 1168 (m).

HRMS (ESI-TOF) m/z: $[M+H]^+$ Calcd for $C_{10}H_{15}O$ 151.1117; Found 151.1119.

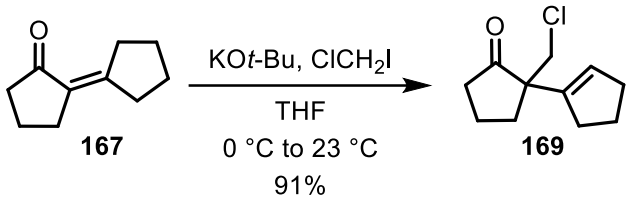

1-(chloromethyl)-[1,1'-bi(cyclopentan)]-1'-en-2-one (169)

Compound **167** was prepared according to literature precedent.[3] To a solution of **167** (100 mg, 0.67 mmol, 1 eq) in THF (6.7 mL) was added potassium *tert*-butoxide solution (1.0 M in THF, 640 µL, 0.64 mmol, 0.96 eq) at 0 °C (ice water bath). The ice bath was removed, and the solution stirred at ambient conditions for 30 minutes, and then re-cooled to 0 °C by ice bath. Thereafter, chloroiodomethane (55 µL, 0.76 mmol, 1.13 eq) was added dropwise and the solution monitored by TLC for consumption of starting material while slowly warming to room temperature. After 3 hours, the reaction was quenched by addition of aqueous potassium hydroxide (1 M in water, 2.0 mL, 2.0 mmol, 3 eq) and then neutralized with 1 M HCl. † The mixture was extracted with diethyl ether (3 x 10 mL) and the combined organics dried on $MgSO_4$, filtered, and concentrated to provide crude material. This residue was further purified by flash chromatography on silica (grading from hexanes to 5% ethyl acetate in hexanes) to afford **169** (120 mg, 0.6 mmol, 91%) as a deep brown oil.

R_f: (10% ethyl acetate in hexanes, $KMnO_4$): 0.53

^1H NMR (400 MHz, $CDCl_3$) δ 5.62 (t, J = 2.1 Hz, 1H), 3.73 (d, J = 10.9 Hz, 1H), 3.59 (d, J = 10.9 Hz, 1H), 2.44 – 2.09 (m, 8H), 2.06 – 1.75 (m, 4H).

$^{13}C\{^1H\}$ NMR (101 MHz, $CDCl_3$) δ 216.2, 140.2, 129.8, 56.8, 47.6, 37.8, 32.5, 31.7, 31.4, 23.2, 18.9.

FTIR (neat), cm^{-1}: 3054 (w), 2954 (s), 2891(m), 2847 (m), 1738 (s), 1637 (w), 1404 (m), 1282 (m), 1153 (s).

HRMS (ESI-TOF) m/z: $[M+H]^+$ Calcd for $C_{11}H_{16}ClO$ 199.0884; Found 199.0884.

† The presence of DMSO was critical for the fragmentation to occur. The quench using potassium hydroxide was initially an attempt to induce fragmentation but was unsuccessful.

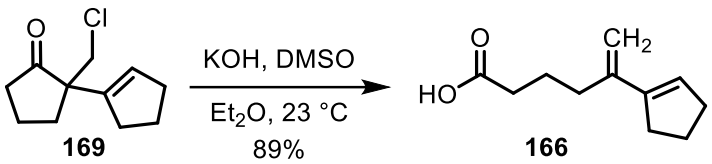

169 166

5-(cyclopent-1-en-1-yl)hex-5-enoic acid (166) from 1-(chloromethyl)-[1,1'-bi(cyclopentan)]-1'-en-2-one (169)

Compound **169** (21 mg, 0.11 mmol, 1 eq) was dissolved in anhydrous diethyl ether (340 µL) and powdered potassium hydroxide (pellets ground with mortar and pestle, 18 mg, 0.32 mmol, 3 eq) was added followed by anhydrous DMSO (90 µL). This mixture stirred for 3 days while monitoring by TLC for starting material consumption, and then quenched with 1 M HCl (3 mL). The mixture was extracted into diethyl ether (3 x 3 mL), and the combined organics washed with water and brine (3 mL). The organic phase was dried on $MgSO_4$, filtered, and concentrated to afford dienoic acid **1** (17 mg, 0.09 mmol, 89%). The material was spectroscopically identical to **166**.

Appendix A. Catalog of Spectra

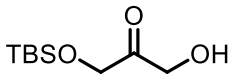
O
TBSO
OH

60

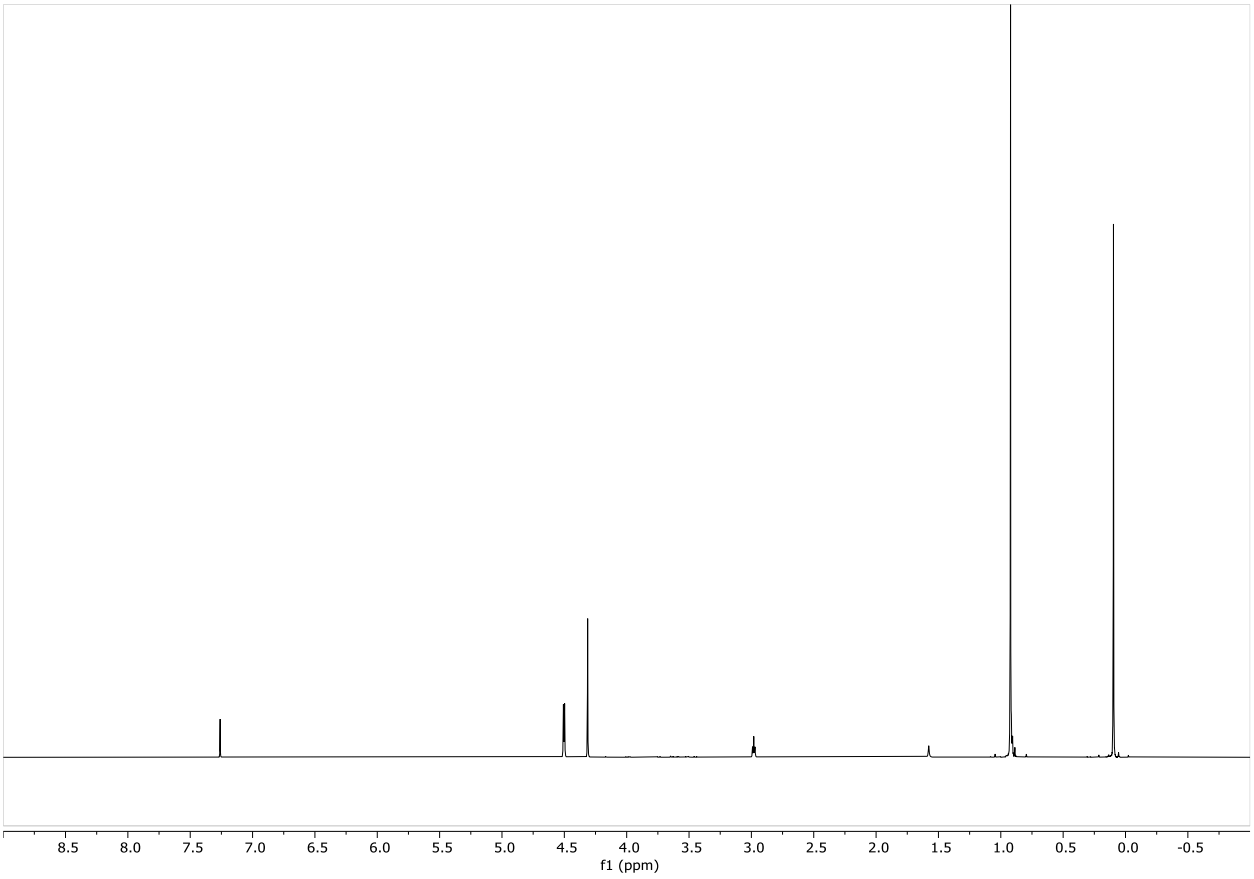
8.5
8.0
7.5
7.0
6.5
6.0
5.5
5.0
4.5
4.0
3.5
3.0
2.5
2.0
1.5
1.0
0.5
0.0
-0.5
f1 (ppm)

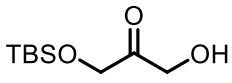
O
TBSO
OH

60

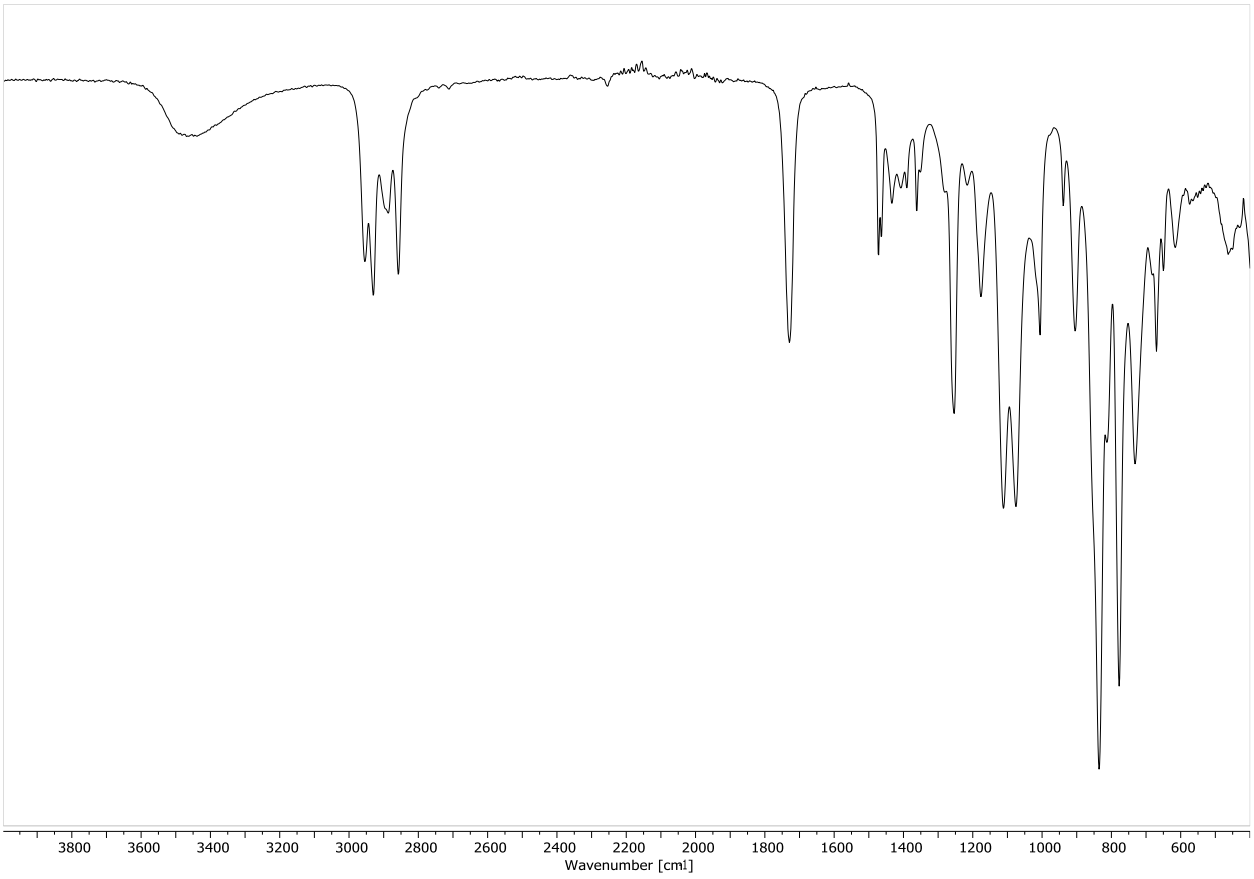
3800
3600
3400
3200
3000
2800
2600
2400
2200
2000
1800
1600
1400
1200
1000
800
600
Wavenumber [cm-1]

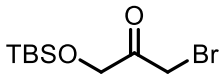
O
TBSO
Br

61

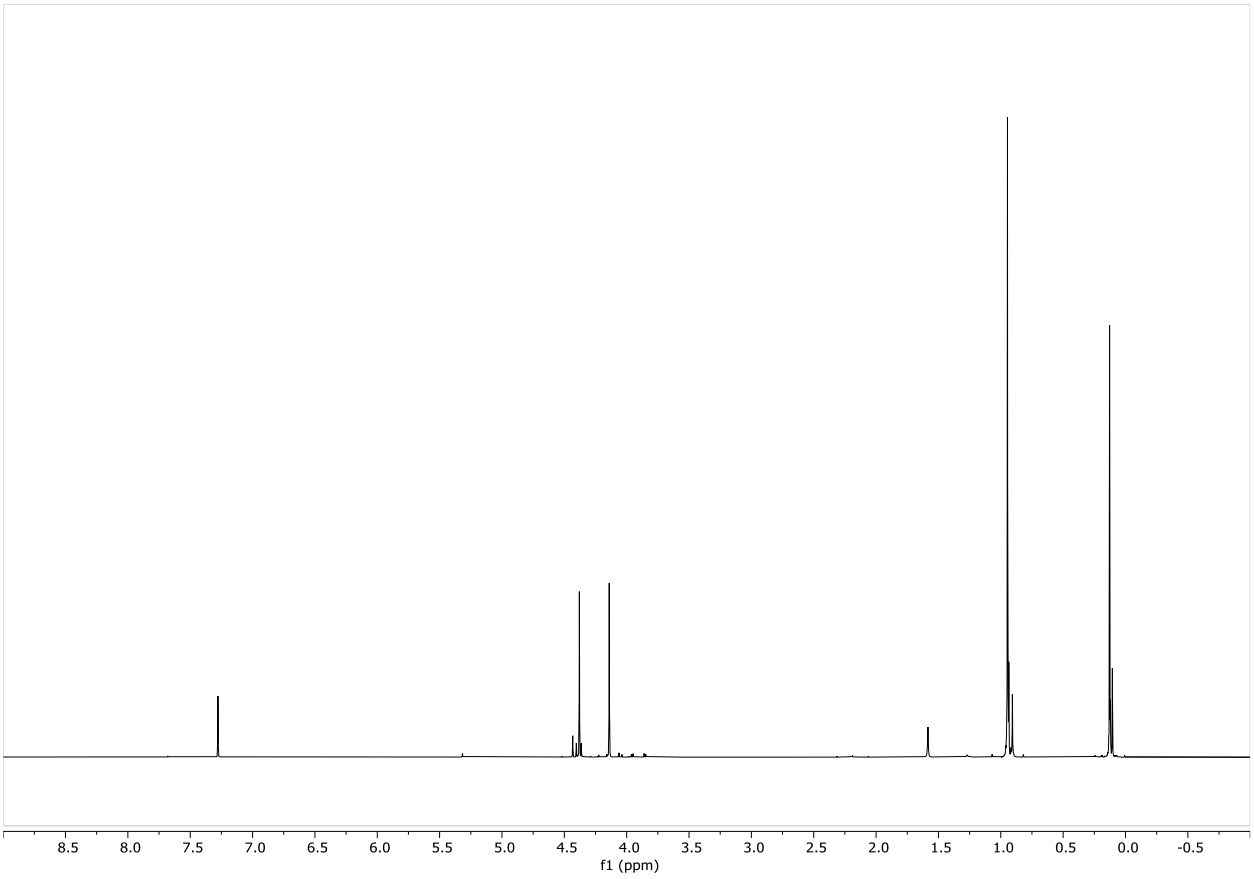
8.5
8.0
7.5
7.0
6.5
6.0
5.5
5.0
4.5
4.0
3.5
3.0
2.5
2.0
1.5
1.0
0.5
0.0
-0.5
f1 (ppm)

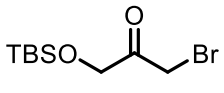
O
TBSO
Br

61

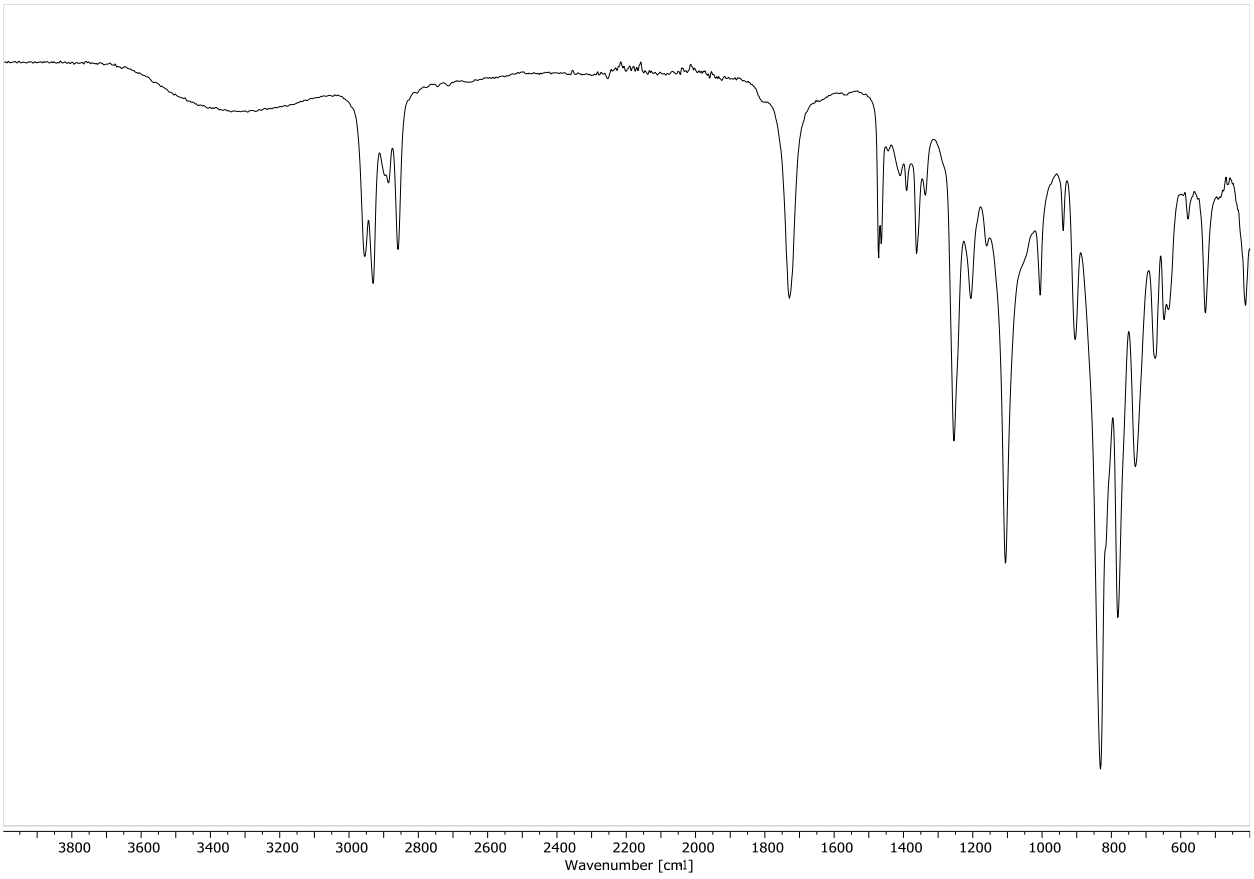
3800
3600
3400
3200
3000
2800
2600
2400
2200
2000
1800
1600
1400
1200
1000
800
600
Wavenumber [cm-1]

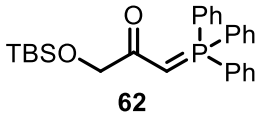
O
Ph
Ph
TBSO
P
Ph

62

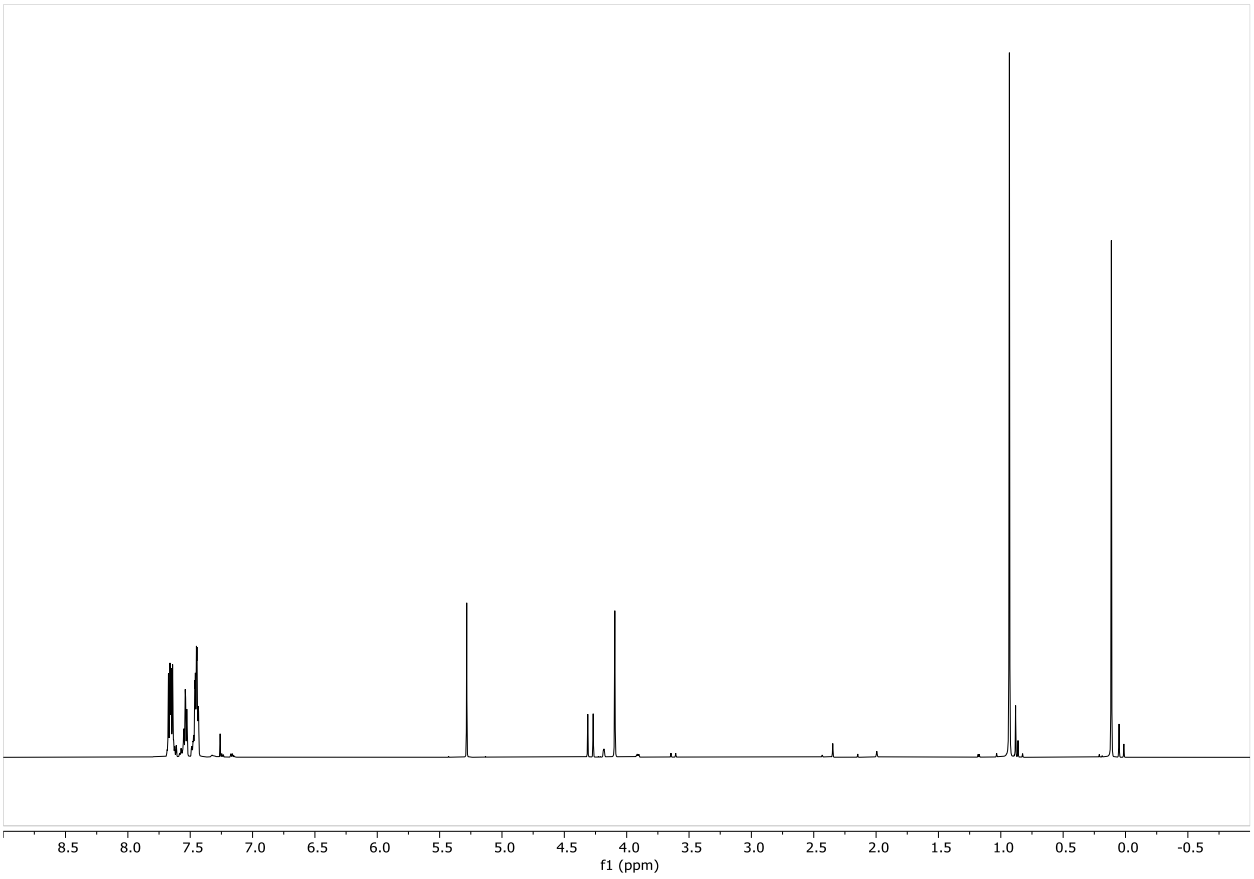
8.5
8.0
7.5
7.0
6.5
6.0
5.5
5.0
4.5
4.0
3.5
3.0
2.5
2.0
1.5
1.0
0.5
0.0
-0.5
f1 (ppm)

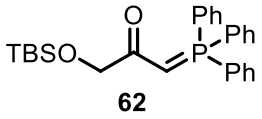
O
Ph
Ph
TBSO
P
Ph

62

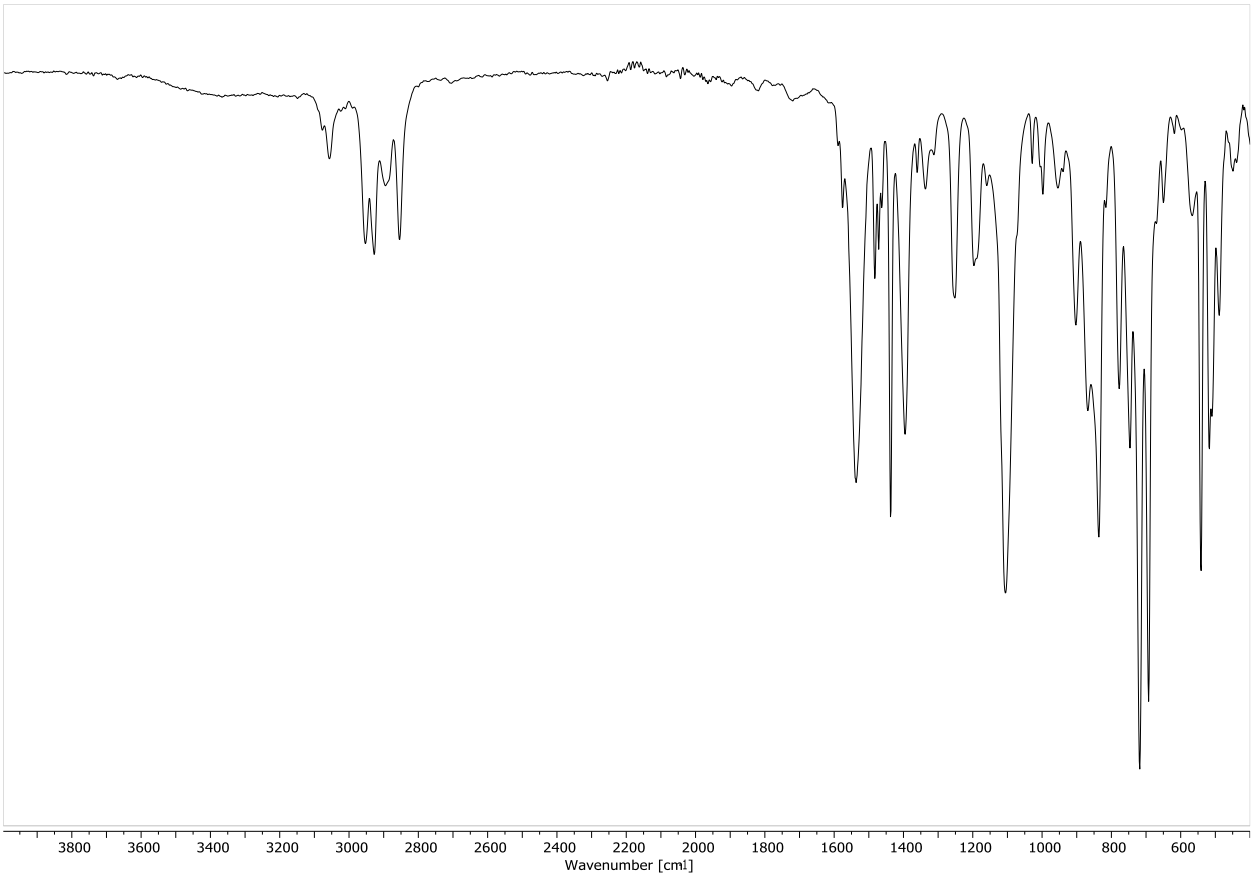
3800
3600
3400
3200
3000
2800
2600
2400
2200
2000
1800
1600
1400
1200
1000
800
600
Wavenumber [cm-1]

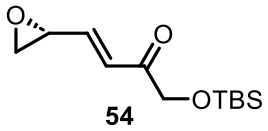

54

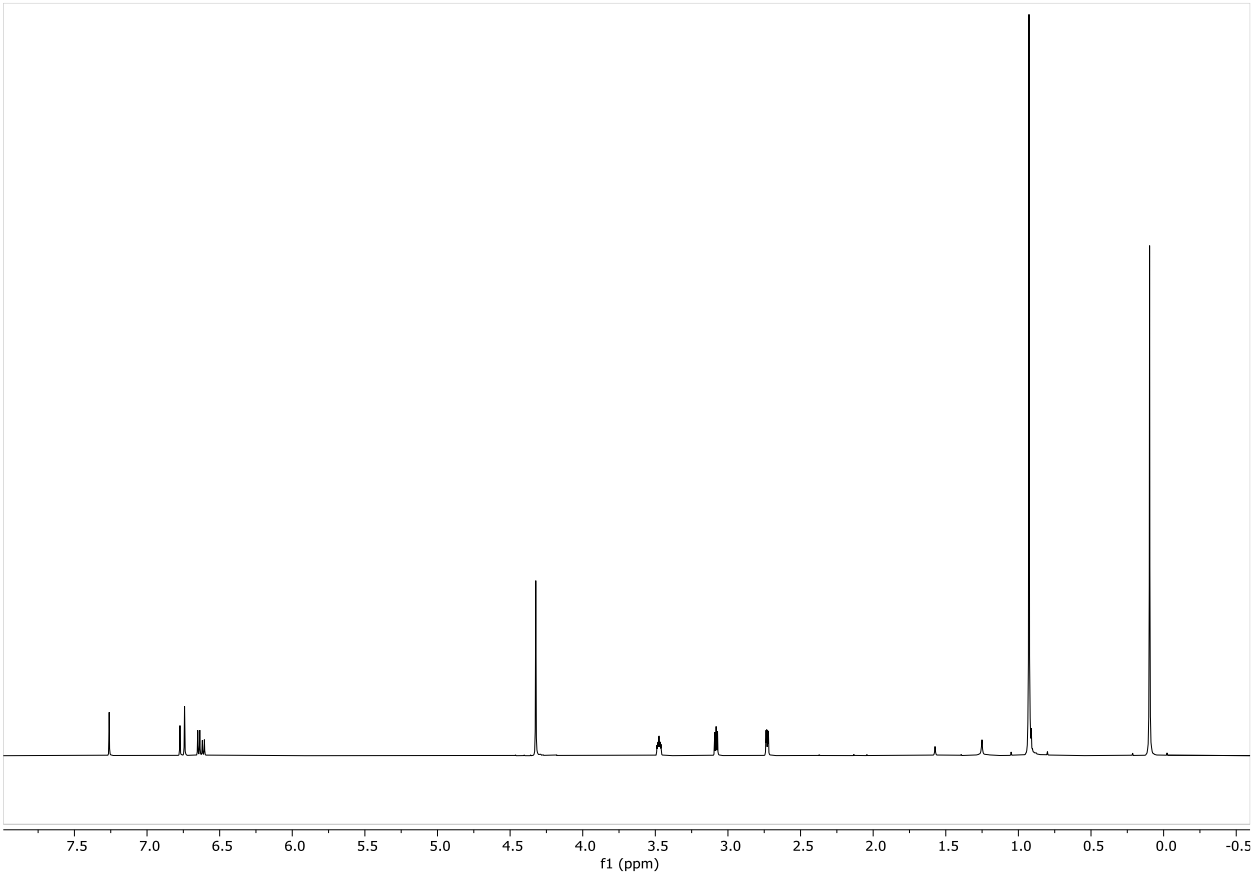

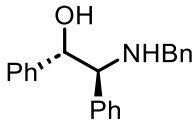

55

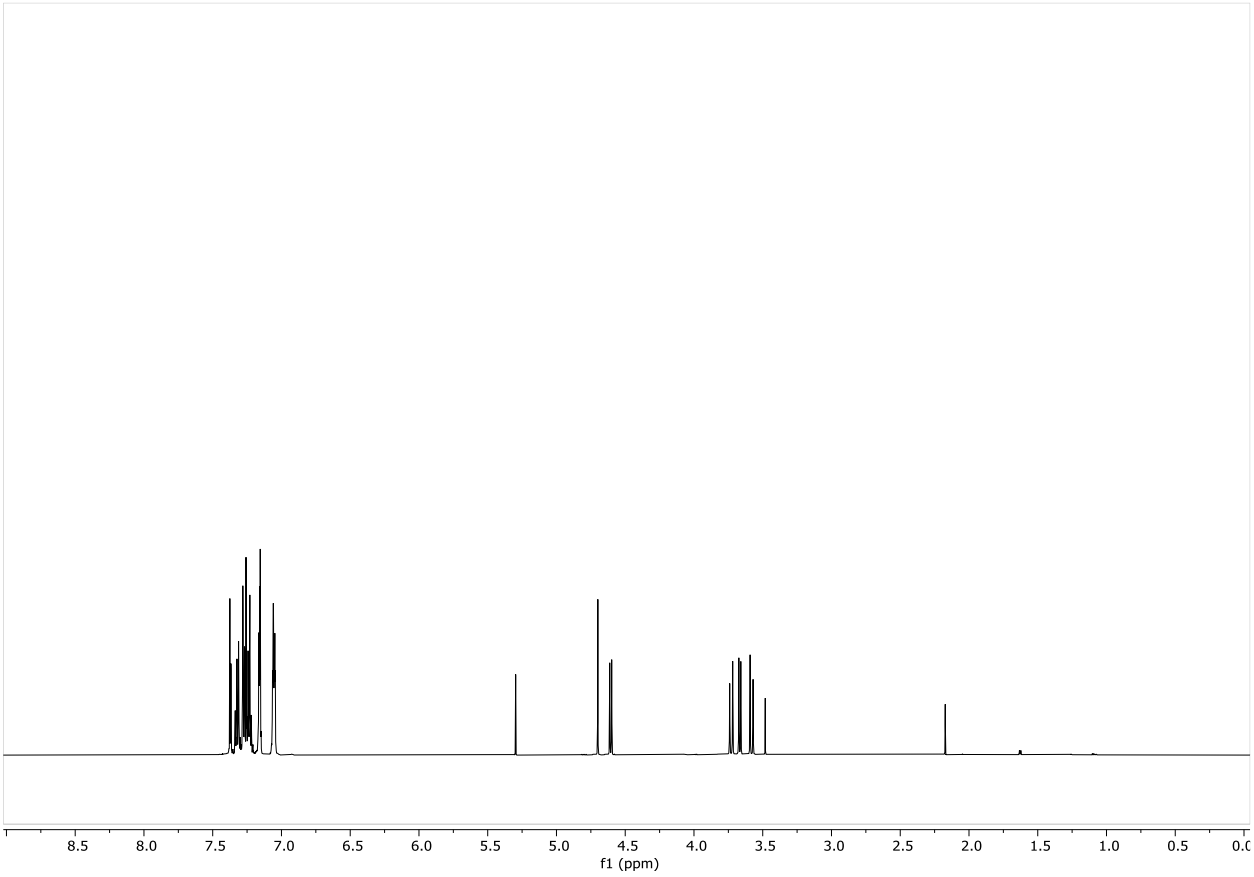

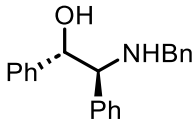
OH
NHBn
Ph
Ph

55

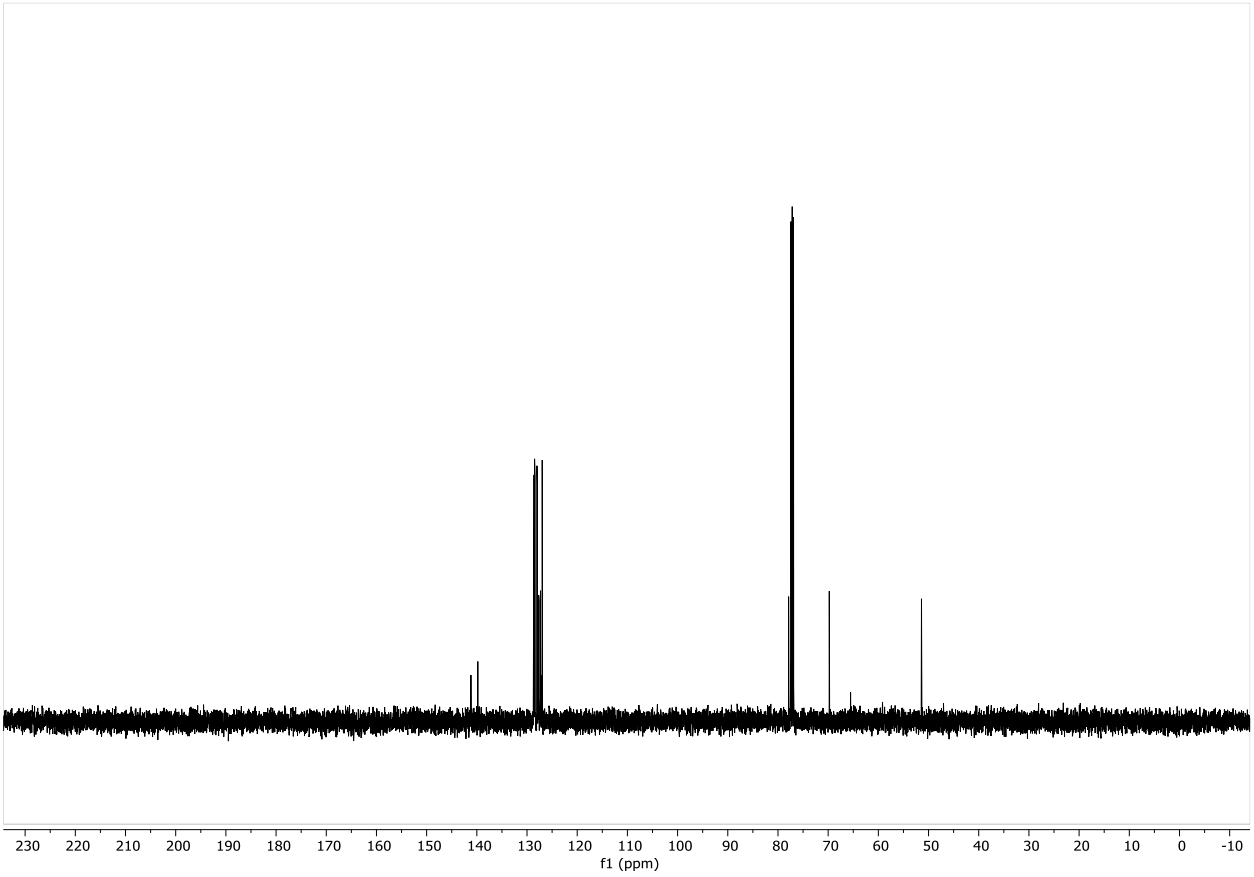
230 220 210 200 190 180 170 160 150 140 130 120 110 100 90 80 70 60 50 40 30 20 10 0 -10
f1 (ppm)

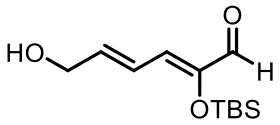
HO
O
H
OTBS

66

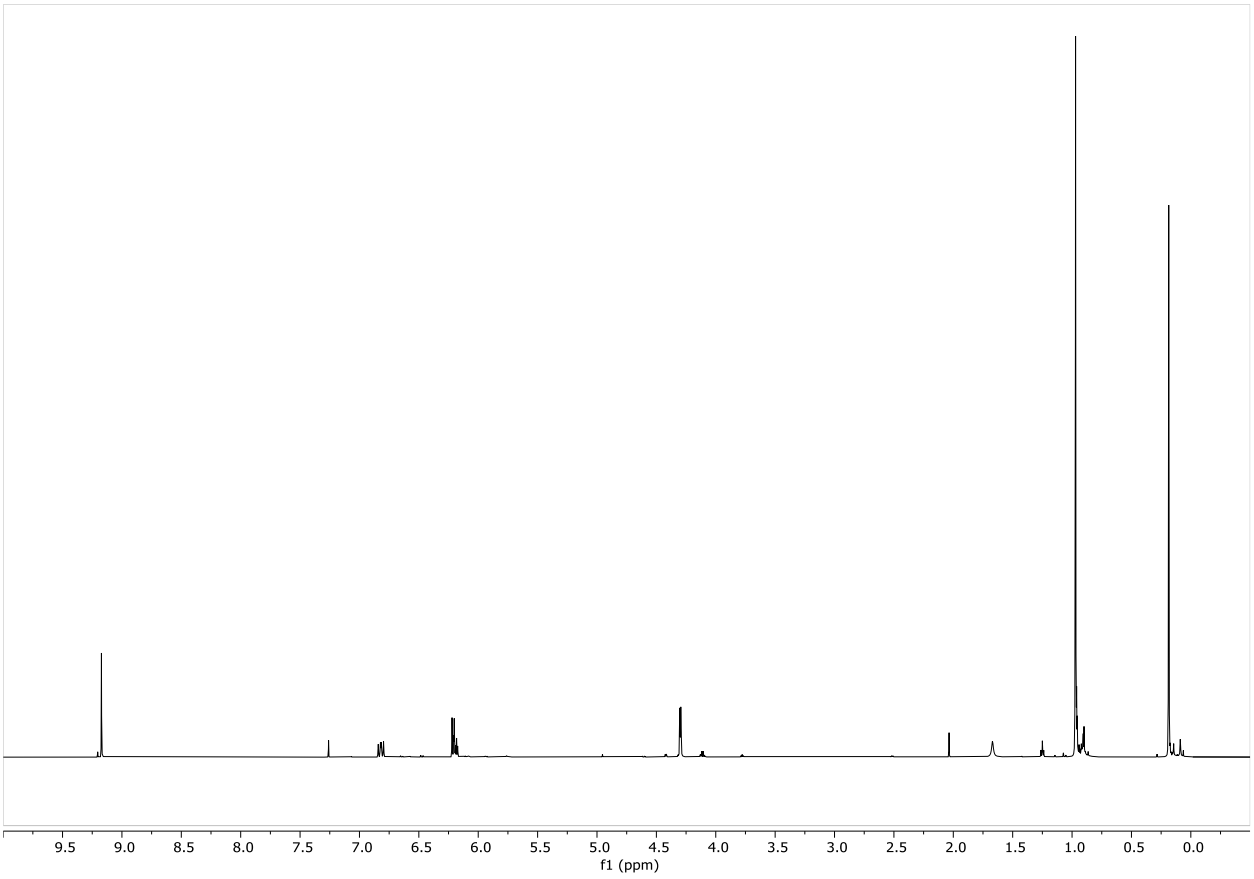
9.5
9.0
8.5
8.0
7.5
7.0
6.5
6.0
5.5
5.0
4.5
4.0
3.5
3.0
2.5
2.0
1.5
1.0
0.5
0.0
f1 (ppm)

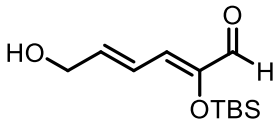
HO
O
H
OTBS

66

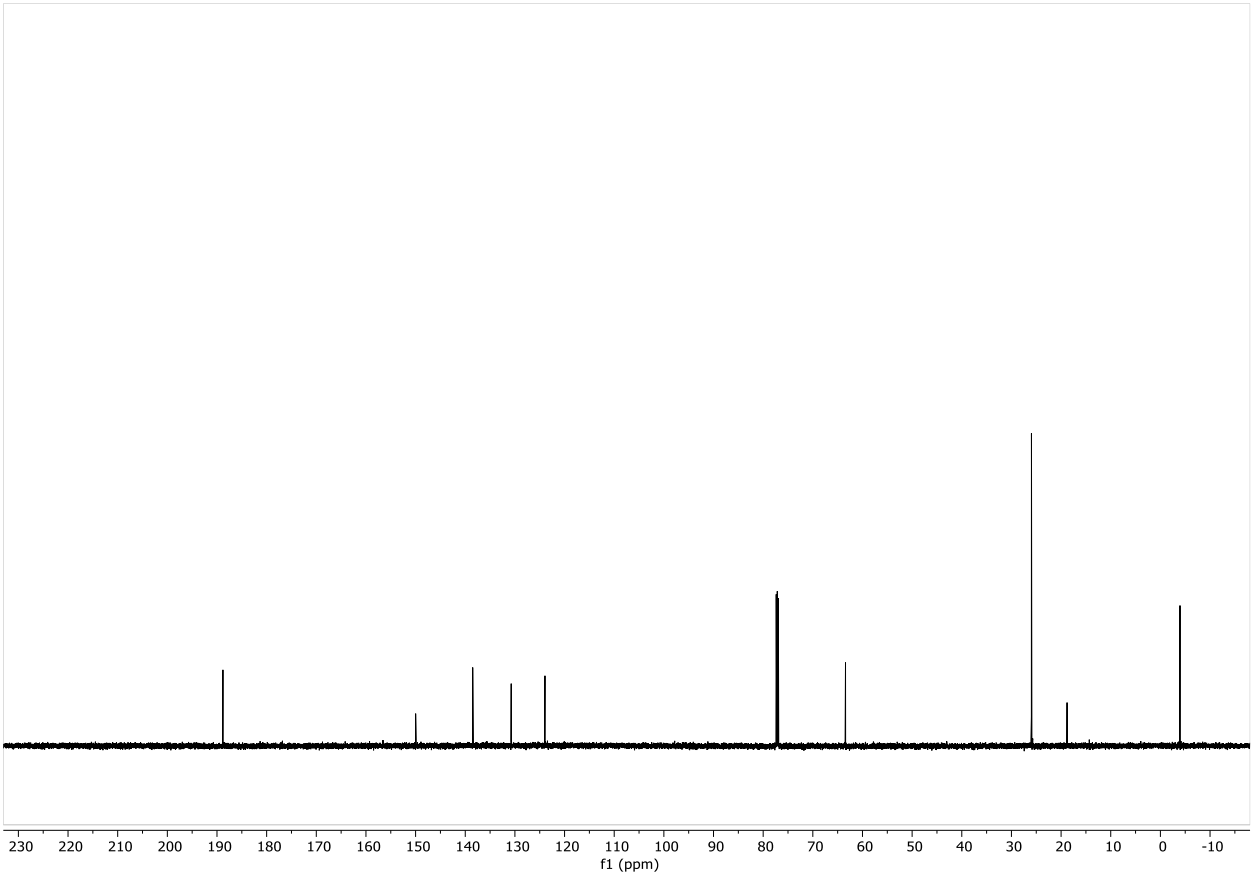
230 220 210 200 190 180 170 160 150 140 130 120 110 100 90 80 70 60 50 40 30 20 10 0 -10
f1 (ppm)

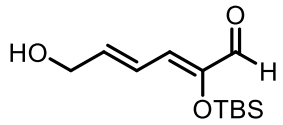

66

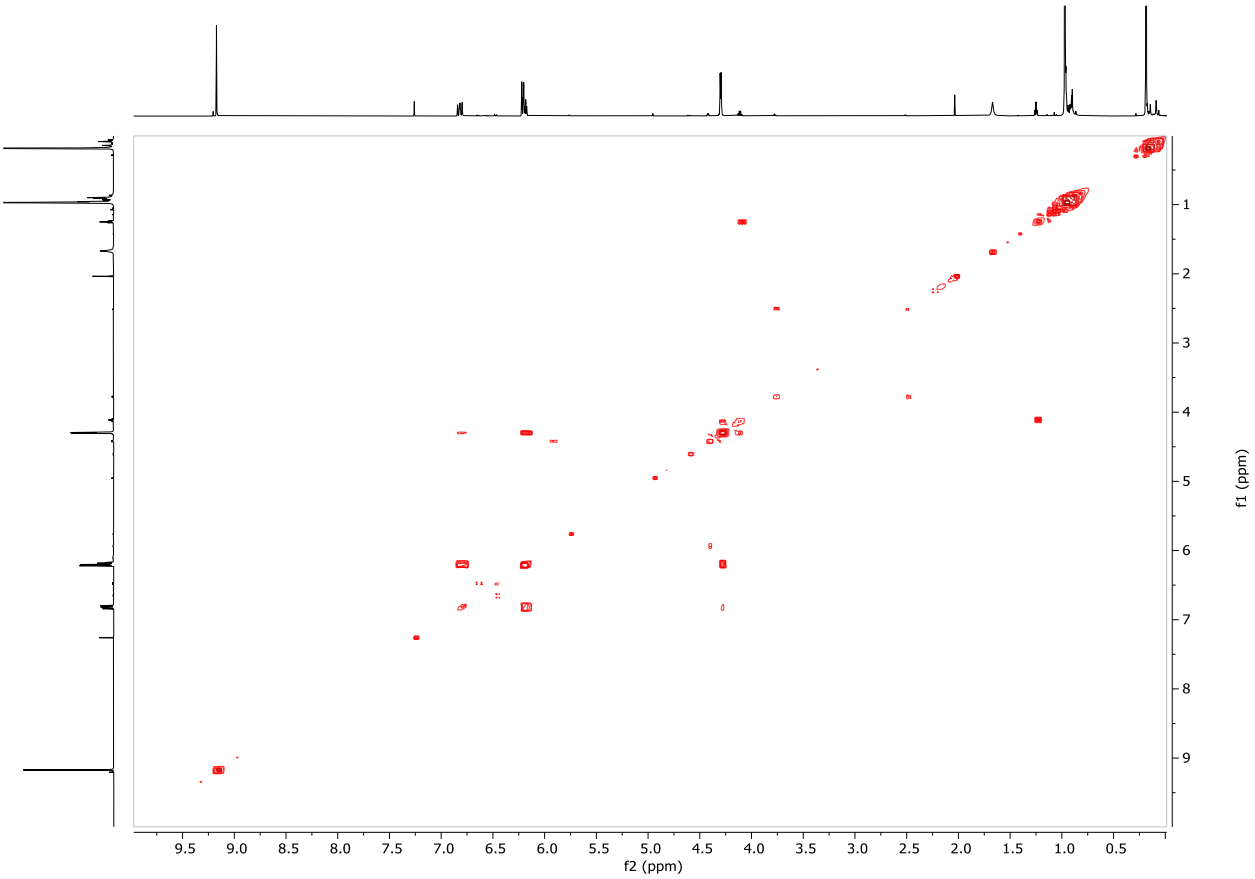

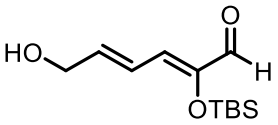
HO
O
H
OTBS

66

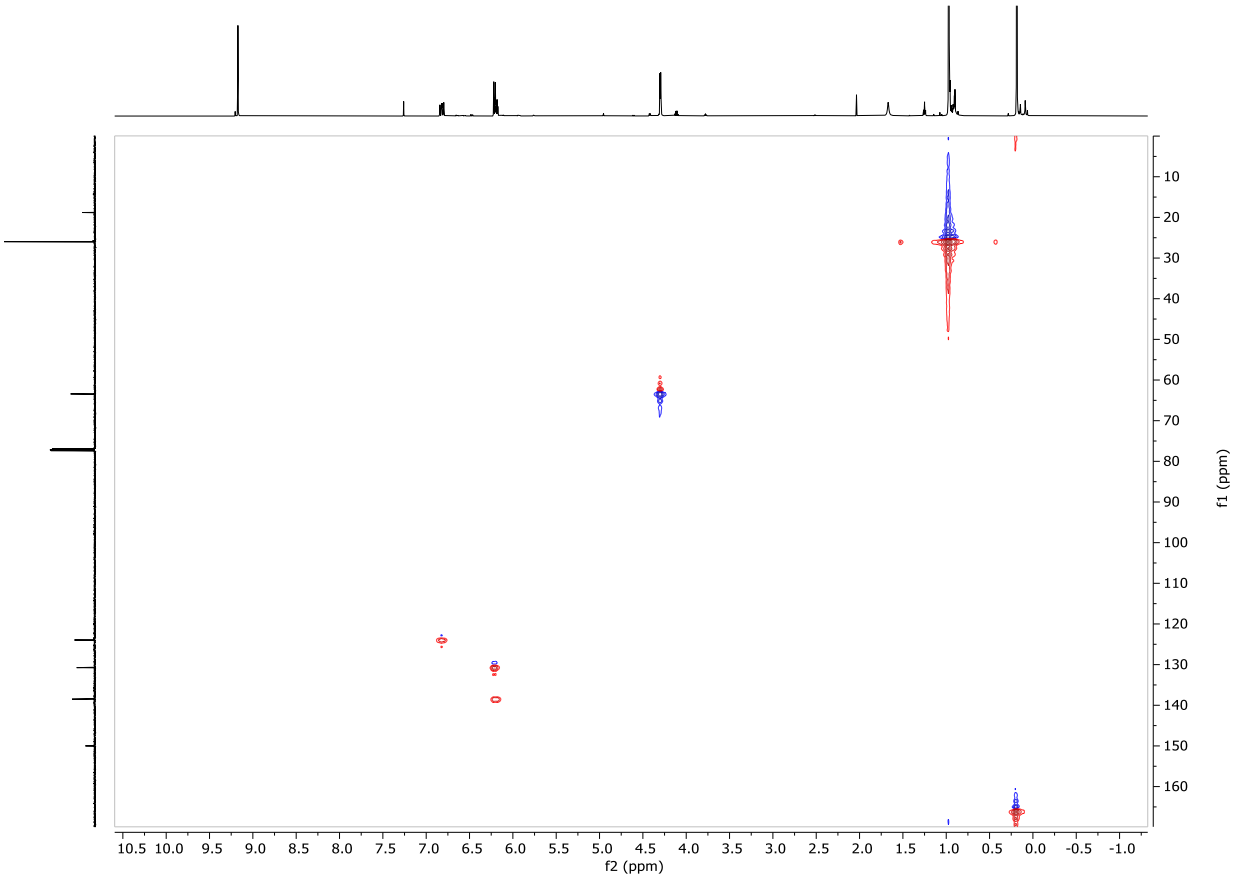
10.5 10.0 9.5 9.0 8.5 8.0 7.5 7.0 6.5 6.0 5.5 5.0 4.5 4.0 3.5 3.0 2.5 2.0 1.5 1.0 0.5 0.0 -0.5 -1.0
f2 (ppm)
10 20 30 40 50 60 70 80 90 100 110 120 130 140 150 160
f1 (ppm)

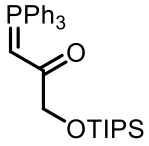
PPh3
O
OTIPS

67

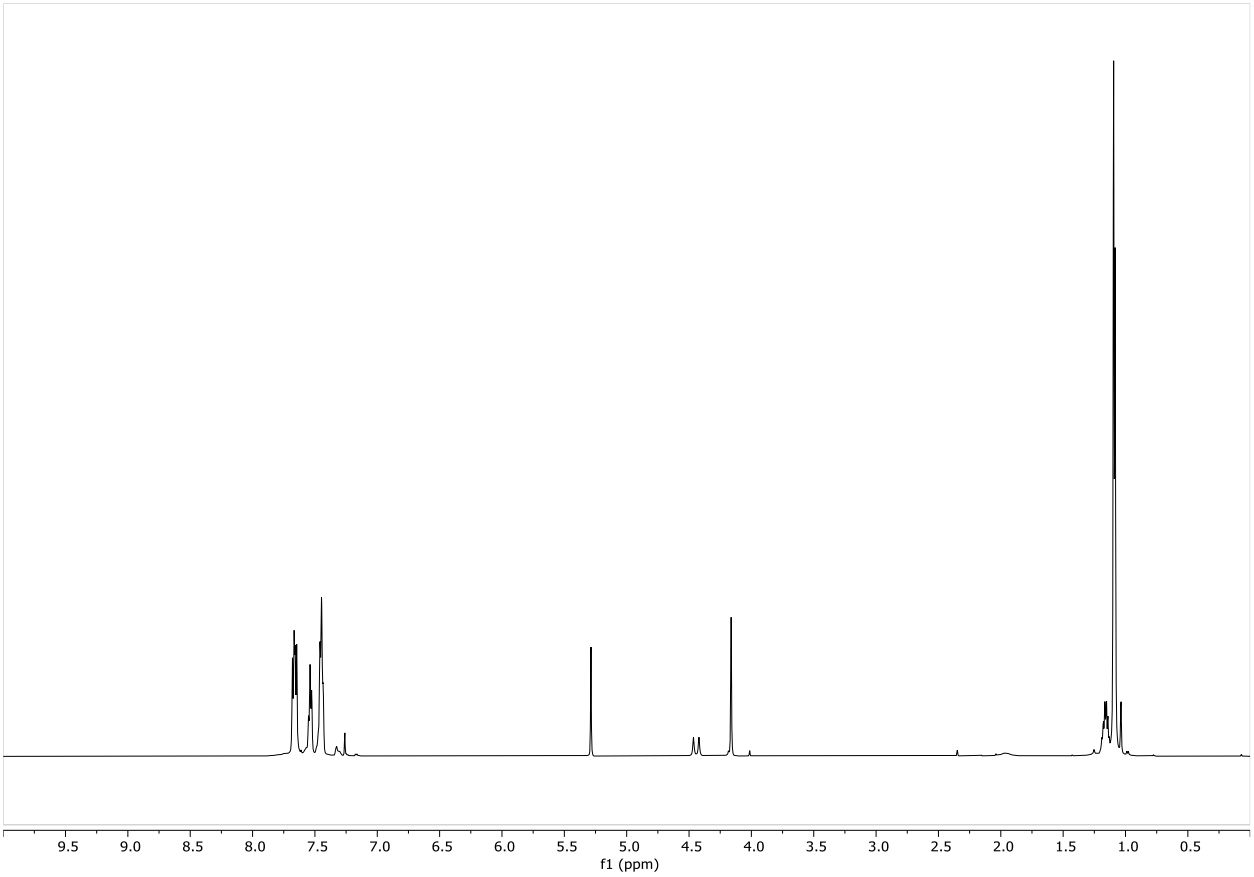
9.5
9.0
8.5
8.0
7.5
7.0
6.5
6.0
5.5
5.0
4.5
4.0
3.5
3.0
2.5
2.0
1.5
1.0
0.5
f1 (ppm)

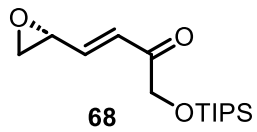

68

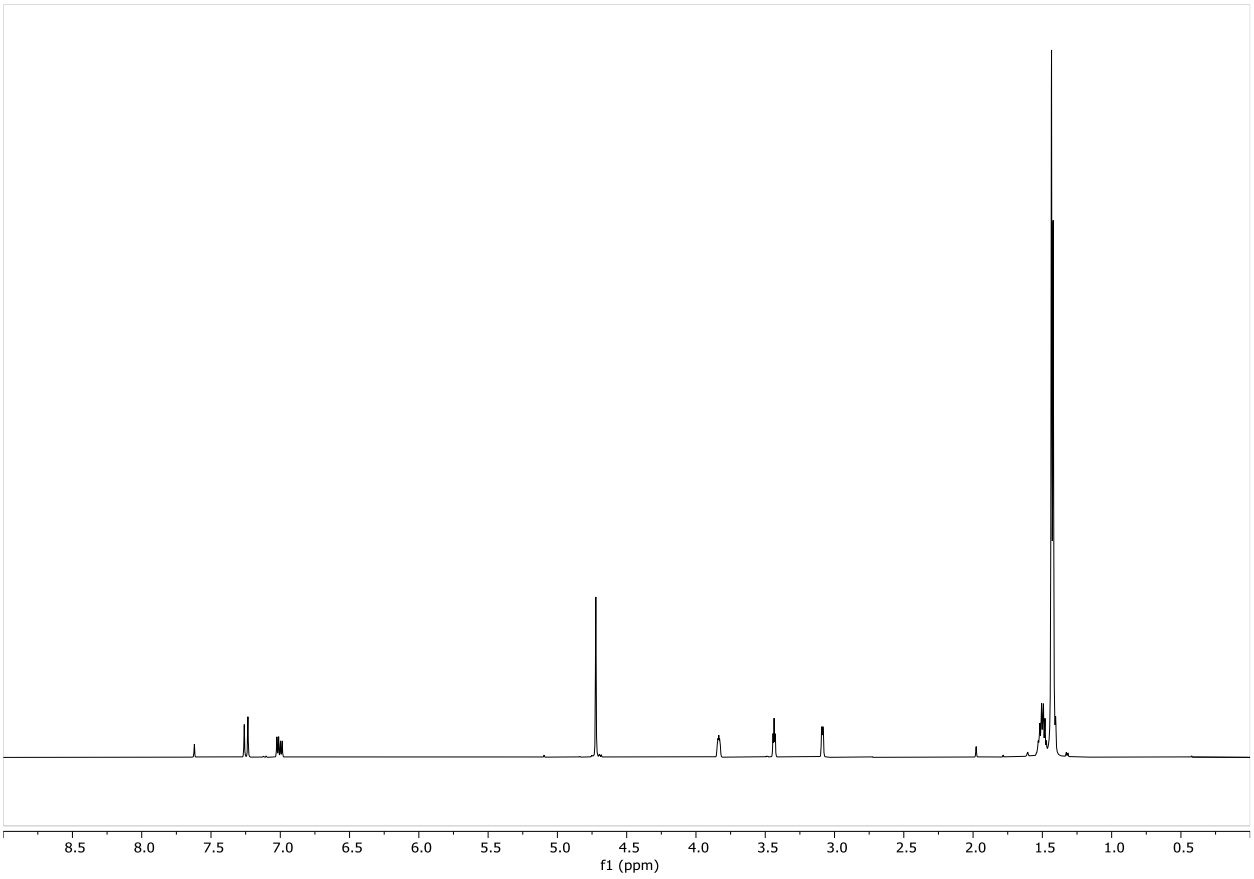

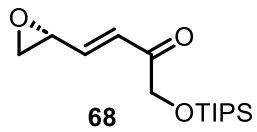
O
O
OTIPS

68

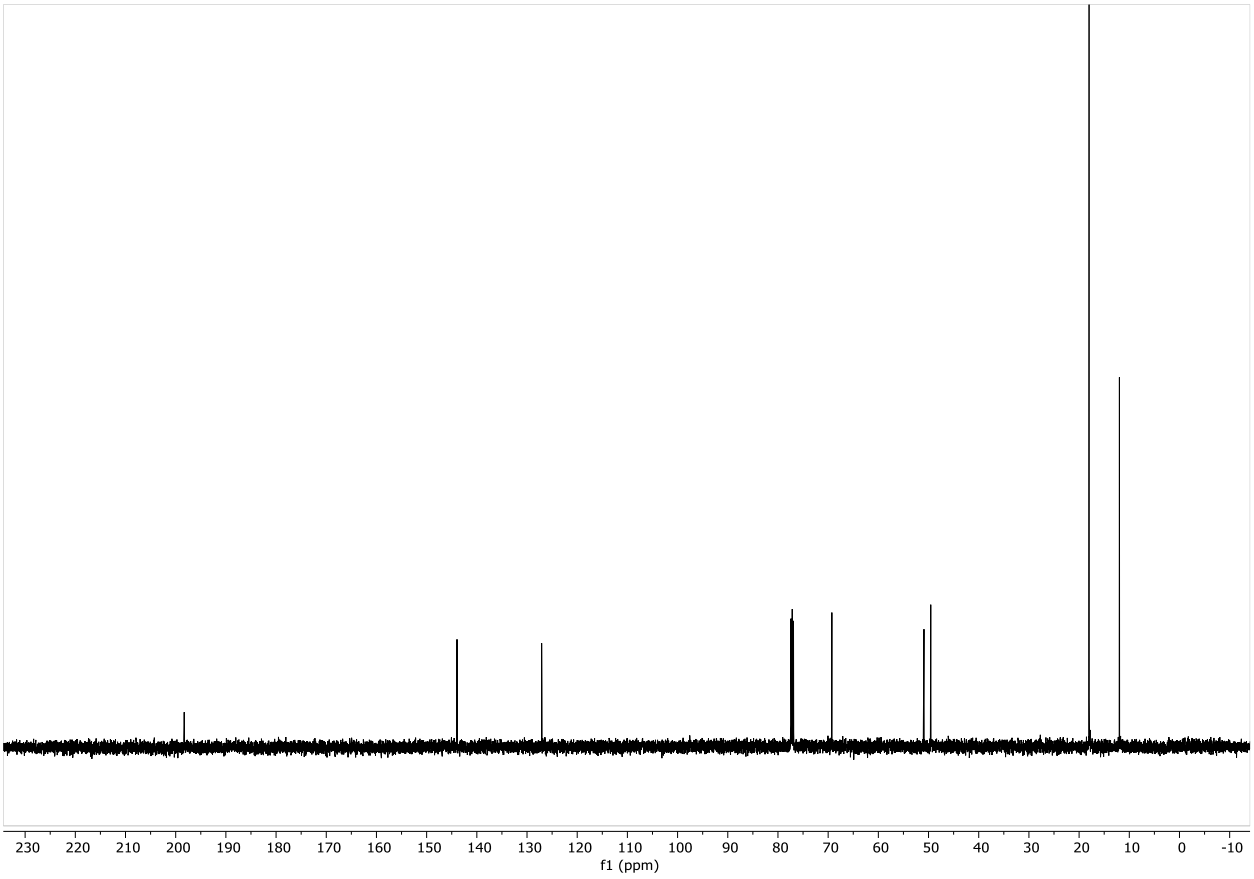
230 220 210 200 190 180 170 160 150 140 130 120 110 100 90 80 70 60 50 40 30 20 10 0 -10
f1 (ppm)

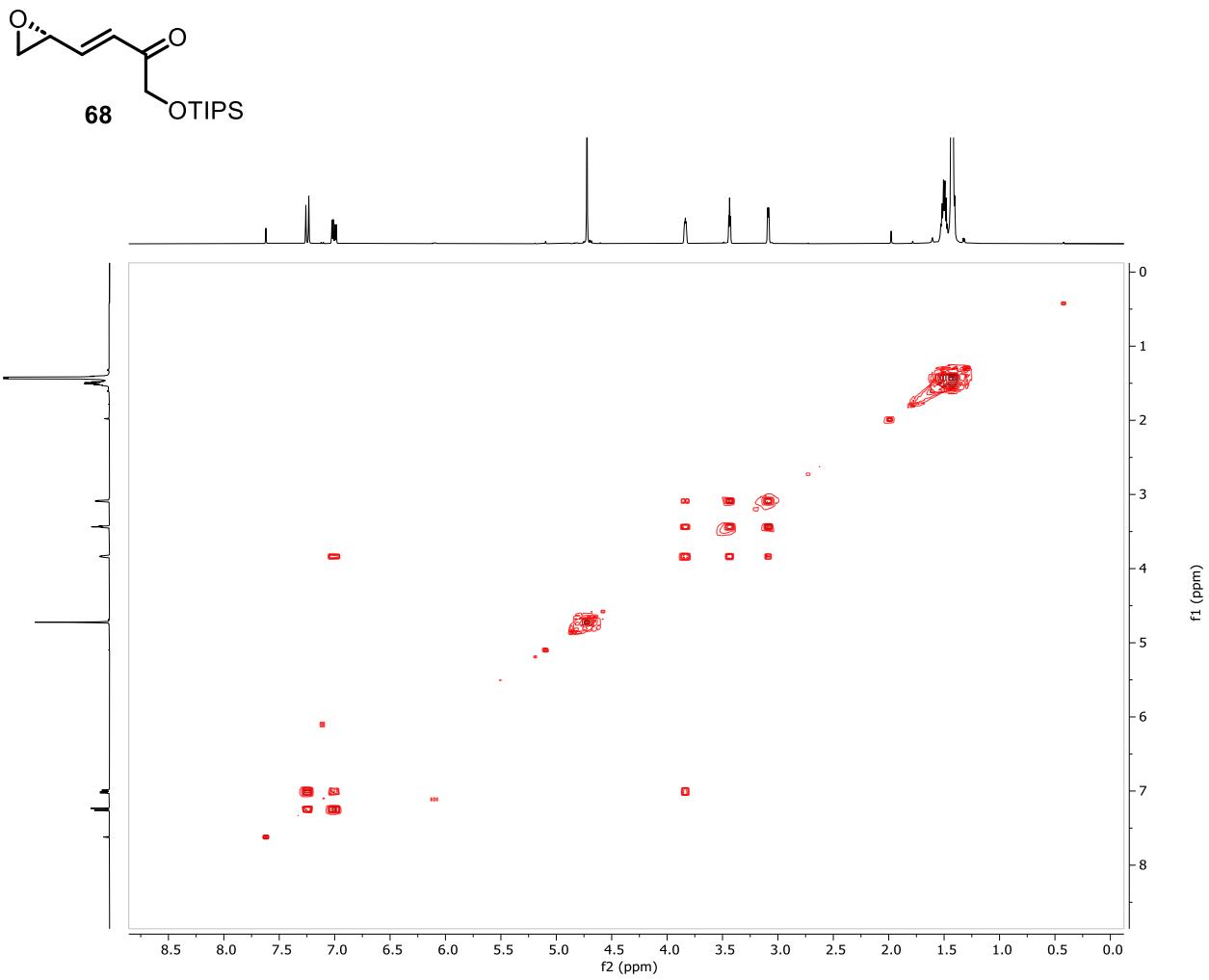
O
O
OTIPS
68
f2 (ppm)
f1 (ppm)

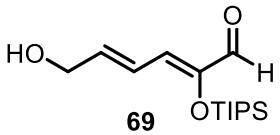
HO
O
H
OTIPS

69

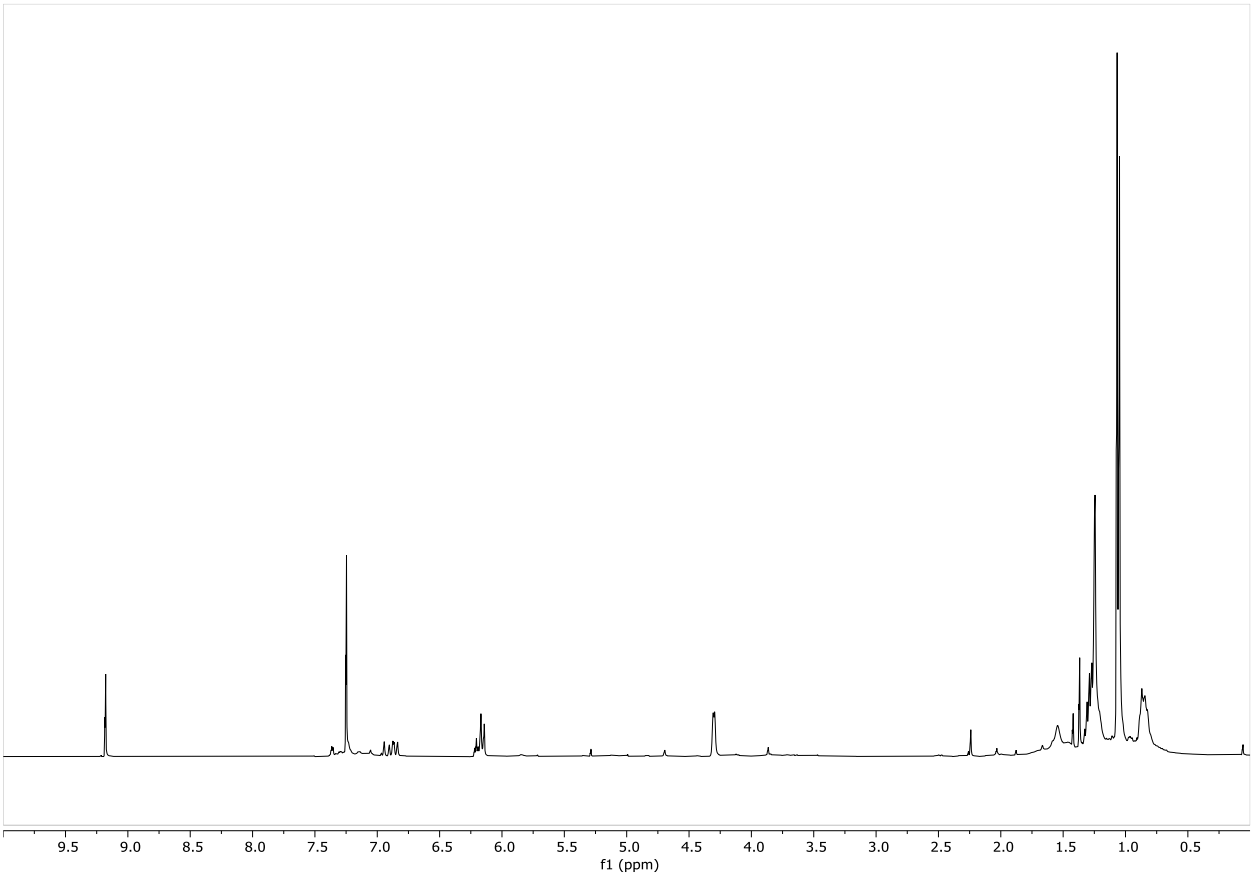
9.5
9.0
8.5
8.0
7.5
7.0
6.5
6.0
5.5
5.0
4.5
4.0
3.5
3.0
2.5
2.0
1.5
1.0
0.5
f1 (ppm)

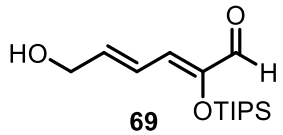
HO
O
H
OTIPS

69

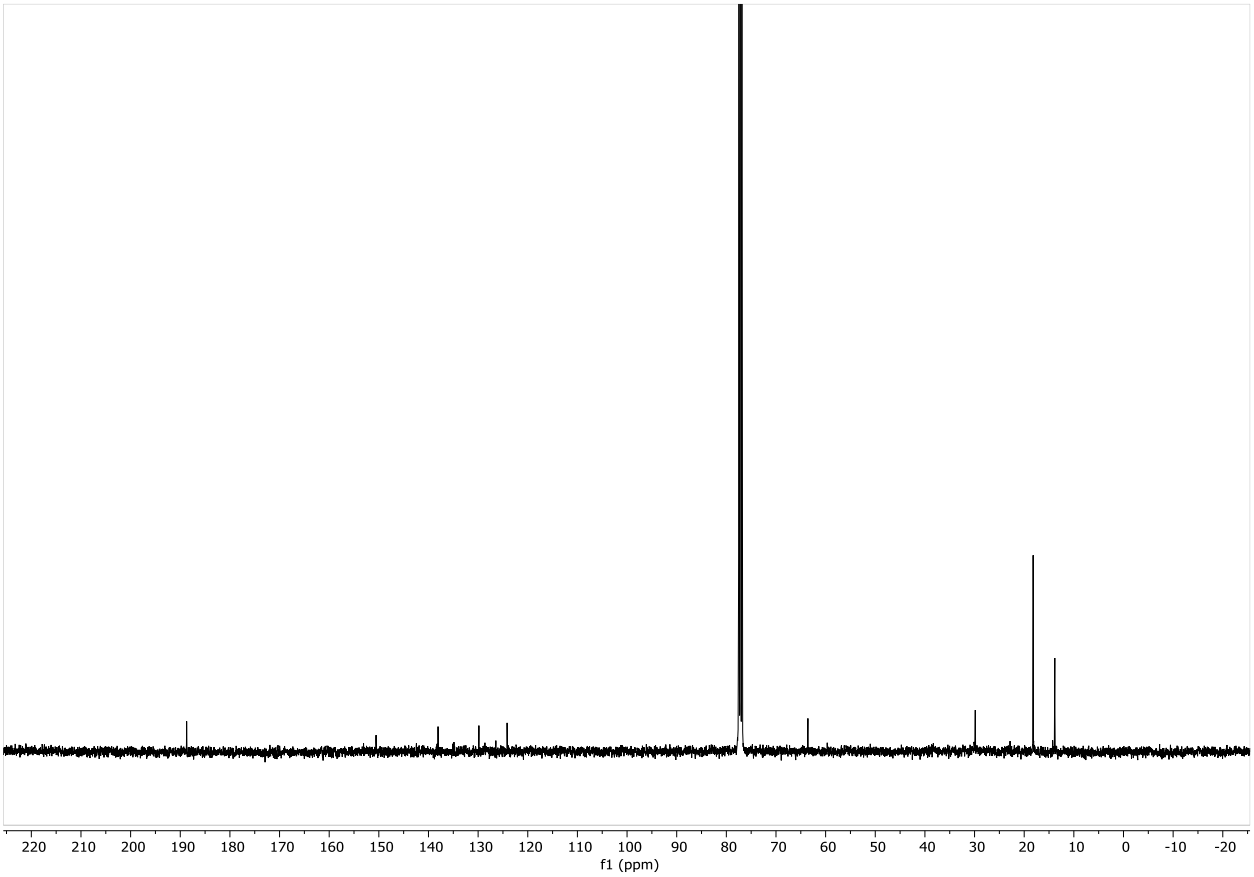
220 210 200 190 180 170 160 150 140 130 120 110 100 90 80 70 60 50 40 30 20 10 0 -10 -20
f1 (ppm)

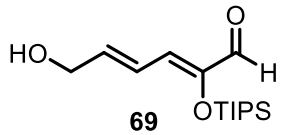
HO
O
H
OTIPS

69

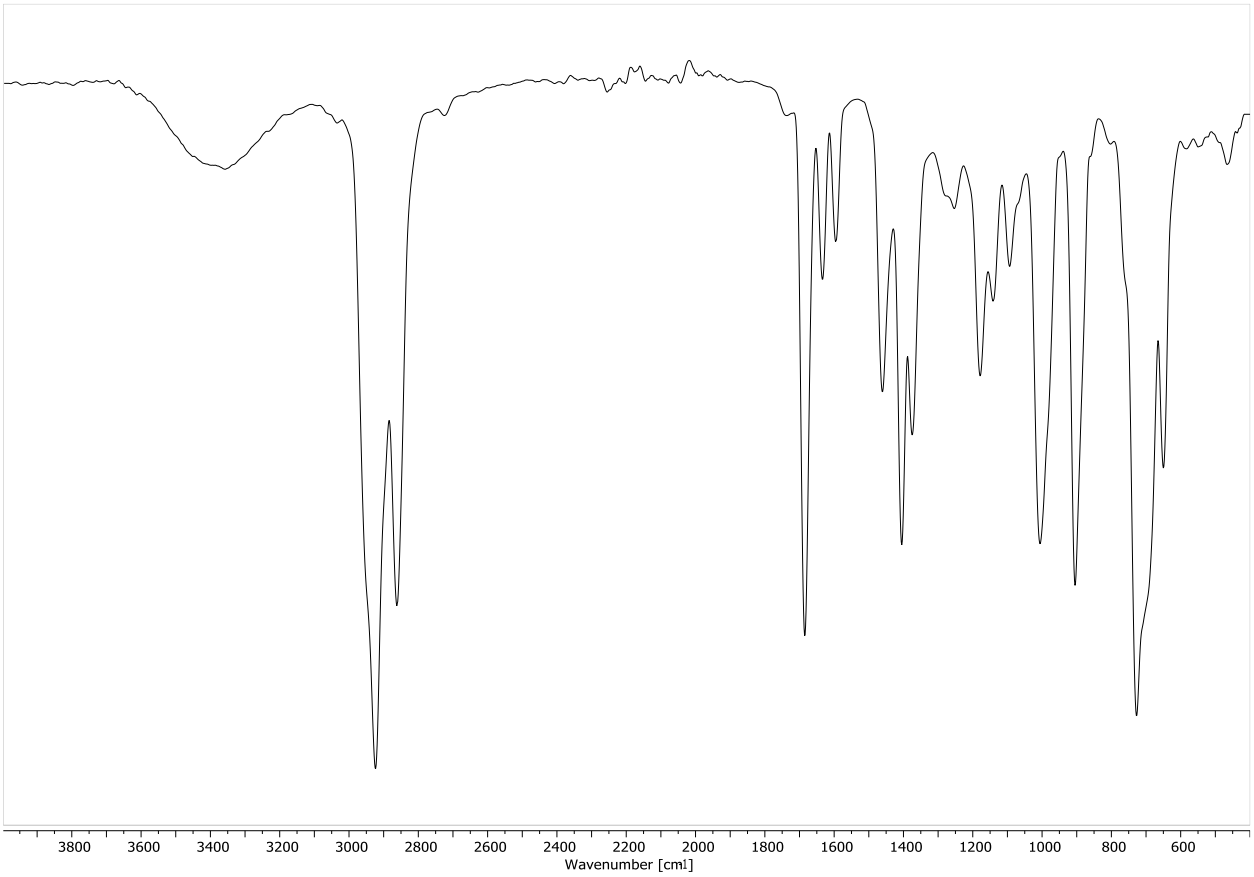
3800
3600
3400
3200
3000
2800
2600
2400
2200
2000
1800
1600
1400
1200
1000
800
600
Wavenumber [cm-1]

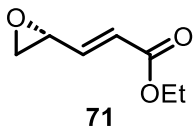

71

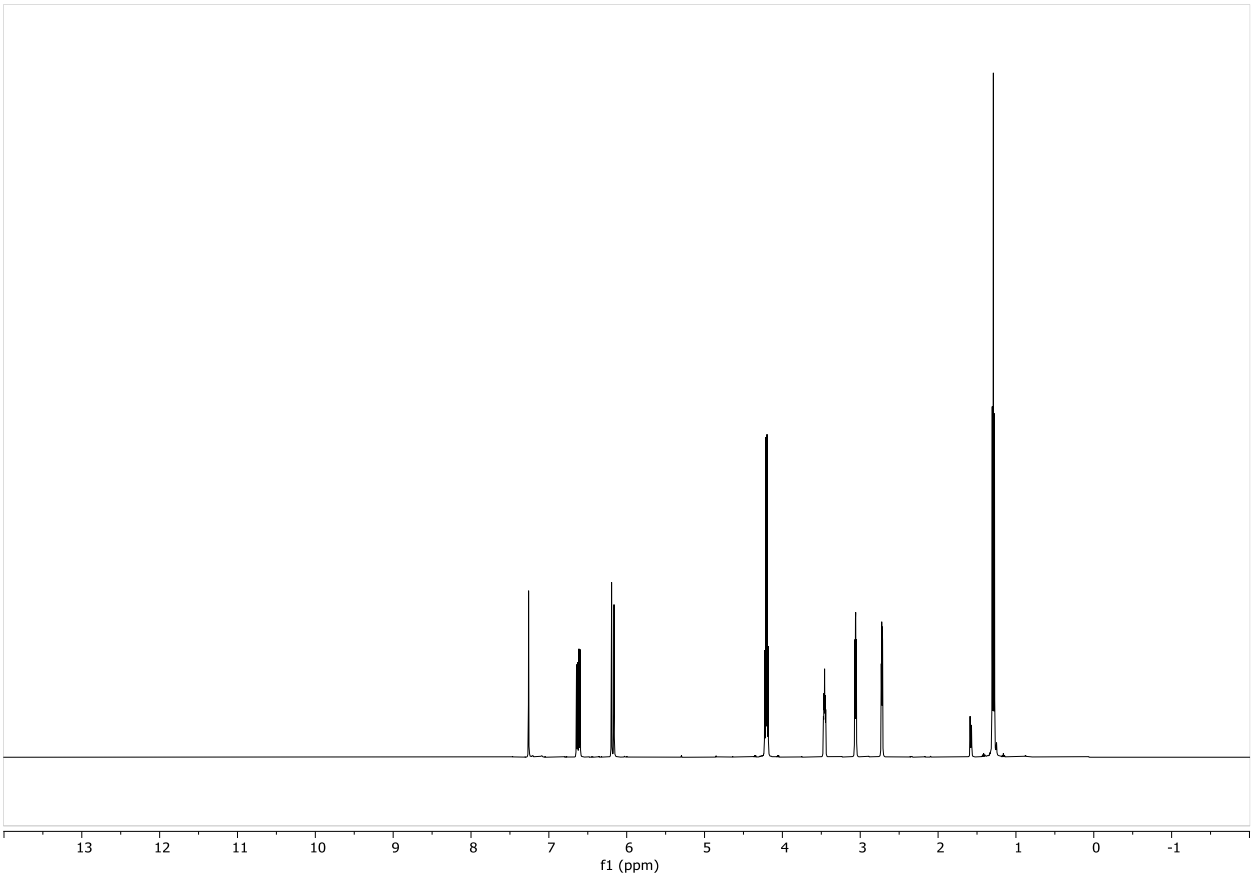

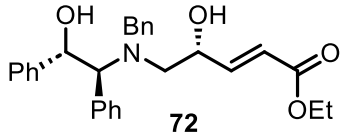
OH
Bn
OH
Ph
N
O
Ph
OEt

72

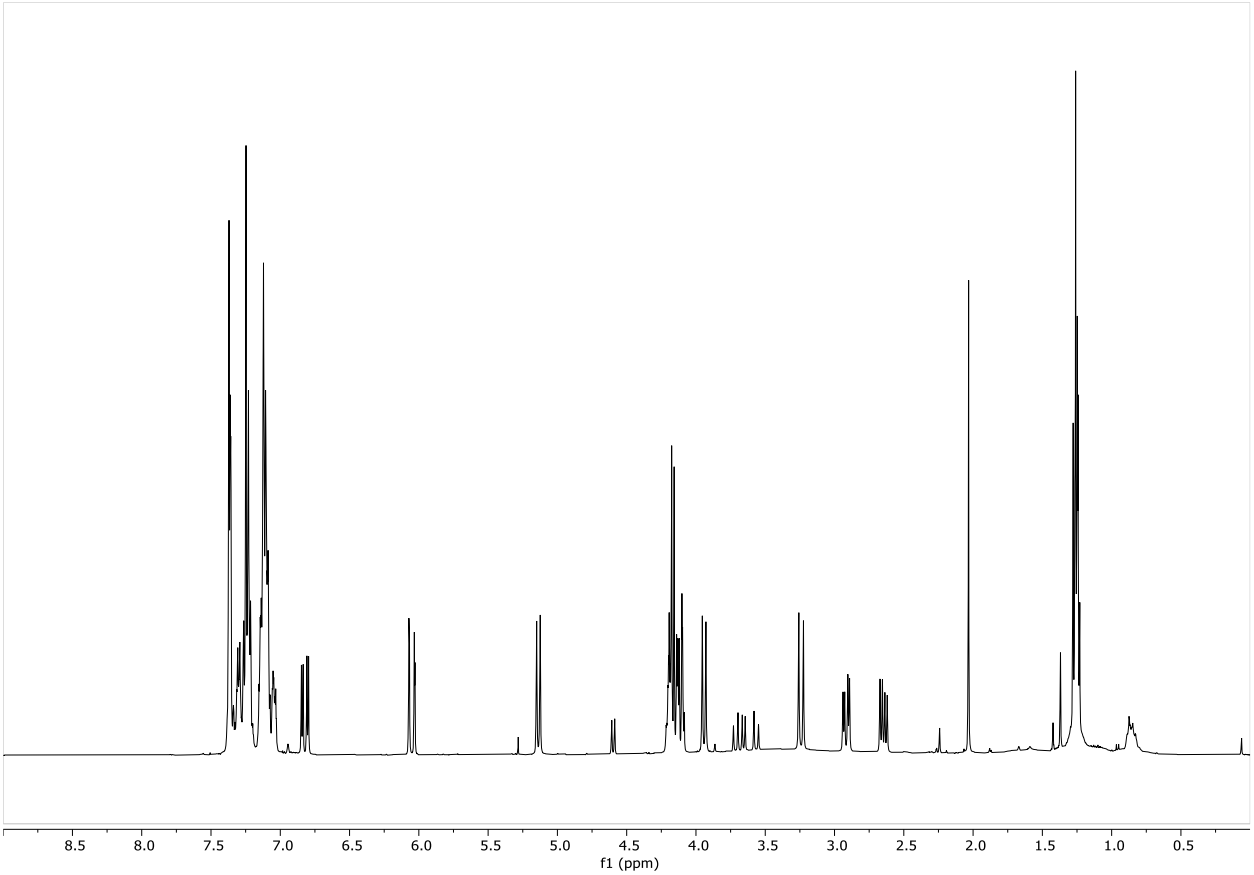
8.5
8.0
7.5
7.0
6.5
6.0
5.5
5.0
4.5
4.0
3.5
3.0
2.5
2.0
1.5
1.0
0.5
f1 (ppm)

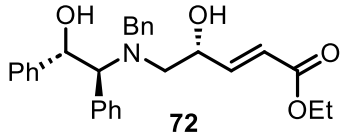
OH
Bn
OH
Ph
N
O
Ph
OEt

72

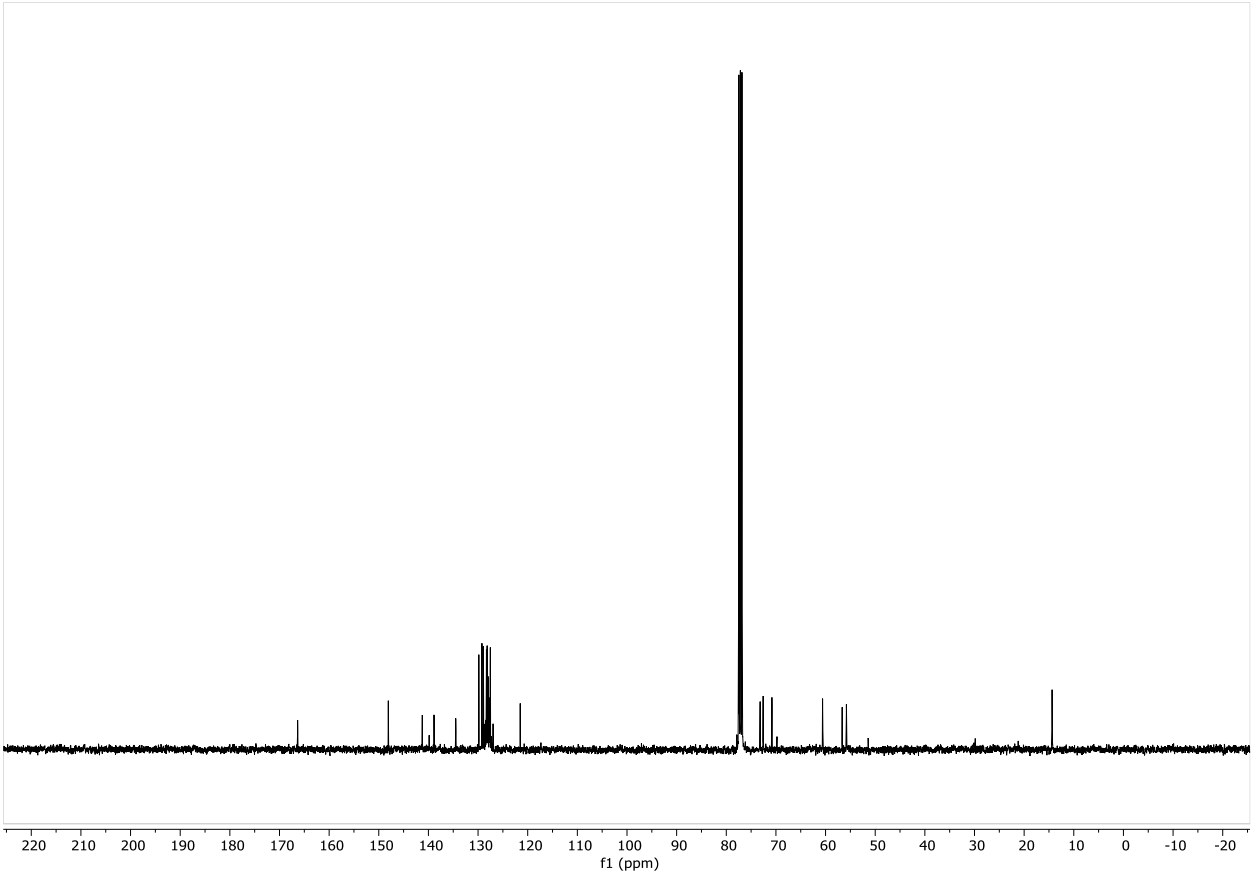
220 210 200 190 180 170 160 150 140 130 120 110 100 90 80 70 60 50 40 30 20 10 0 -10 -20
f1 (ppm)

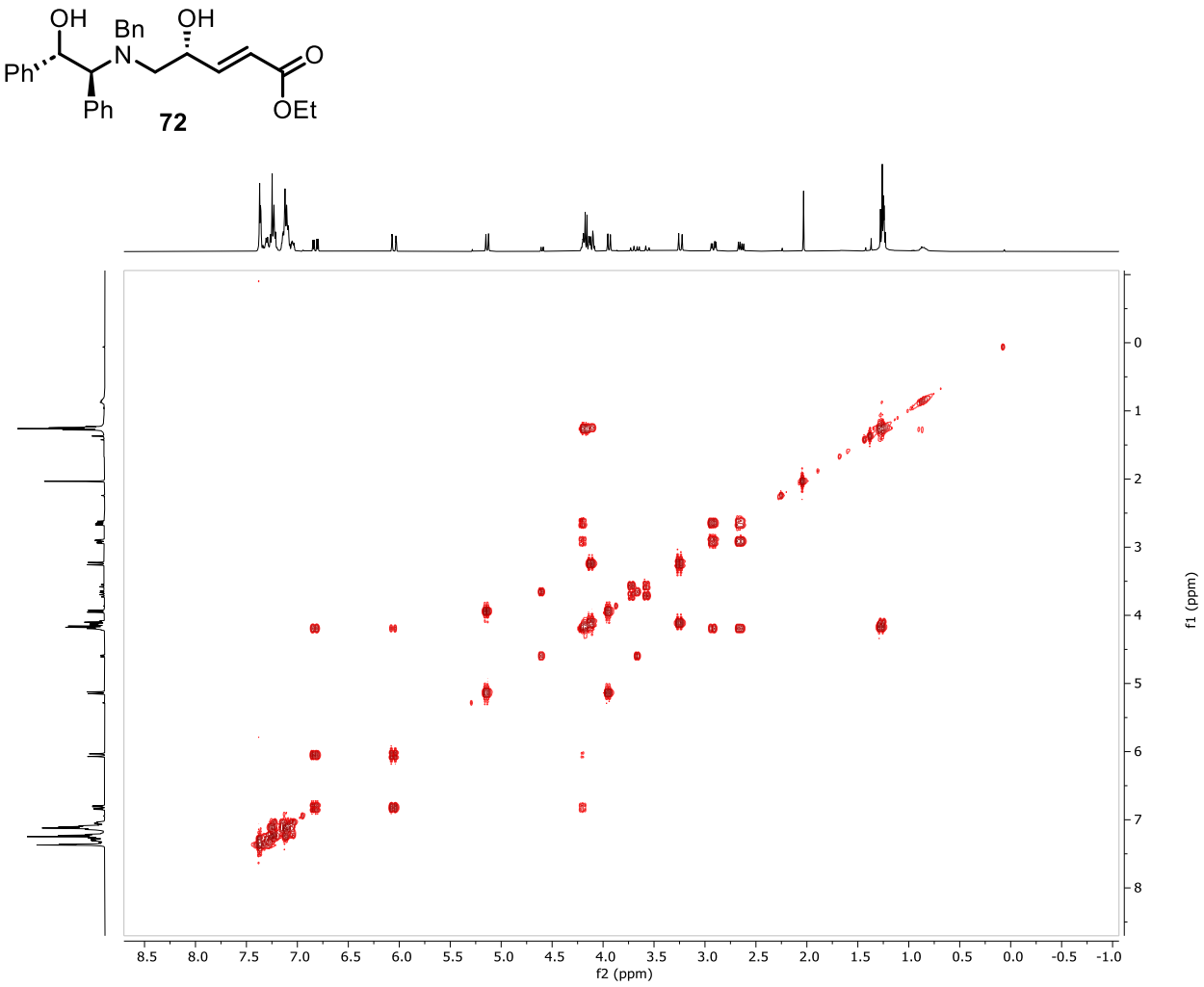
OH
Bn
OH
Ph
N
O
Ph
OEt
72
f1 (ppm)
f2 (ppm)

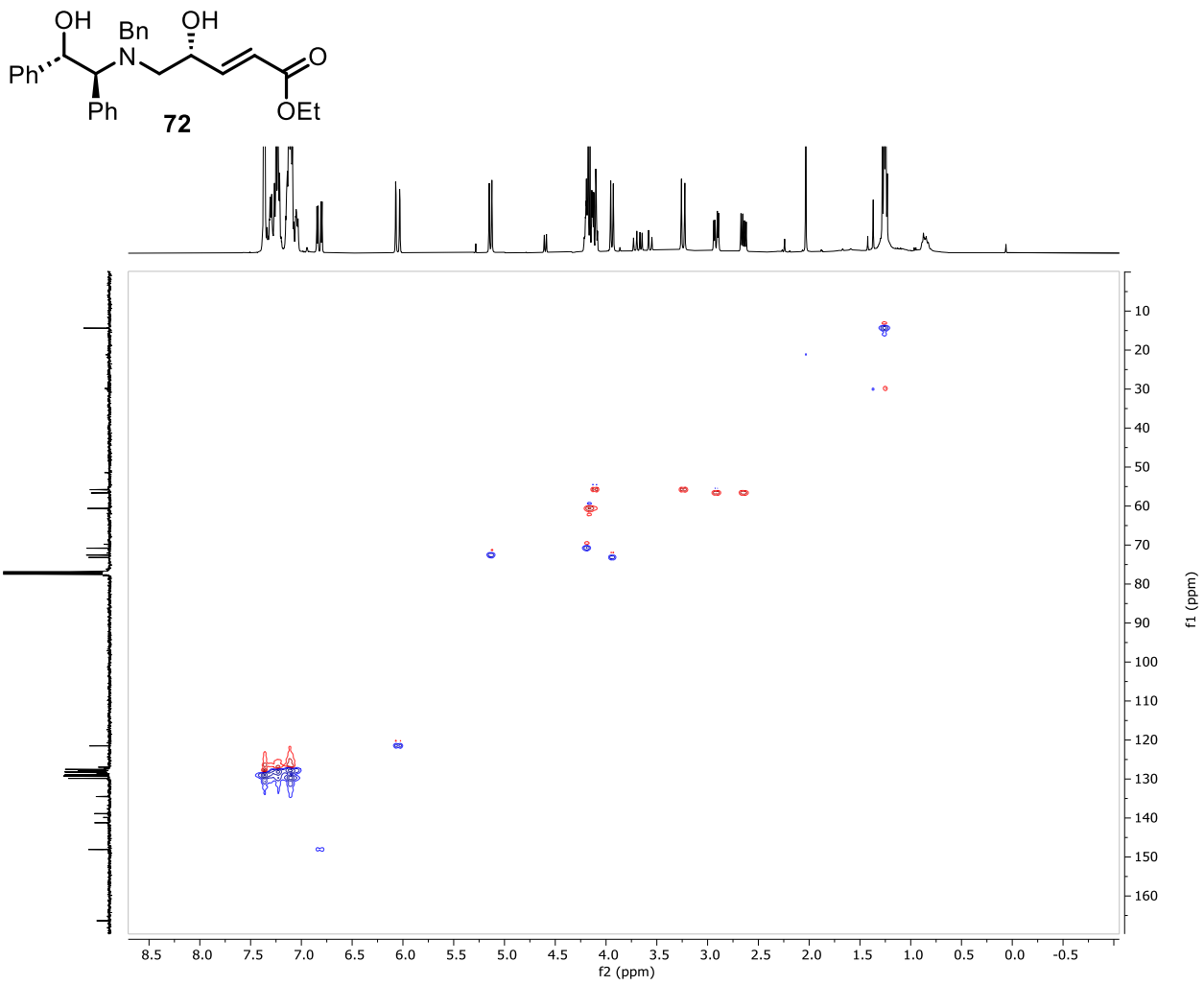
OH
Bn
OH
Ph
N
O
Ph
OEt
72
f1 (ppm)
f2 (ppm)

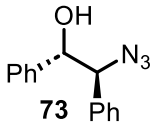

73

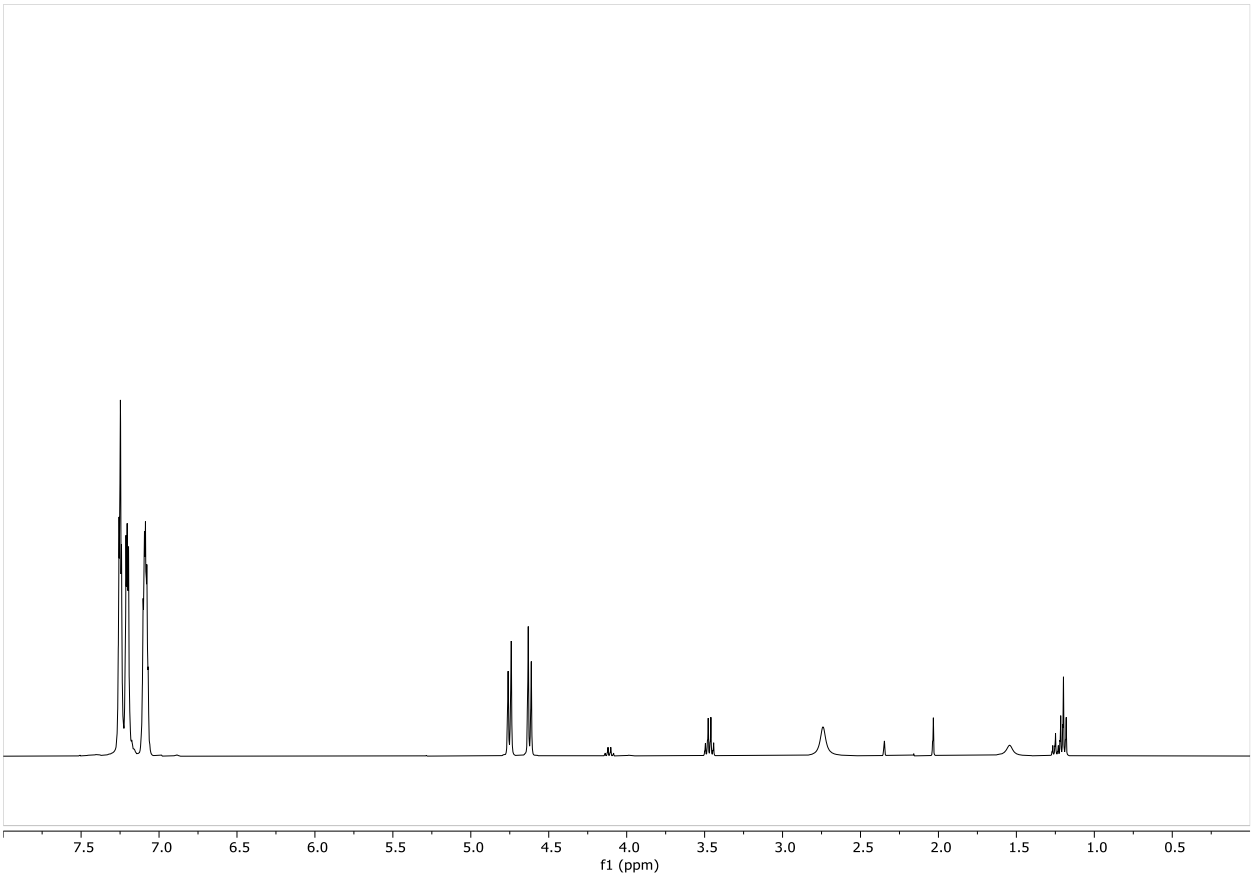

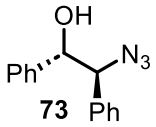
OH
N3
Ph
Ph

73

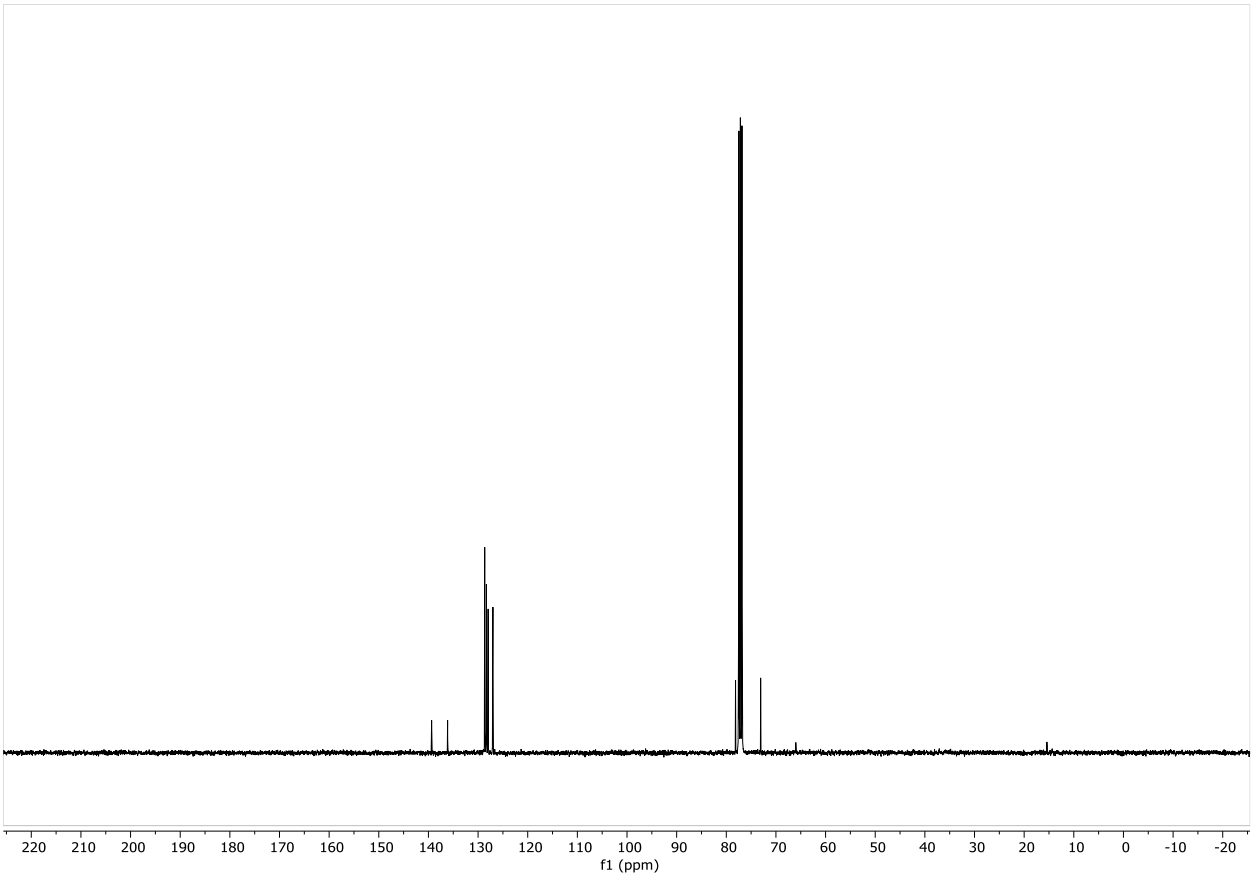
220 210 200 190 180 170 160 150 140 130 120 110 100 90 80 70 60 50 40 30 20 10 0 -10 -20
f1 (ppm)

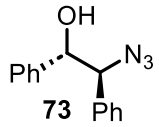
OH
N3
Ph
Ph

73

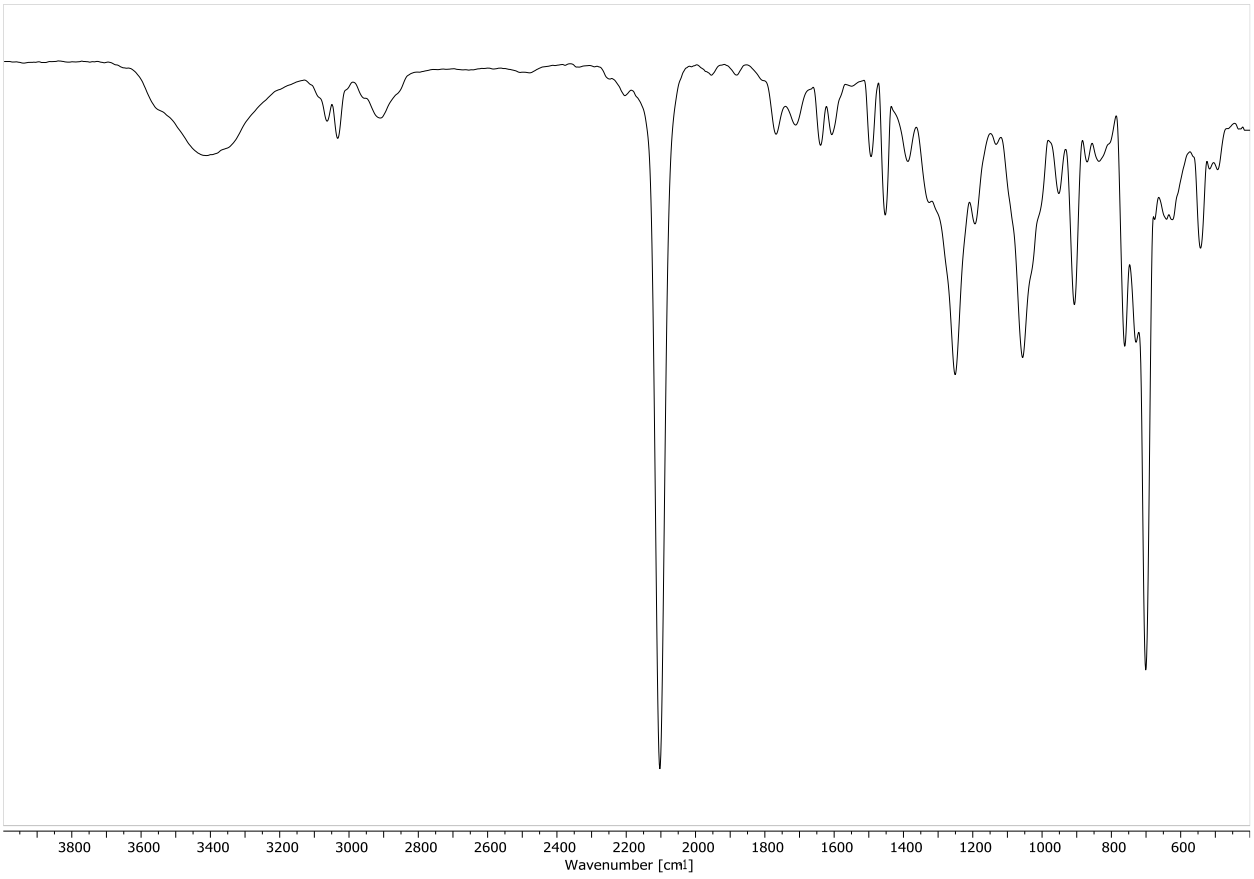
3800
3600
3400
3200
3000
2800
2600
2400
2200
2000
1800
1600
1400
1200
1000
800
600
Wavenumber [cm-1]

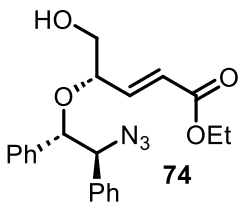
HO
O
O
N3
OEt
Ph
Ph

74

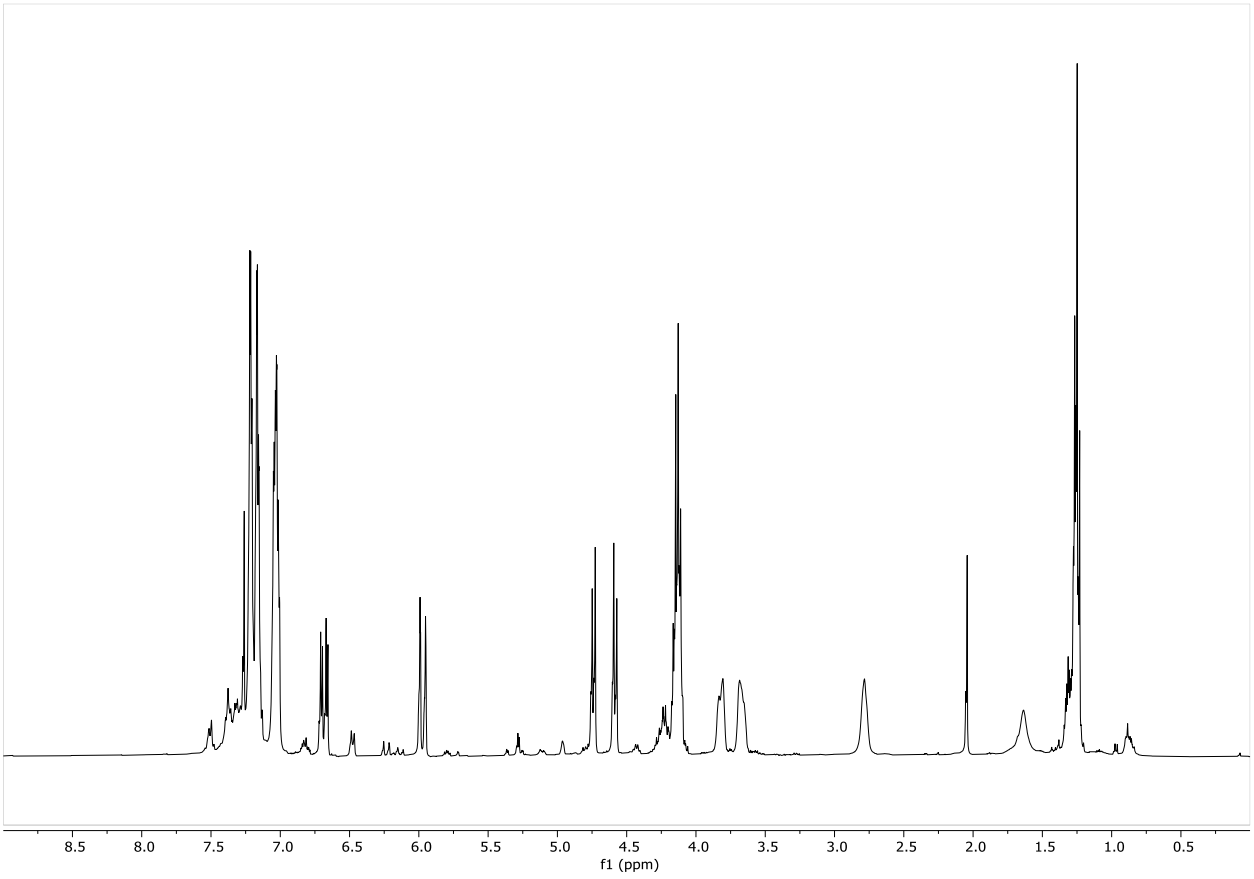
8.5
8.0
7.5
7.0
6.5
6.0
5.5
5.0
4.5
4.0
3.5
3.0
2.5
2.0
1.5
1.0
0.5
f1 (ppm)

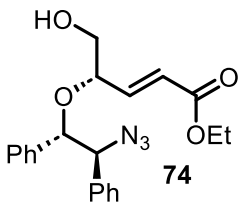
HO
O
O
N3
OEt
Ph
Ph

74

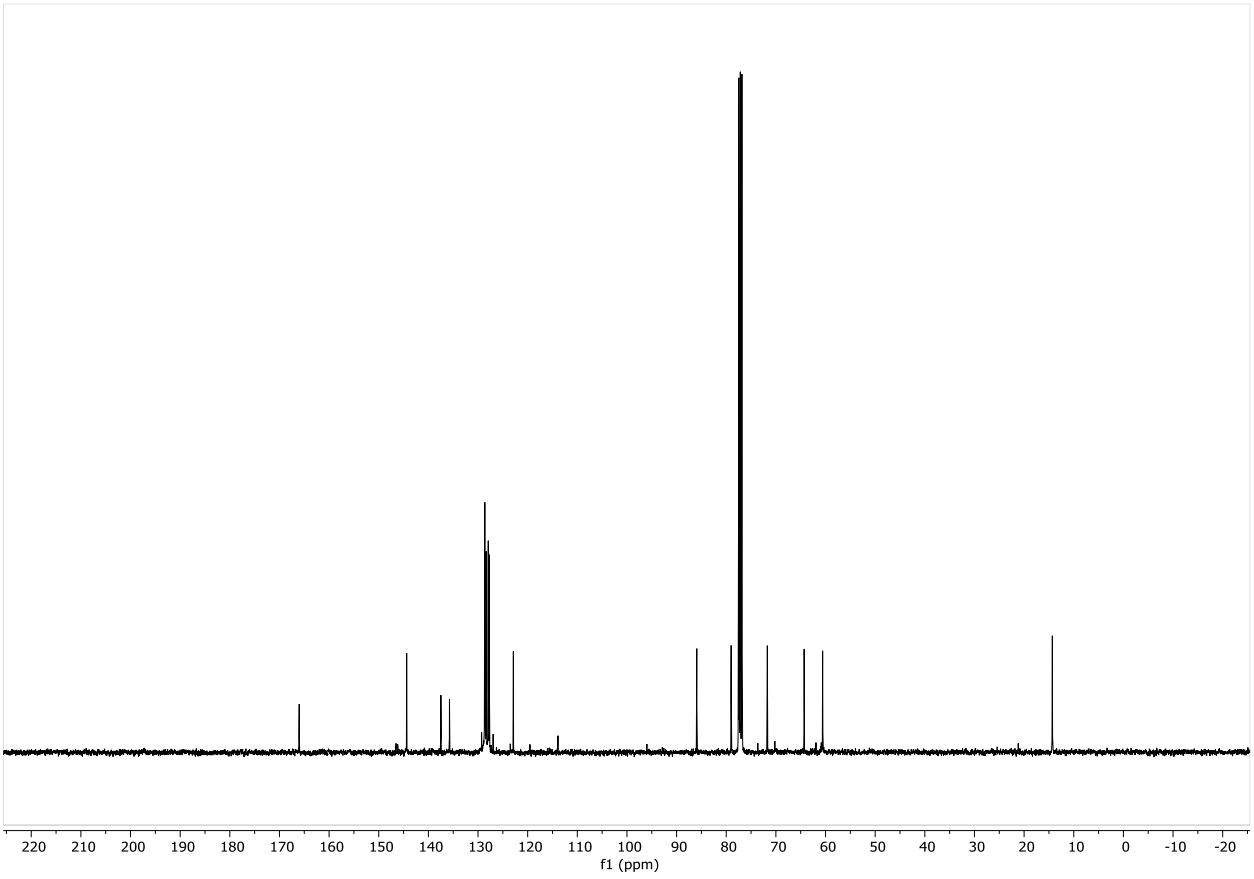
220 210 200 190 180 170 160 150 140 130 120 110 100 90 80 70 60 50 40 30 20 10 0 -10 -20
f1 (ppm)

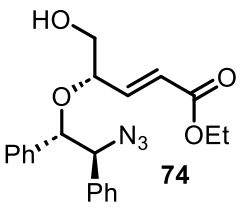
HO
O
O
OEt
N3
Ph
Ph

74

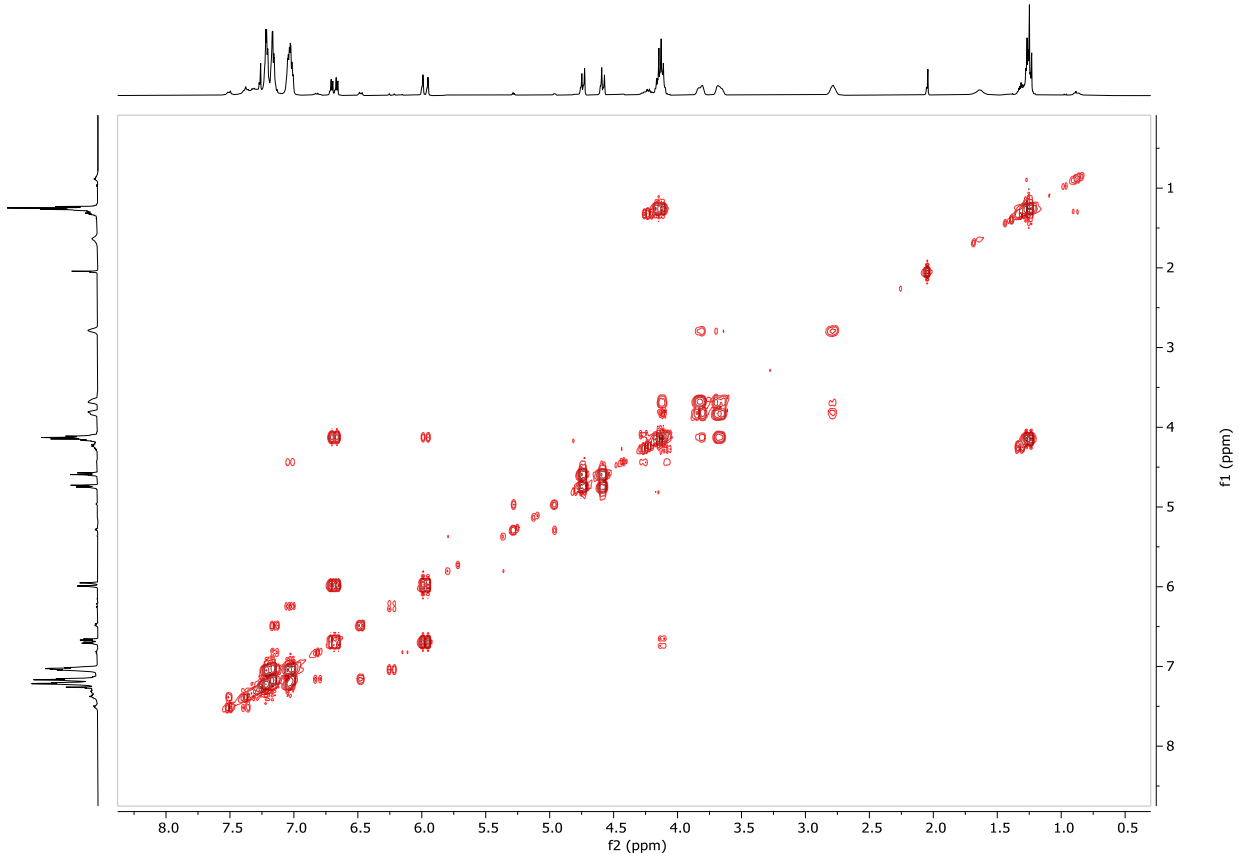
8.0
7.5
7.0
6.5
6.0
5.5
5.0
4.5
4.0
3.5
3.0
2.5
2.0
1.5
1.0
0.5
f2 (ppm)
1
2
3
4
5
6
7
8
f1 (ppm)

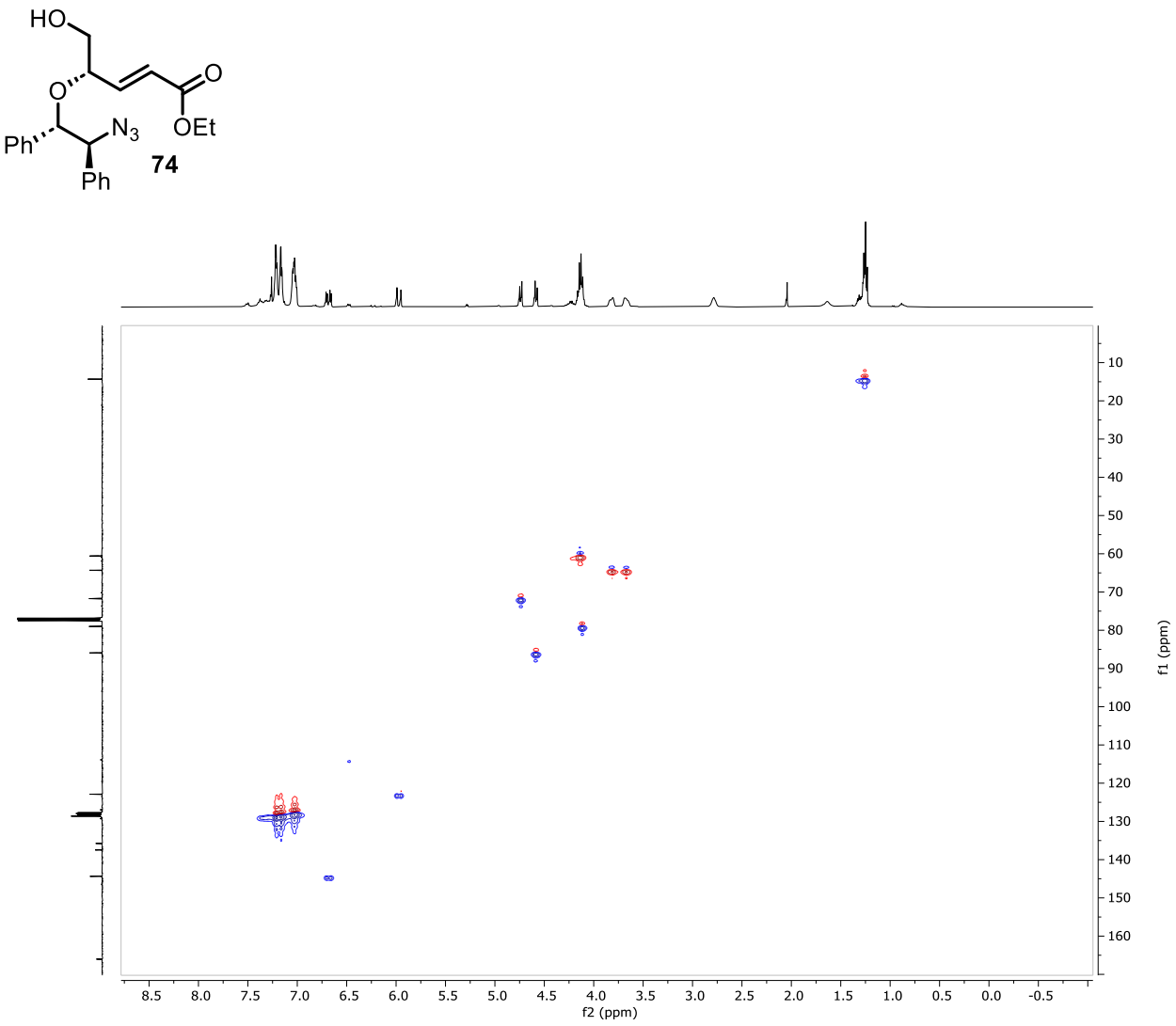
HO
O
O
OEt
N3
Ph
Ph
74
f2 (ppm)
f1 (ppm)

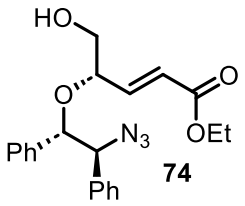
HO
O
O
N3
OEt
Ph
Ph

74

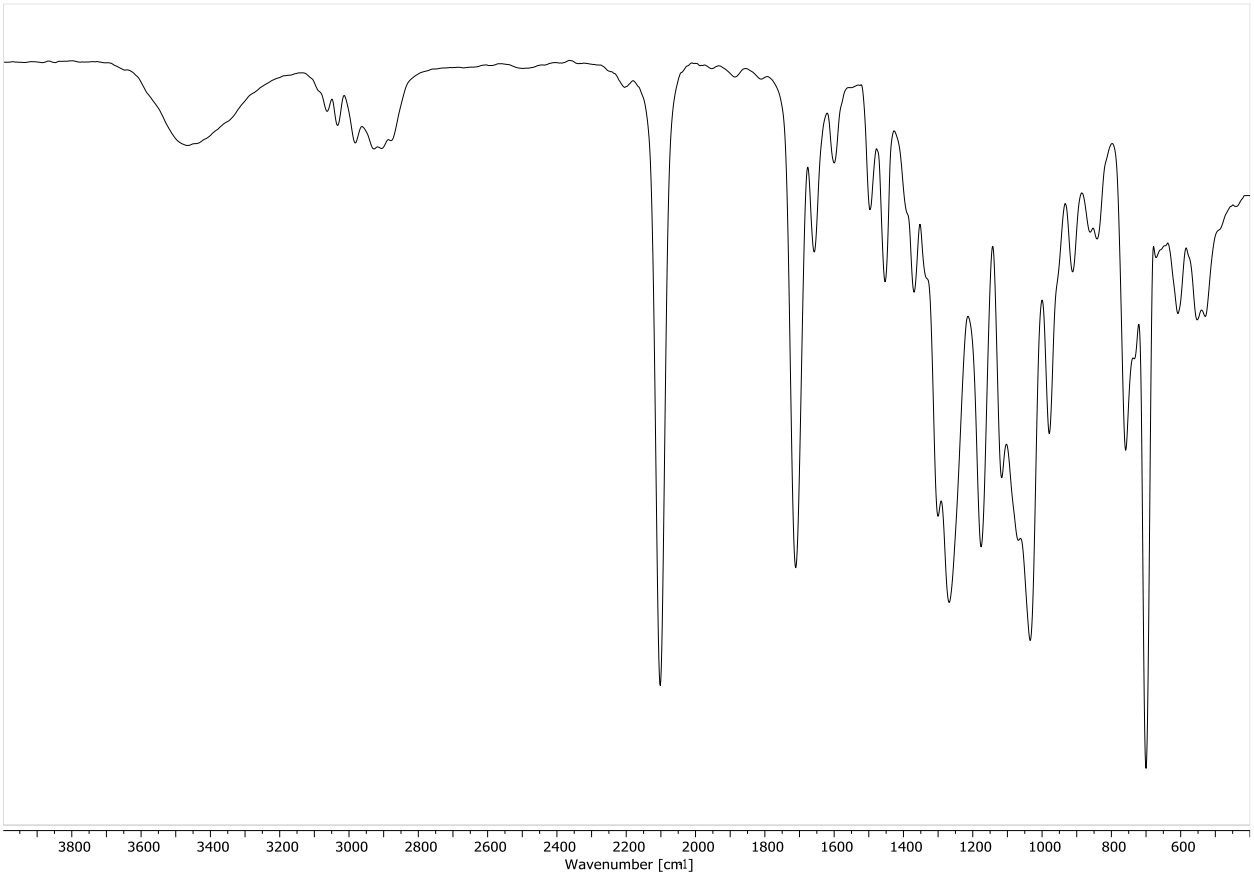
3800
3600
3400
3200
3000
2800
2600
2400
2200
2000
1800
1600
1400
1200
1000
800
600
Wavenumber [cm-1]

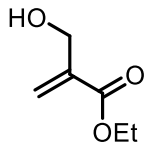

77

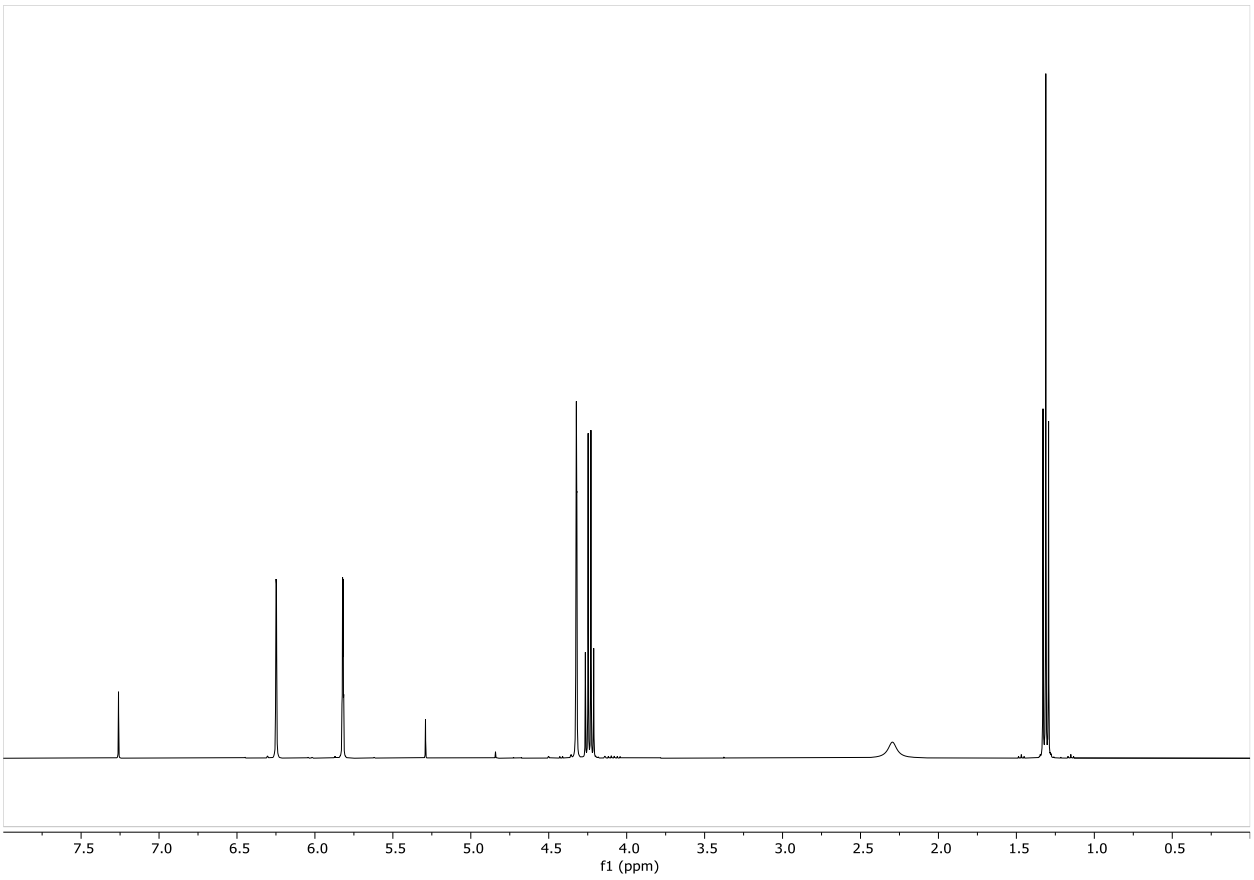

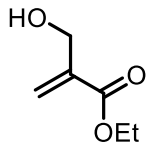
HO
O
OEt

77

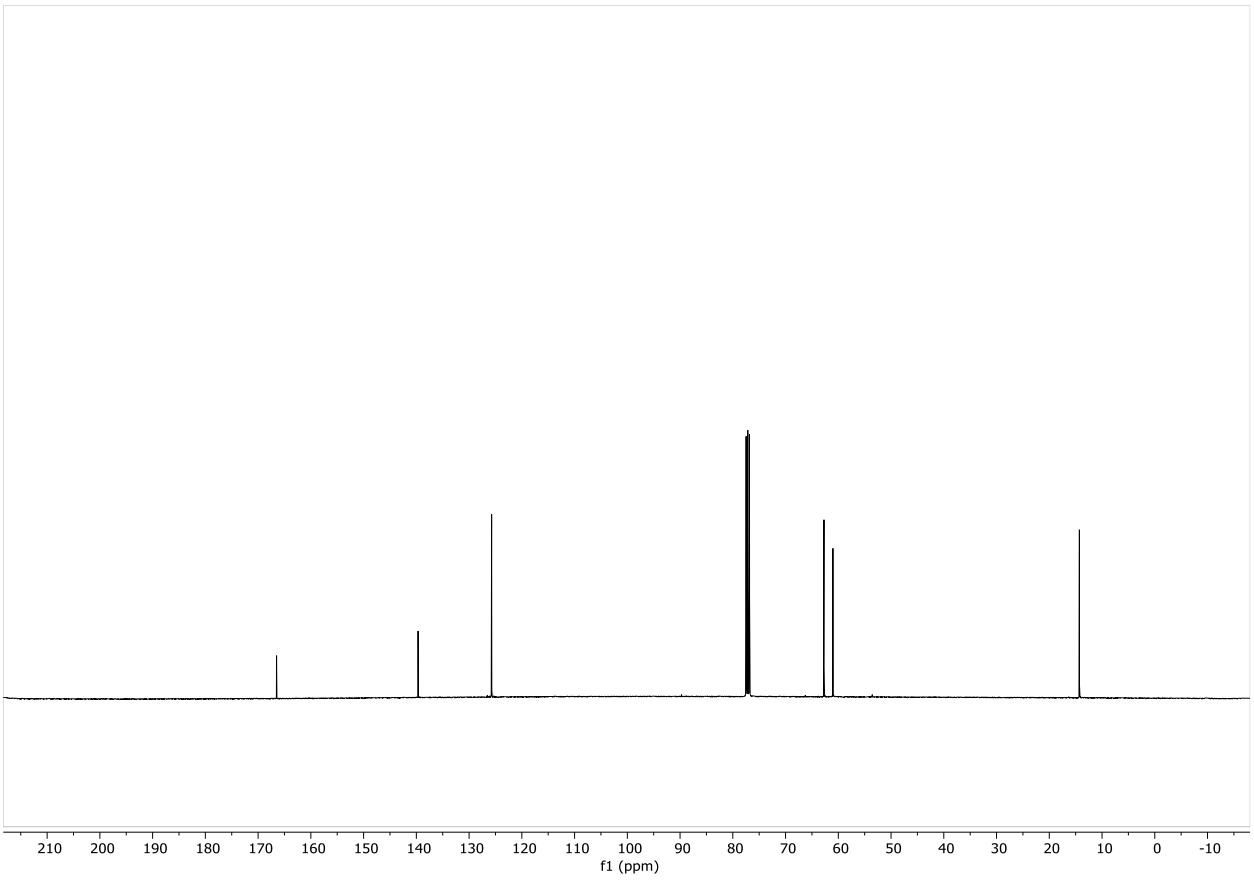
210
200
190
180
170
160
150
140
130
120
110
100
90
80
70
60
50
40
30
20
10
0
-10
f1 (ppm)

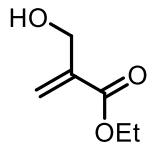
HO
O
OEt

77

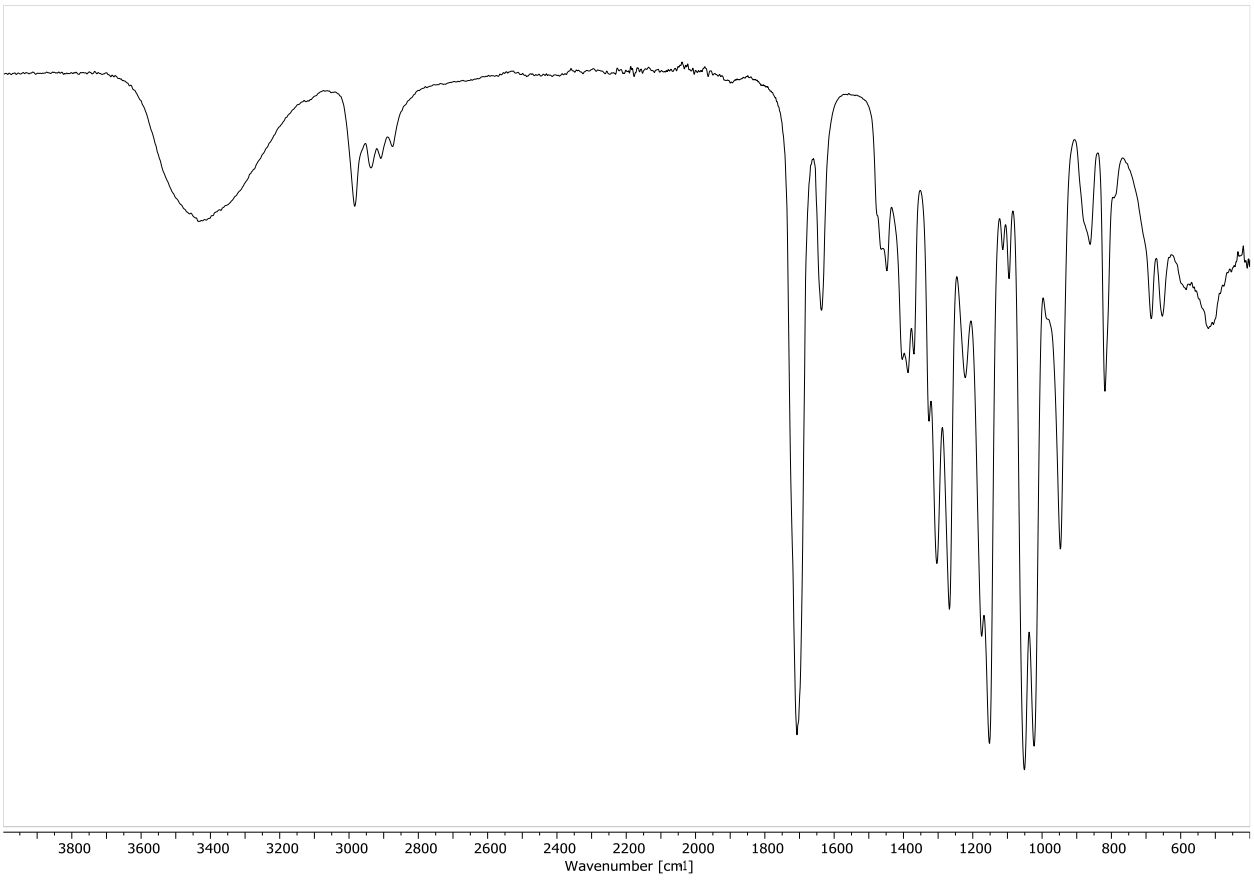
3800
3600
3400
3200
3000
2800
2600
2400
2200
2000
1800
1600
1400
1200
1000
800
600
Wavenumber [cm-1]

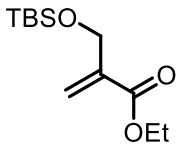

78

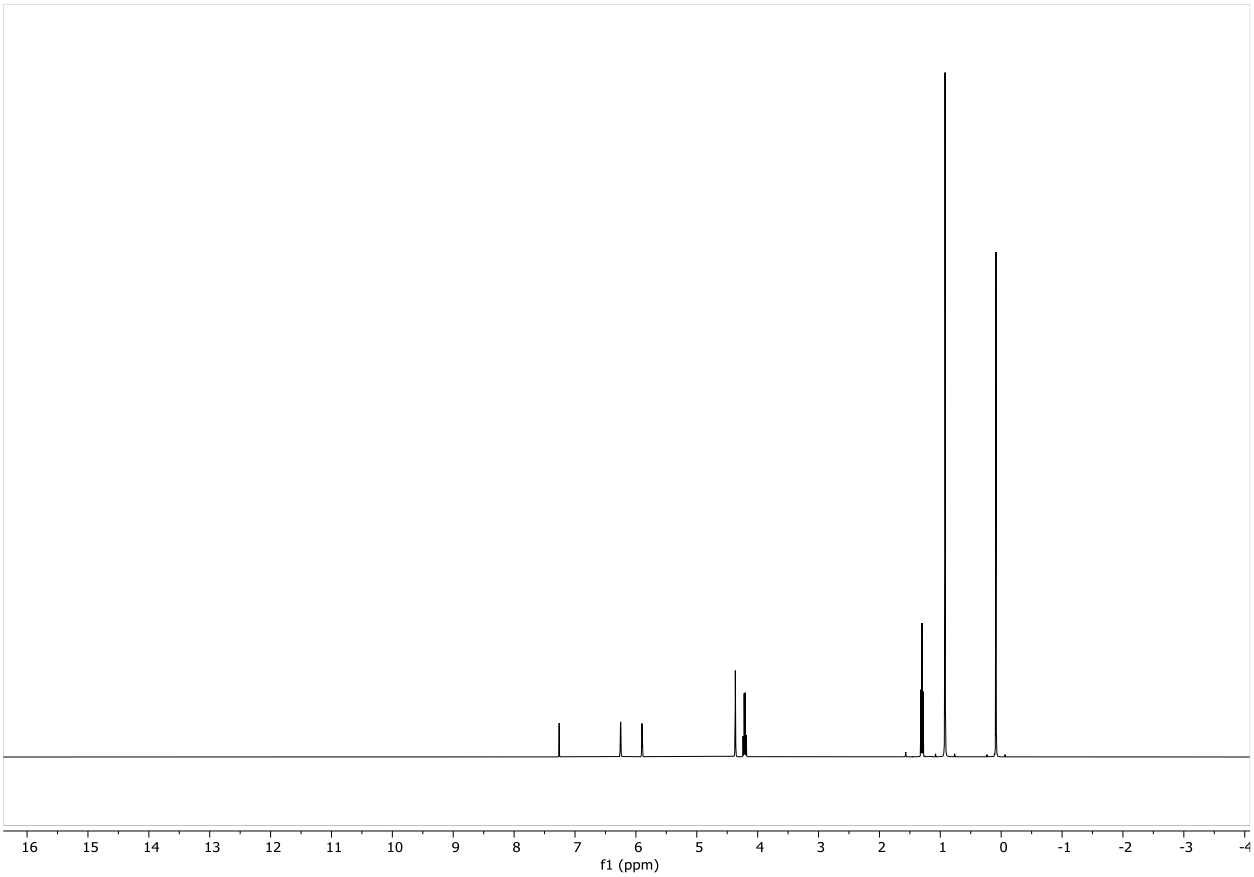

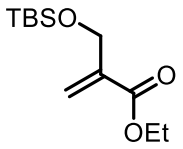
TBSO
O
OEt

78

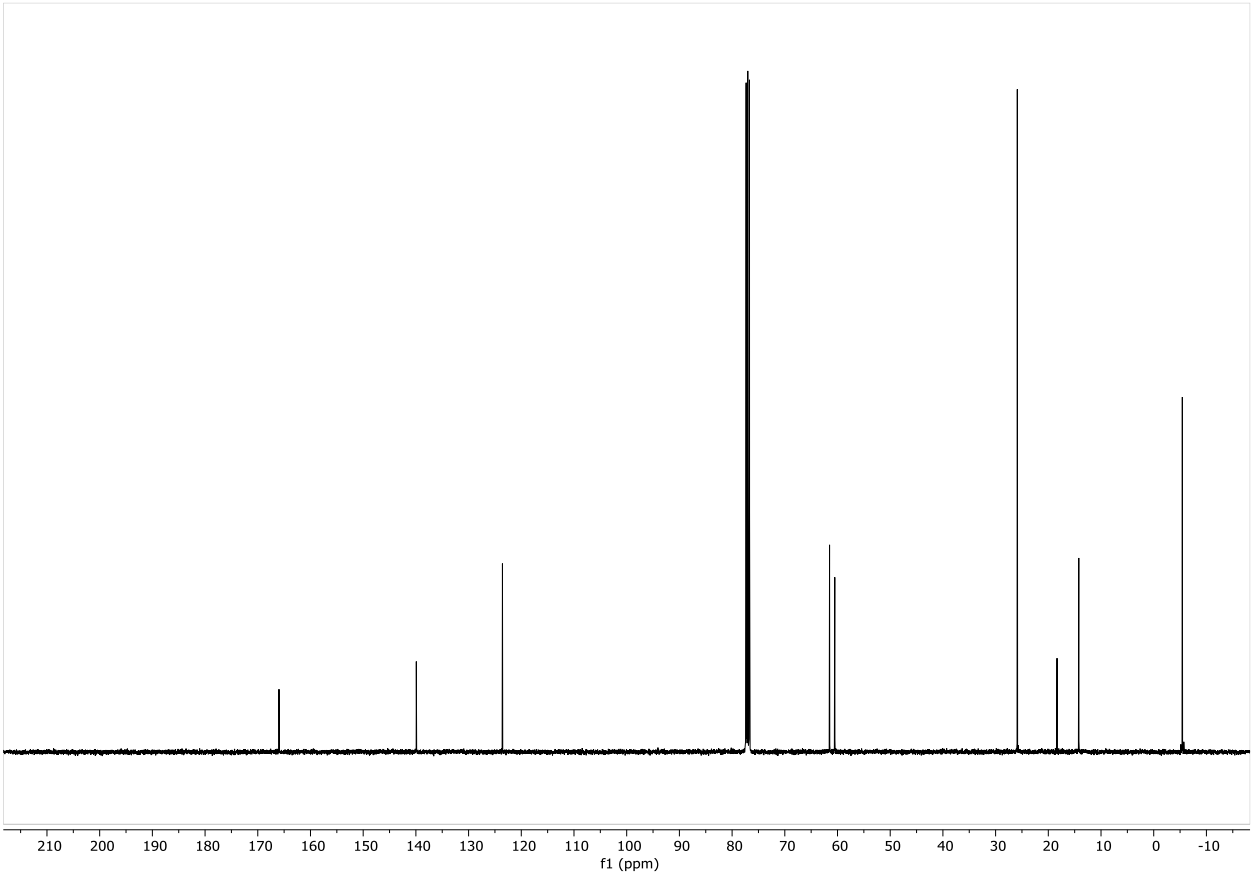
210
200
190
180
170
160
150
140
130
120
110
100
90
80
70
60
50
40
30
20
10
0
-10
f1 (ppm)

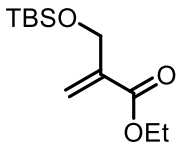
TBSO
O
OEt

78

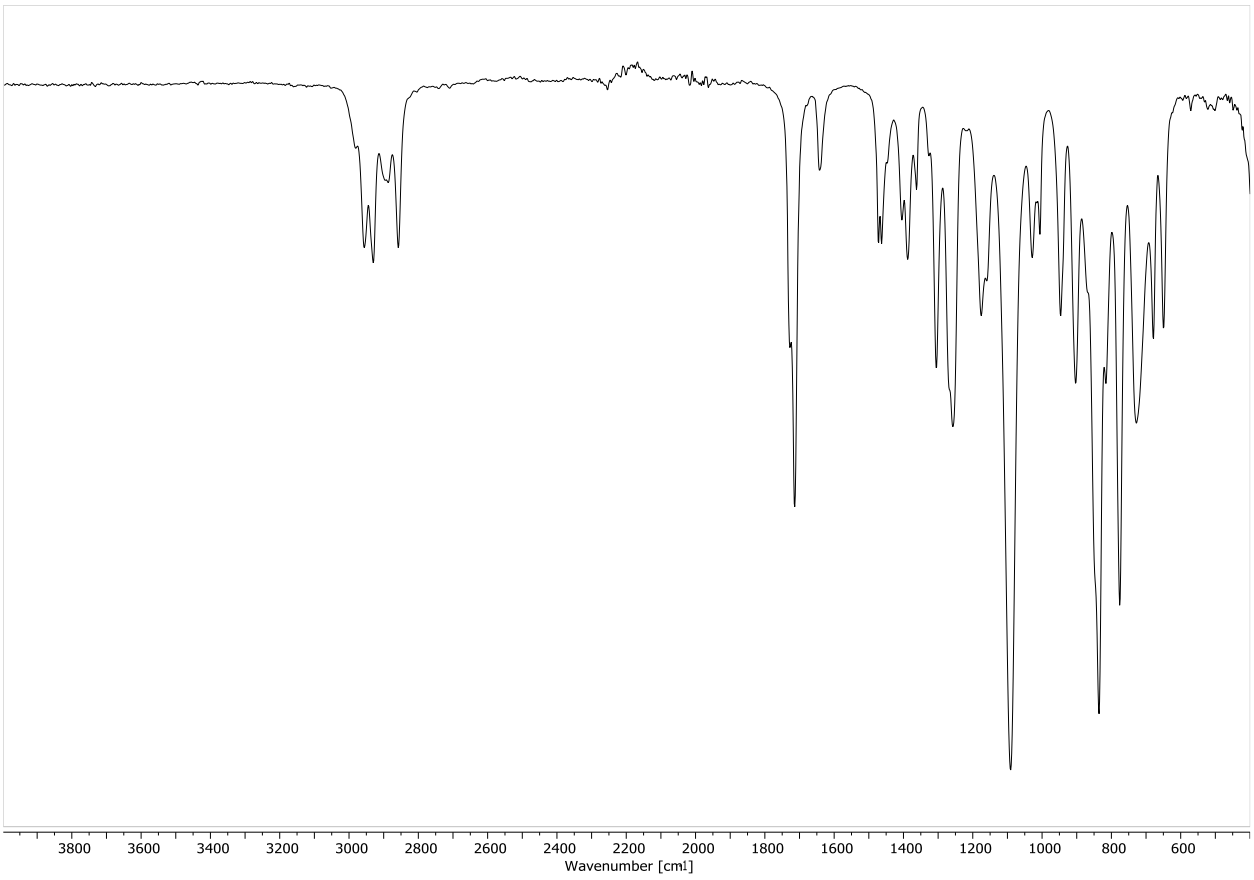
3800
3600
3400
3200
3000
2800
2600
2400
2200
2000
1800
1600
1400
1200
1000
800
600
Wavenumber [cm-1]

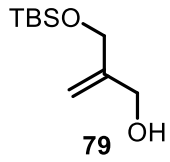

79

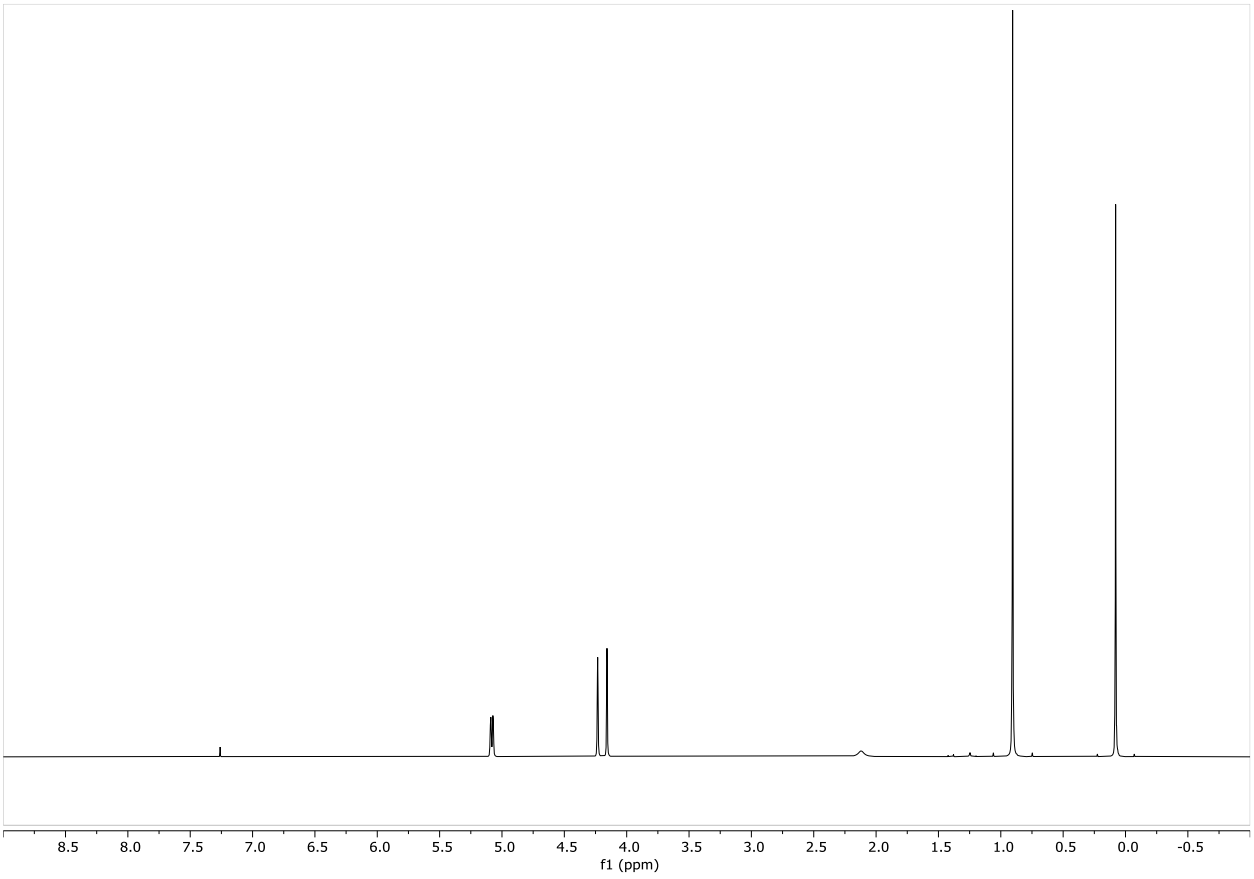

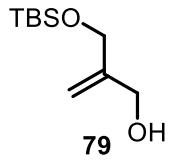
TBSO
OH

79

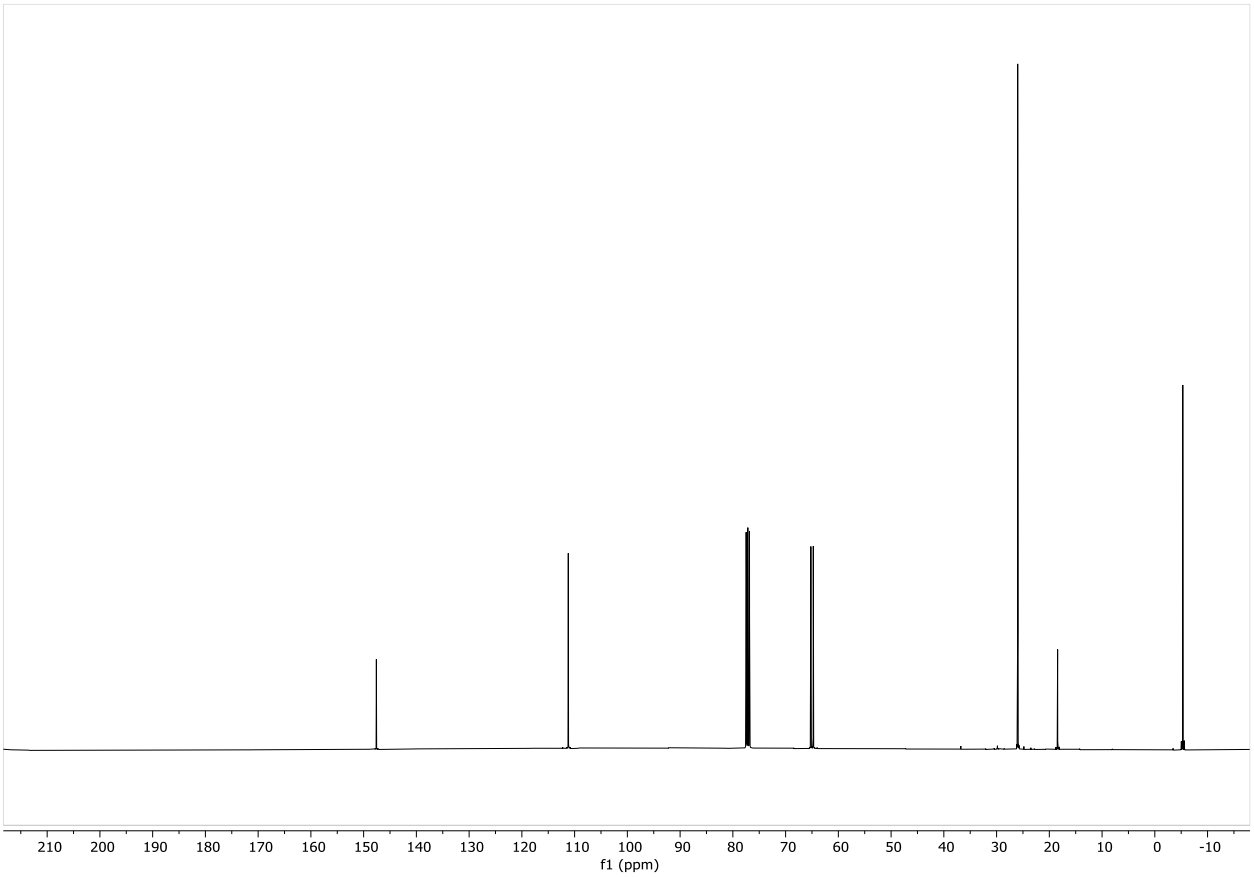
210
200
190
180
170
160
150
140
130
120
110
100
90
80
70
60
50
40
30
20
10
0
-10
f1 (ppm)

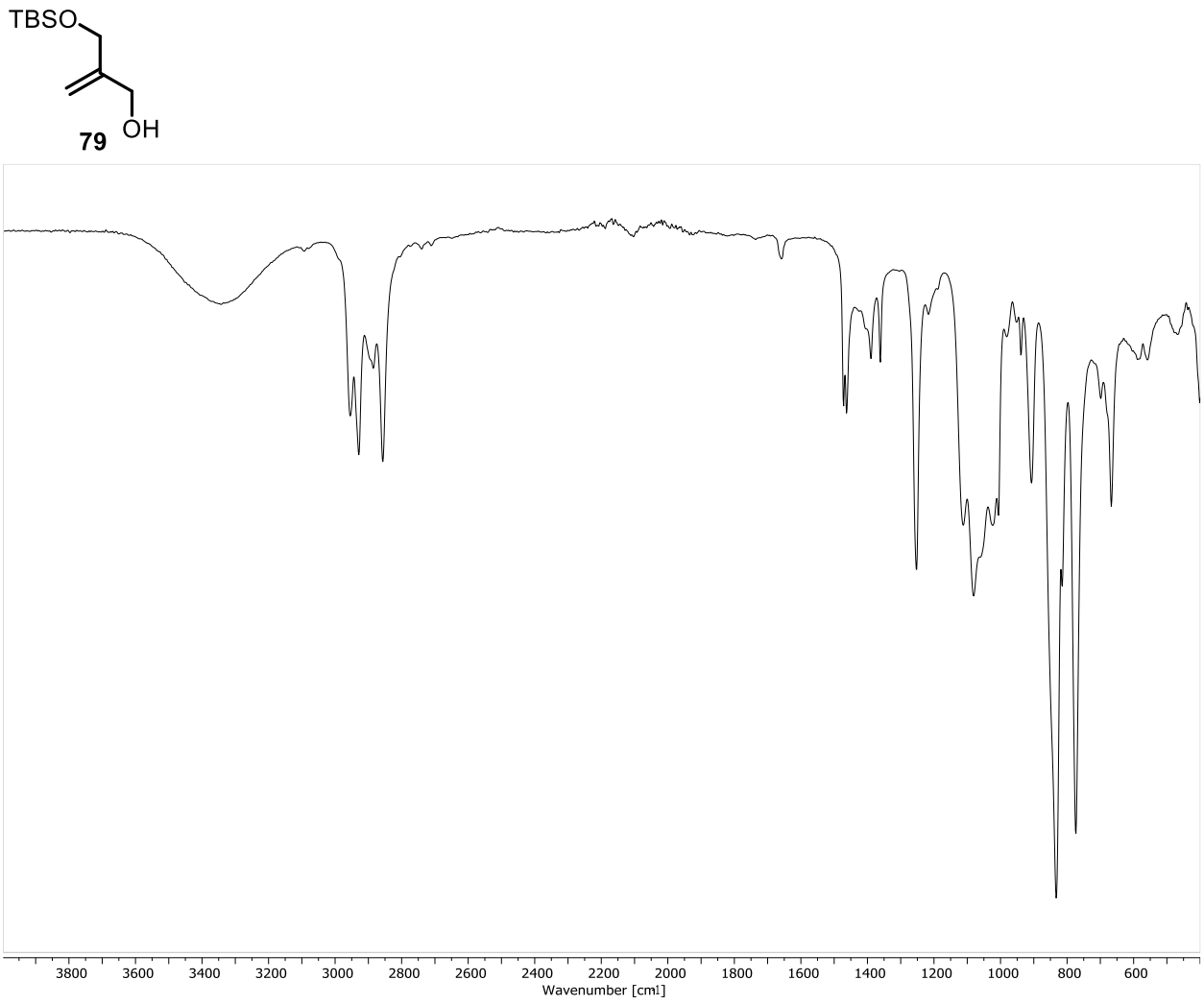
TBSO
OH
79
3800
3600
3400
3200
3000
2800
2600
2400
2200
2000
1800
1600
1400
1200
1000
800
600
Wavenumber [cm-1]

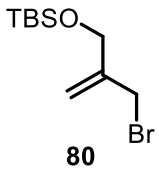

80

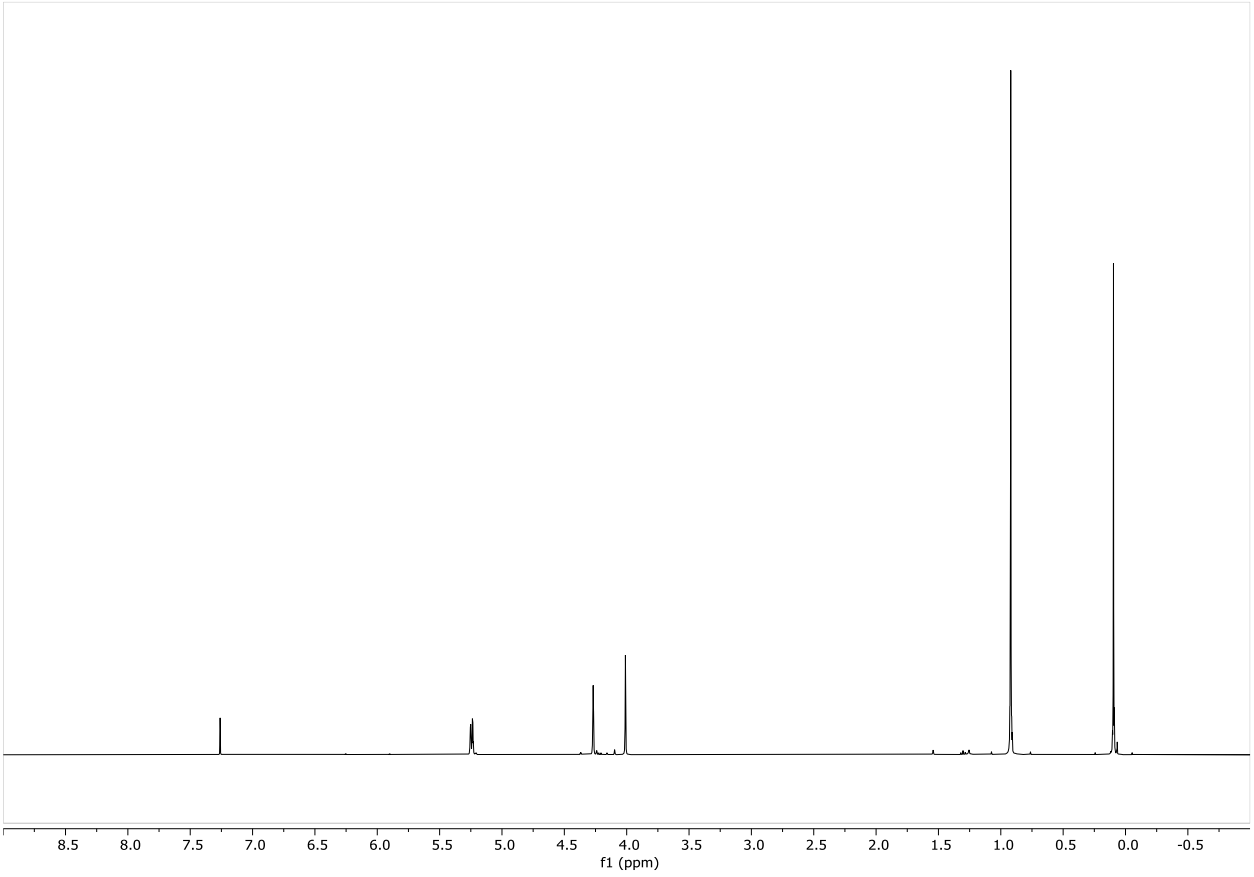

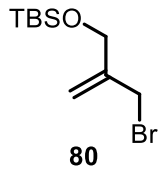
TBSO
Br

80

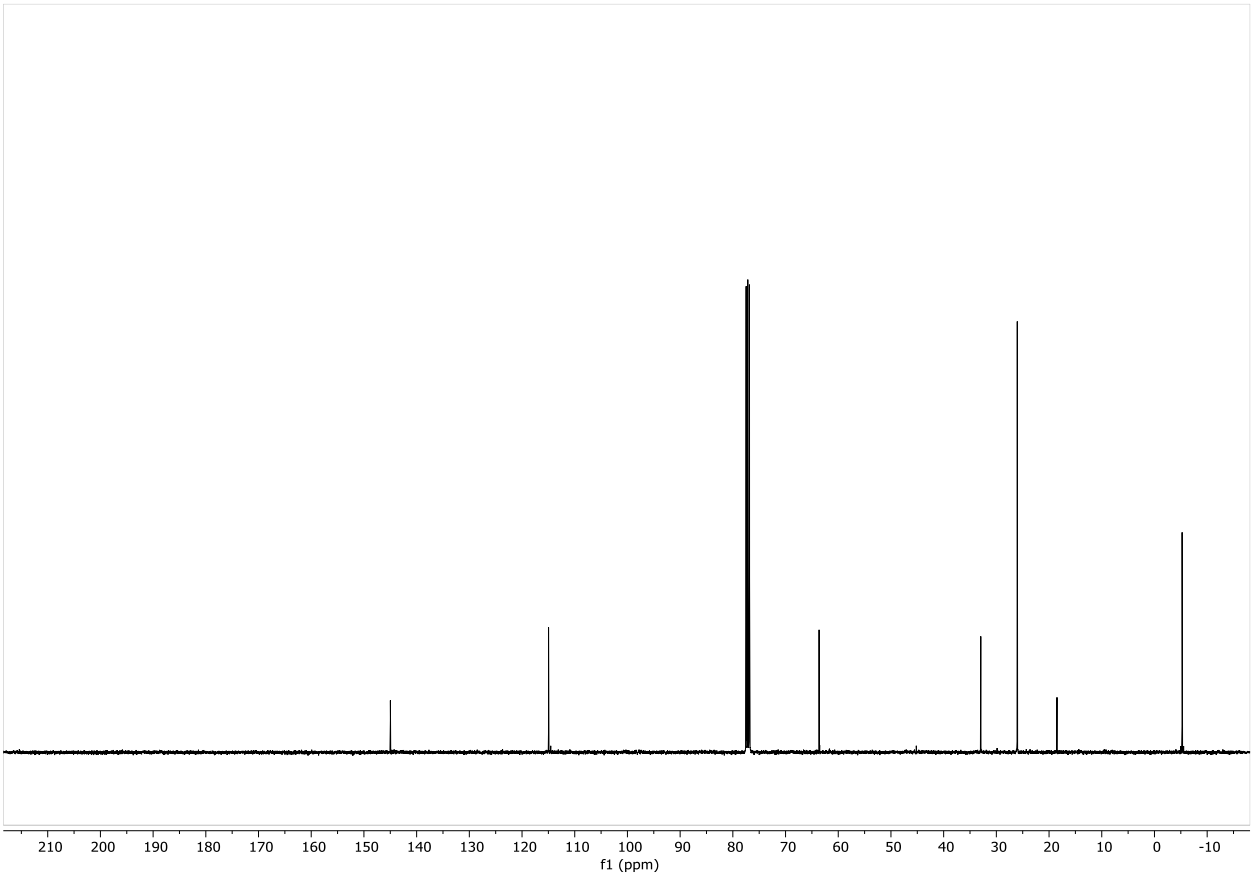
210
200
190
180
170
160
150
140
130
120
110
100
90
80
70
60
50
40
30
20
10
0
-10
f1 (ppm)

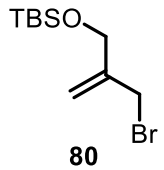
TBSO
Br

80

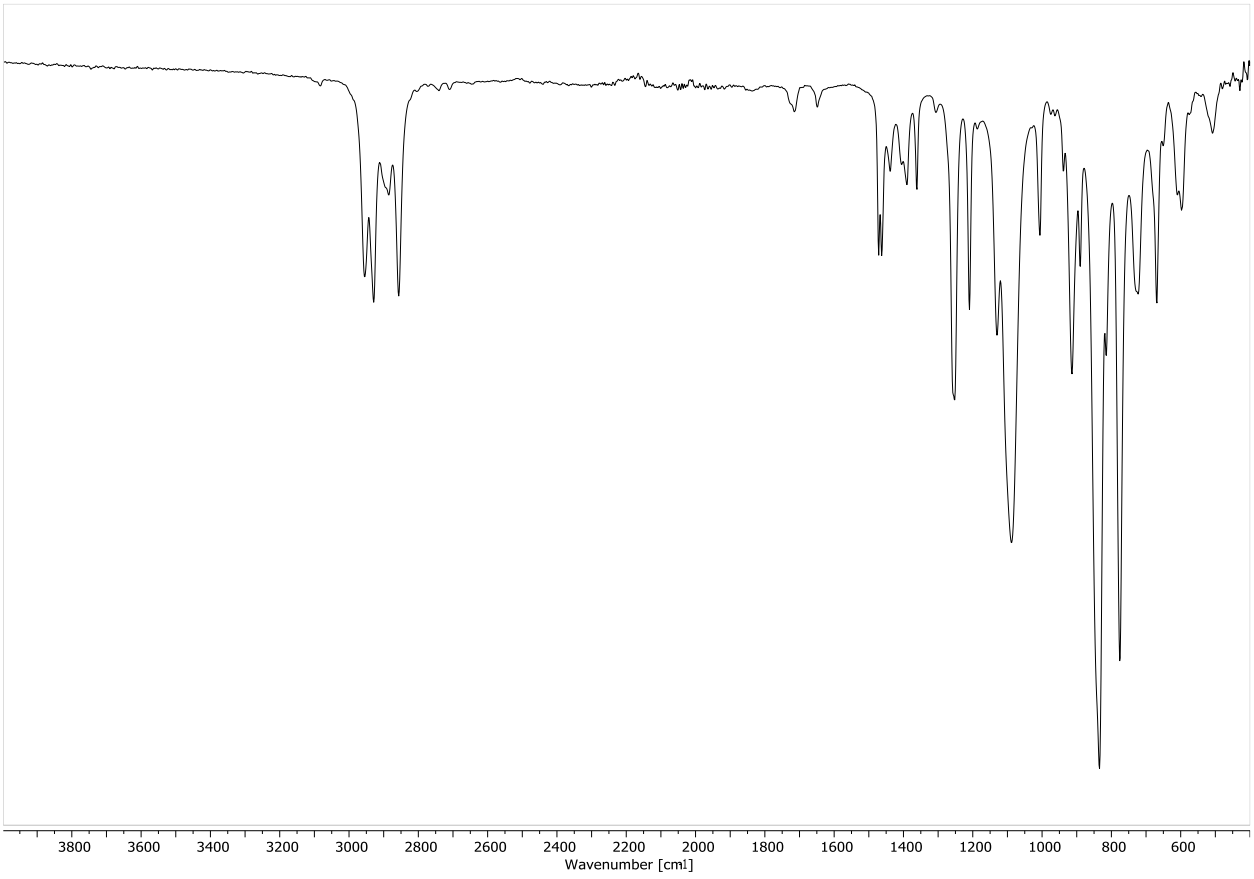
3800
3600
3400
3200
3000
2800
2600
2400
2200
2000
1800
1600
1400
1200
1000
800
600
Wavenumber [cm-1]

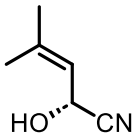

82

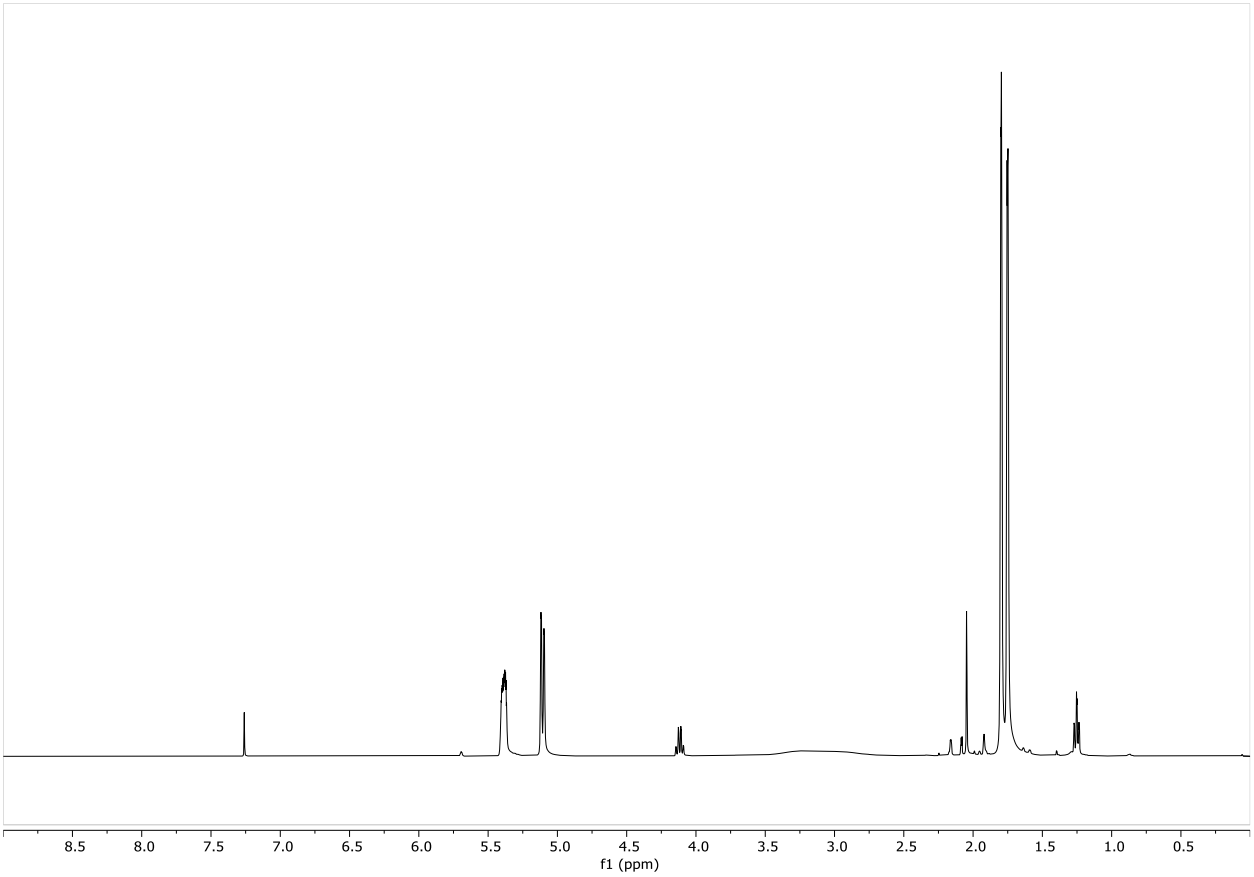

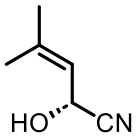
HO
CN

82

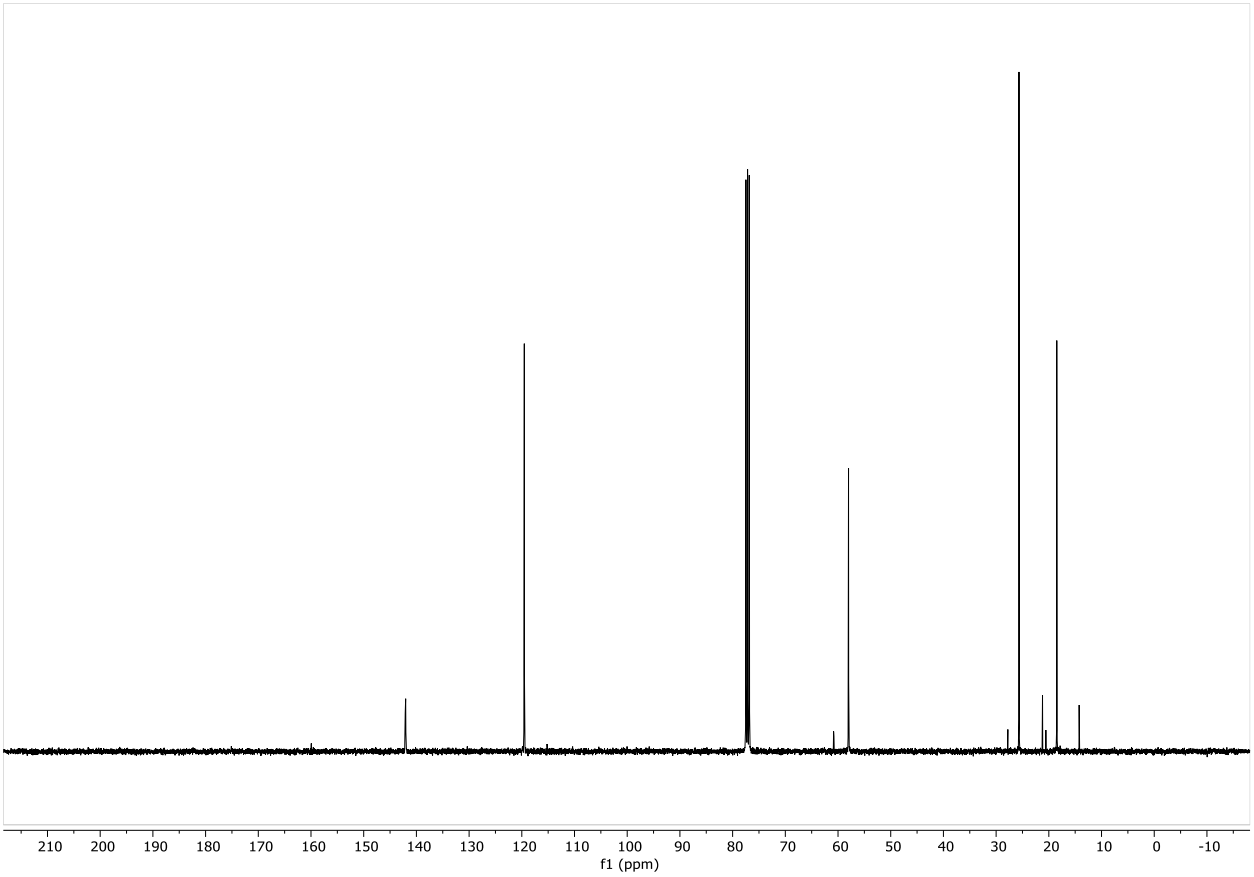
210
200
190
180
170
160
150
140
130
120
110
100
90
80
70
60
50
40
30
20
10
0
-10
f1 (ppm)

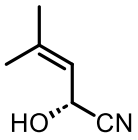
HO
CN

82

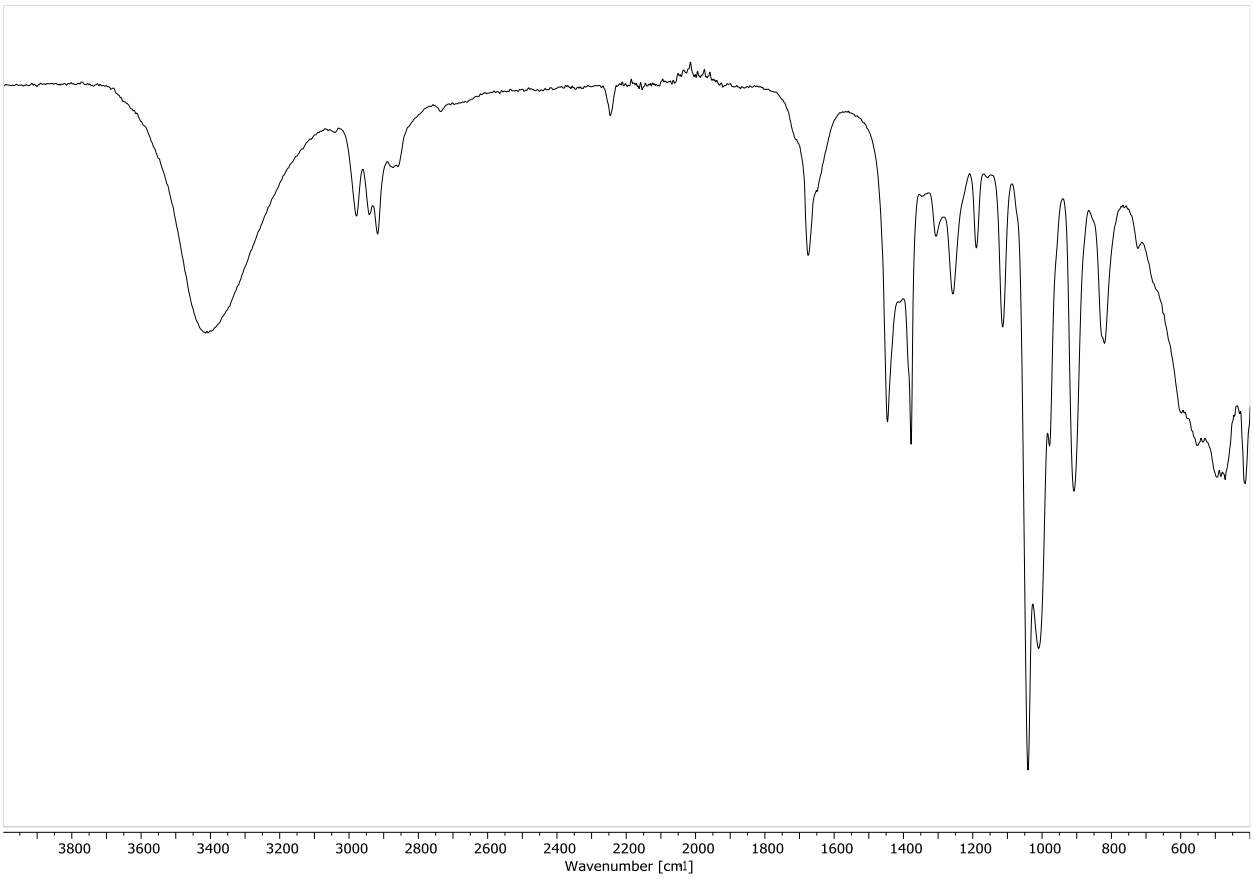
3800
3600
3400
3200
3000
2800
2600
2400
2200
2000
1800
1600
1400
1200
1000
800
600
Wavenumber [cm-1]

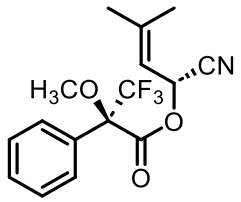
H3CO
CF3
CN
O
O

82m

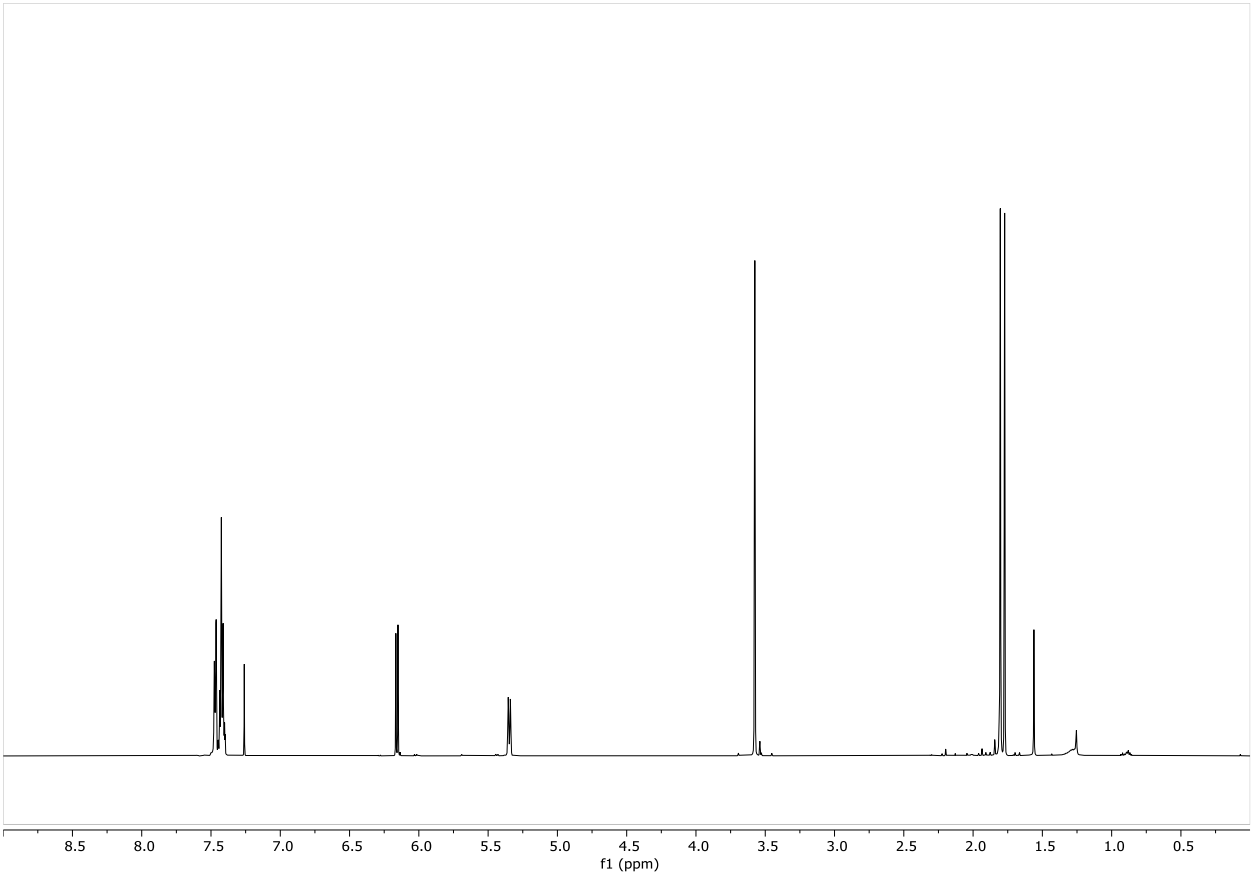
8.5
8.0
7.5
7.0
6.5
6.0
5.5
5.0
4.5
4.0
3.5
3.0
2.5
2.0
1.5
1.0
0.5
f1 (ppm)

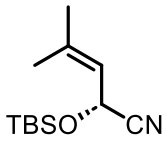

83

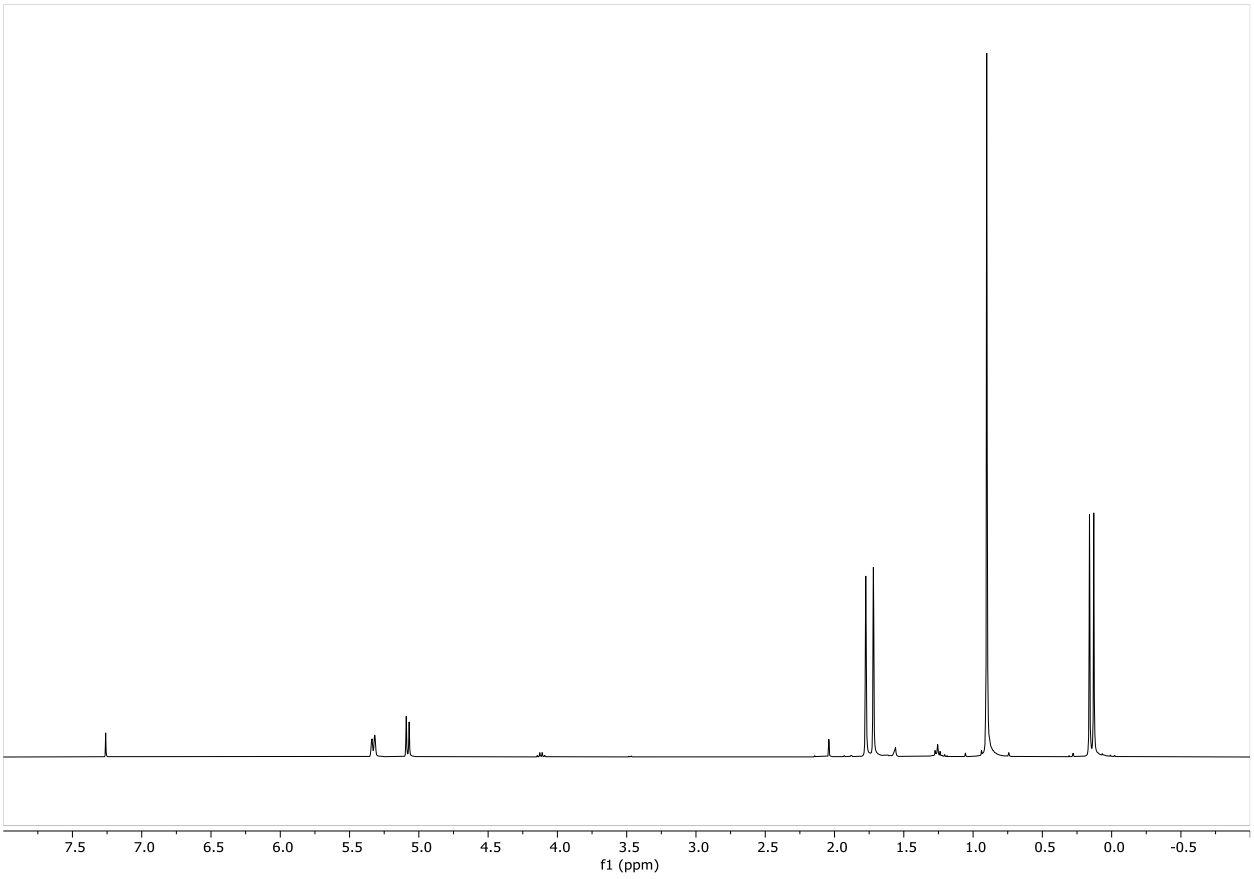

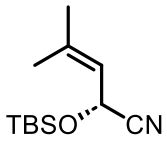
TBSO
CN

83

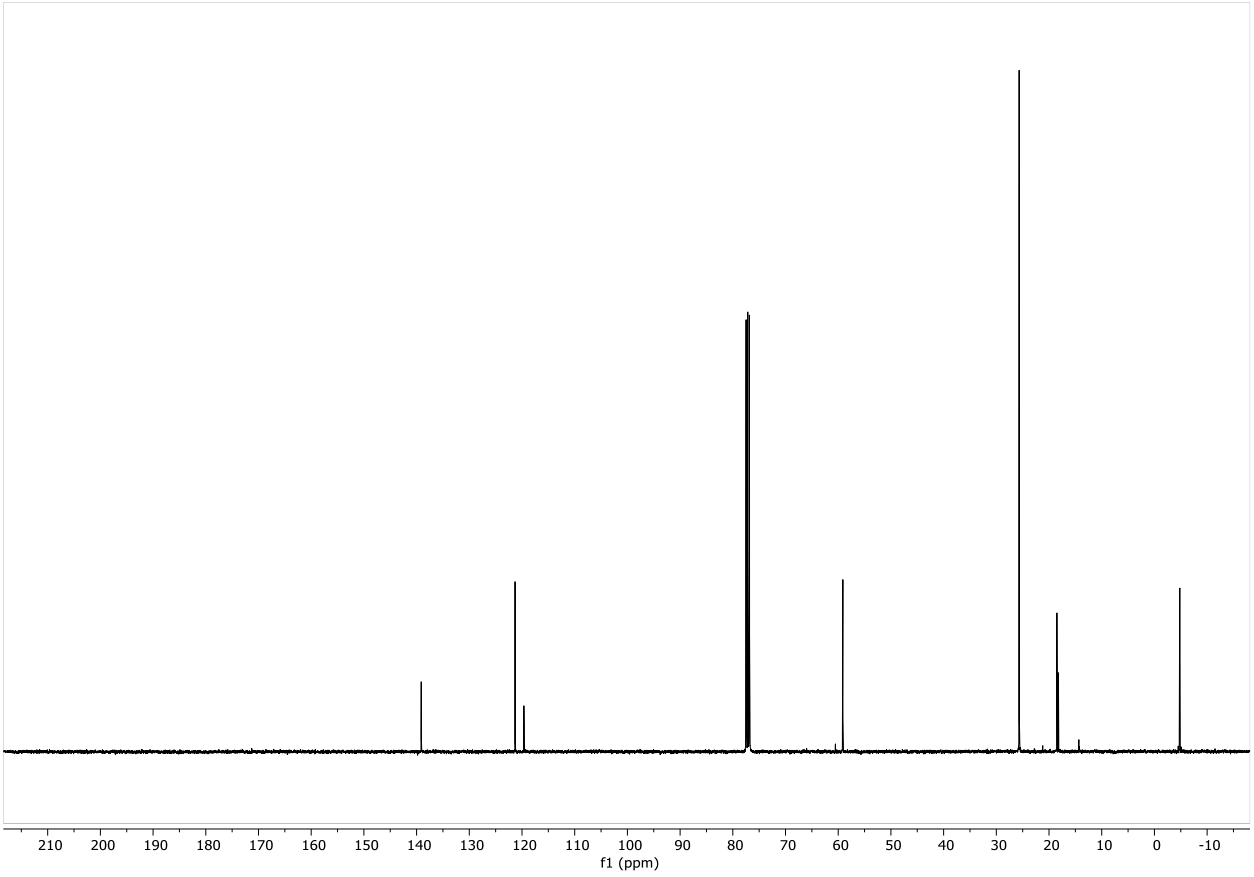
210
200
190
180
170
160
150
140
130
120
110
100
90
80
70
60
50
40
30
20
10
0
-10
f1 (ppm)

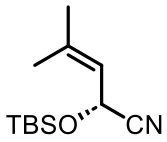
TBSO
CN

83

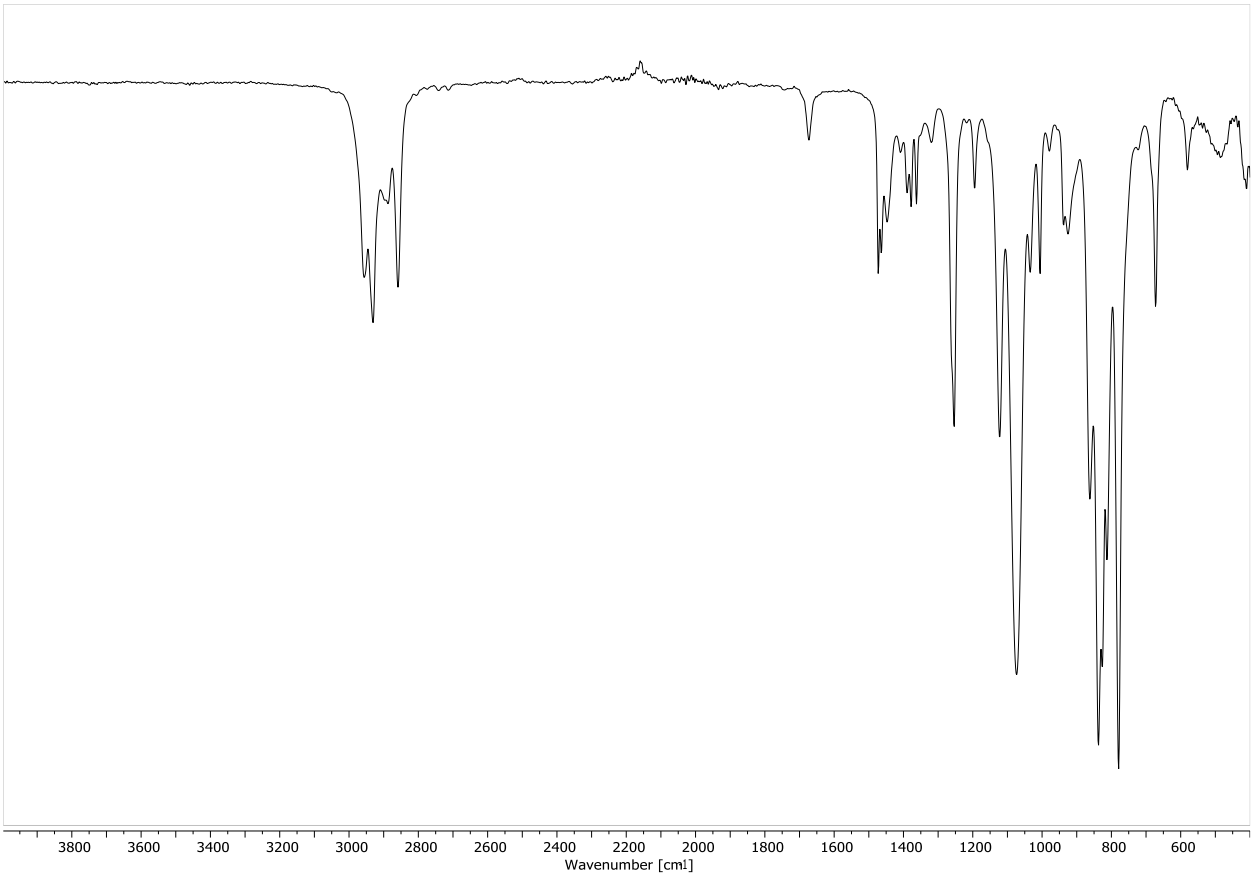
3800
3600
3400
3200
3000
2800
2600
2400
2200
2000
1800
1600
1400
1200
1000
800
600
Wavenumber [cm-1]

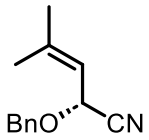

88

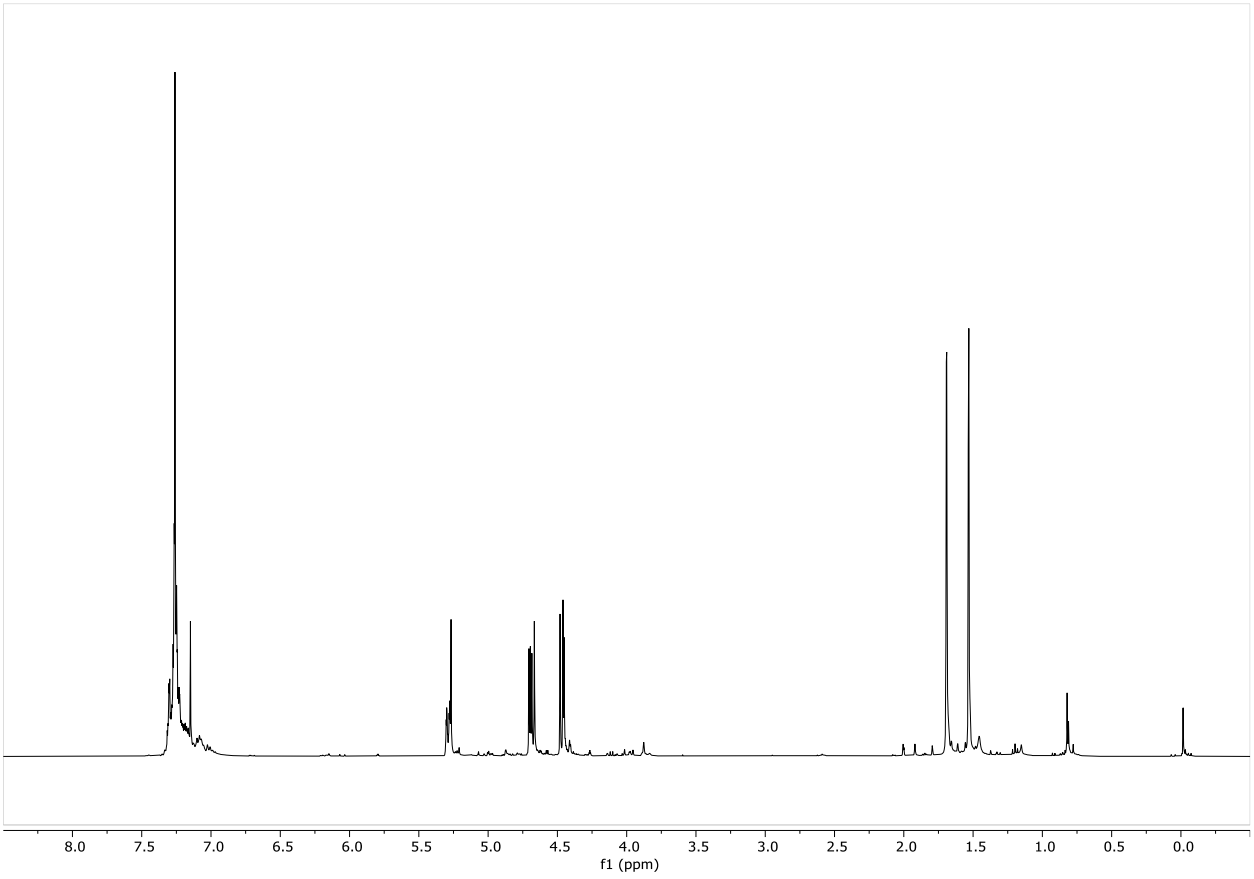

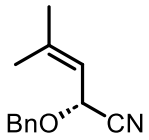
BnO
CN

88

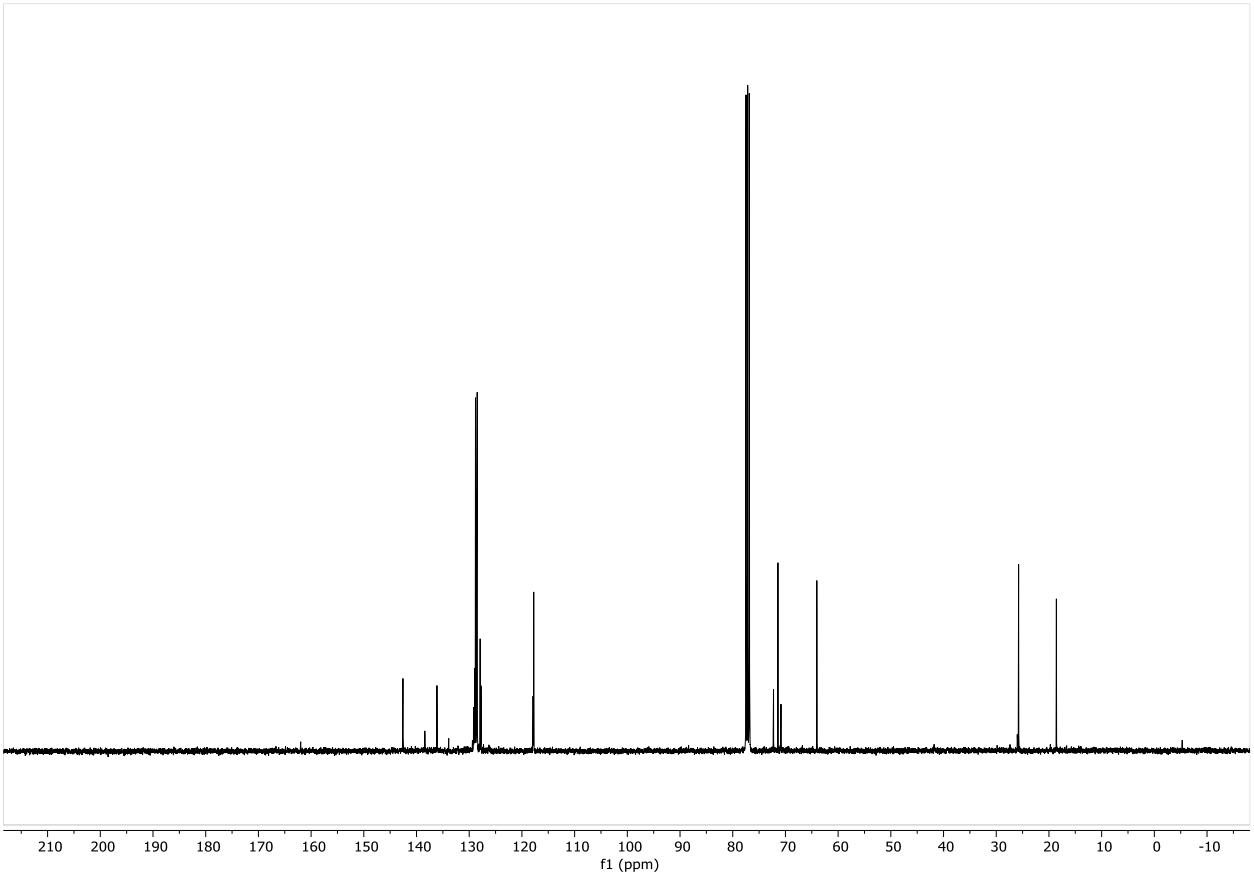
210
200
190
180
170
160
150
140
130
120
110
100
90
80
70
60
50
40
30
20
10
0
-10
f1 (ppm)

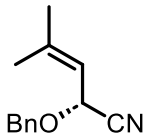
BnO
CN

88

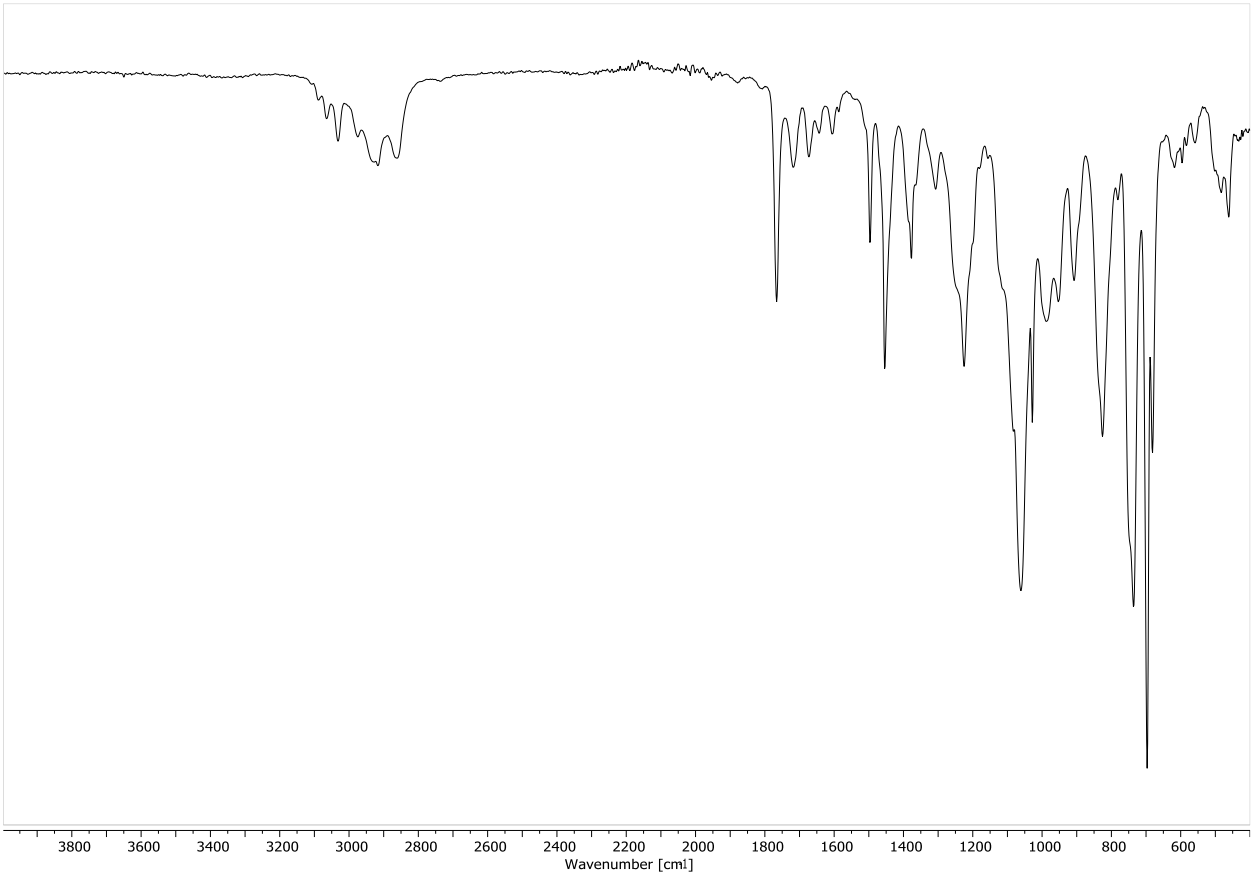
3800
3600
3400
3200
3000
2800
2600
2400
2200
2000
1800
1600
1400
1200
1000
800
600
Wavenumber [cm-1]

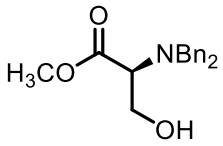

90

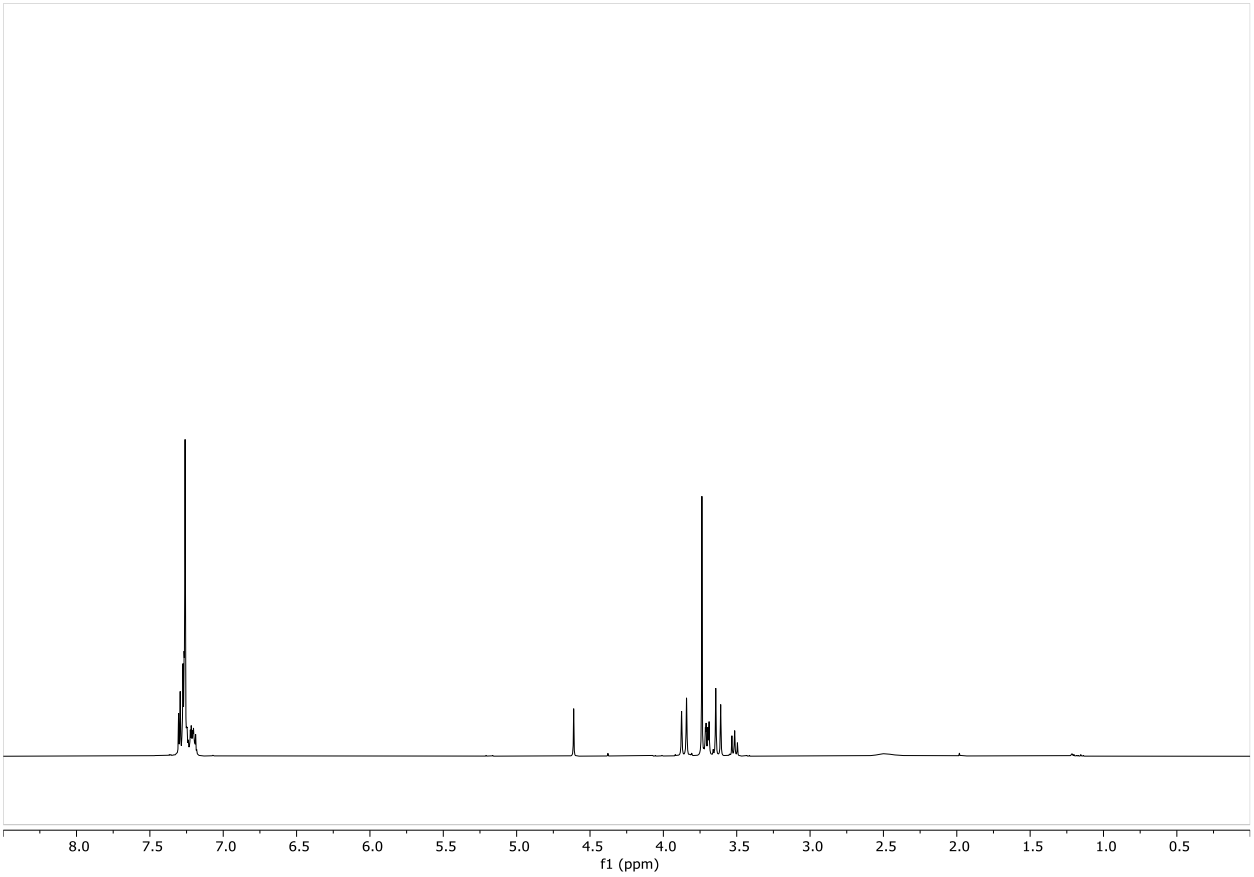

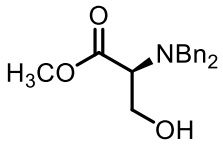
O
NBn2
H3CO
OH

90

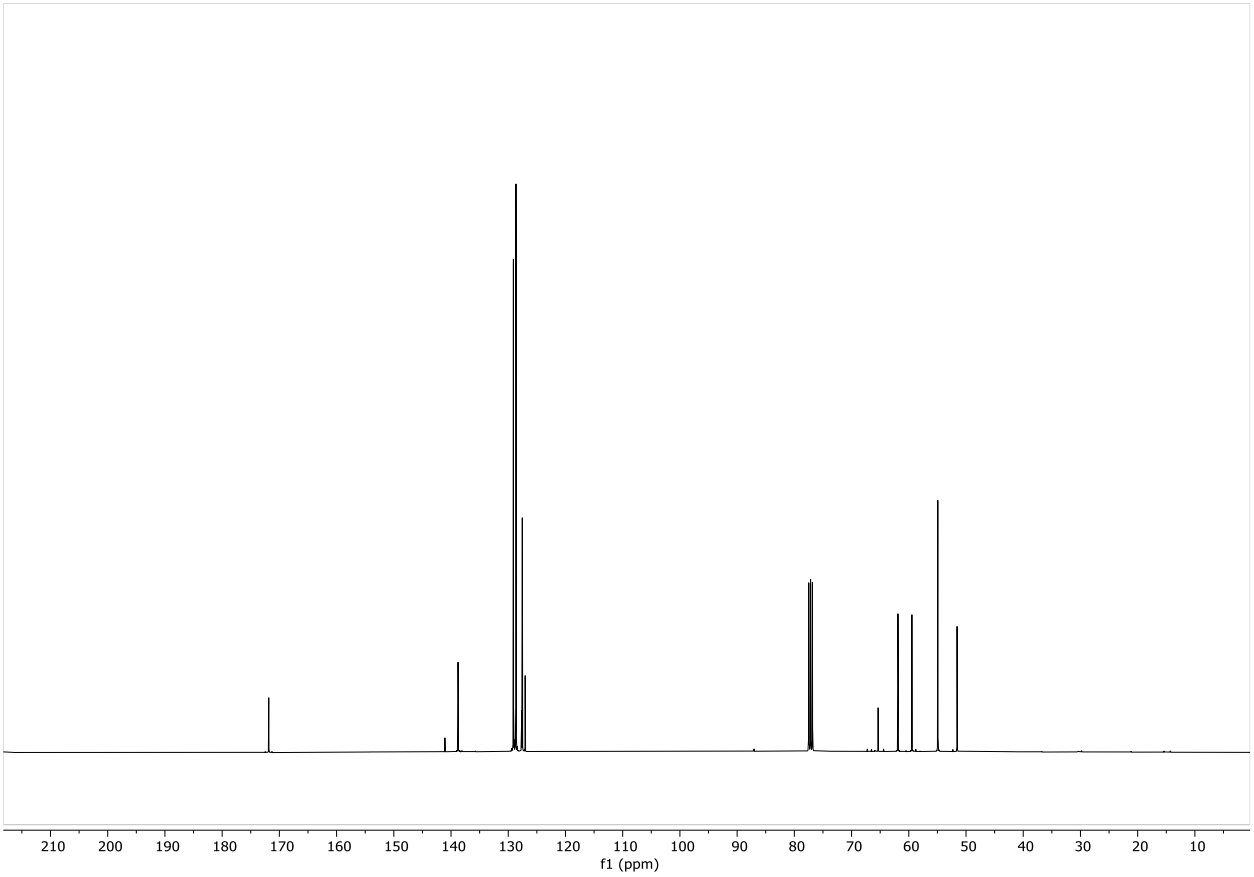
210
200
190
180
170
160
150
140
130
120
110
100
90
80
70
60
50
40
30
20
10
f1 (ppm)

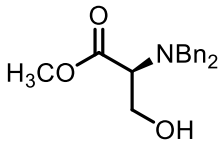
O
H3CO
NBn2
OH

90

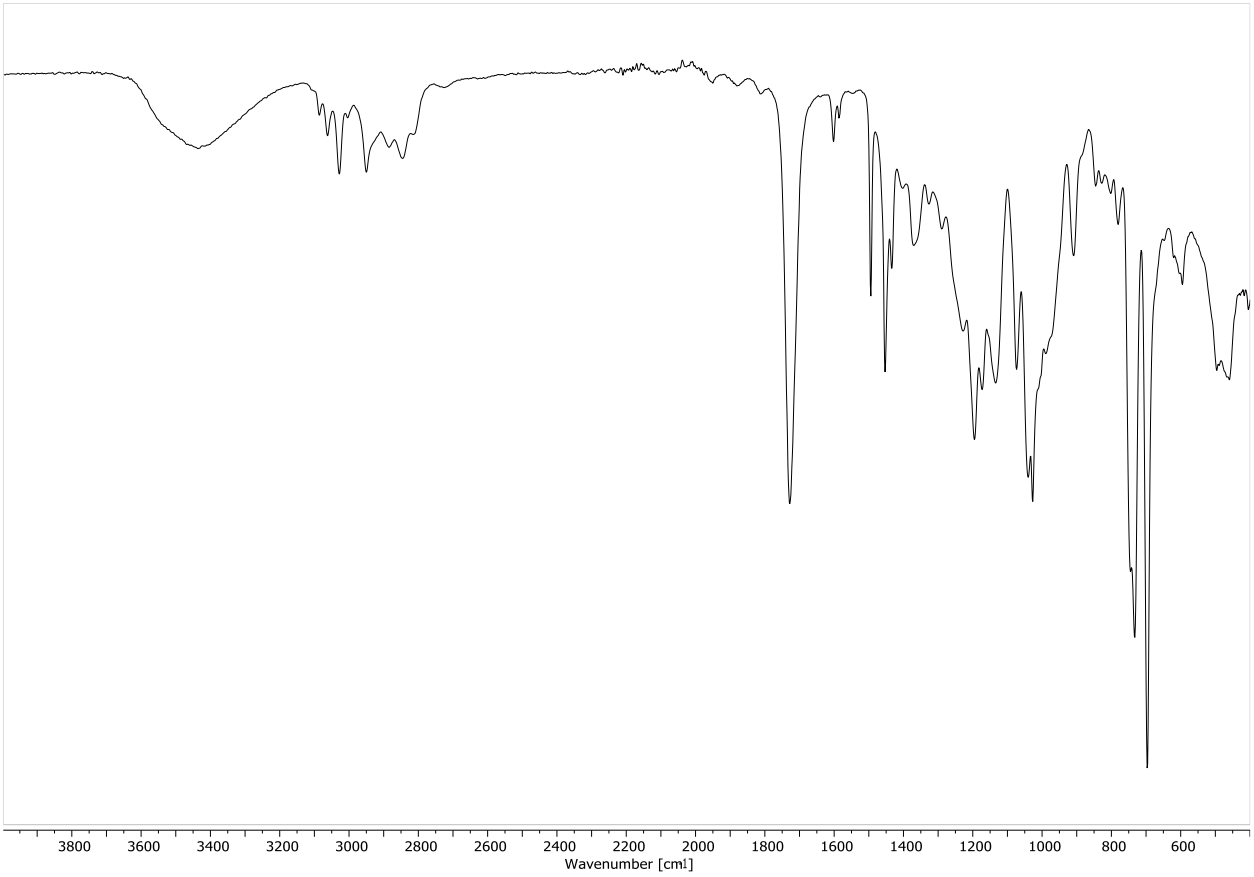
3800
3600
3400
3200
3000
2800
2600
2400
2200
2000
1800
1600
1400
1200
1000
800
600
Wavenumber [cm-1]

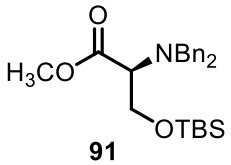
O
H3CO
NBn2
OTBS

91

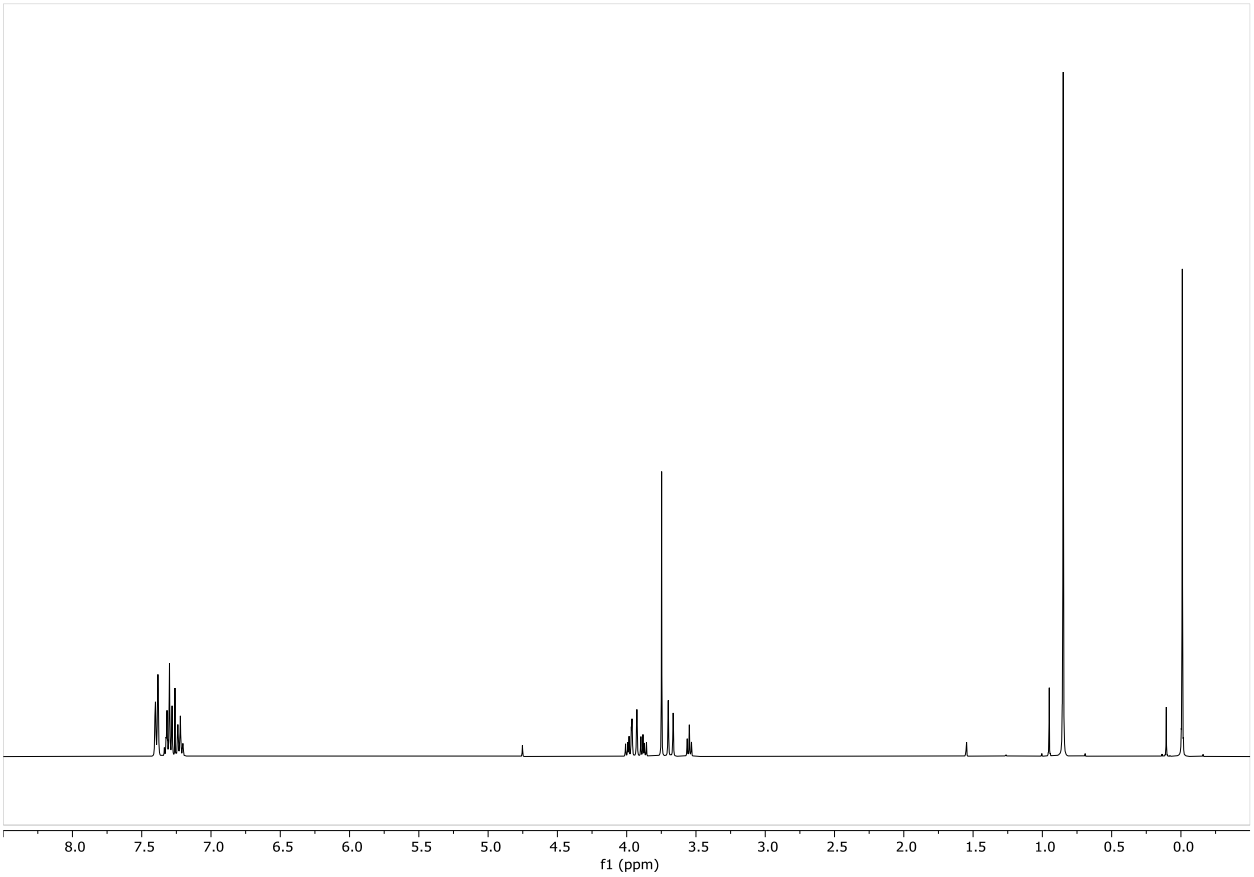
8.0
7.5
7.0
6.5
6.0
5.5
5.0
4.5
4.0
3.5
3.0
2.5
2.0
1.5
1.0
0.5
0.0
f1 (ppm)

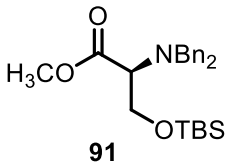
O
H3CO
NBn2
OTBS

91

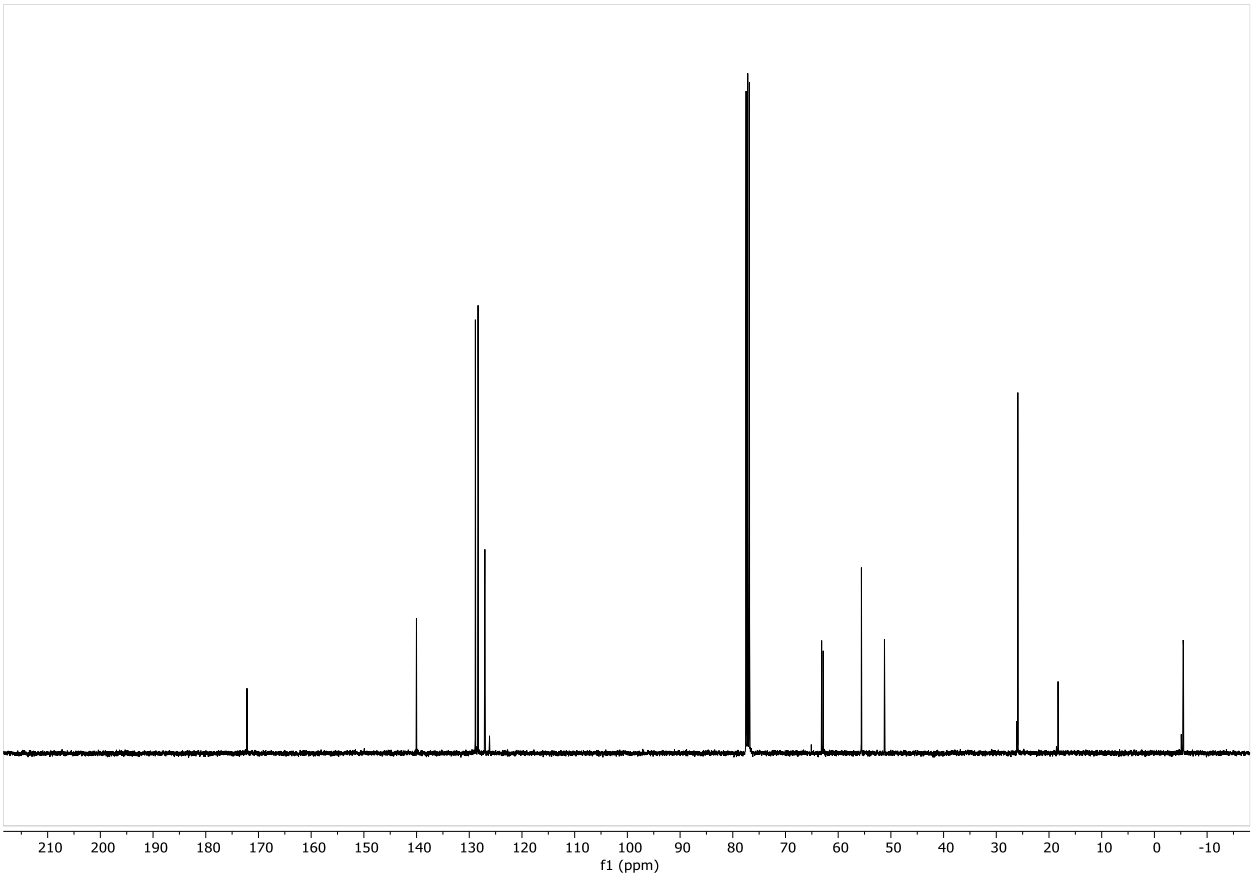
210 200 190 180 170 160 150 140 130 120 110 100 90 80 70 60 50 40 30 20 10 0 -10
f1 (ppm)

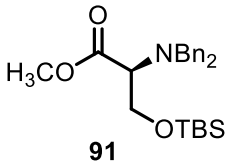
O
H3CO
NBn2
OTBS

91

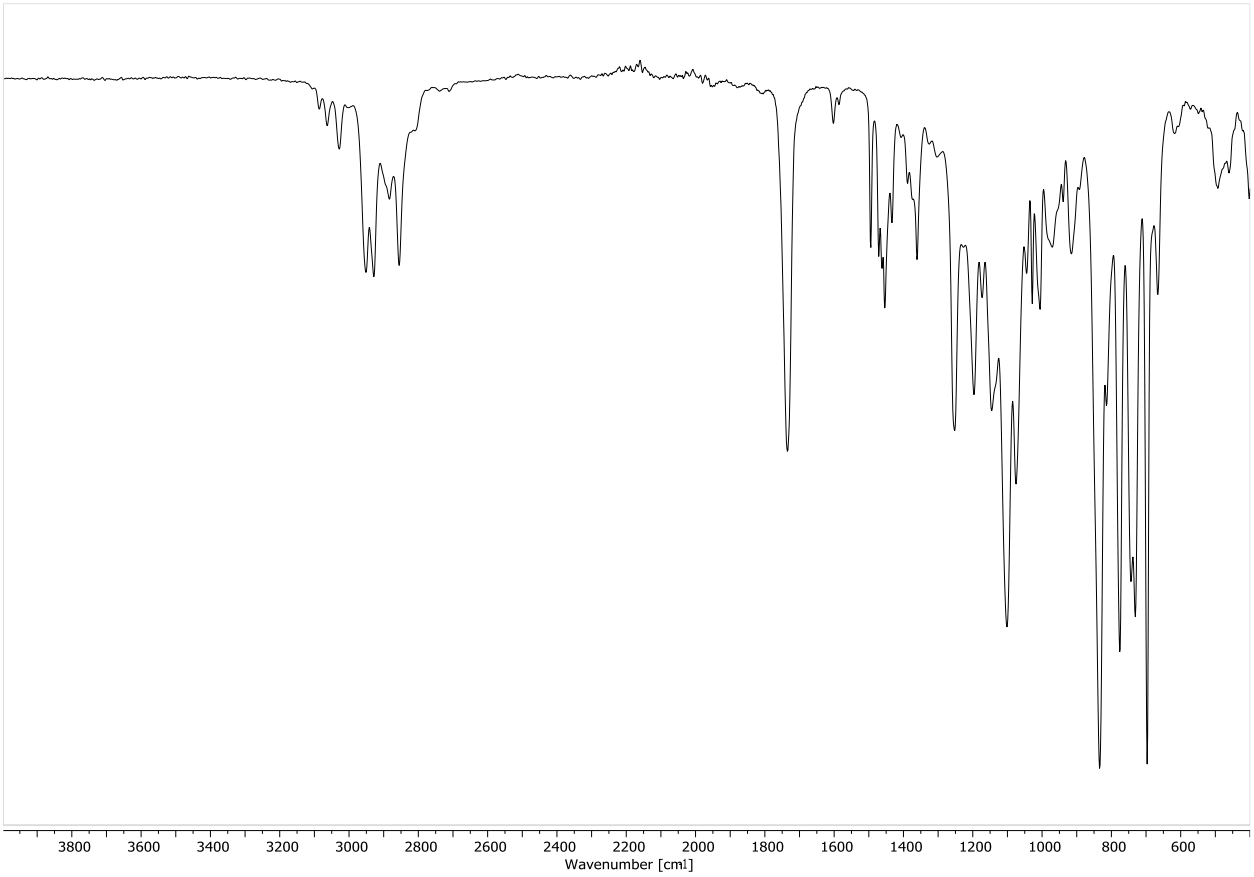
3800
3600
3400
3200
3000
2800
2600
2400
2200
2000
1800
1600
1400
1200
1000
800
600
Wavenumber [cm-1]

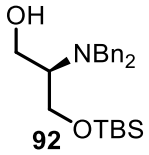

92

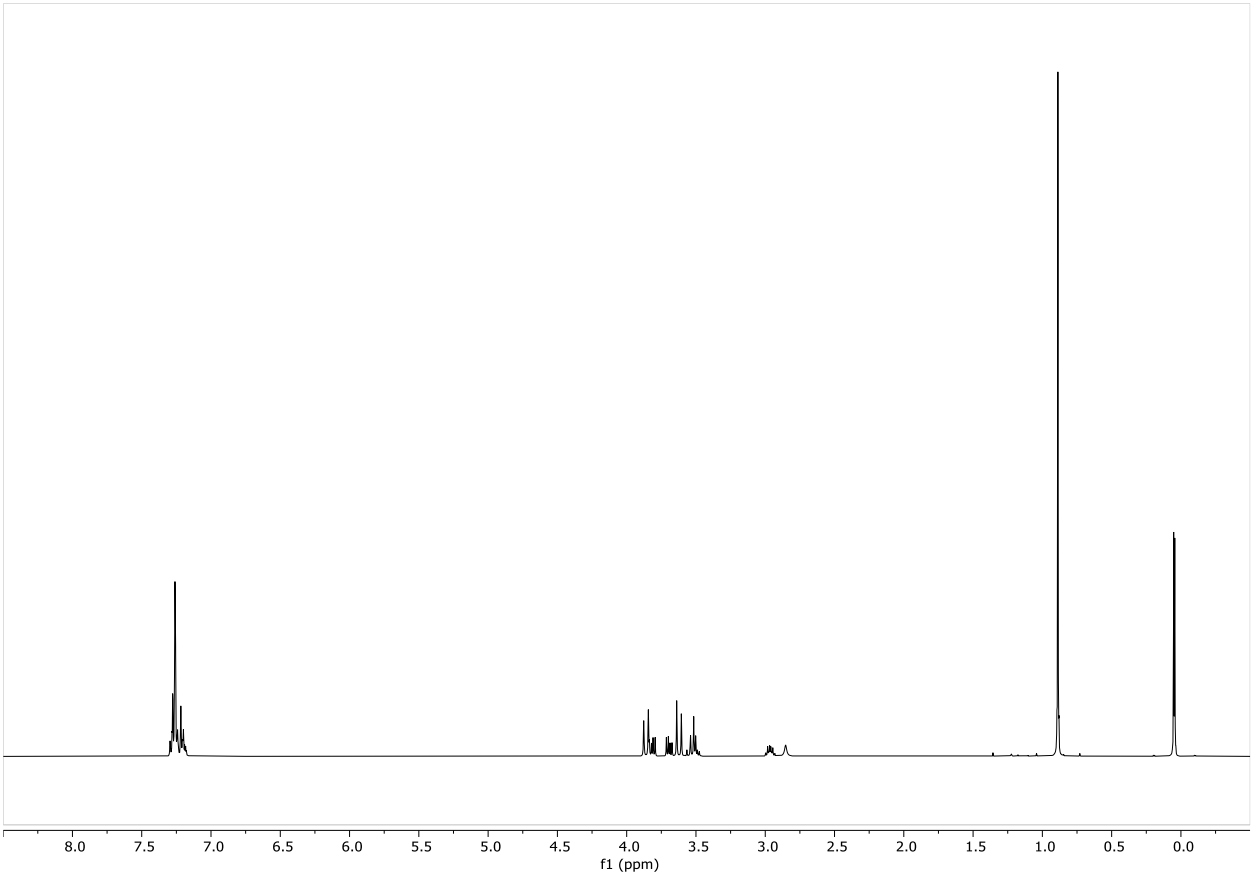

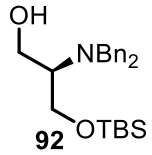
OH
NBn2
OTBS

92

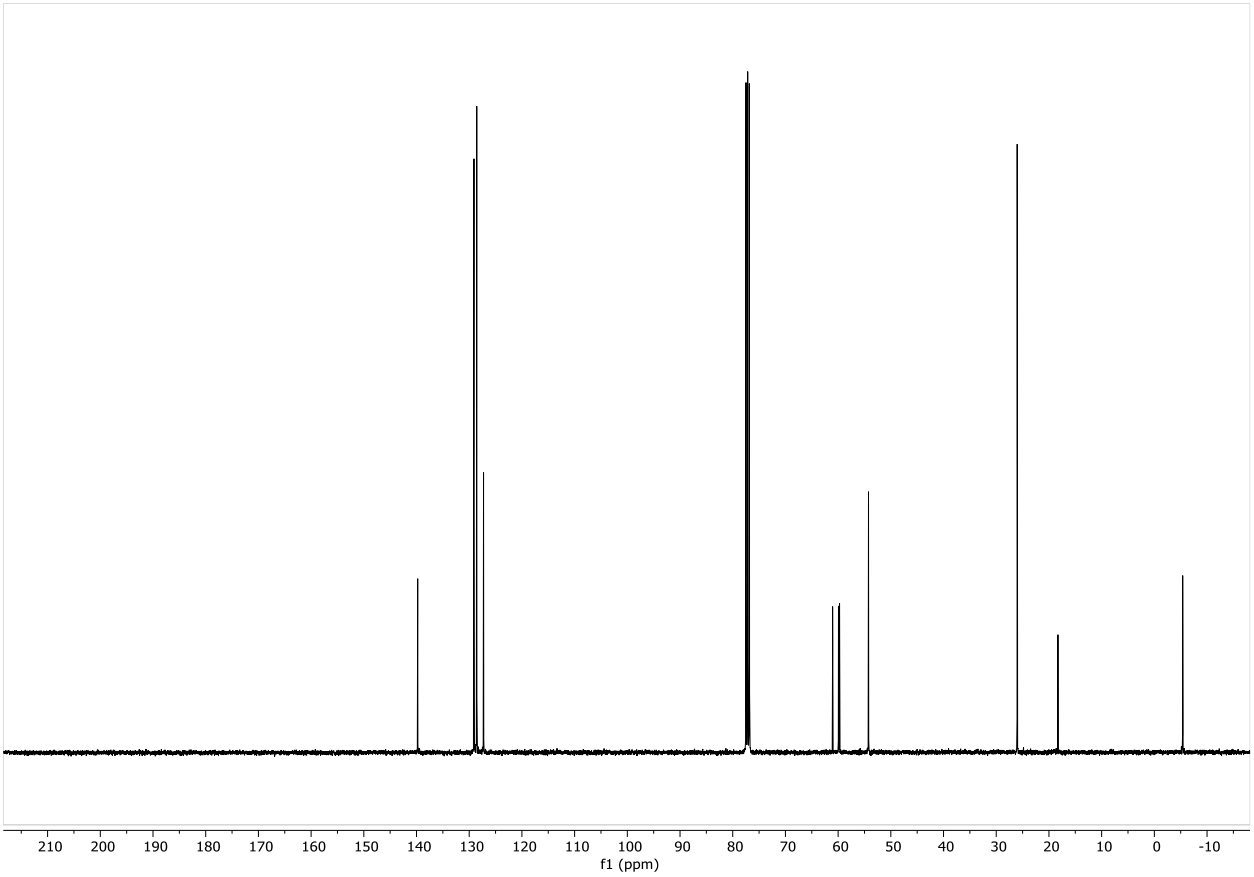
210
200
190
180
170
160
150
140
130
120
110
100
90
80
70
60
50
40
30
20
10
0
-10
f1 (ppm)

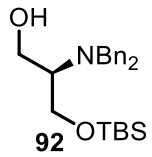
OH
NBn2
OTBS

92

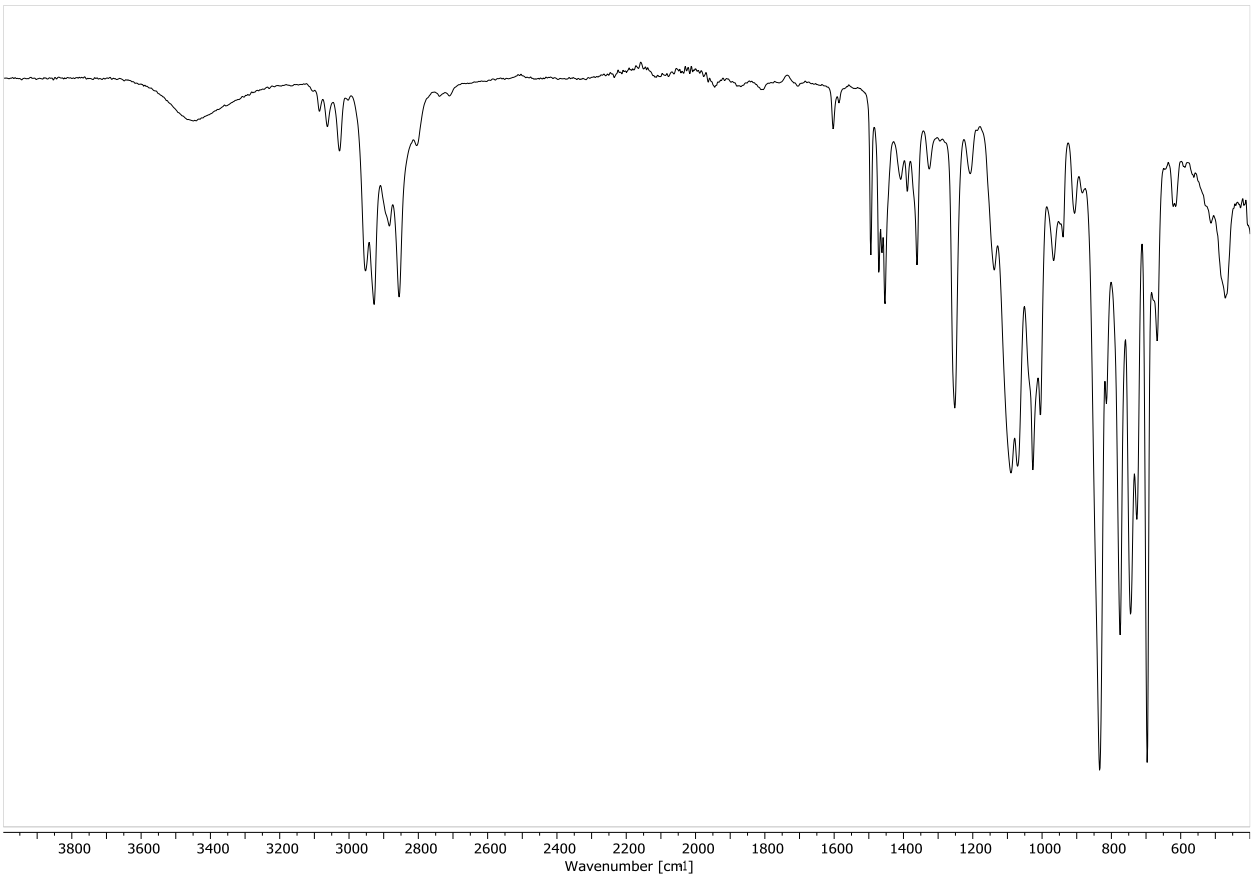
3800
3600
3400
3200
3000
2800
2600
2400
2200
2000
1800
1600
1400
1200
1000
800
600
Wavenumber [cm-1]

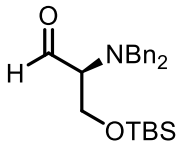
O
H
NBn2
OTBS

93

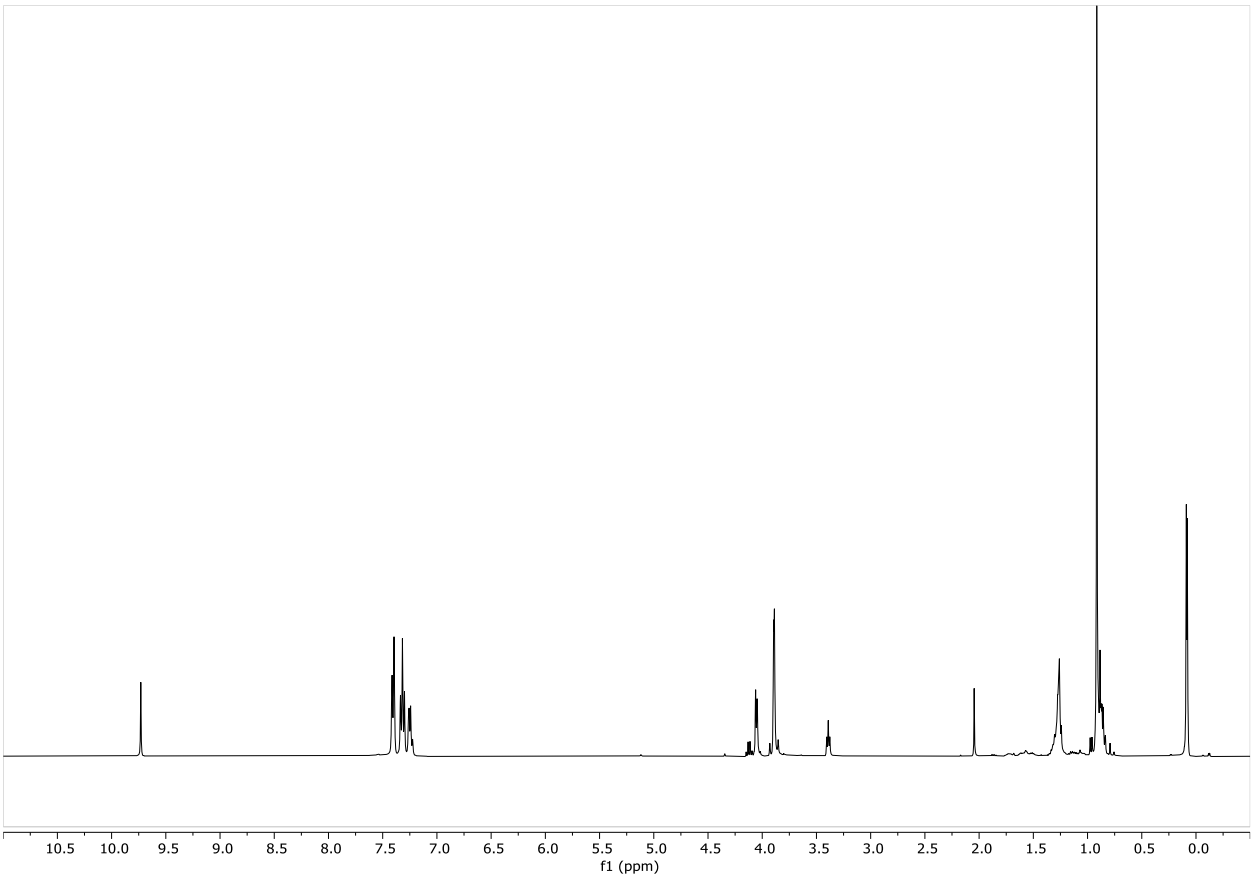
10.5
10.0
9.5
9.0
8.5
8.0
7.5
7.0
6.5
6.0
5.5
5.0
4.5
4.0
3.5
3.0
2.5
2.0
1.5
1.0
0.5
0.0
f1 (ppm)

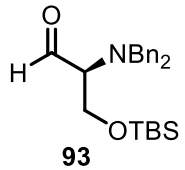
O
H
NBn2
OTBS

93

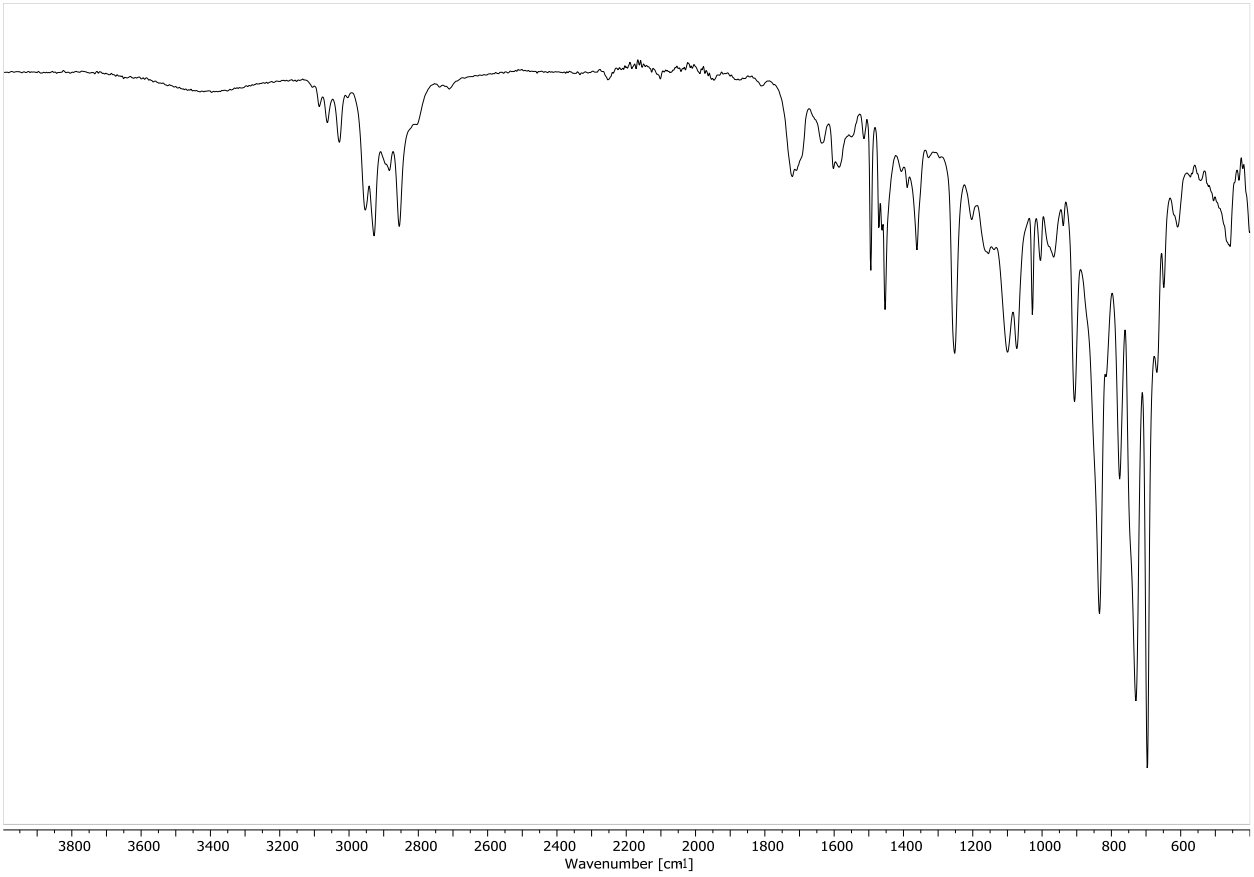
3800
3600
3400
3200
3000
2800
2600
2400
2200
2000
1800
1600
1400
1200
1000
800
600
Wavenumber [cm-1]

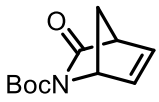

96

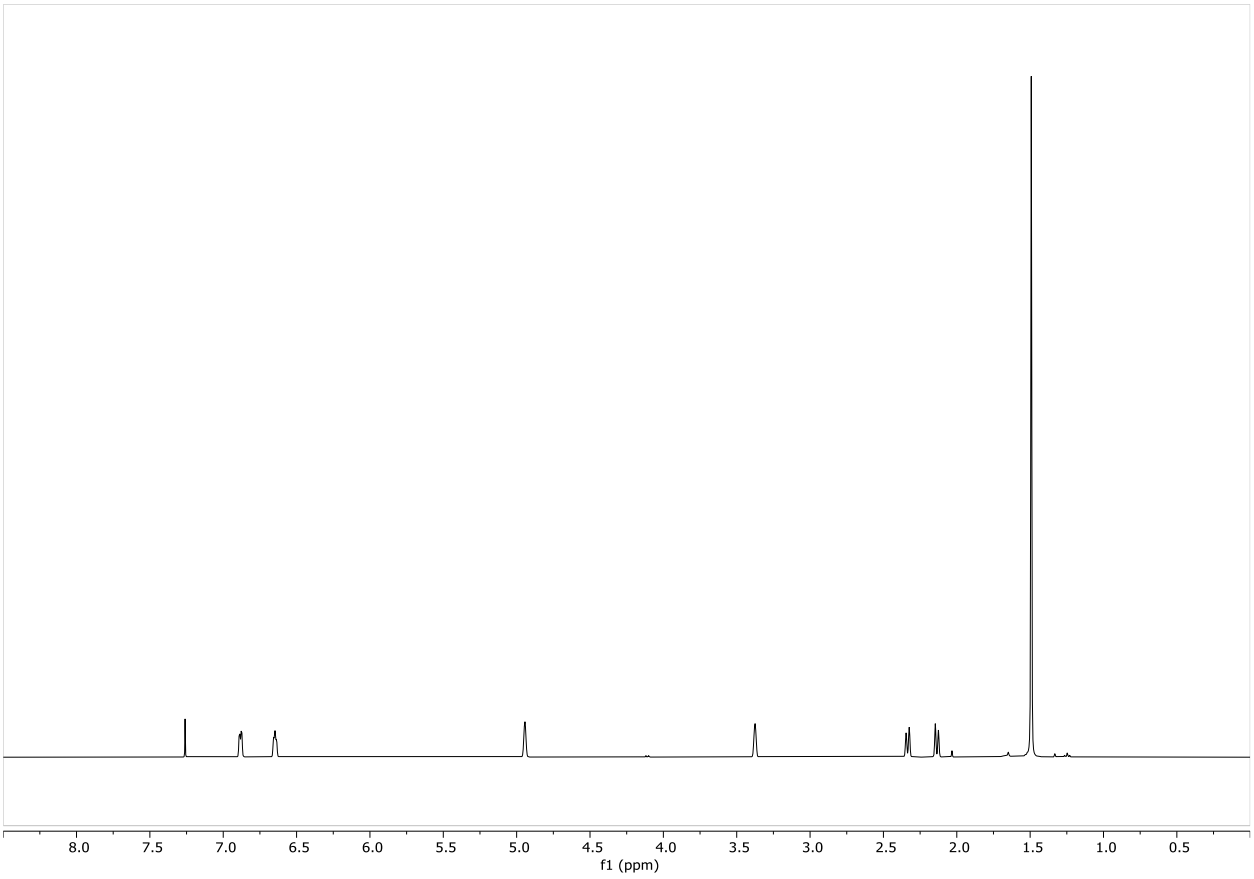

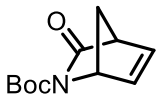
O
BocN

96

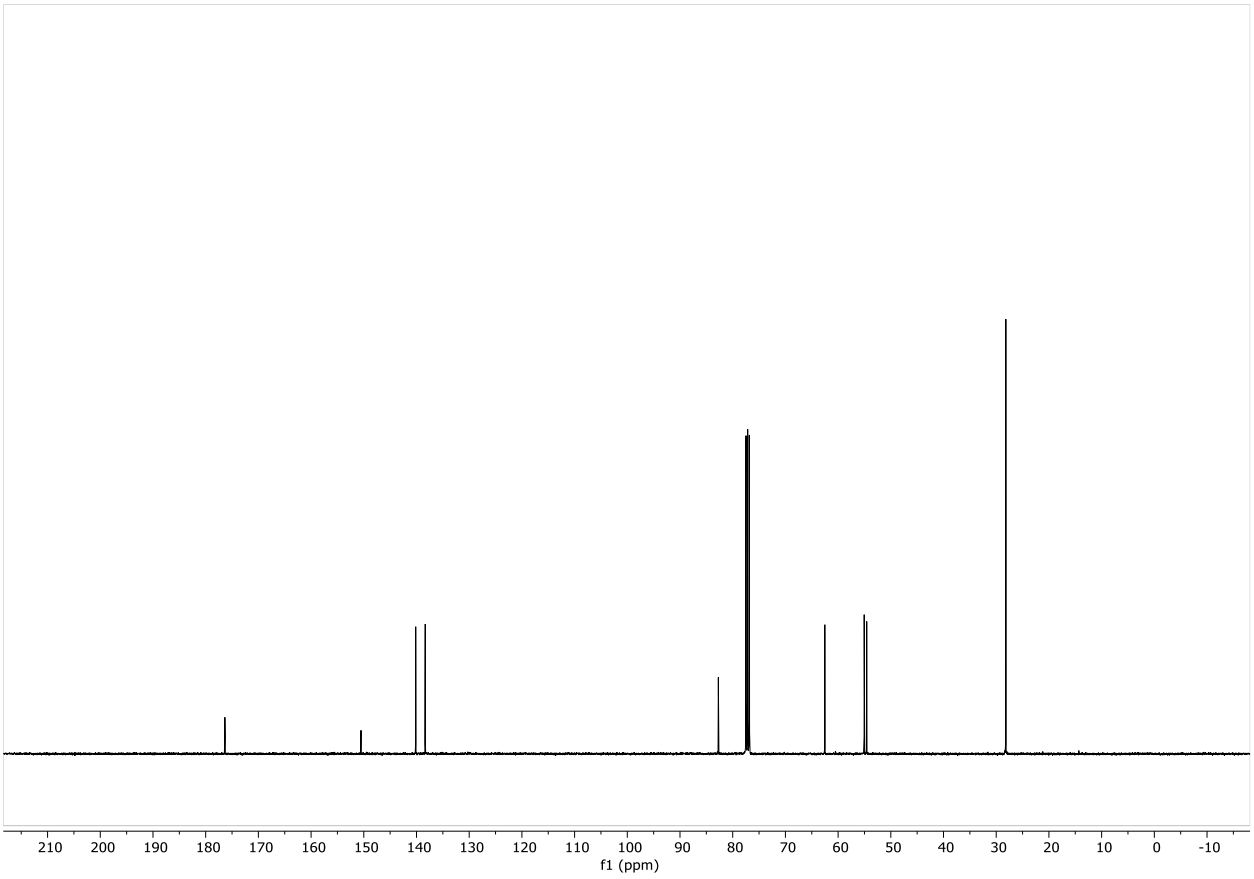
210
200
190
180
170
160
150
140
130
120
110
100
90
80
70
60
50
40
30
20
10
0
-10
f1 (ppm)

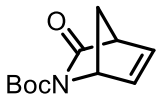
O
BocN

96

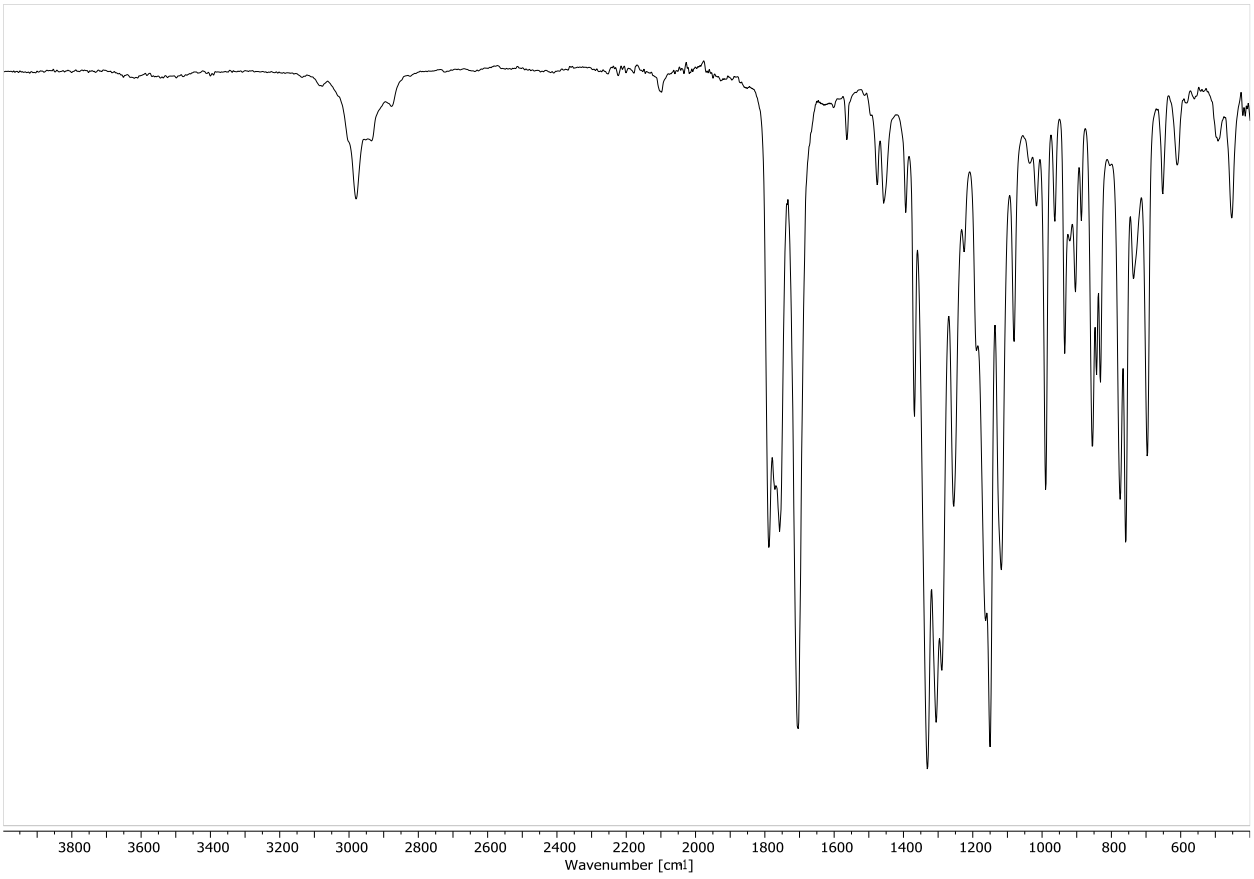
3800
3600
3400
3200
3000
2800
2600
2400
2200
2000
1800
1600
1400
1200
1000
800
600
Wavenumber [cm-1]

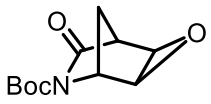

97

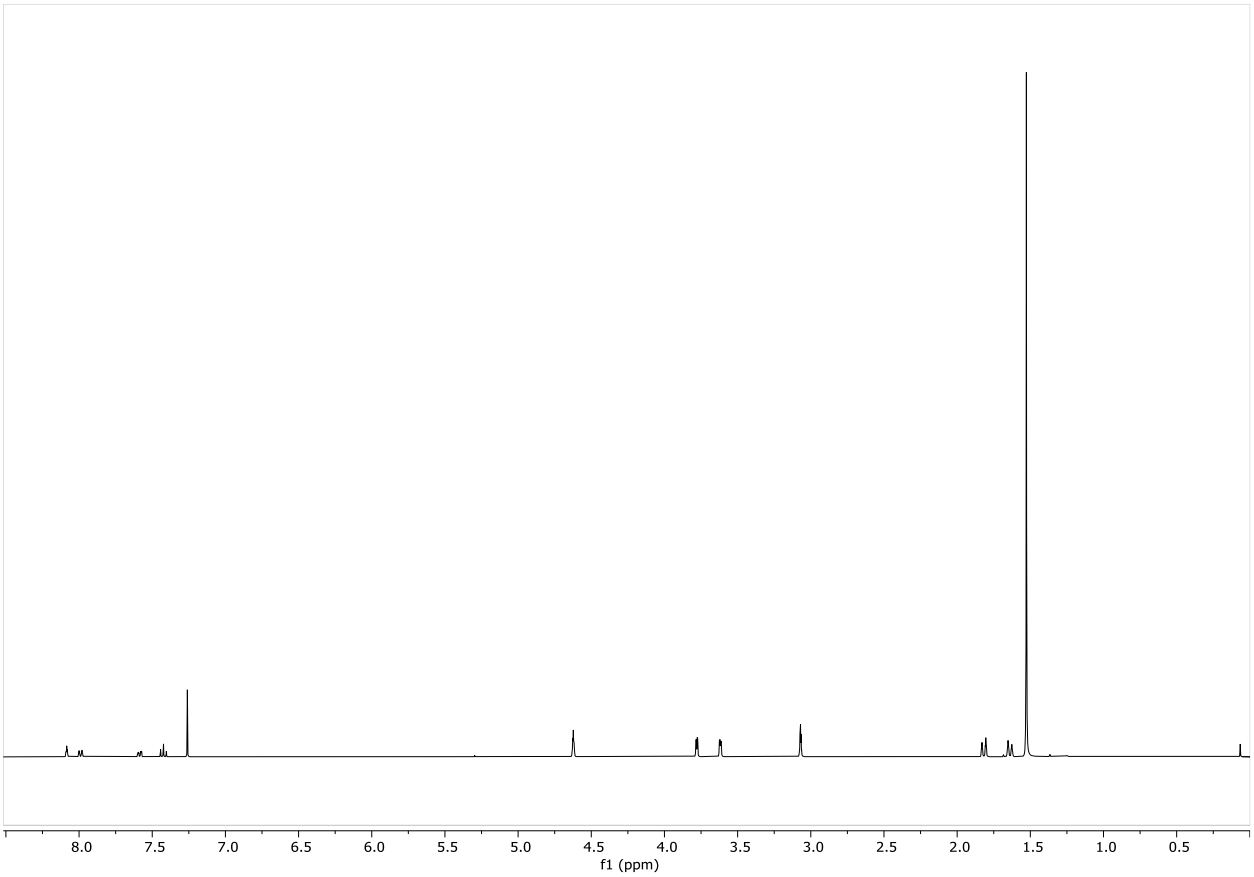

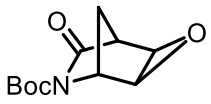
O
O
BocN

97

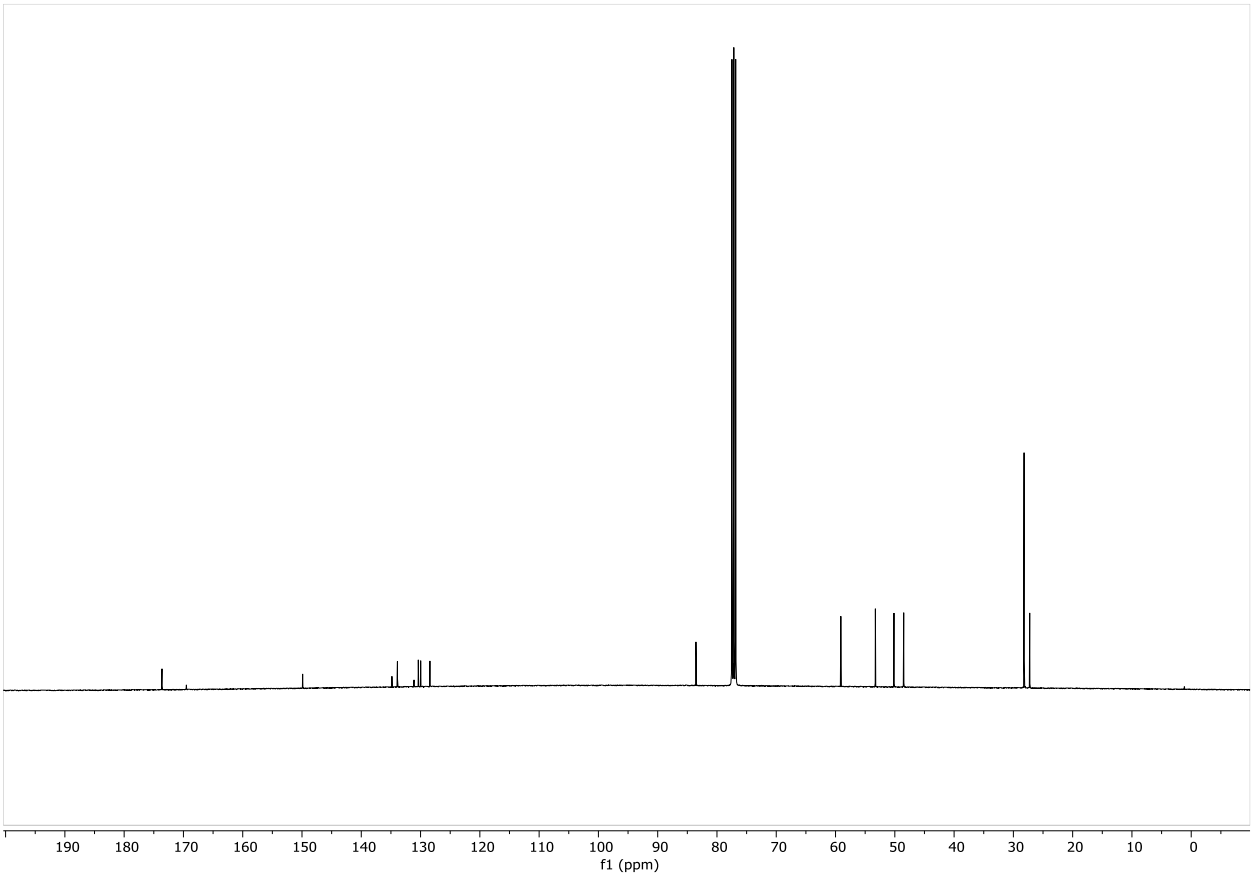
190
180
170
160
150
140
130
120
110
100
90
80
70
60
50
40
30
20
10
0
f1 (ppm)

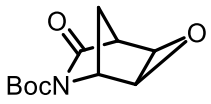
O
O
BocN

97

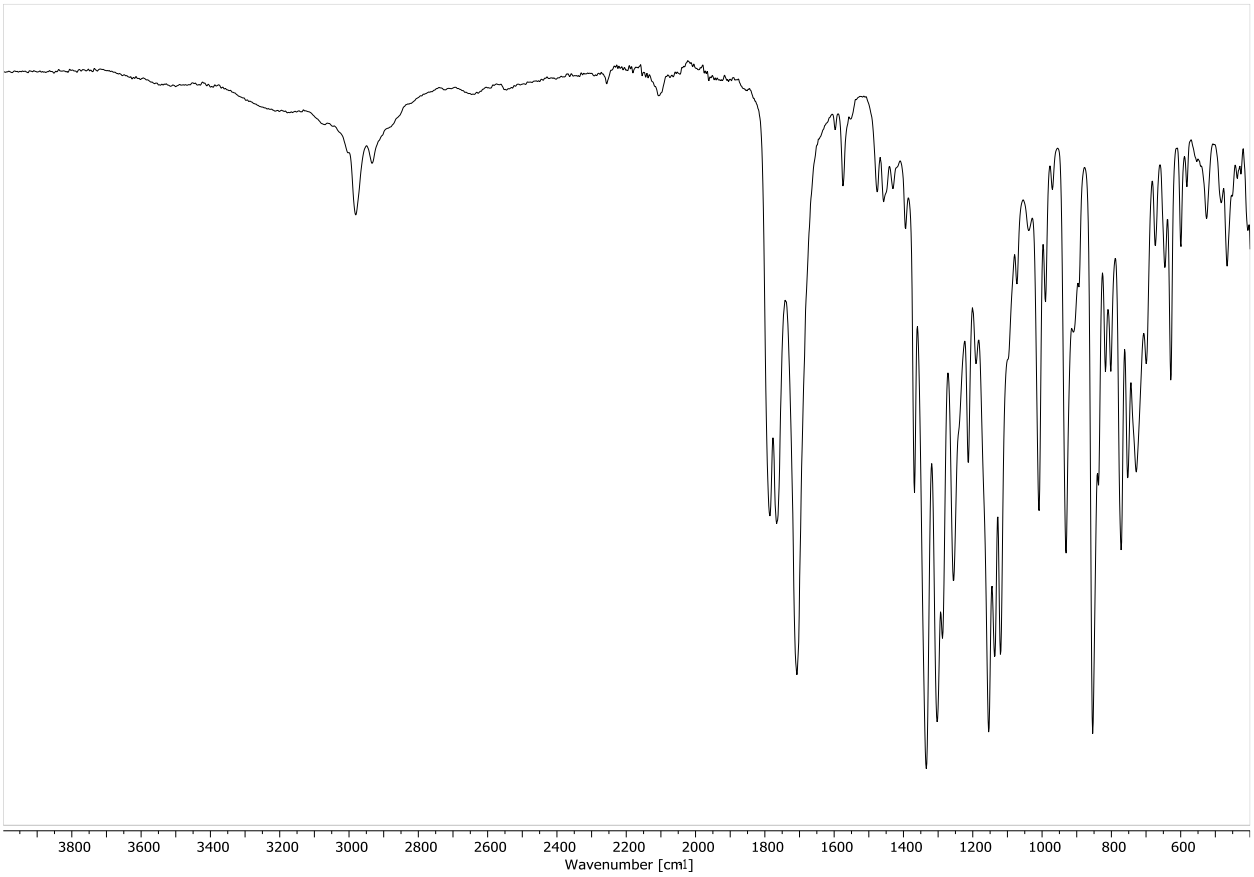
3800
3600
3400
3200
3000
2800
2600
2400
2200
2000
1800
1600
1400
1200
1000
800
600
Wavenumber [cm-1]

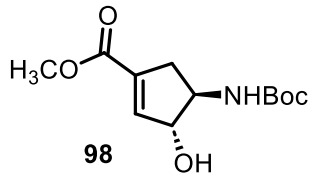

98

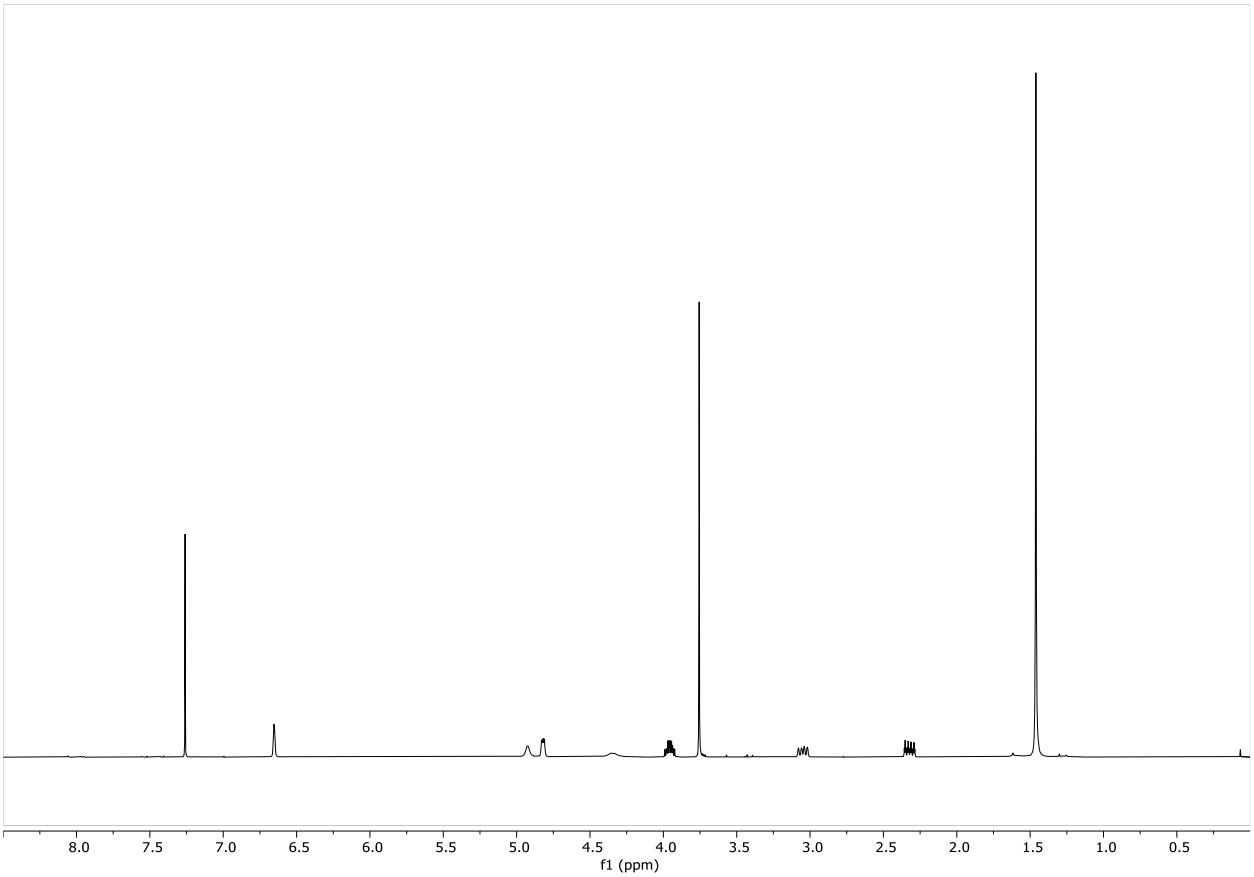

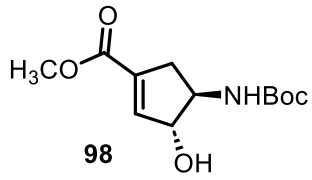
O
H3CO
NHBoc
OH

98

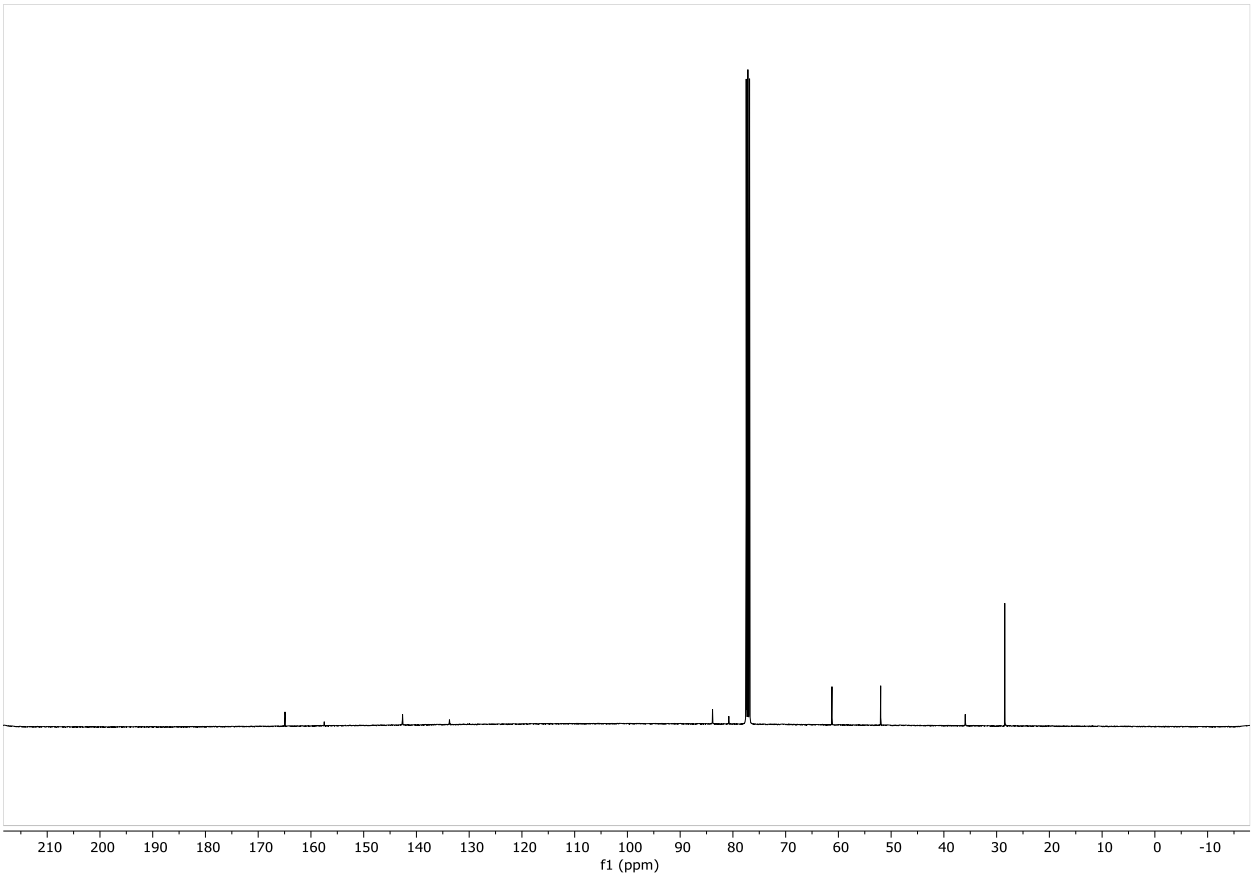
210 200 190 180 170 160 150 140 130 120 110 100 90 80 70 60 50 40 30 20 10 0 -10
f1 (ppm)

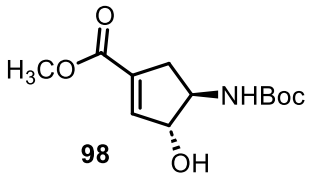
O
H3CO
NHBoc
OH

98

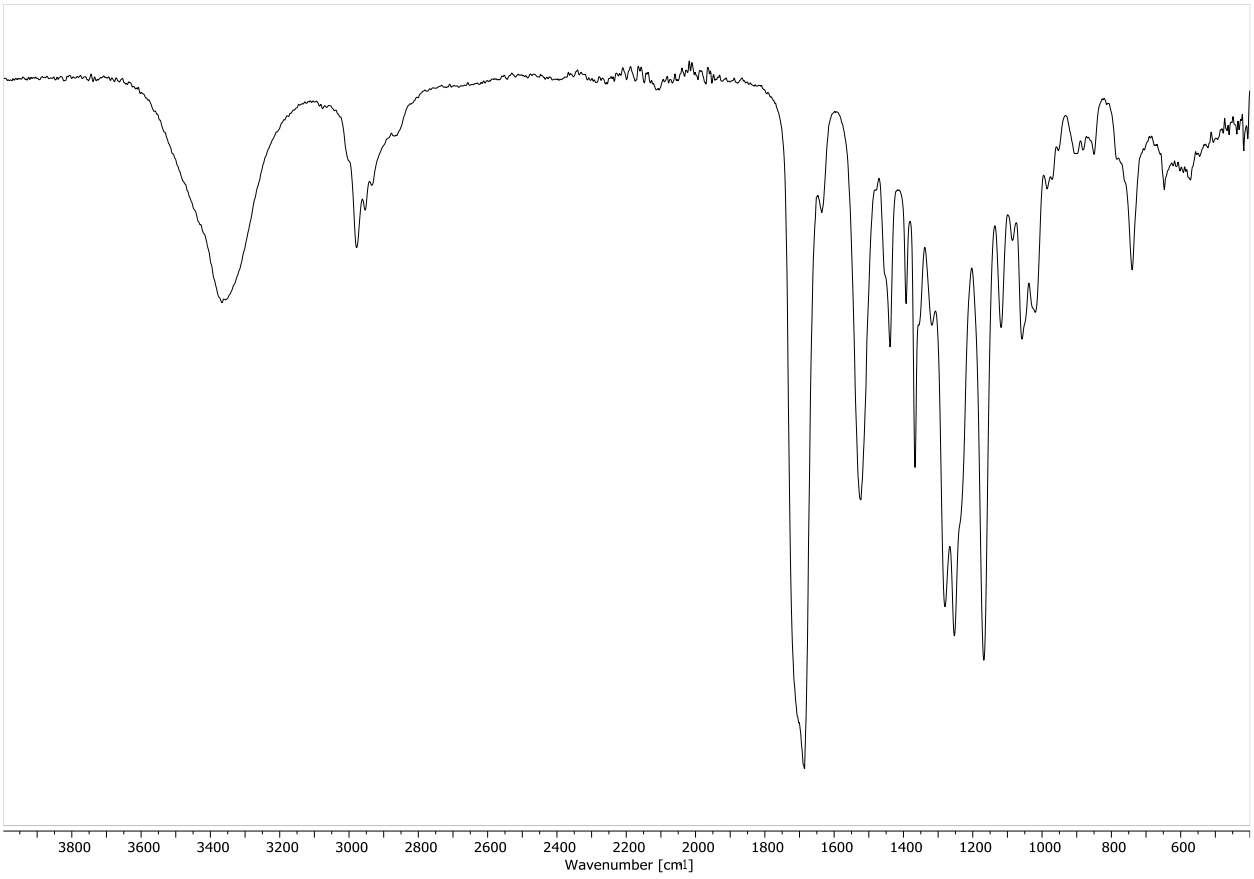
3800
3600
3400
3200
3000
2800
2600
2400
2200
2000
1800
1600
1400
1200
1000
800
600
Wavenumber [cm-1]

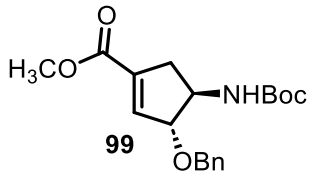
O
H3CO
NHBoc
OBn

99

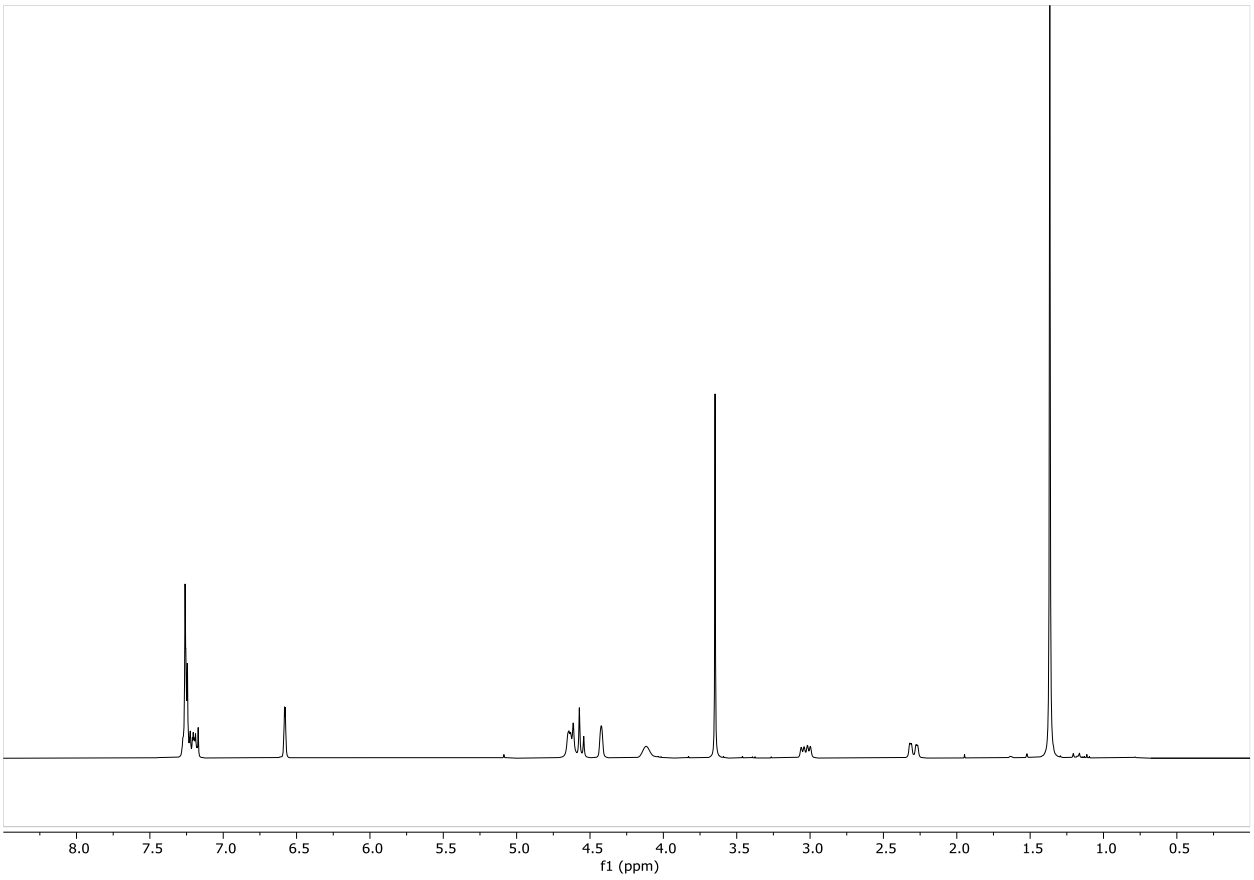
8.0
7.5
7.0
6.5
6.0
5.5
5.0
4.5
4.0
3.5
3.0
2.5
2.0
1.5
1.0
0.5
f1 (ppm)

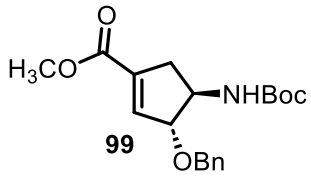
O
H3CO
NHBoc
OBn

99

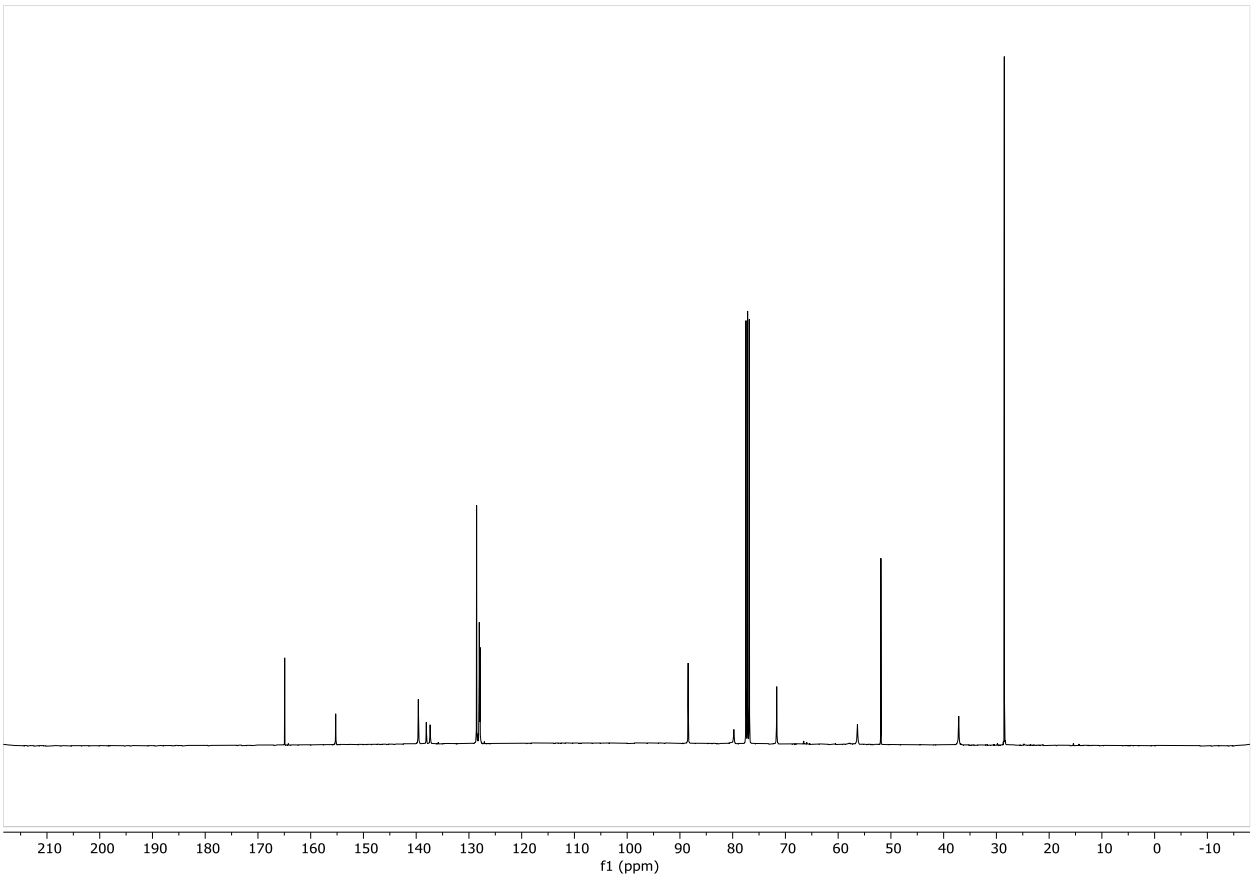
210 200 190 180 170 160 150 140 130 120 110 100 90 80 70 60 50 40 30 20 10 0 -10
f1 (ppm)

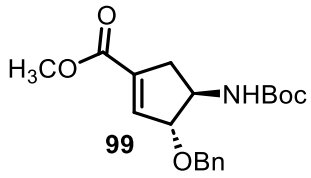
O
H3CO
NHBoc
OBn

99

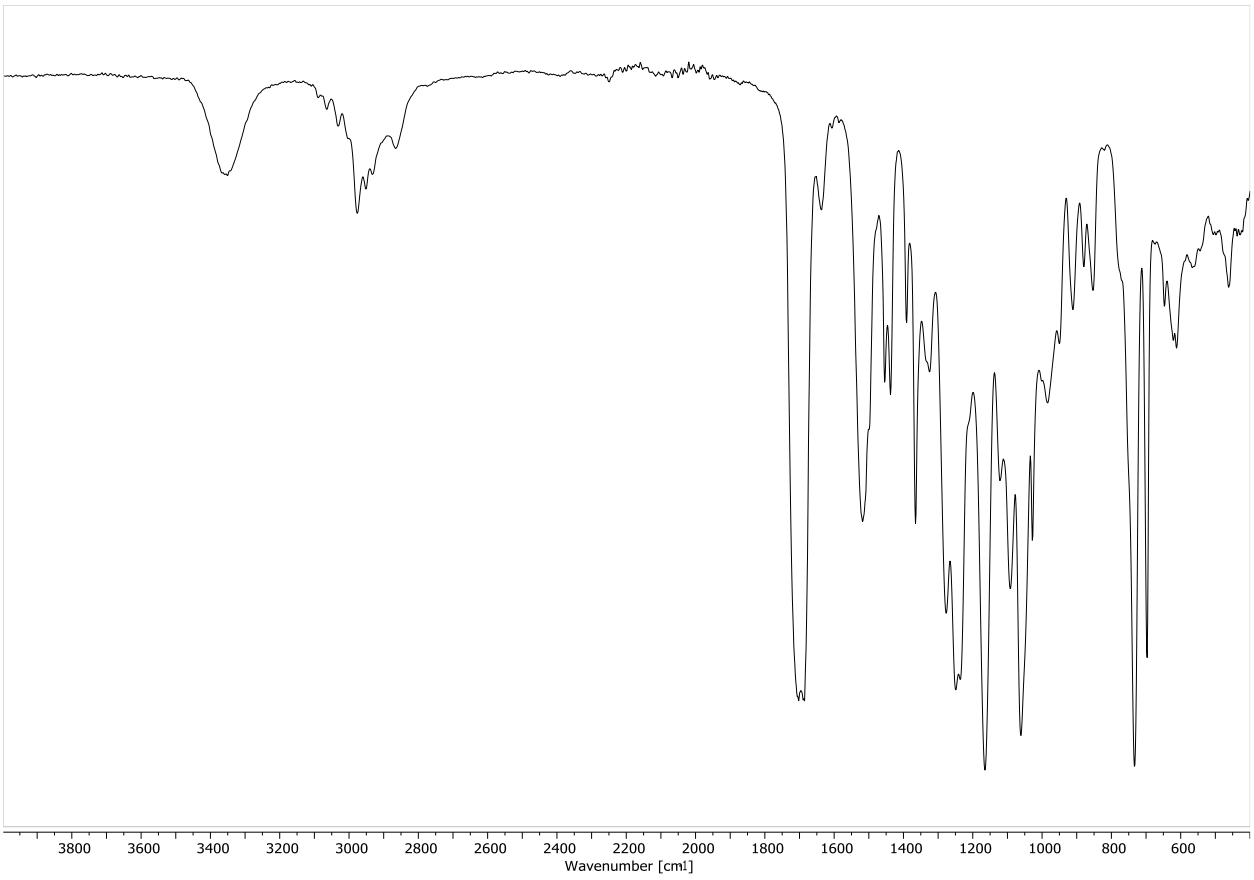
3800
3600
3400
3200
3000
2800
2600
2400
2200
2000
1800
1600
1400
1200
1000
800
600
Wavenumber [cm-1]

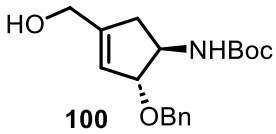
HO
NHBoc
OBn

100

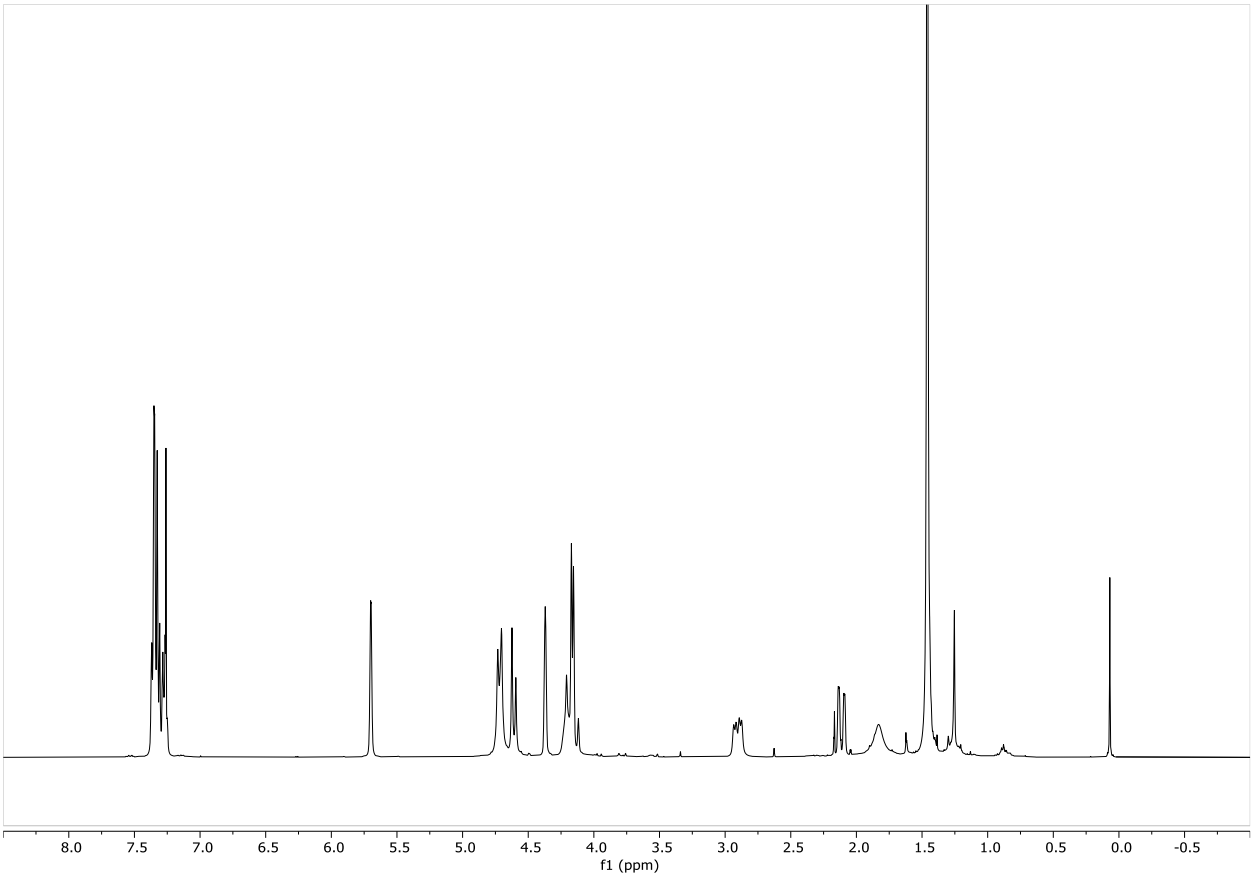
8.0
7.5
7.0
6.5
6.0
5.5
5.0
4.5
4.0
3.5
3.0
2.5
2.0
1.5
1.0
0.5
0.0
-0.5
f1 (ppm)

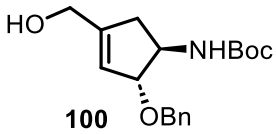
HO
NHBoc
OBn

100

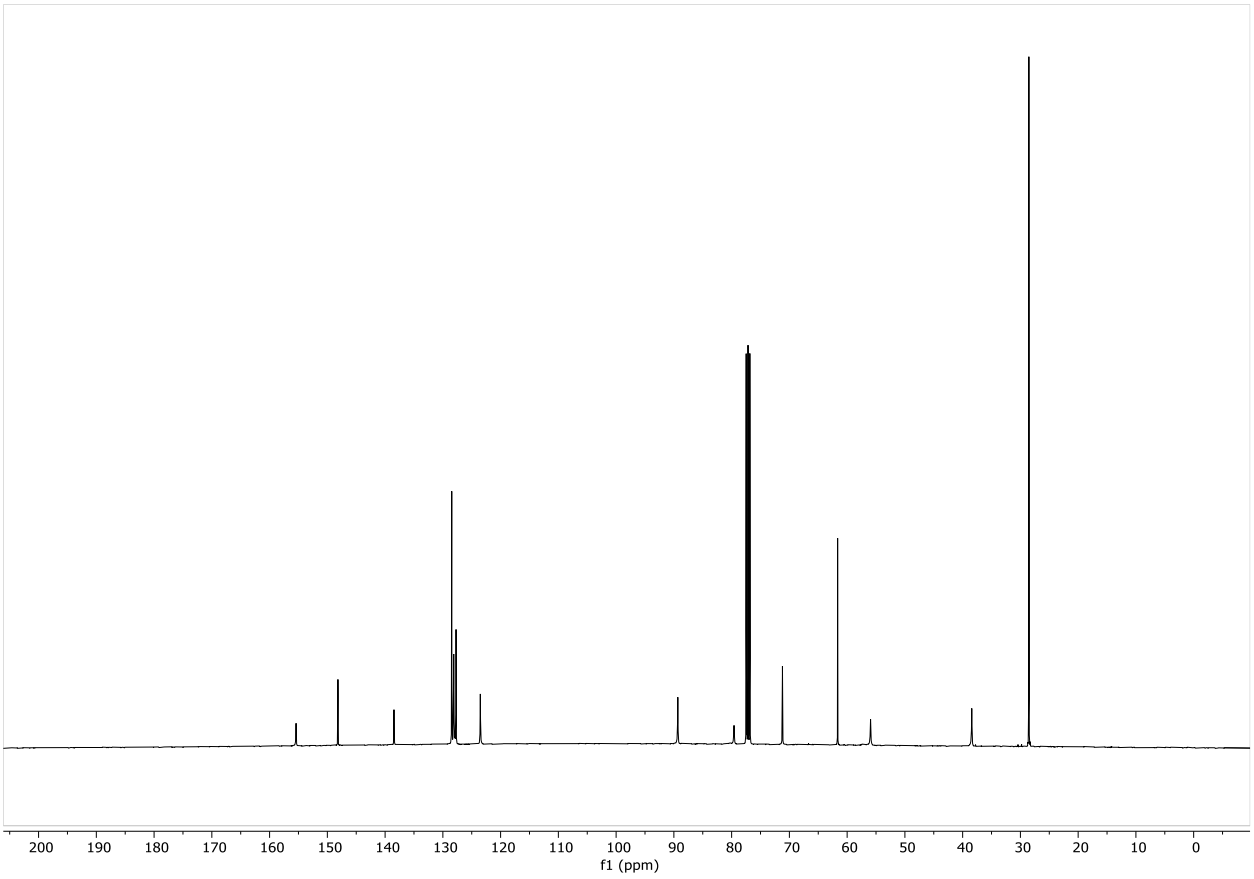
200
190
180
170
160
150
140
130
120
110
100
90
80
70
60
50
40
30
20
10
0
f1 (ppm)

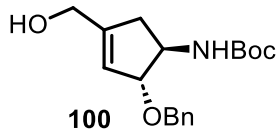
HO
NHBoc
OBn

100

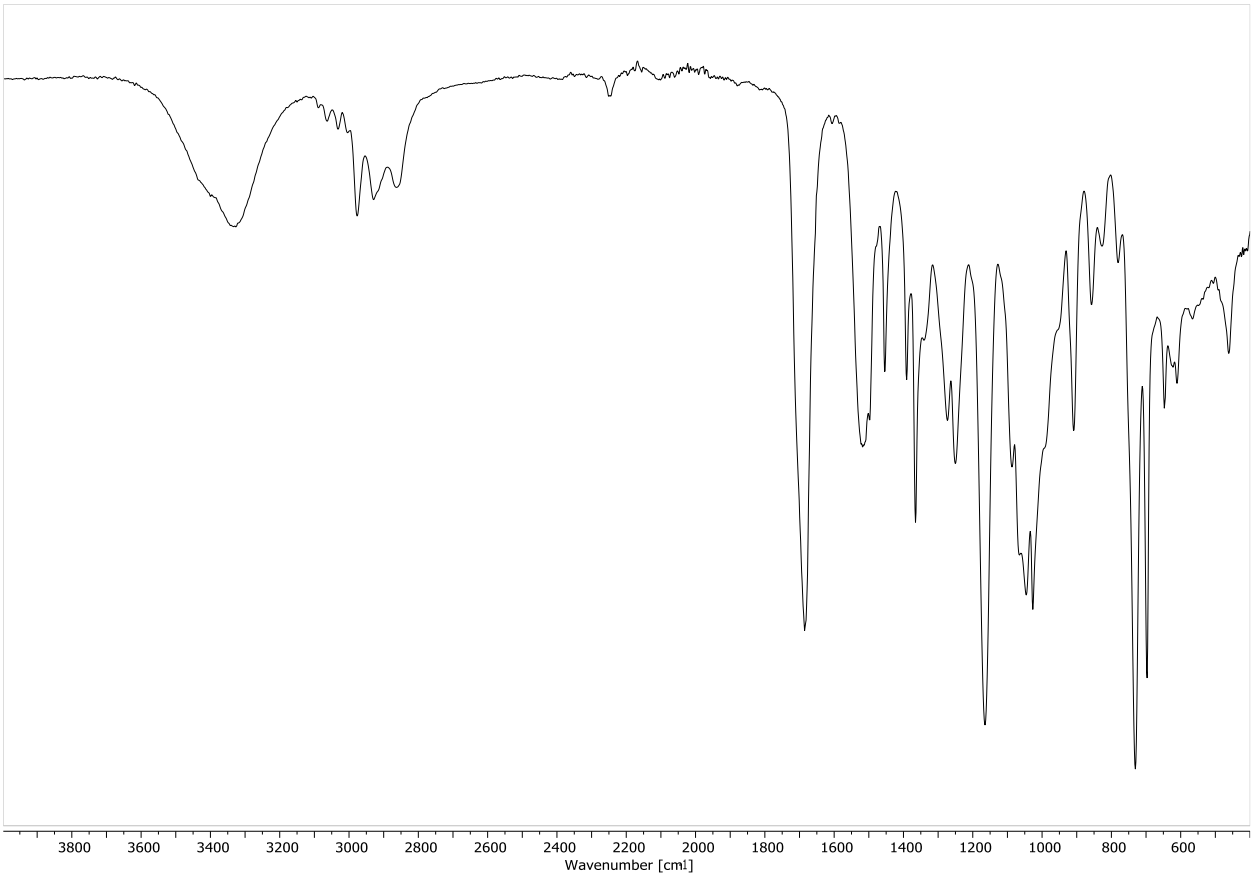
3800
3600
3400
3200
3000
2800
2600
2400
2200
2000
1800
1600
1400
1200
1000
800
600
Wavenumber [cm-1]

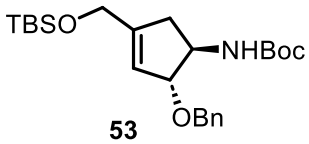
TBSO
NHBoc
OBn

53

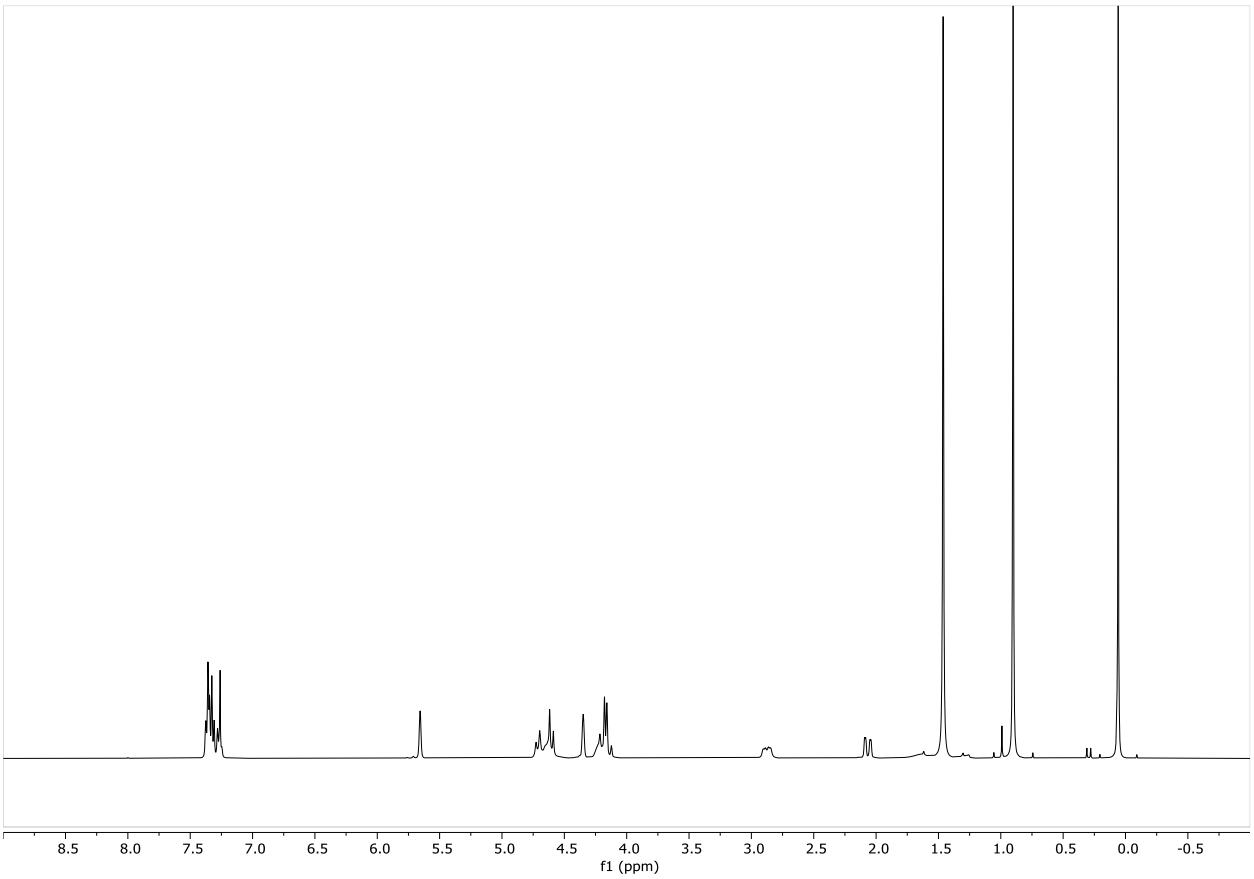
8.5
8.0
7.5
7.0
6.5
6.0
5.5
5.0
4.5
4.0
3.5
3.0
2.5
2.0
1.5
1.0
0.5
0.0
-0.5
f1 (ppm)

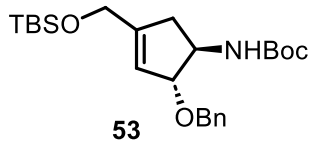
TBSO
NHBoc
OBn

53

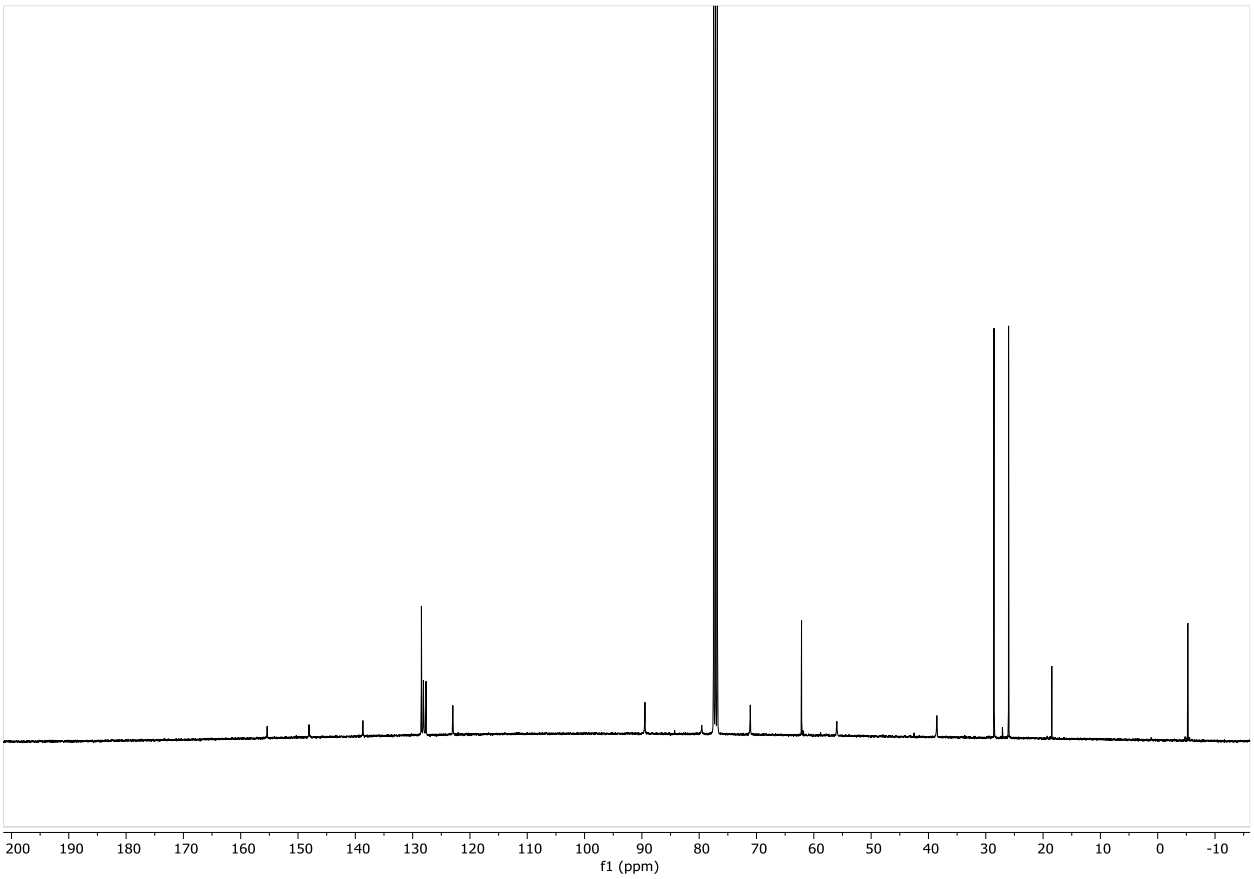
200
190
180
170
160
150
140
130
120
110
100
90
80
70
60
50
40
30
20
10
0
-10
f1 (ppm)

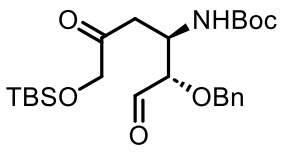
O
NHBoc
TBSO
OBn
O

50

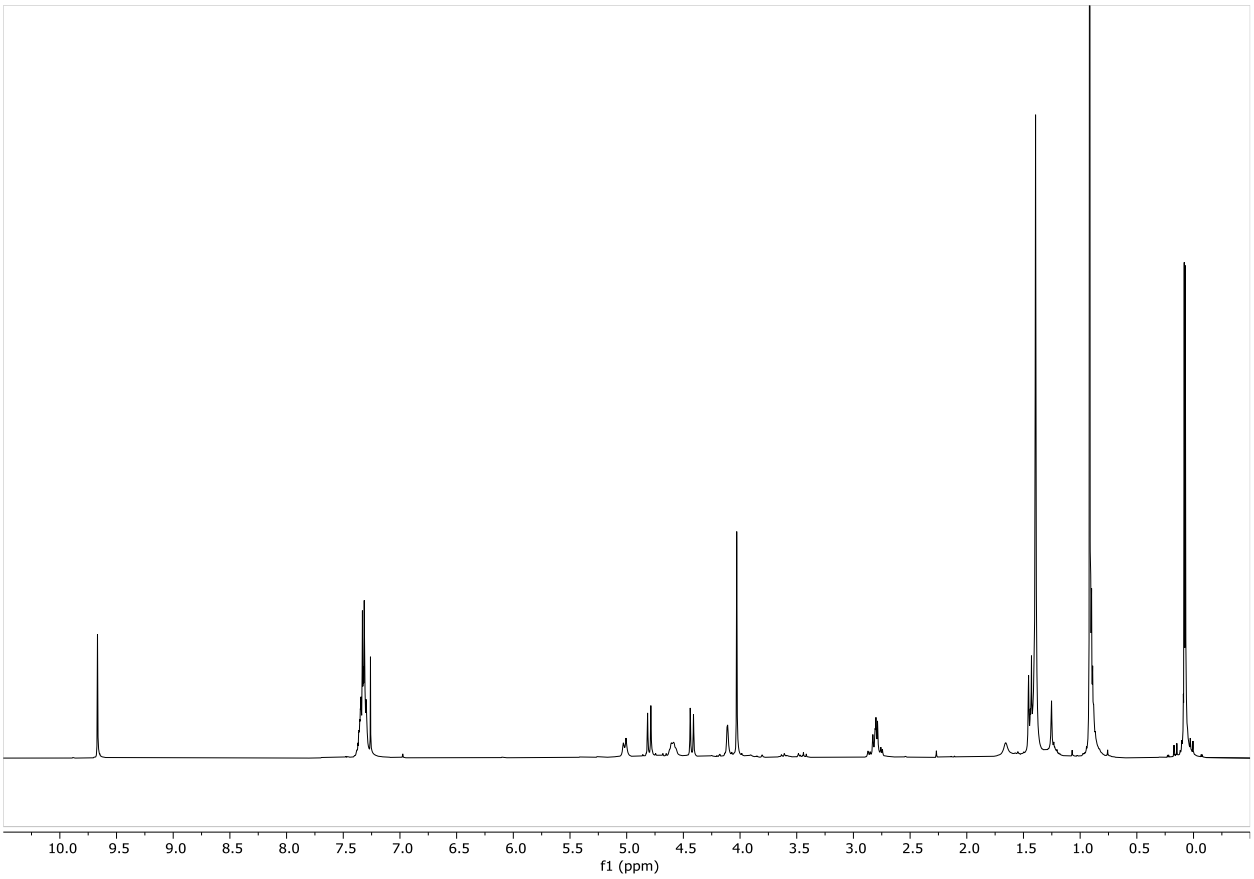
10.0
9.5
9.0
8.5
8.0
7.5
7.0
6.5
6.0
5.5
5.0
4.5
4.0
3.5
3.0
2.5
2.0
1.5
1.0
0.5
0.0
f1 (ppm)

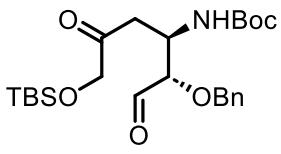
O
NHBoc
TBSO
OBn
O

50

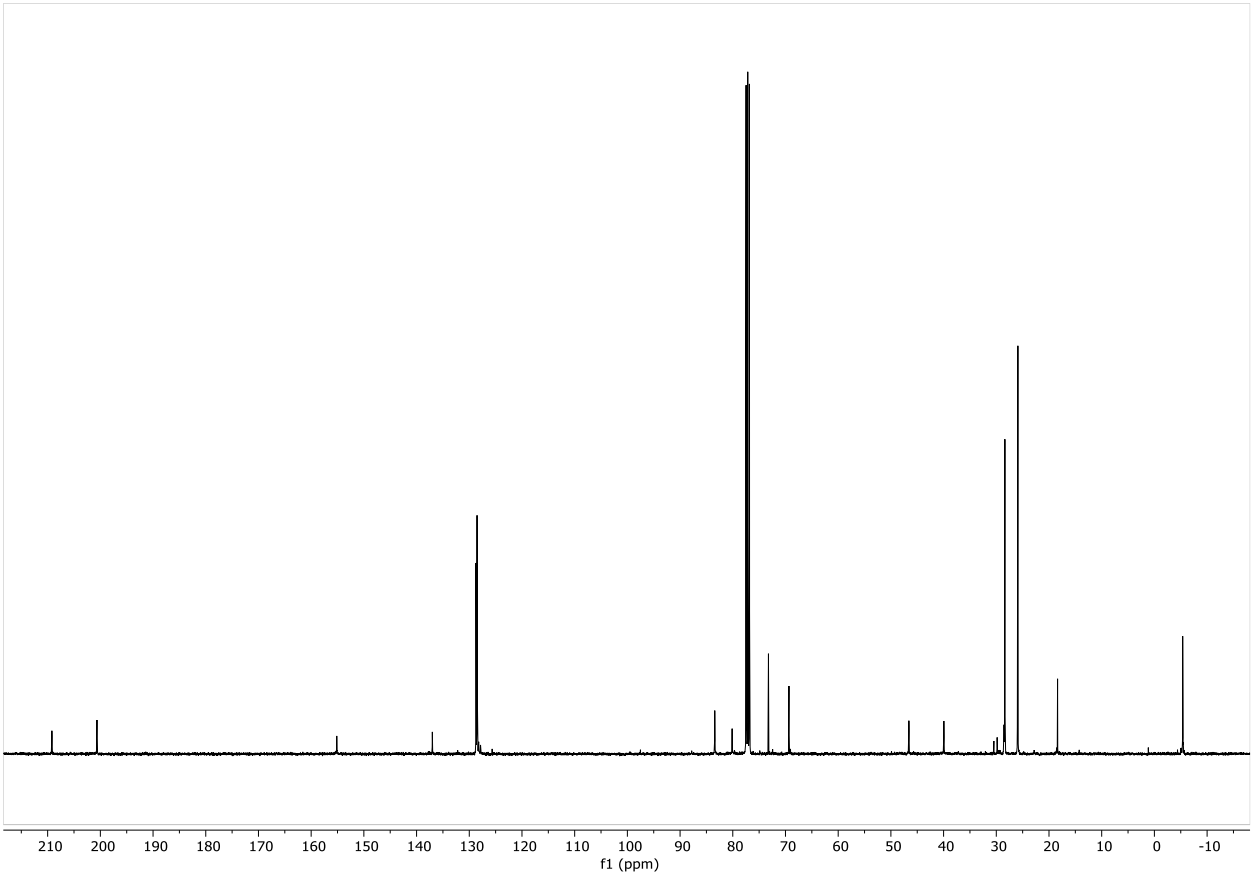
210
200
190
180
170
160
150
140
130
120
110
100
90
80
70
60
50
40
30
20
10
0
-10
f1 (ppm)

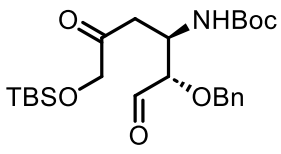
O
NHBoc
TBSO
OBn
O

50

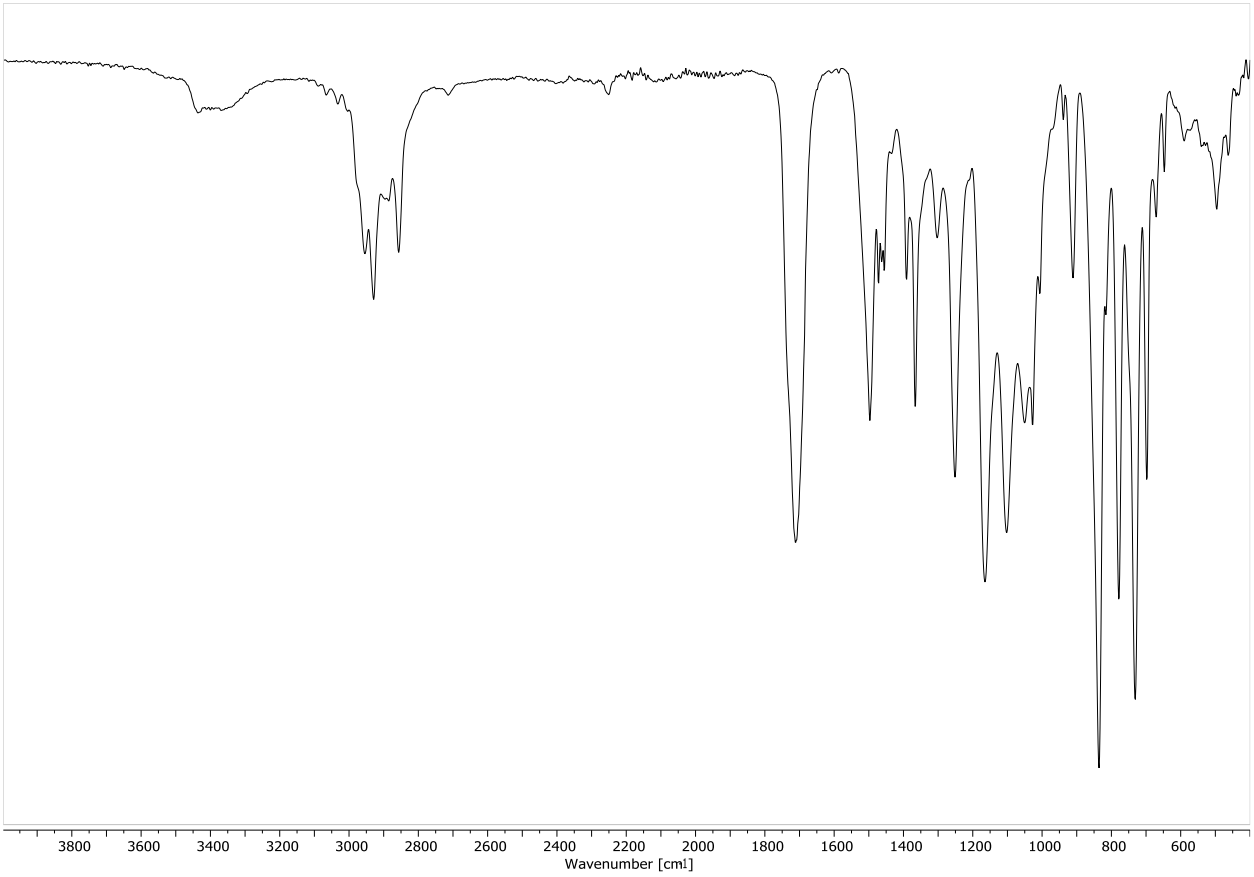
3800
3600
3400
3200
3000
2800
2600
2400
2200
2000
1800
1600
1400
1200
1000
800
600
Wavenumber [cm-1]

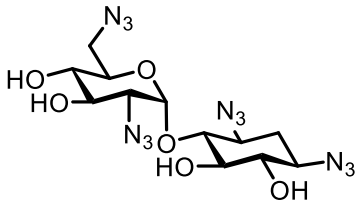
N3
HO
HO
O
N3
N3
O
HO
N3
OH

102

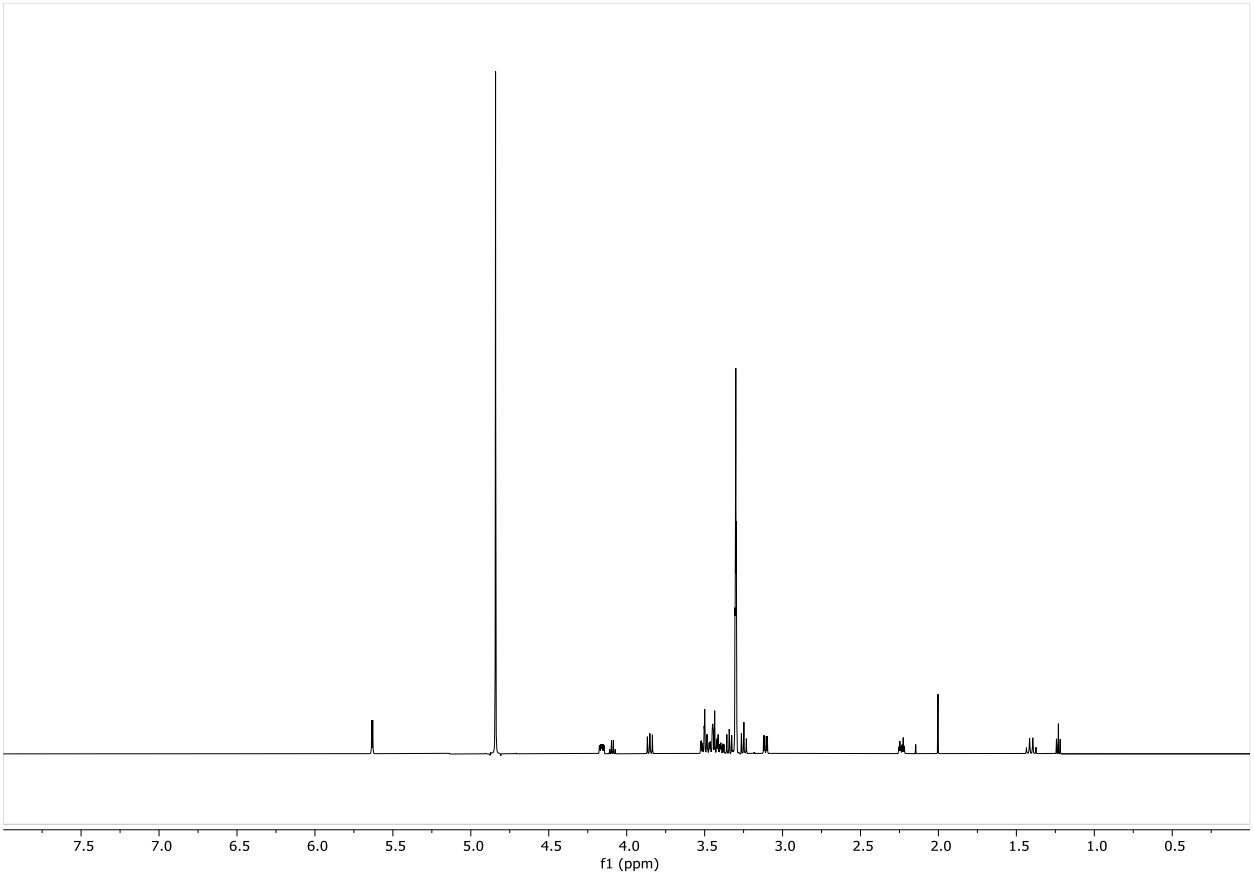
7.5
7.0
6.5
6.0
5.5
5.0
4.5
4.0
3.5
3.0
2.5
2.0
1.5
1.0
0.5
f1 (ppm)

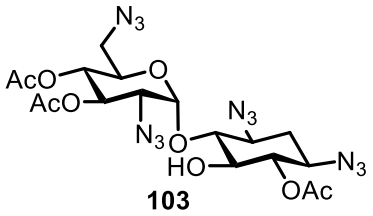
N3
AcO
AcO
O
N3
O
N3
HO
N3
OAc

103

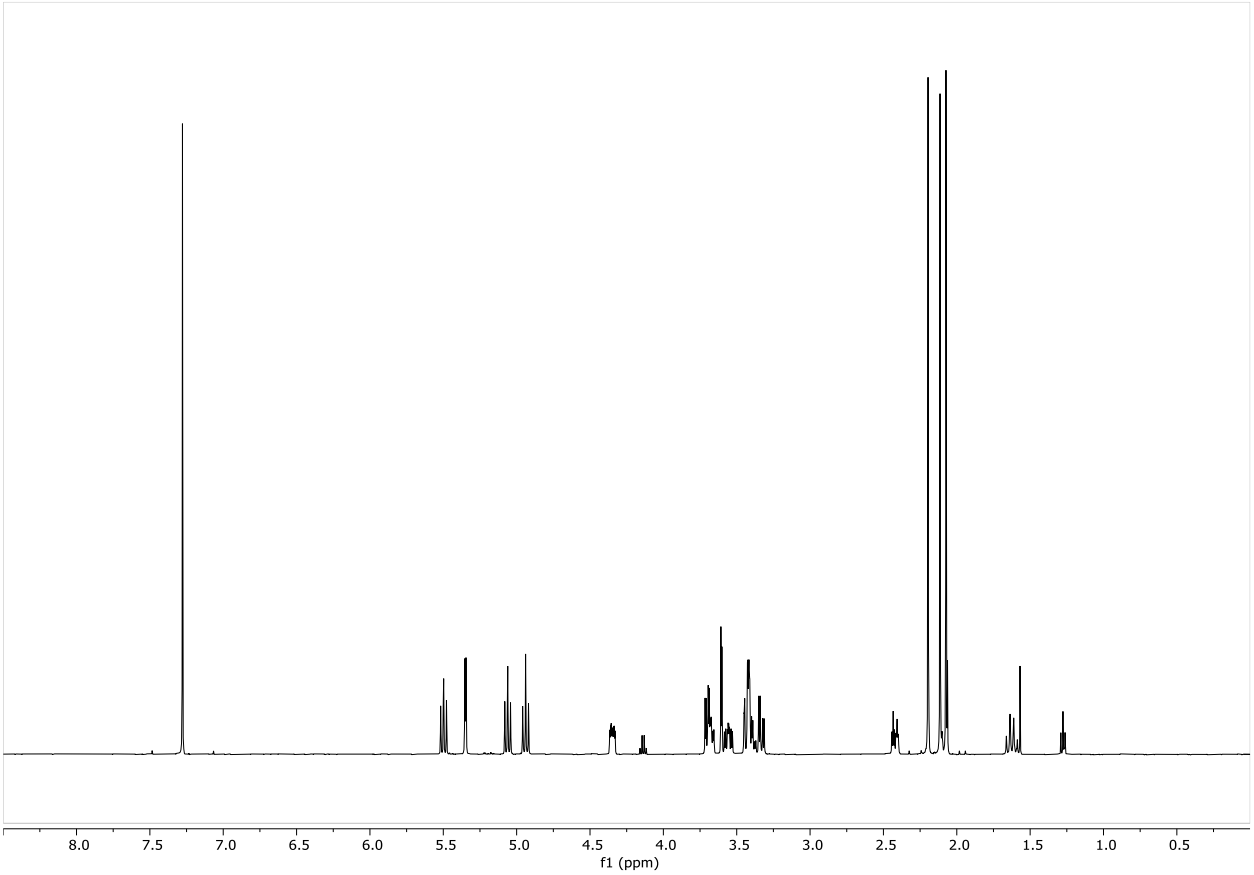
8.0
7.5
7.0
6.5
6.0
5.5
5.0
4.5
4.0
3.5
3.0
2.5
2.0
1.5
1.0
0.5
f1 (ppm)

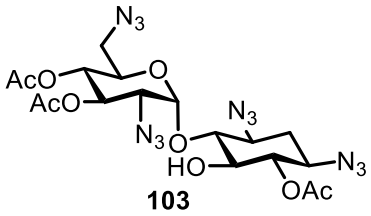
N3
AcO
AcO
O
N3
O
N3
HO
N3
OAc

103

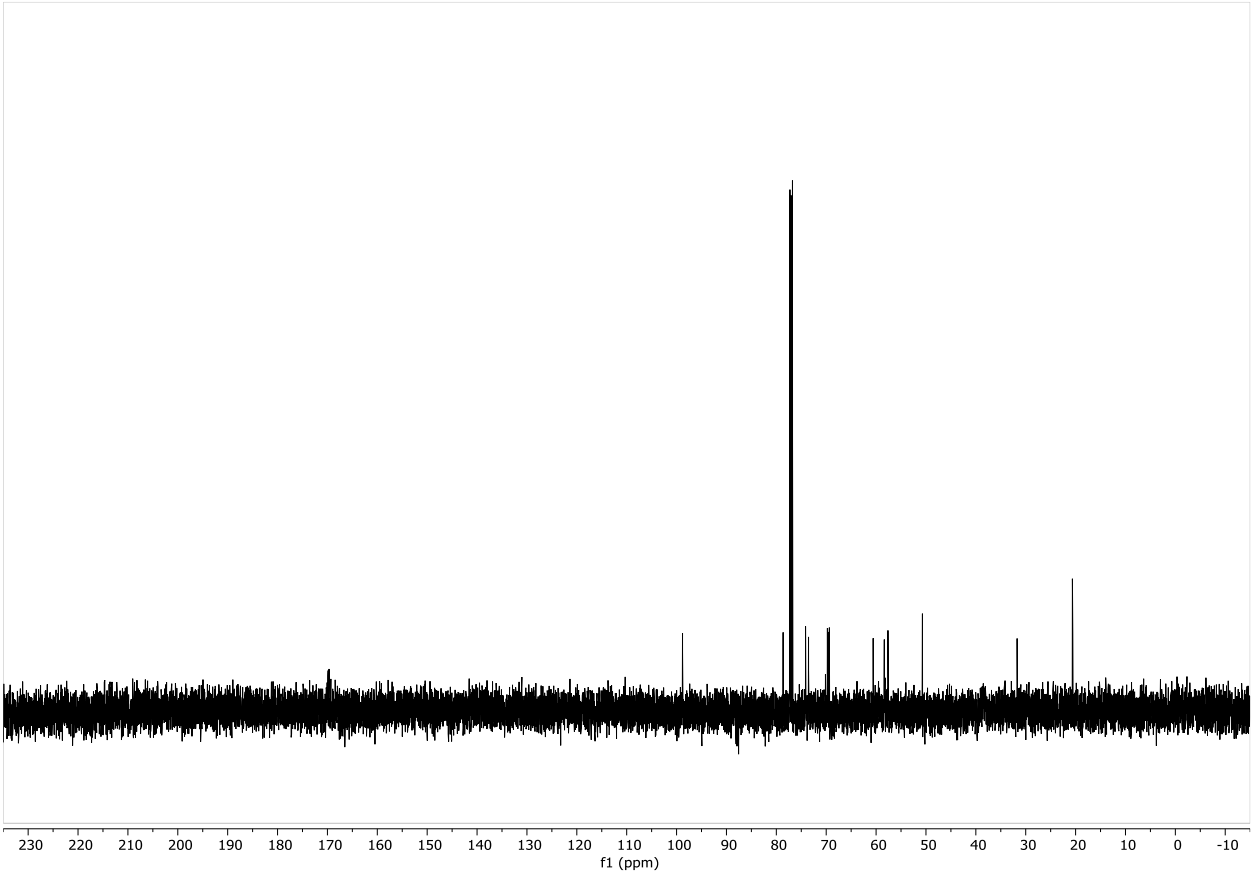
230 220 210 200 190 180 170 160 150 140 130 120 110 100 90 80 70 60 50 40 30 20 10 0 -10
f1 (ppm)

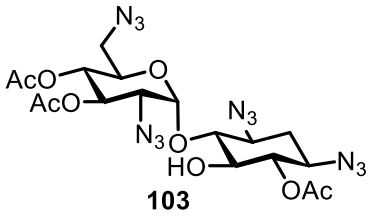
N3
AcO
AcO
O
N3
O
N3
HO
N3
OAc

103

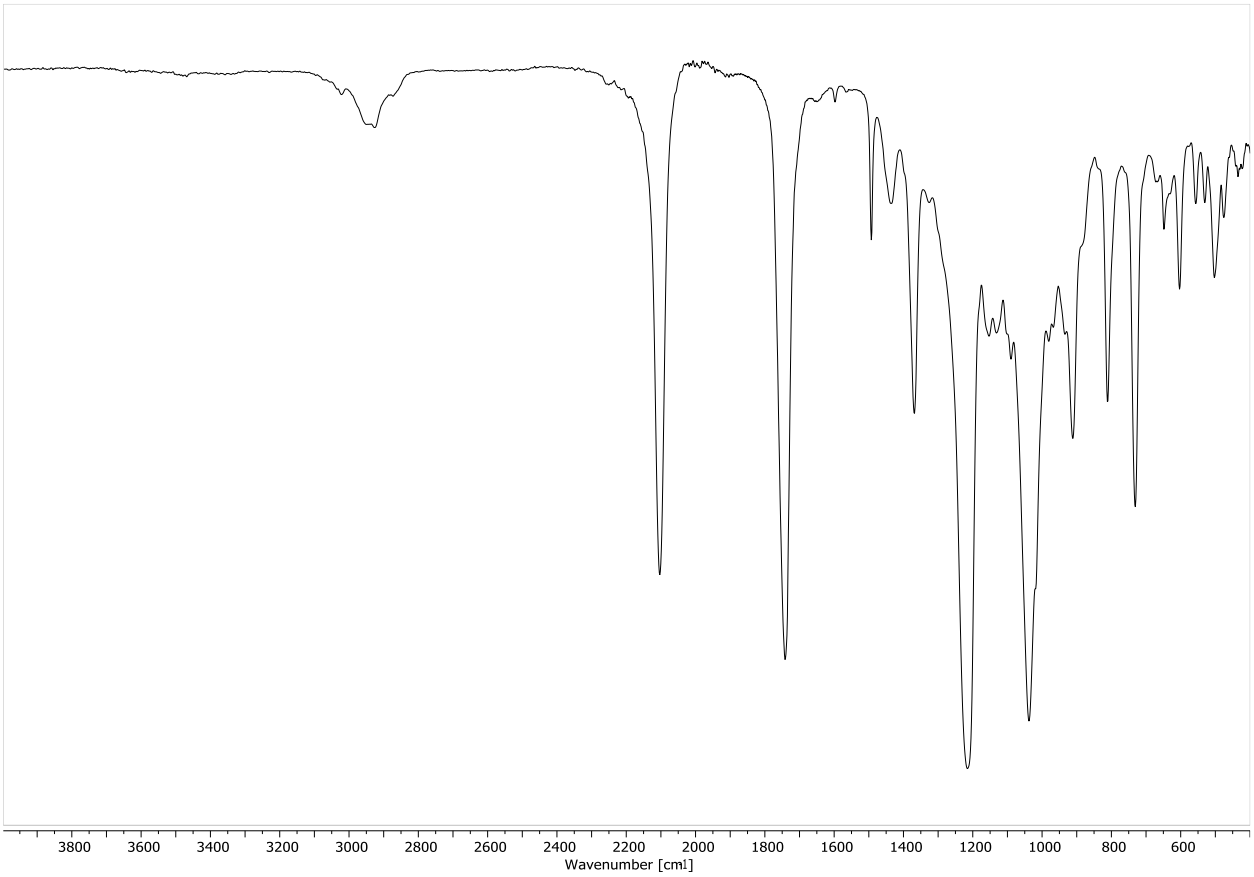
3800
3600
3400
3200
3000
2800
2600
2400
2200
2000
1800
1600
1400
1200
1000
800
600
Wavenumber [cm-1]

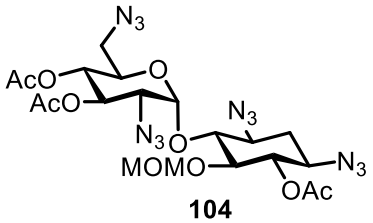
N3
AcO
AcO
O
N3
N3
O
MOMO
N3
OAc

104

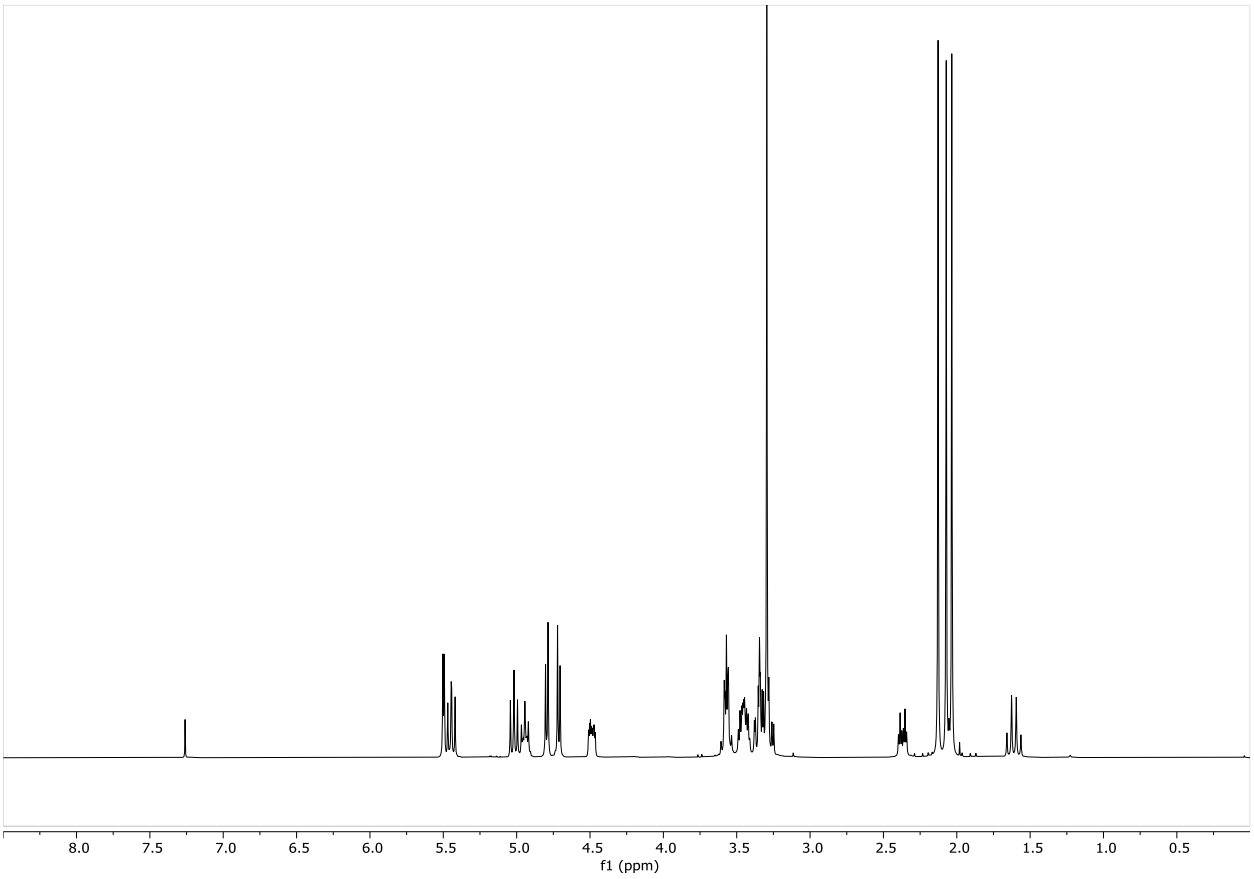
8.0
7.5
7.0
6.5
6.0
5.5
5.0
4.5
4.0
3.5
3.0
2.5
2.0
1.5
1.0
0.5
f1 (ppm)

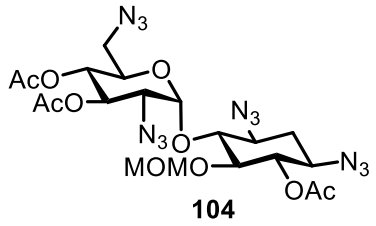
N3
AcO
AcO
O
N3
N3
O
MOMO
N3
OAc

104

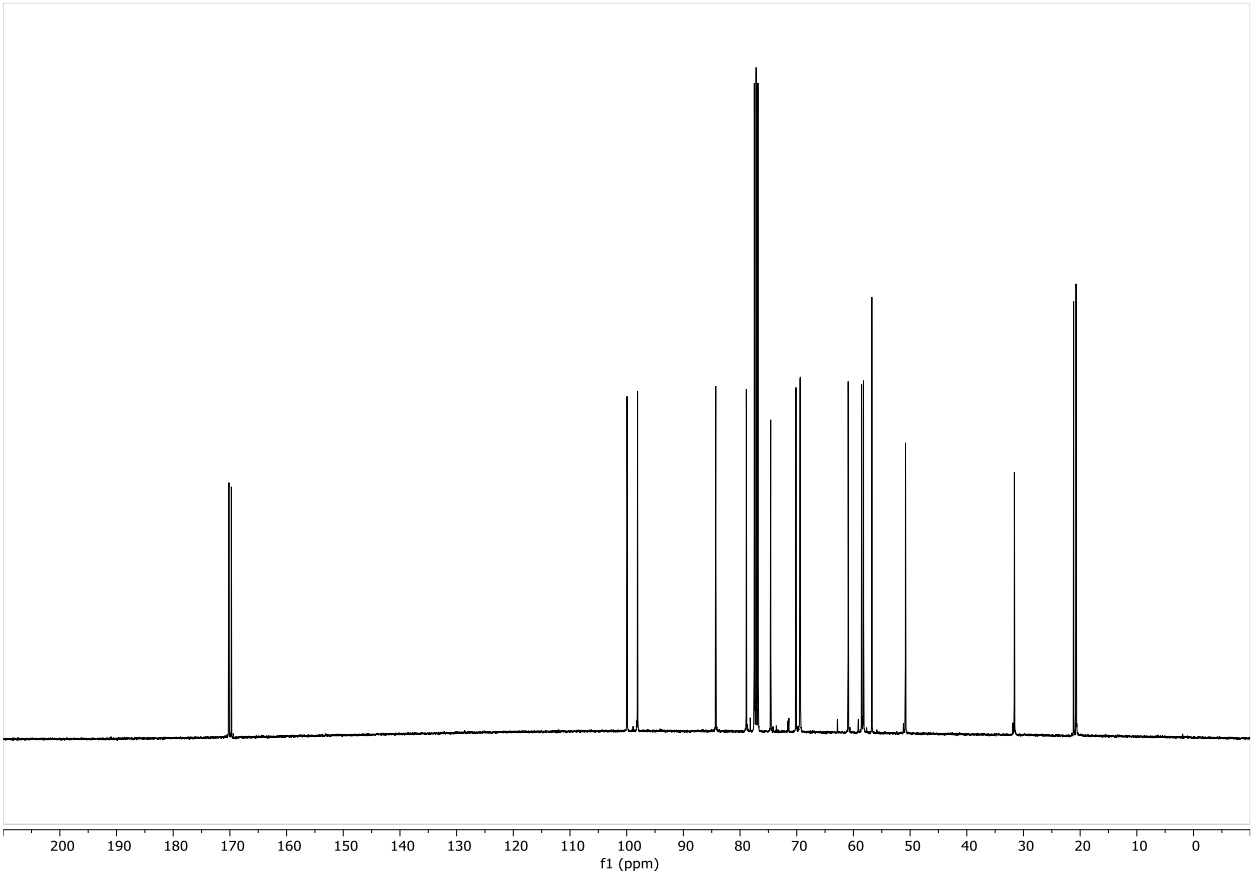
200
190
180
170
160
150
140
130
120
110
100
90
80
70
60
50
40
30
20
10
0
f1 (ppm)

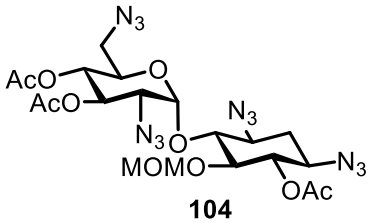
N3
AcO
AcO
O
N3
N3
O
MOMO
N3
OAc

104

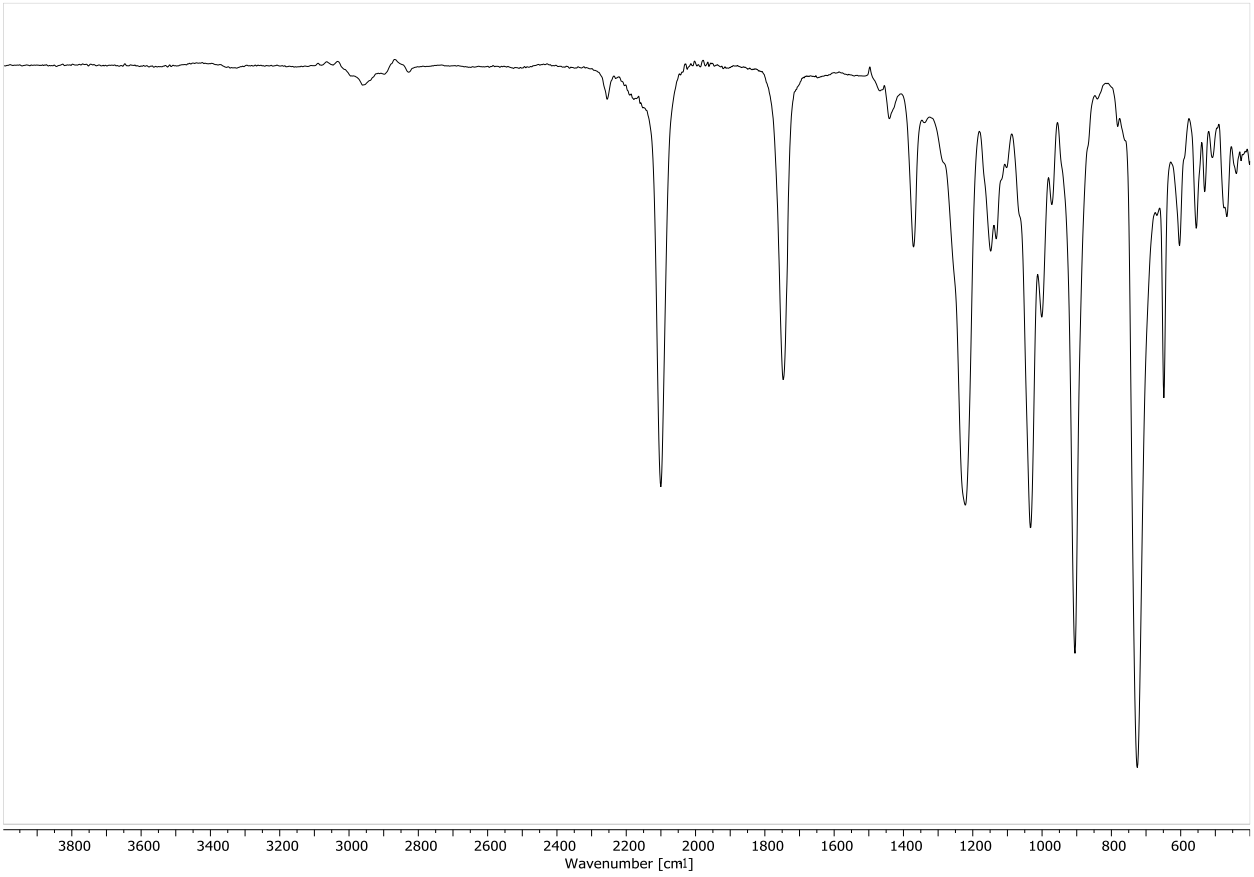
3800
3600
3400
3200
3000
2800
2600
2400
2200
2000
1800
1600
1400
1200
1000
800
600
Wavenumber [cm-1]

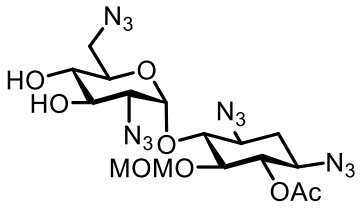
N3
HO
HO
O
N3
N3
O
MOMO
N3
OAc

105

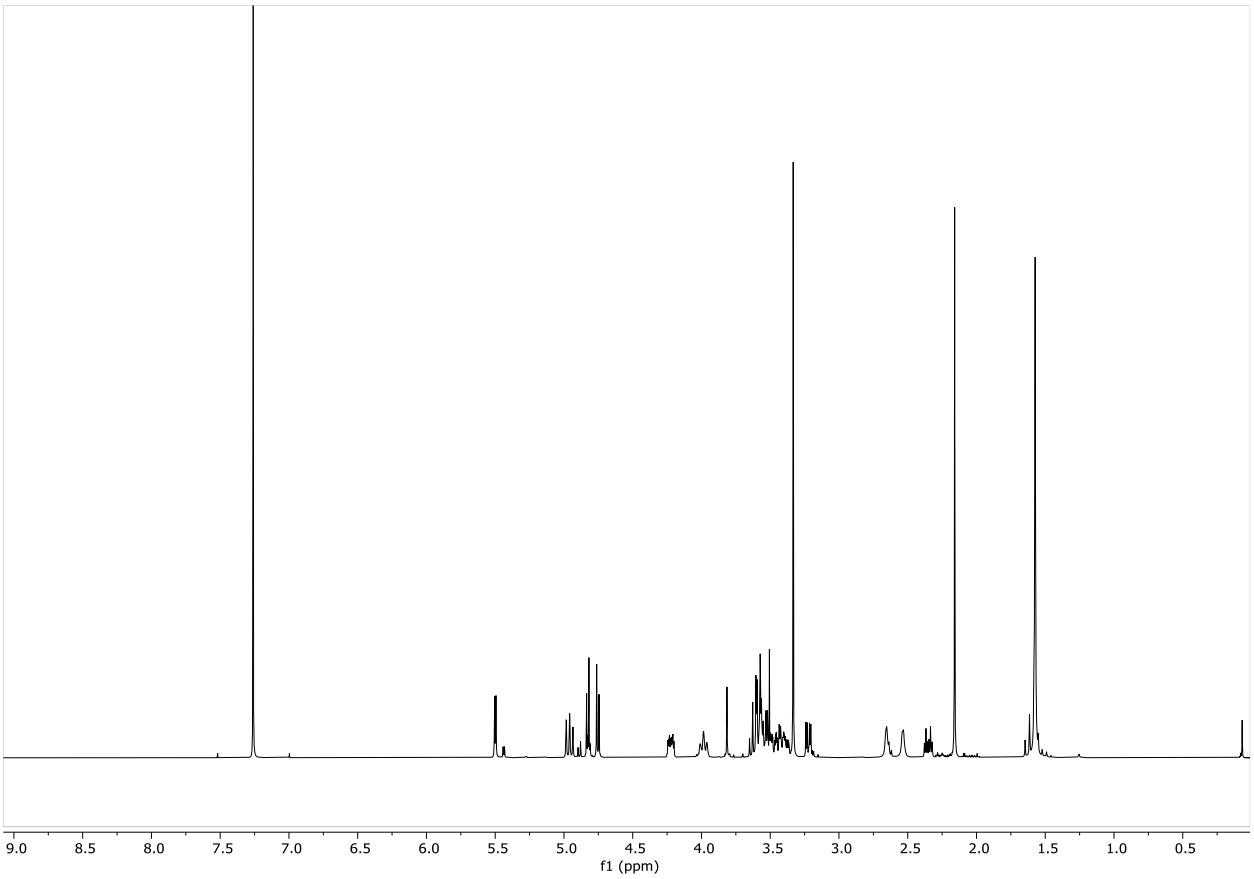
9.0
8.5
8.0
7.5
7.0
6.5
6.0
5.5
5.0
4.5
4.0
3.5
3.0
2.5
2.0
1.5
1.0
0.5
f1 (ppm)

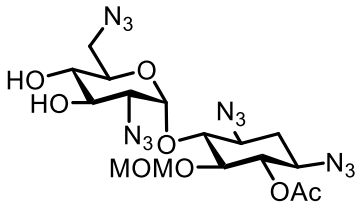
N3
HO
HO
O
N3
N3
O
MOMO
N3
OAc

105

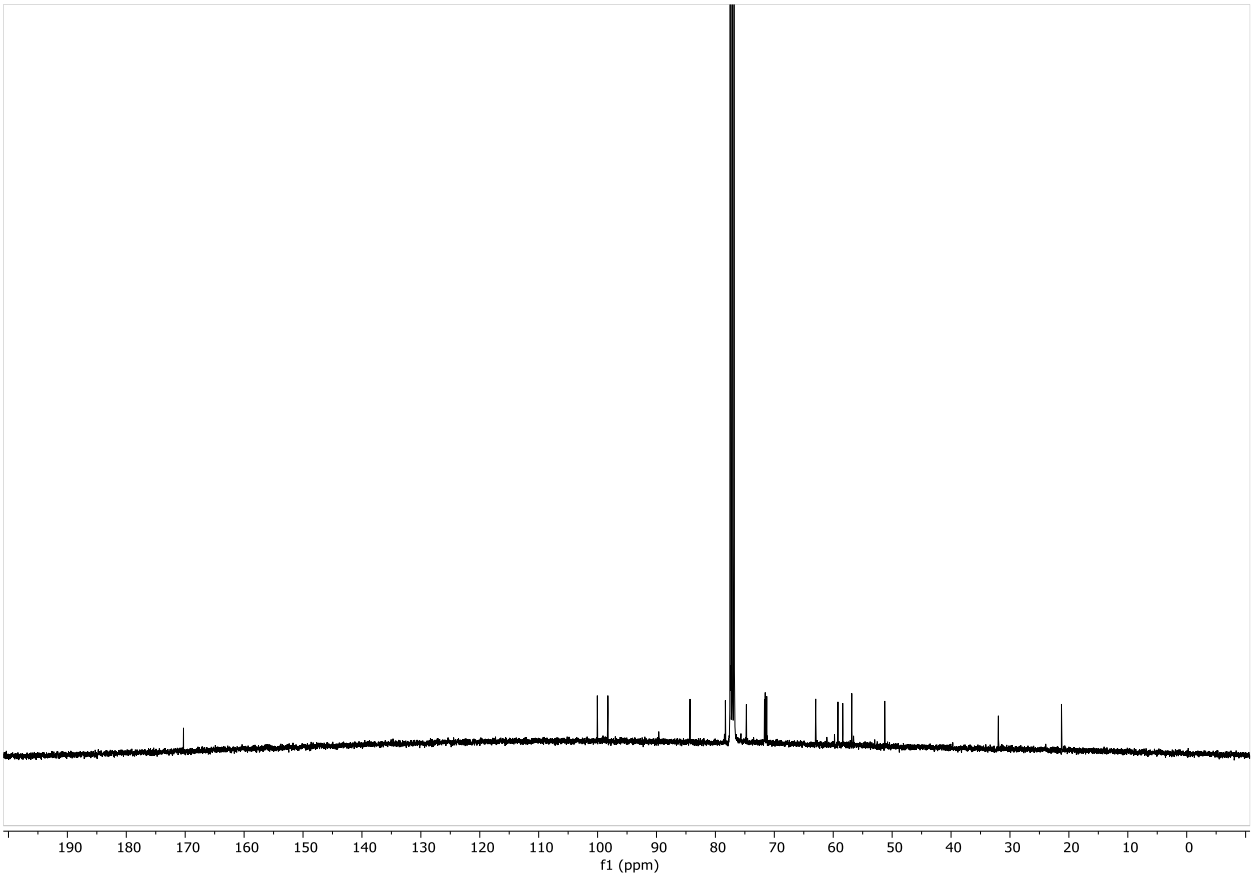
190
180
170
160
150
140
130
120
110
100
90
80
70
60
50
40
30
20
10
0
f1 (ppm)

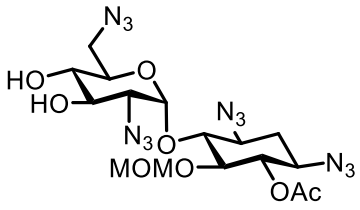
N3
HO
HO
O
N3
N3
O
MOMO
N3
OAc

105

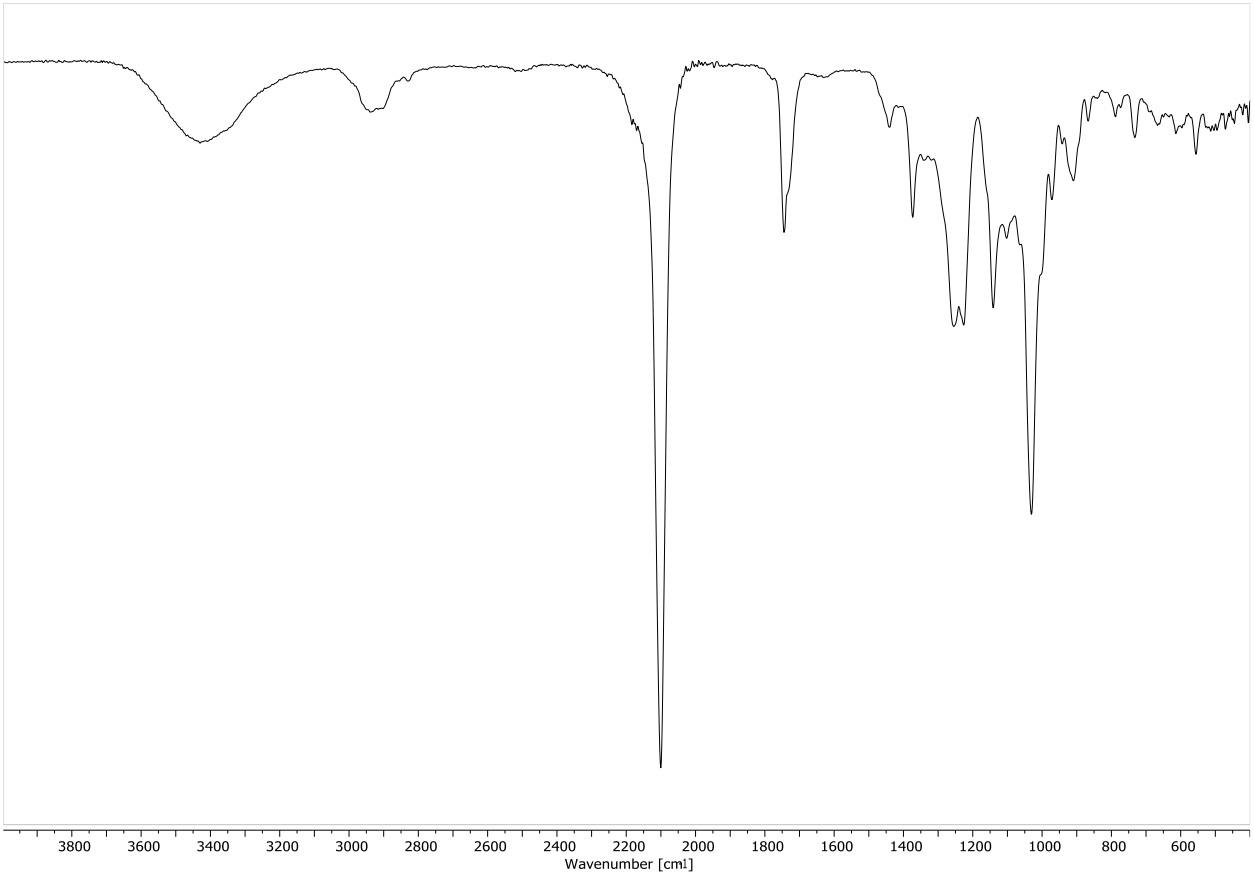
3800
3600
3400
3200
3000
2800
2600
2400
2200
2000
1800
1600
1400
1200
1000
800
600
Wavenumber [cm-1]

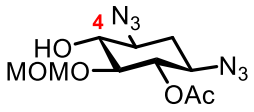
4
N3
HO
MOMO
N3
OAc

106

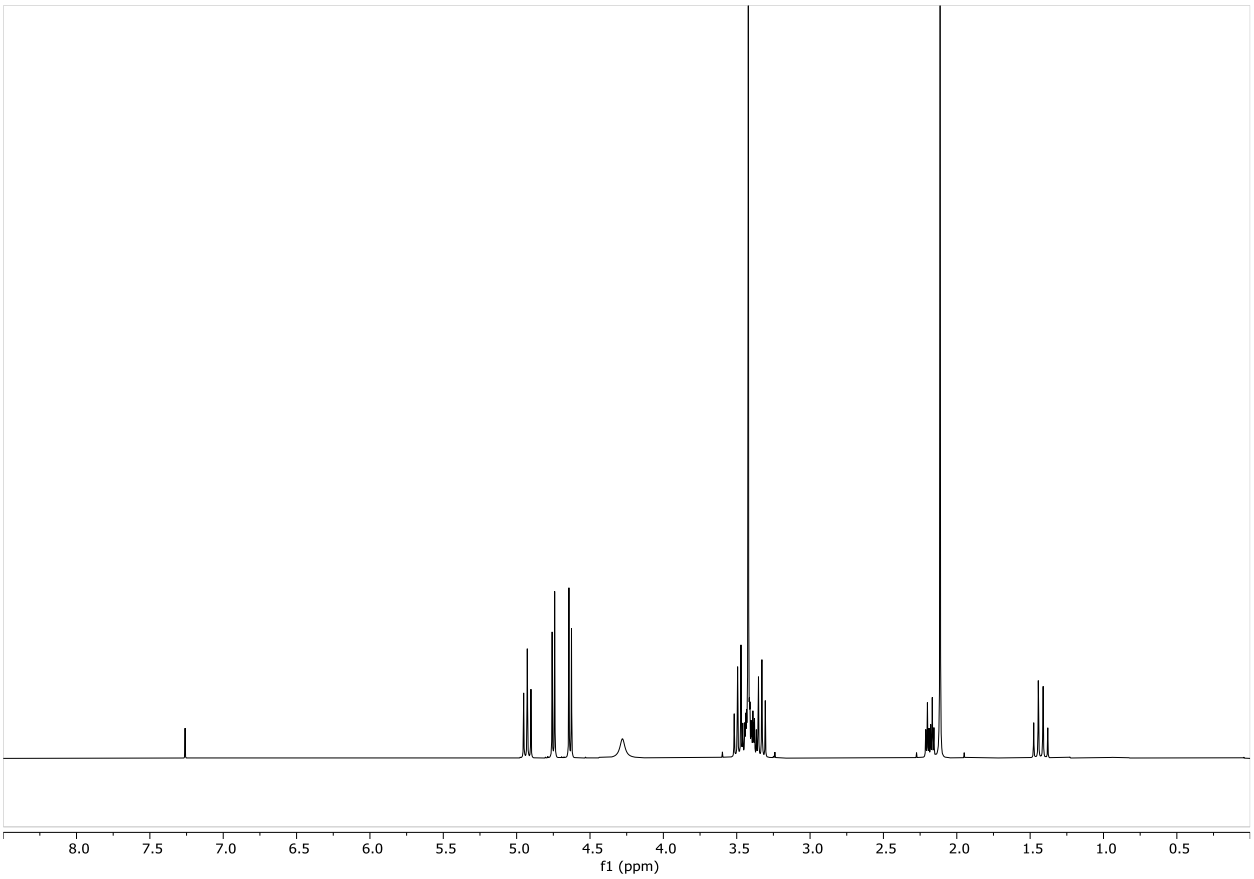
8.0
7.5
7.0
6.5
6.0
5.5
5.0
4.5
4.0
3.5
3.0
2.5
2.0
1.5
1.0
0.5
f1 (ppm)

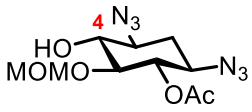
4
N3
HO
MOMO
N3
OAc

106

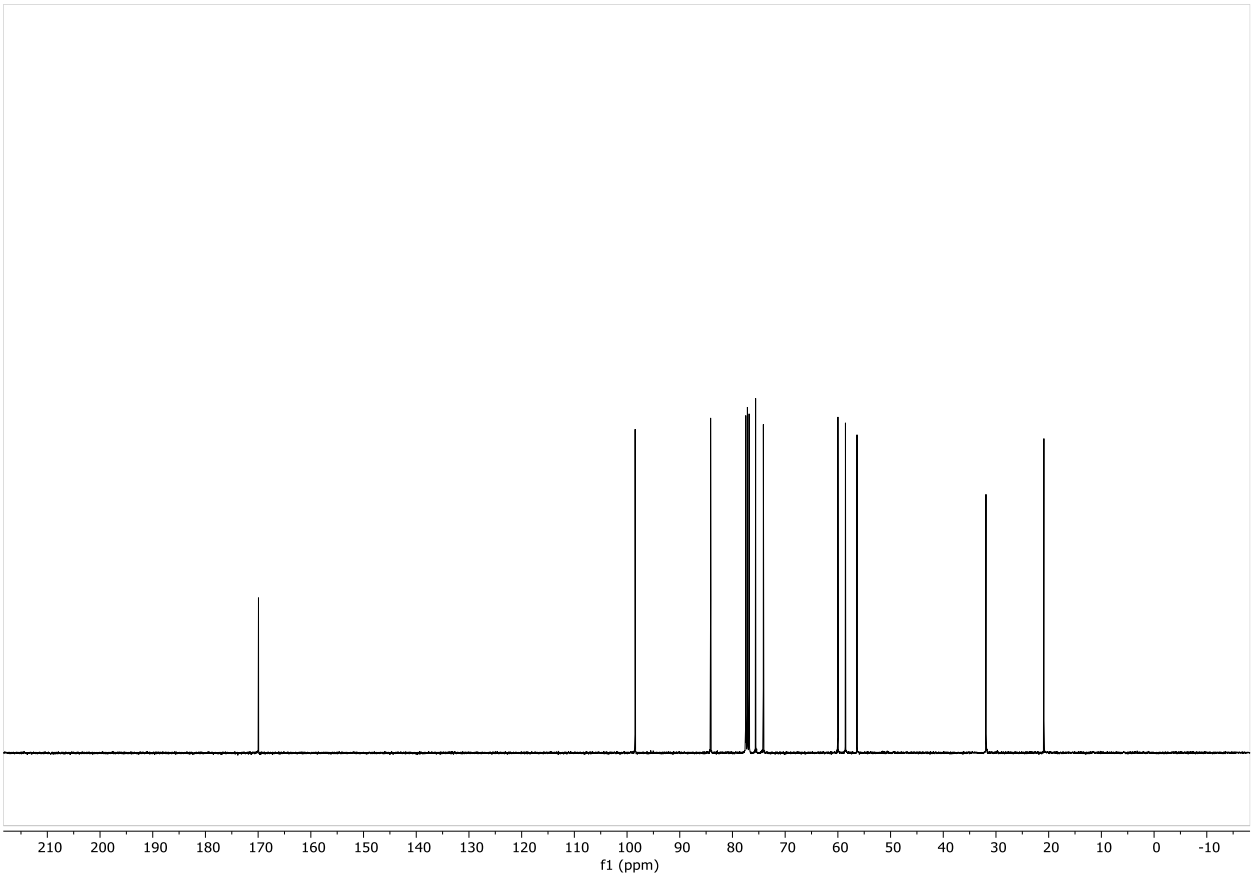
210
200
190
180
170
160
150
140
130
120
110
100
90
80
70
60
50
40
30
20
10
0
-10
f1 (ppm)

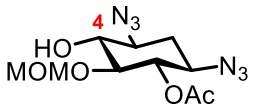
4
N3
HO
MOMO
N3
OAc

106

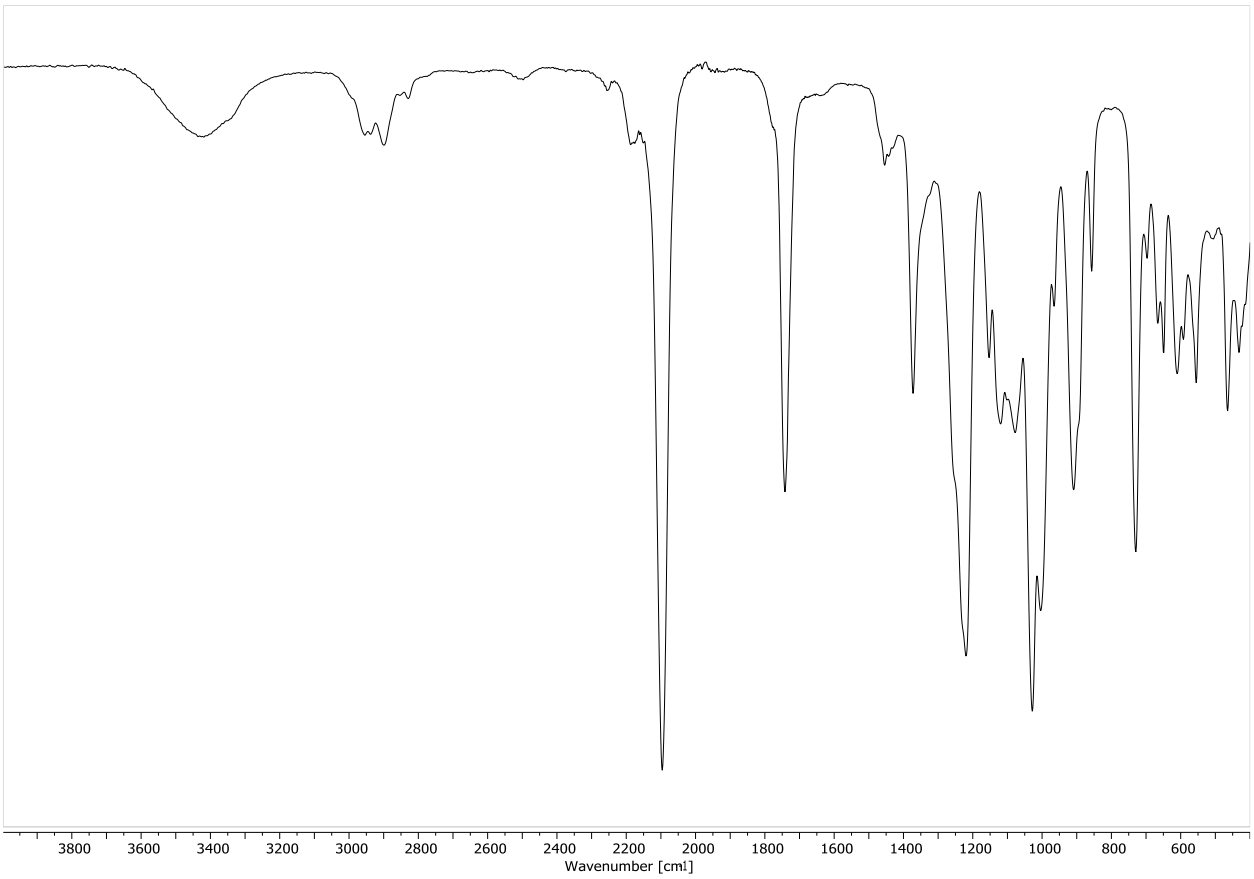
3800
3600
3400
3200
3000
2800
2600
2400
2200
2000
1800
1600
1400
1200
1000
800
600
Wavenumber [cm-1]

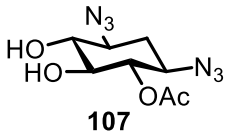

107

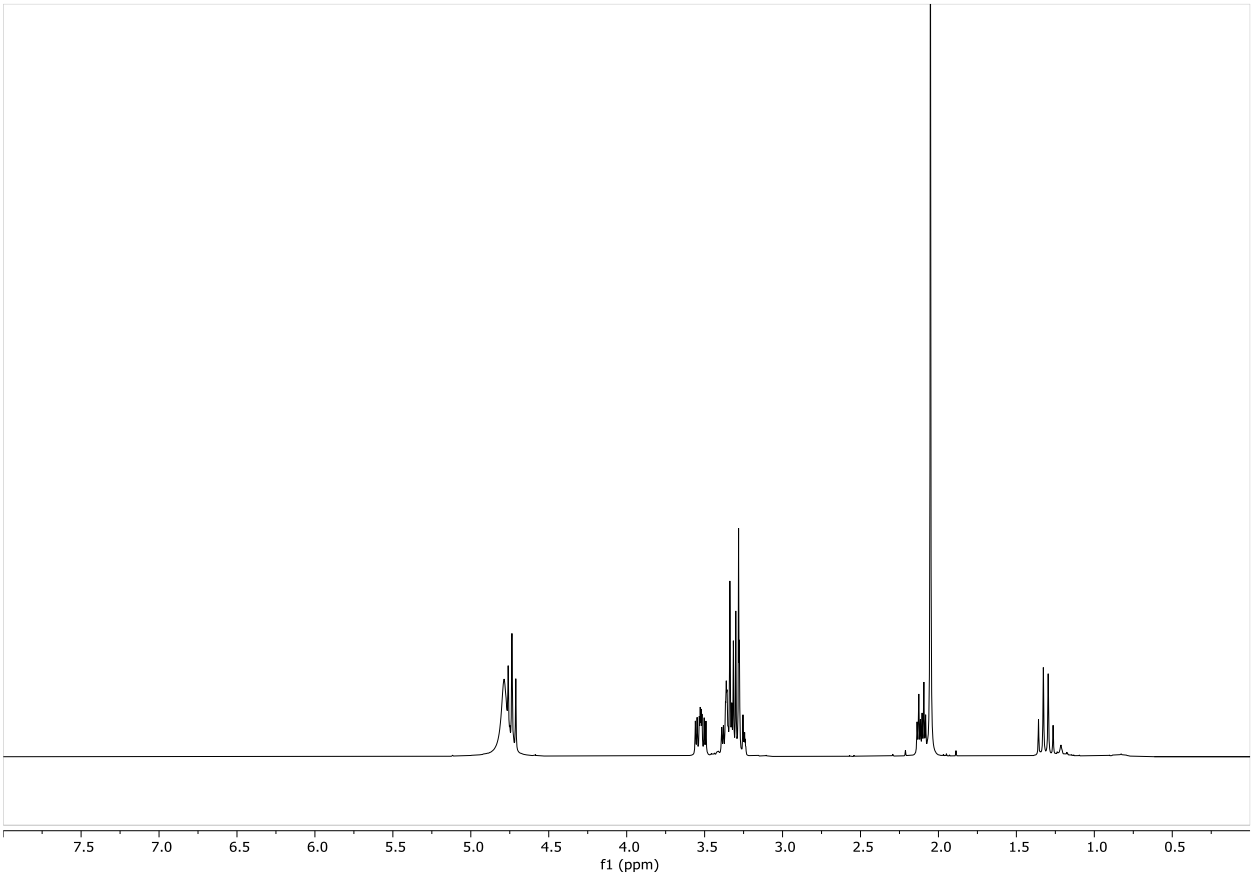

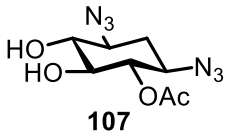
N3
HO
HO
N3
OAc

107

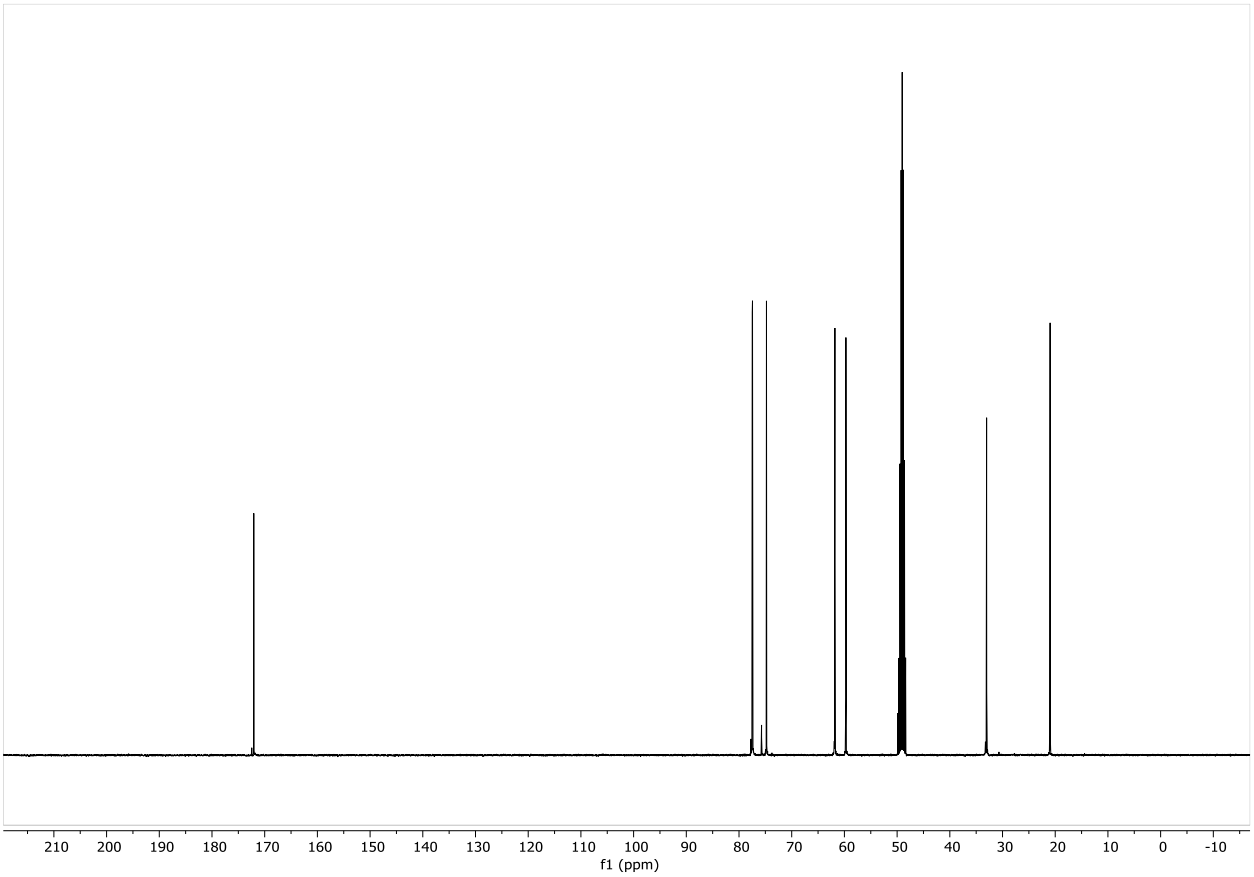
210
200
190
180
170
160
150
140
130
120
110
100
90
80
70
60
50
40
30
20
10
0
-10
f1 (ppm)

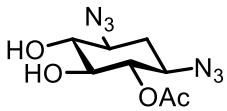
N3
HO
HO
N3
OAc

107

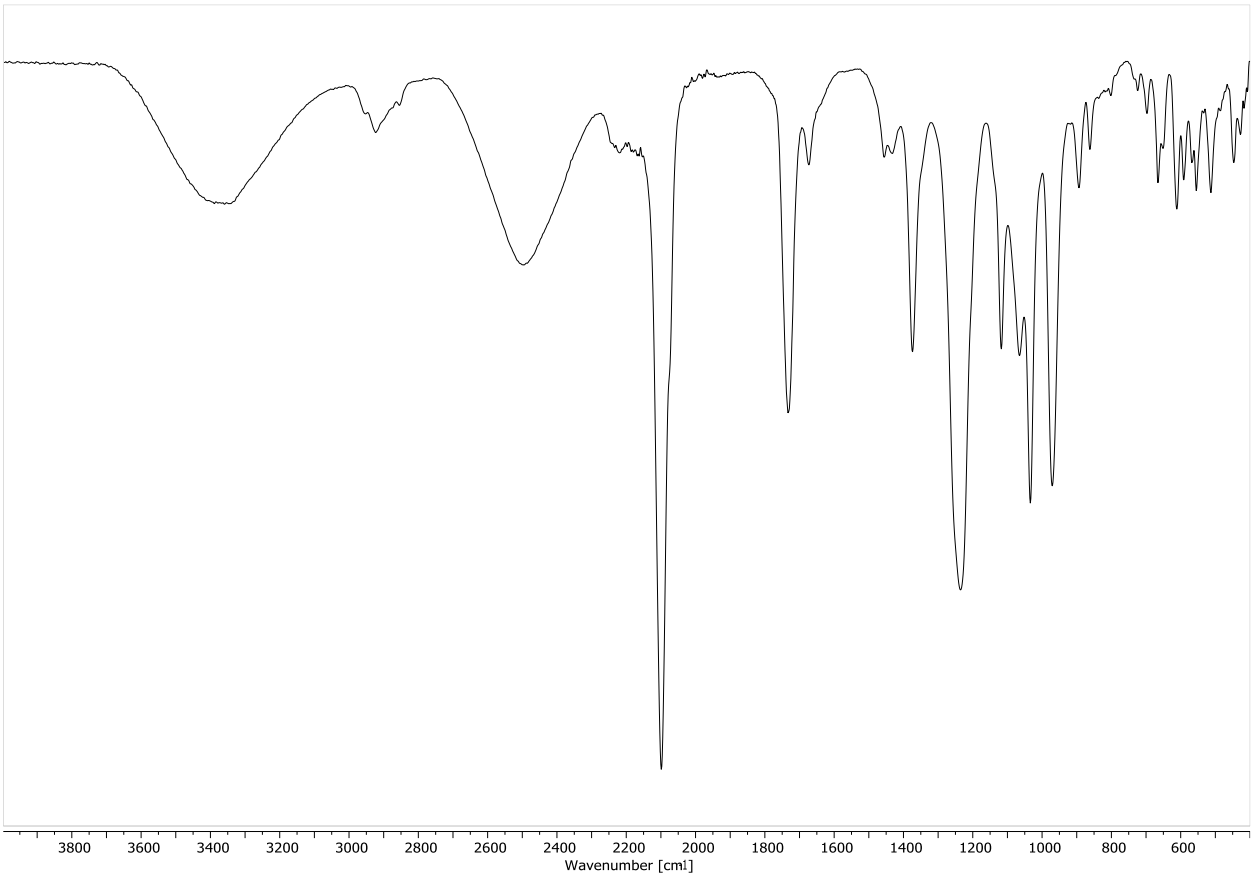
3800
3600
3400
3200
3000
2800
2600
2400
2200
2000
1800
1600
1400
1200
1000
800
600
Wavenumber [cm-1]

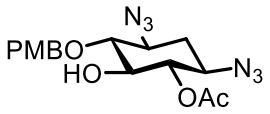
N3
PMBO
HO
N3
OAc

108

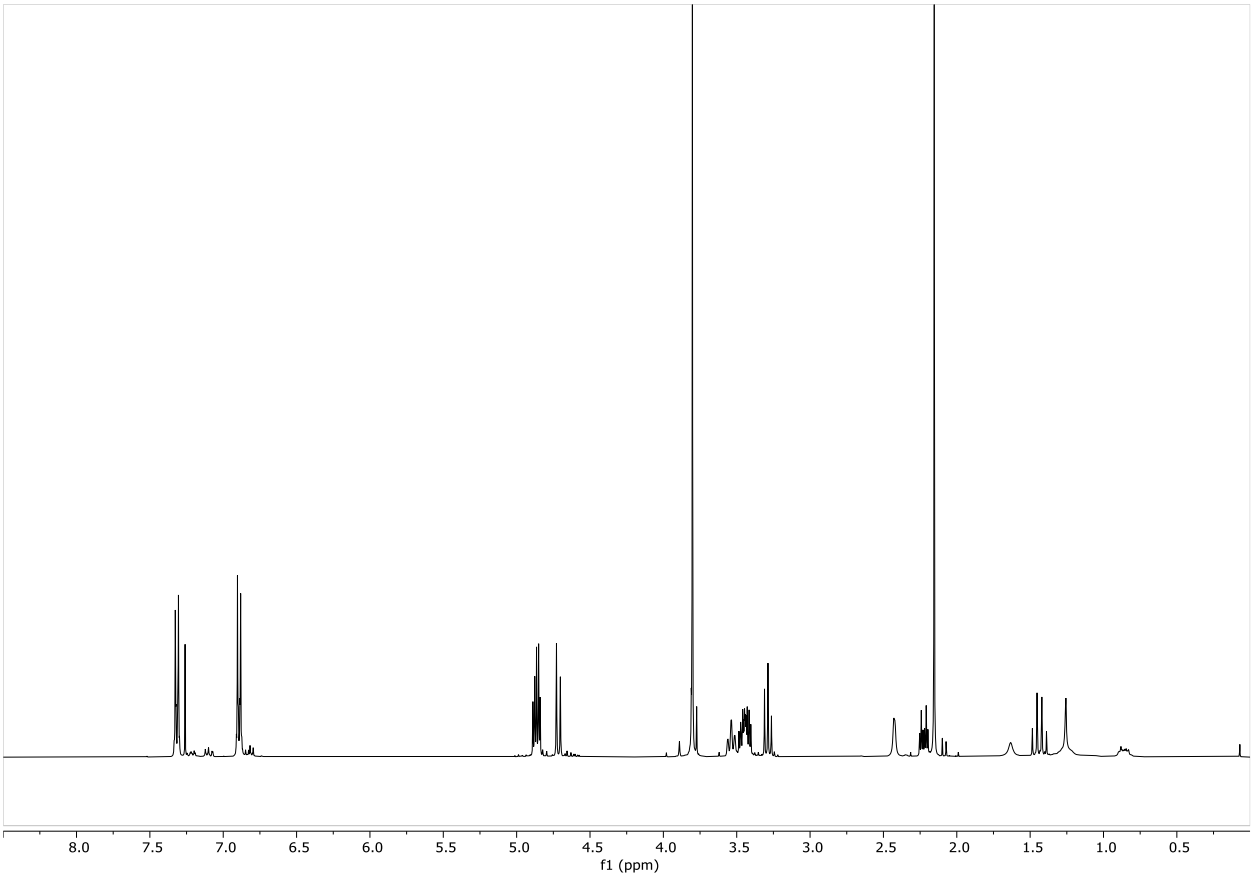
8.0
7.5
7.0
6.5
6.0
5.5
5.0
4.5
4.0
3.5
3.0
2.5
2.0
1.5
1.0
0.5
f1 (ppm)

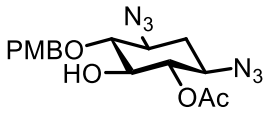
N3
PMBO
HO
N3
OAc

108

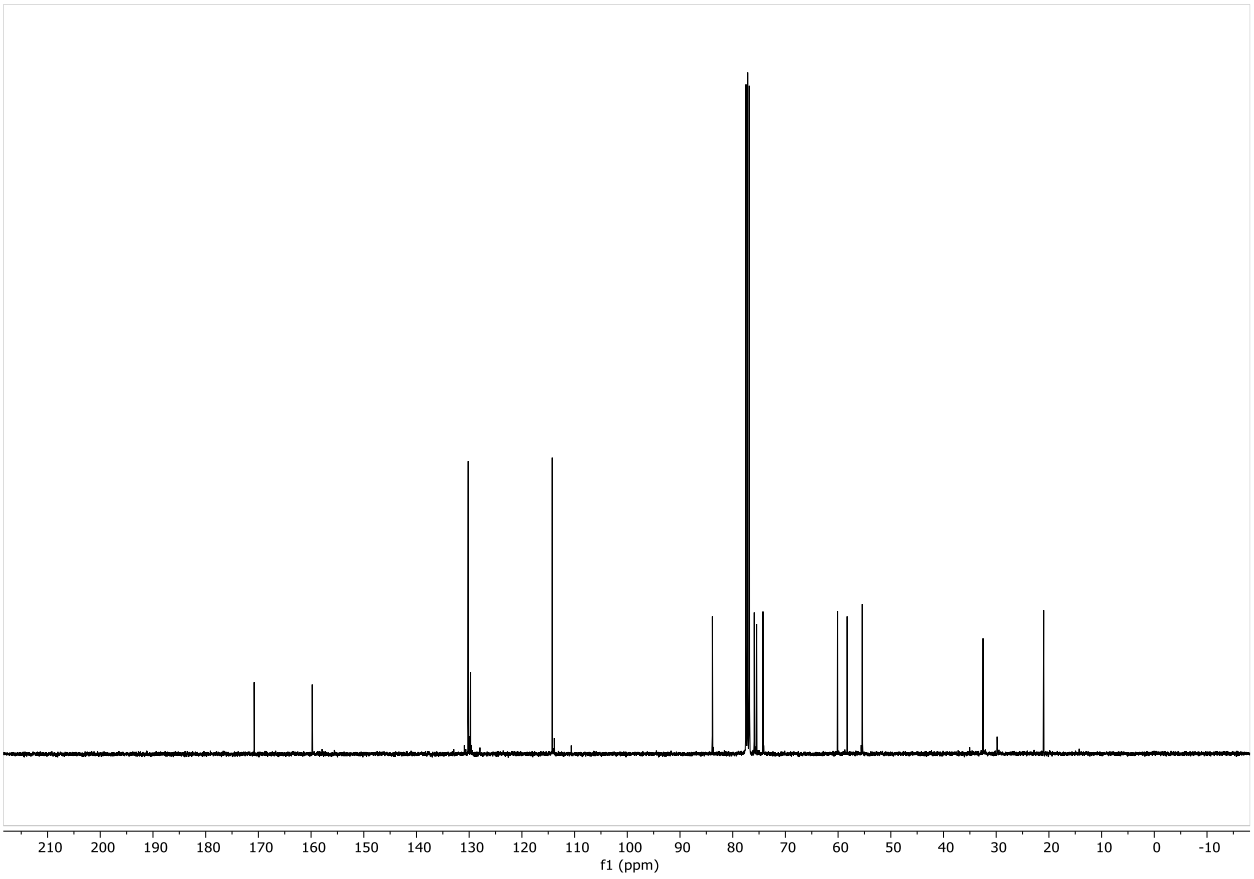
210
200
190
180
170
160
150
140
130
120
110
100
90
80
70
60
50
40
30
20
10
0
-10
f1 (ppm)

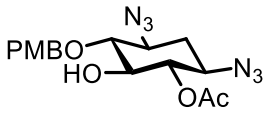
N3
PMBO
HO
N3
OAc

108

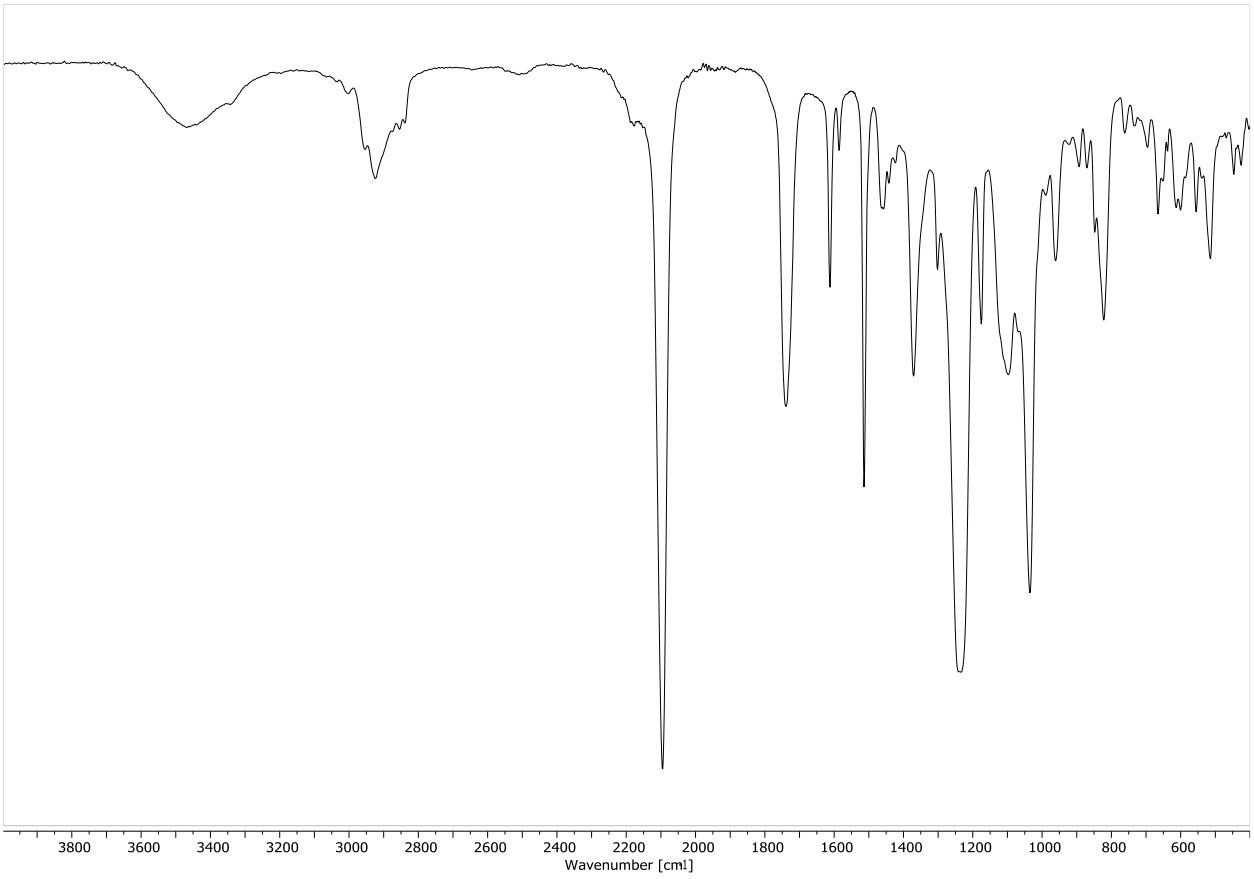
3800
3600
3400
3200
3000
2800
2600
2400
2200
2000
1800
1600
1400
1200
1000
800
600
Wavenumber [cm-1]

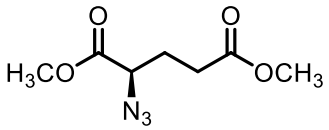

117

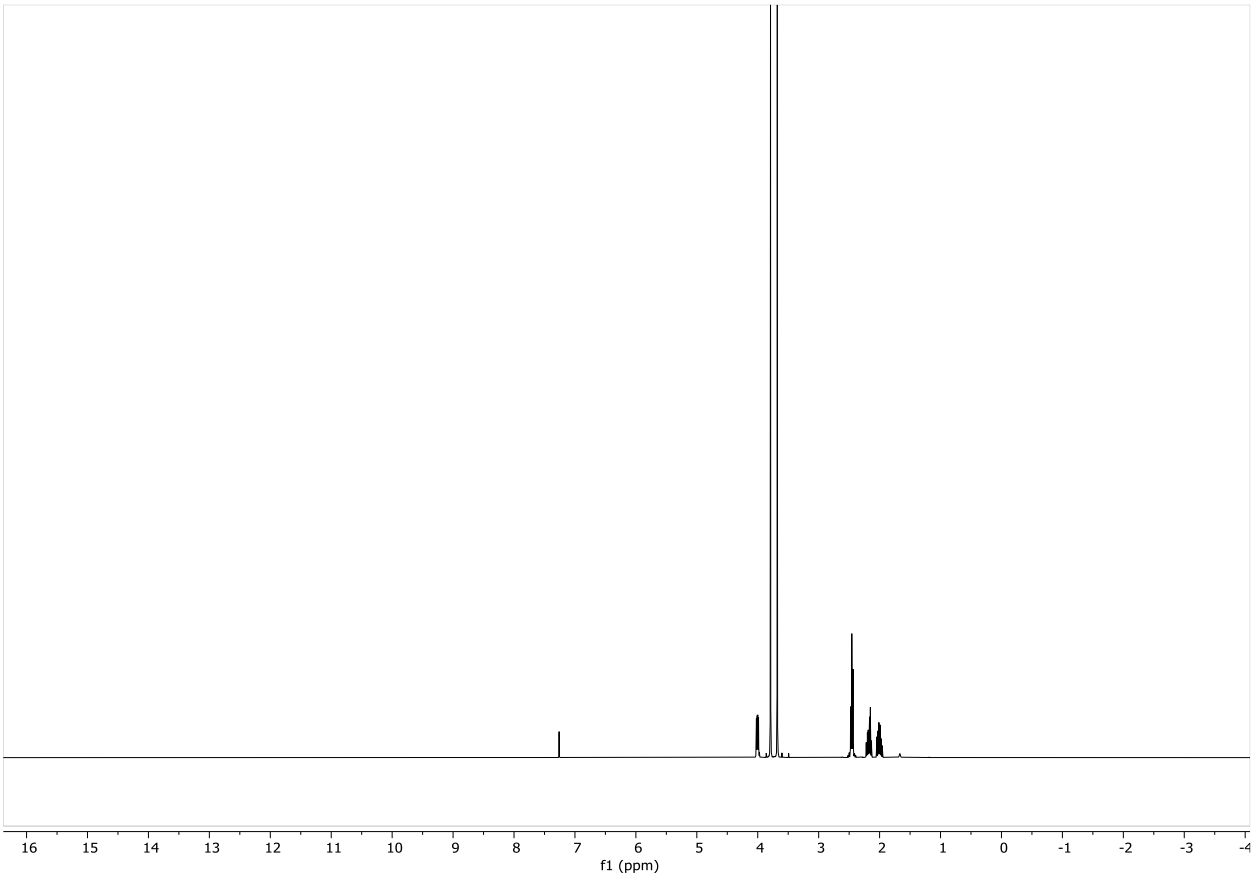

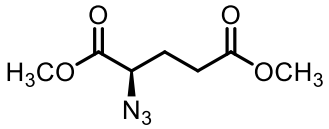
O
O
H3CO
OCH3
N3

117

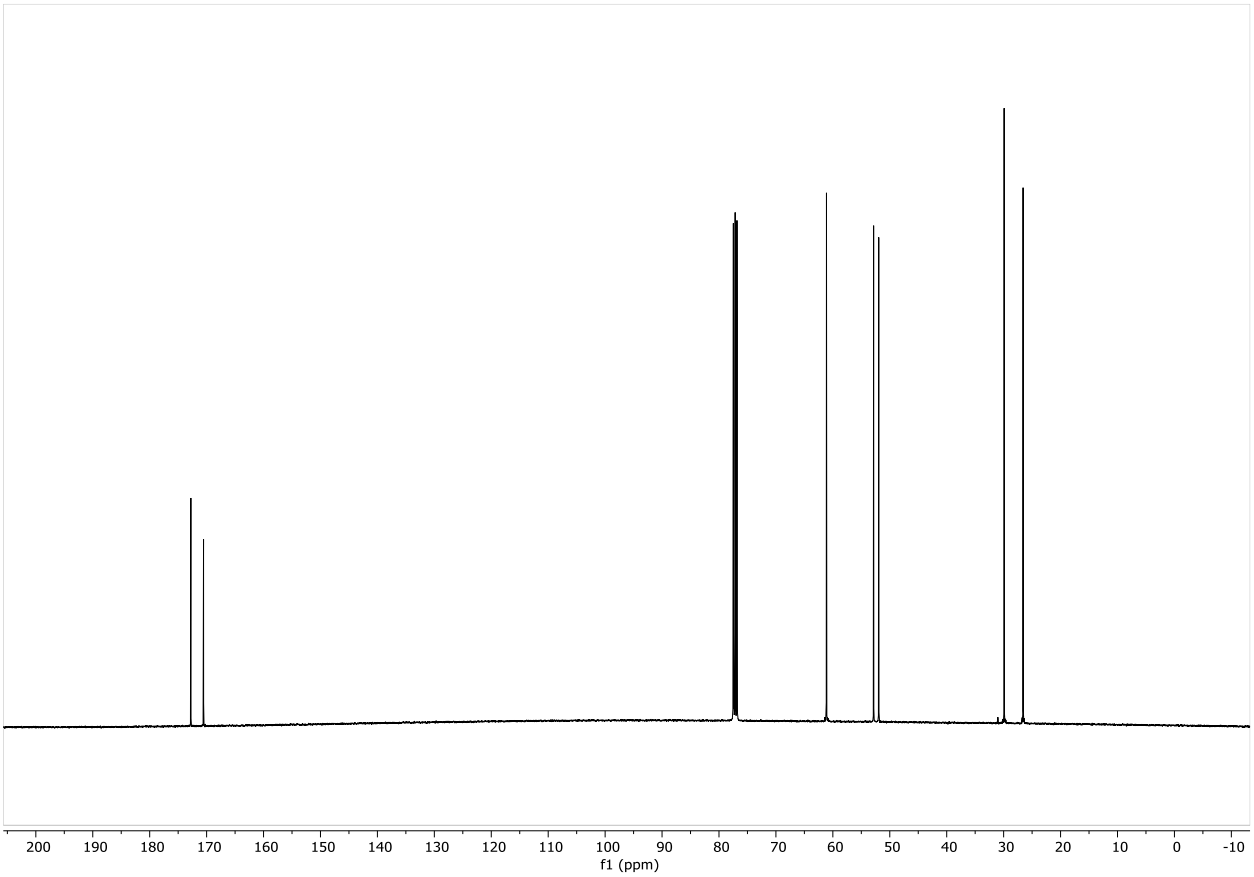
200
190
180
170
160
150
140
130
120
110
100
90
80
70
60
50
40
30
20
10
0
-10
f1 (ppm)

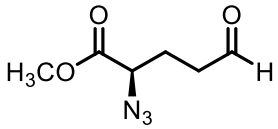
O
O
H3CO
H
N3

118

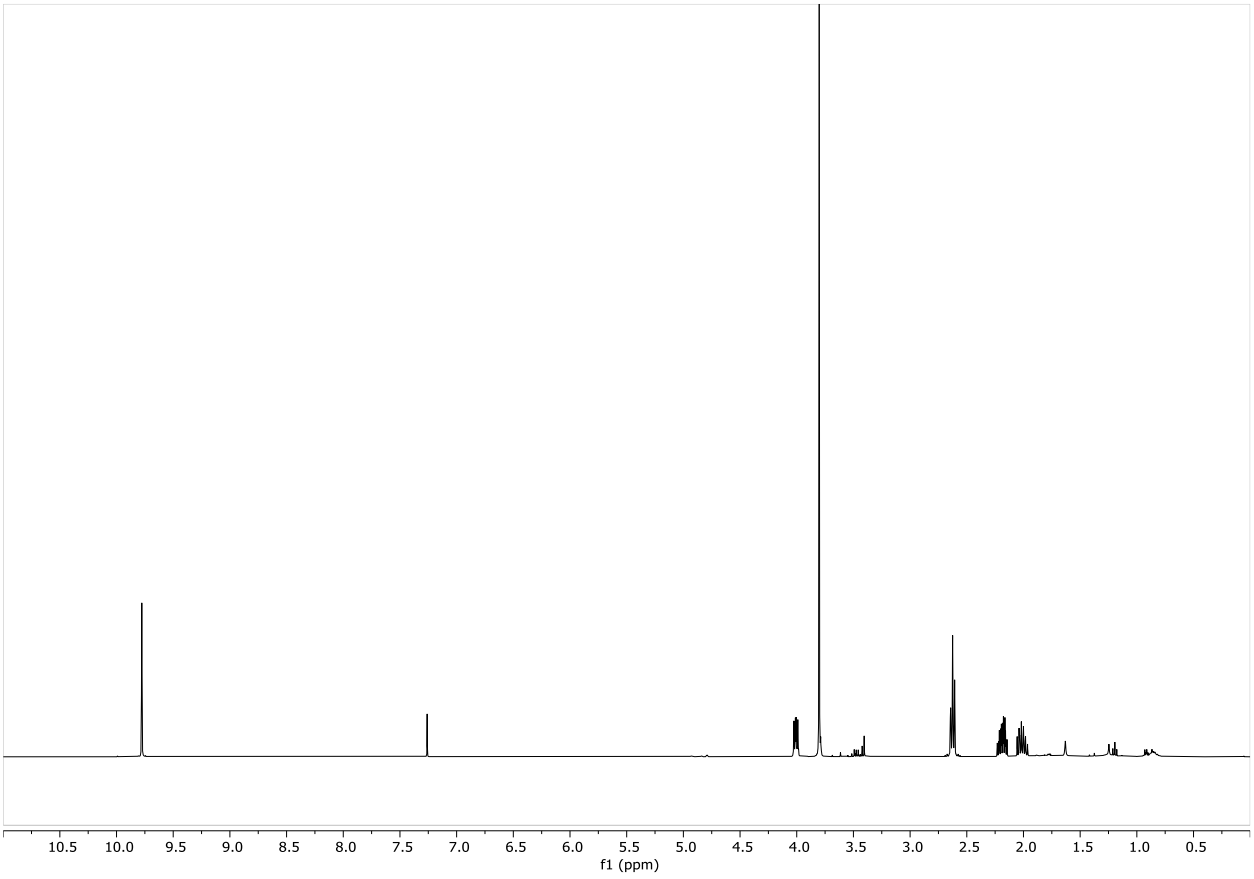
10.5
10.0
9.5
9.0
8.5
8.0
7.5
7.0
6.5
6.0
5.5
5.0
4.5
4.0
3.5
3.0
2.5
2.0
1.5
1.0
0.5
f1 (ppm)

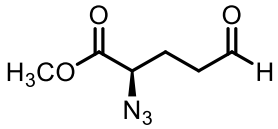
O
O
H3CO
H
N3

118

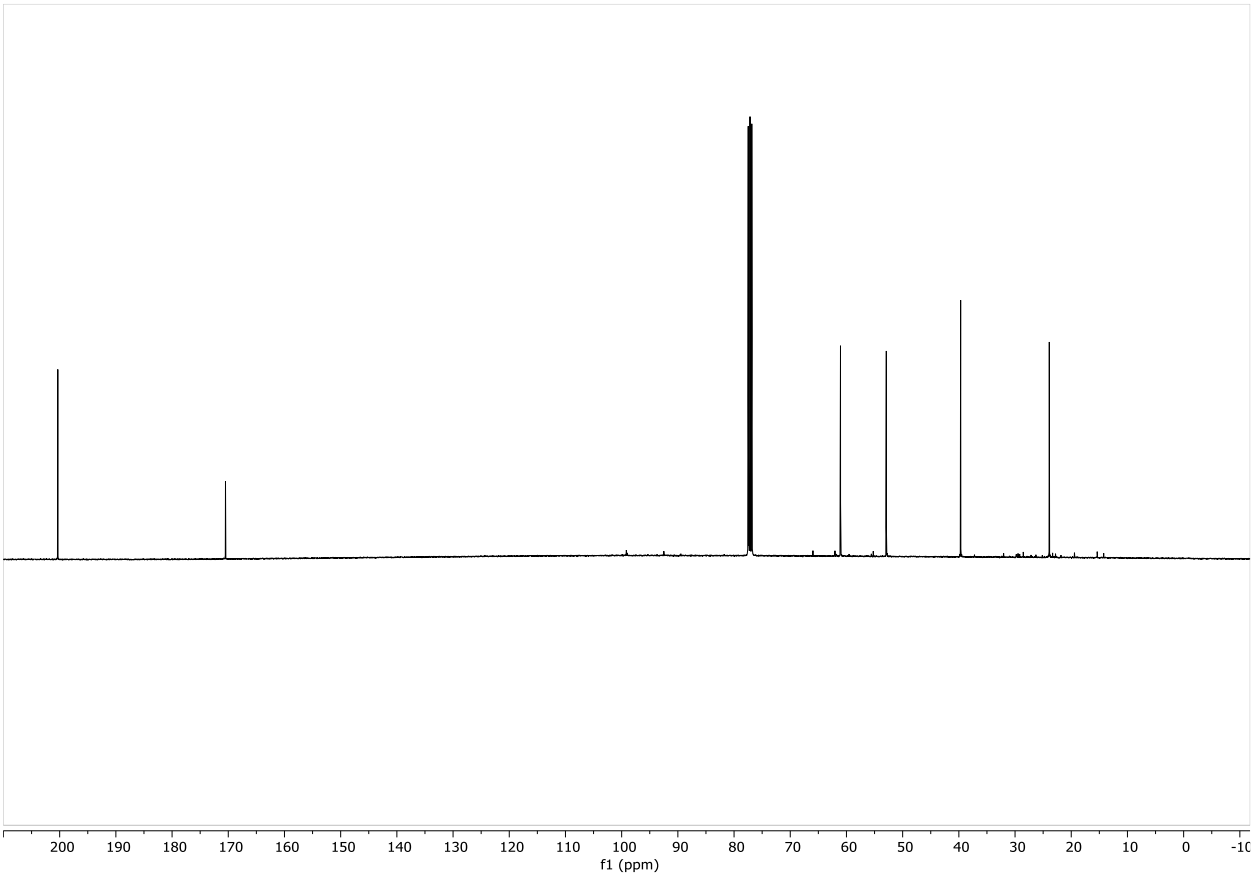
200
190
180
170
160
150
140
130
120
110
100
90
80
70
60
50
40
30
20
10
0
f1 (ppm)

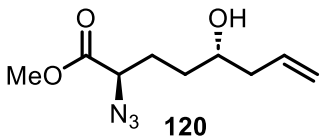

120

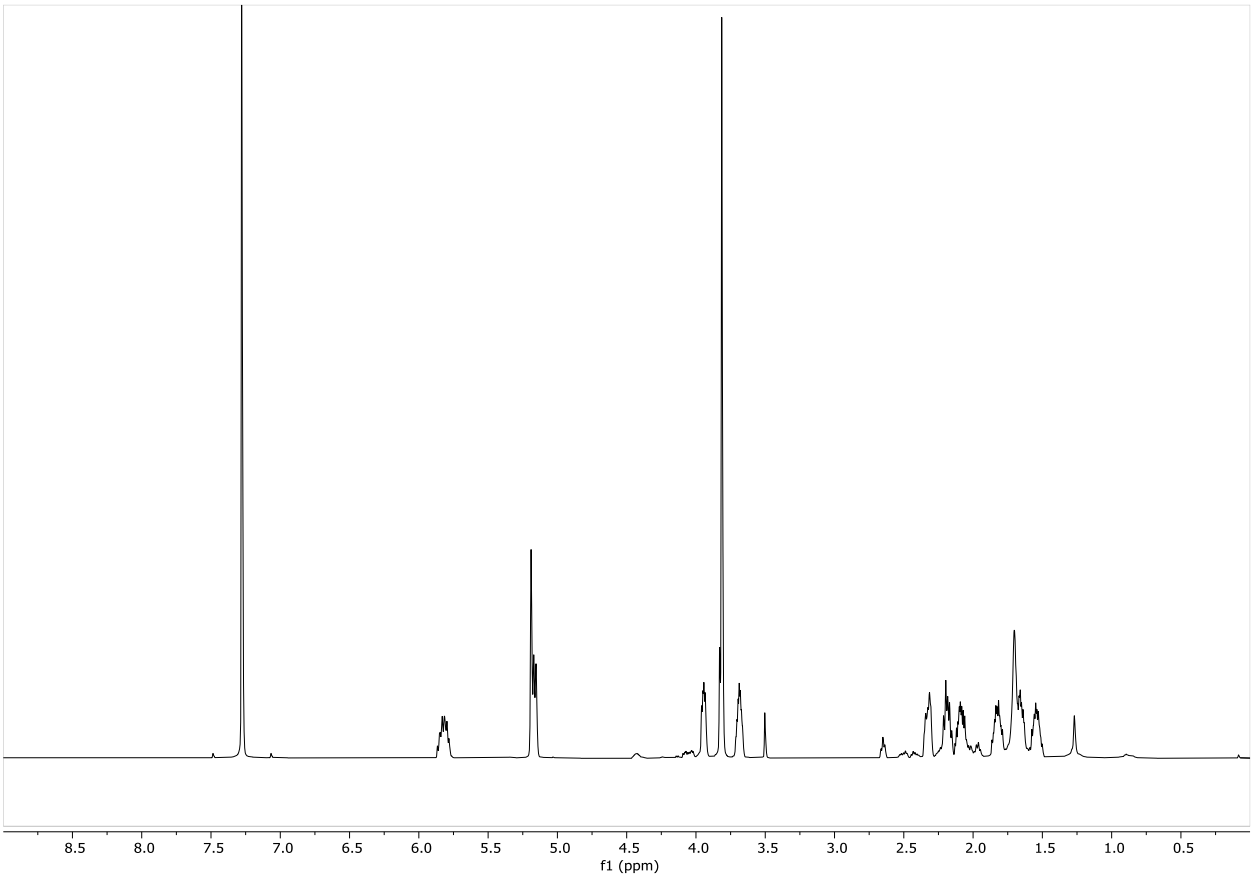

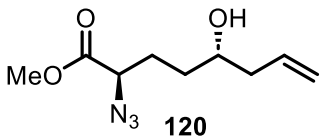
O
OH
MeO
N3

120

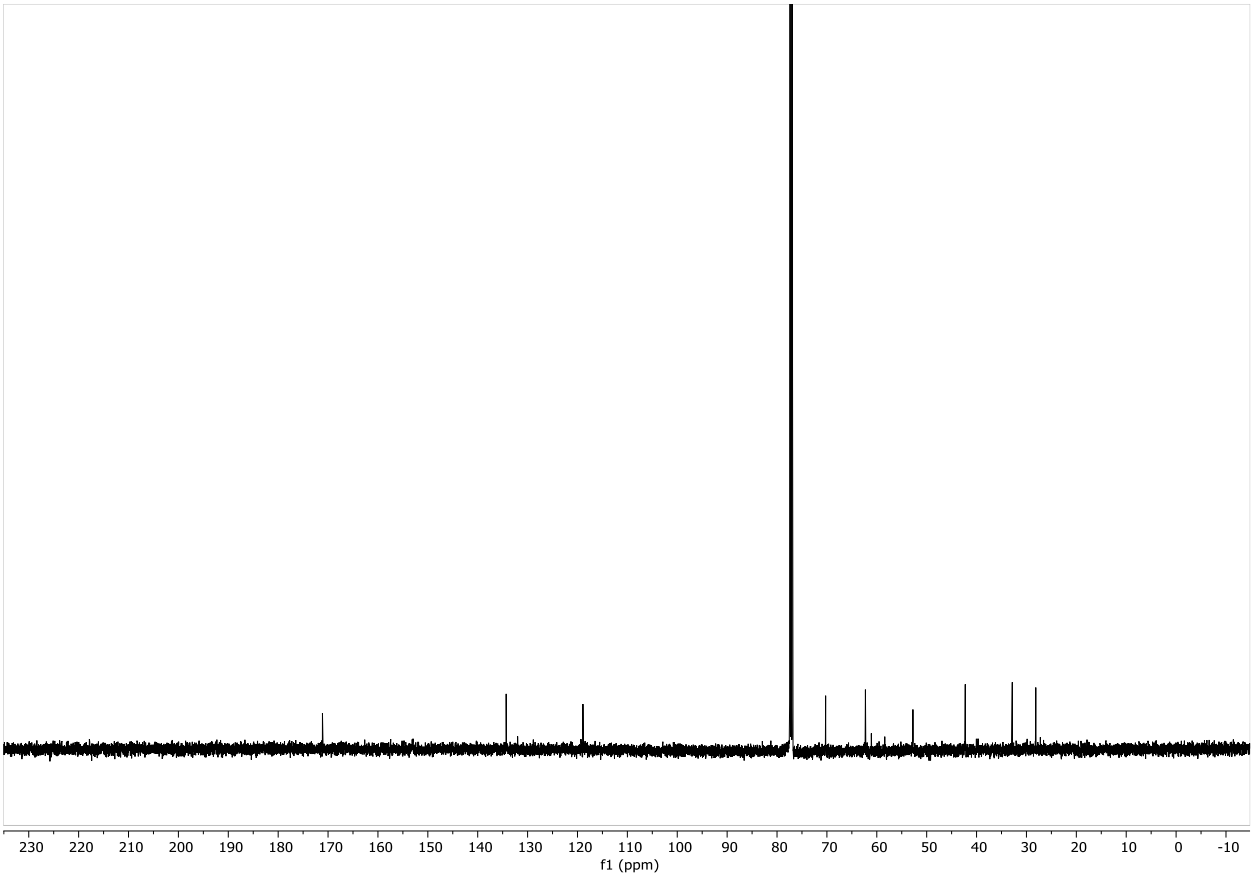
230 220 210 200 190 180 170 160 150 140 130 120 110 100 90 80 70 60 50 40 30 20 10 0 -10
f1 (ppm)

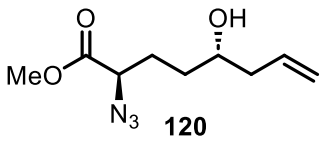
O
OH
MeO
N3

120

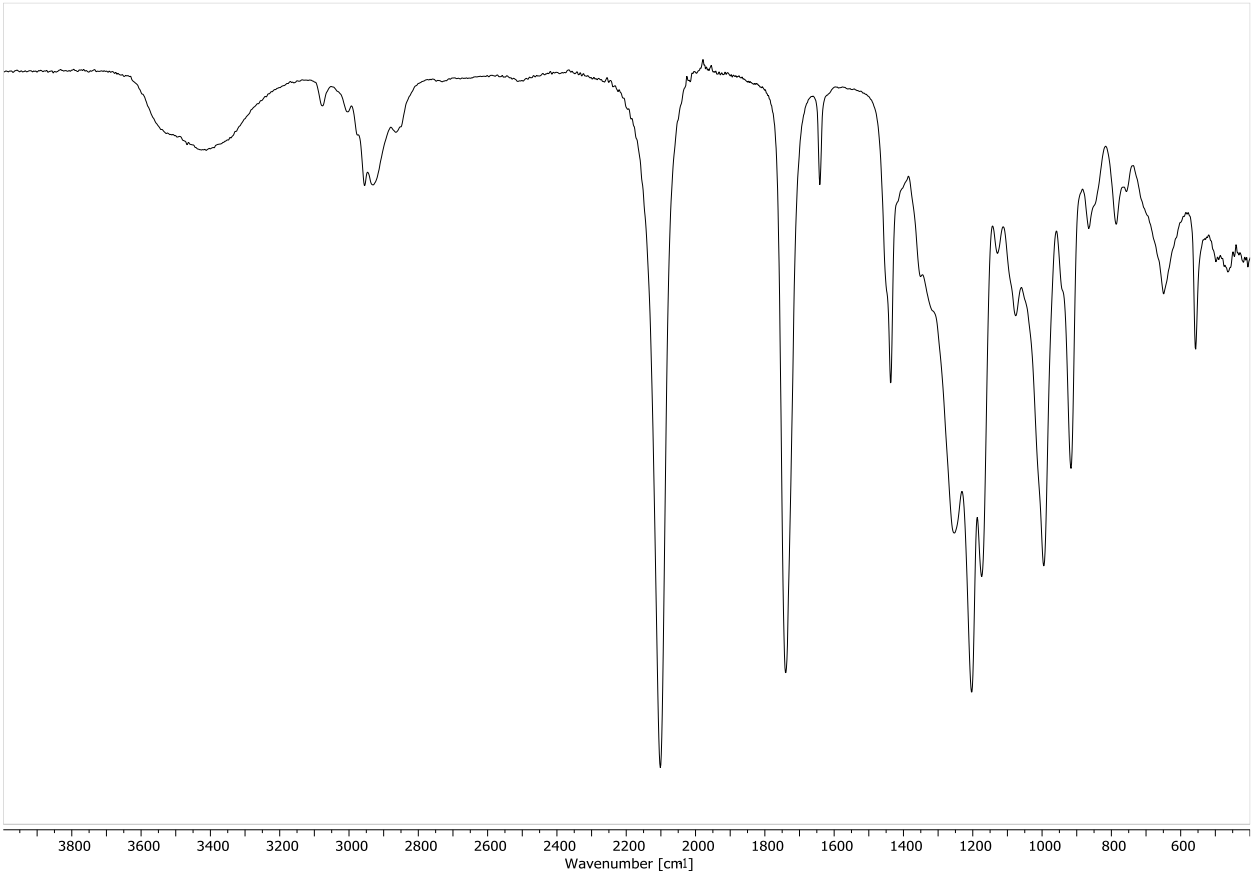
3800
3600
3400
3200
3000
2800
2600
2400
2200
2000
1800
1600
1400
1200
1000
800
600
Wavenumber [cm-1]

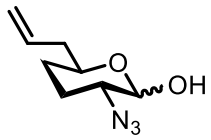

120.2

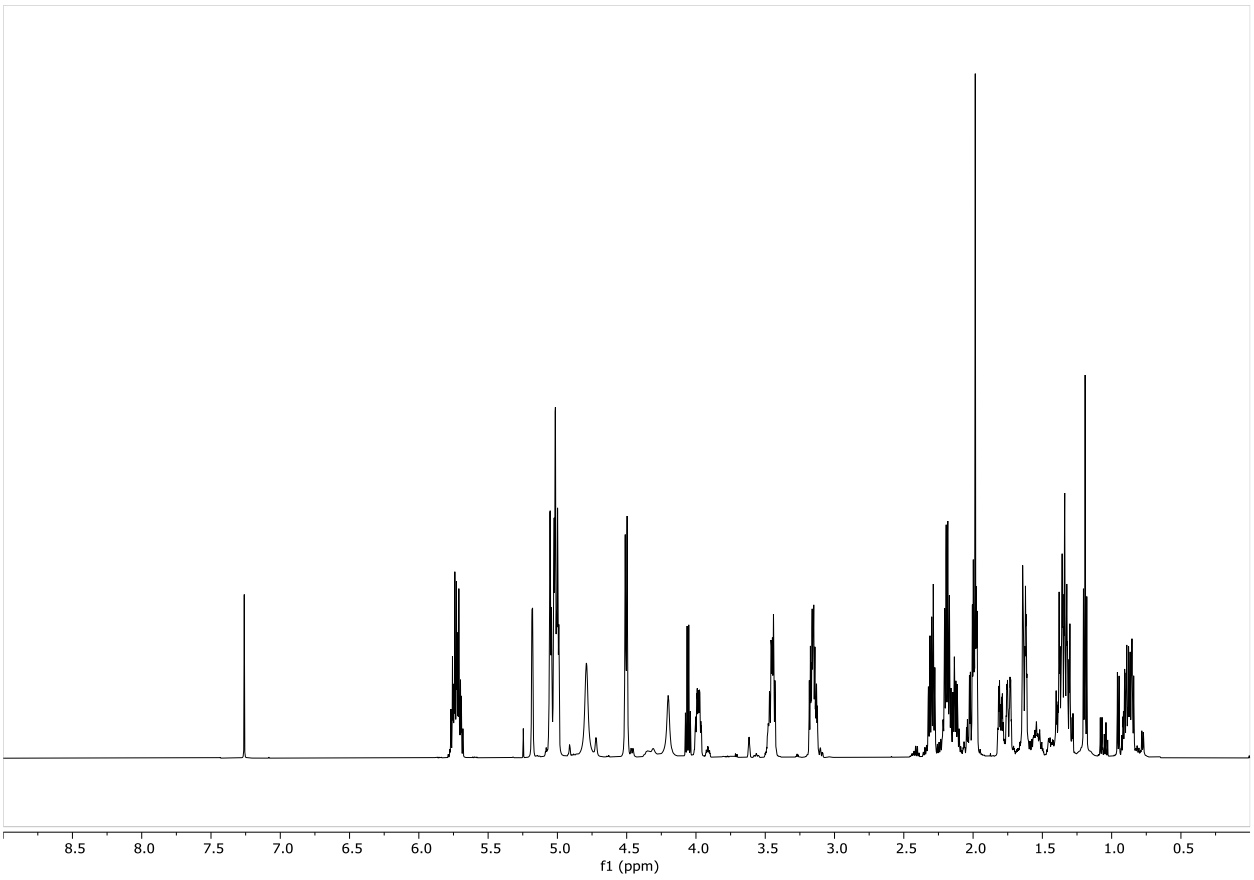

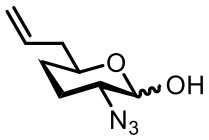
O
OH
N3

120.2

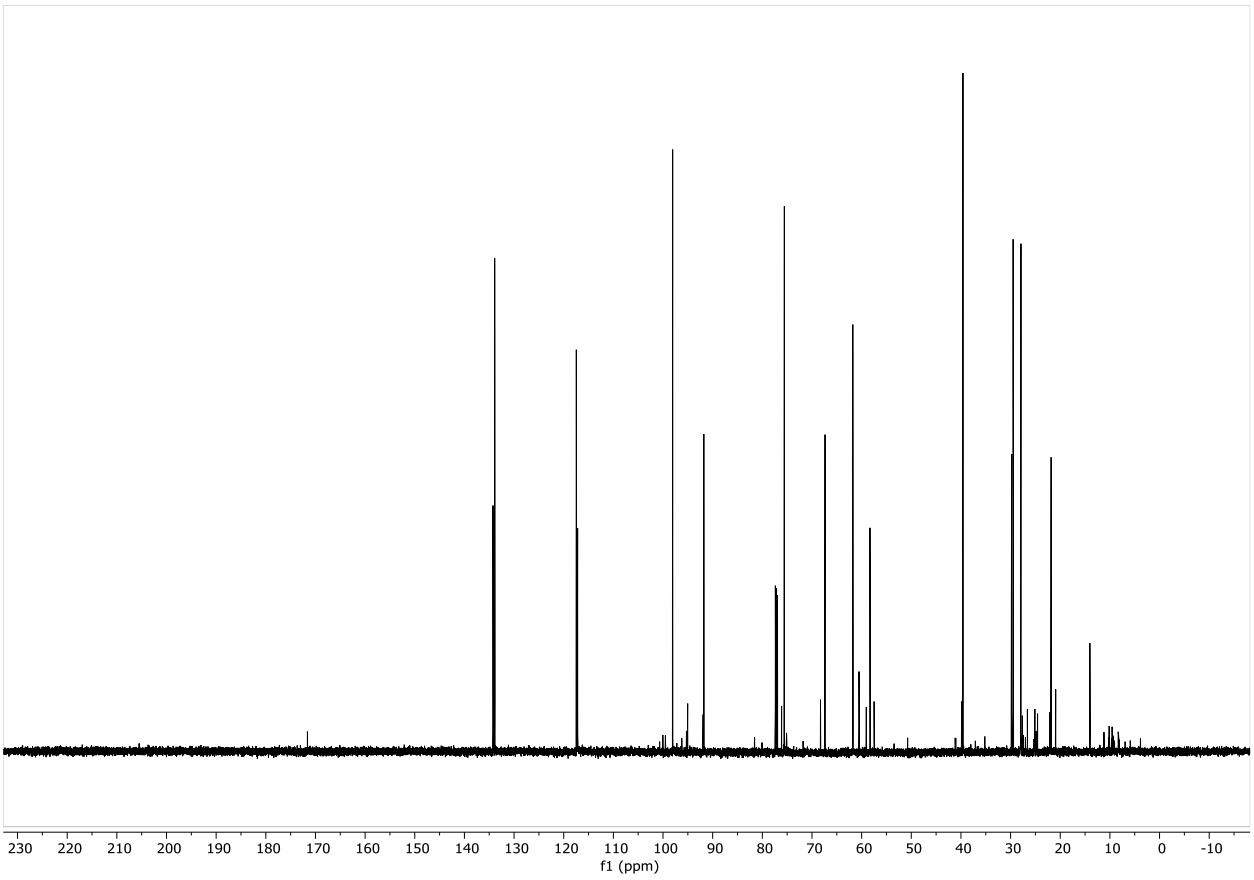
230 220 210 200 190 180 170 160 150 140 130 120 110 100 90 80 70 60 50 40 30 20 10 0 -10
f1 (ppm)

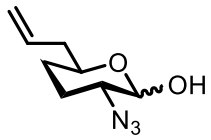
O
OH
N3

120.2

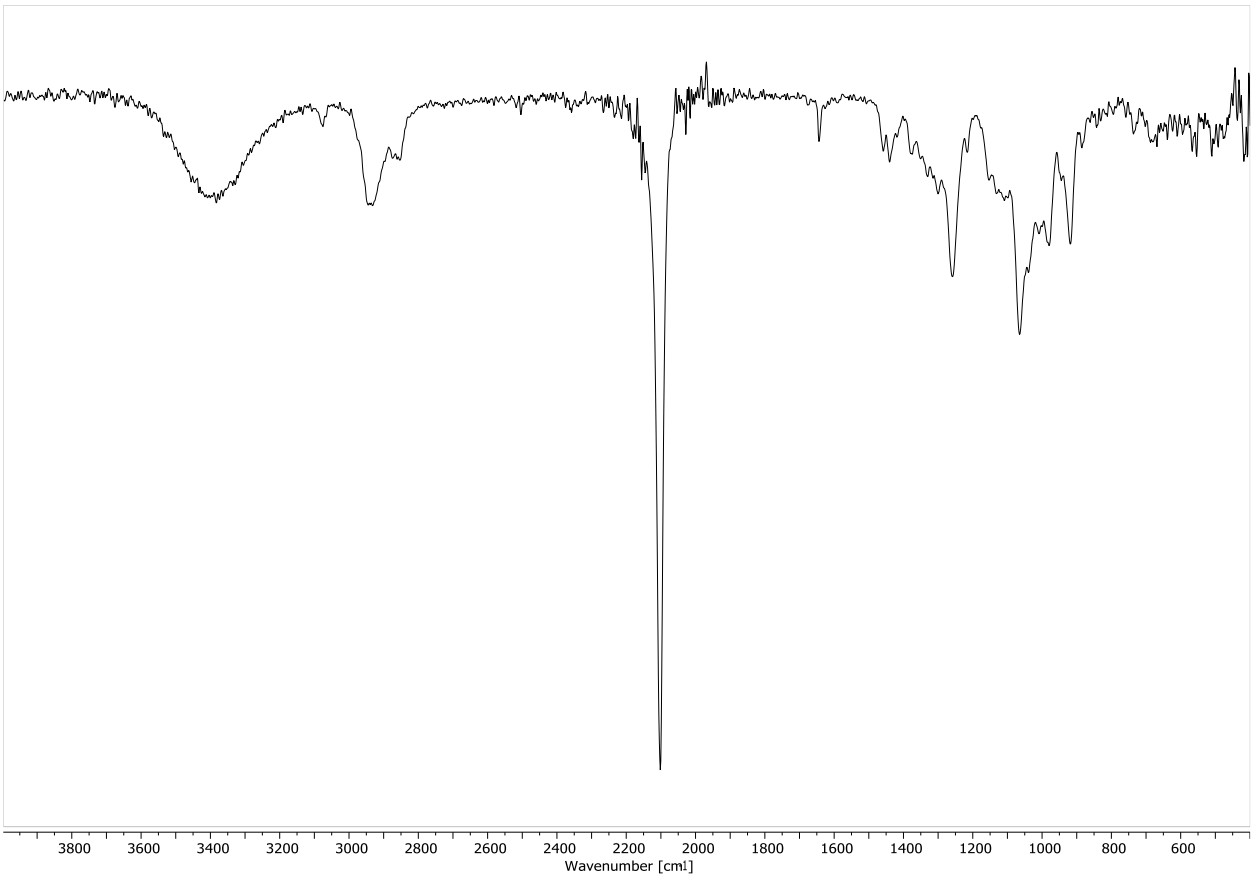
3800
3600
3400
3200
3000
2800
2600
2400
2200
2000
1800
1600
1400
1200
1000
800
600
Wavenumber [cm-1]

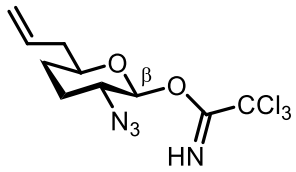
O
β
O
CCl3
N3
HN

121

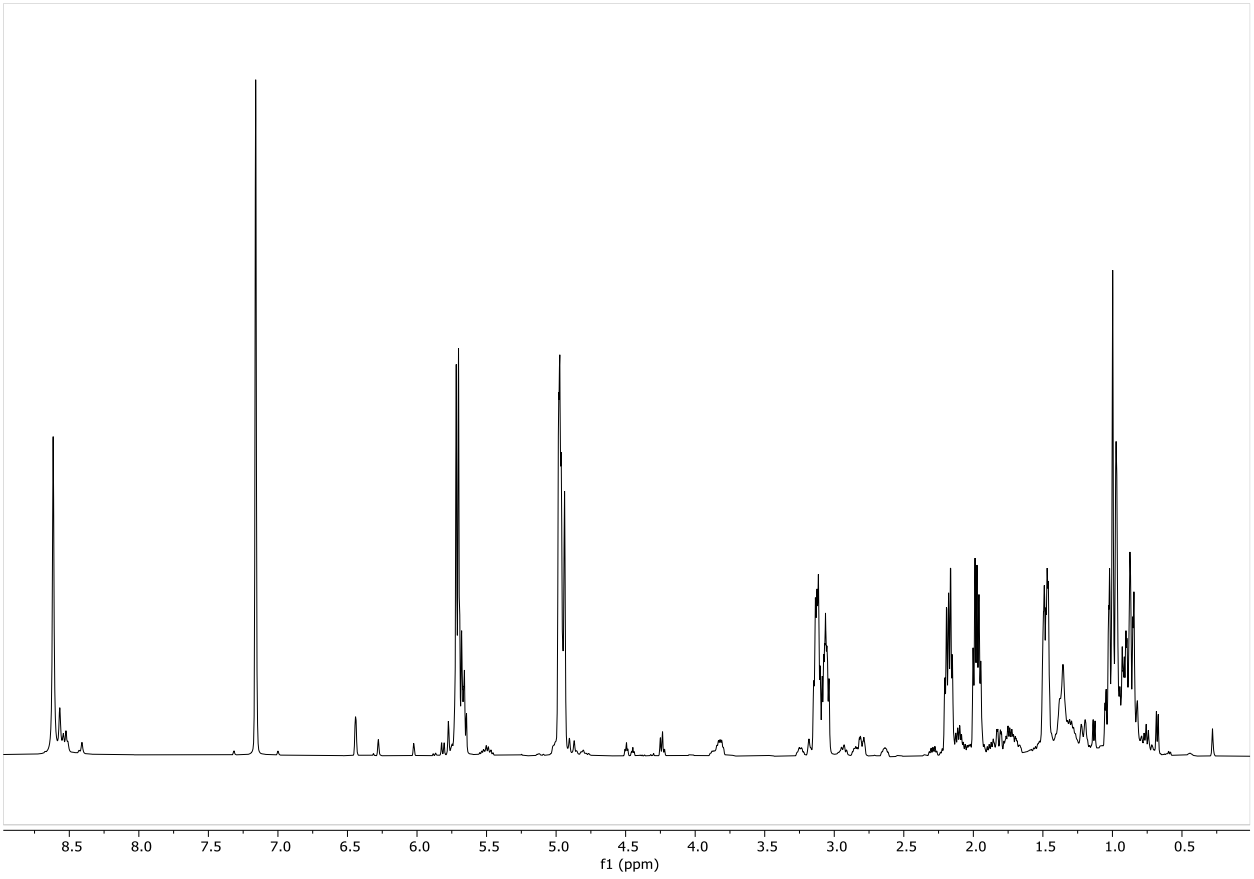
8.5
8.0
7.5
7.0
6.5
6.0
5.5
5.0
4.5
4.0
3.5
3.0
2.5
2.0
1.5
1.0
0.5
f1 (ppm)

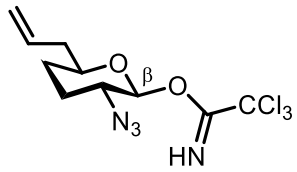
O
β
O
CCl3
N3
HN

121

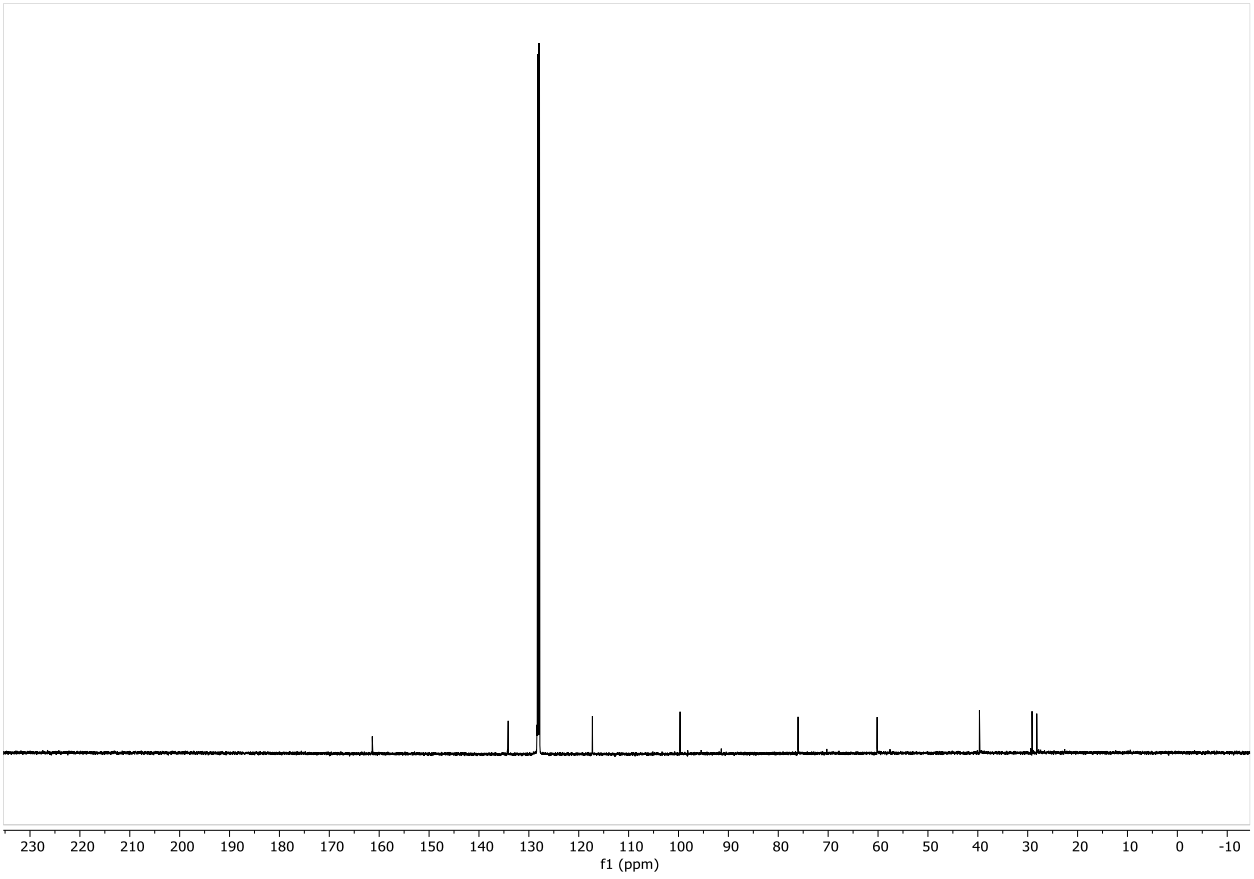
230 220 210 200 190 180 170 160 150 140 130 120 110 100 90 80 70 60 50 40 30 20 10 0 -10
f1 (ppm)

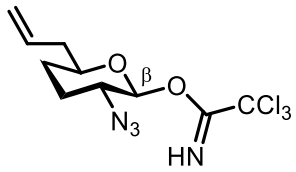
O
β
O
CCl3
N3
HN

121

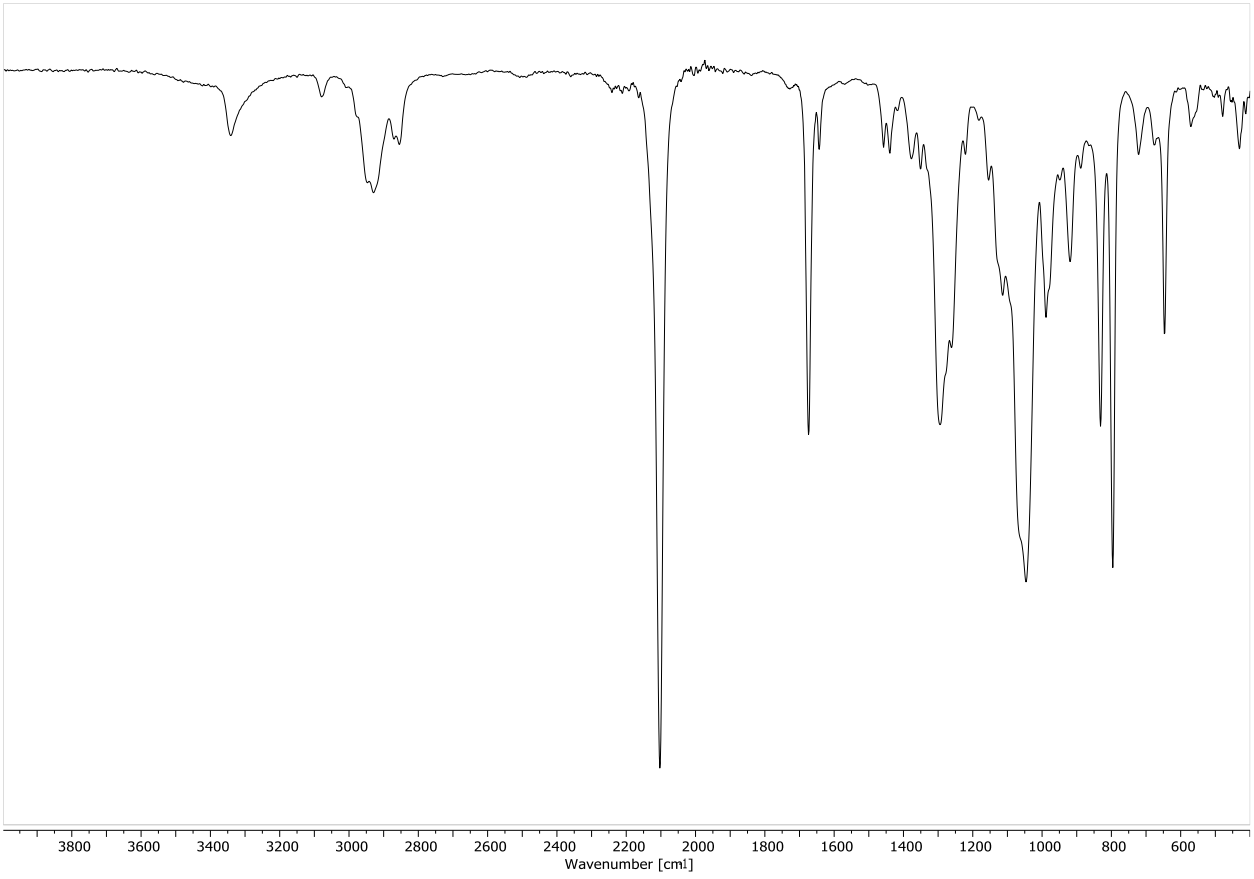
3800
3600
3400
3200
3000
2800
2600
2400
2200
2000
1800
1600
1400
1200
1000
800
600
Wavenumber [cm-1]

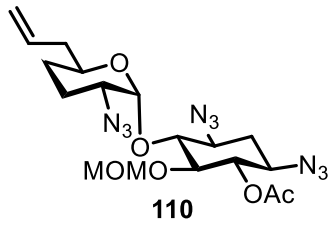
O
N3
N3
O
MOMO
N3
OAc

110

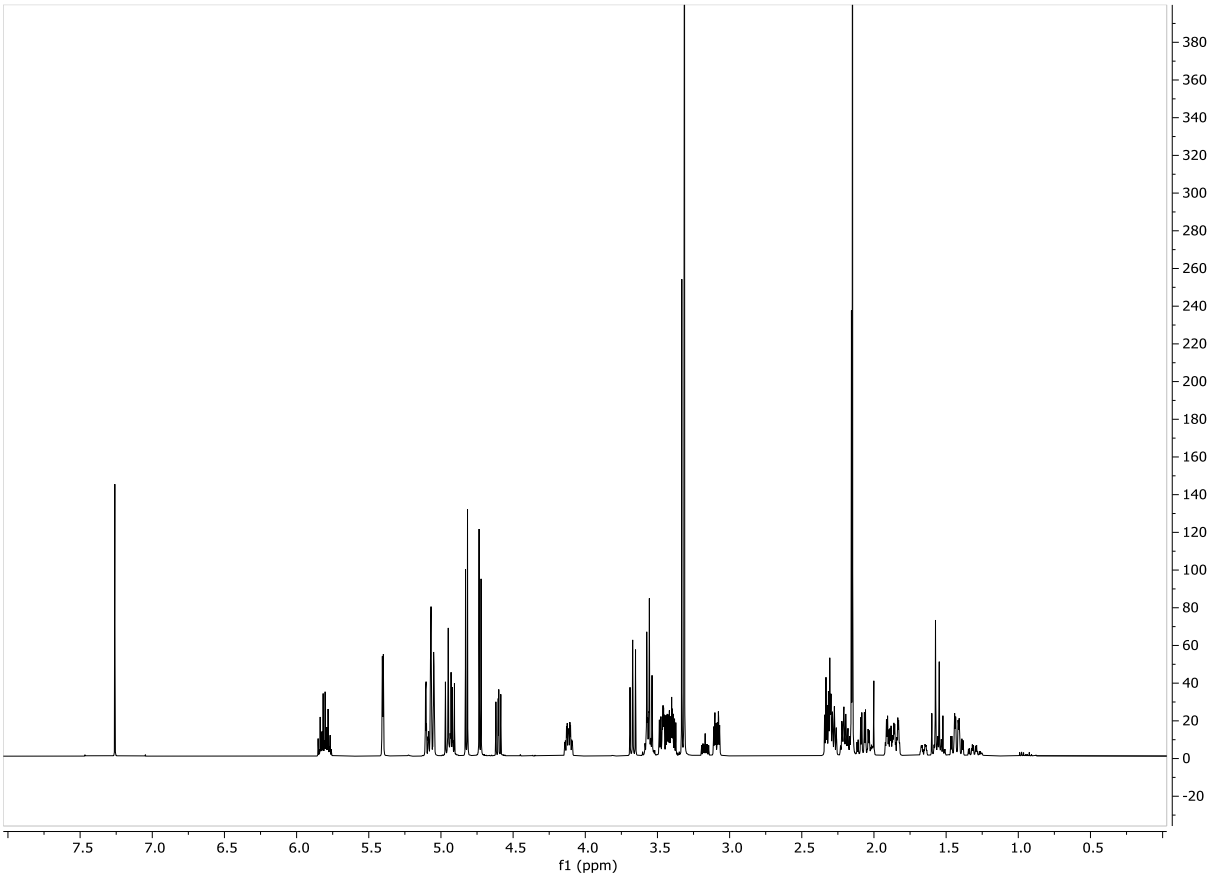
380
360
340
320
300
280
260
240
220
200
180
160
140
120
100
80
60
40
20
0
-20
7.5
7.0
6.5
6.0
5.5
5.0
4.5
4.0
3.5
3.0
2.5
2.0
1.5
1.0
0.5
f1 (ppm)

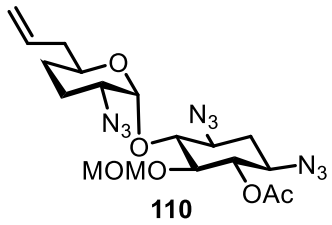
O
N3
N3
O
MOMO
N3
OAc

110

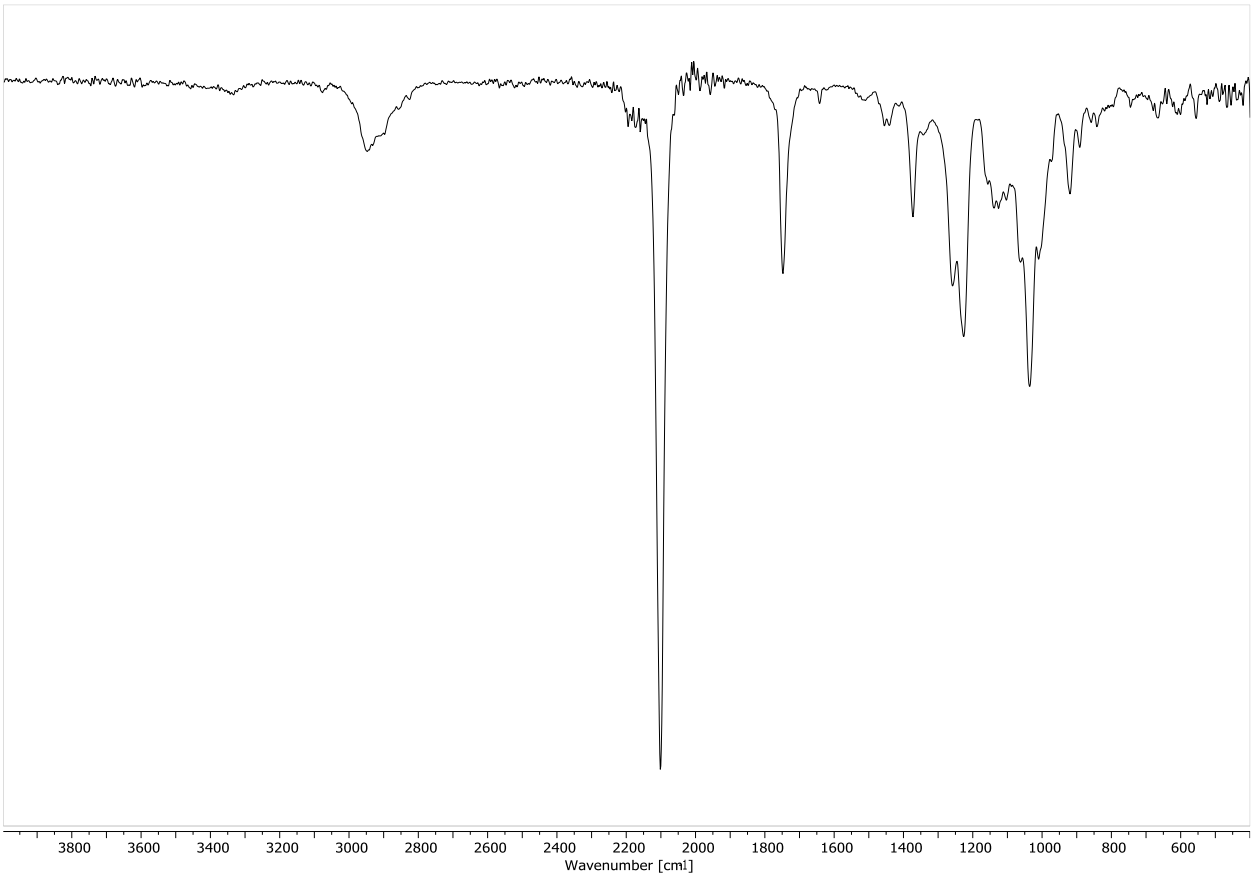
3800
3600
3400
3200
3000
2800
2600
2400
2200
2000
1800
1600
1400
1200
1000
800
600
Wavenumber [cm-1]

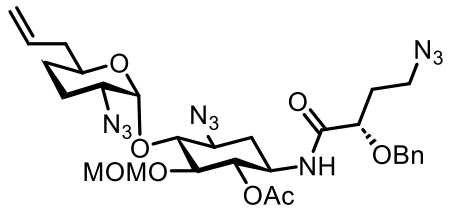
O
N3
O
MOMO
N3
OAc
NH
O
OBn
N3

123

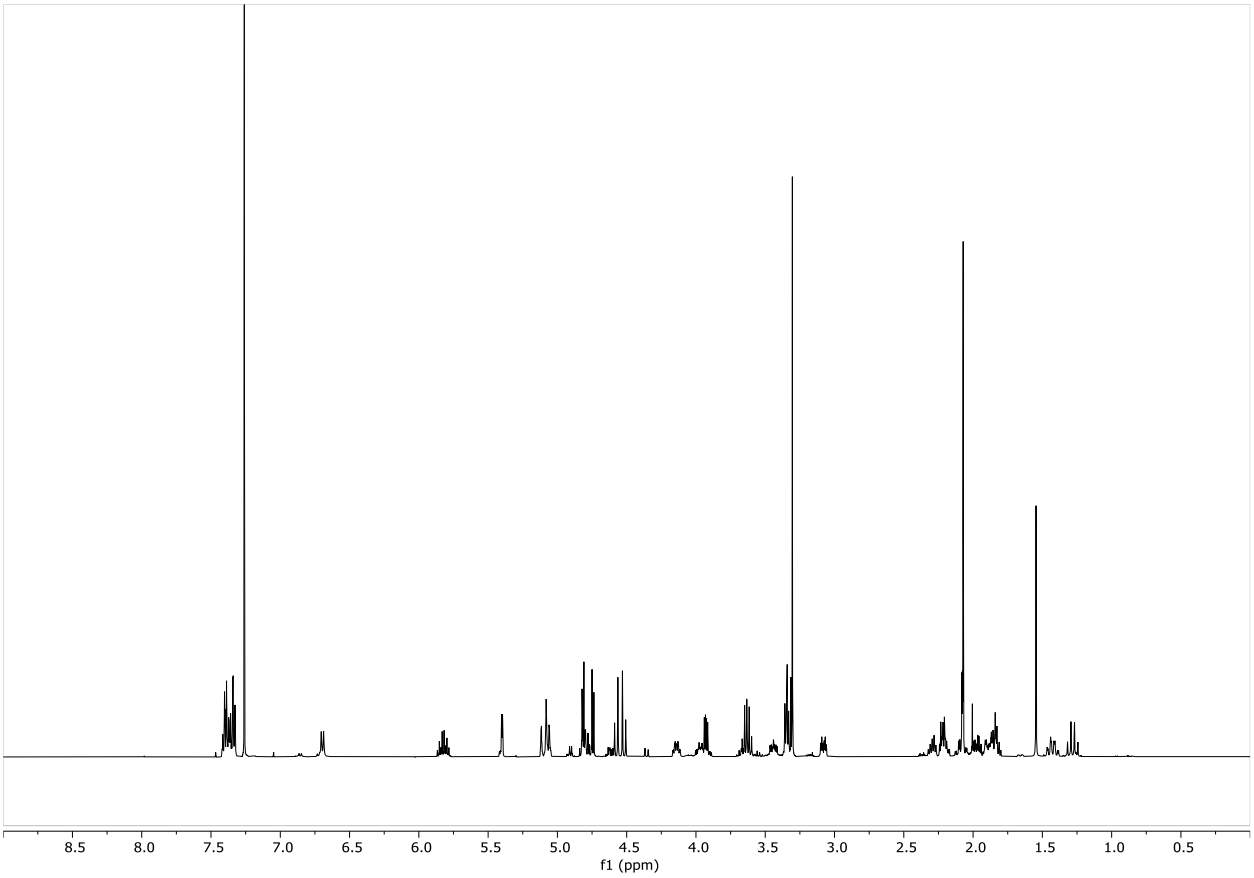
8.5
8.0
7.5
7.0
6.5
6.0
5.5
5.0
4.5
4.0
3.5
3.0
2.5
2.0
1.5
1.0
0.5
f1 (ppm)

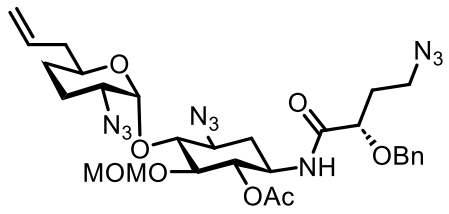
O
N3
N3
O
MOMO
N3
O
NH
OBn
OAc

123

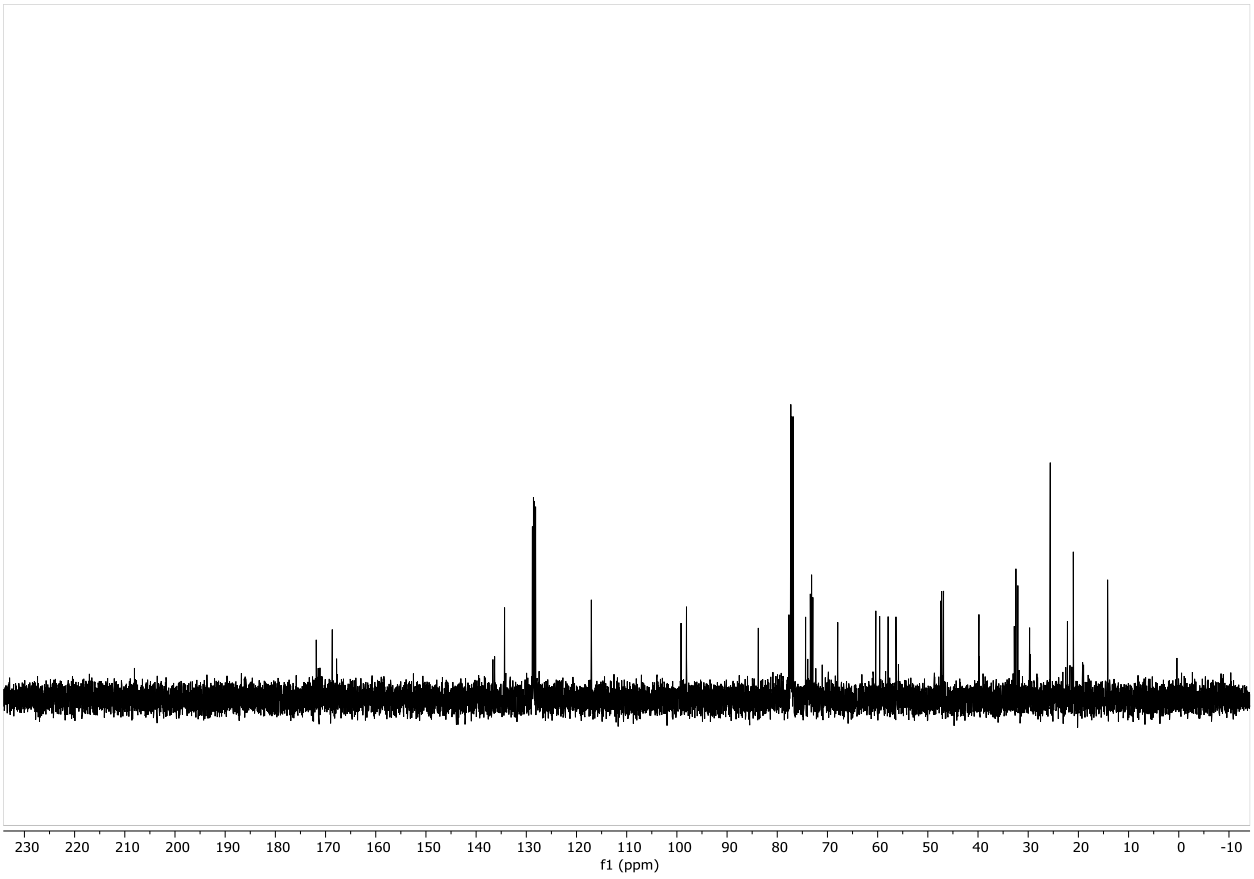
230 220 210 200 190 180 170 160 150 140 130 120 110 100 90 80 70 60 50 40 30 20 10 0 -10
f1 (ppm)

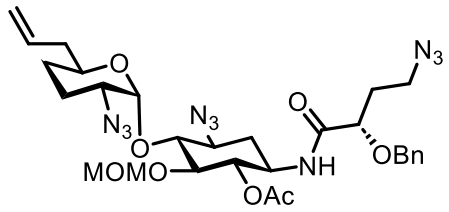
O
N3
O
MOMO
N3
NH
O
OAc
N3
OBn

123

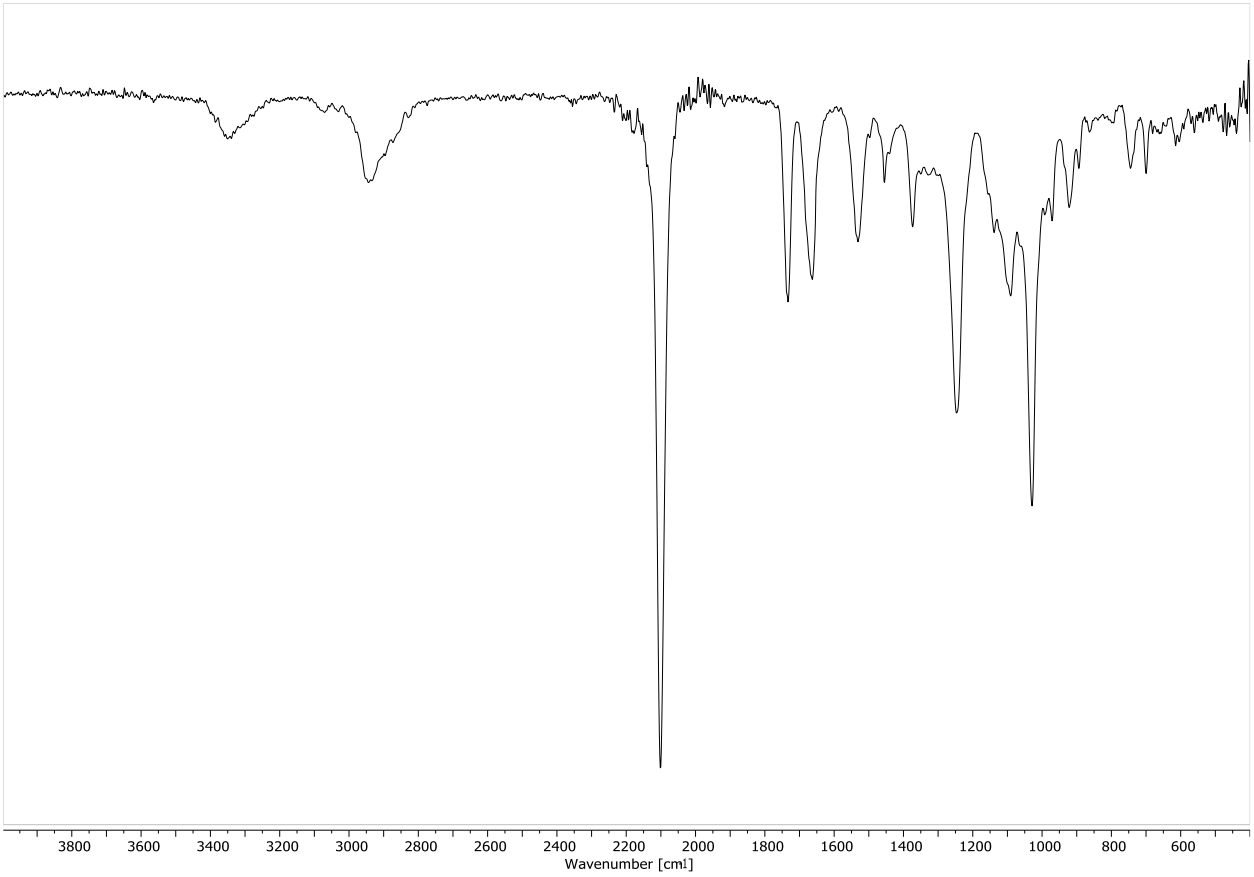
3800
3600
3400
3200
3000
2800
2600
2400
2200
2000
1800
1600
1400
1200
1000
800
600
Wavenumber [cm-1]

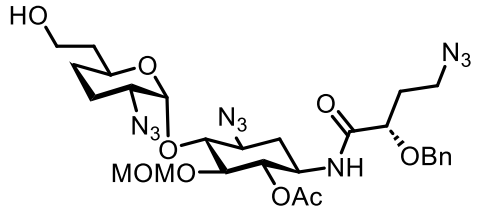
HO
O
N3
O
MOMO
N3
O
NH
OBn
N3
OAc

124

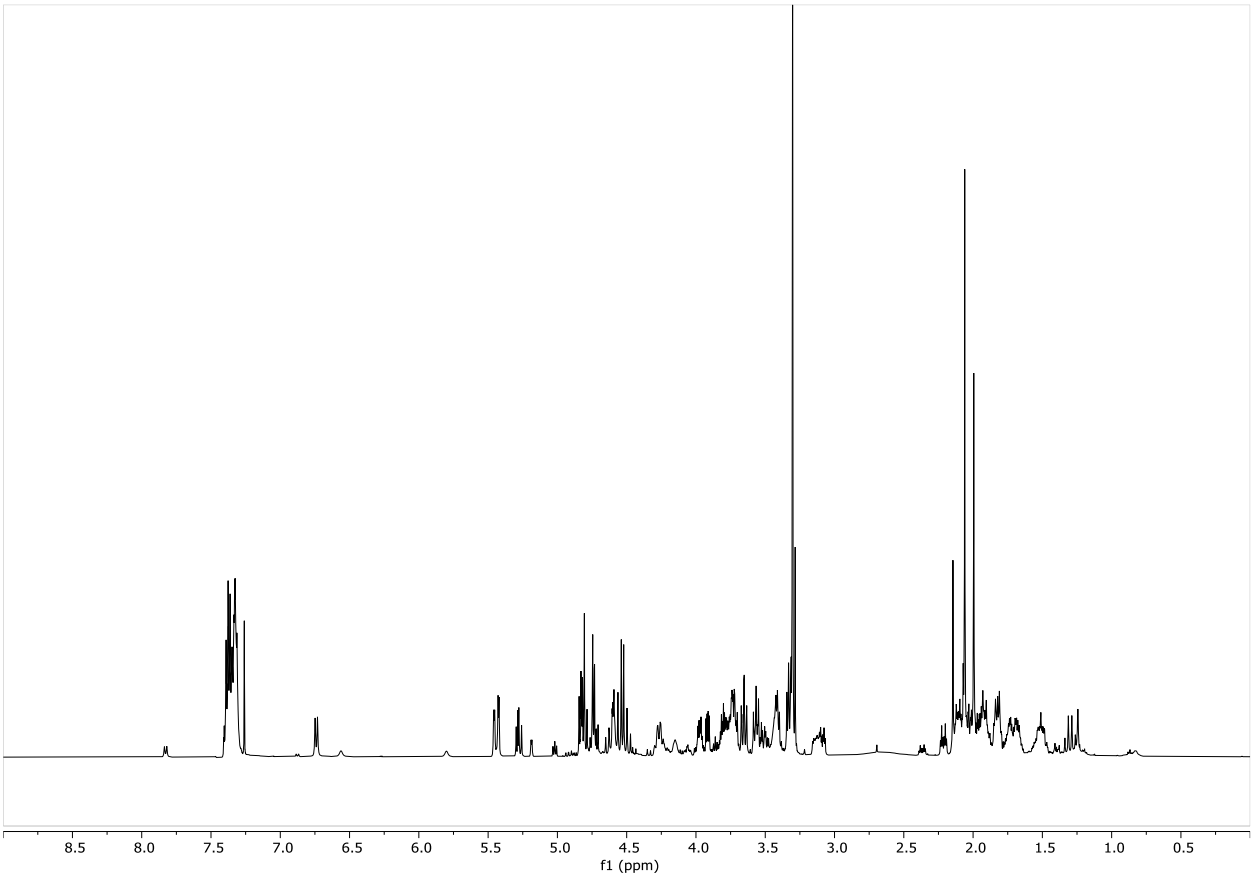
8.5
8.0
7.5
7.0
6.5
6.0
5.5
5.0
4.5
4.0
3.5
3.0
2.5
2.0
1.5
1.0
0.5
f1 (ppm)

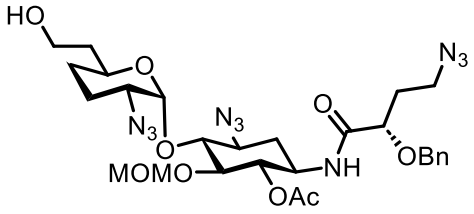
HO
O
N3
N3
O
MOMO
N3
O
NH
OBn
N3
OAc

124

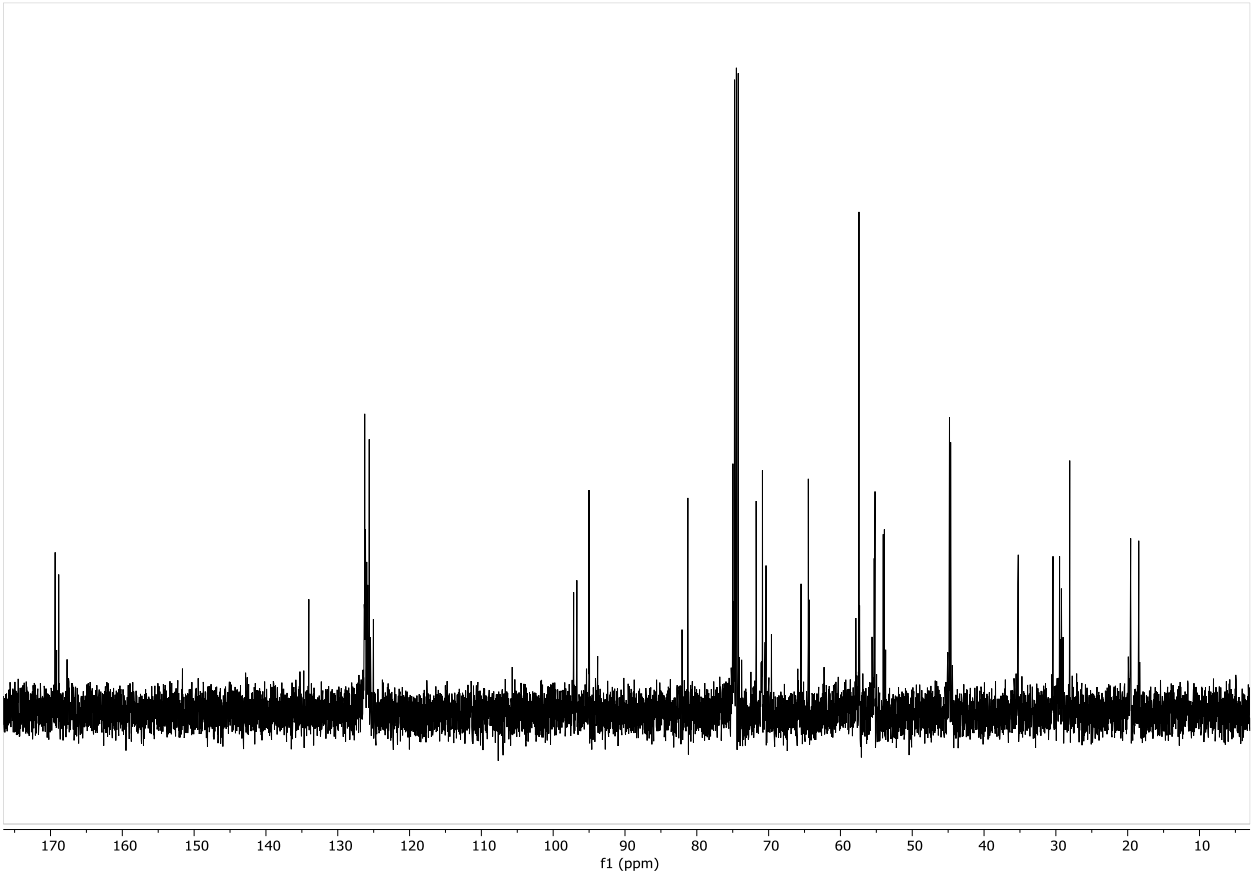
170
160
150
140
130
120
110
100
90
80
70
60
50
40
30
20
10
f1 (ppm)

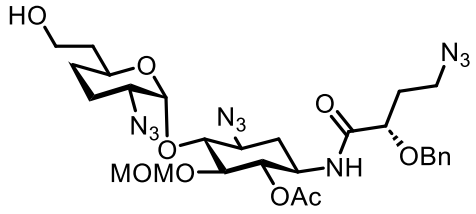
HO
O
N3
N3
O
MOMO
N3
O
NH
OBn
OAc

124

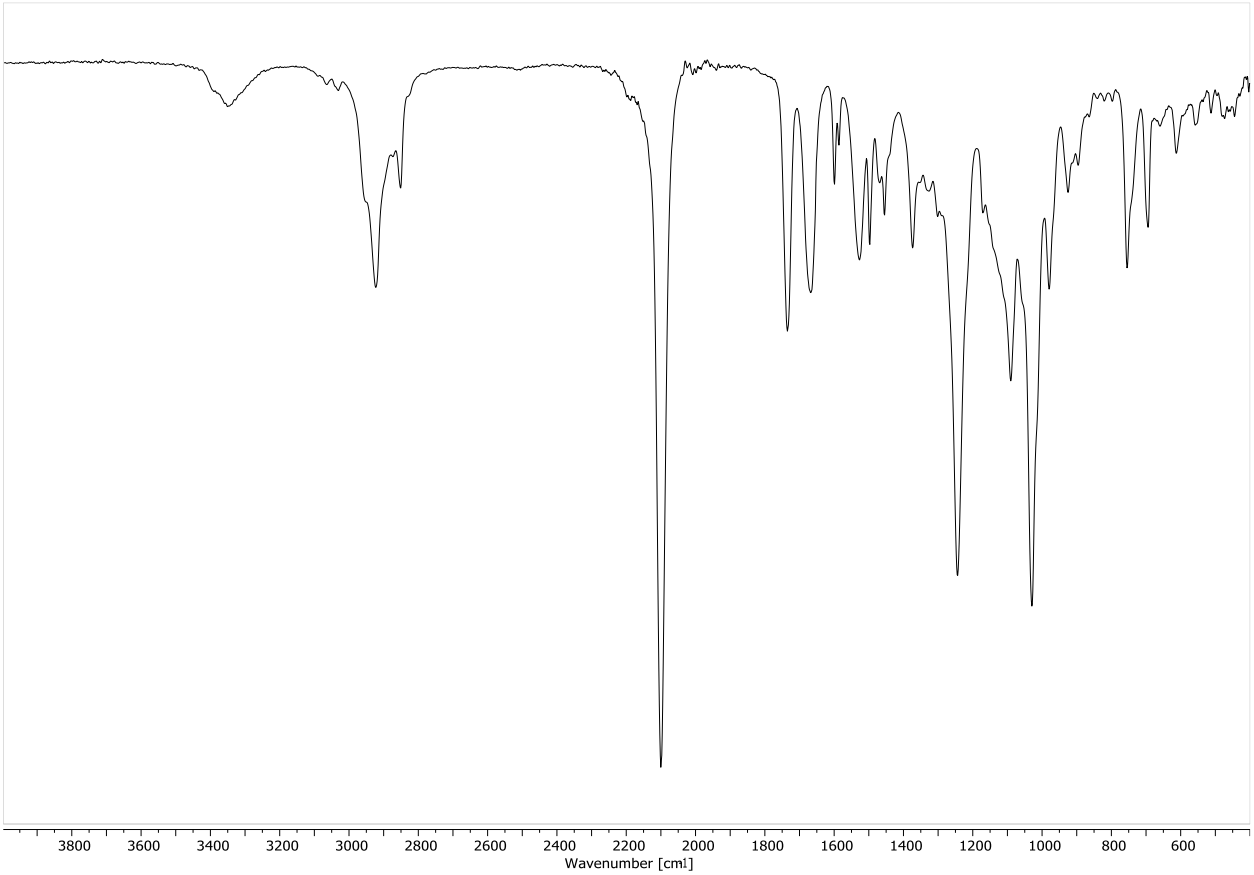
3800
3600
3400
3200
3000
2800
2600
2400
2200
2000
1800
1600
1400
1200
1000
800
600
Wavenumber [cm-1]

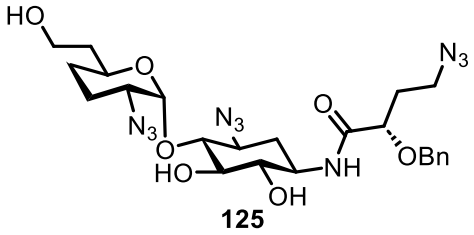
HO
O
N3
O
HO
N3
OH
NH
O
OBn
N3

125

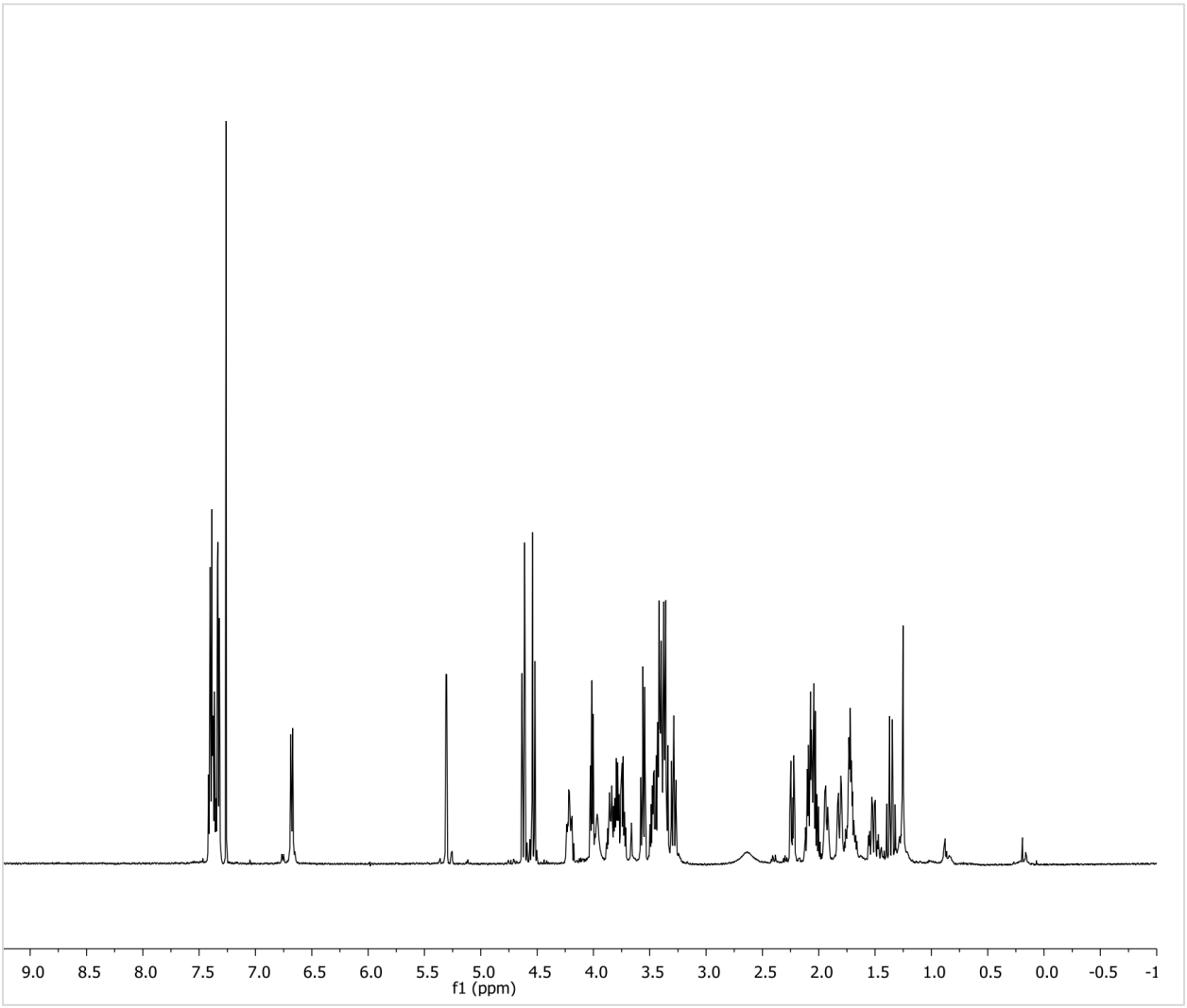
9.0
8.5
8.0
7.5
7.0
6.5
6.0
5.5
5.0
4.5
4.0
3.5
3.0
2.5
2.0
1.5
1.0
0.5
0.0
-0.5
-1
f1 (ppm)

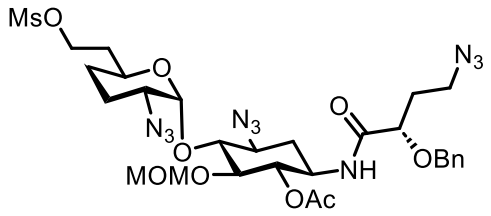
MsO
O
N3
O
N3
MOMO
OAc
N3
O
NH
OBn
N3

126

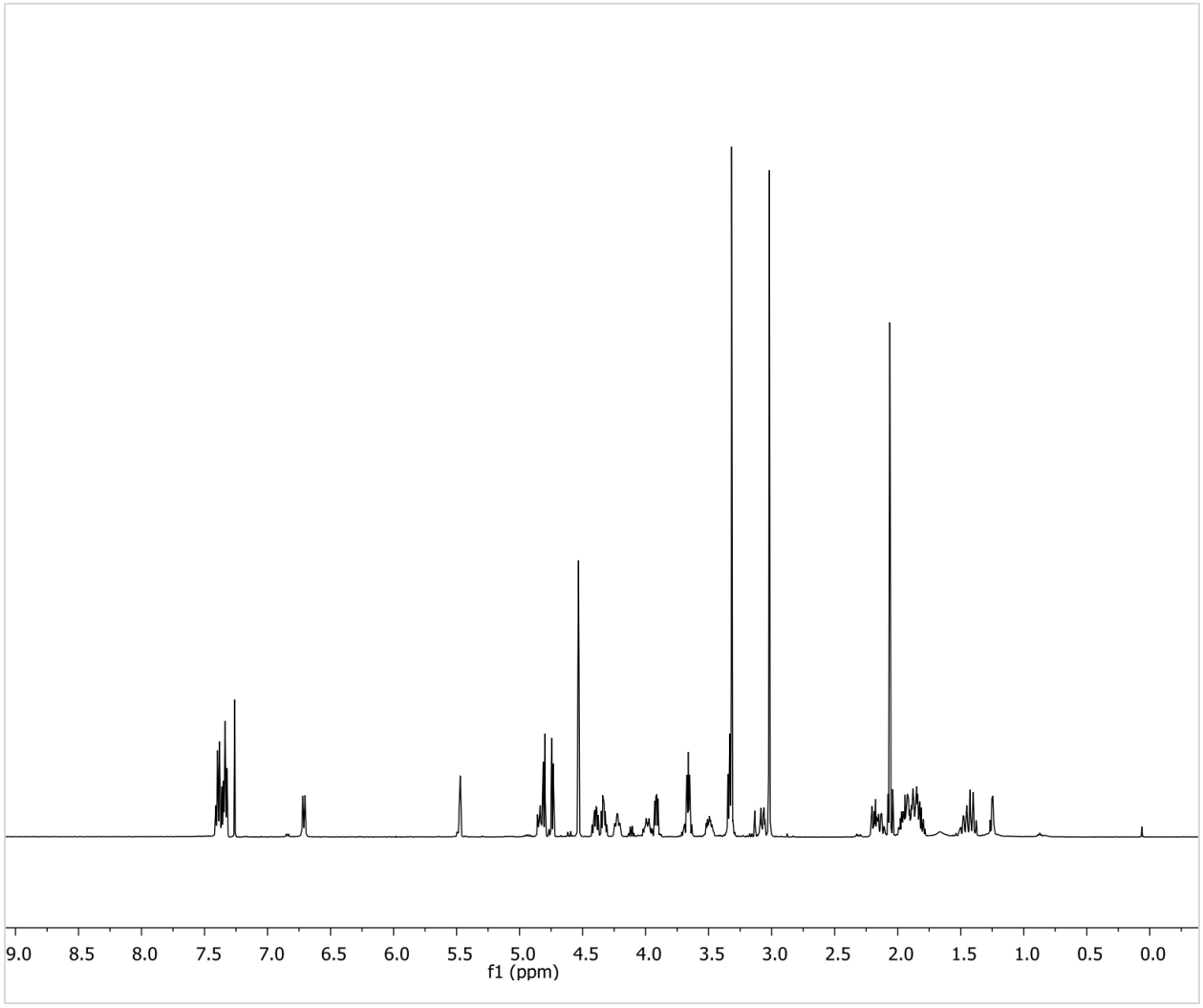
9.0
8.5
8.0
7.5
7.0
6.5
6.0
5.5
5.0
4.5
4.0
3.5
3.0
2.5
2.0
1.5
1.0
0.5
0.0
f1 (ppm)

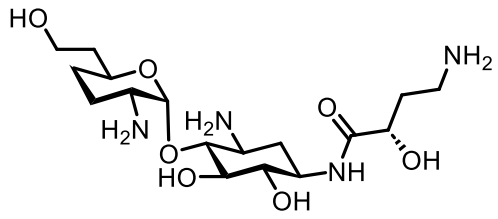
HO
O
H2N
H2N
O
HO
OH
NH
O
OH
NH2

127

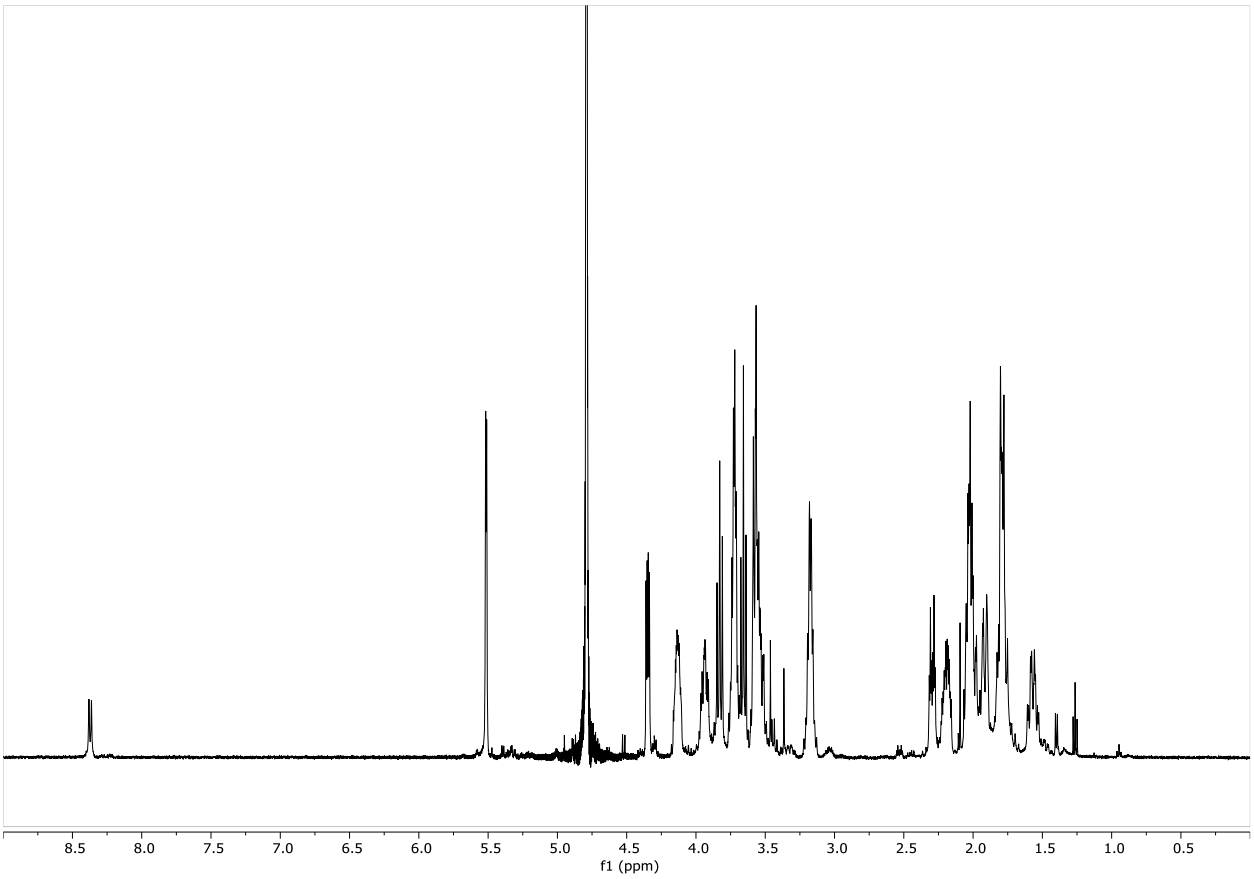
8.5
8.0
7.5
7.0
6.5
6.0
5.5
5.0
4.5
4.0
3.5
3.0
2.5
2.0
1.5
1.0
0.5
f1 (ppm)

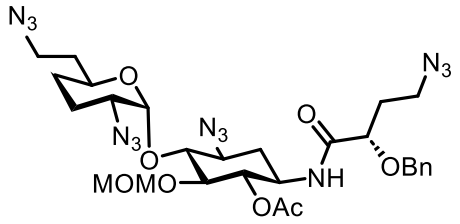
N3
O
N3
O
N3
MOMO
OAc
NH
O
OBn
N3

128

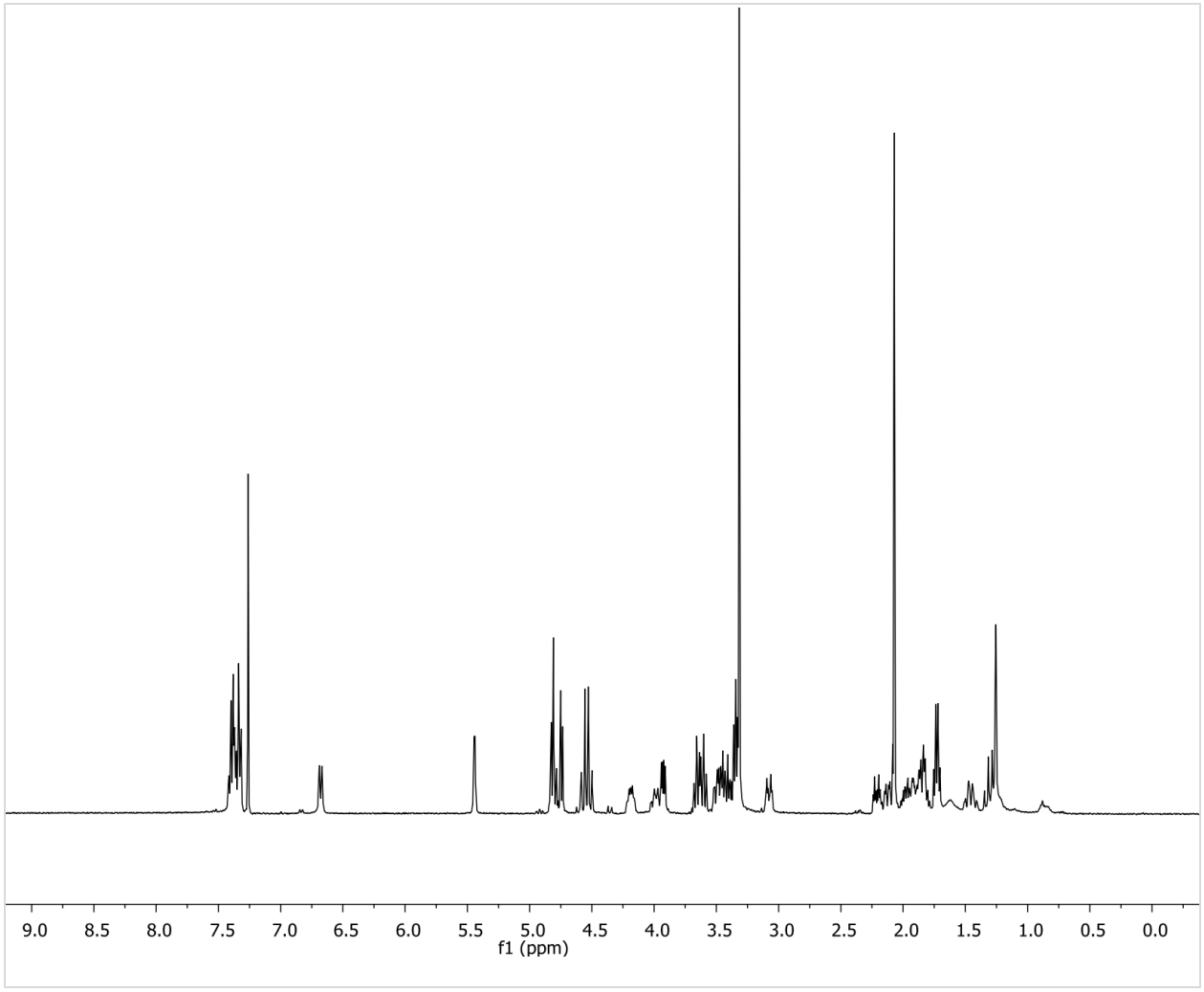
9.0
8.5
8.0
7.5
7.0
6.5
6.0
5.5
5.0
4.5
4.0
3.5
3.0
2.5
2.0
1.5
1.0
0.5
0.0
f1 (ppm)

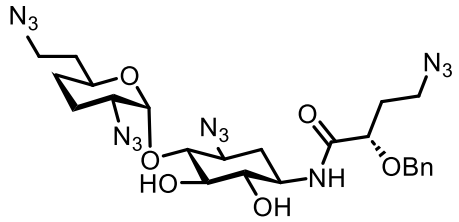

129

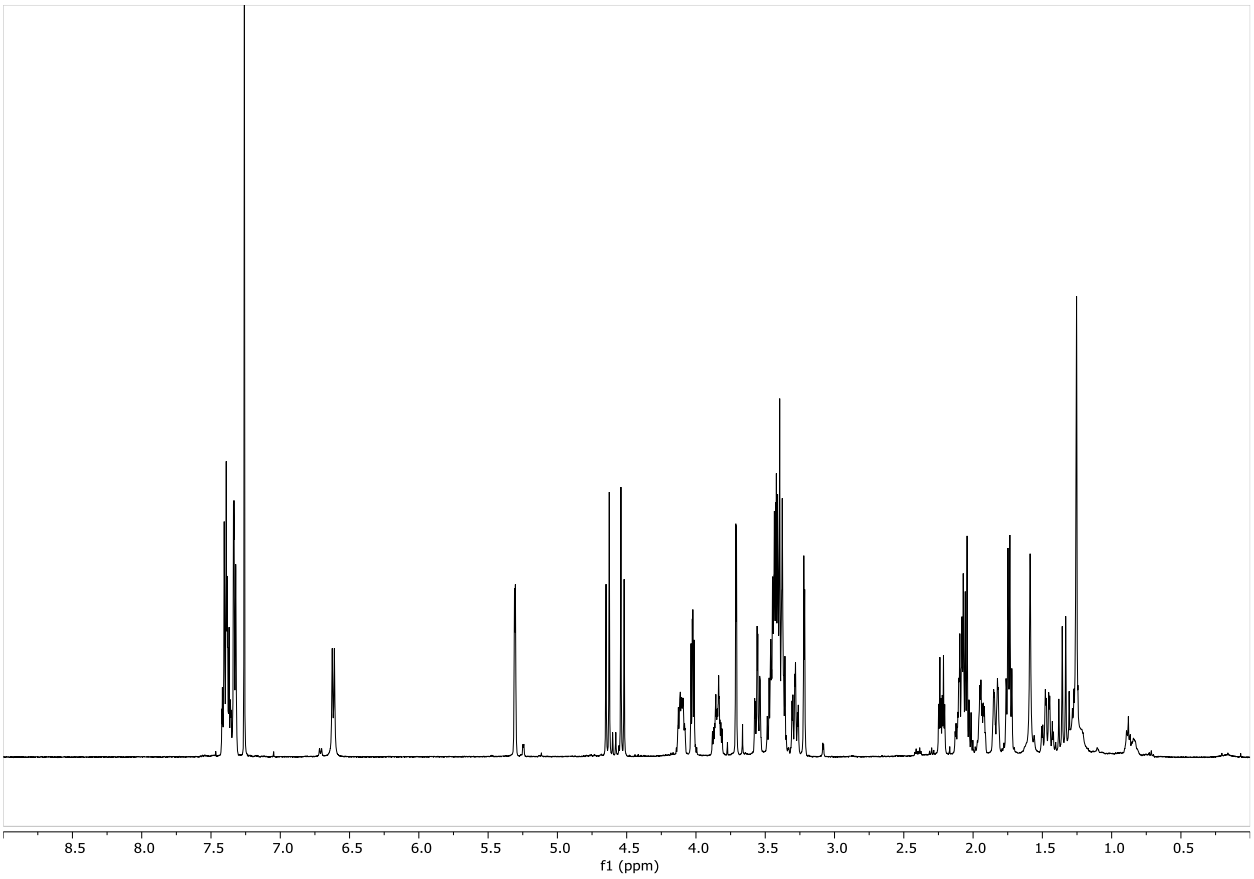

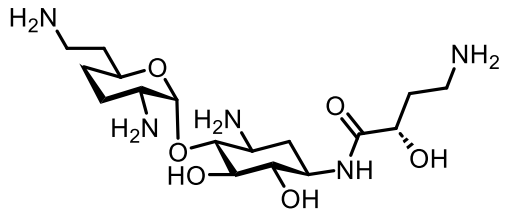
H2N
O
H2N
H2N
O
HO
OH
NH
O
OH
NH2

130

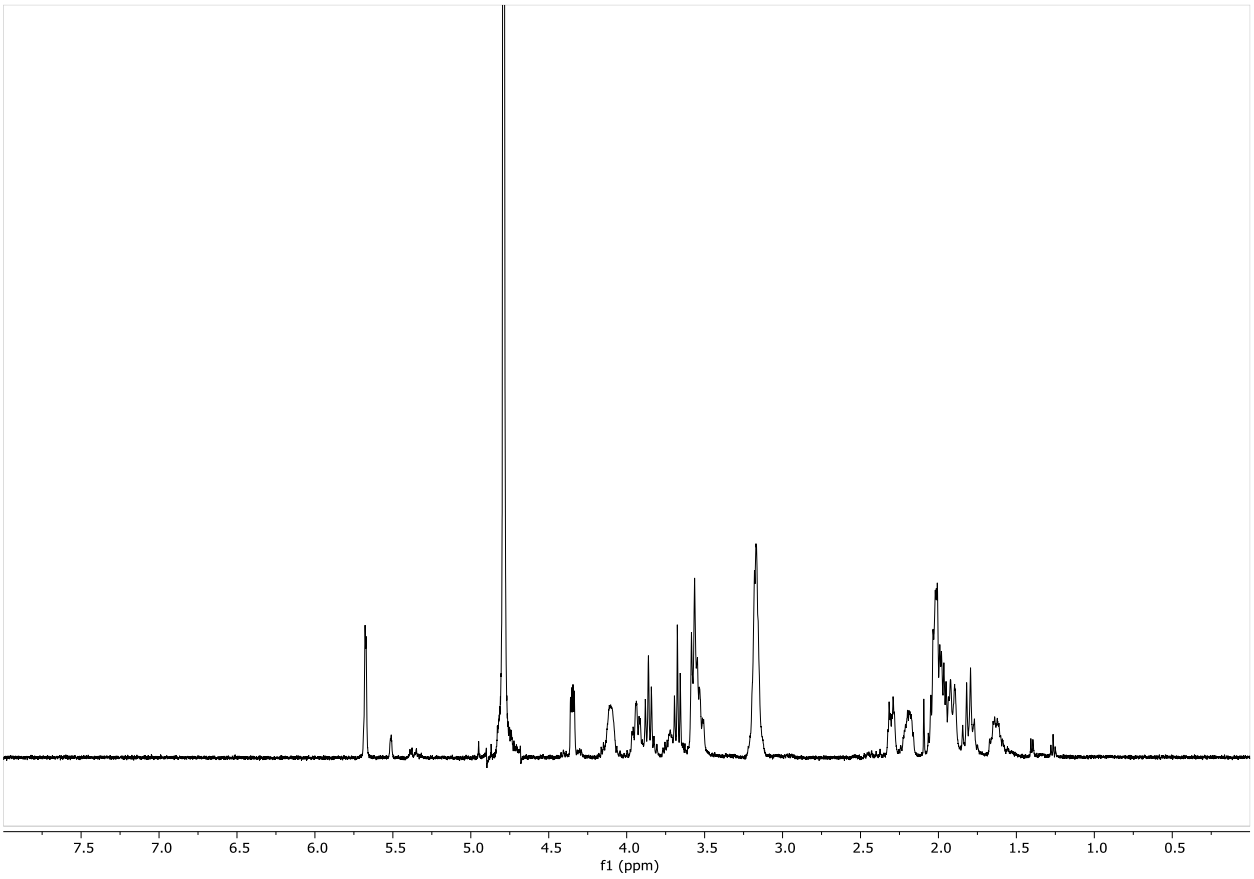
7.5
7.0
6.5
6.0
5.5
5.0
4.5
4.0
3.5
3.0
2.5
2.0
1.5
1.0
0.5
f1 (ppm)

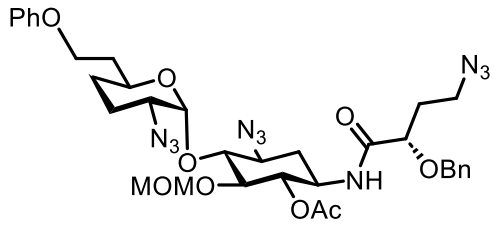
PhO
O
N3
N3
O
MOMO
N3
O
NH
OBn
N3
OAc

131

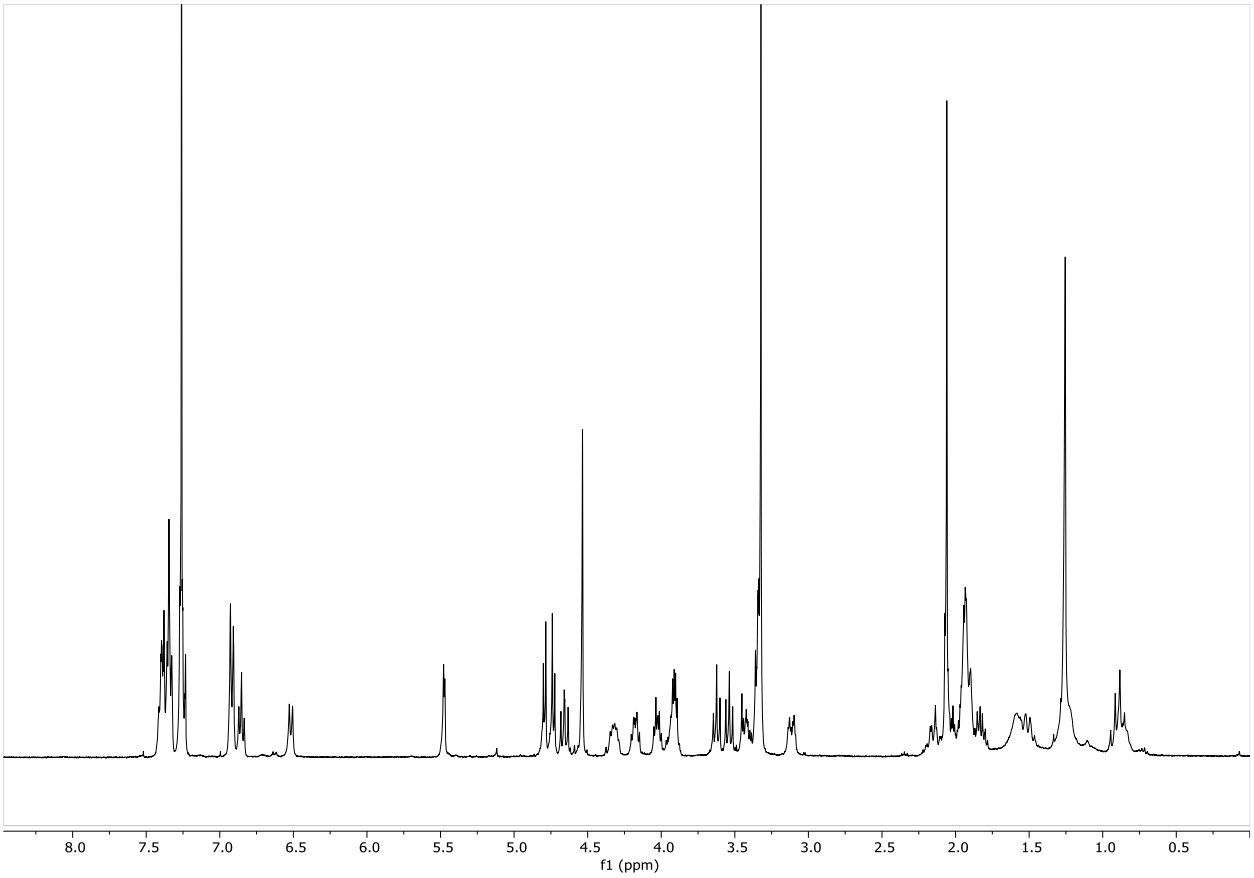
8.0
7.5
7.0
6.5
6.0
5.5
5.0
4.5
4.0
3.5
3.0
2.5
2.0
1.5
1.0
0.5
f1 (ppm)

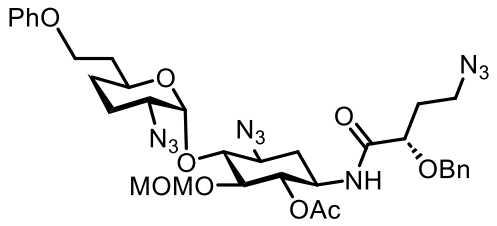
PhO
O
N3
N3
O
MOMO
N3
O
NH
OBn
N3
OAc

131

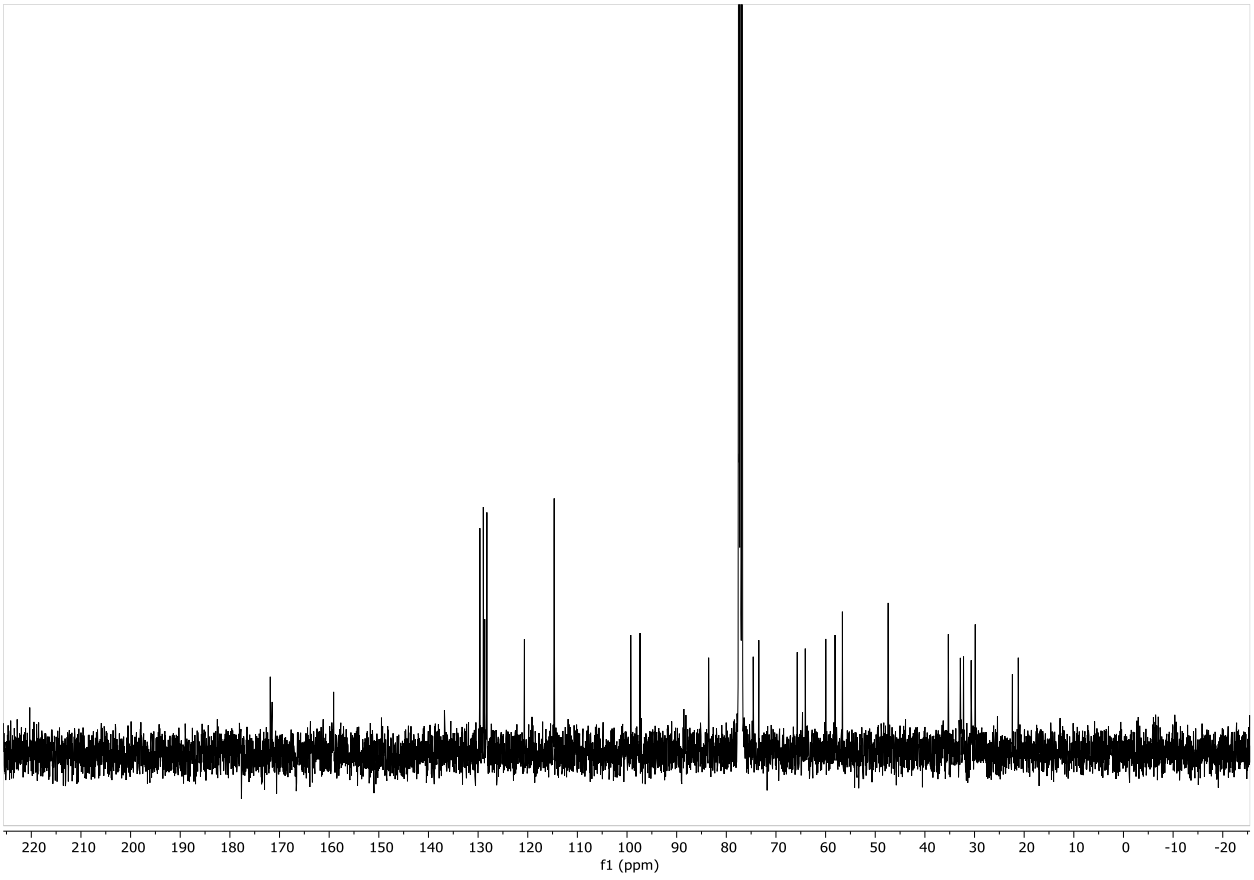
220 210 200 190 180 170 160 150 140 130 120 110 100 90 80 70 60 50 40 30 20 10 0 -10 -20
f1 (ppm)

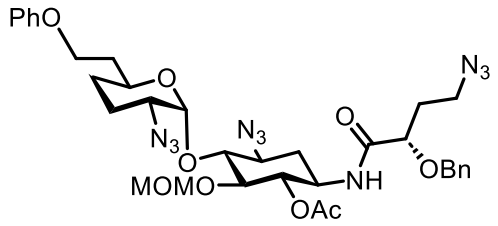
PhO
O
N3
N3
O
MOMO
N3
O
NH
OBn
N3
OAc

131

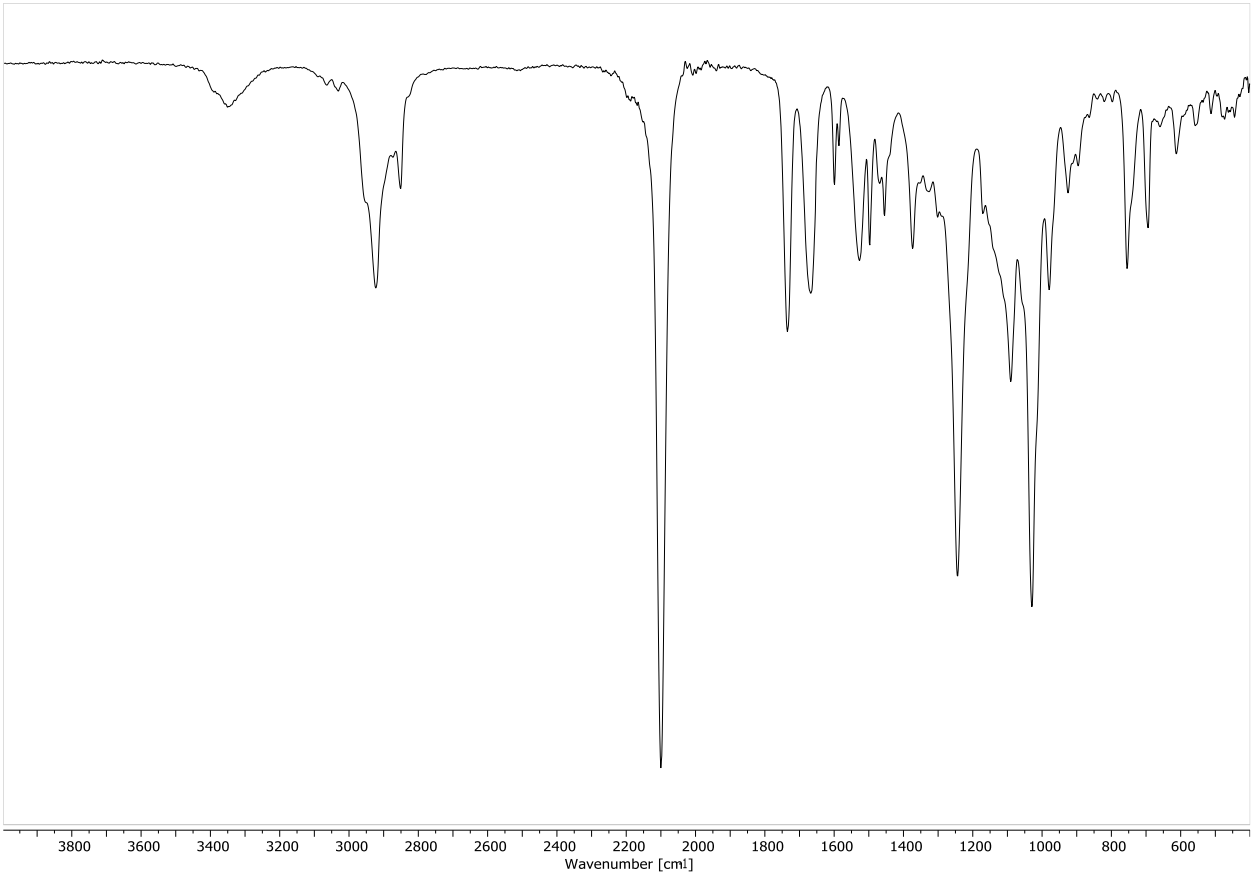
3800
3600
3400
3200
3000
2800
2600
2400
2200
2000
1800
1600
1400
1200
1000
800
600
Wavenumber [cm-1]

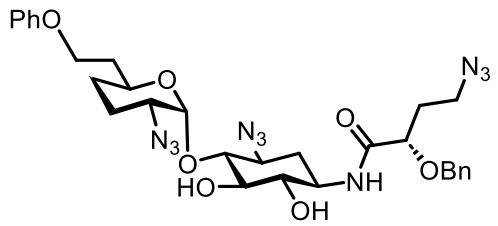
PhO
O
N3
O
HO
N3
OH
NH
O
OBn
N3

132

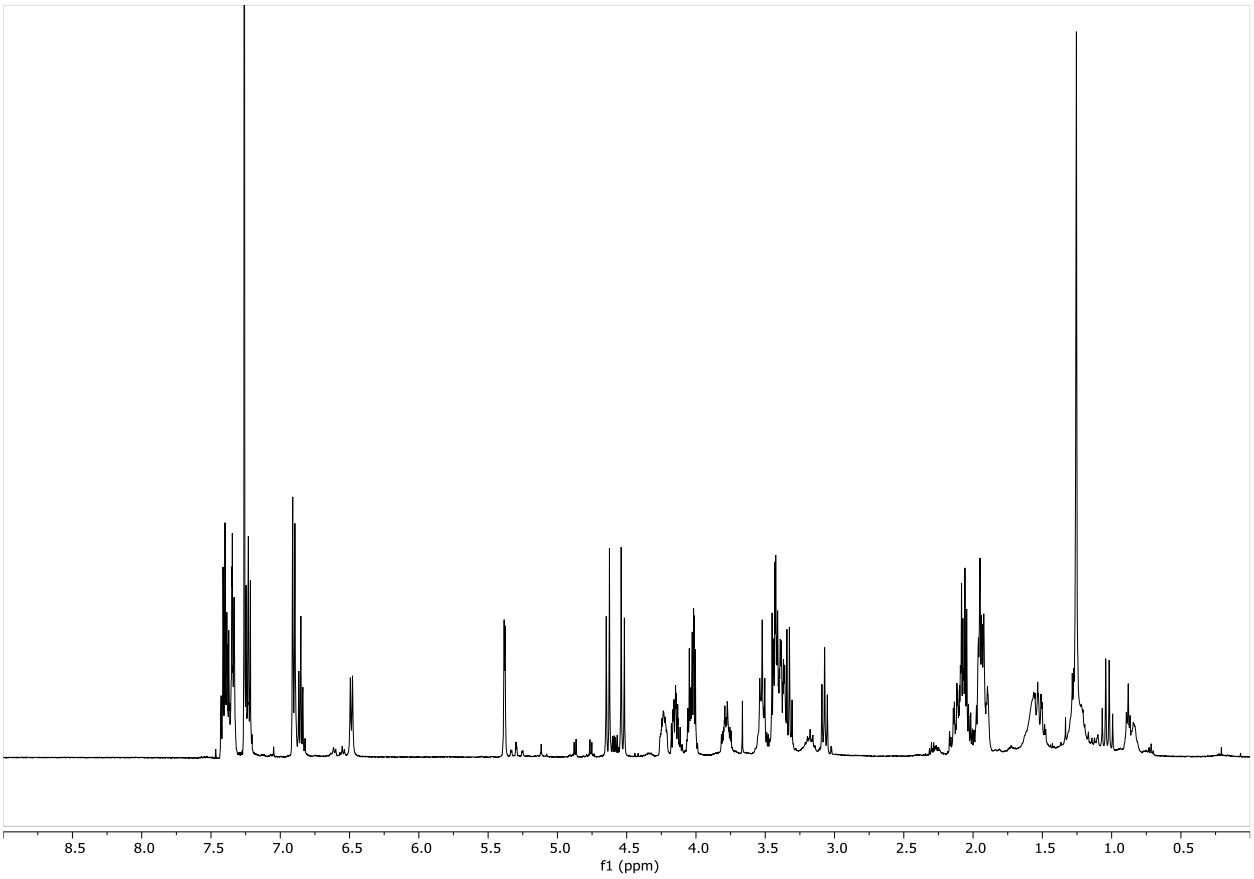
8.5
8.0
7.5
7.0
6.5
6.0
5.5
5.0
4.5
4.0
3.5
3.0
2.5
2.0
1.5
1.0
0.5
f1 (ppm)

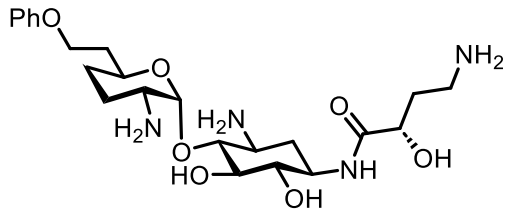
PhO
O
H_2N
H_2N
O
HO
OH
H_2N
NH
O
OH
NH_2

133

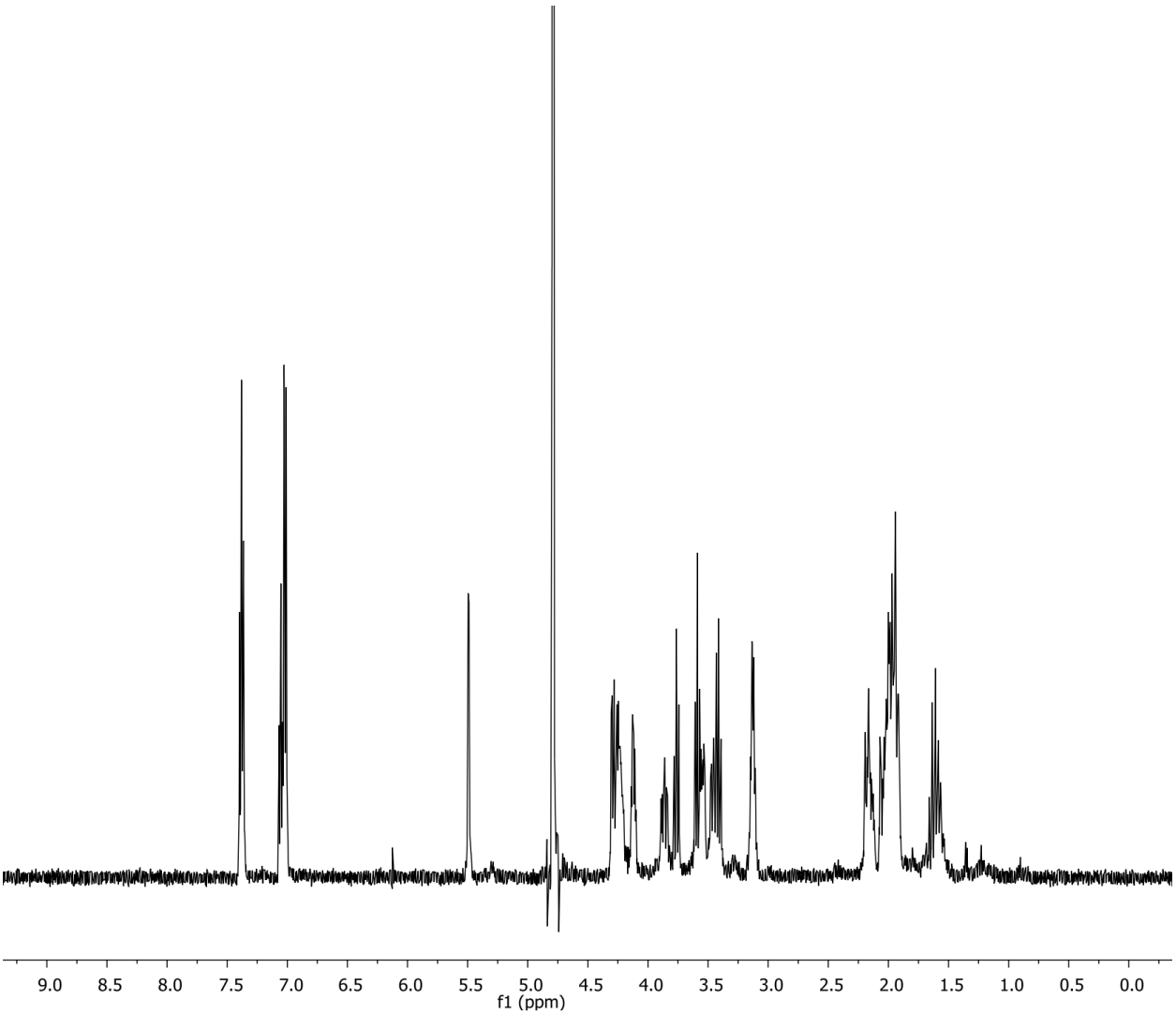
9.0
8.5
8.0
7.5
7.0
6.5
6.0
5.5
5.0
4.5
4.0
3.5
3.0
2.5
2.0
1.5
1.0
0.5
0.0
f1 (ppm)

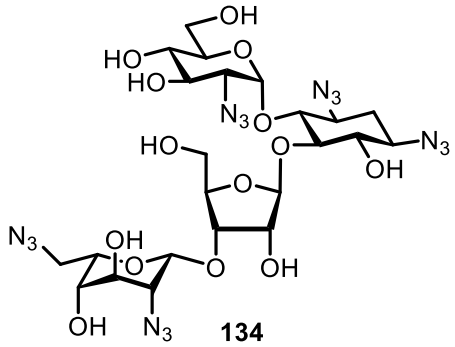
OH
HO
O
HO
N3
N3
O
N3
HO
O
OH
O
N3
OH
O
O
OH
OH
N3

134

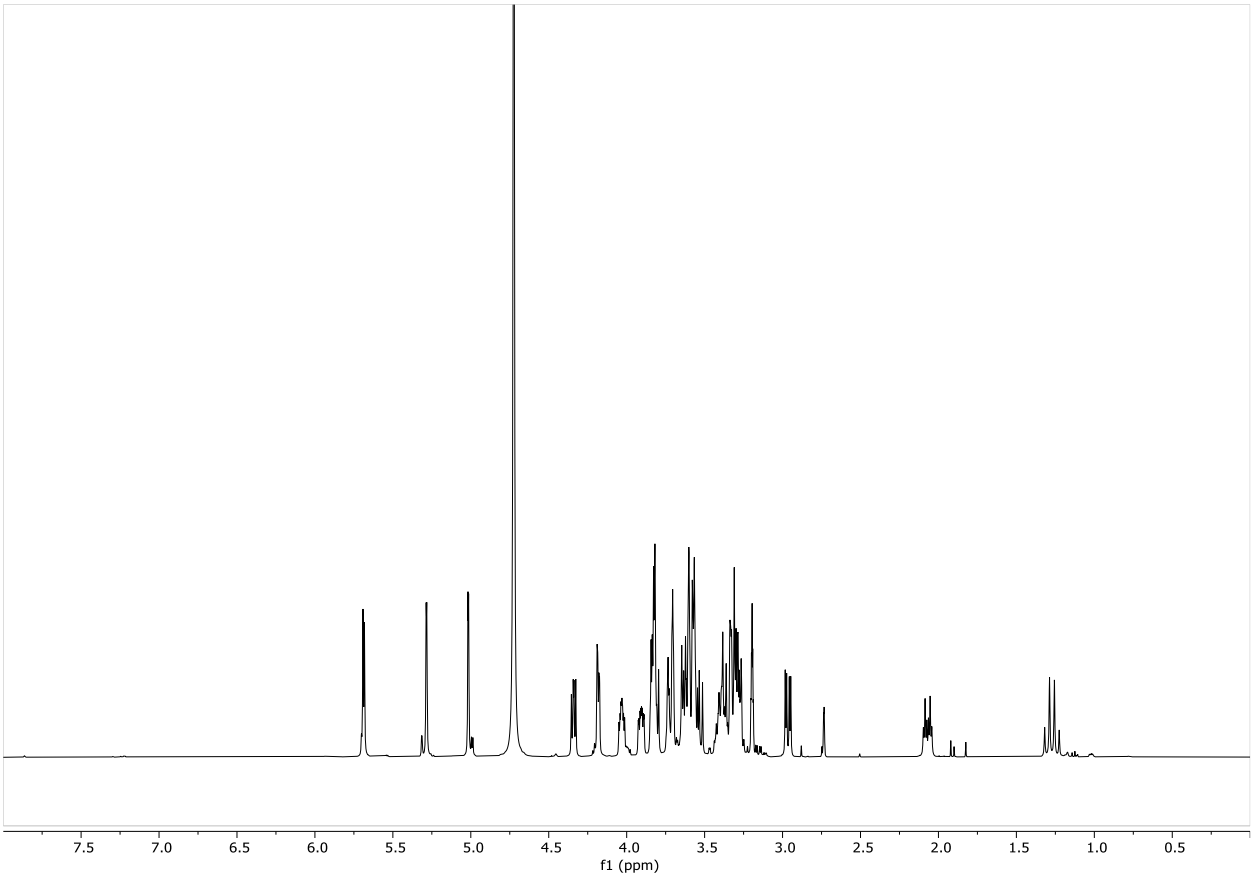
7.5
7.0
6.5
6.0
5.5
5.0
4.5
4.0
3.5
3.0
2.5
2.0
1.5
1.0
0.5
f1 (ppm)

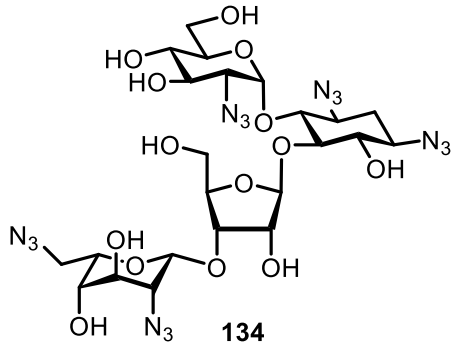
OH
HO
HO
O
N3
N3
O
N3
HO
O
O
OH
O
N3
OH
O
O
OH
OH
N3

134

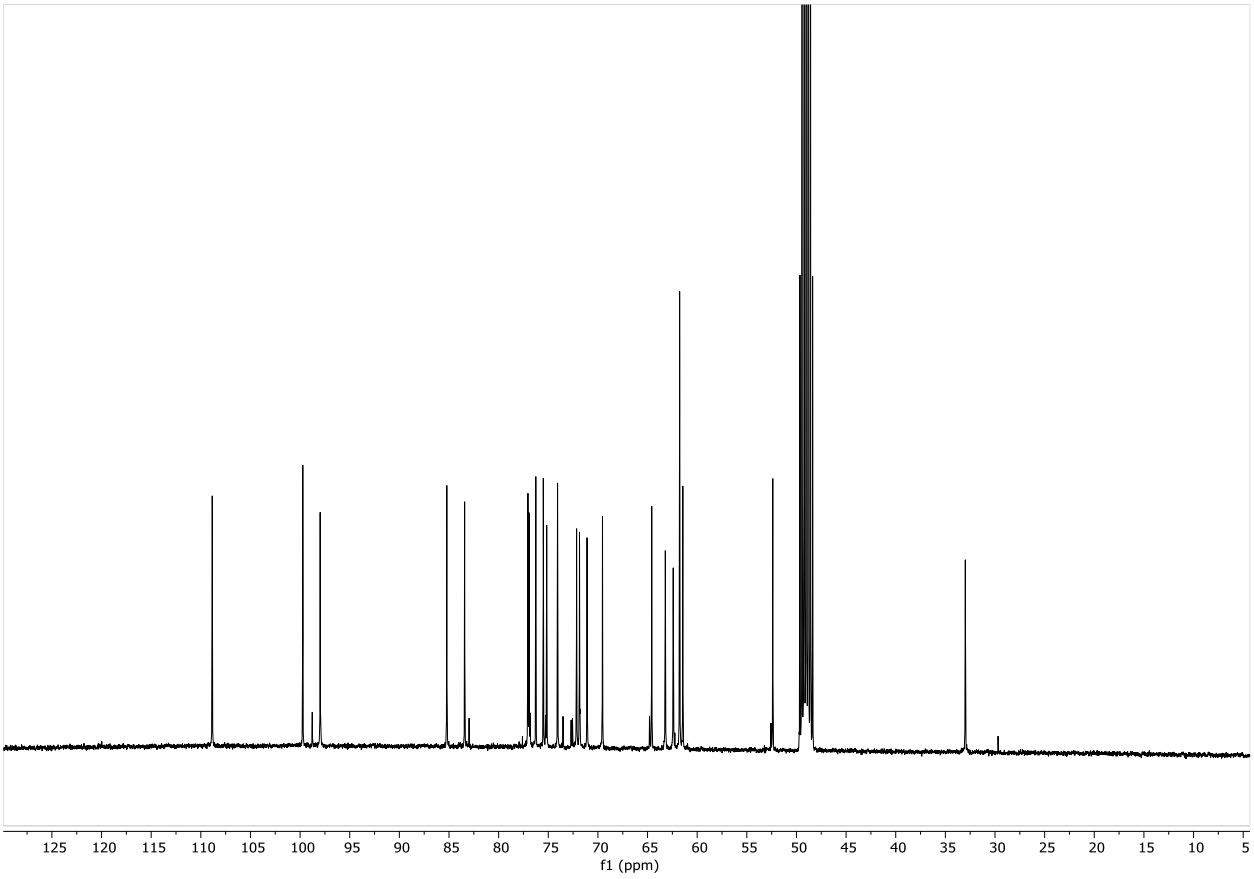
125 120 115 110 105 100 95 90 85 80 75 70 65 60 55 50 45 40 35 30 25 20 15 10 5
f1 (ppm)

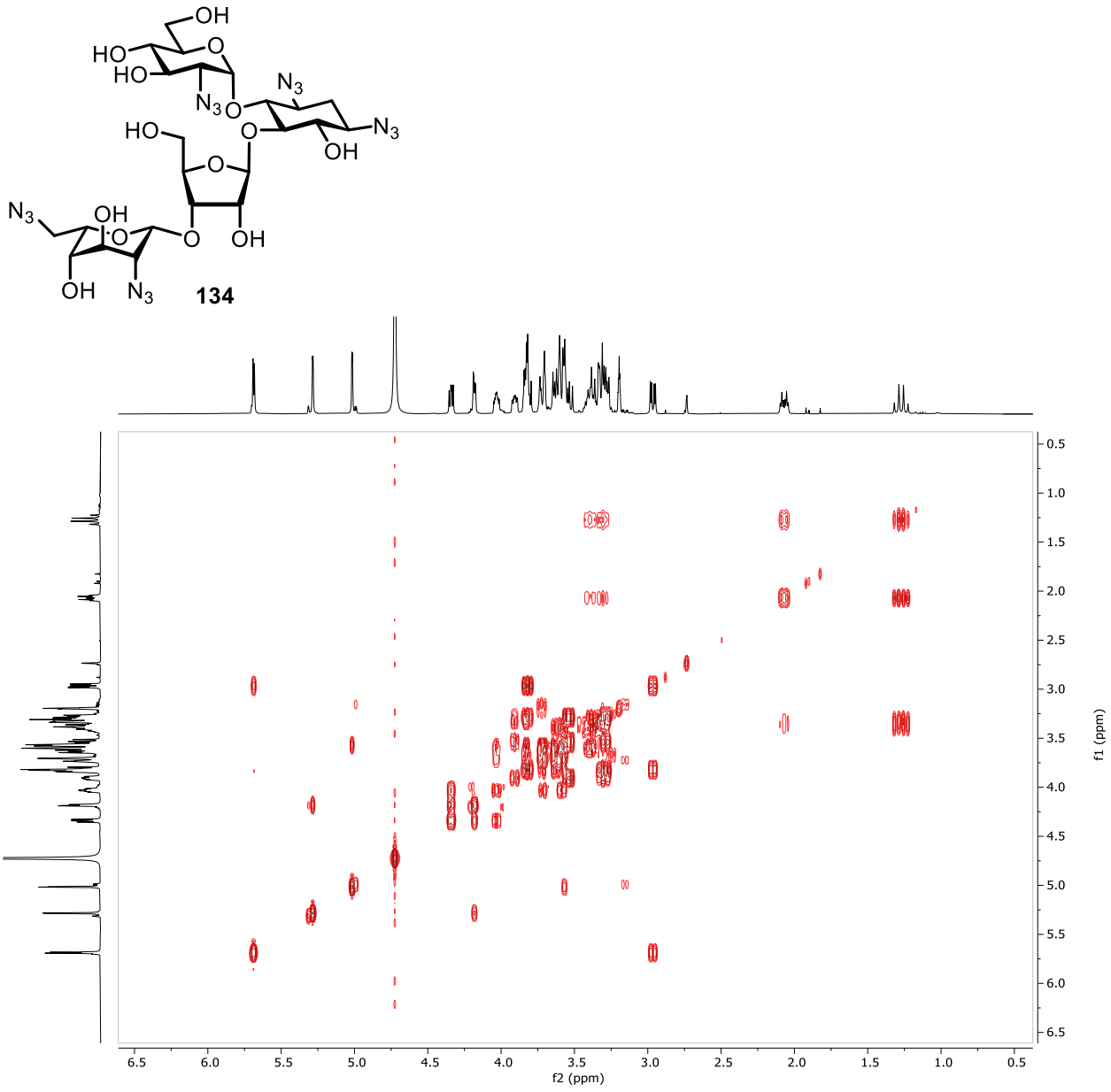
OH
HO
O
HO
N3
N3
O
N3
HO
O
O
N3
OH
N3
OH
O
O
OH
OH
N3
134
f2 (ppm)
f1 (ppm)

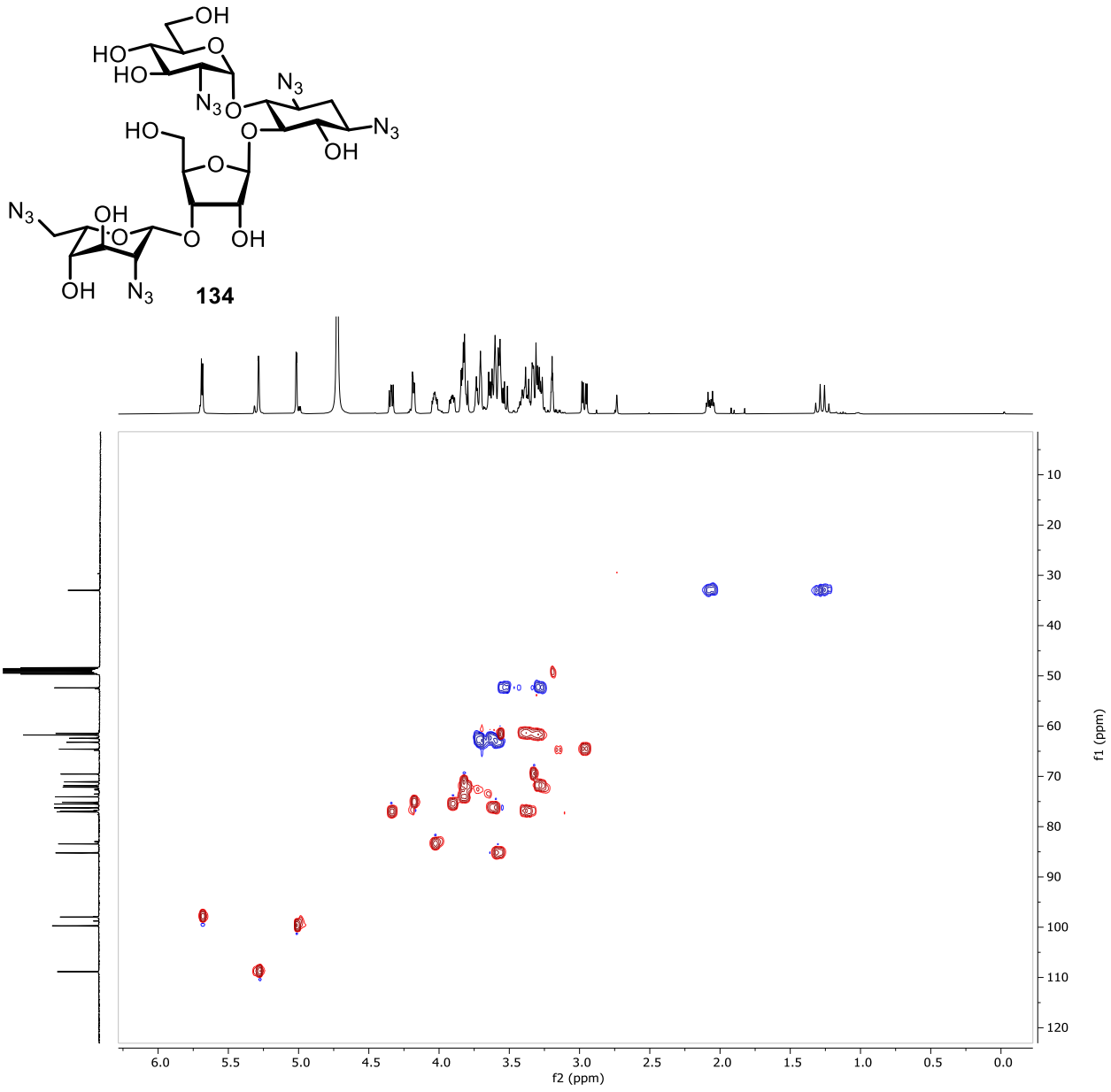
OH
HO
O
HO
N3
N3
O
N3
HO
O
O
N3
OH
N3
OH
O
O
OH
OH
N3
134
f2 (ppm)
f1 (ppm)

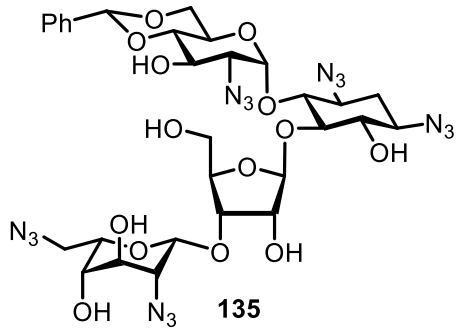
Ph
O
O
O
HO
N3
N3
O
HO
O
O
N3
OH
N3
OH
O
O
OH
OH
N3

135

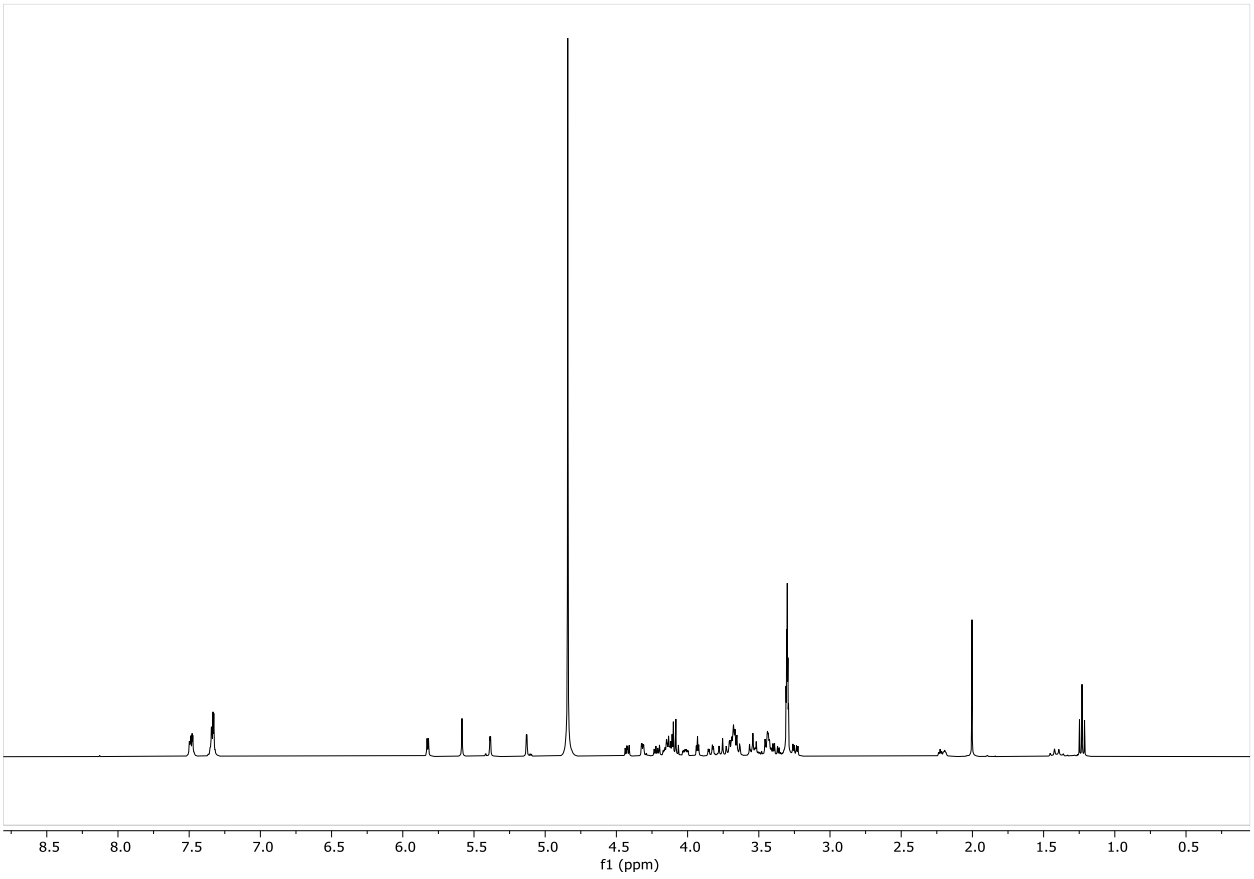
8.5
8.0
7.5
7.0
6.5
6.0
5.5
5.0
4.5
4.0
3.5
3.0
2.5
2.0
1.5
1.0
0.5
f1 (ppm)

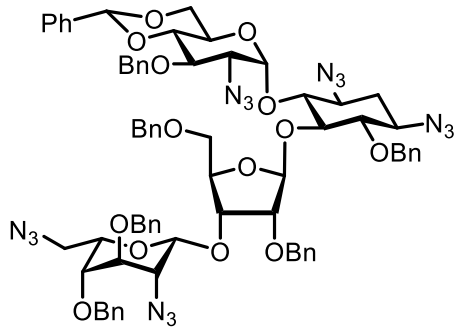
Ph
O
O
O
BnO
N3
N3
O
N3
BnO
O
OBn
O
N3
OBn
O
O
OBn
OBn
N3

136

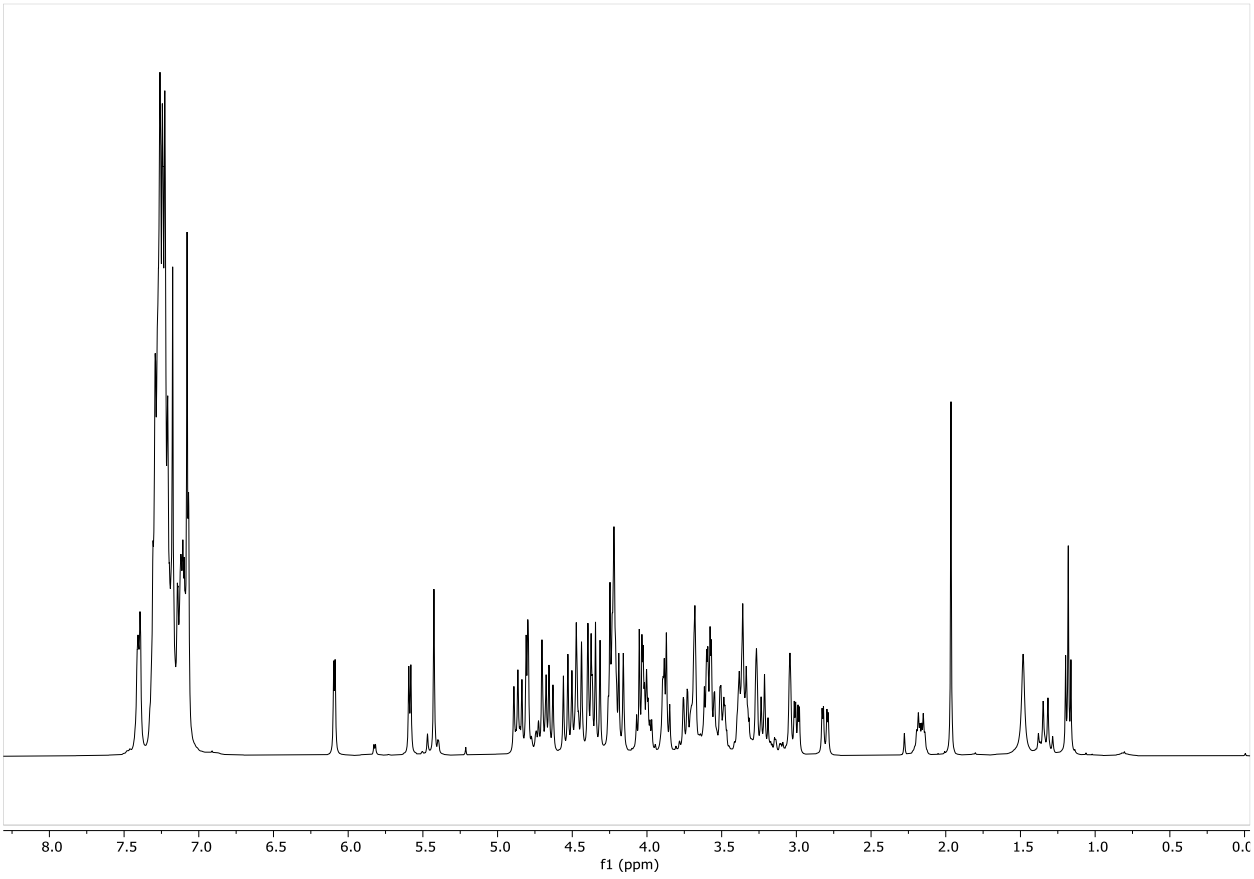
8.0
7.5
7.0
6.5
6.0
5.5
5.0
4.5
4.0
3.5
3.0
2.5
2.0
1.5
1.0
0.5
f1 (ppm)

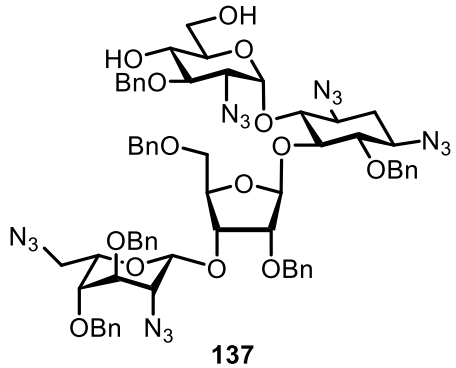
OH
HO
O
BnO
N3
N3
O
N3
BnO
O
OBn
O
N3
OBn
O
O
OBn
OBn
N3

137

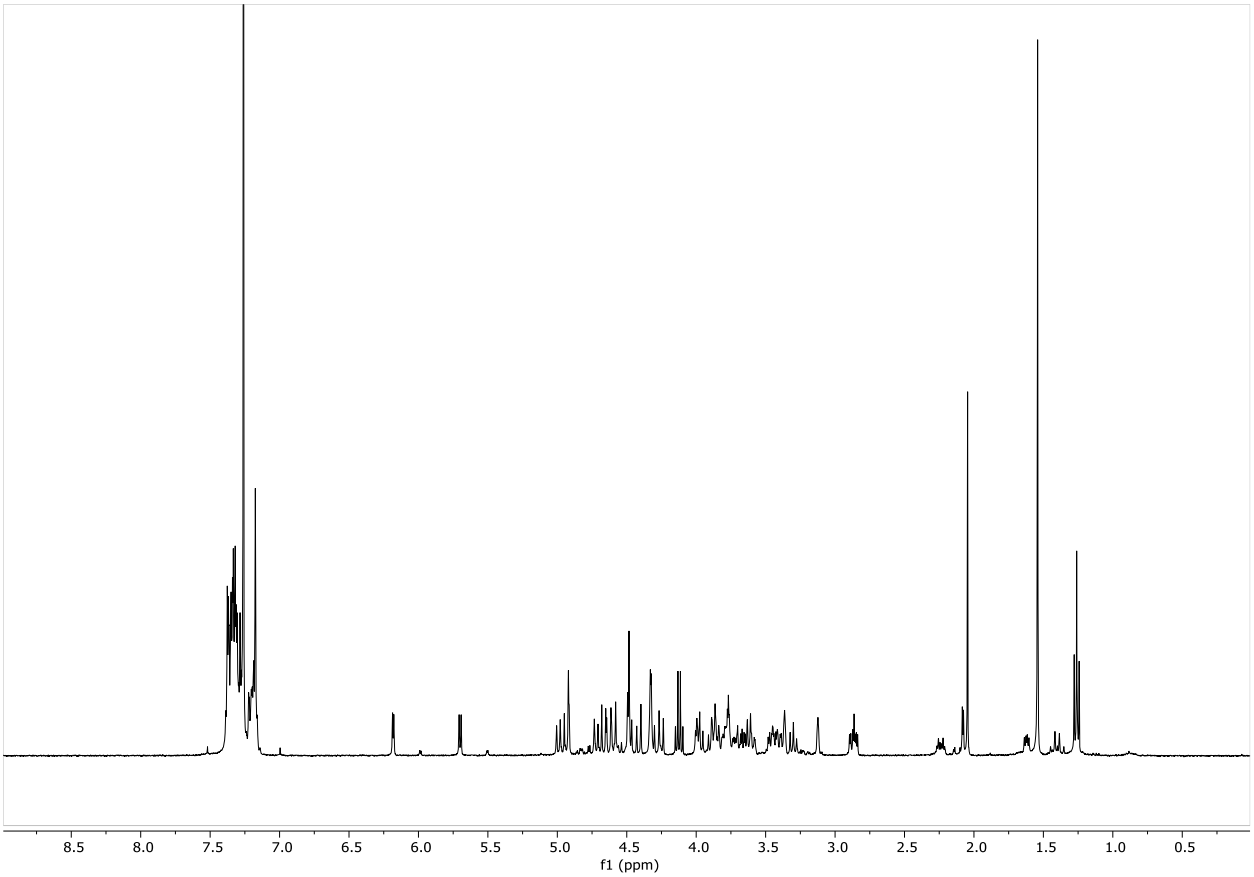
8.5
8.0
7.5
7.0
6.5
6.0
5.5
5.0
4.5
4.0
3.5
3.0
2.5
2.0
1.5
1.0
0.5
f1 (ppm)

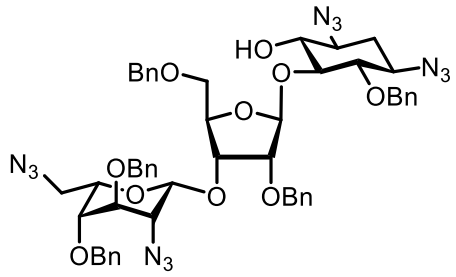
N3
HO
BnO
O
N3
OBn
O
N3
OBn
O
O
OBn
OBn
N3

113

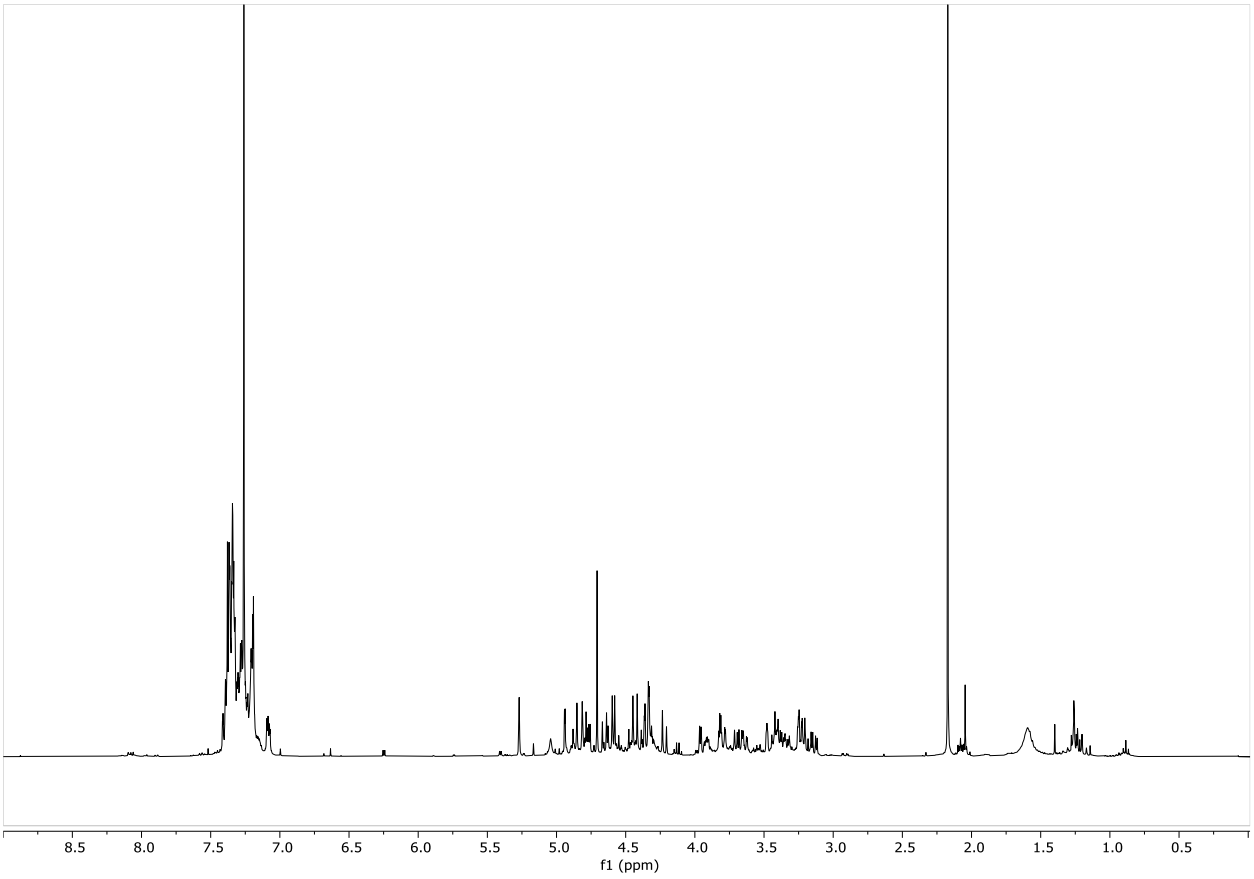
8.5
8.0
7.5
7.0
6.5
6.0
5.5
5.0
4.5
4.0
3.5
3.0
2.5
2.0
1.5
1.0
0.5
f1 (ppm)

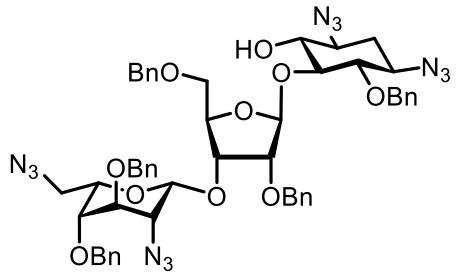
N3
HO
BnO
O
N3
OBn
O
N3
OBn
O
O
OBn
OBn
N3

113

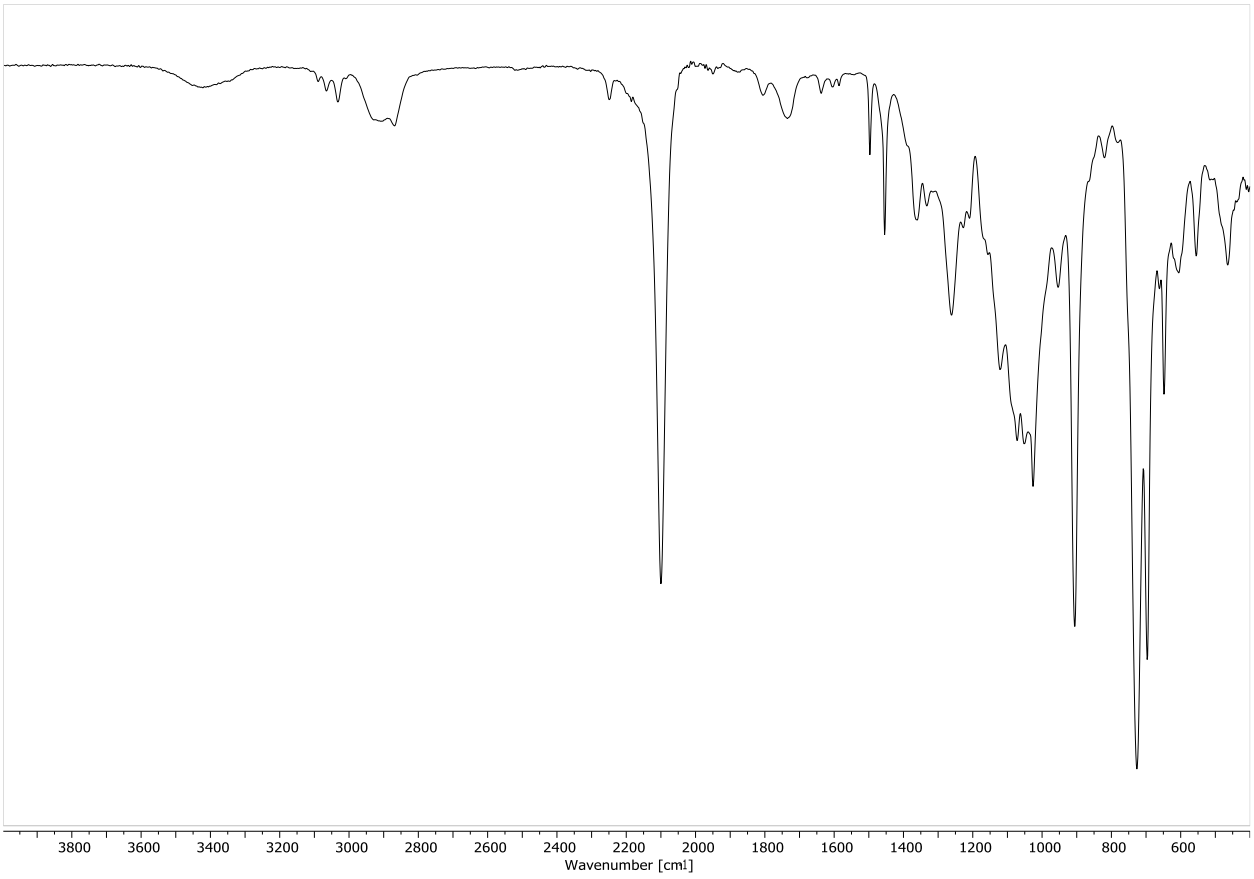
3800
3600
3400
3200
3000
2800
2600
2400
2200
2000
1800
1600
1400
1200
1000
800
600
Wavenumber [cm-1]

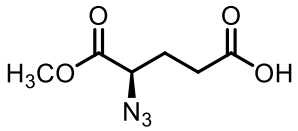

138

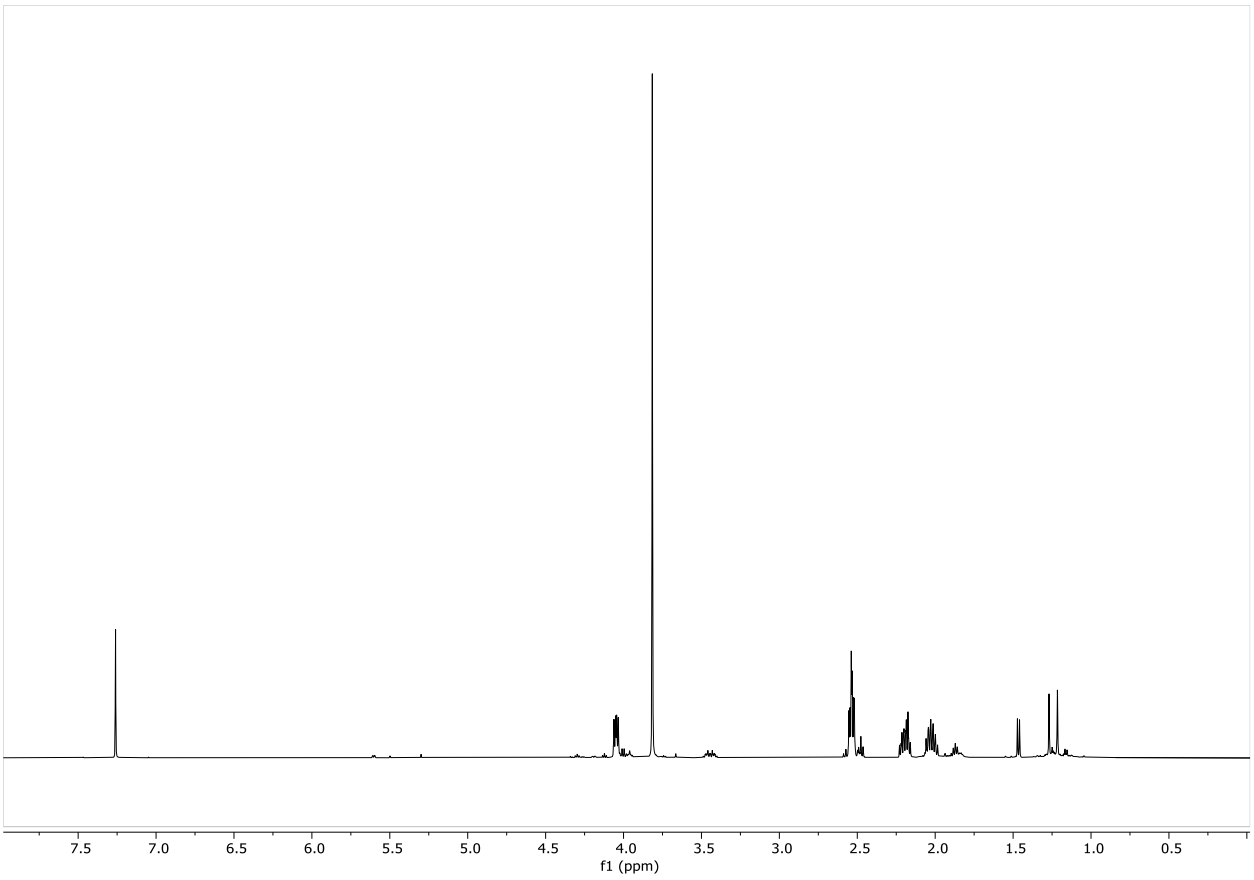

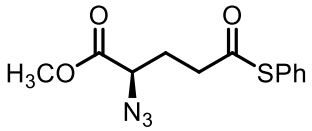
O
O
H3CO
SPh
N3

139

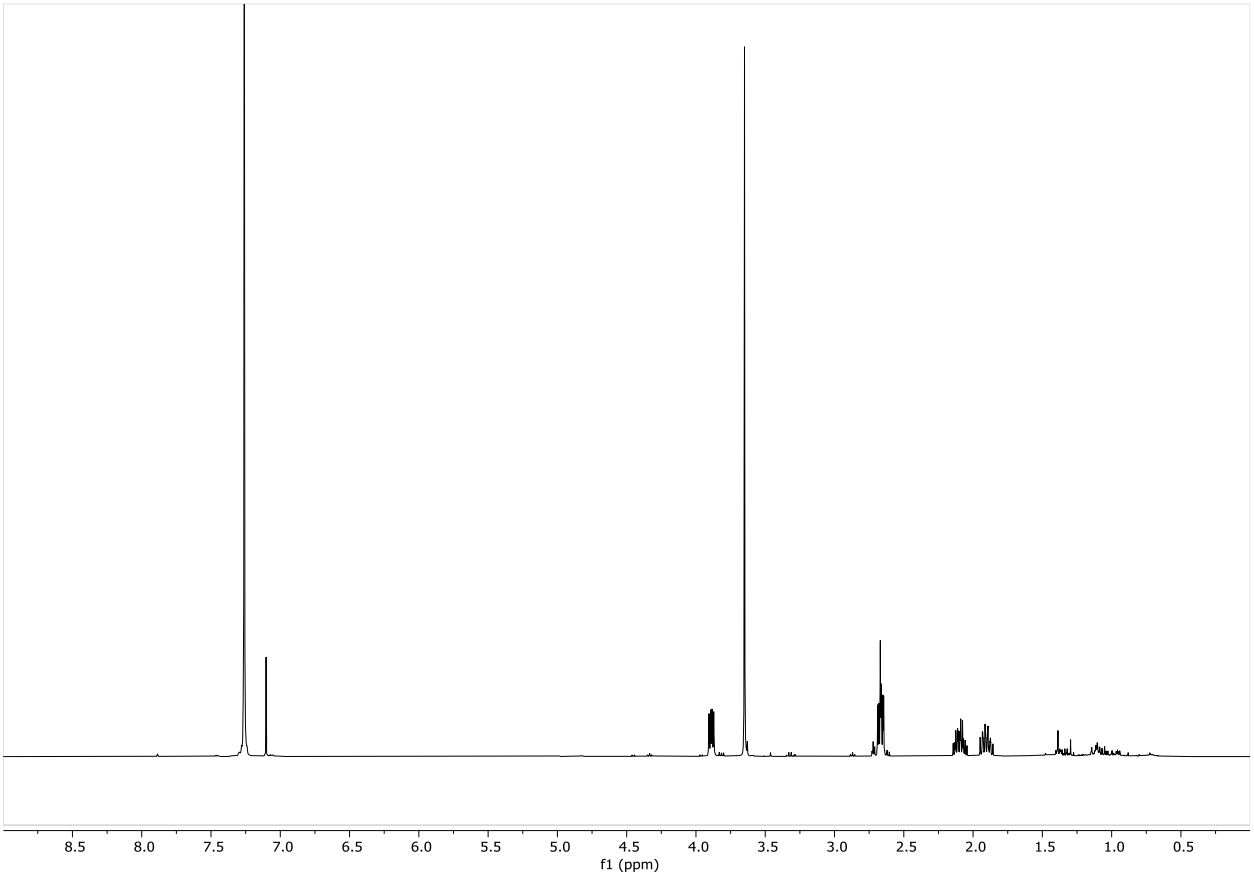
8.5
8.0
7.5
7.0
6.5
6.0
5.5
5.0
4.5
4.0
3.5
3.0
2.5
2.0
1.5
1.0
0.5
f1 (ppm)

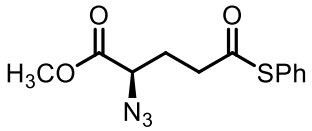
O
O
H3CO
SPh
N3

139

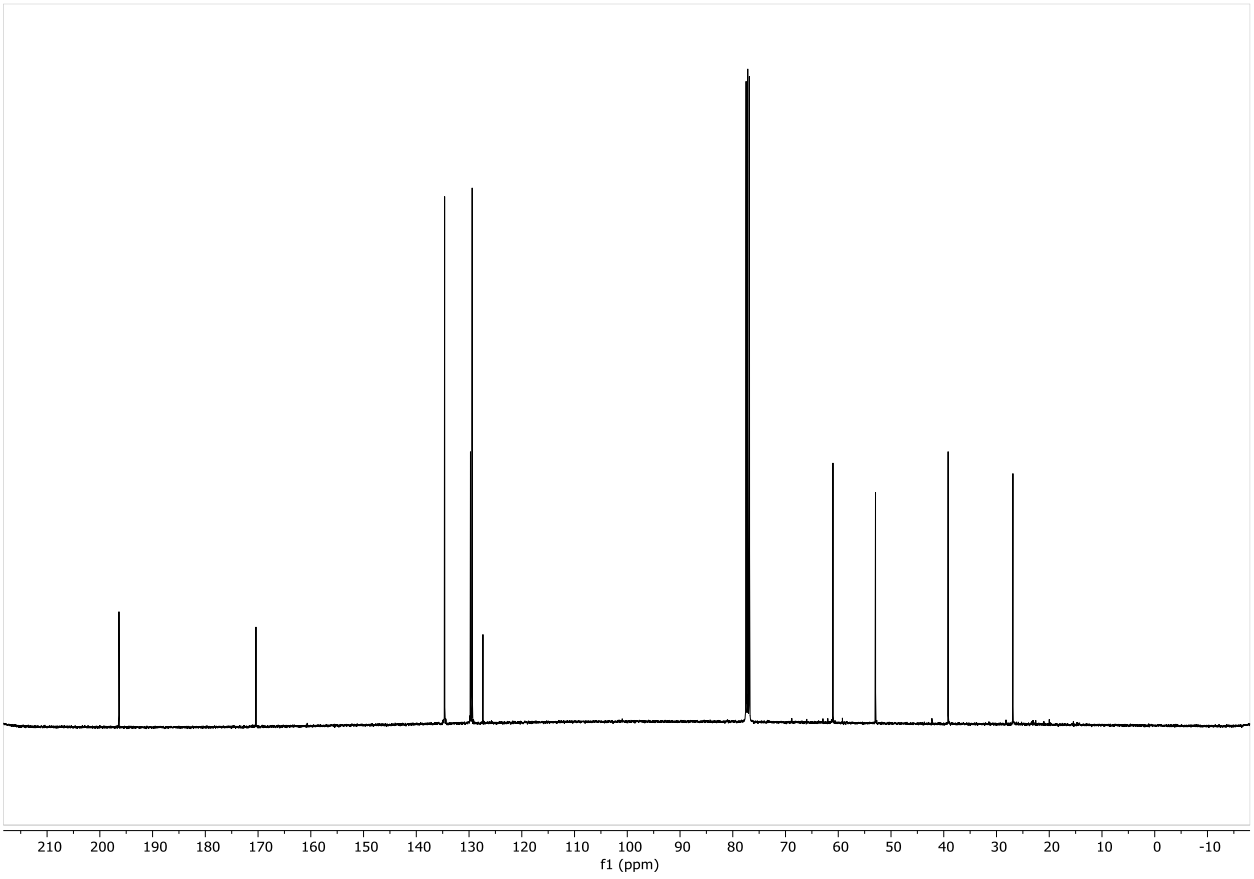
210
200
190
180
170
160
150
140
130
120
110
100
90
80
70
60
50
40
30
20
10
0
-10
f1 (ppm)

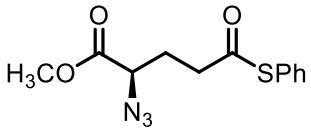
O
O
H3CO
SPh
N3

139

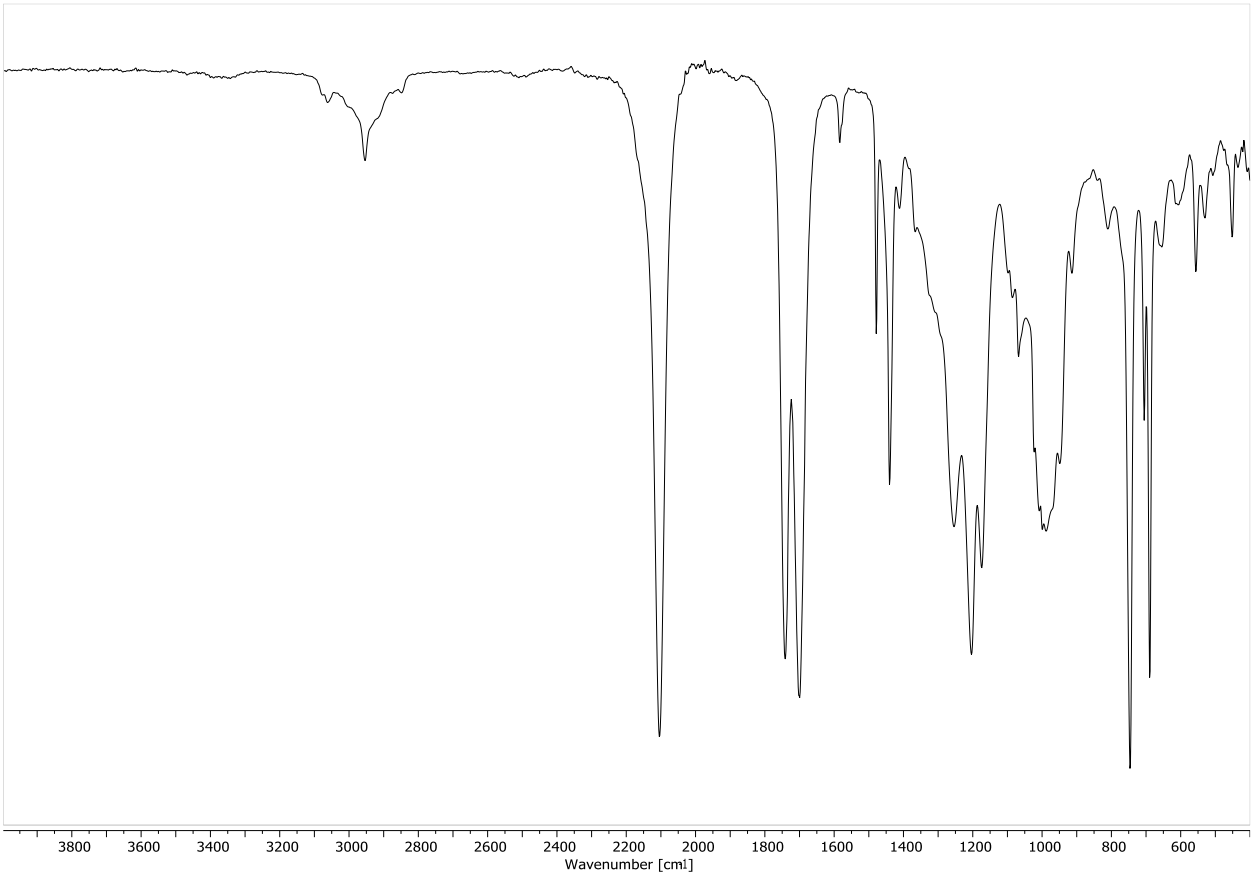
3800
3600
3400
3200
3000
2800
2600
2400
2200
2000
1800
1600
1400
1200
1000
800
600
Wavenumber [cm-1]

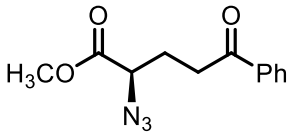

140

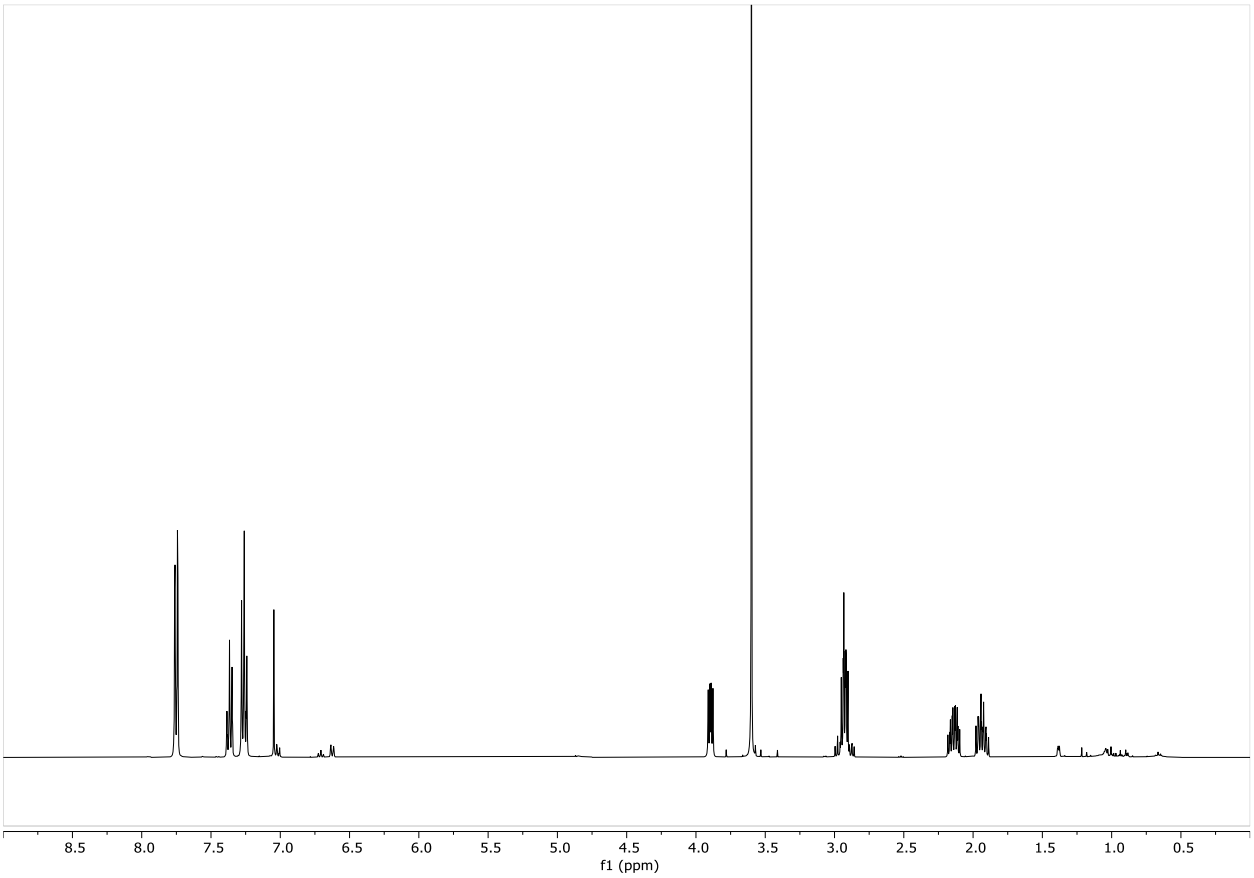

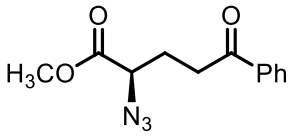
O
O
H3CO
Ph
N3

140

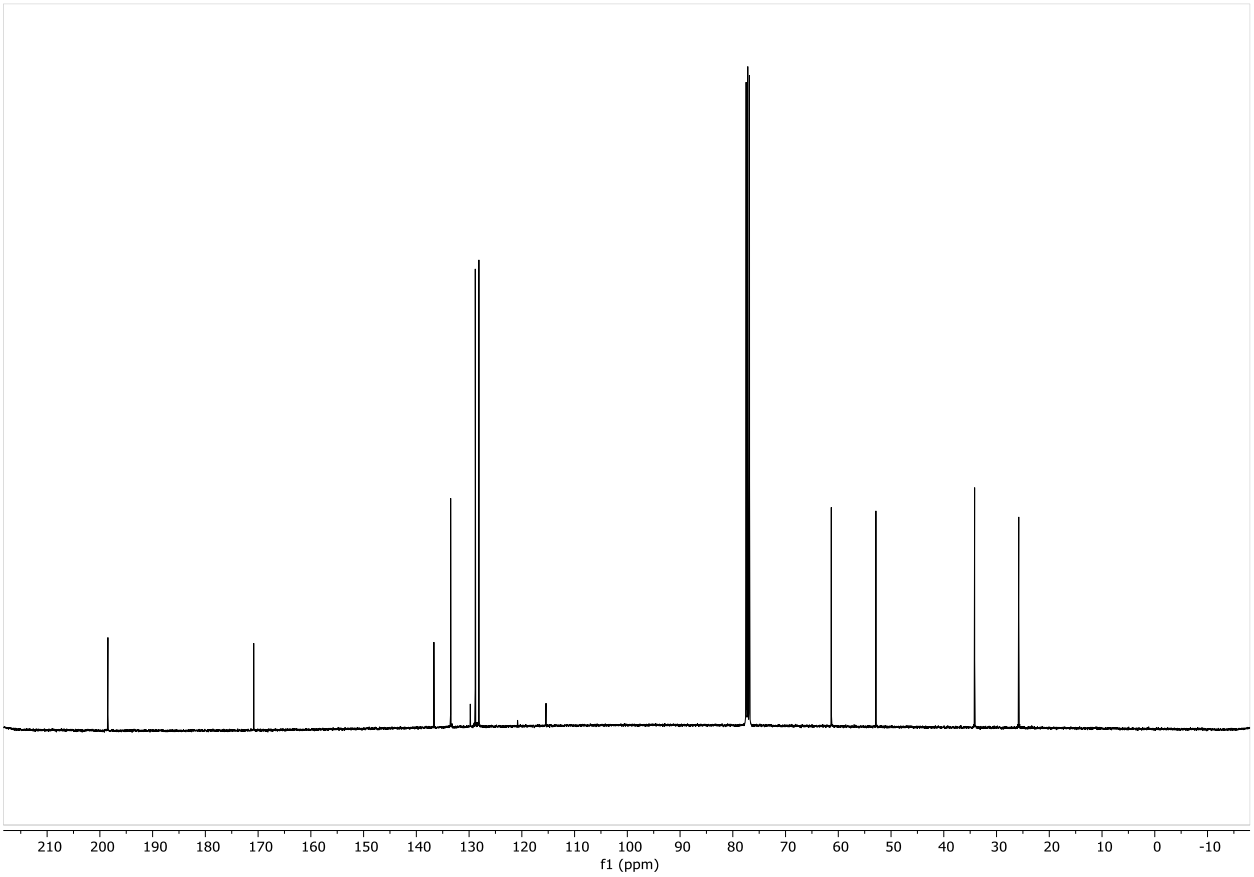
210
200
190
180
170
160
150
140
130
120
110
100
90
80
70
60
50
40
30
20
10
0
-10
f1 (ppm)

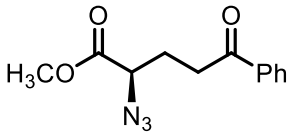
O
O
H3CO
Ph
N3

140

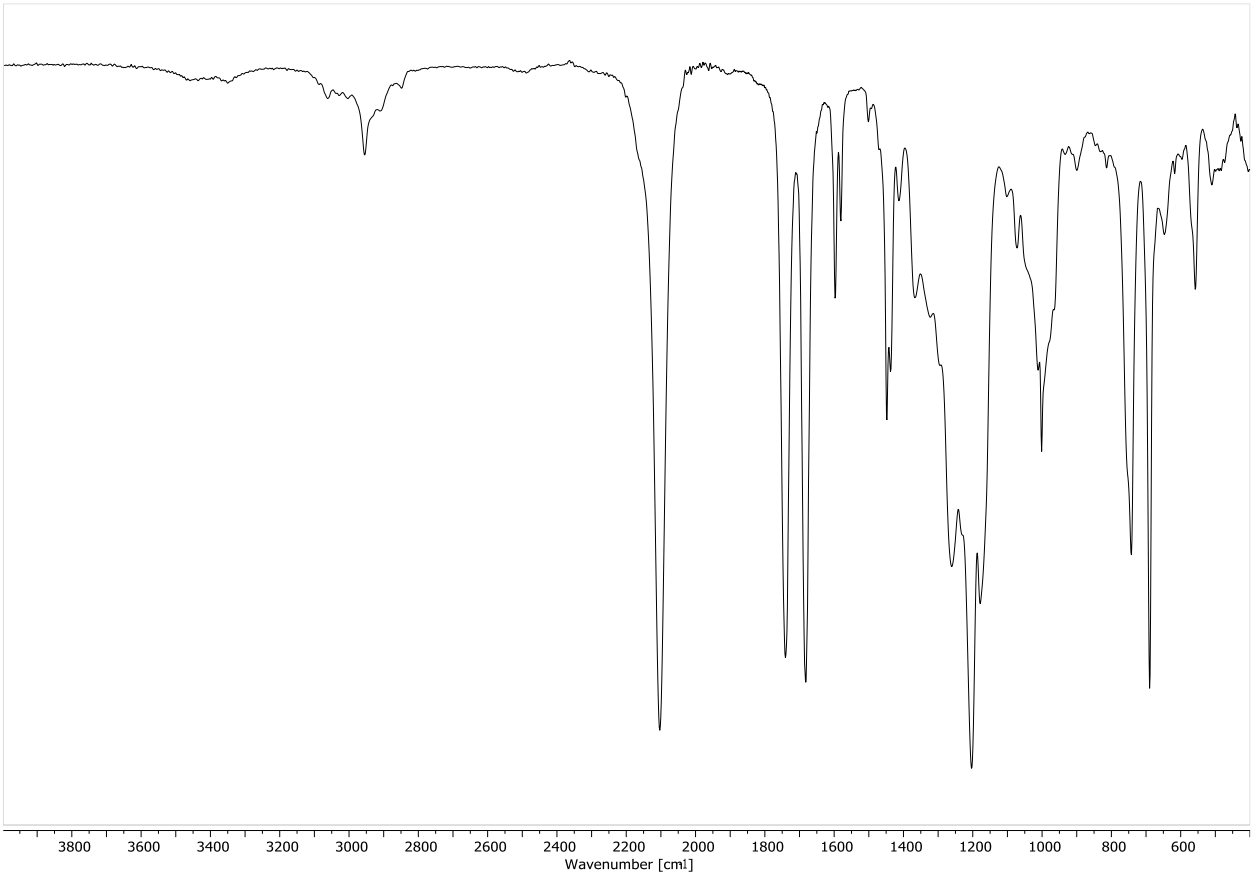
3800
3600
3400
3200
3000
2800
2600
2400
2200
2000
1800
1600
1400
1200
1000
800
600
Wavenumber [cm-1]

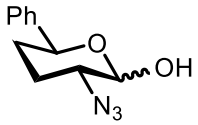

142

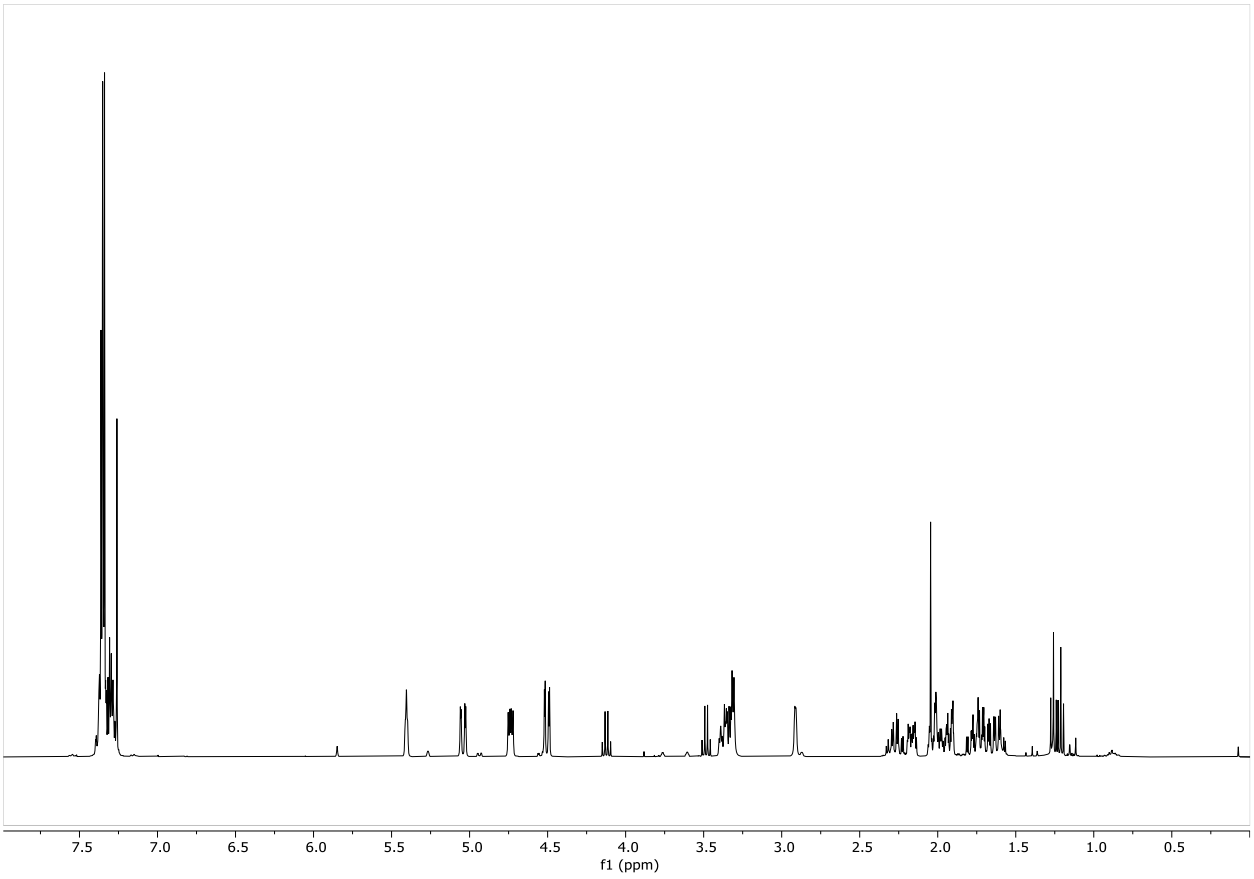

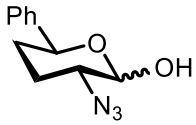
Ph
O
OH
N3

142

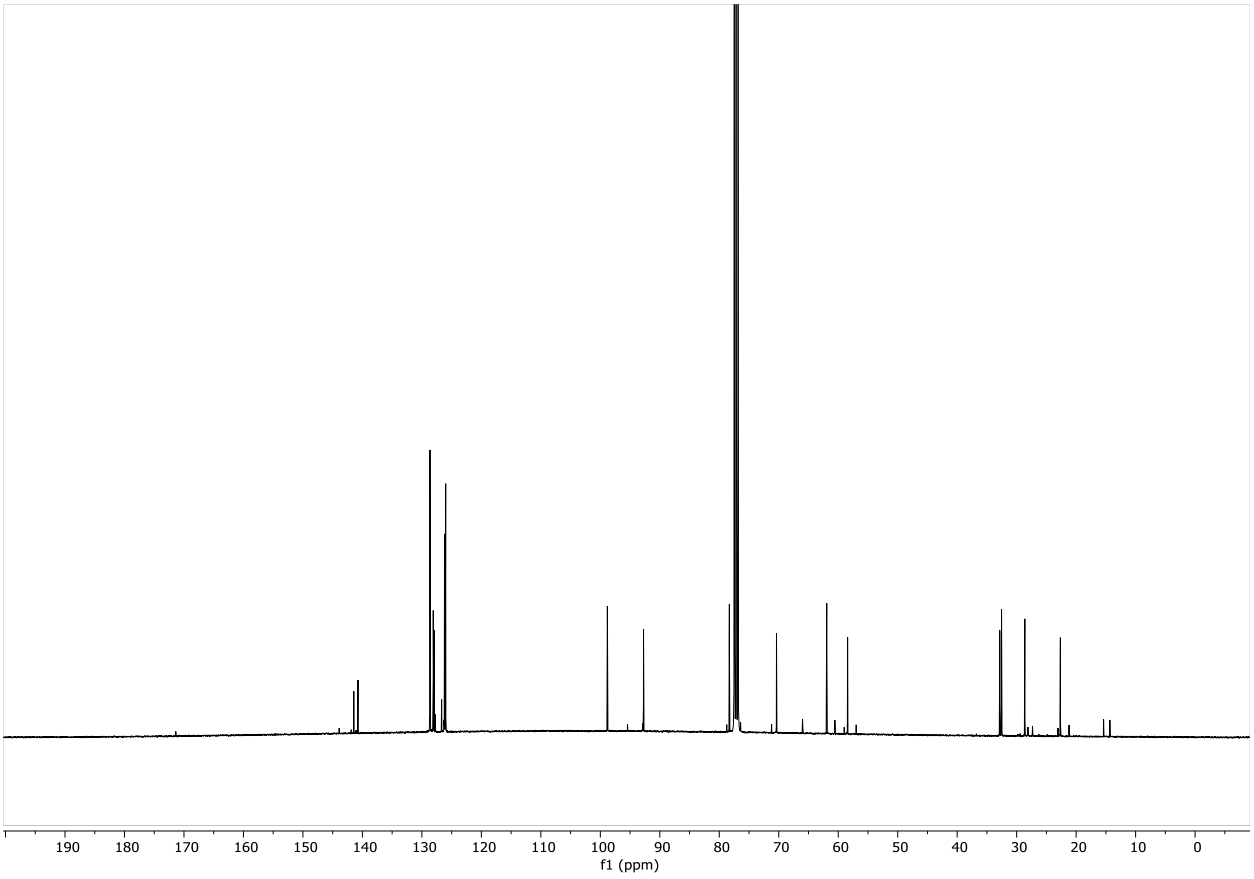
190
180
170
160
150
140
130
120
110
100
90
80
70
60
50
40
30
20
10
0
f1 (ppm)

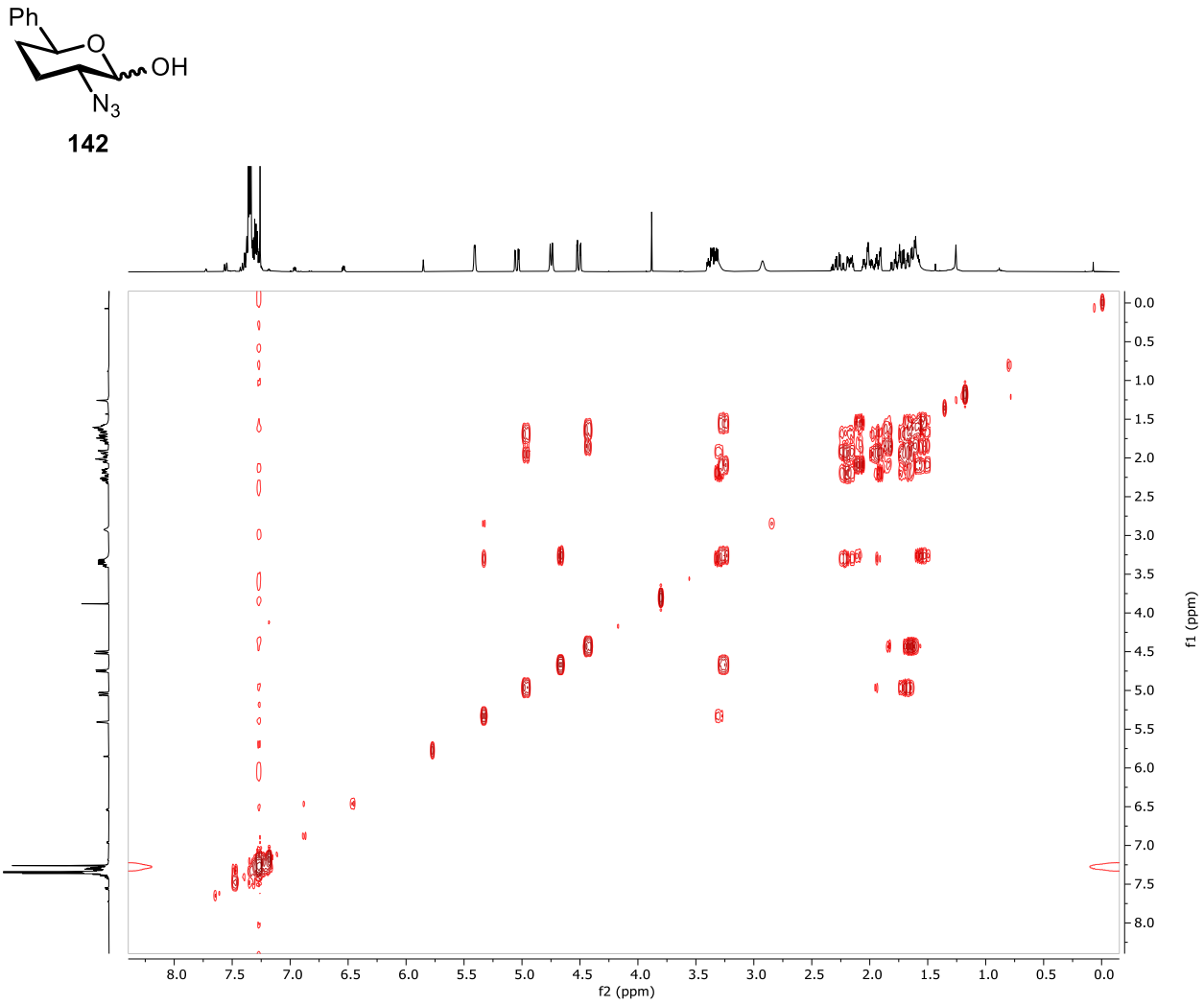
Ph
O
OH
N3
142
f2 (ppm)
f1 (ppm)

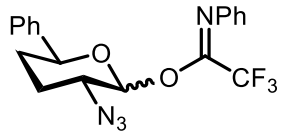
Ph
O
NPh
O
CF3
N3

114

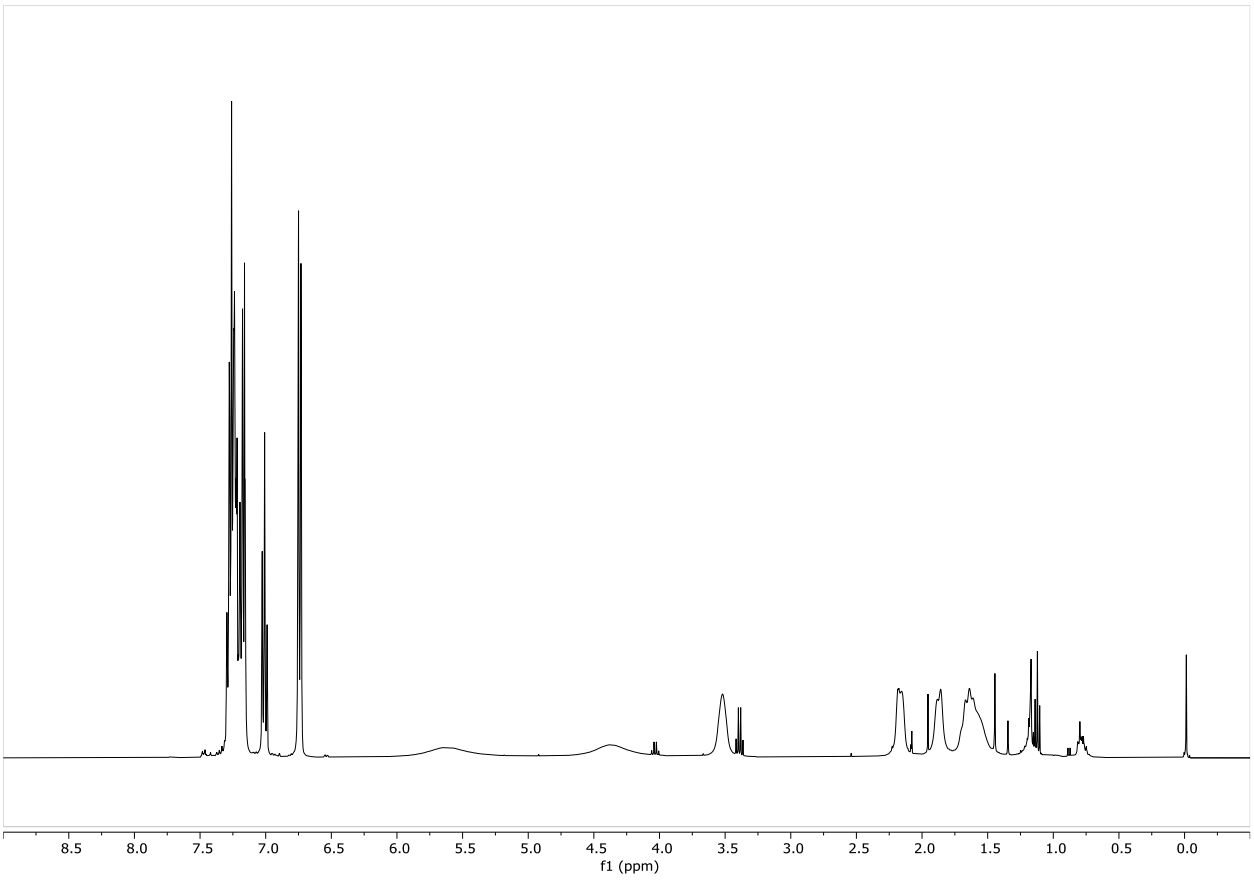
8.5
8.0
7.5
7.0
6.5
6.0
5.5
5.0
4.5
4.0
3.5
3.0
2.5
2.0
1.5
1.0
0.5
0.0
f1 (ppm)

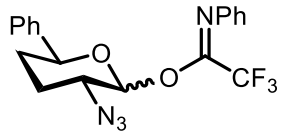
Ph
O
NPh
O
CF3
N3

114

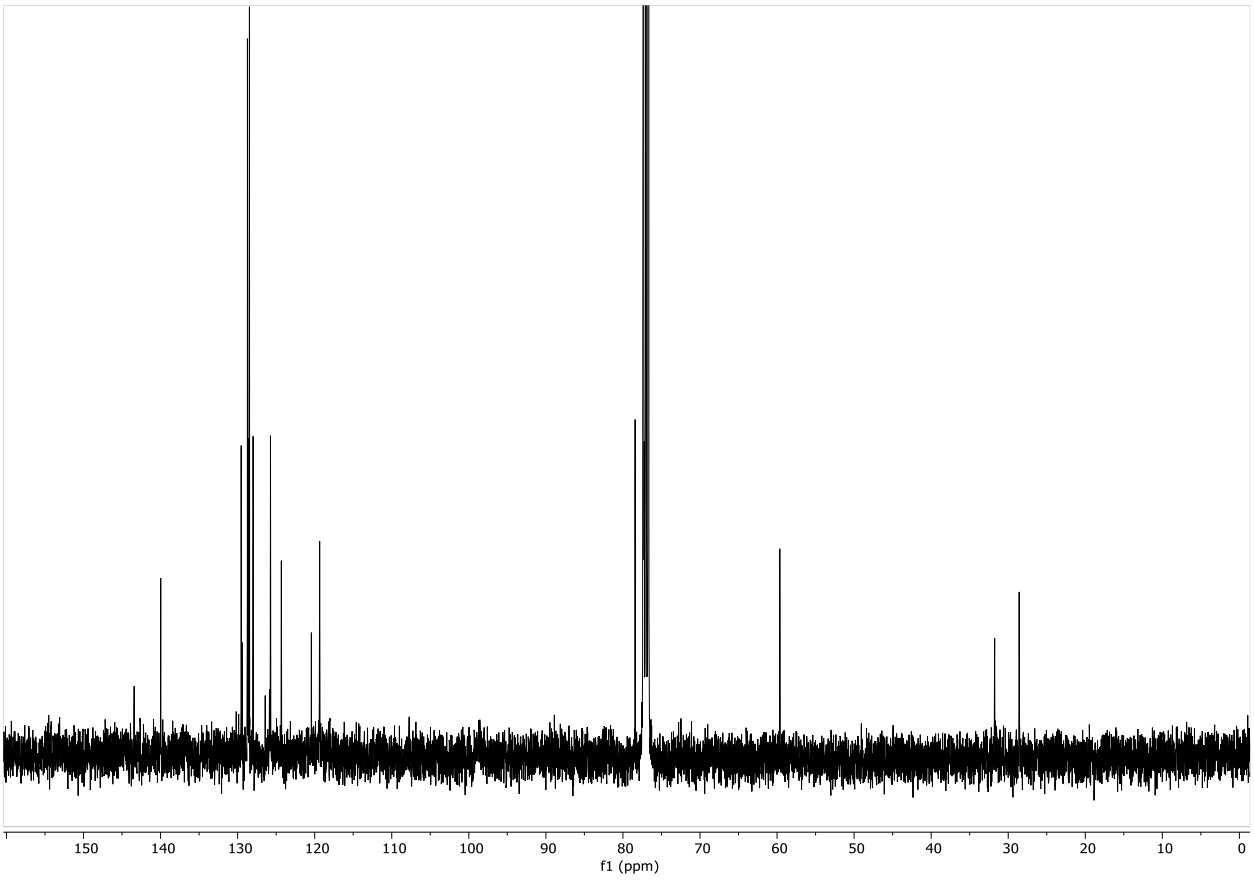
150
140
130
120
110
100
90
80
70
60
50
40
30
20
10
0
f1 (ppm)

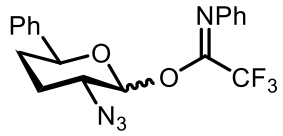
Ph
O
NPh
O
CF3
N3

114

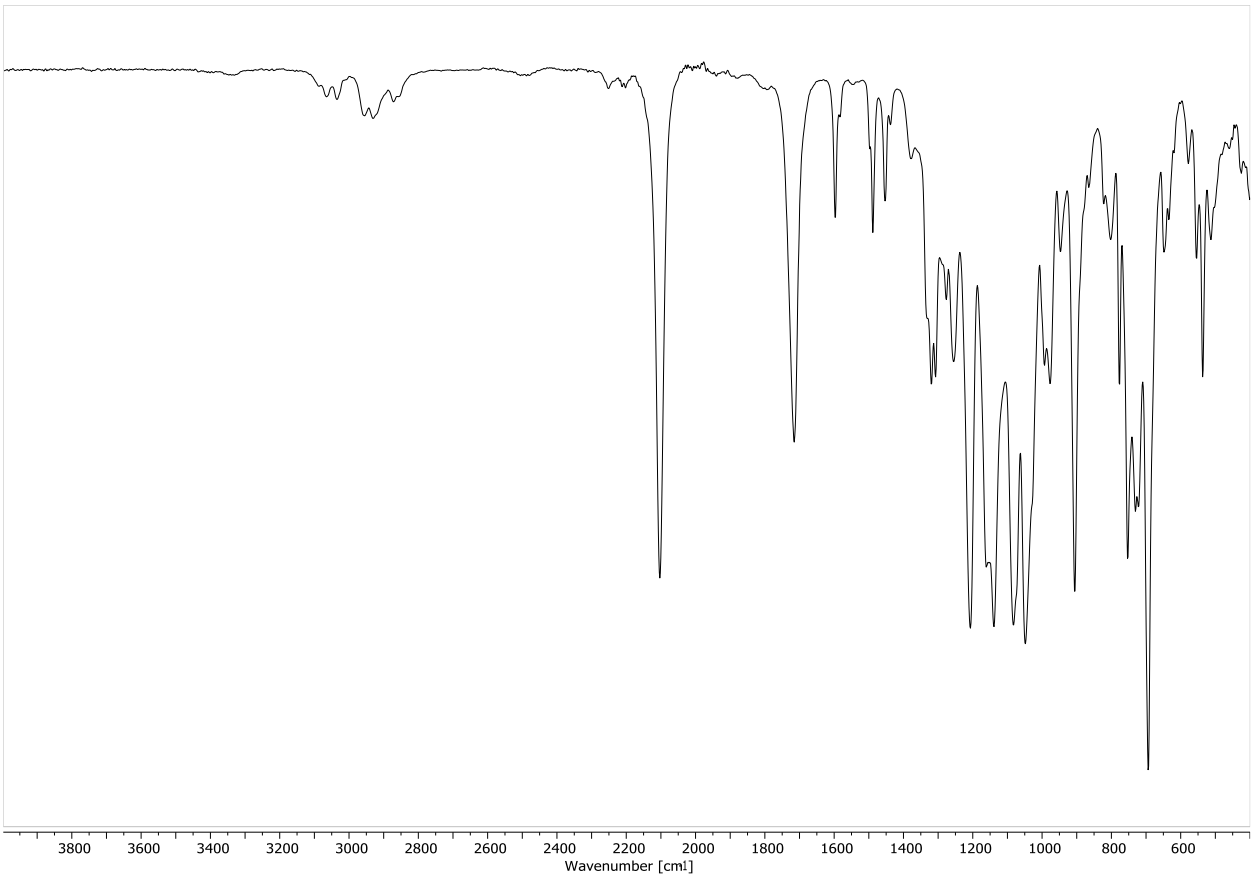
3800
3600
3400
3200
3000
2800
2600
2400
2200
2000
1800
1600
1400
1200
1000
800
600
Wavenumber [cm-1]

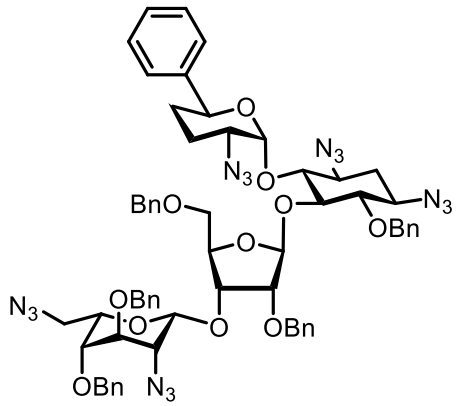
O
N3
N3
O
N3
BnO
O
OBn
O
N3
OBn
O
O
OBn
OBn
N3

115

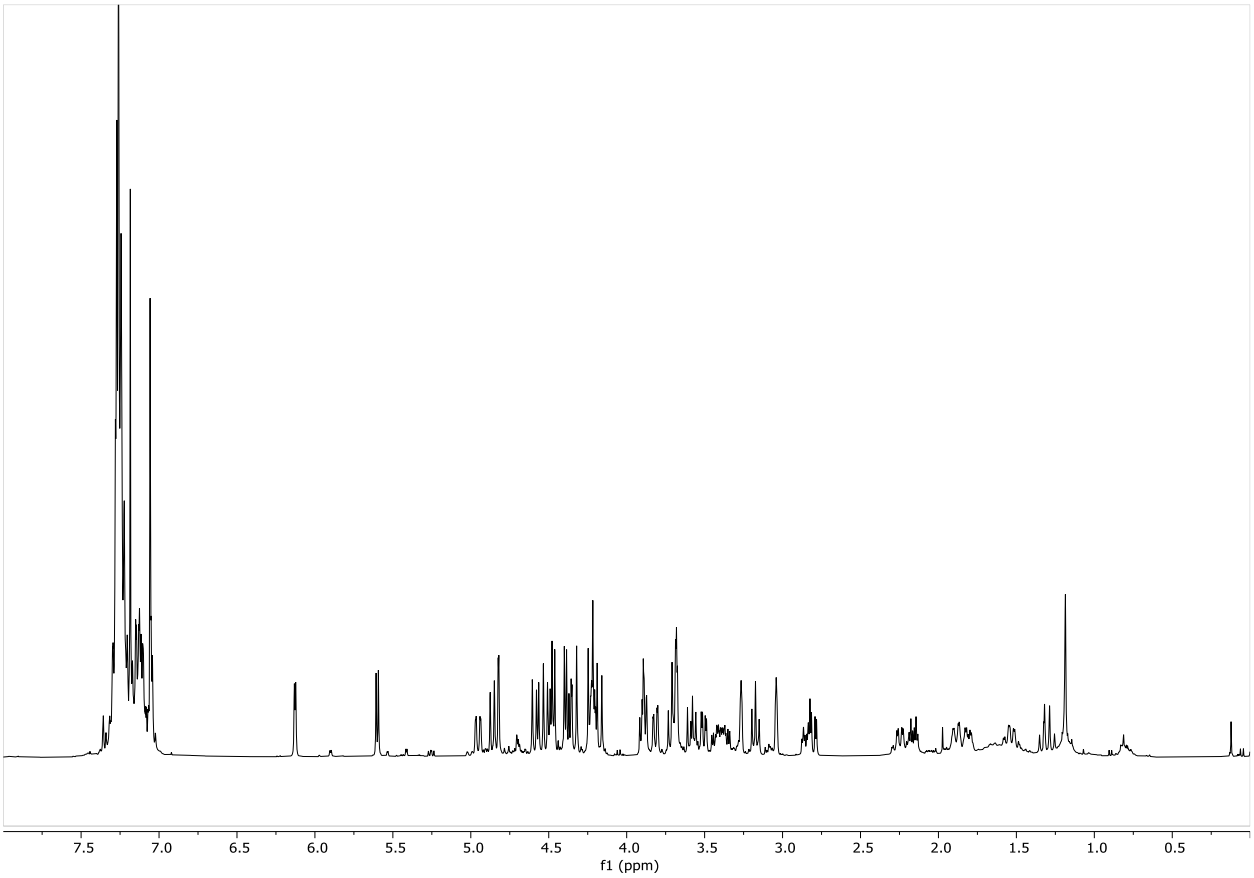
7.5
7.0
6.5
6.0
5.5
5.0
4.5
4.0
3.5
3.0
2.5
2.0
1.5
1.0
0.5
f1 (ppm)

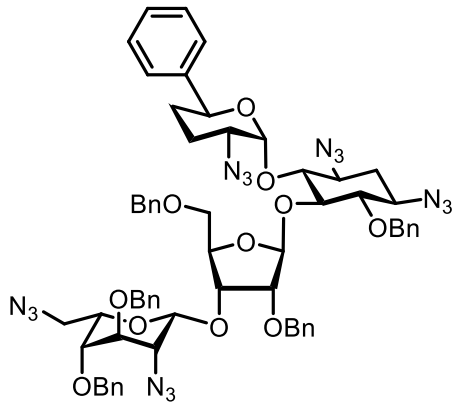
O
N3
N3
O
N3
BnO
O
OBn
O
N3
OBn
O
O
OBn
OBn
N3

115

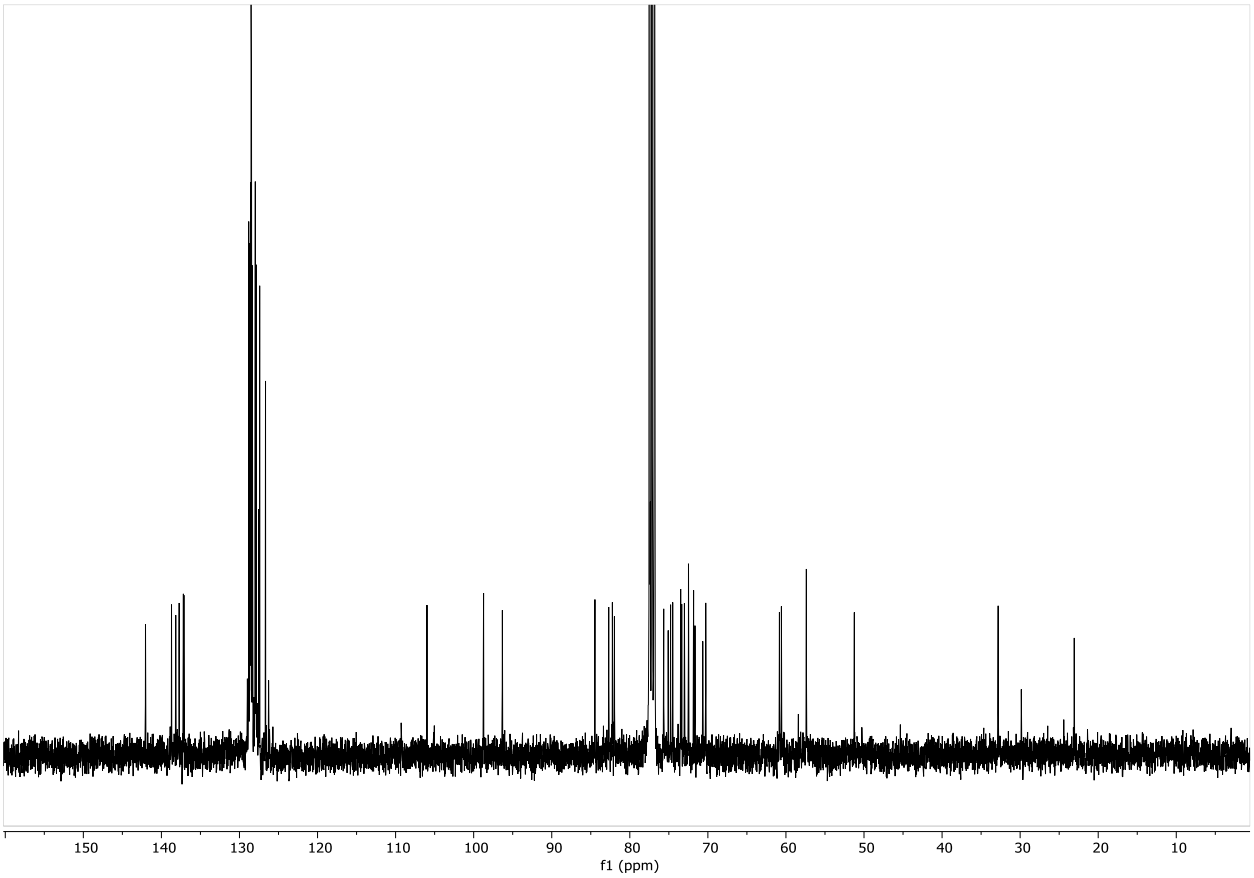
150
140
130
120
110
100
90
80
70
60
50
40
30
20
10
f1 (ppm)

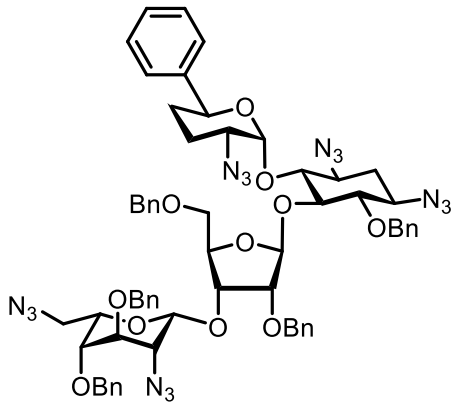
O
N3
N3
O
N3
BnO
O
OBn
O
N3
OBn
O
O
OBn
OBn
N3

115

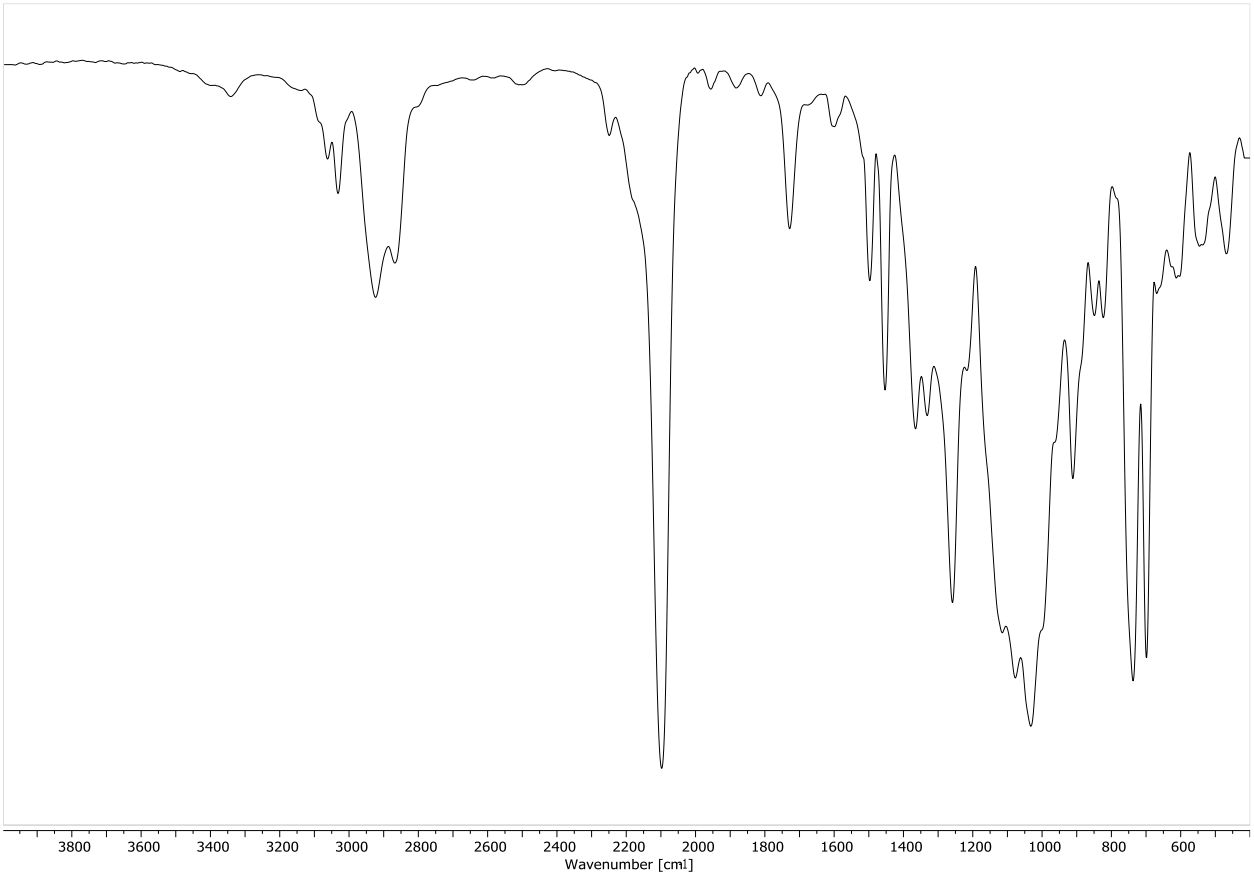
3800
3600
3400
3200
3000
2800
2600
2400
2200
2000
1800
1600
1400
1200
1000
800
600
Wavenumber [cm-1]

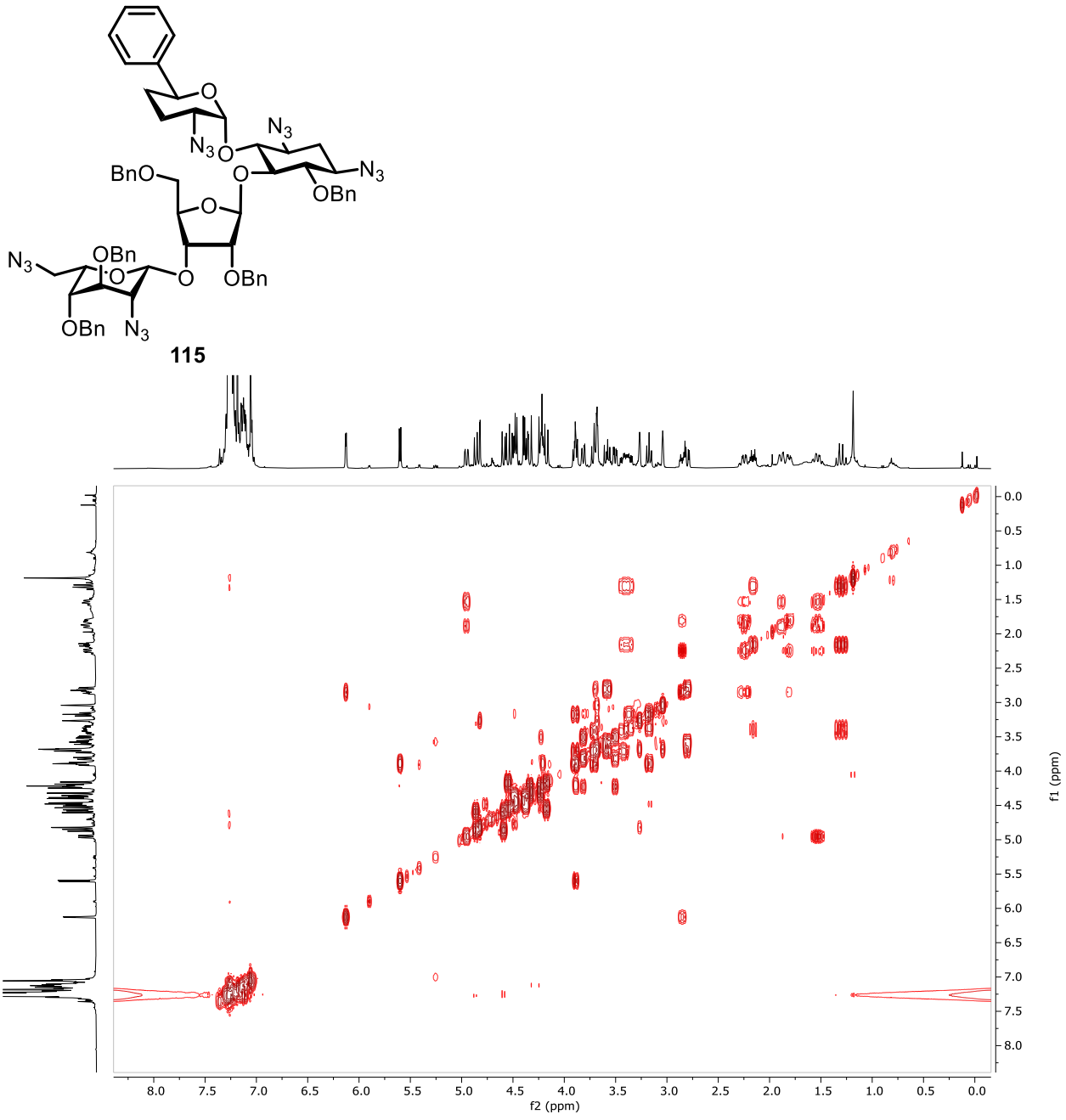

115

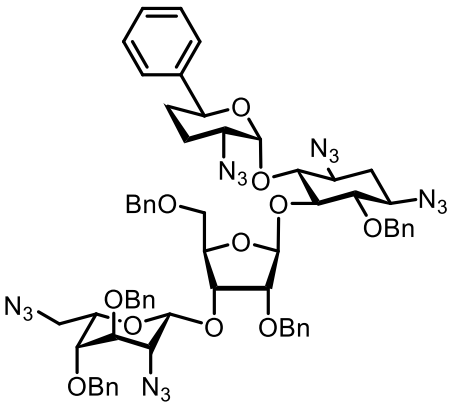
O
N3
N3
O
N3
BnO
O
OBn
O
N3
OBn
O
O
OBn
OBn
N3

115

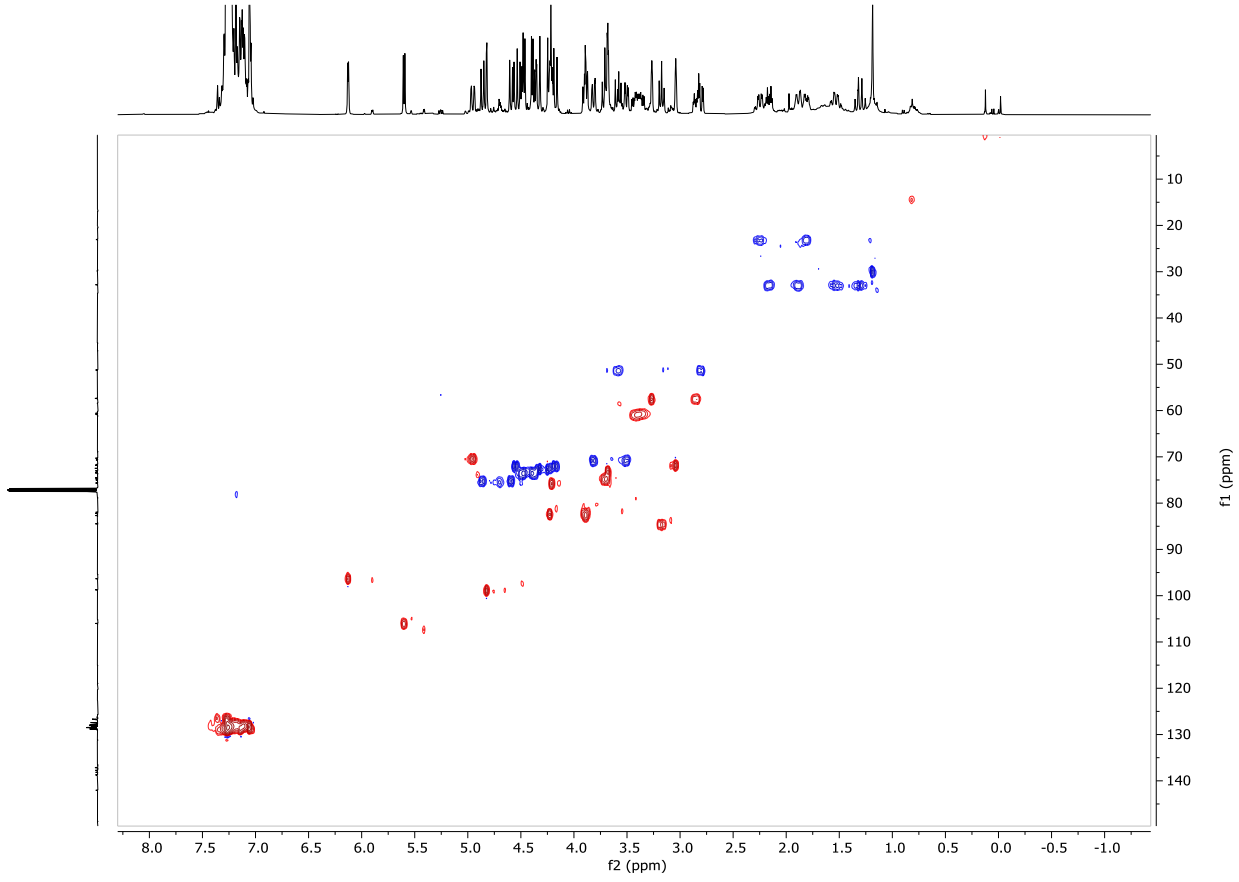
10
20
30
40
50
60
70
80
90
100
110
120
130
140
f1 (ppm)
8.0
7.5
7.0
6.5
6.0
5.5
5.0
4.5
4.0
3.5
3.0
2.5
2.0
1.5
1.0
0.5
0.0
-0.5
-1.0
f2 (ppm)

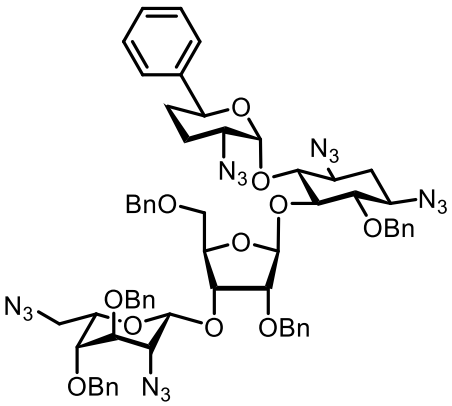
O
N3
N3
O
N3
BnO
O
OBn
O
N3
OBn
O
O
OBn
OBn
N3

115

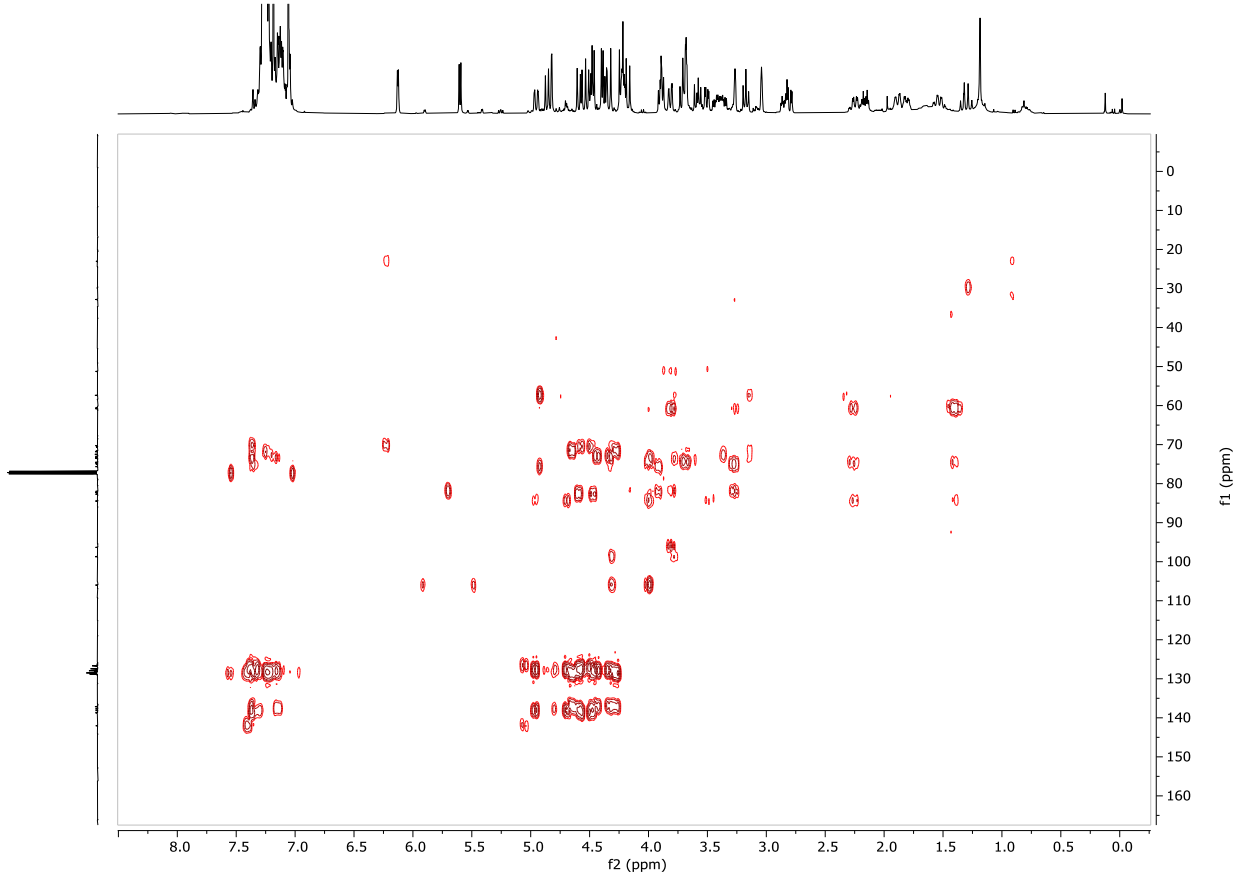
0
10
20
30
40
50
60
70
80
90
100
110
120
130
140
150
160
f1 (ppm)
8.0
7.5
7.0
6.5
6.0
5.5
5.0
4.5
4.0
3.5
3.0
2.5
2.0
1.5
1.0
0.5
0.0
f2 (ppm)

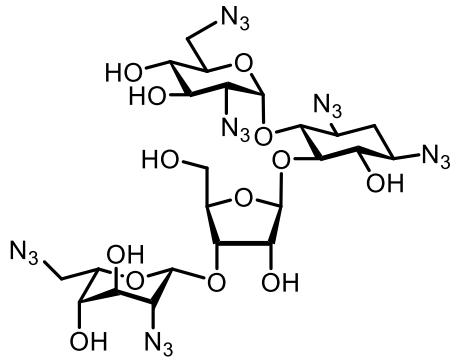
N3
HO
O
HO
N3
N3
O
HO
O
N3
OH
O
N3
OH
O
O
OH
OH
N3

145

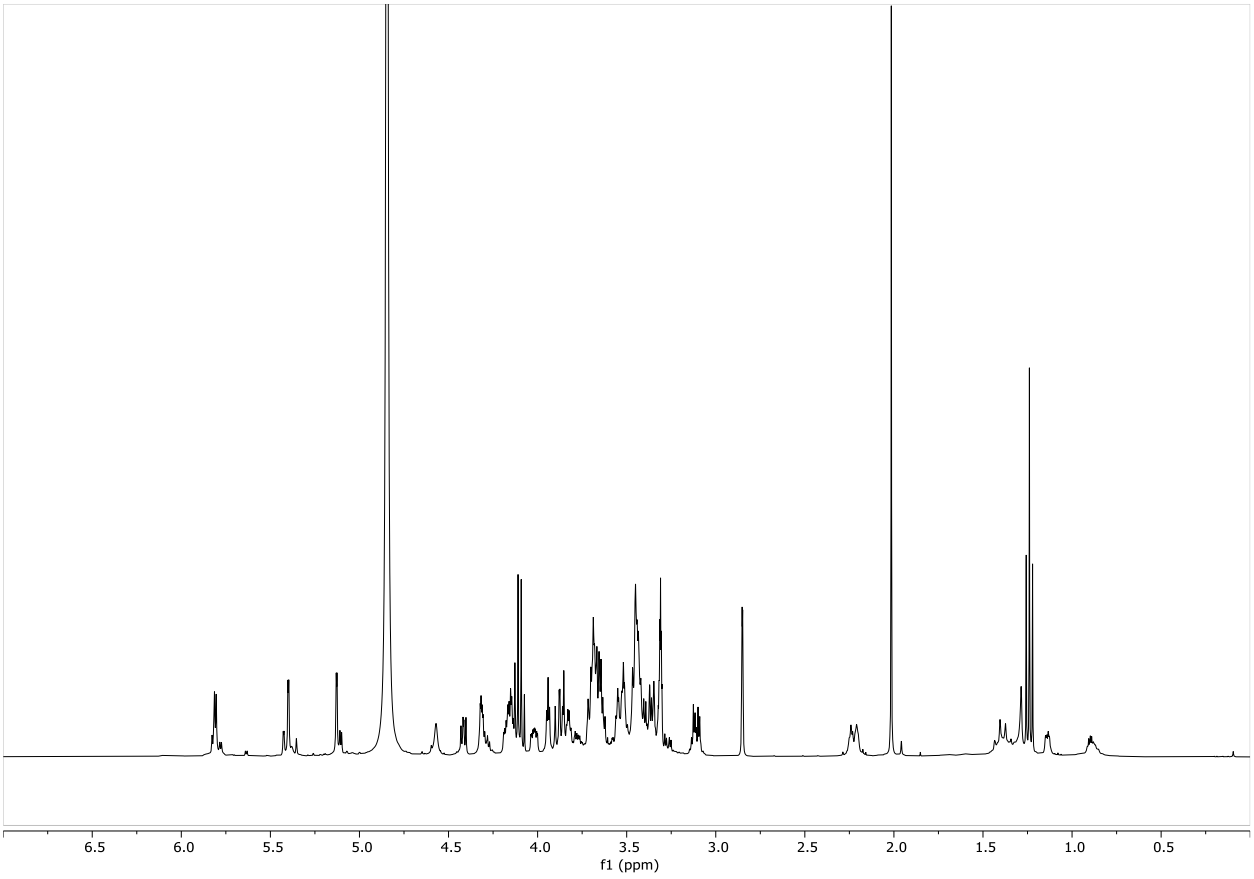
6.5
6.0
5.5
5.0
4.5
4.0
3.5
3.0
2.5
2.0
1.5
1.0
0.5
f1 (ppm)

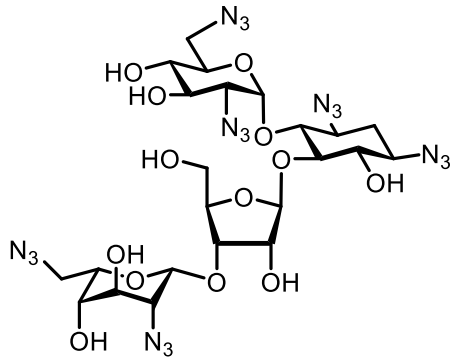
N3
HO
O
HO
N3
N3
O
HO
O
N3
OH
O
N3
OH
O
O
OH
OH
N3

145

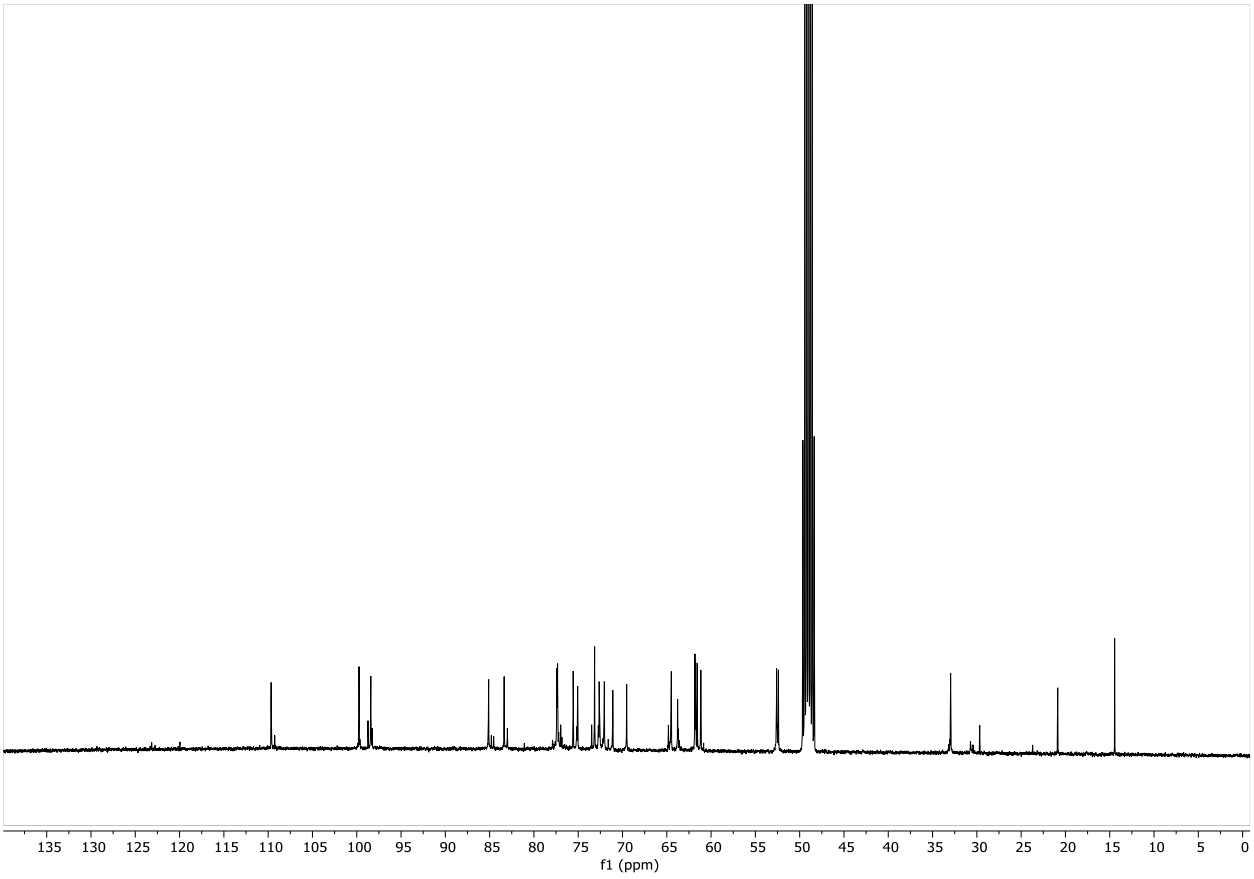
135 130 125 120 115 110 105 100 95 90 85 80 75 70 65 60 55 50 45 40 35 30 25 20 15 10 5 0
f1 (ppm)

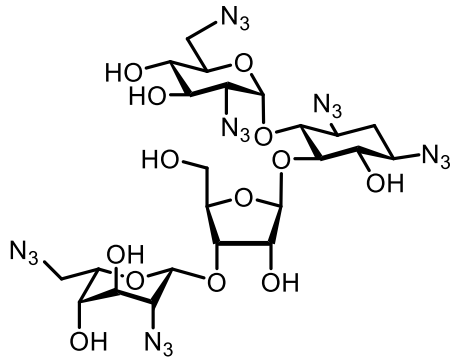
N3
HO
HO
O
N3
N3
O
HO
O
N3
OH
O
N3
OH
O
O
OH
OH
N3

145

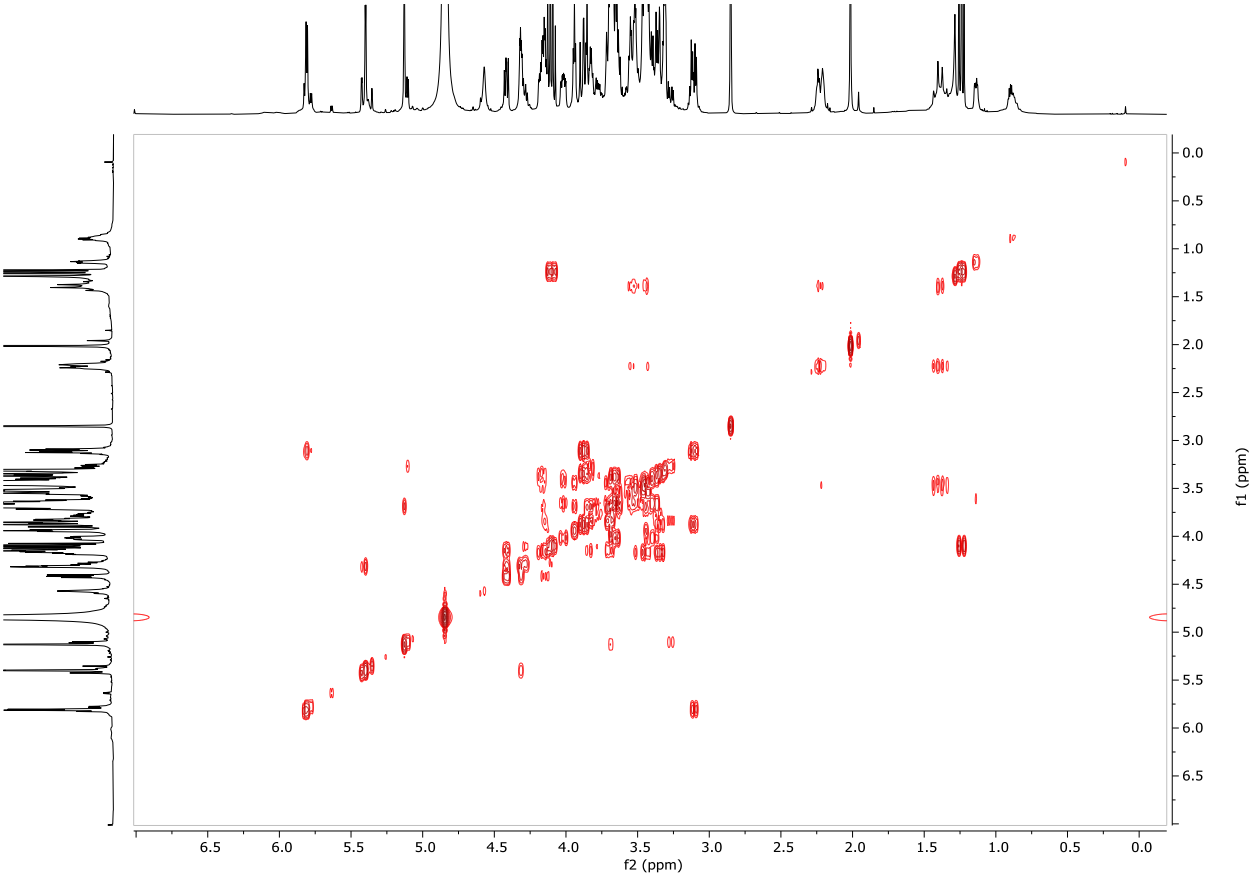
0.0
0.5
1.0
1.5
2.0
2.5
3.0
3.5
4.0
4.5
5.0
5.5
6.0
6.5
f1 (ppm)
6.5
6.0
5.5
5.0
4.5
4.0
3.5
3.0
2.5
2.0
1.5
1.0
0.5
0.0
f2 (ppm)

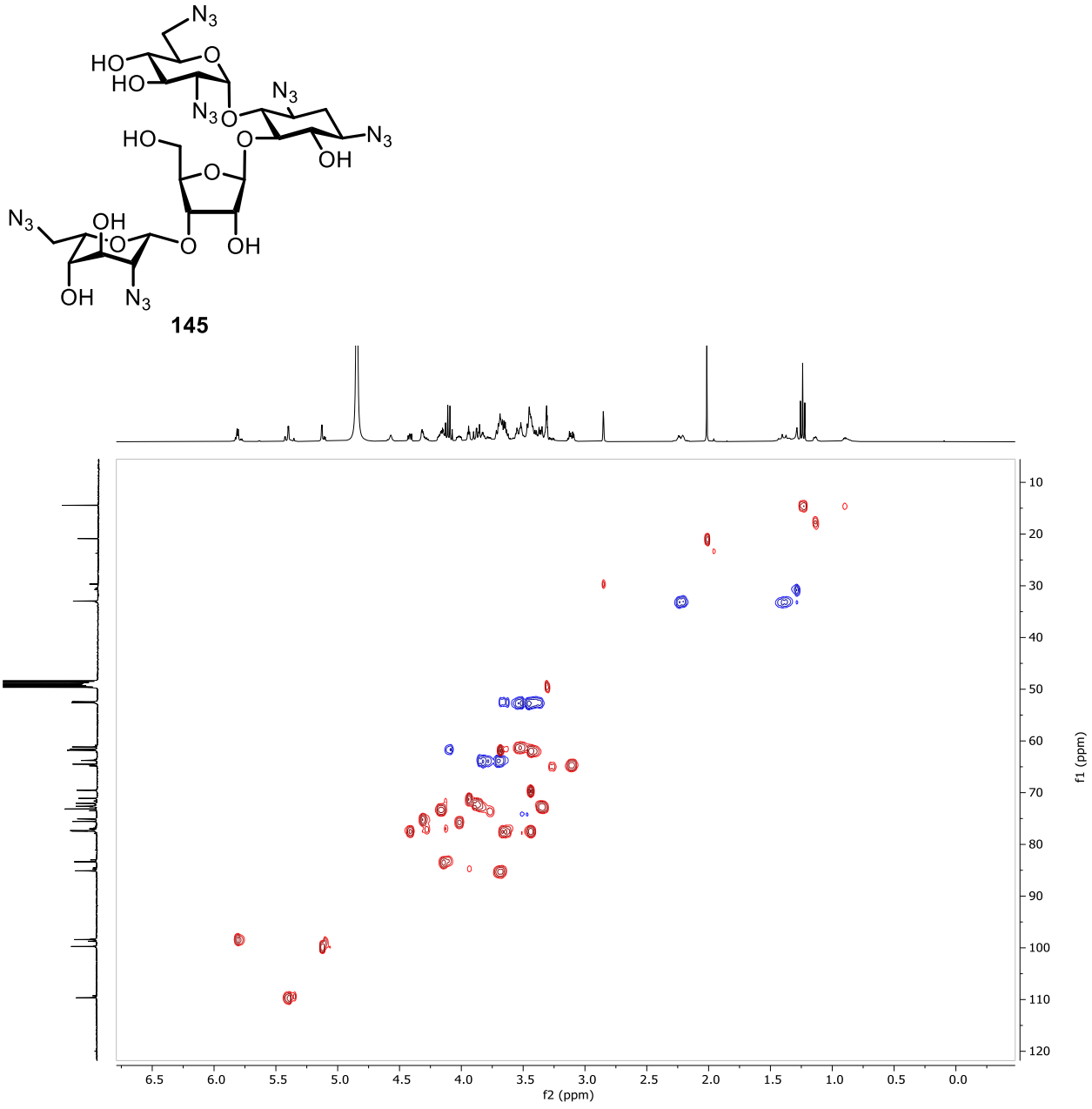
N3
HO
HO
O
N3
O
N3
HO
O
N3
OH
O
N3
OH
O
O
OH
OH
N3
145
f2 (ppm)
f1 (ppm)

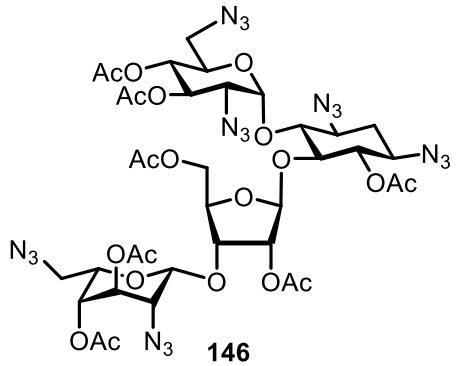
N3
AcO
AcO
O
N3
N3
O
AcO
O
N3
OAc
O
N3
OAc
O
O
OAc
OAc
N3

146

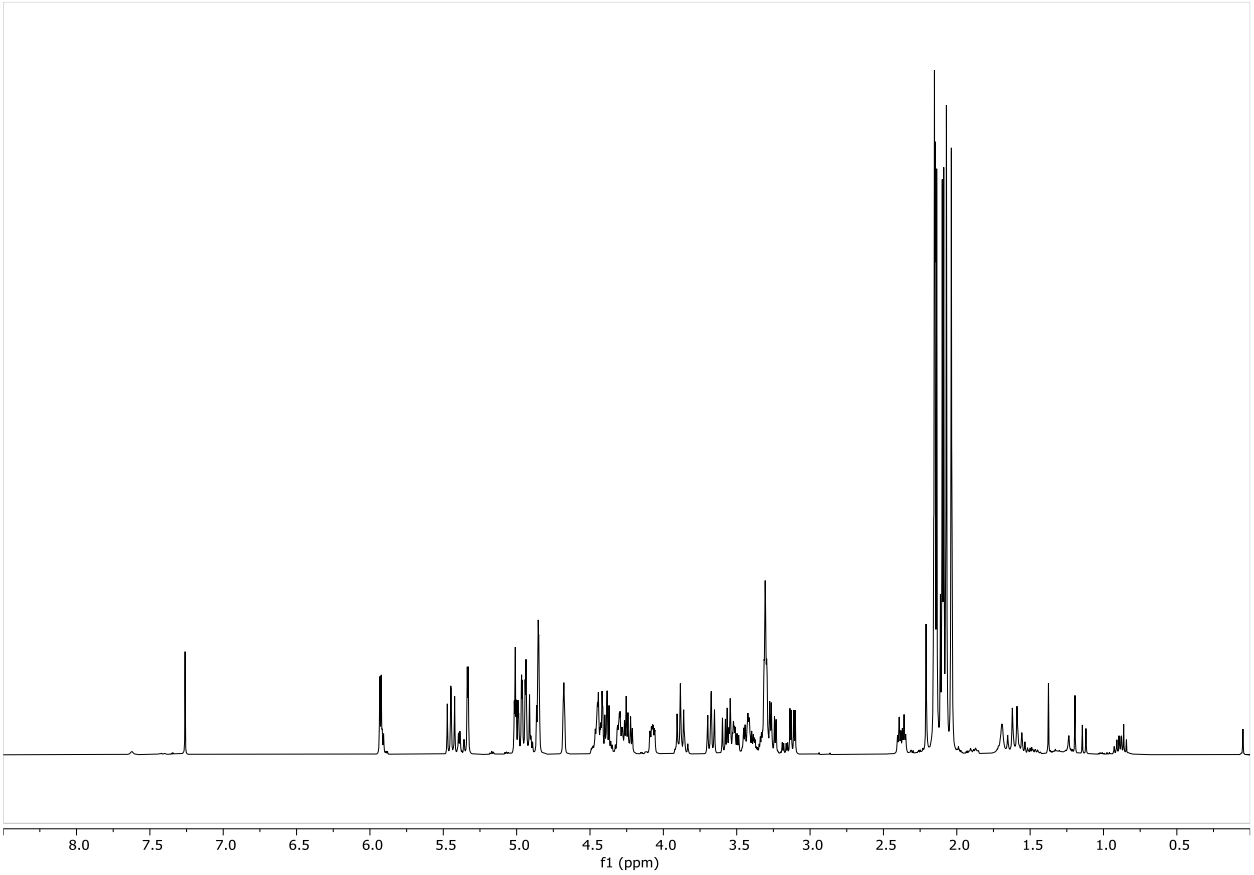
8.0
7.5
7.0
6.5
6.0
5.5
5.0
4.5
4.0
3.5
3.0
2.5
2.0
1.5
1.0
0.5
f1 (ppm)

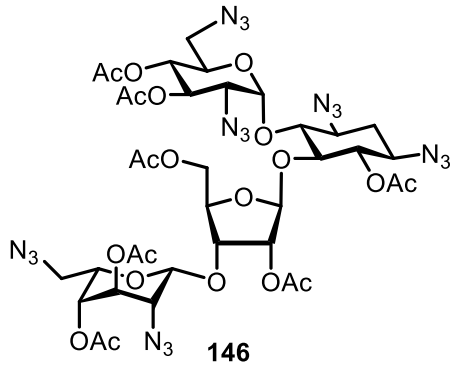
N3
AcO
AcO
O
N3
N3
O
AcO
O
N3
OAc
O
N3
OAc
O
O
OAc
OAc
N3

146

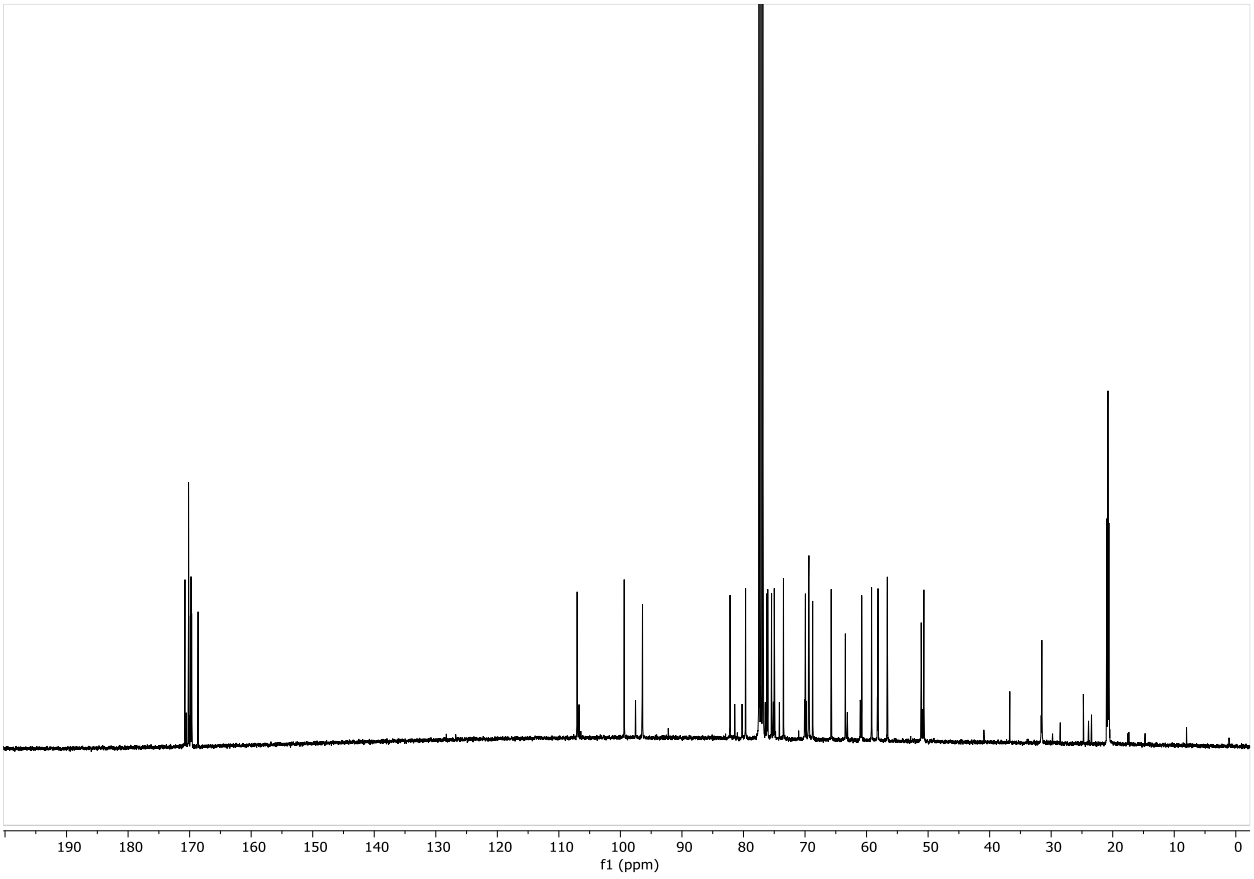
190
180
170
160
150
140
130
120
110
100
90
80
70
60
50
40
30
20
10
0
f1 (ppm)

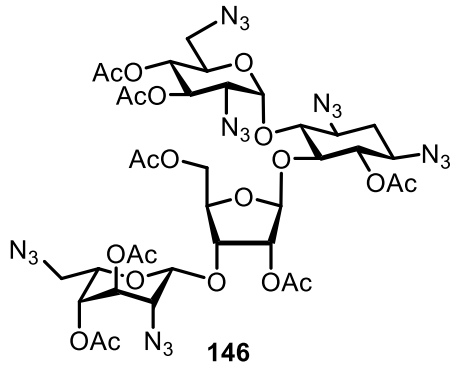
N3
AcO
AcO
O
N3
N3
O
AcO
O
N3
OAc
O
N3
OAc
O
O
OAc
OAc
N3

146

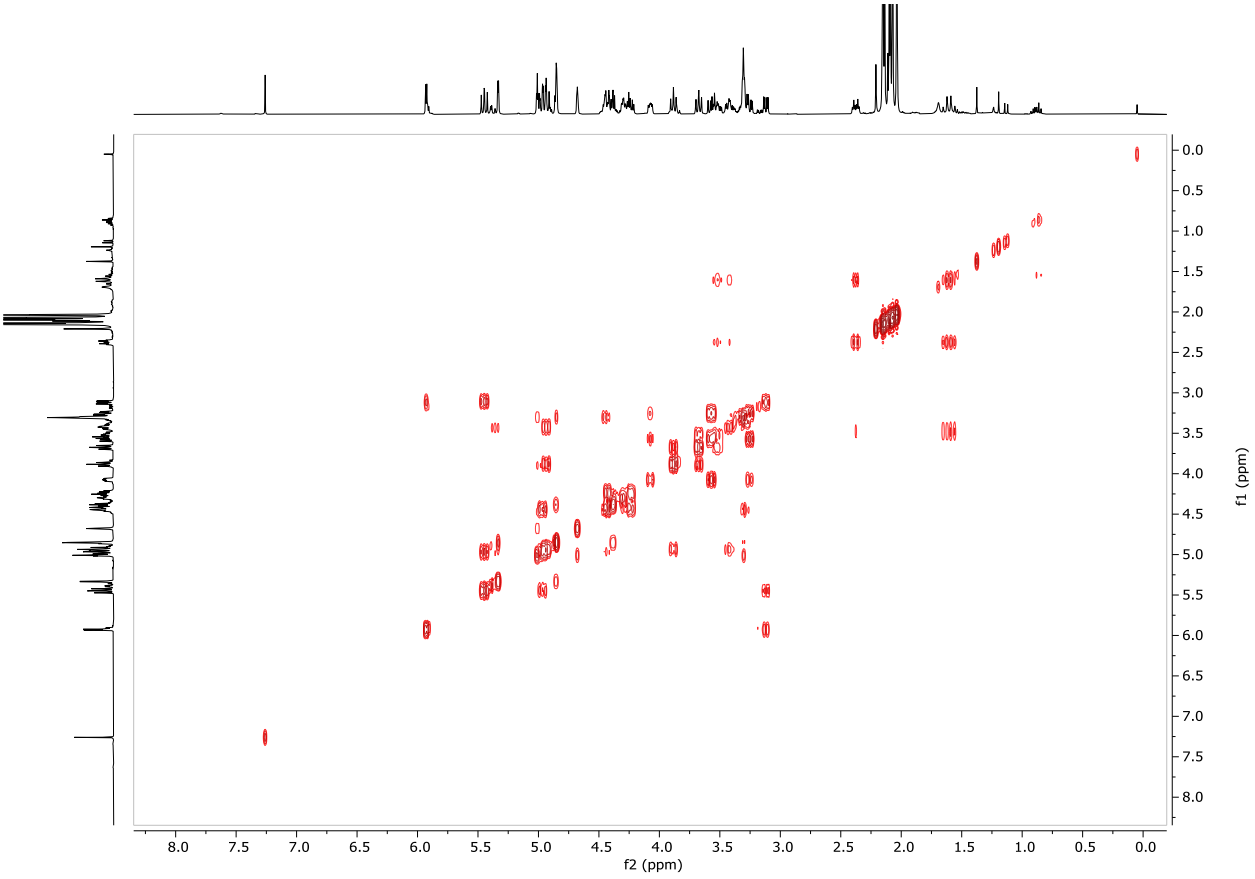
f2 (ppm)
f1 (ppm)
8.0
7.5
7.0
6.5
6.0
5.5
5.0
4.5
4.0
3.5
3.0
2.5
2.0
1.5
1.0
0.5
0.0

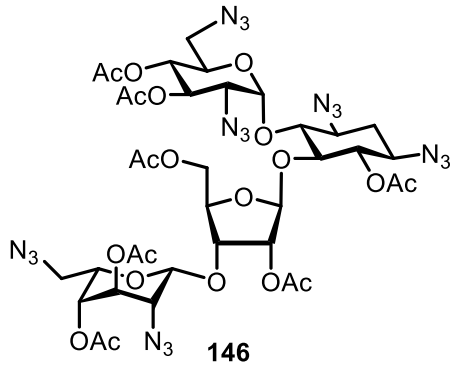
N3
AcO
AcO
O
N3
N3
O
AcO
O
N3
OAc
O
N3
OAc
O
O
OAc
OAc
N3

146

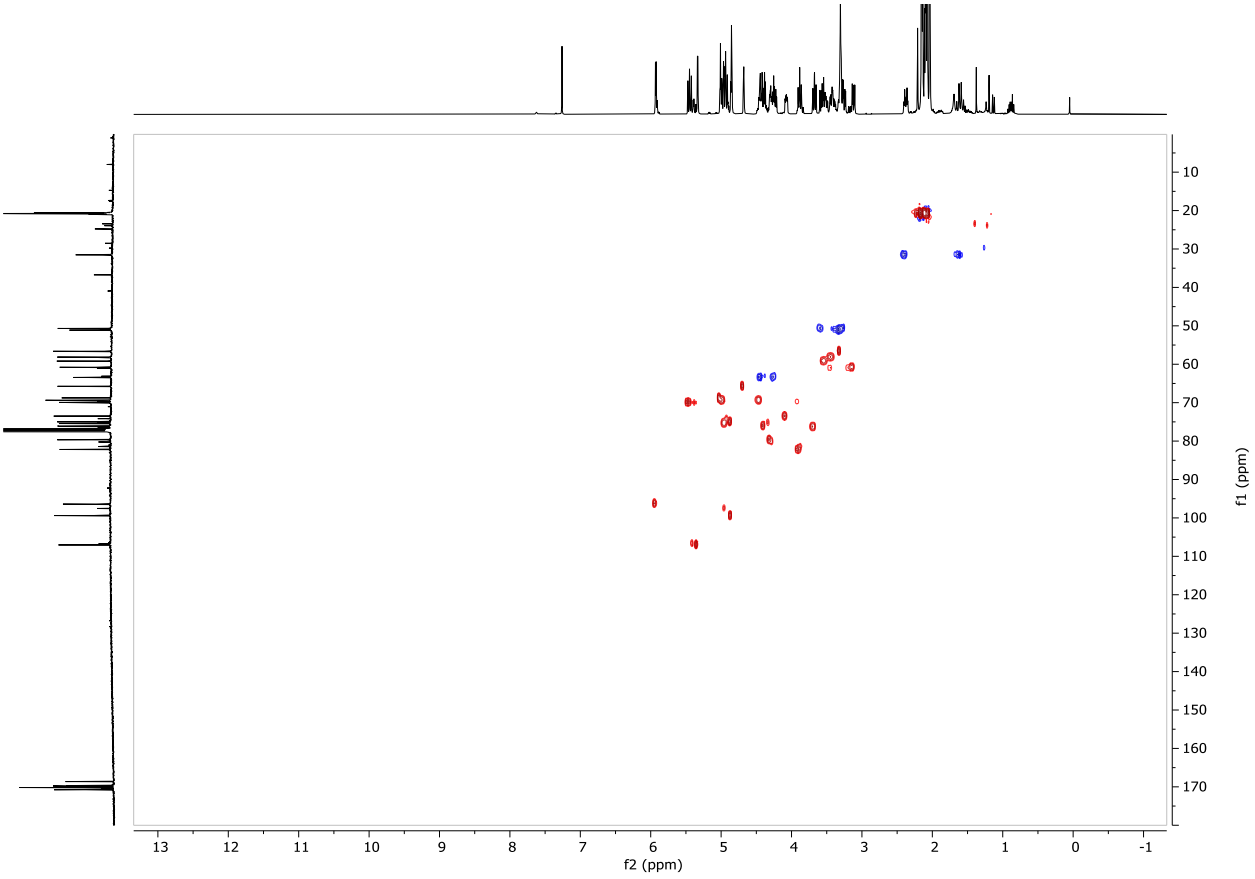
10
20
30
40
50
60
70
80
90
100
110
120
130
140
150
160
170
f1 (ppm)
13
12
11
10
9
8
7
6
5
4
3
2
1
0
-1
f2 (ppm)

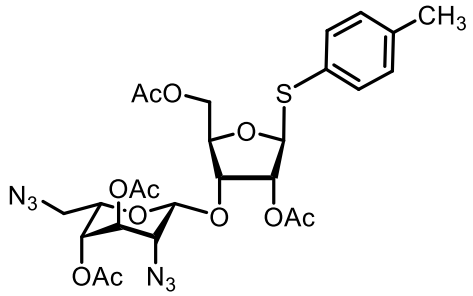
CH3
AcO
S
O
OAc
N3
O
O
OAc
OAc
N3

147

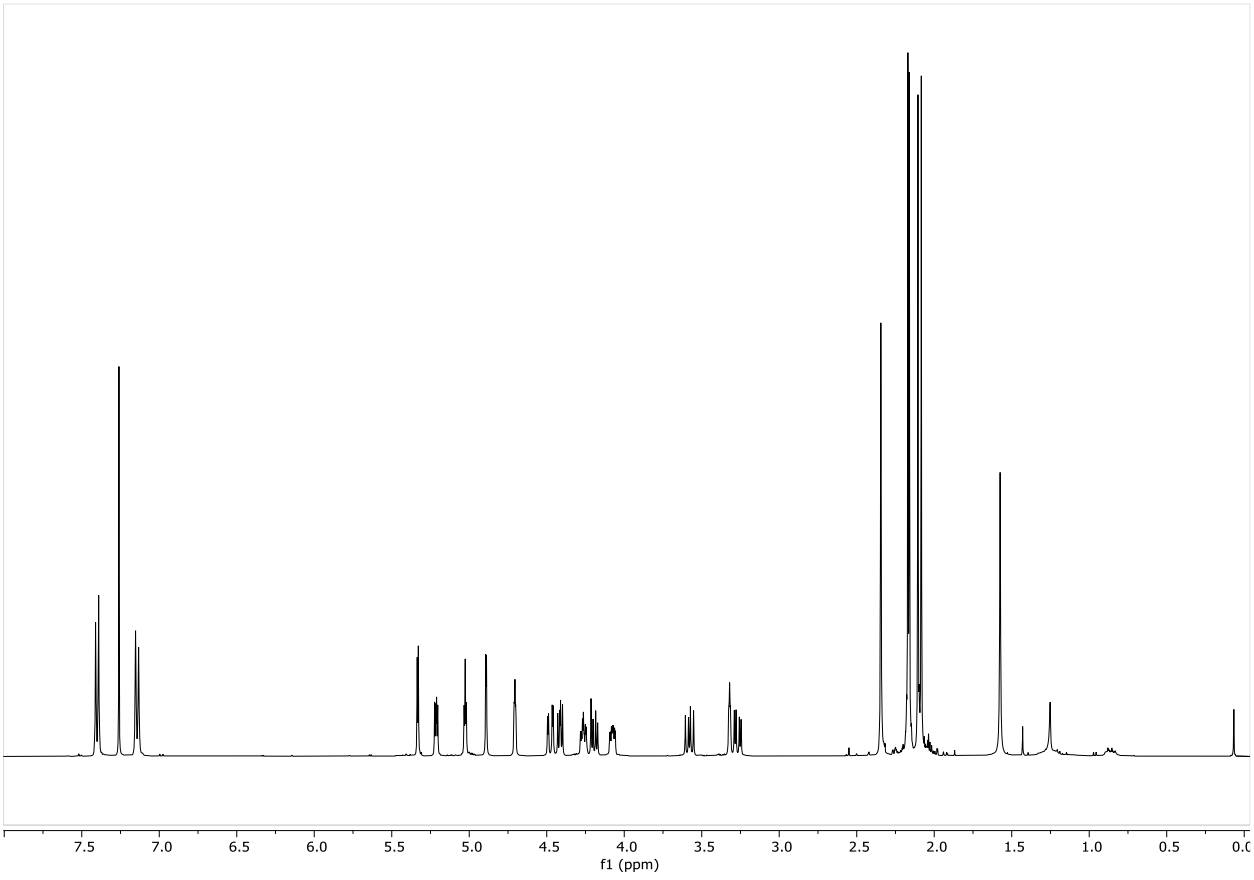
7.5
7.0
6.5
6.0
5.5
5.0
4.5
4.0
3.5
3.0
2.5
2.0
1.5
1.0
0.5
f1 (ppm)

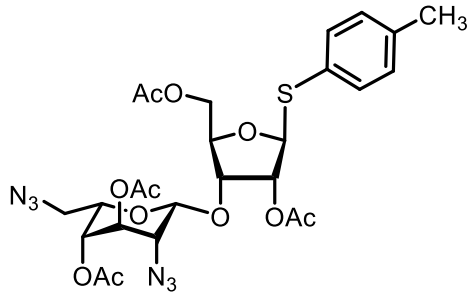
CH3
AcO
S
O
OAc
N3
O
O
OAc
OAc
N3

147

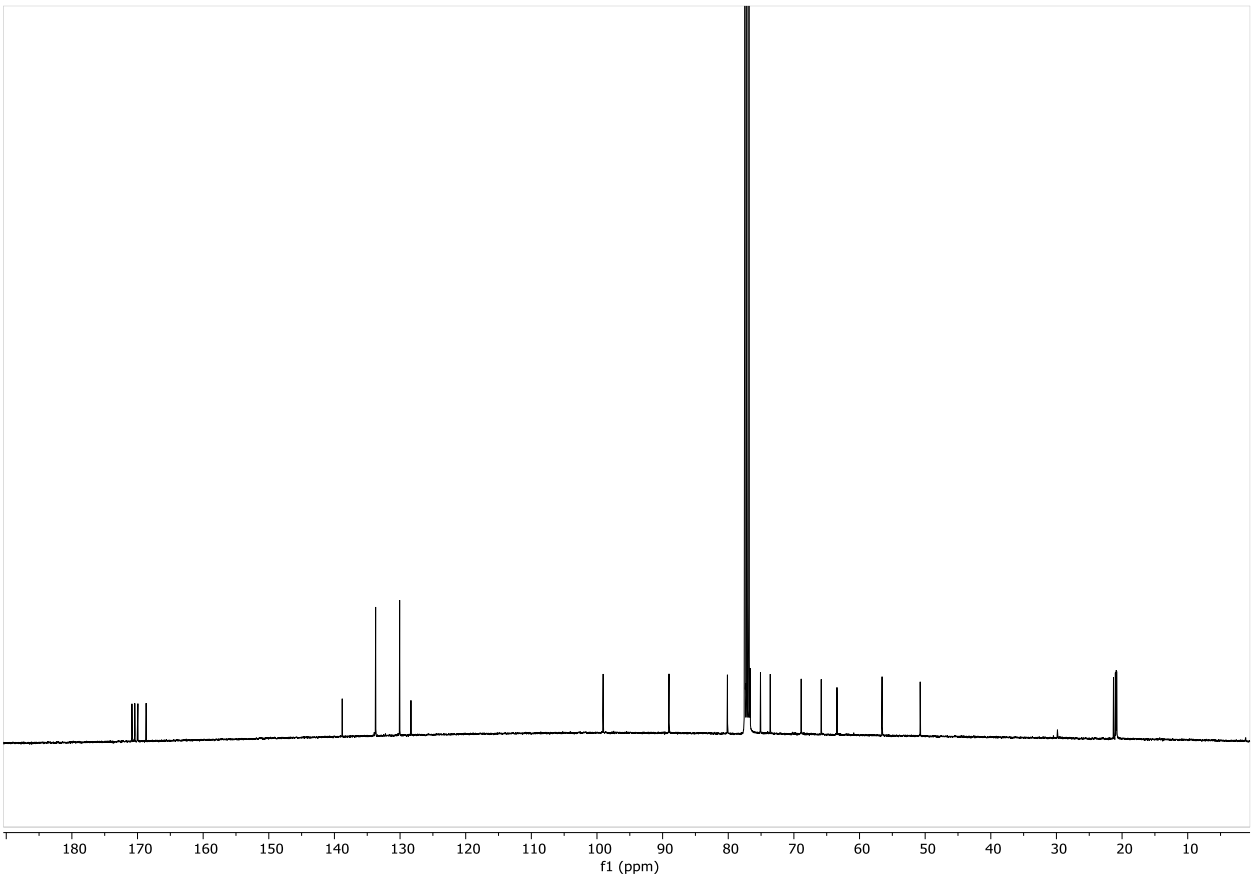
180
170
160
150
140
130
120
110
100
90
80
70
60
50
40
30
20
10
f1 (ppm)

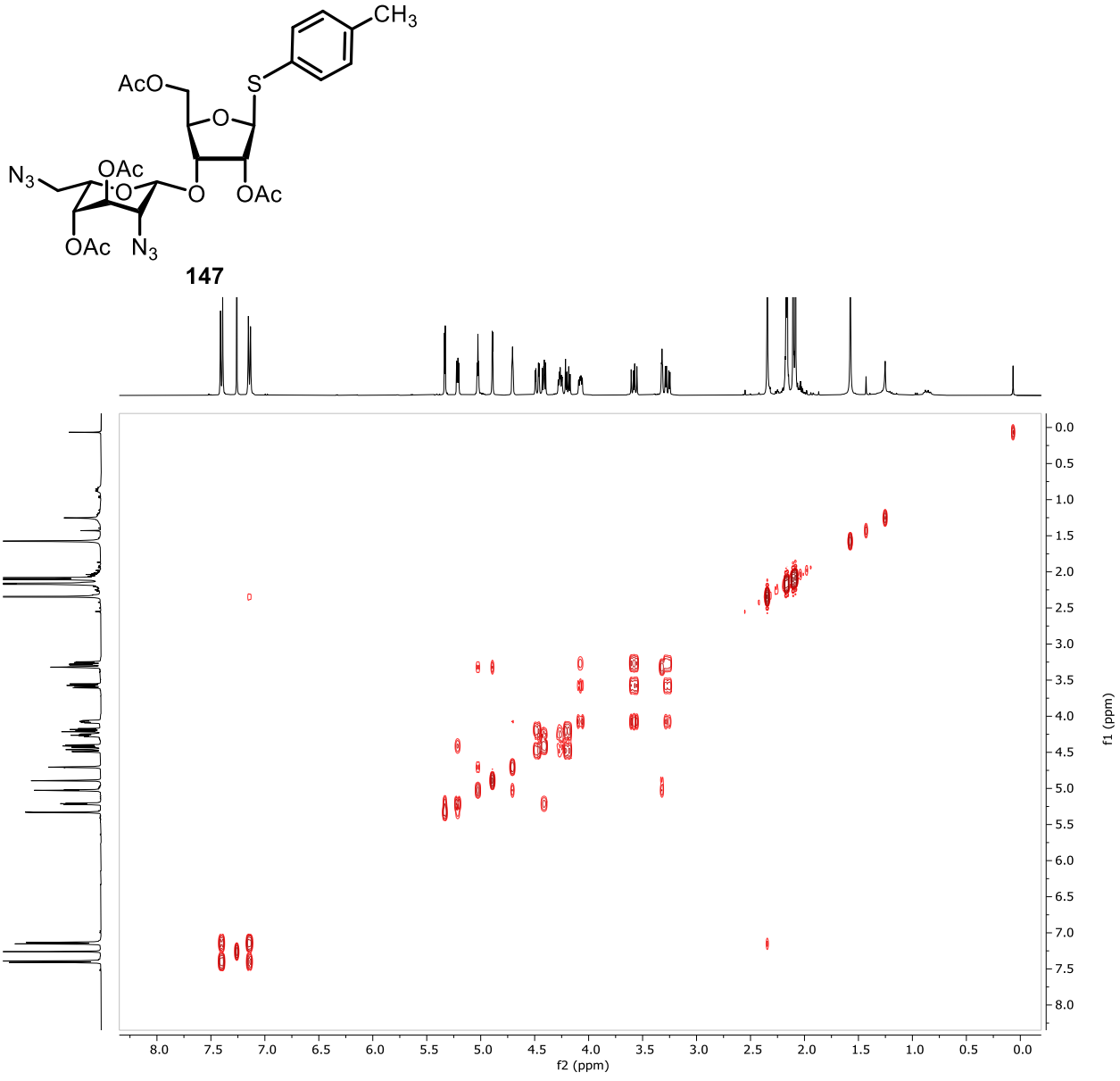
CH3
AcO
S
O
OAc
N3
OAc
O
O
OAc
OAc
N3
147
f1 (ppm)
f2 (ppm)

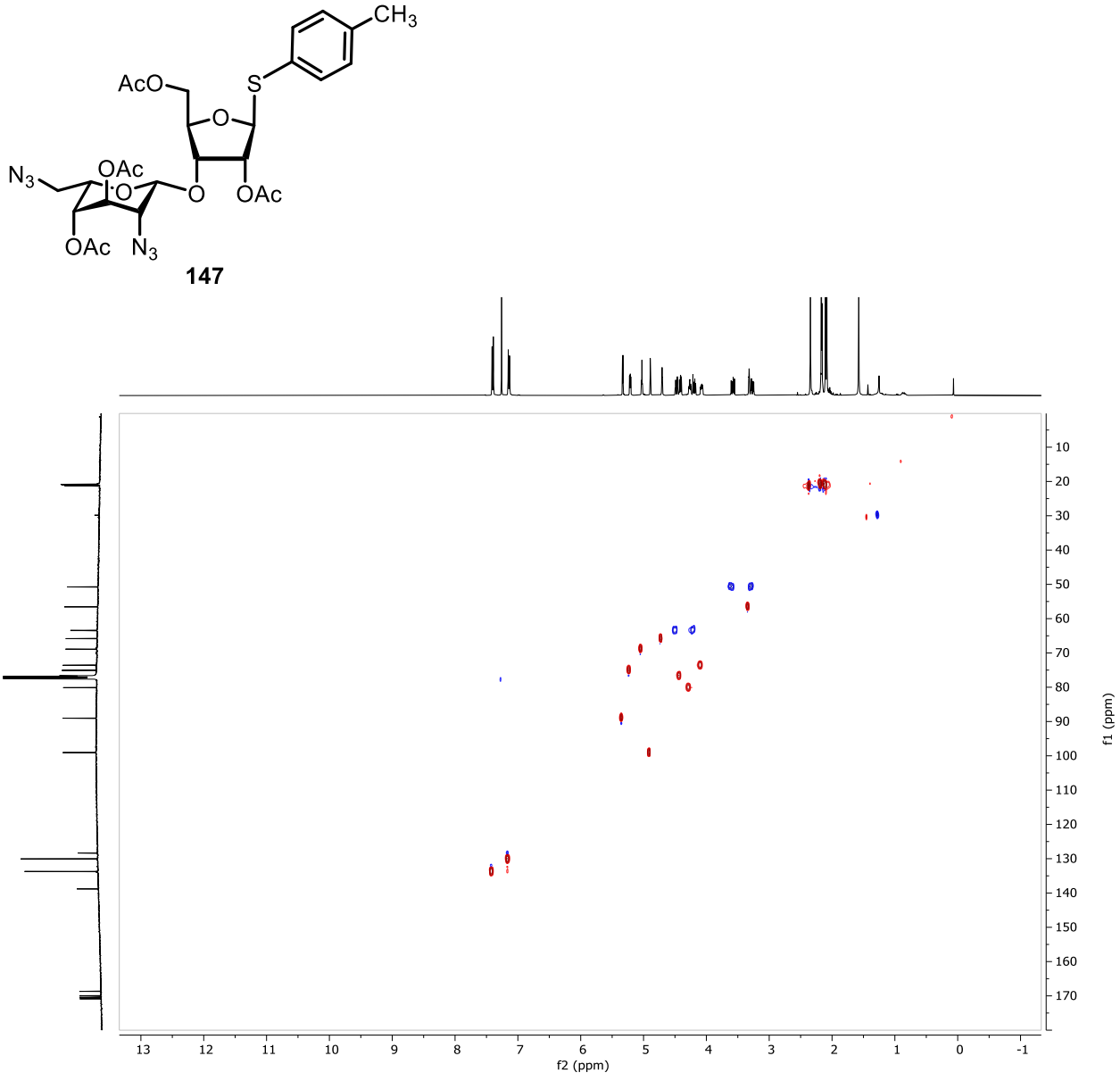
CH3
AcO
S
O
OAc
N3
O
O
OAc
OAc
N3
147
f1 (ppm)
f2 (ppm)

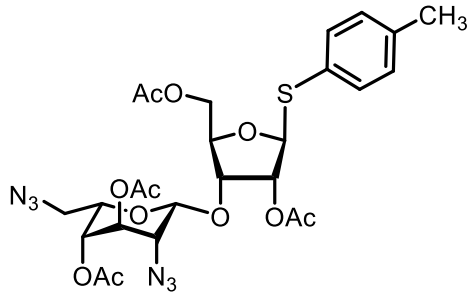
CH3
AcO
S
O
OAc
N3
O
O
OAc
OAc
N3

147

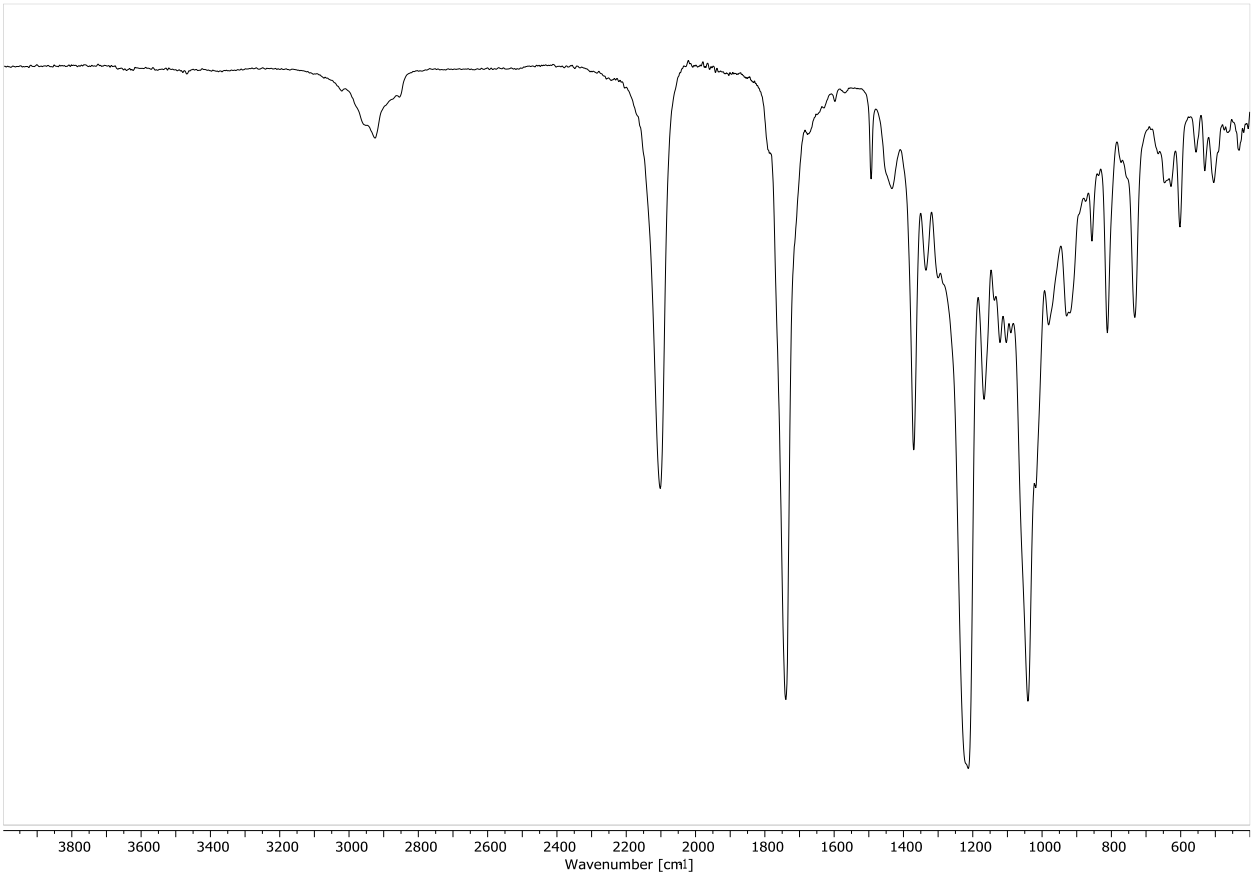
3800
3600
3400
3200
3000
2800
2600
2400
2200
2000
1800
1600
1400
1200
1000
800
600
Wavenumber [cm-1]

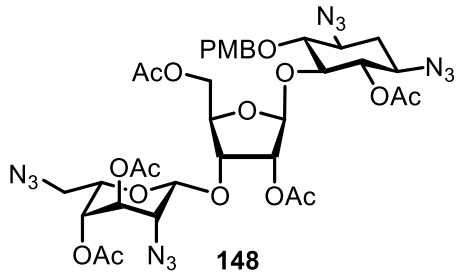
N3
PMBO
AcO
O
N3
OAc
O
OAc
N3
O
O
OAc
OAc
N3

148

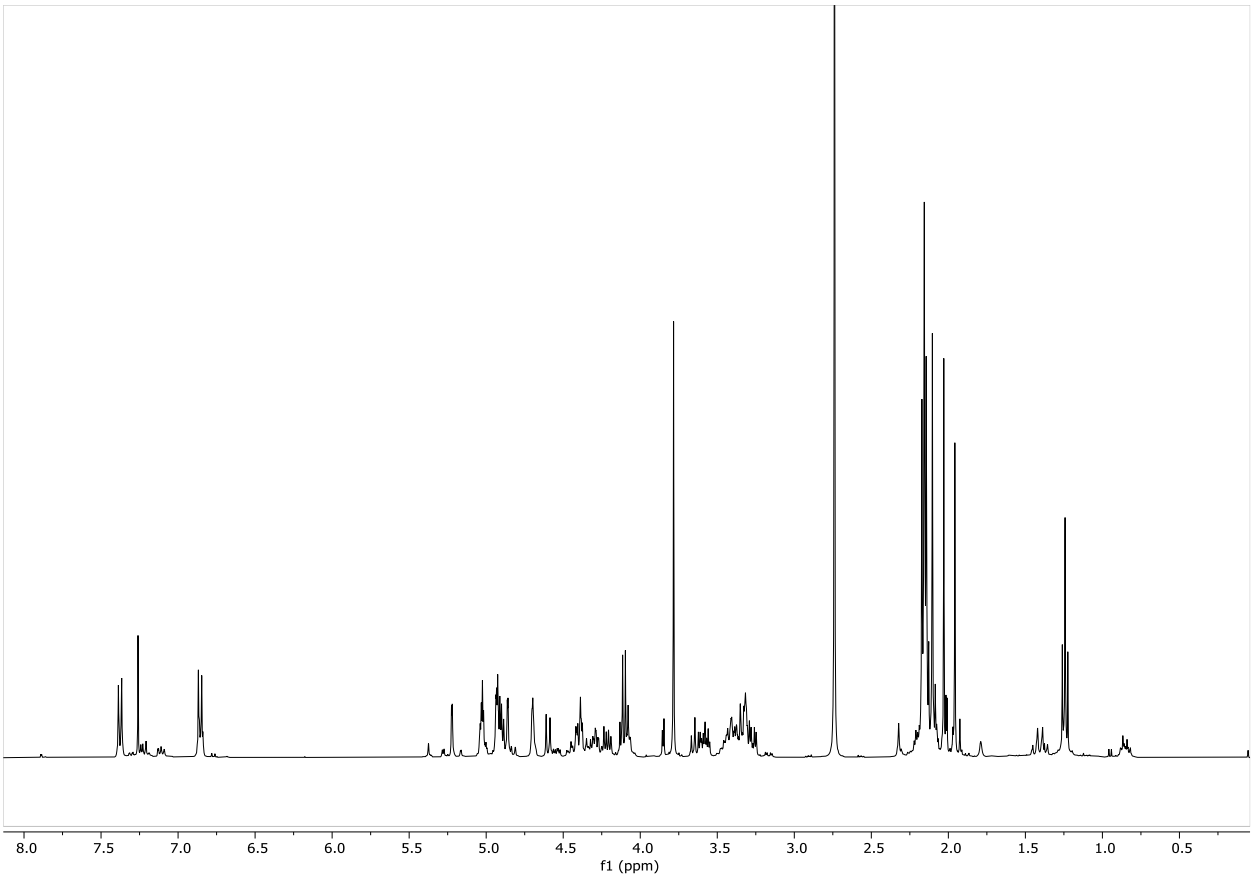
8.0
7.5
7.0
6.5
6.0
5.5
5.0
4.5
4.0
3.5
3.0
2.5
2.0
1.5
1.0
0.5
f1 (ppm)

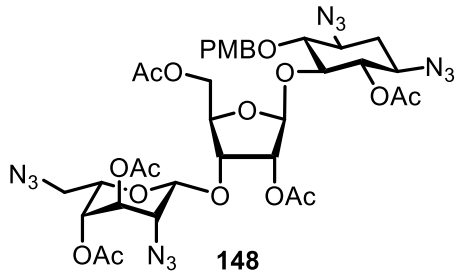
N3
PMBO
AcO
O
N3
OAc
O
OAc
N3
O
O
OAc
OAc
N3

148

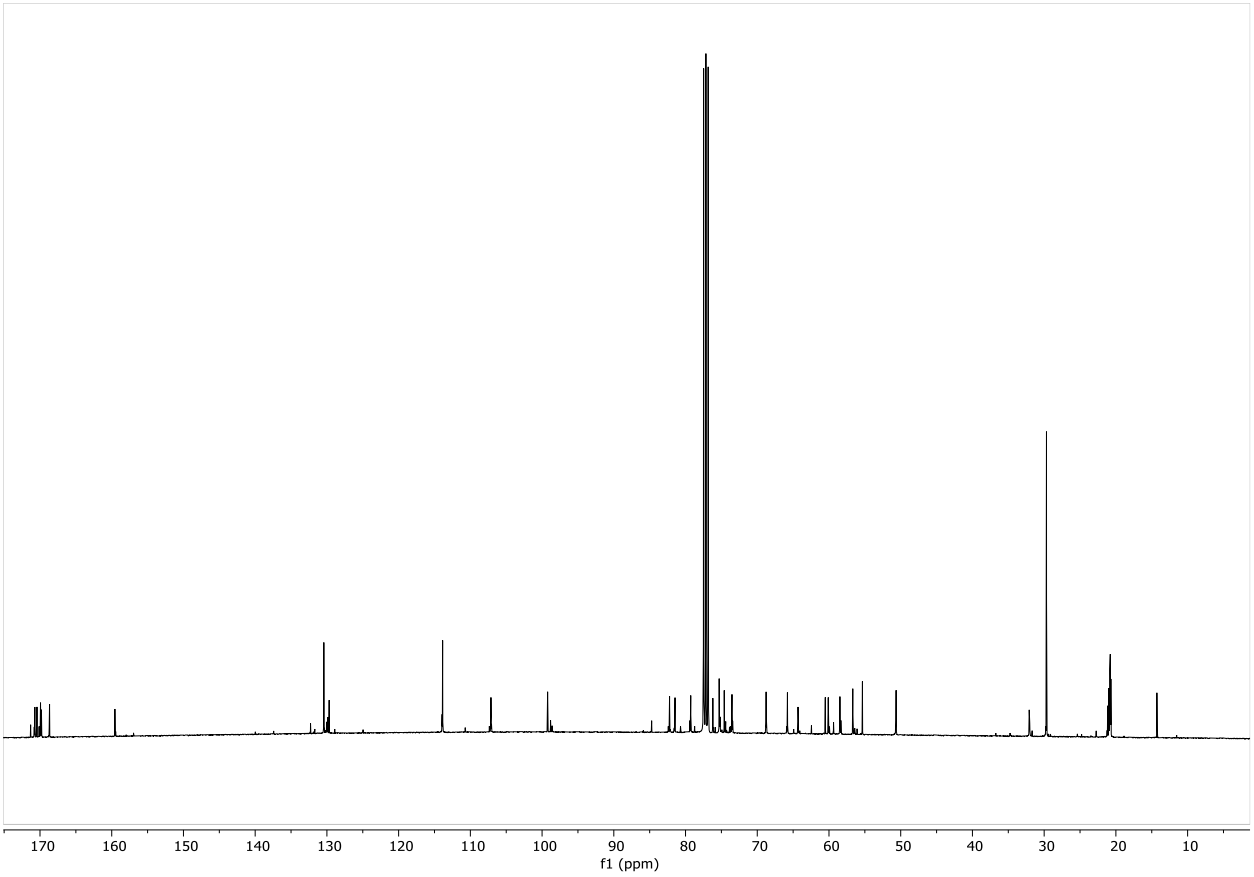
170
160
150
140
130
120
110
100
90
80
70
60
50
40
30
20
10
f1 (ppm)

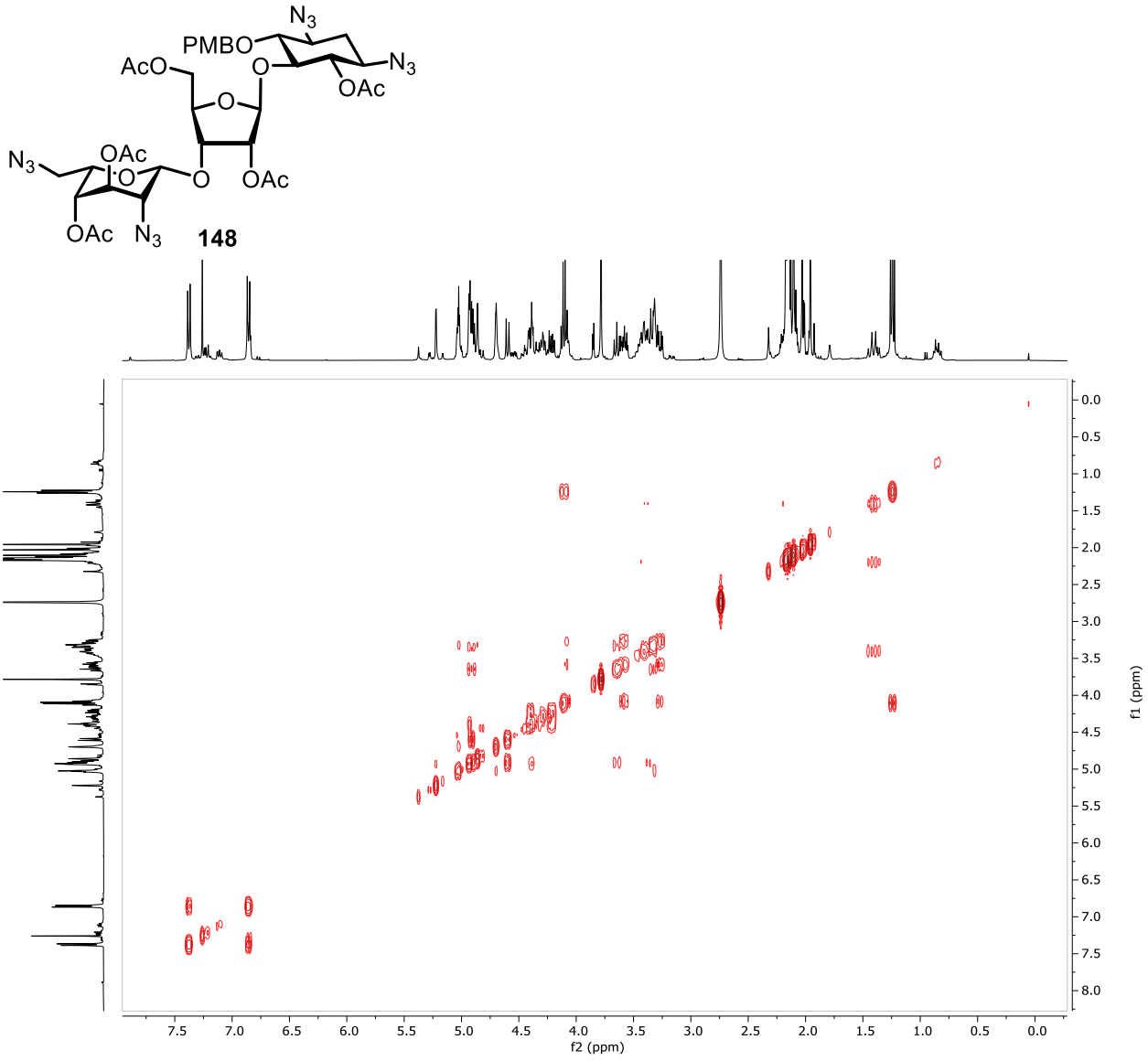
N3
PMBO
AcO
O
N3
OAc
O
N3
OAc
O
O
OAc
OAc
N3
148
f2 (ppm)
f1 (ppm)

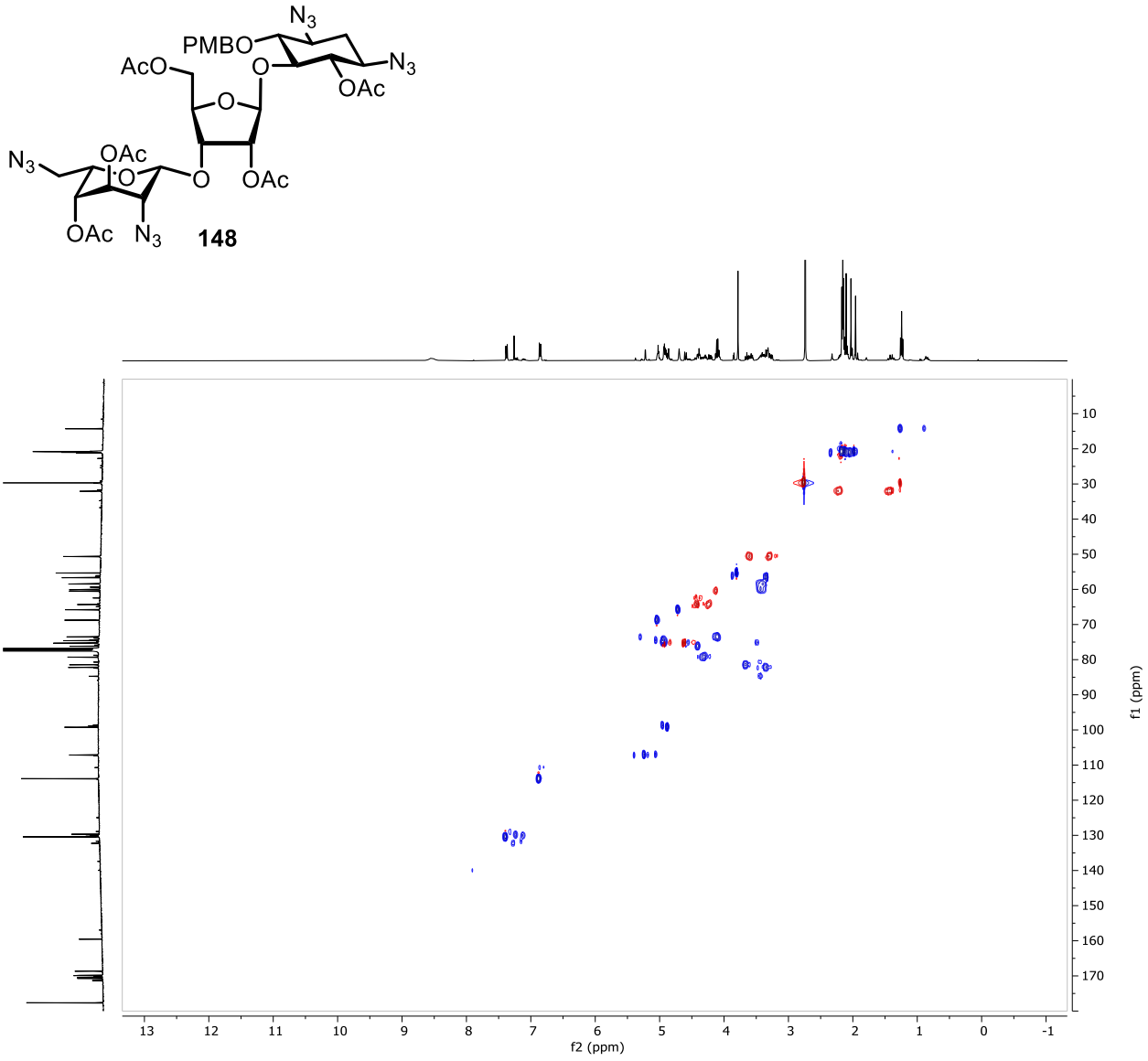
N3
PMBO
AcO
O
N3
OAc
O
OAc
N3
O
O
OAc
OAc
N3
148
f2 (ppm)
f1 (ppm)

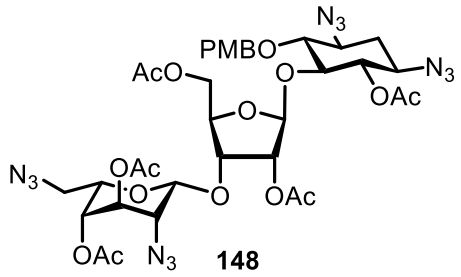
N3
PMBO
AcO
O
N3
OAc
O
OAc
N3
O
O
OAc
OAc
N3

148

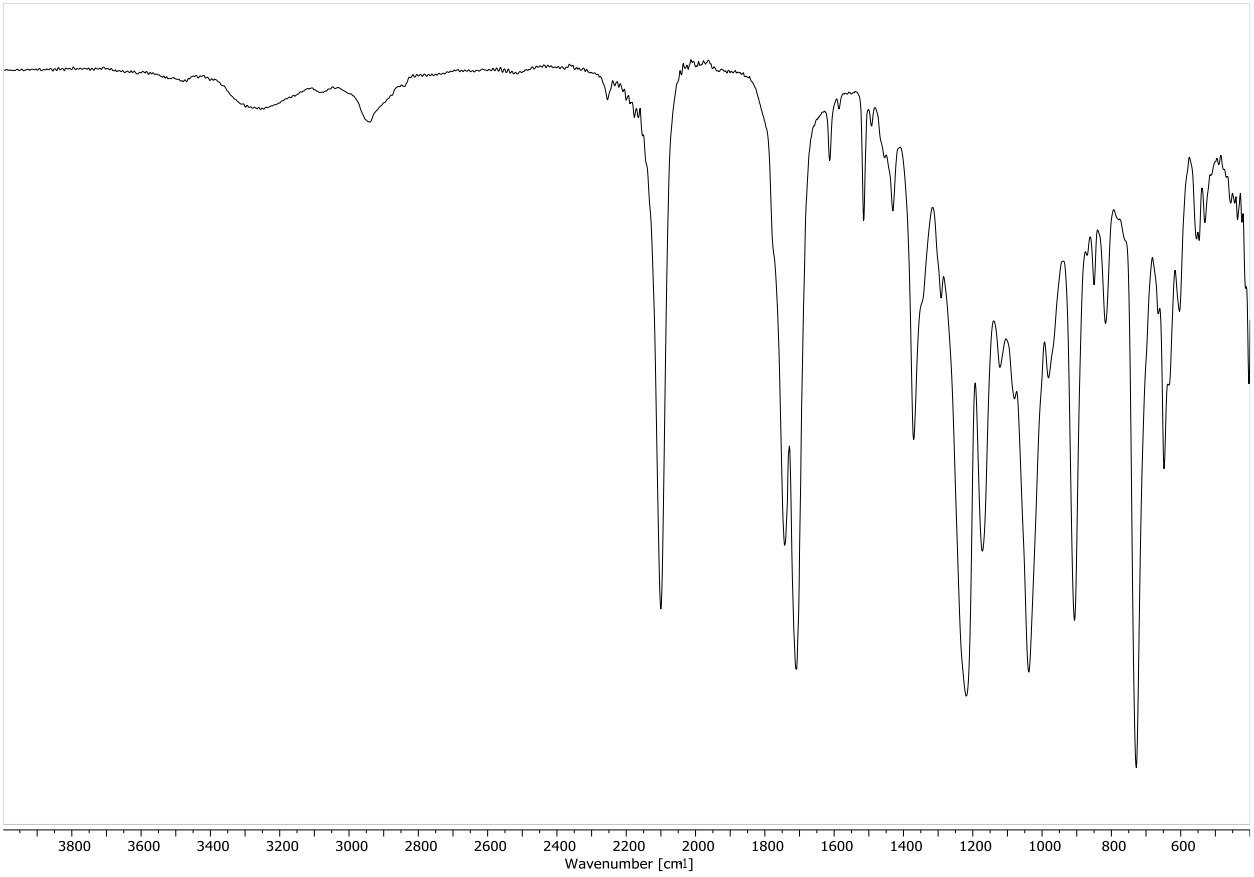
3800
3600
3400
3200
3000
2800
2600
2400
2200
2000
1800
1600
1400
1200
1000
800
600
Wavenumber [cm-1]

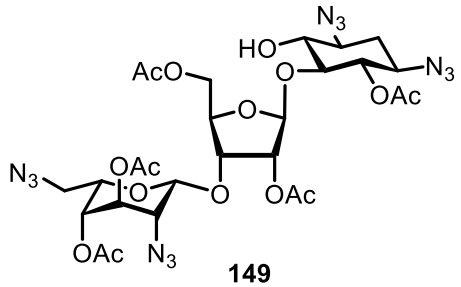
N3
HO
AcO
O
N3
OAc
O
OAc
N3
O
O
OAc
OAc
N3

149

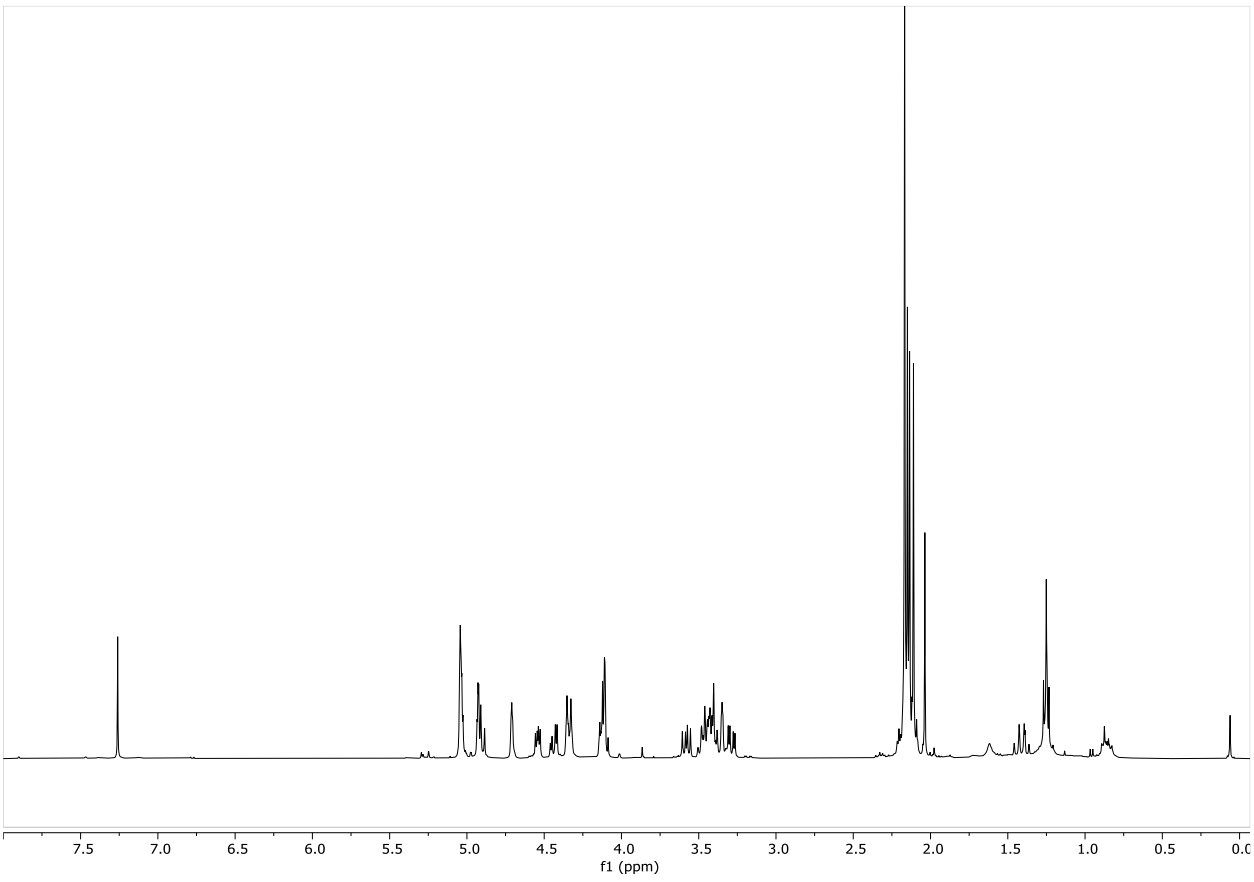
7.5
7.0
6.5
6.0
5.5
5.0
4.5
4.0
3.5
3.0
2.5
2.0
1.5
1.0
0.5
f1 (ppm)

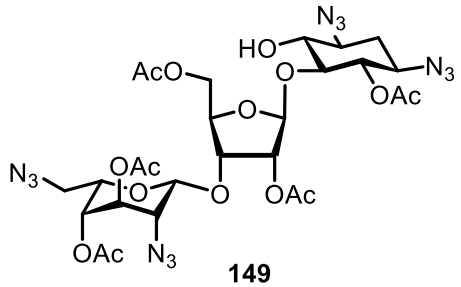
N3
HO
AcO
O
N3
OAc
O
OAc
N3
O
O
OAc
OAc
N3

149

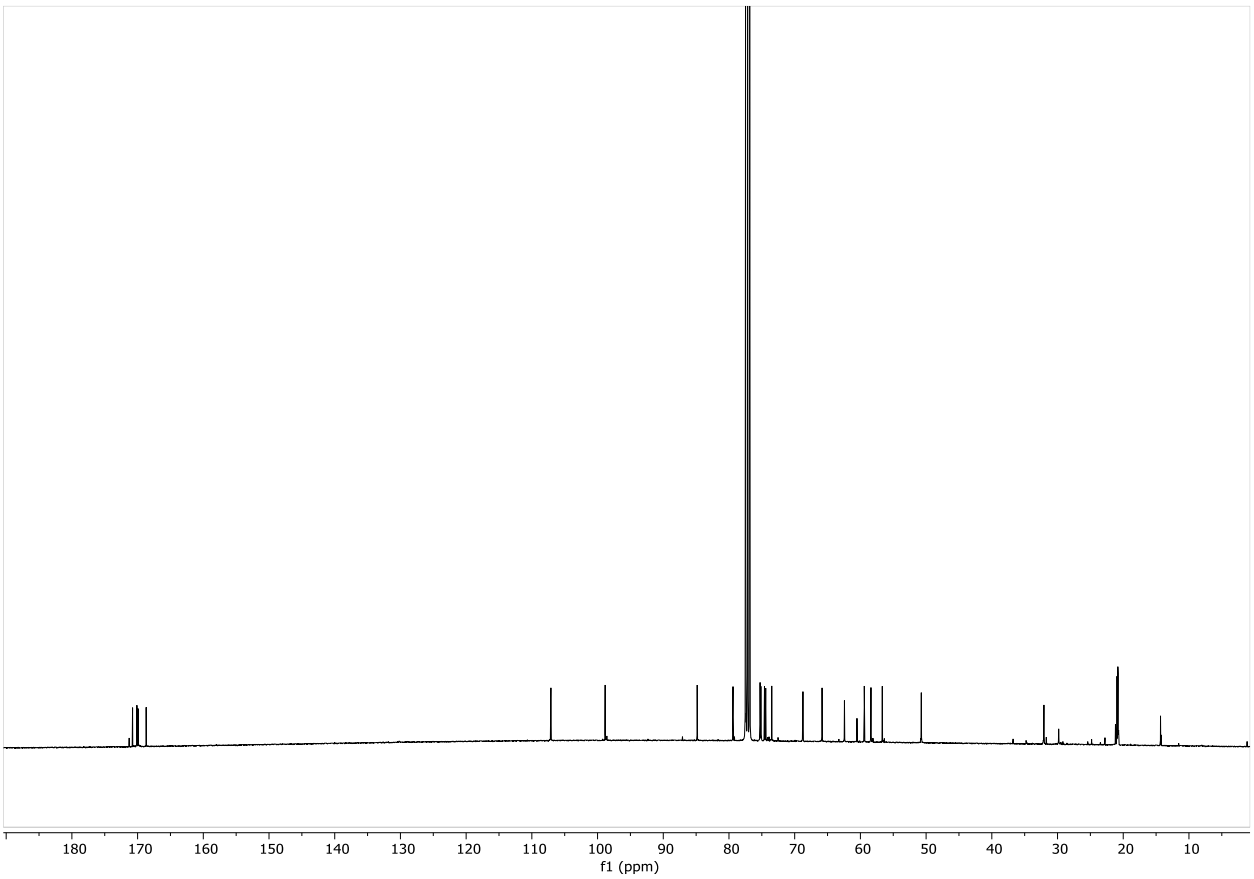
180
170
160
150
140
130
120
110
100
90
80
70
60
50
40
30
20
10
f1 (ppm)

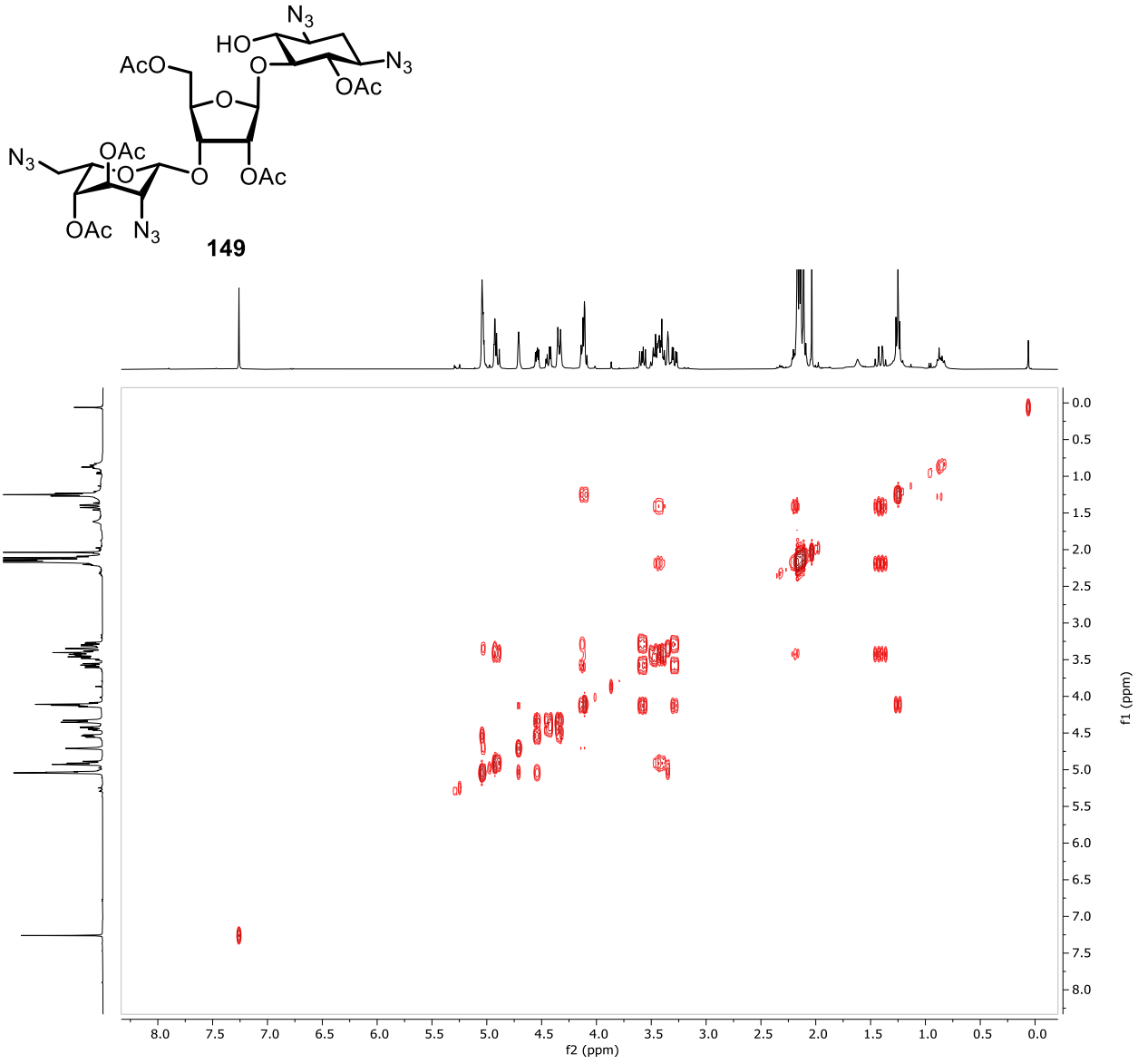
N3
HO
AcO
O
N3
OAc
O
OAc
N3
O
O
OAc
OAc
N3
149
f2 (ppm)
f1 (ppm)

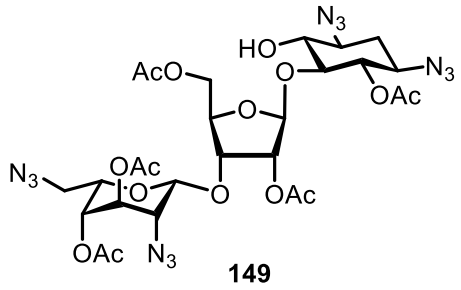
N3
HO
AcO
O
N3
OAc
O
OAc
N3
O
O
OAc
OAc
N3

149

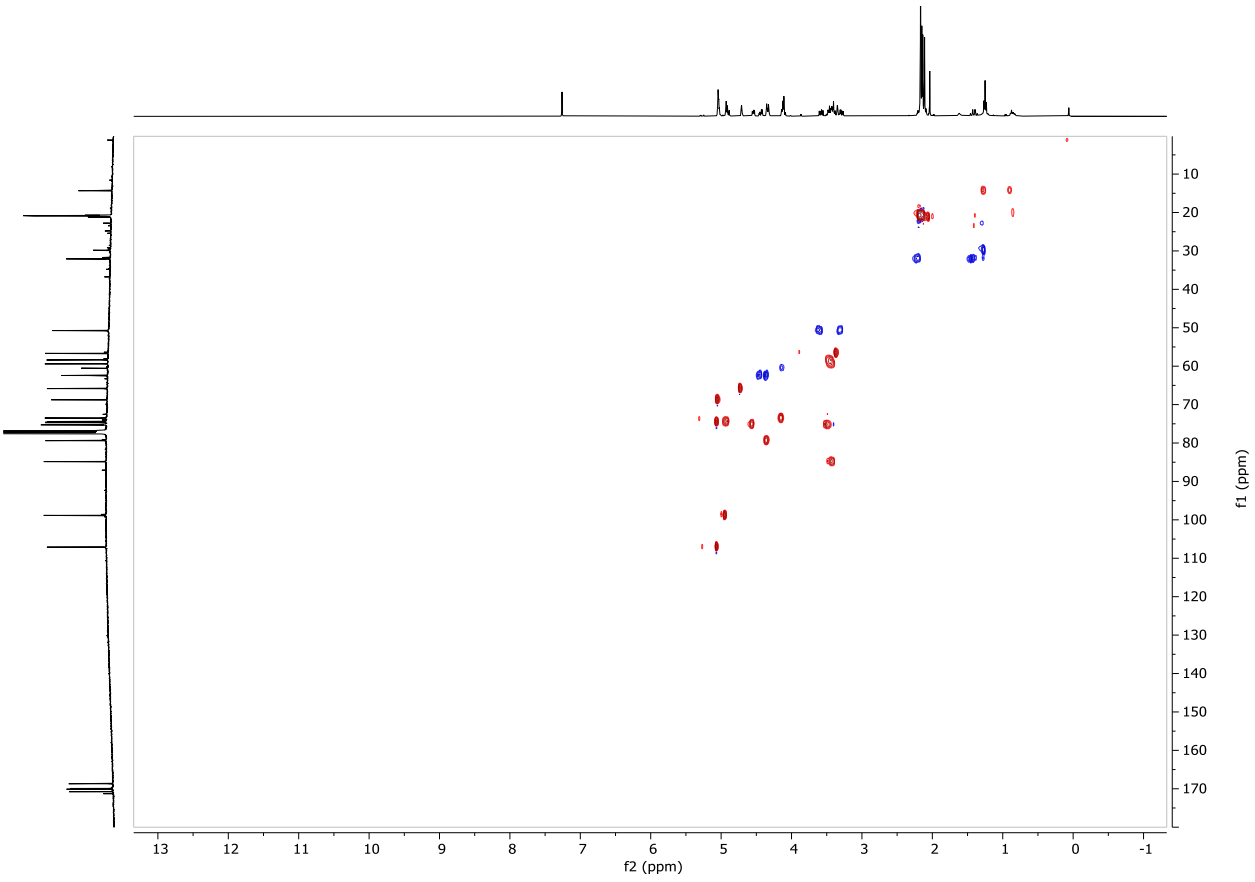
13
12
11
10
9
8
7
6
5
4
3
2
1
0
-1
f2 (ppm)
10
20
30
40
50
60
70
80
90
100
110
120
130
140
150
160
170
f1 (ppm)

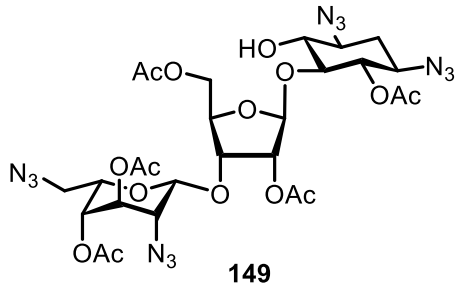
N3
HO
AcO
O
N3
OAc
O
OAc
N3
O
O
OAc
OAc
N3

149

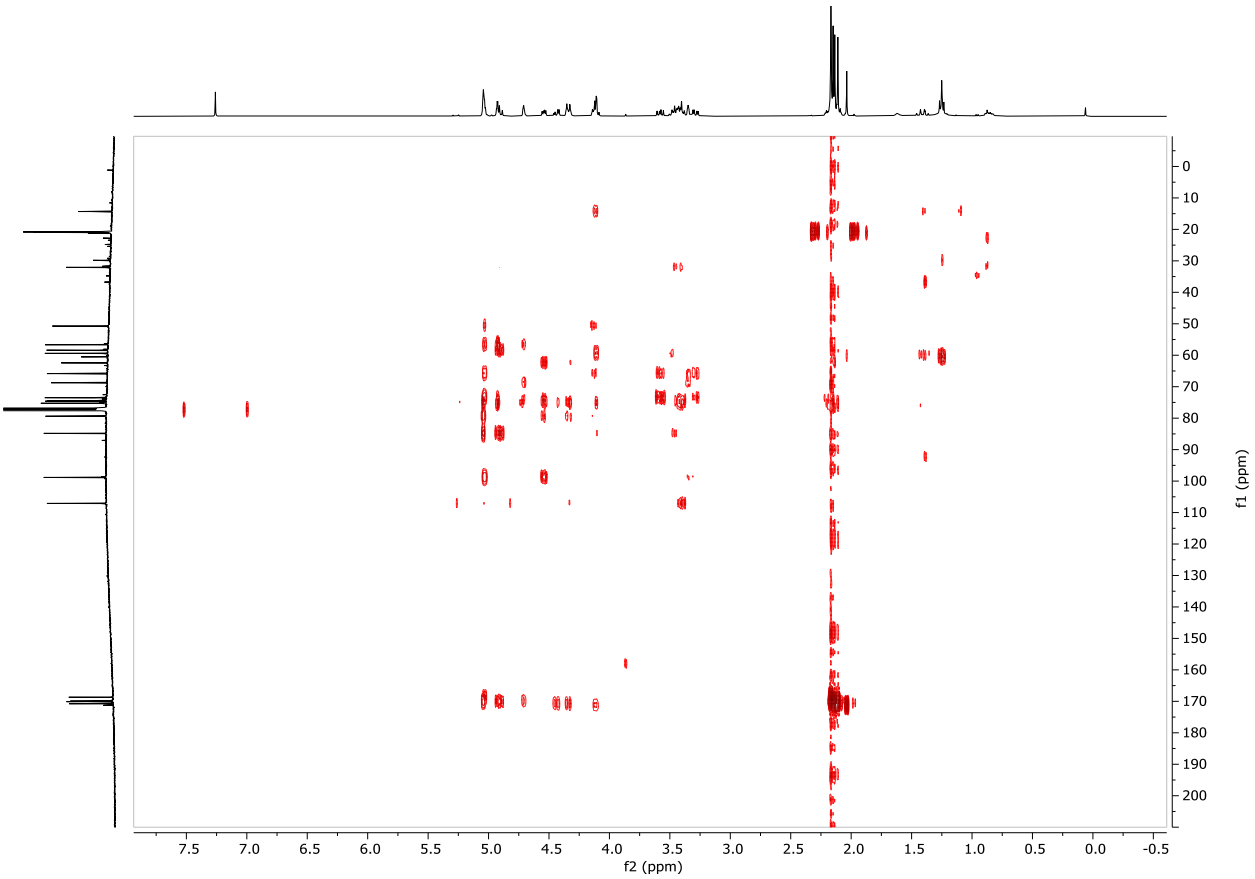
7.5
7.0
6.5
6.0
5.5
5.0
4.5
4.0
3.5
3.0
2.5
2.0
1.5
1.0
0.5
0.0
-0.5
f2 (ppm)
0
10
20
30
40
50
60
70
80
90
100
110
120
130
140
150
160
170
180
190
200
f1 (ppm)

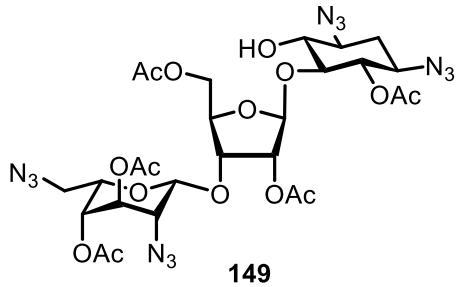
N3
HO
AcO
O
N3
OAc
O
OAc
N3
O
O
OAc
OAc
N3

149

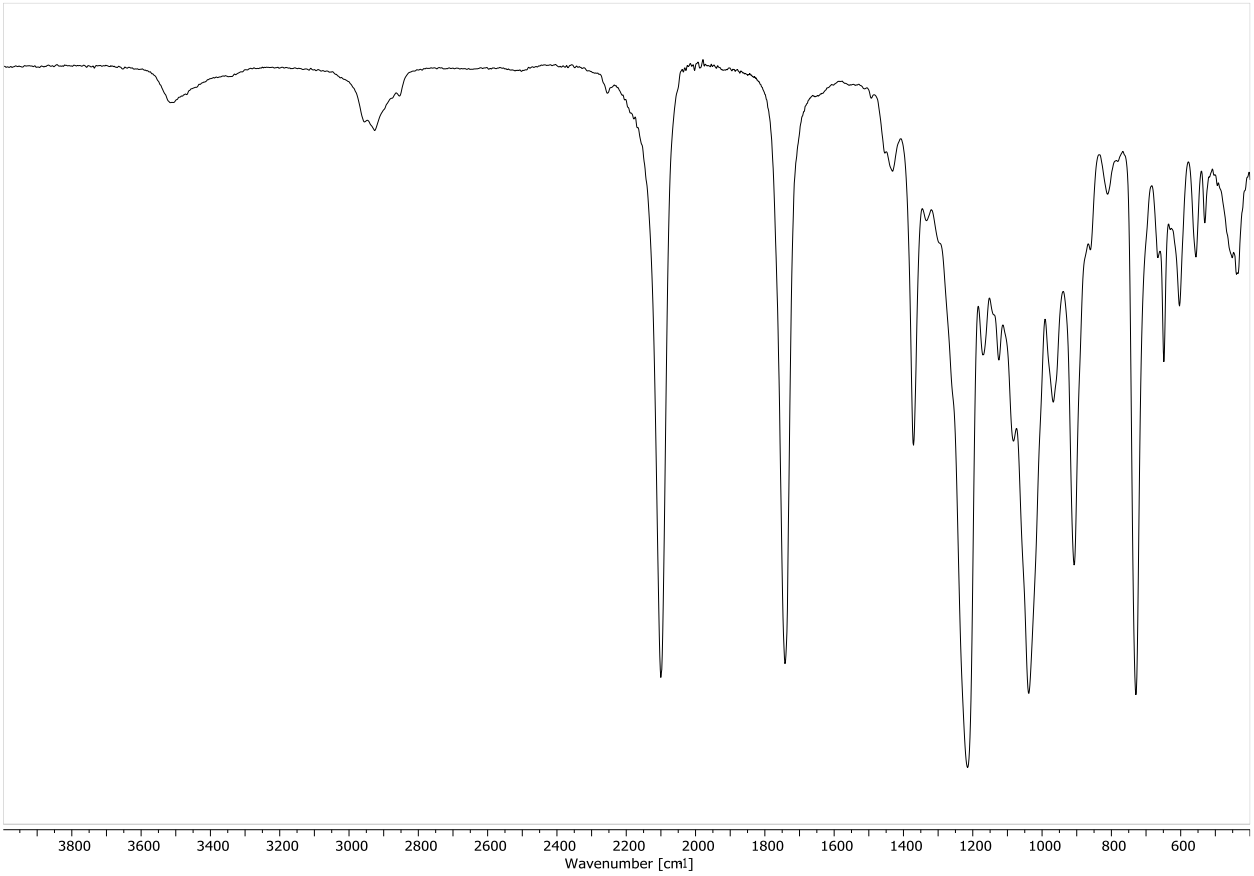
3800
3600
3400
3200
3000
2800
2600
2400
2200
2000
1800
1600
1400
1200
1000
800
600
Wavenumber [cm-1]

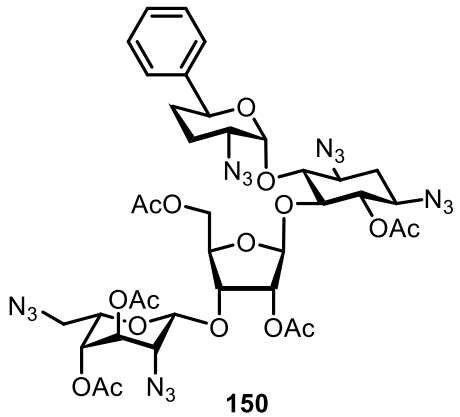
O
N3
N3
O
N3
AcO
O
OAc
O
N3
OAc
O
O
OAc
OAc
N3

150

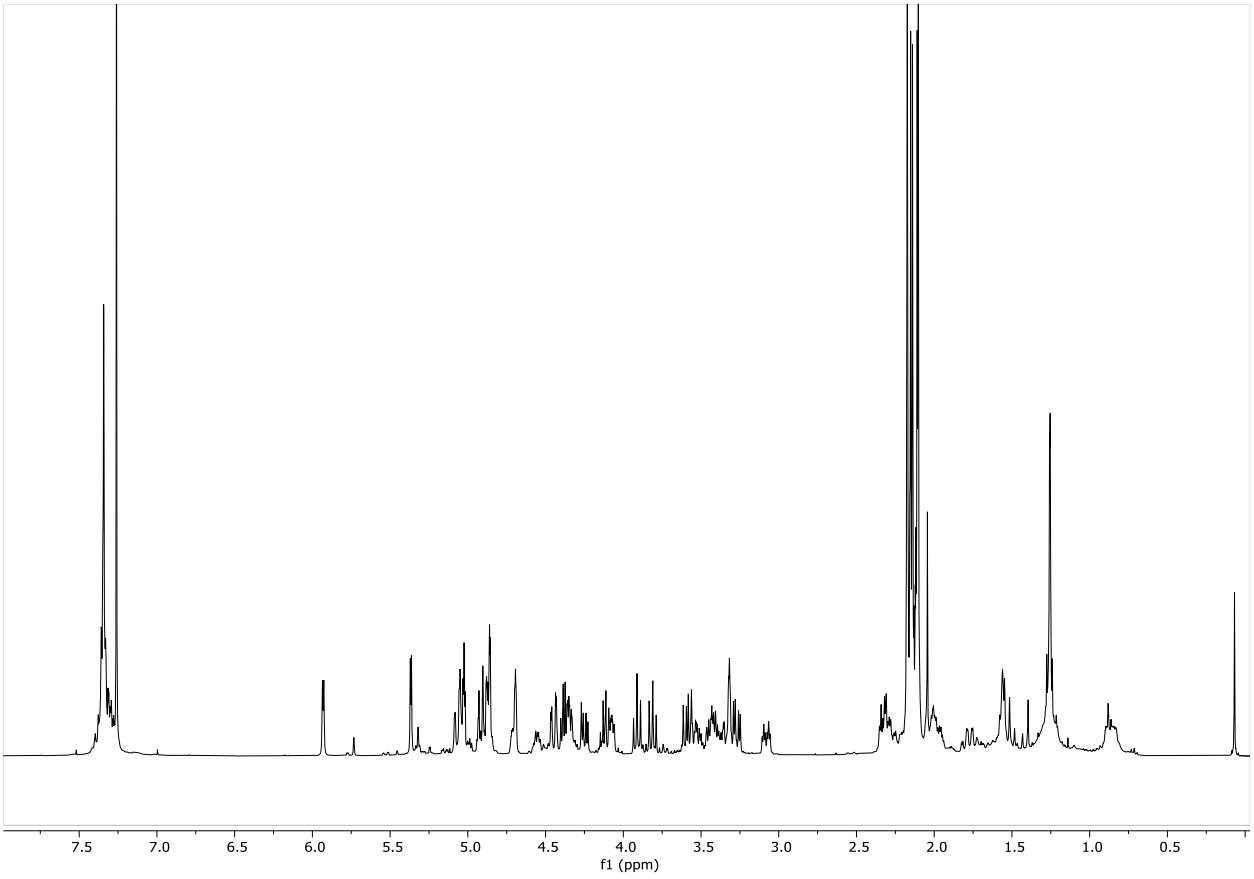
7.5
7.0
6.5
6.0
5.5
5.0
4.5
4.0
3.5
3.0
2.5
2.0
1.5
1.0
0.5
f1 (ppm)

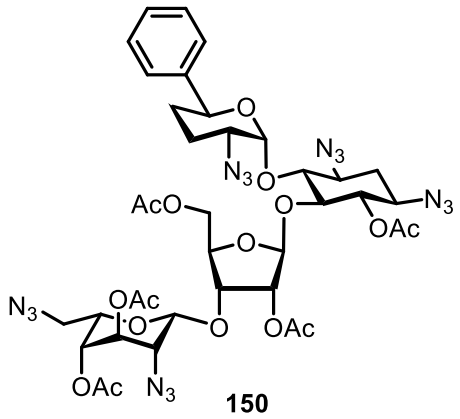

150

MTP-06-064.11.fid

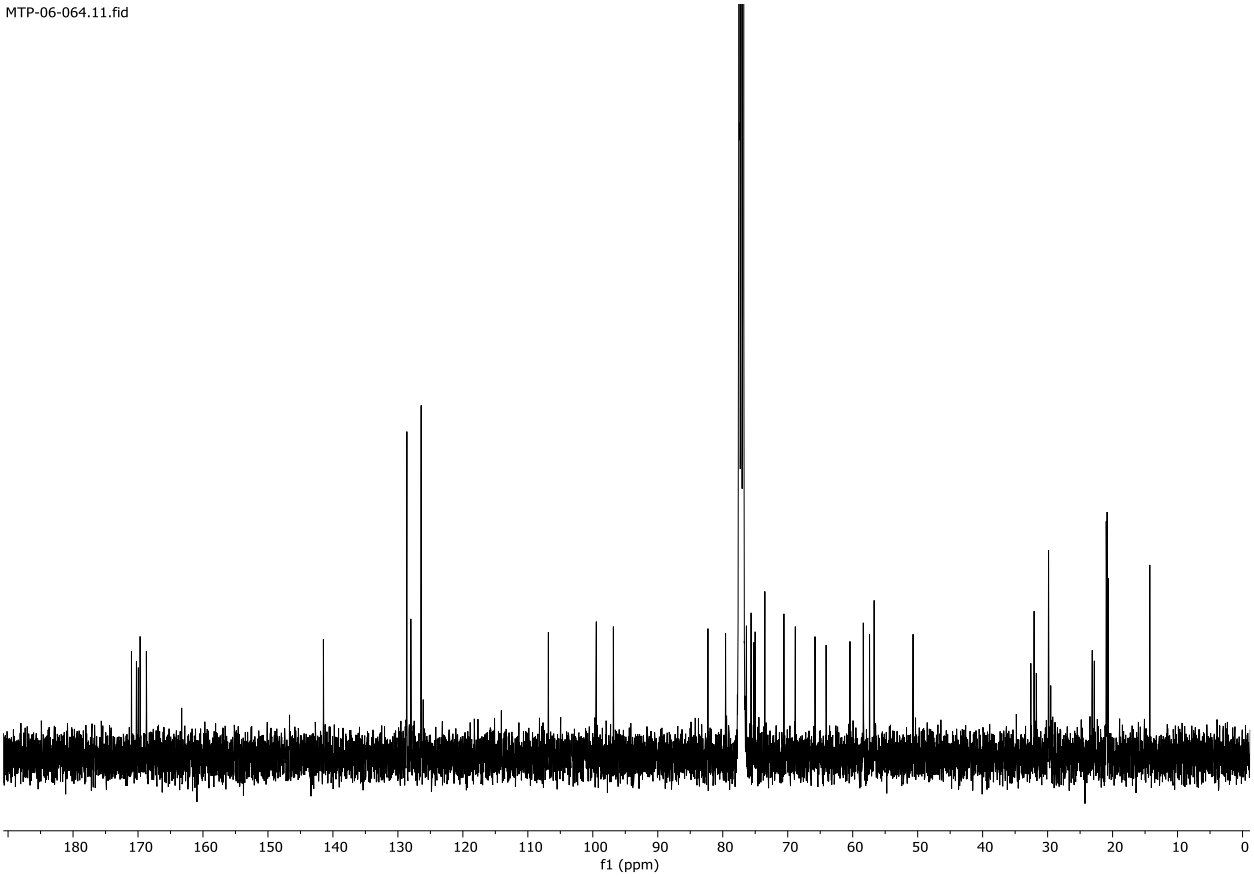

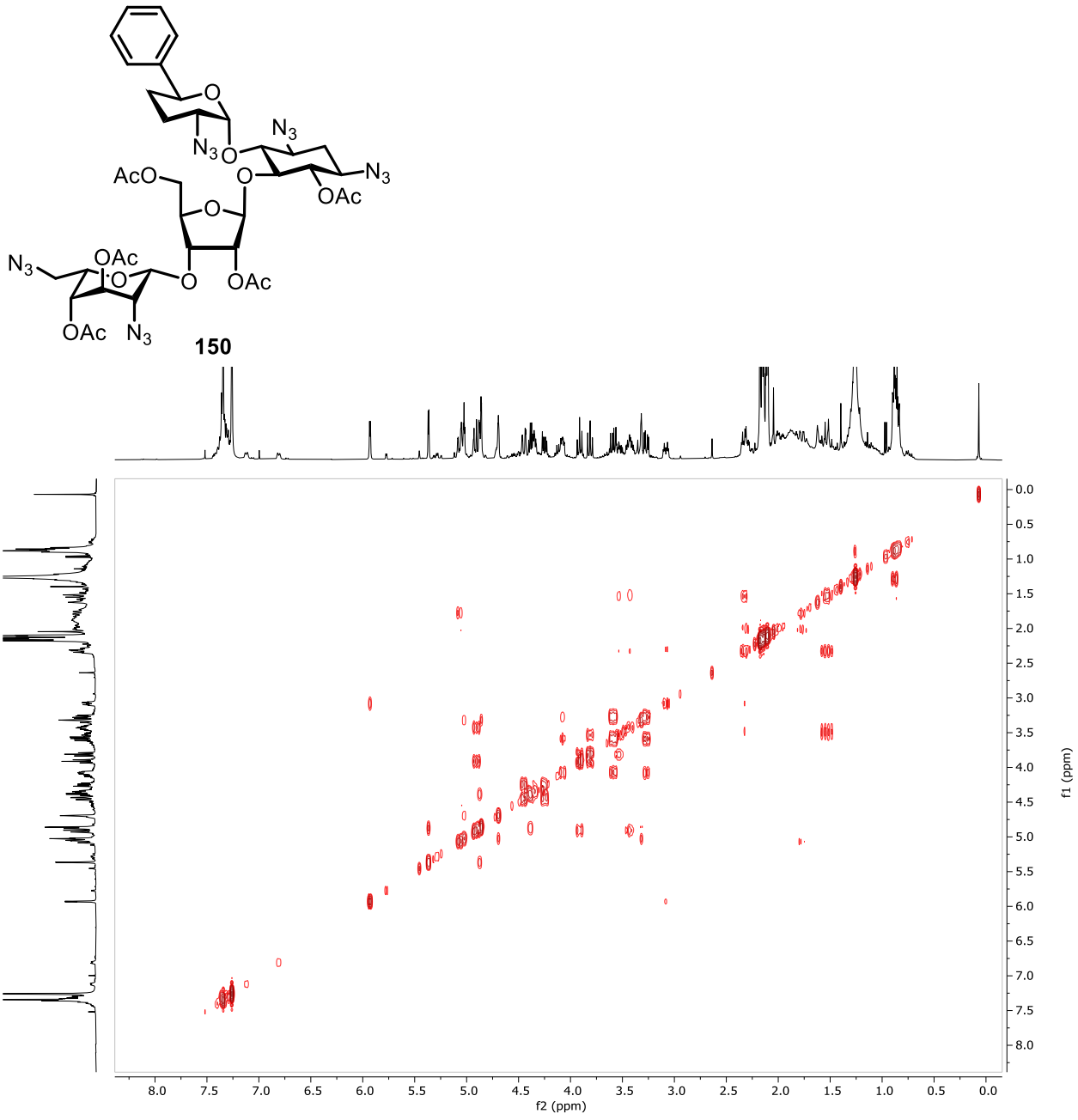
150
f2 (ppm)
f1 (ppm)

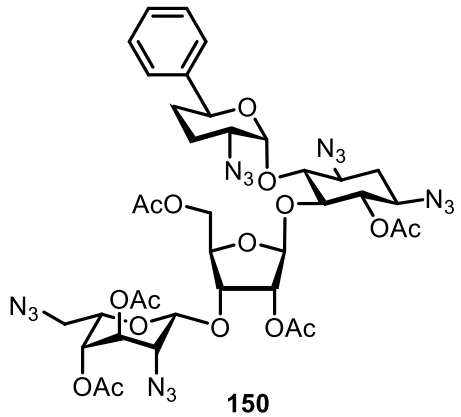
O
N3
N3
O
N3
AcO
O
OAc
O
N3
OAc
O
O
OAc
OAc
N3

150

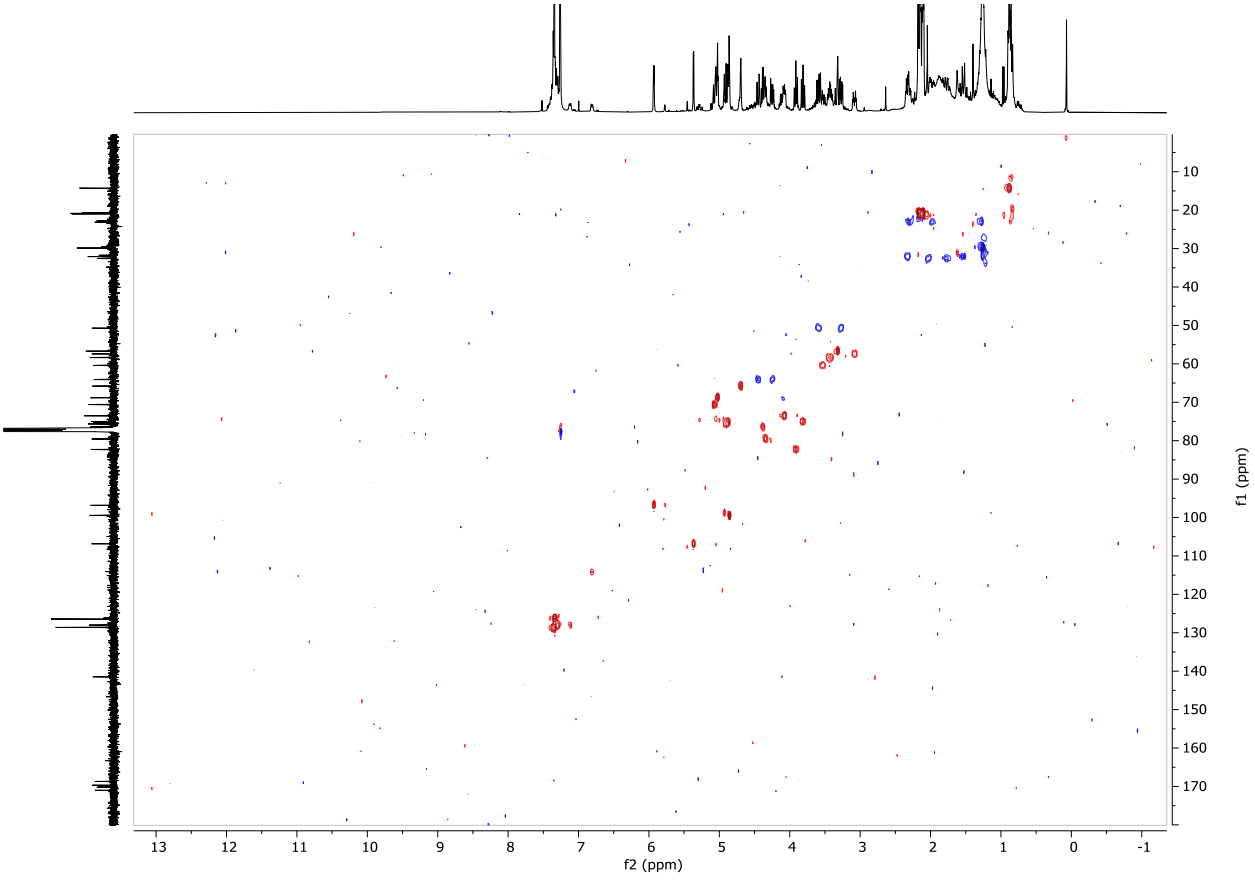
13
12
11
10
9
8
7
6
5
4
3
2
1
0
-1
f2 (ppm)
10
20
30
40
50
60
70
80
90
100
110
120
130
140
150
160
170
f1 (ppm)

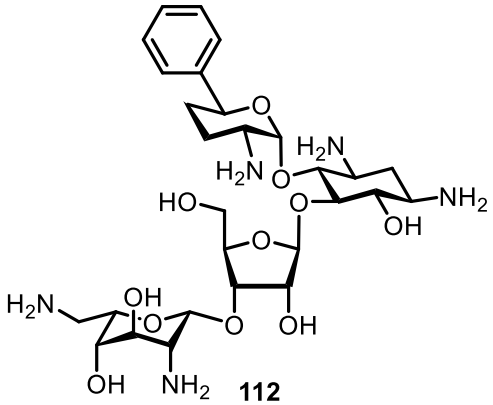
O
H2N
H2N
O
NH2
HO
O
OH
O
H2N
OH
O
O
OH
OH
NH2

112

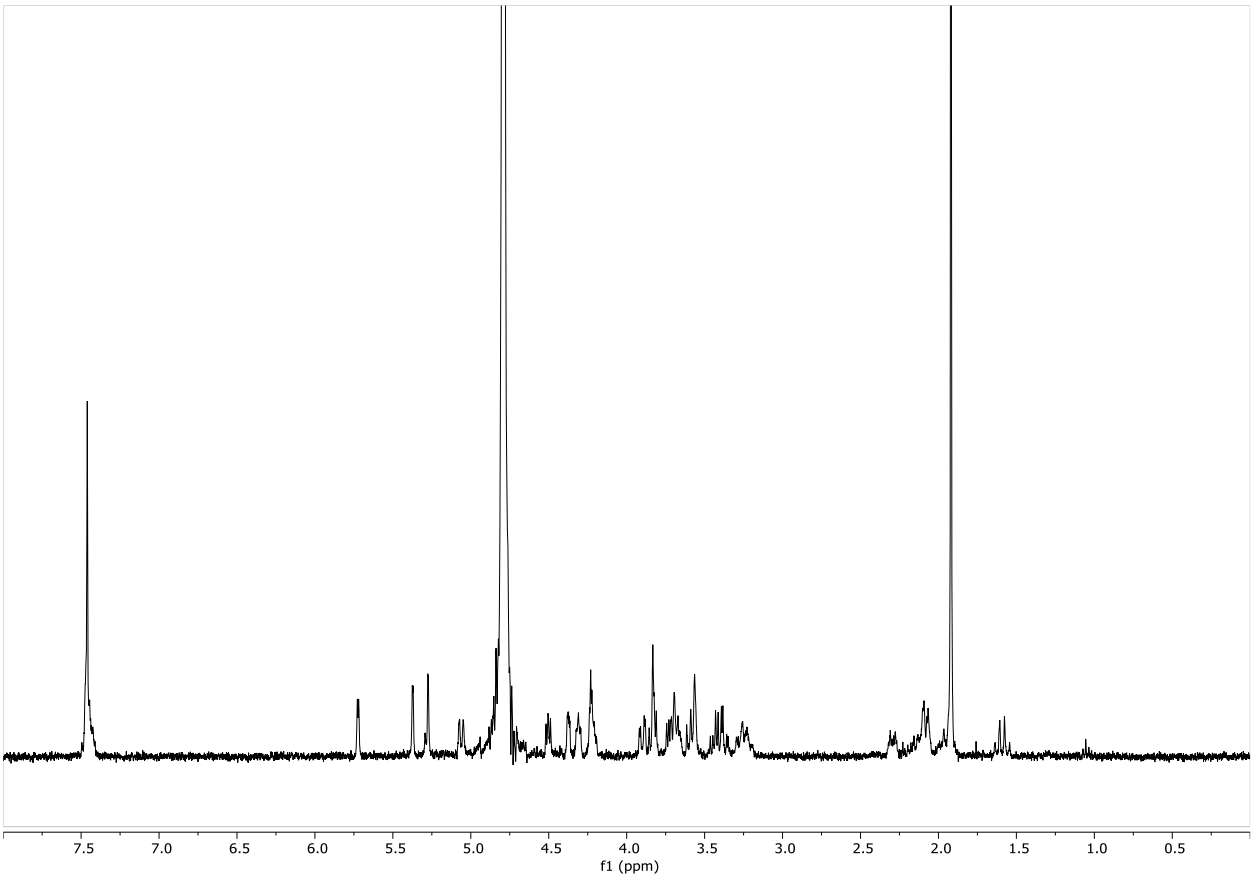
7.5
7.0
6.5
6.0
5.5
5.0
4.5
4.0
3.5
3.0
2.5
2.0
1.5
1.0
0.5
f1 (ppm)

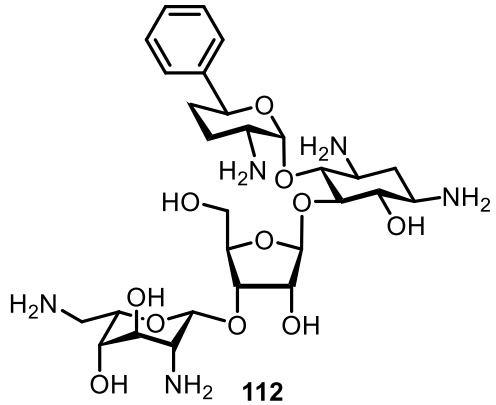
O
H2N
H2N
O
NH2
HO
O
OH
O
H2N
OH
O
O
OH
OH
NH2

112

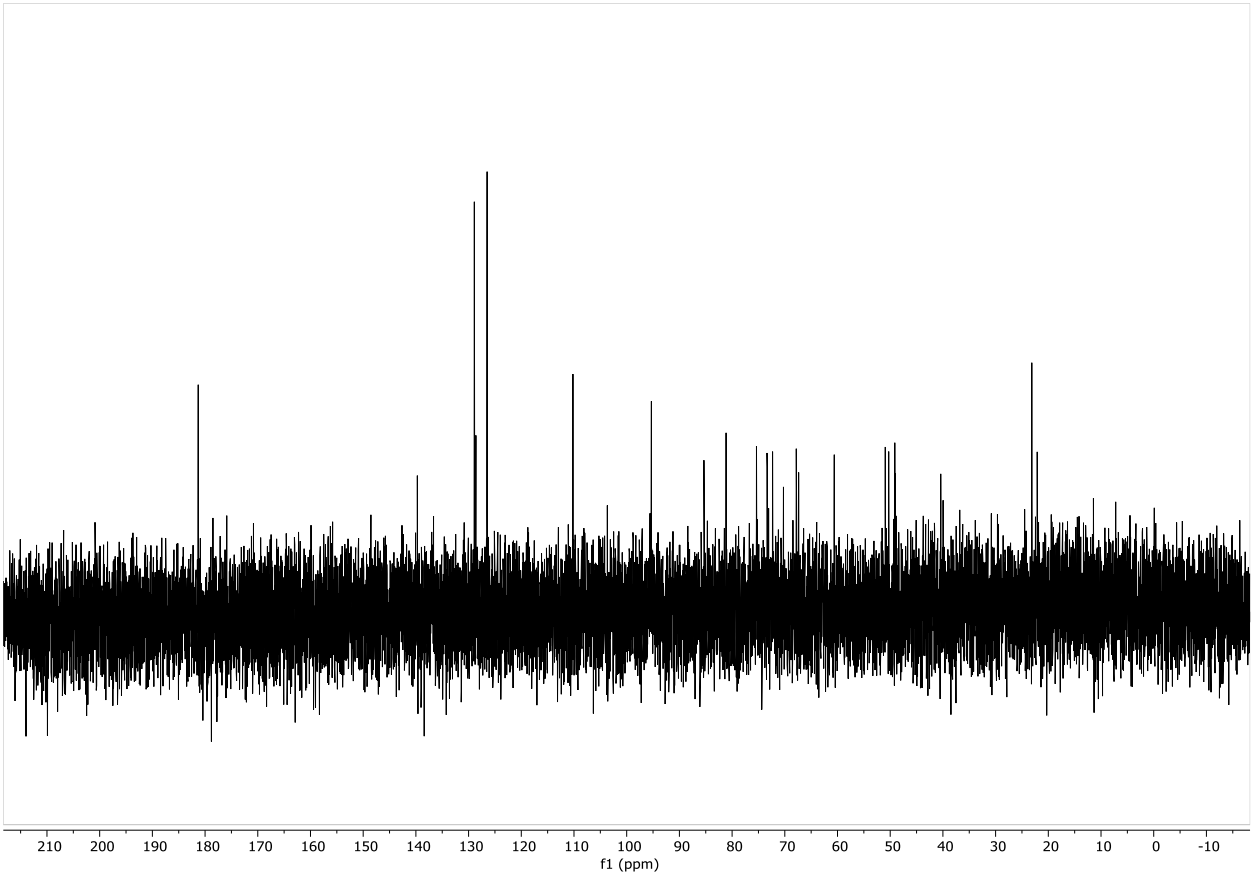
210
200
190
180
170
160
150
140
130
120
110
100
90
80
70
60
50
40
30
20
10
0
-10
f1 (ppm)

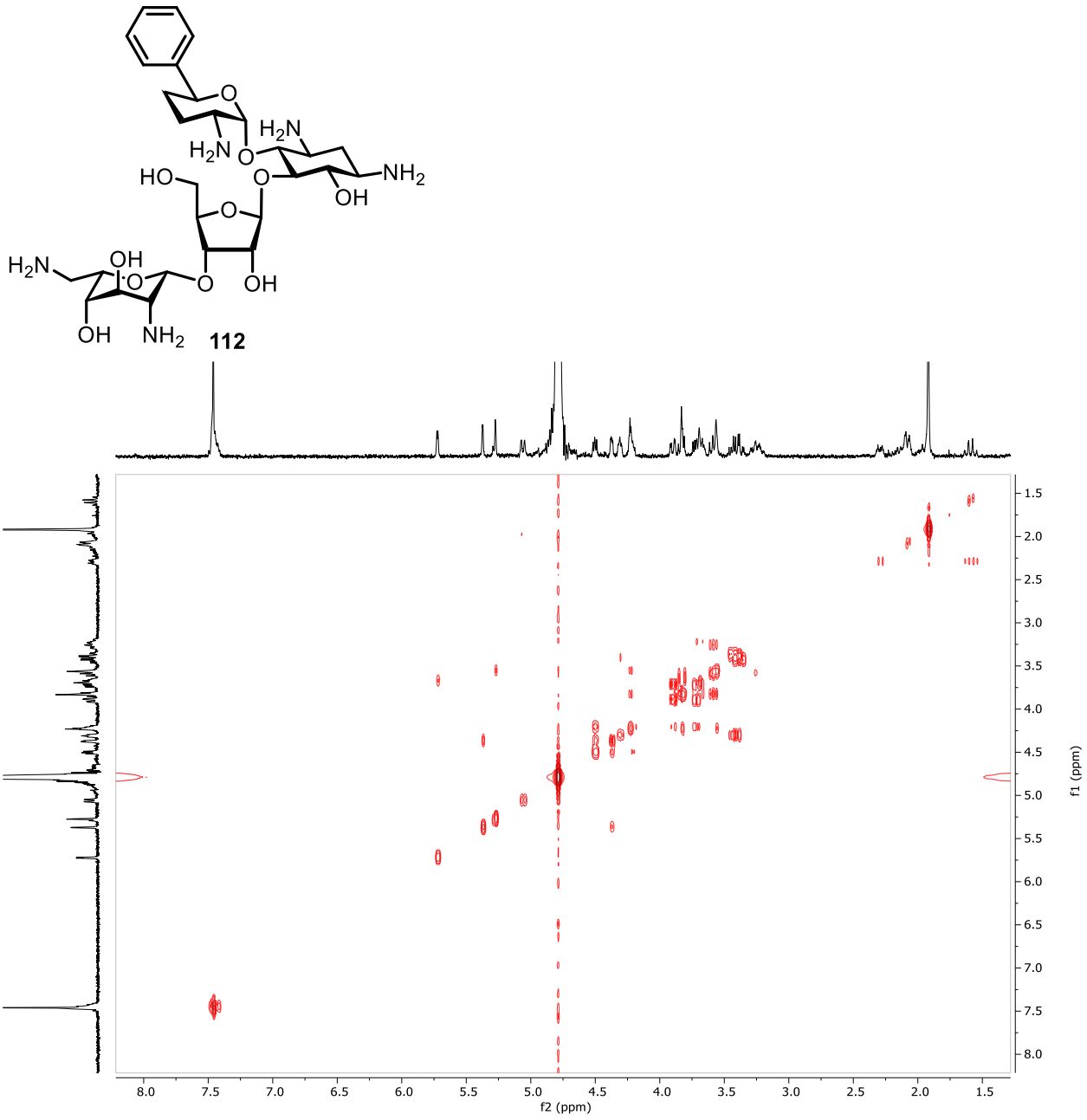
H2N
H2N
O
O
NH2
OH
HO
O
H2N
OH
O
O
OH
OH
NH2
112
f2 (ppm)
f1 (ppm)

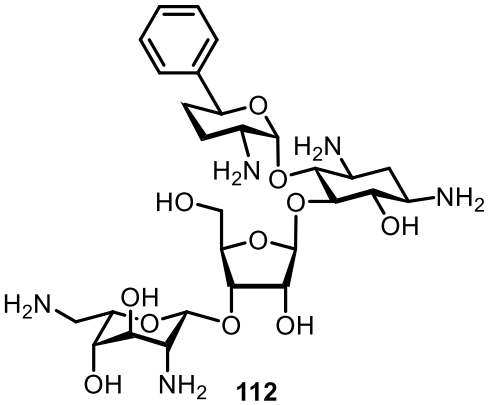
O
H2N
H2N
O
NH2
HO
O
OH
O
H2N
OH
O
O
OH
OH
NH2

112

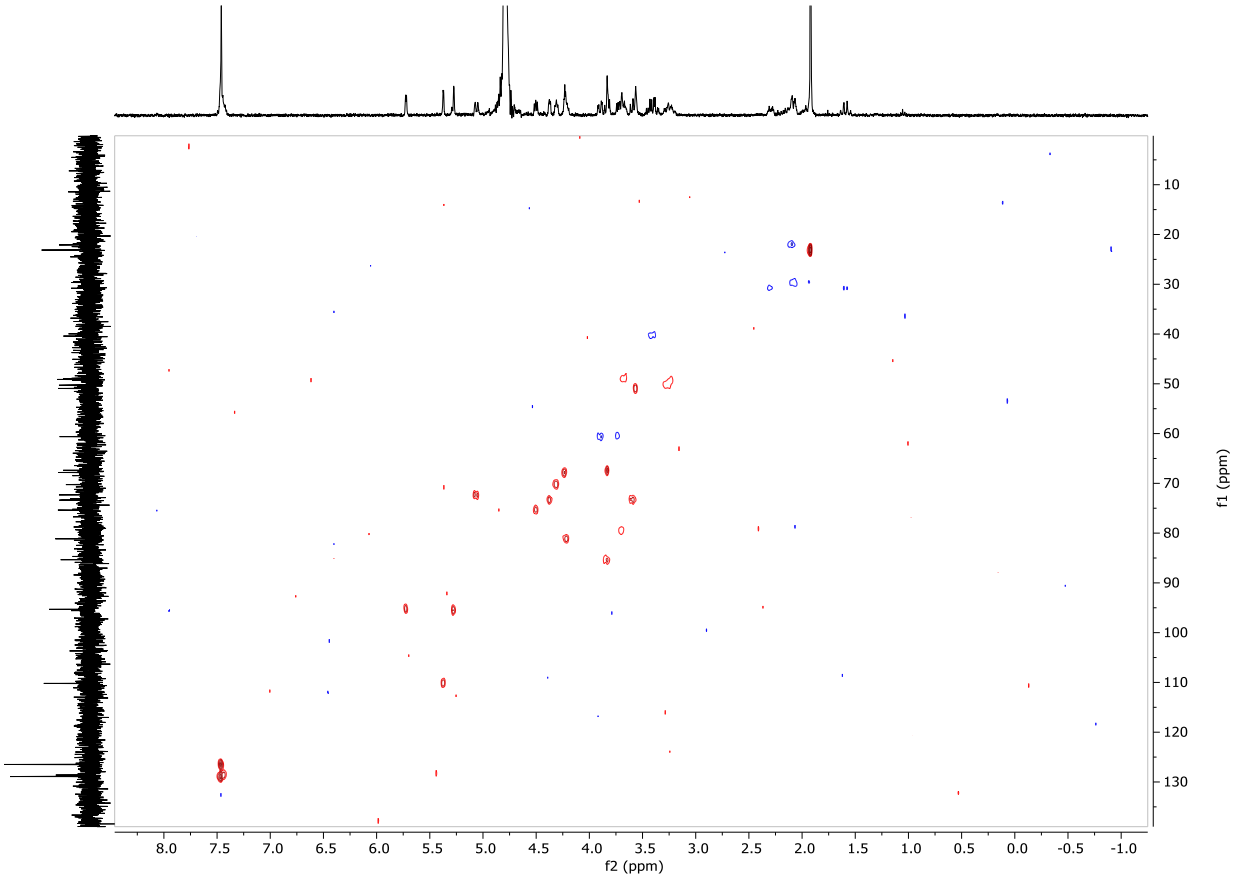
8.0
7.5
7.0
6.5
6.0
5.5
5.0
4.5
4.0
3.5
3.0
2.5
2.0
1.5
1.0
0.5
0.0
-0.5
-1.0
f2 (ppm)
10
20
30
40
50
60
70
80
90
100
110
120
130
f1 (ppm)

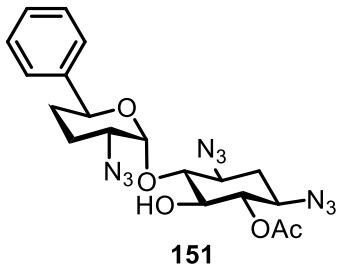
O
N3
N3
O
HO
N3
OAc

151

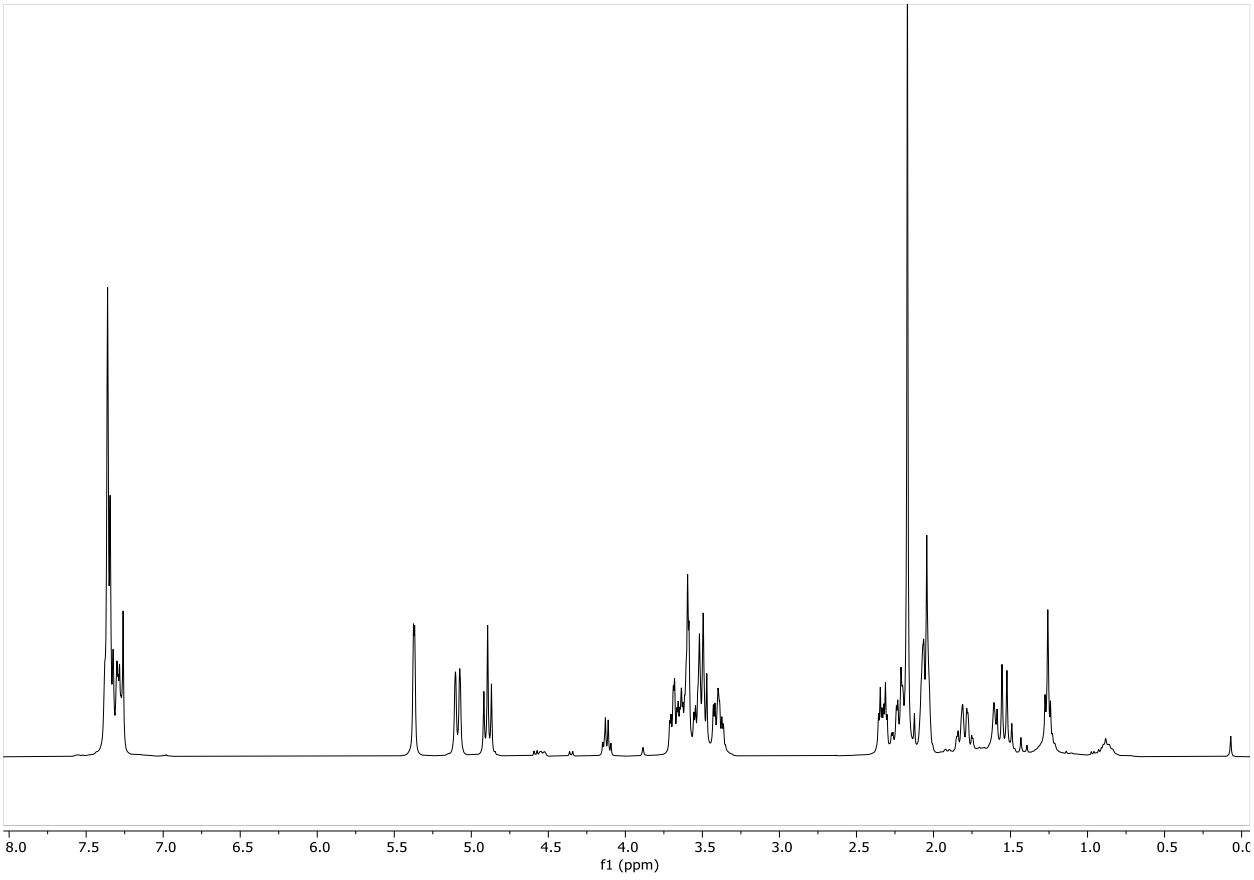
8.0
7.5
7.0
6.5
6.0
5.5
5.0
4.5
4.0
3.5
3.0
2.5
2.0
1.5
1.0
0.5
f1 (ppm)

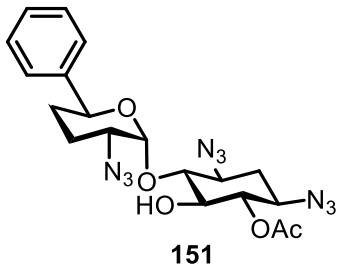
O
N3
N3
O
HO
N3
OAc

151

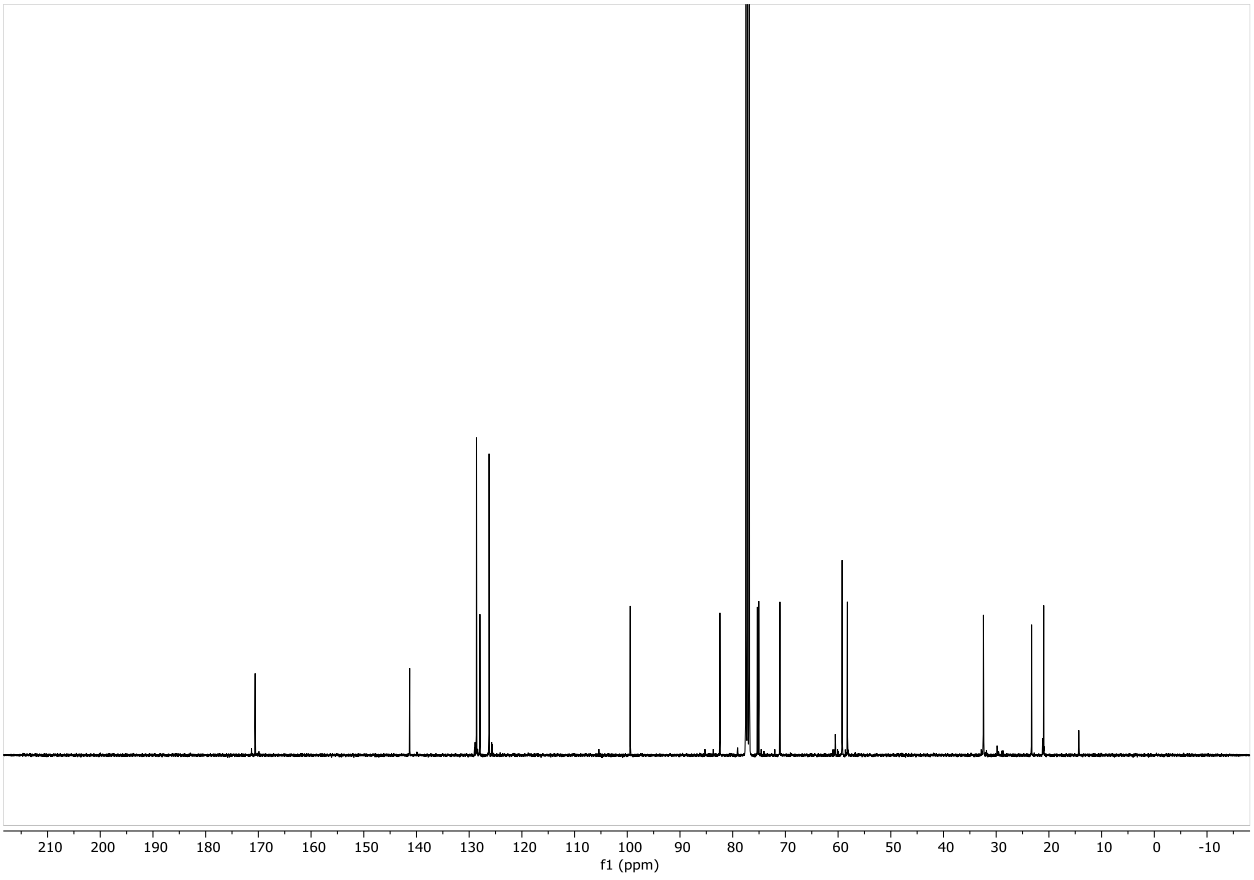
210
200
190
180
170
160
150
140
130
120
110
100
90
80
70
60
50
40
30
20
10
0
-10
f1 (ppm)

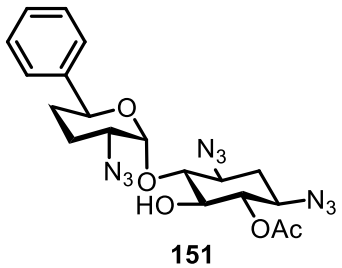
O
N3
N3
O
HO
N3
OAc

151

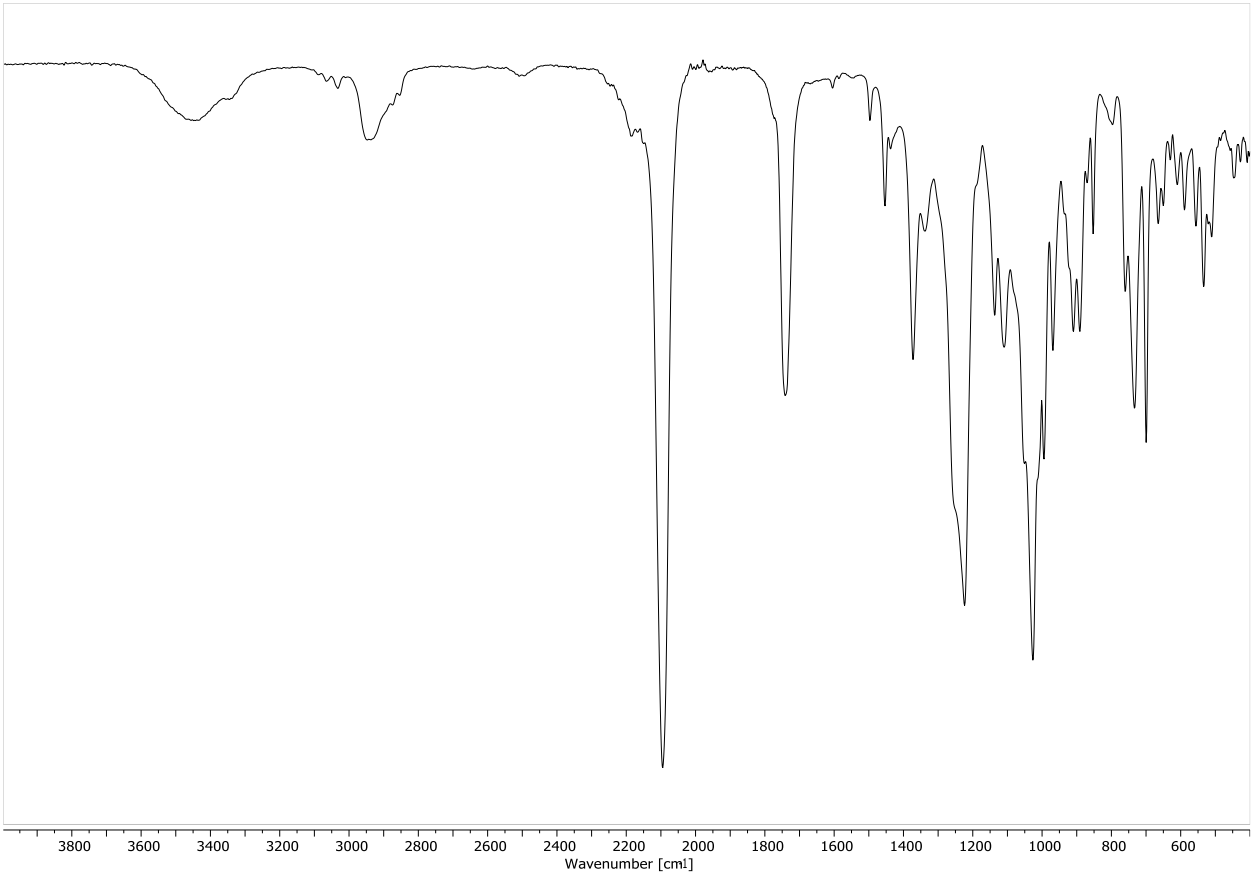
3800
3600
3400
3200
3000
2800
2600
2400
2200
2000
1800
1600
1400
1200
1000
800
600
Wavenumber [cm-1]

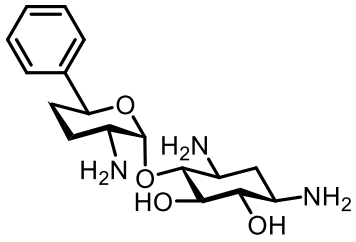
O
H2N
H2N
O
HO
NH2
OH

152

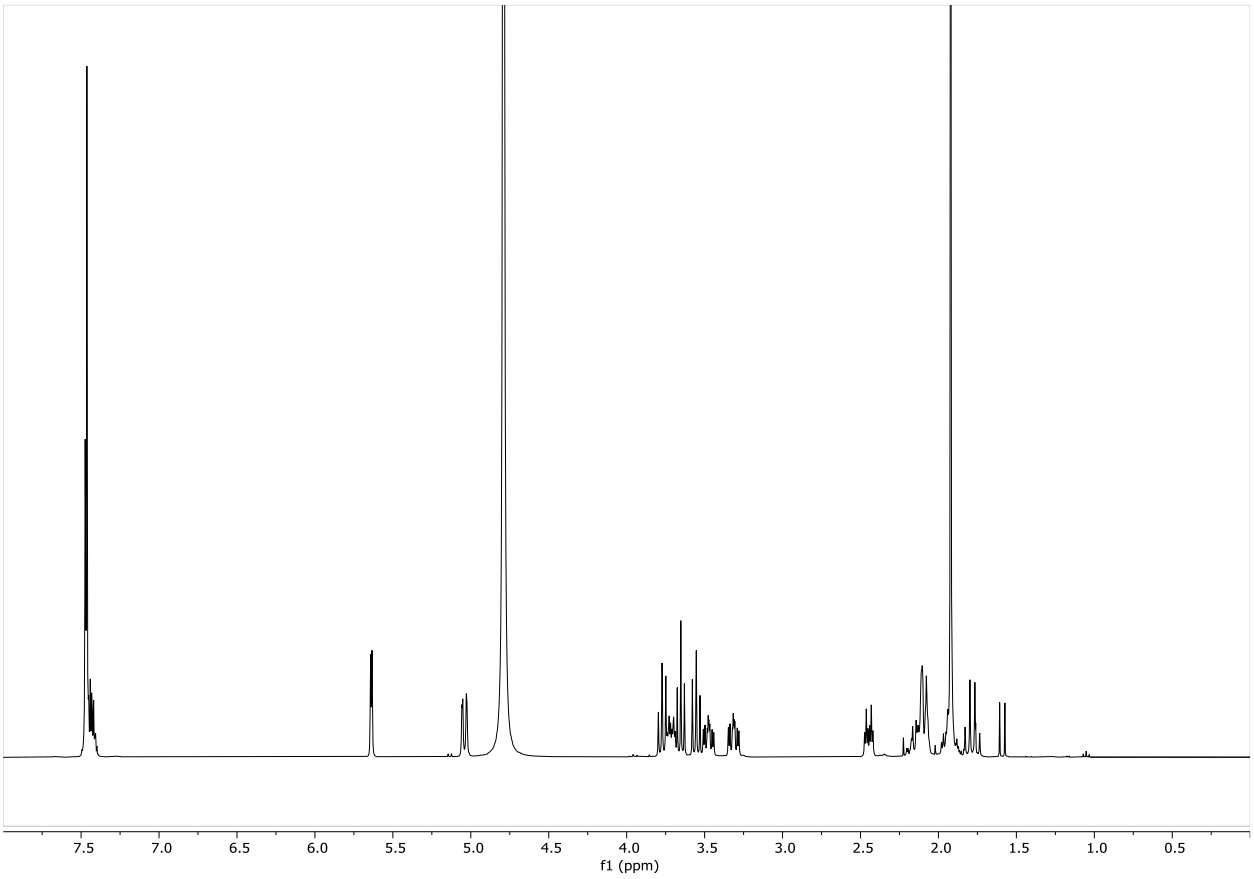
7.5
7.0
6.5
6.0
5.5
5.0
4.5
4.0
3.5
3.0
2.5
2.0
1.5
1.0
0.5
f1 (ppm)

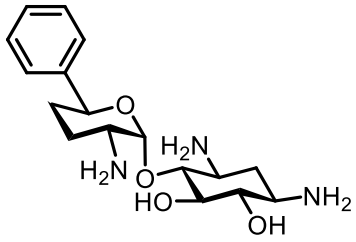
O
H2N
H2N
O
HO
NH2
OH

152

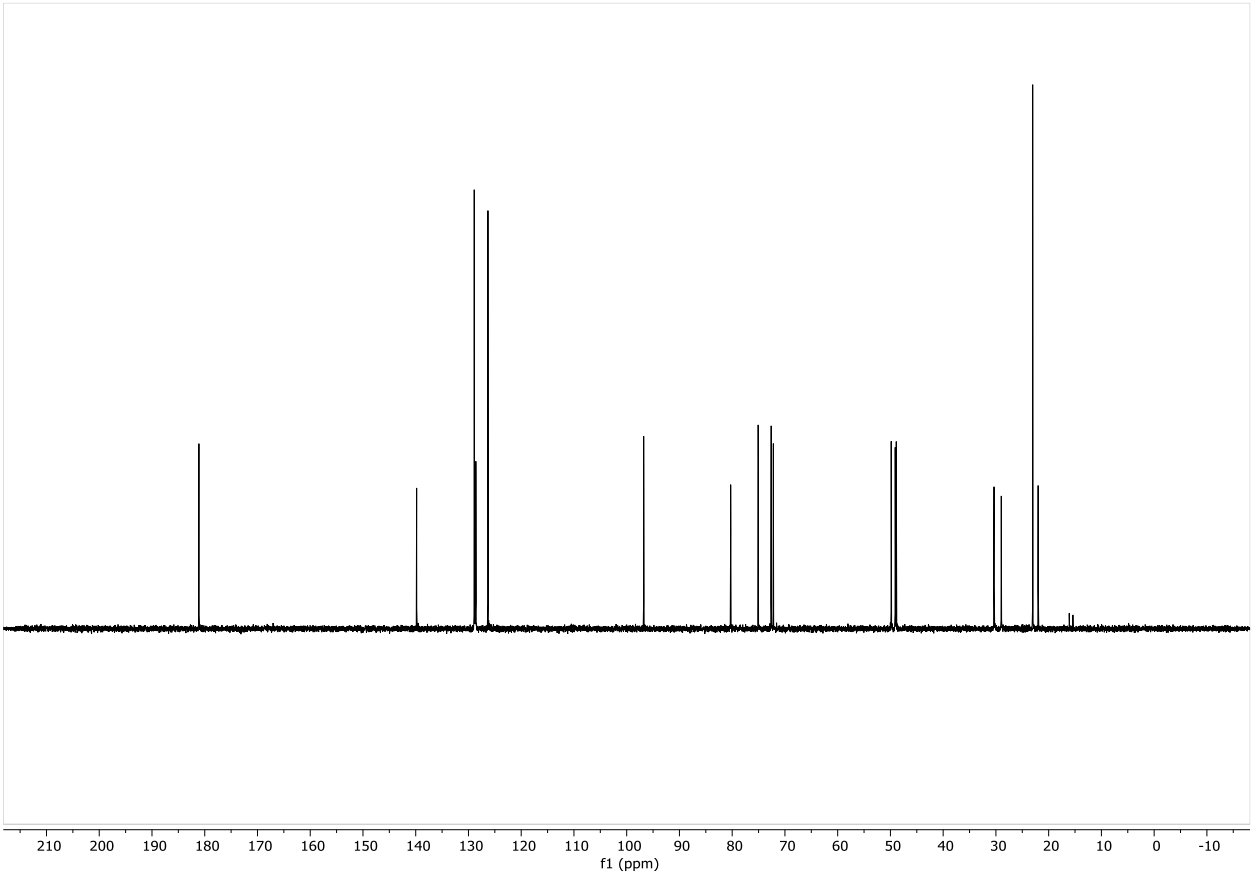
210
200
190
180
170
160
150
140
130
120
110
100
90
80
70
60
50
40
30
20
10
0
-10
f1 (ppm)

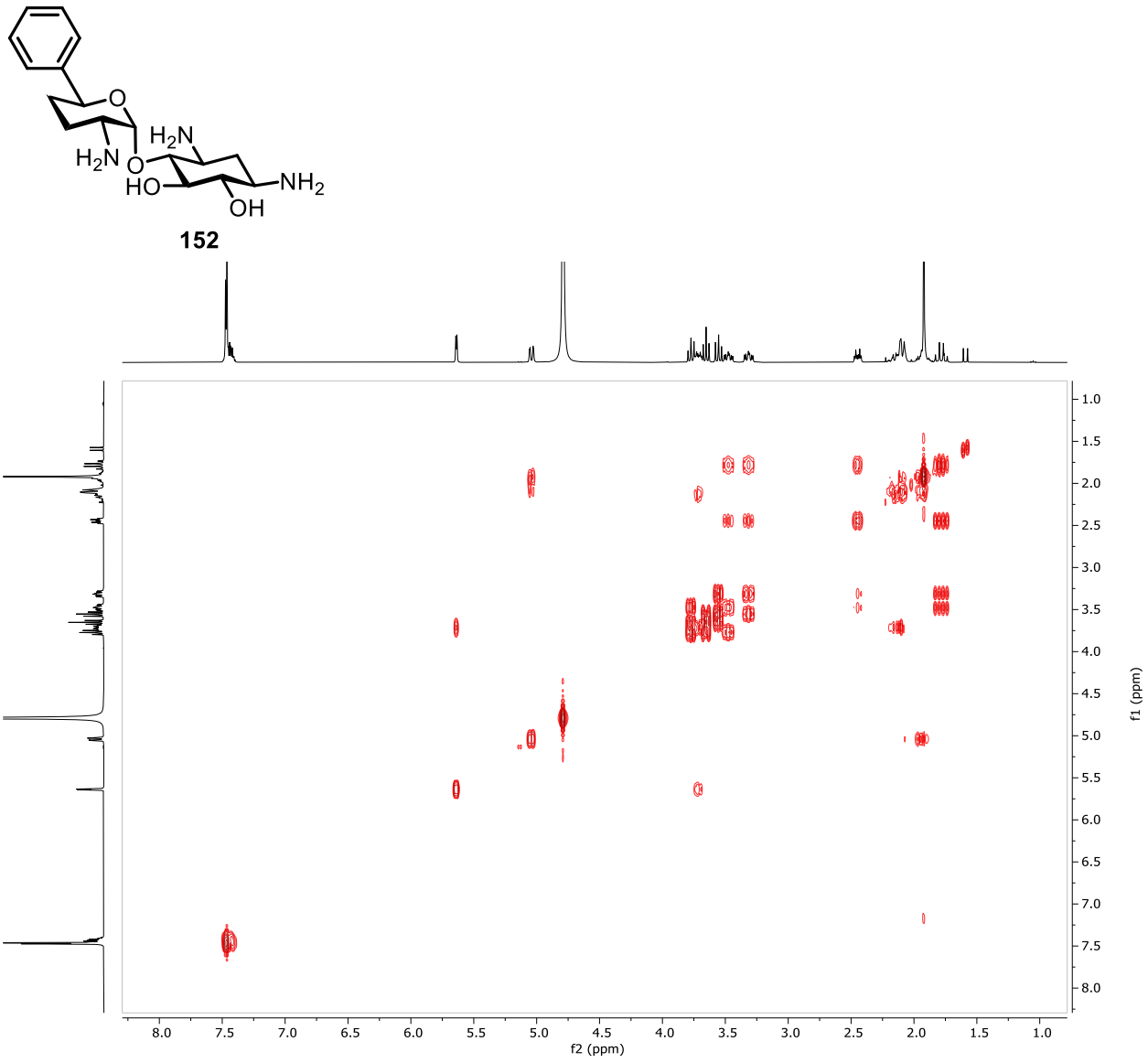

152

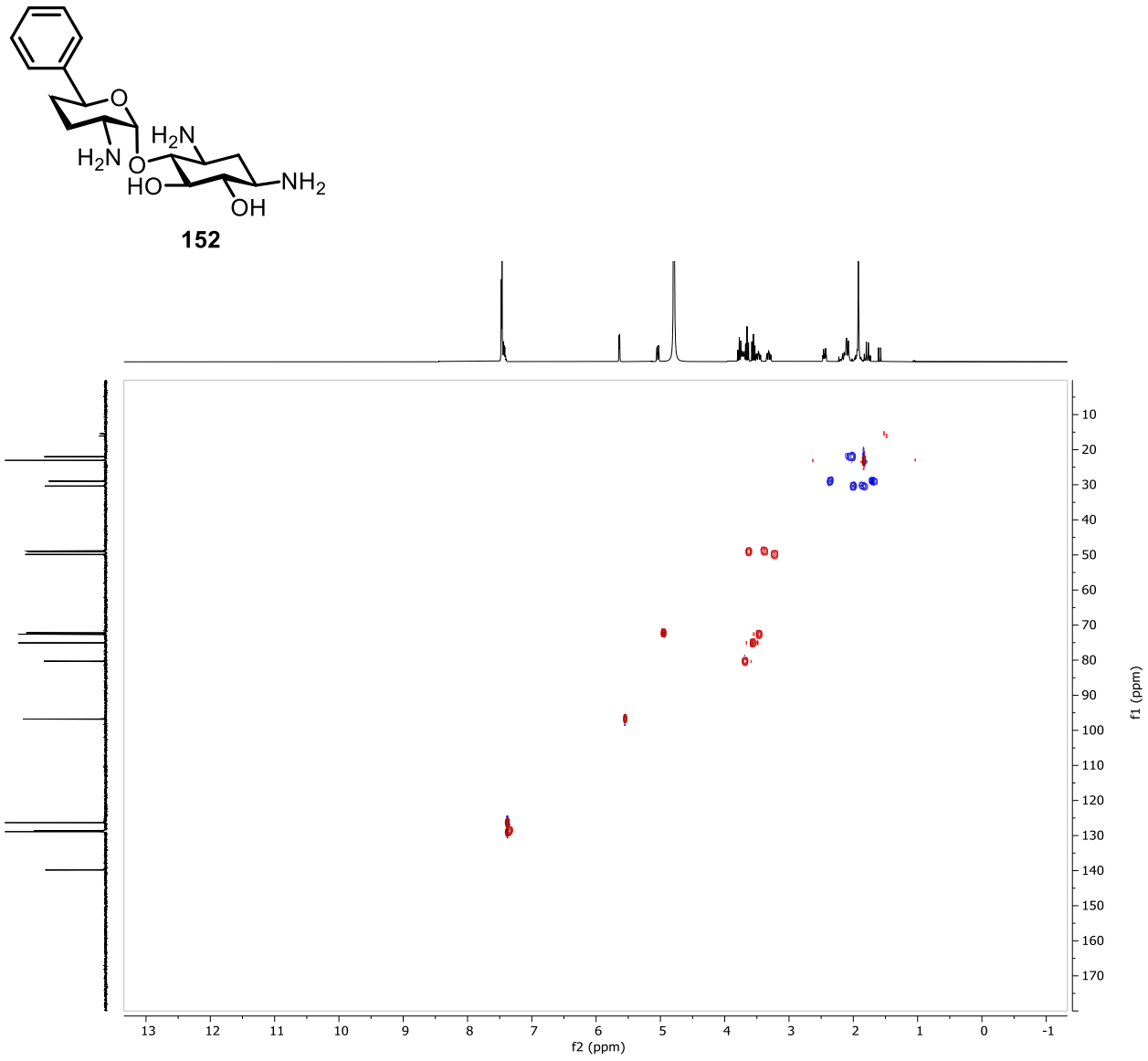
O
H2N
H2N
O
HO
NH2
OH
152
f2 (ppm)
f1 (ppm)

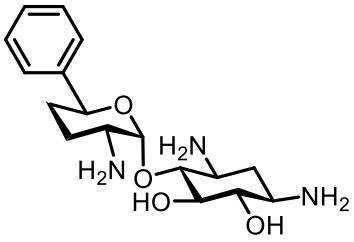
O
H2N
H2N
O
HO
NH2
OH

152

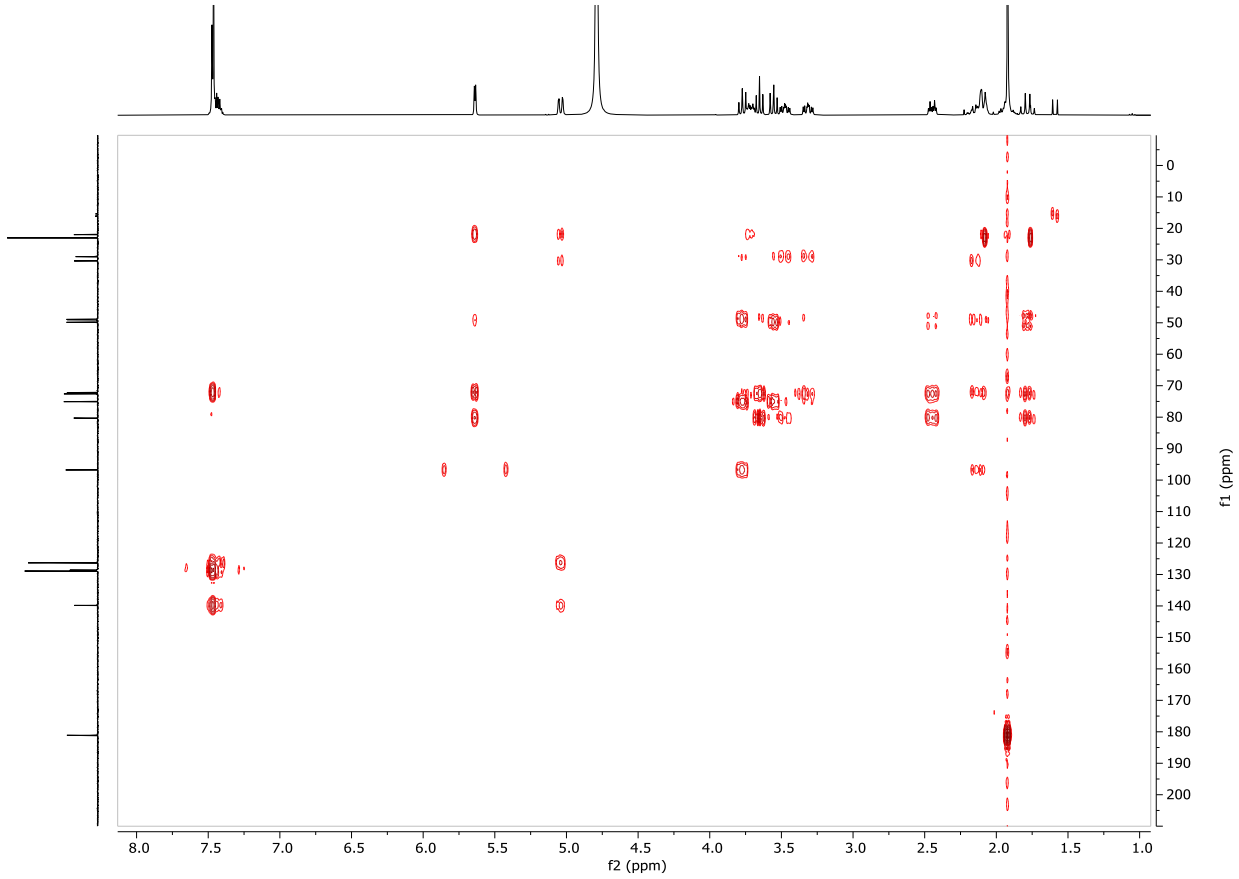
8.0
7.5
7.0
6.5
6.0
5.5
5.0
4.5
4.0
3.5
3.0
2.5
2.0
1.5
1.0
f2 (ppm)
0
10
20
30
40
50
60
70
80
90
100
110
120
130
140
150
160
170
180
190
200
f1 (ppm)

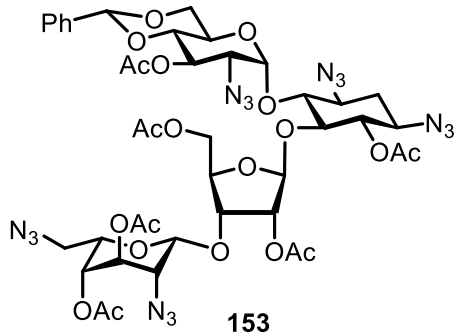
Ph
O
O
AcO
O
N3
N3
O
N3
AcO
O
OAc
O
N3
OAc
O
O
OAc
OAc
N3

153

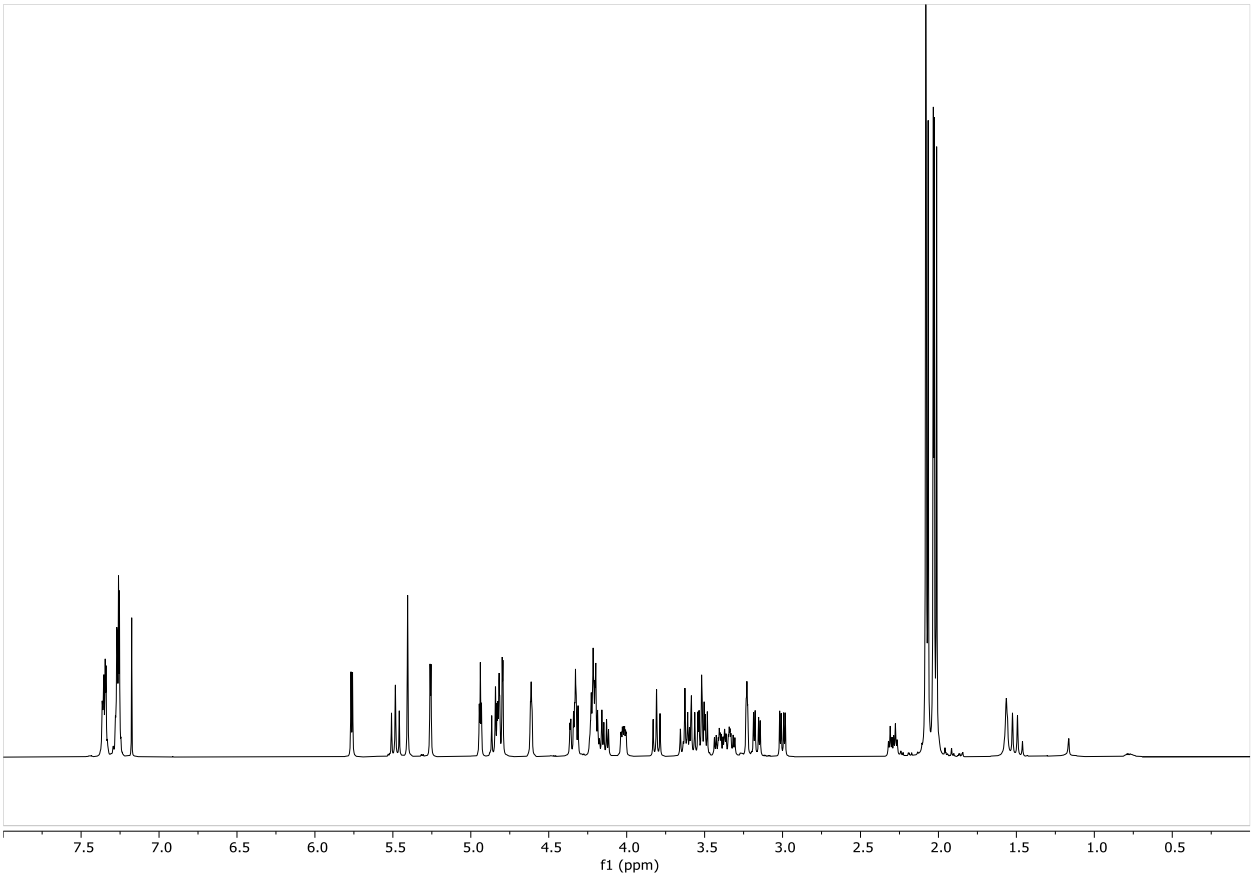
7.5
7.0
6.5
6.0
5.5
5.0
4.5
4.0
3.5
3.0
2.5
2.0
1.5
1.0
0.5
f1 (ppm)

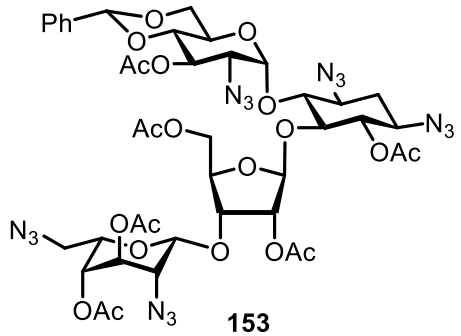
Ph
O
O
O
AcO
N3
N3
O
N3
AcO
O
OAc
O
N3
OAc
O
O
OAc
OAc
N3

153

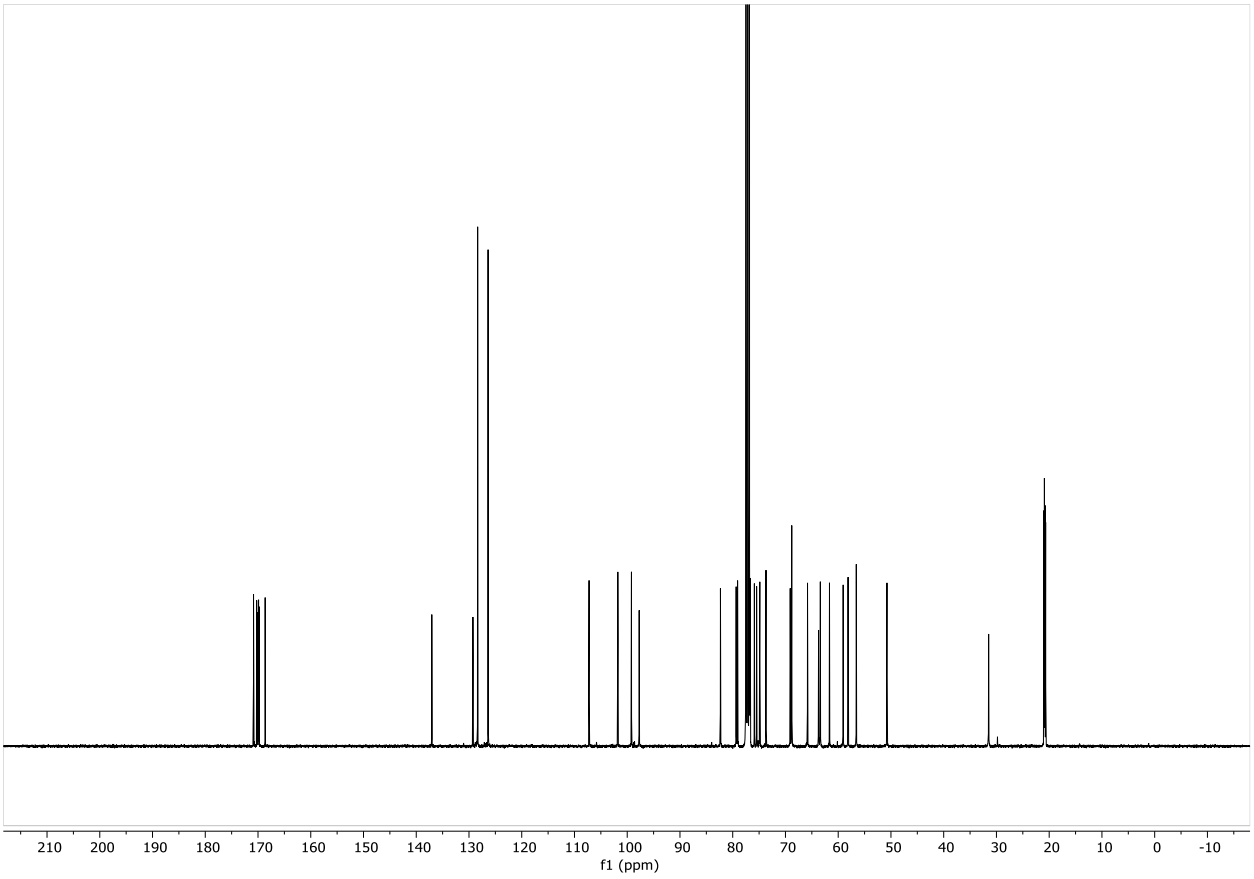
210
200
190
180
170
160
150
140
130
120
110
100
90
80
70
60
50
40
30
20
10
0
-10
f1 (ppm)

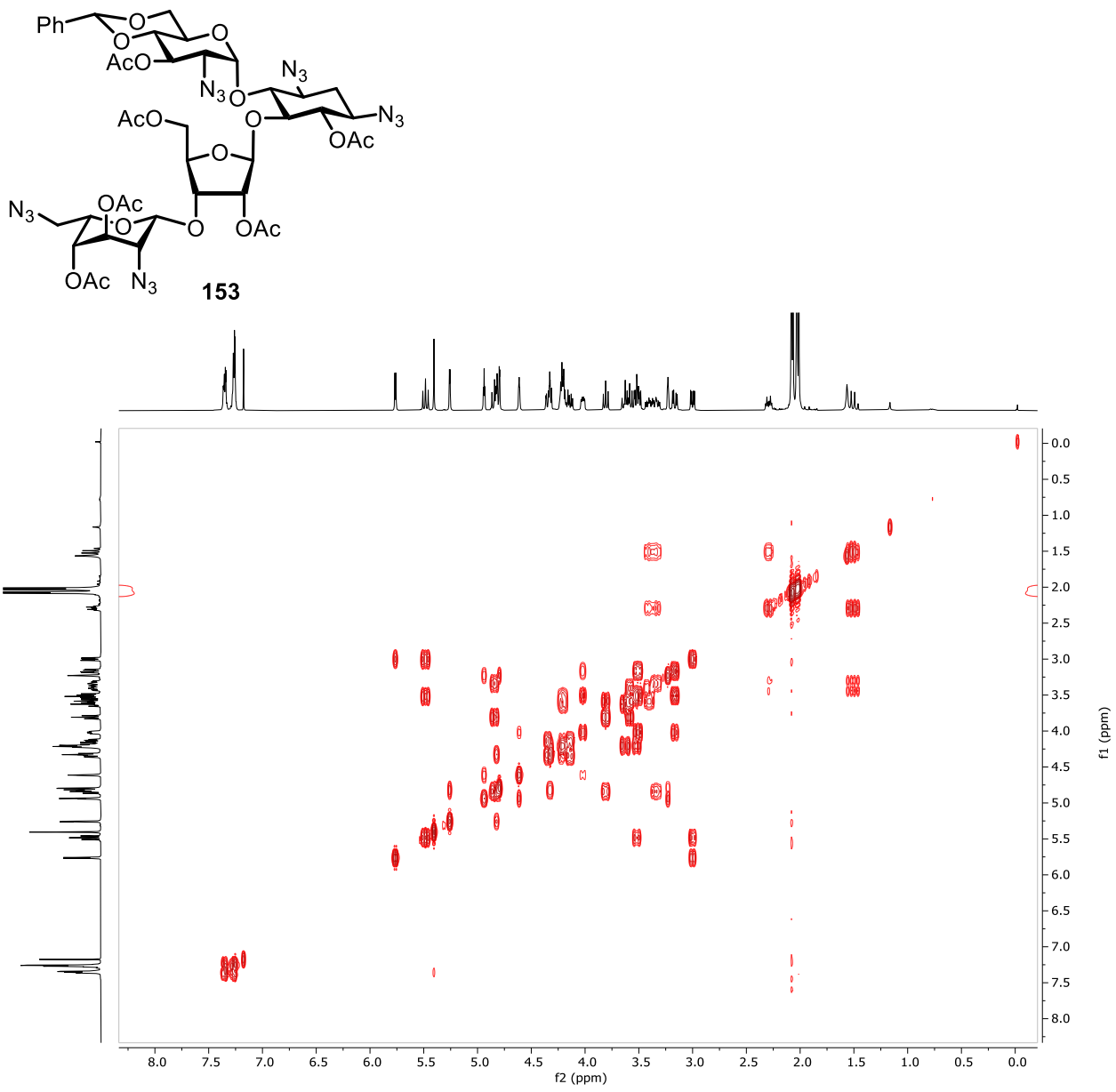
Ph
O
O
AcO
O
N3
N3
O
N3
AcO
O
N3
OAc
O
OAc
N3
OAc
O
O
OAc
OAc
N3
153
f2 (ppm)
f1 (ppm)

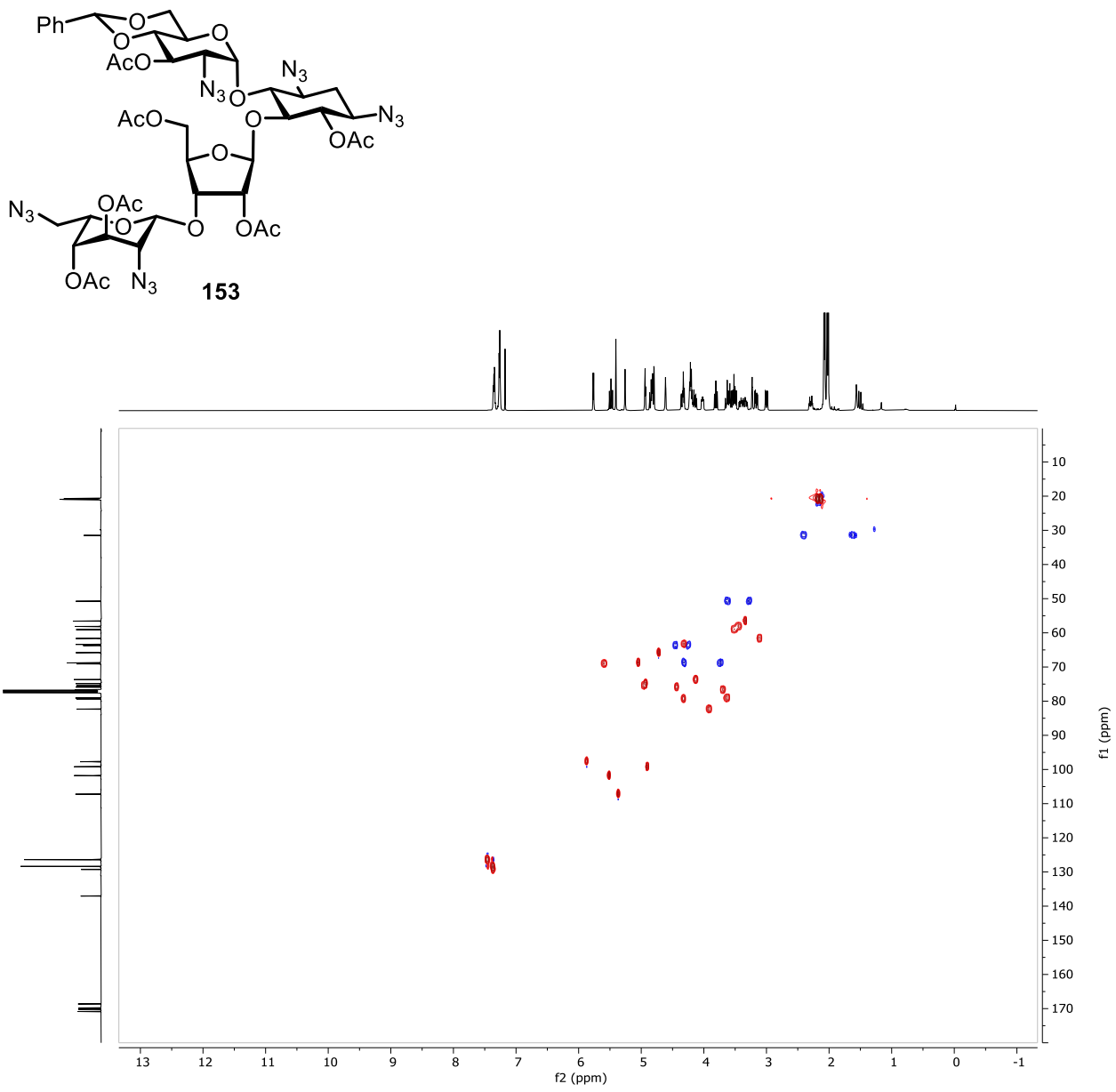
Ph
O
O
AcO
O
N3
N3
O
N3
AcO
O
OAc
O
N3
OAc
O
O
OAc
OAc
N3
153
10
20
30
40
50
60
70
80
90
100
110
120
130
140
150
160
170
f1 (ppm)
13
12
11
10
9
8
7
6
5
4
3
2
1
0
-1
f2 (ppm)

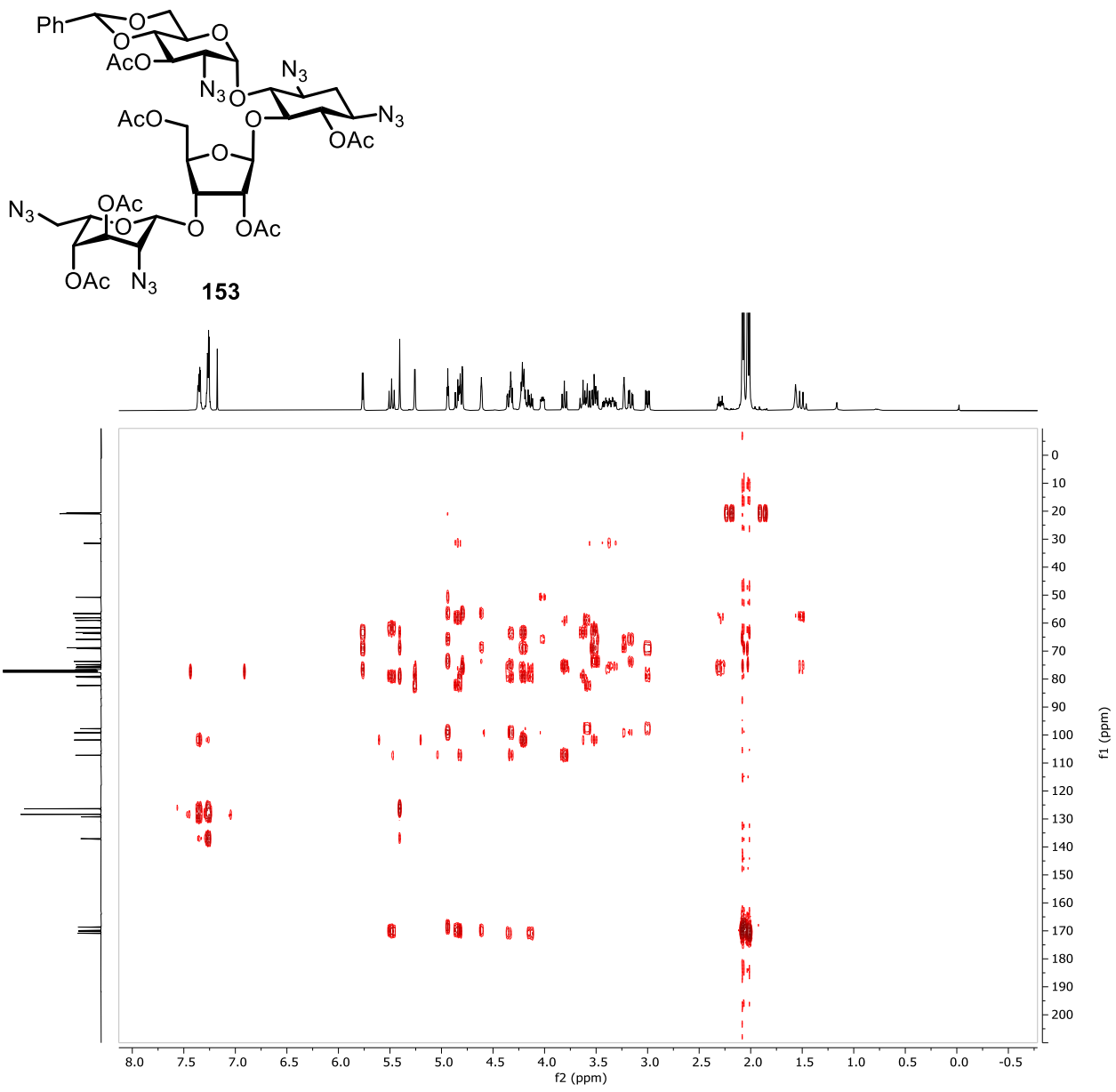
Ph
O
O
AcO
N3
O
N3
N3
O
AcO
O
OAc
O
N3
OAc
O
O
OAc
OAc
N3
153
f2 (ppm)
f1 (ppm)

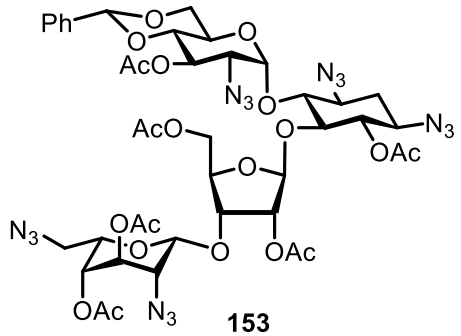
Ph
O
O
AcO
O
N3
N3
O
N3
AcO
O
OAc
O
N3
OAc
O
O
OAc
OAc
N3

153

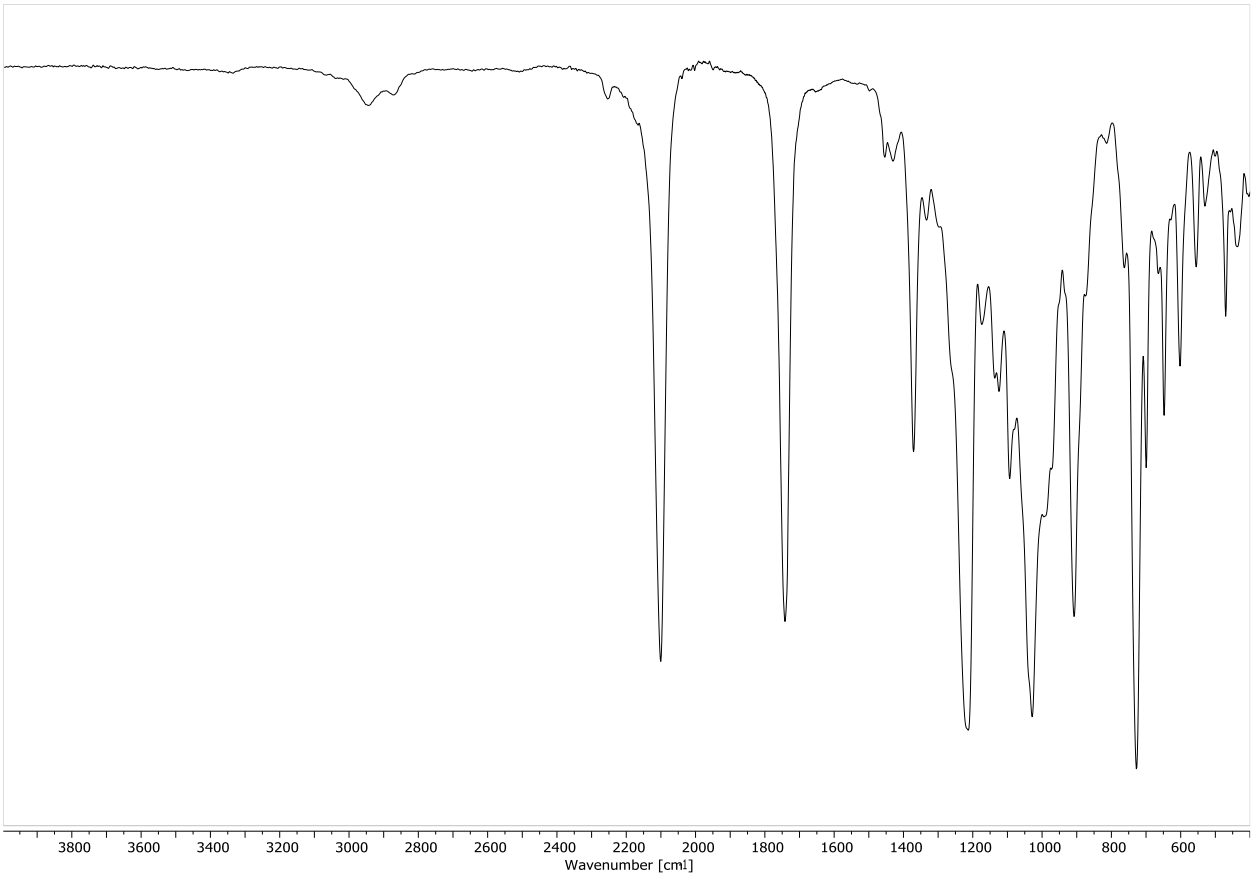
3800
3600
3400
3200
3000
2800
2600
2400
2200
2000
1800
1600
1400
1200
1000
800
600
Wavenumber [cm-1]

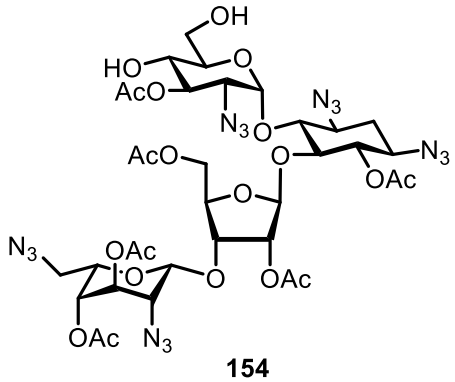
OH
HO
AcO
O
N3
N3
O
N3
AcO
O
N3
OAc
O
N3
OAc
O
O
OAc
OAc
N3

154

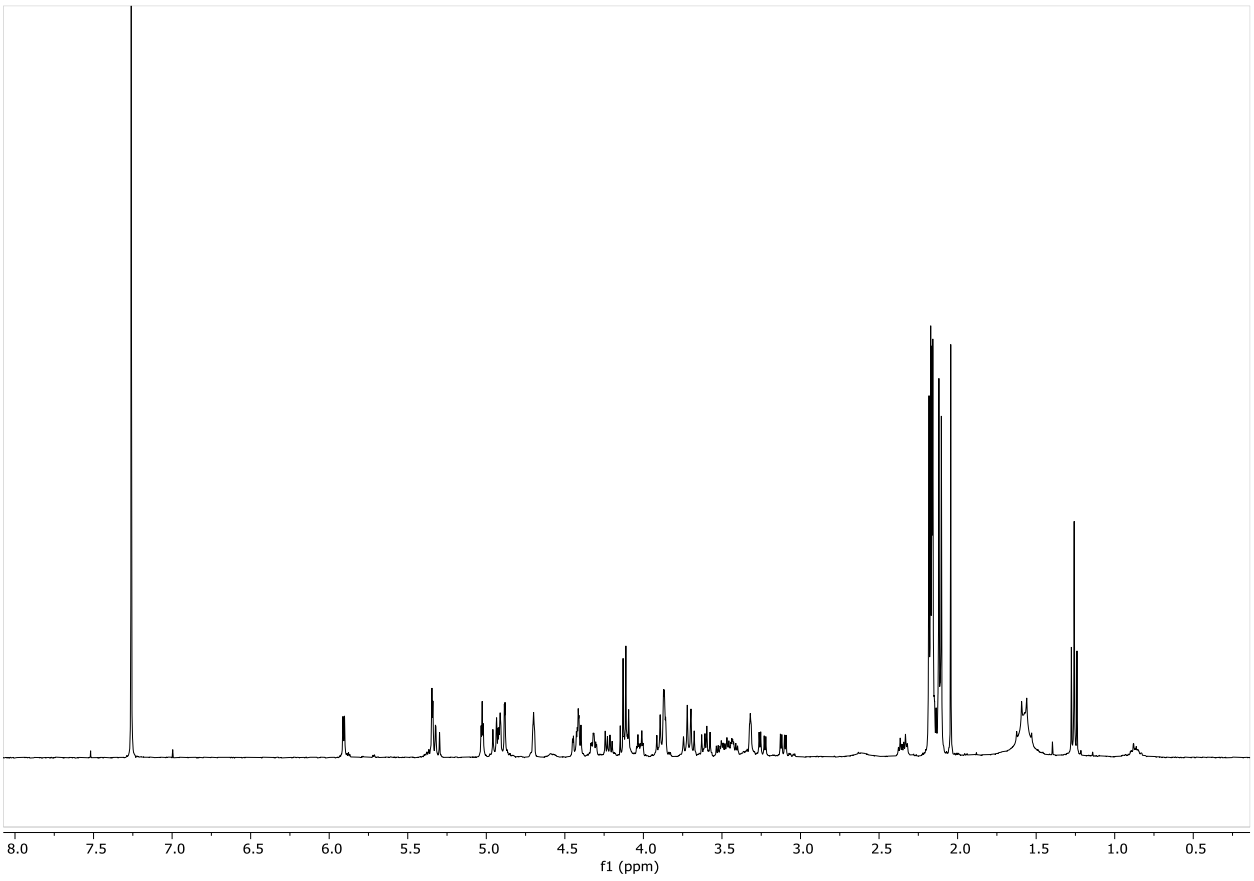
8.0
7.5
7.0
6.5
6.0
5.5
5.0
4.5
4.0
3.5
3.0
2.5
2.0
1.5
1.0
0.5
f1 (ppm)

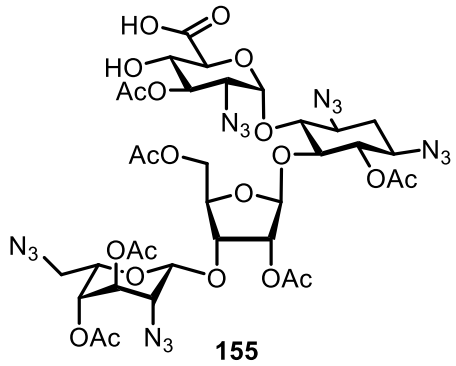
HO
O
HO
O
AcO
N3
N3
O
N3
AcO
O
OAc
O
N3
OAc
O
O
OAc
OAc
N3

155

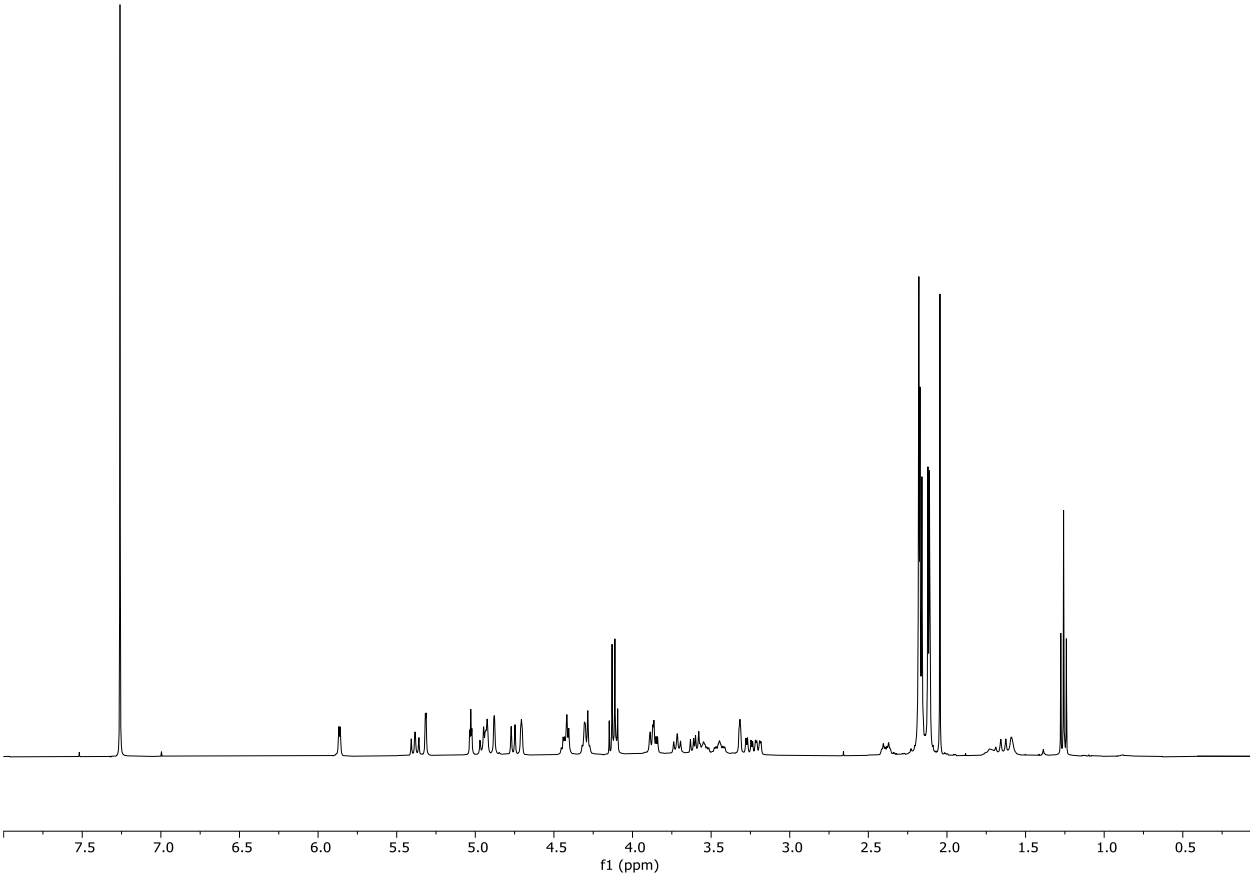
7.5
7.0
6.5
6.0
5.5
5.0
4.5
4.0
3.5
3.0
2.5
2.0
1.5
1.0
0.5
f1 (ppm)

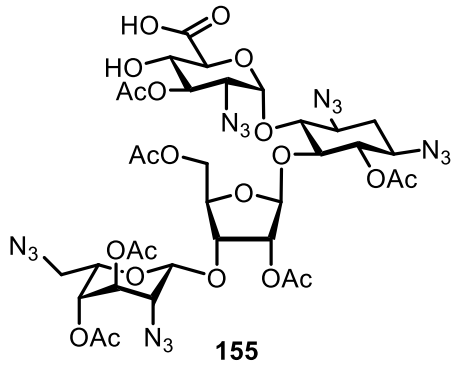
HO
O
HO
O
AcO
N3
N3
O
N3
AcO
O
OAc
O
N3
OAc
O
O
OAc
OAc
N3

155

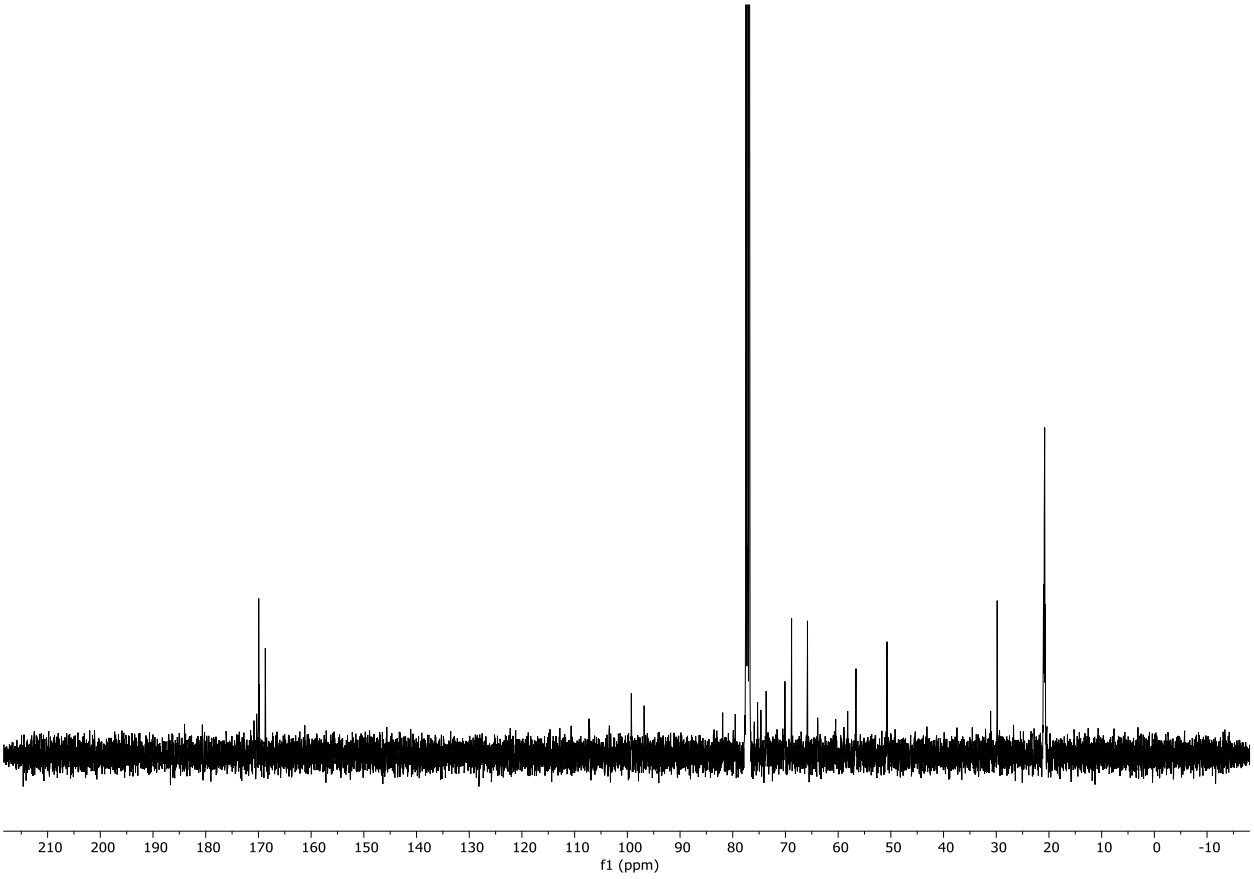
210
200
190
180
170
160
150
140
130
120
110
100
90
80
70
60
50
40
30
20
10
0
-10
f1 (ppm)

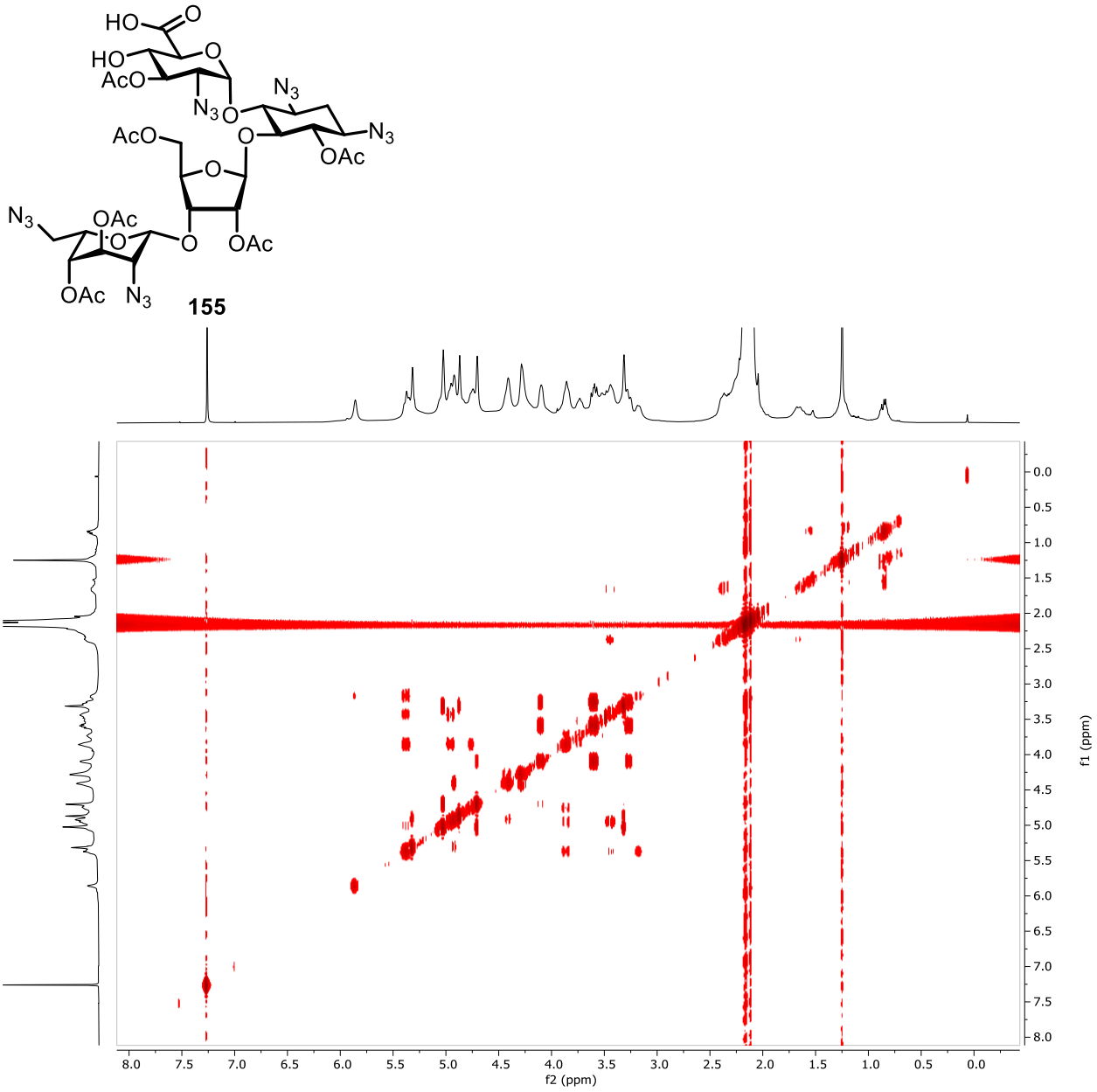
HO
O
HO
O
AcO
N3
N3
O
N3
AcO
O
N3
OAc
O
N3
OAc
O
O
OAc
OAc
N3
155
f2 (ppm)
f1 (ppm)

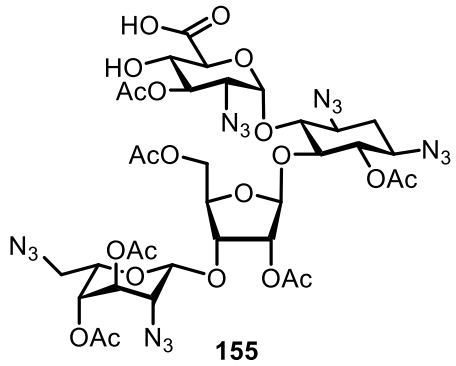
HO
O
HO
O
AcO
N3
N3
O
N3
AcO
O
OAc
O
N3
OAc
O
O
OAc
OAc
N3

155

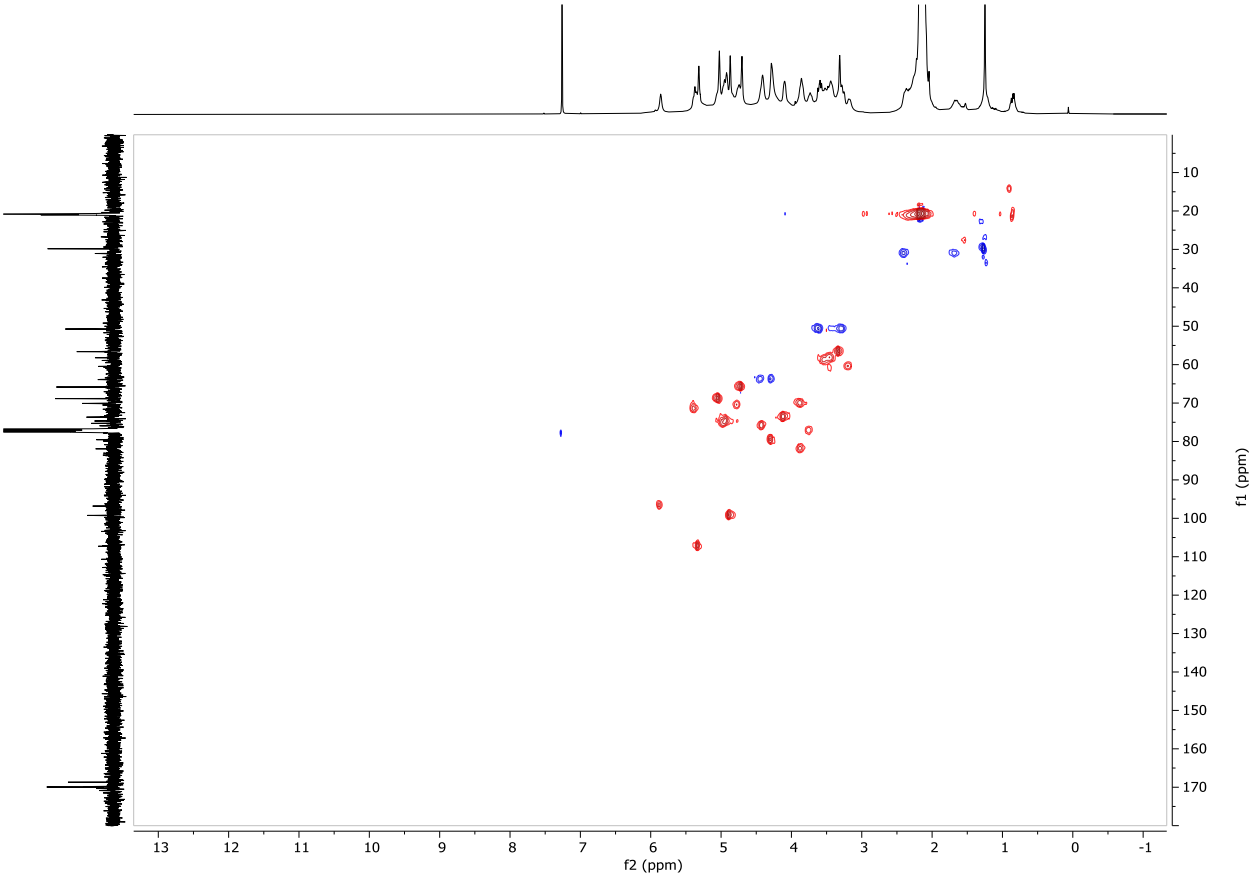
10
20
30
40
50
60
70
80
90
100
110
120
130
140
150
160
170
f1 (ppm)
13
12
11
10
9
8
7
6
5
4
3
2
1
0
-1
f2 (ppm)

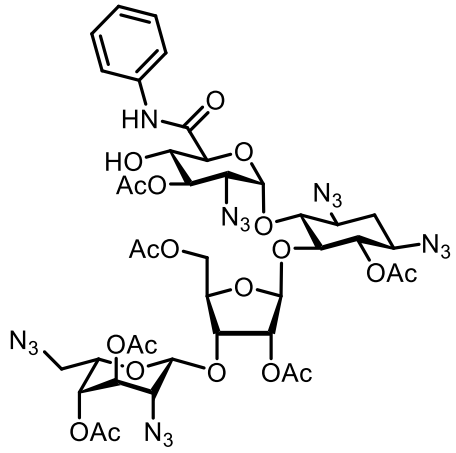
HN
O
HO
AcO
O
N3
N3
O
AcO
O
N3
OAc
O
N3
OAc
O
O
OAc
OAc
N3

156

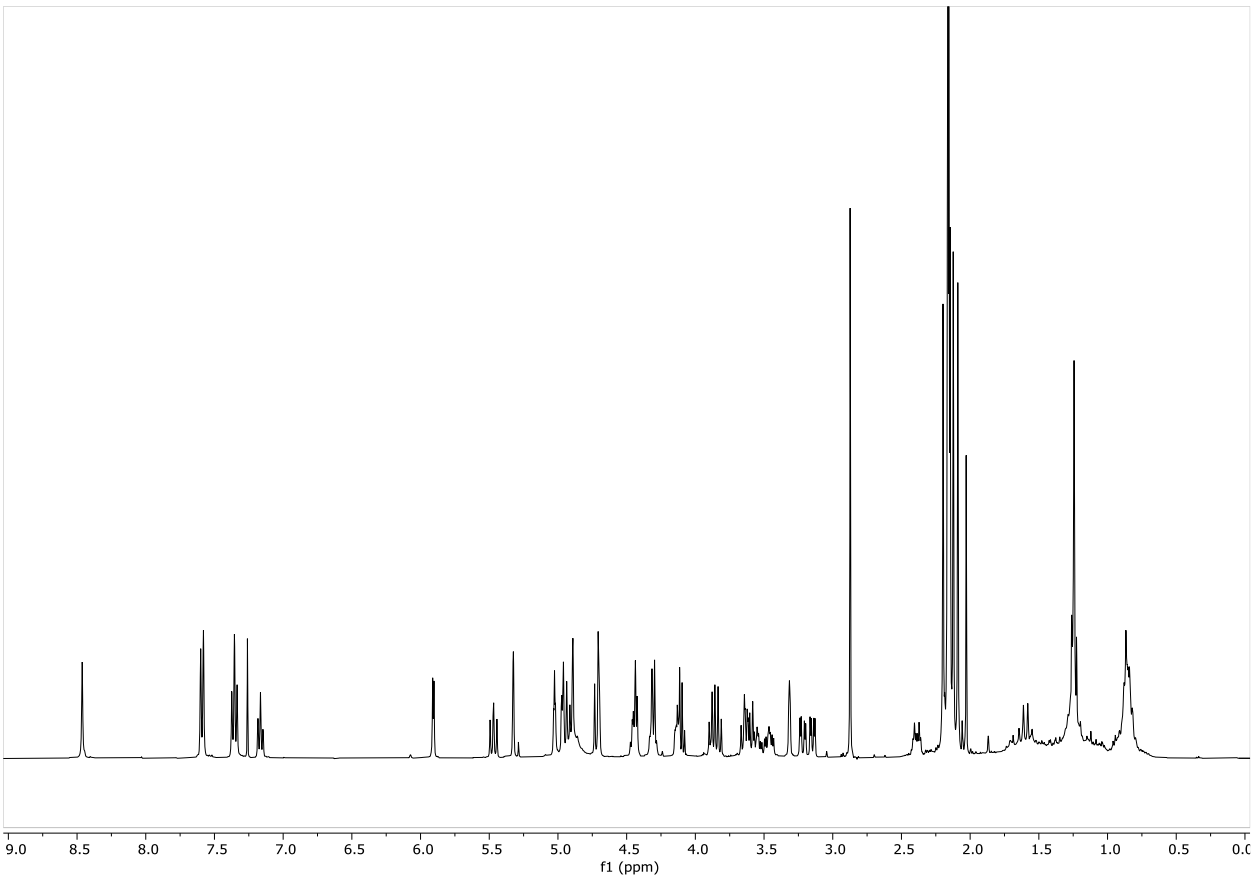
9.0
8.5
8.0
7.5
7.0
6.5
6.0
5.5
5.0
4.5
4.0
3.5
3.0
2.5
2.0
1.5
1.0
0.5
f1 (ppm)

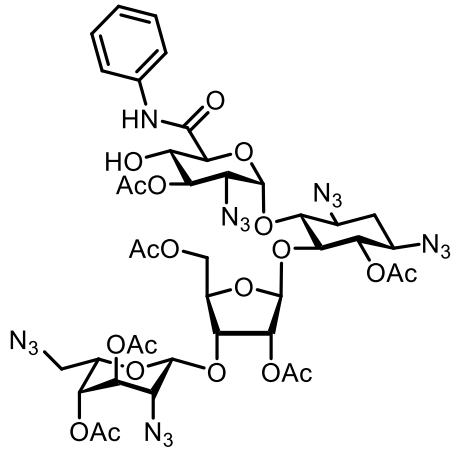
HN
O
HO
AcO
O
N3
N3
O
AcO
O
N3
OAc
O
N3
OAc
O
O
OAc
OAc
N3

156

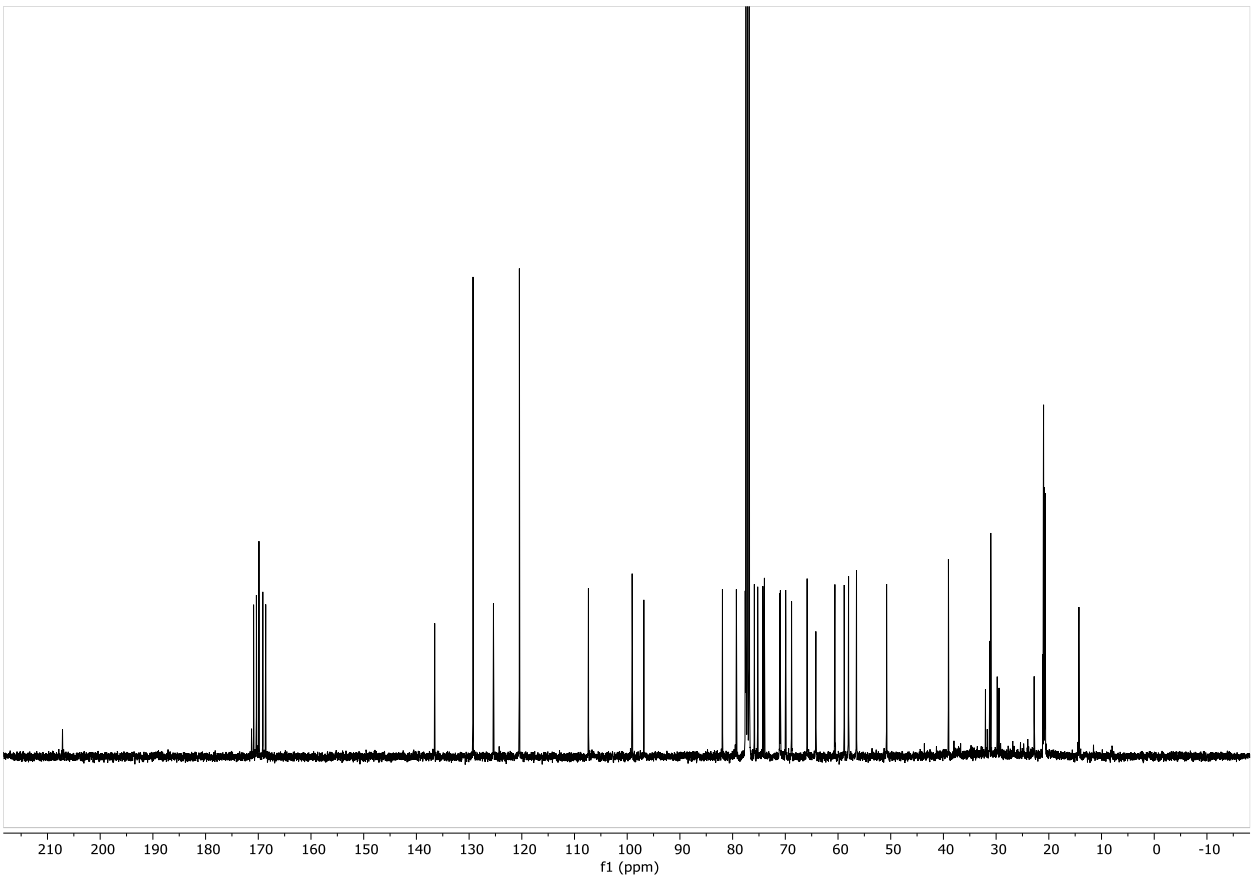
210 200 190 180 170 160 150 140 130 120 110 100 90 80 70 60 50 40 30 20 10 0 -10
f1 (ppm)

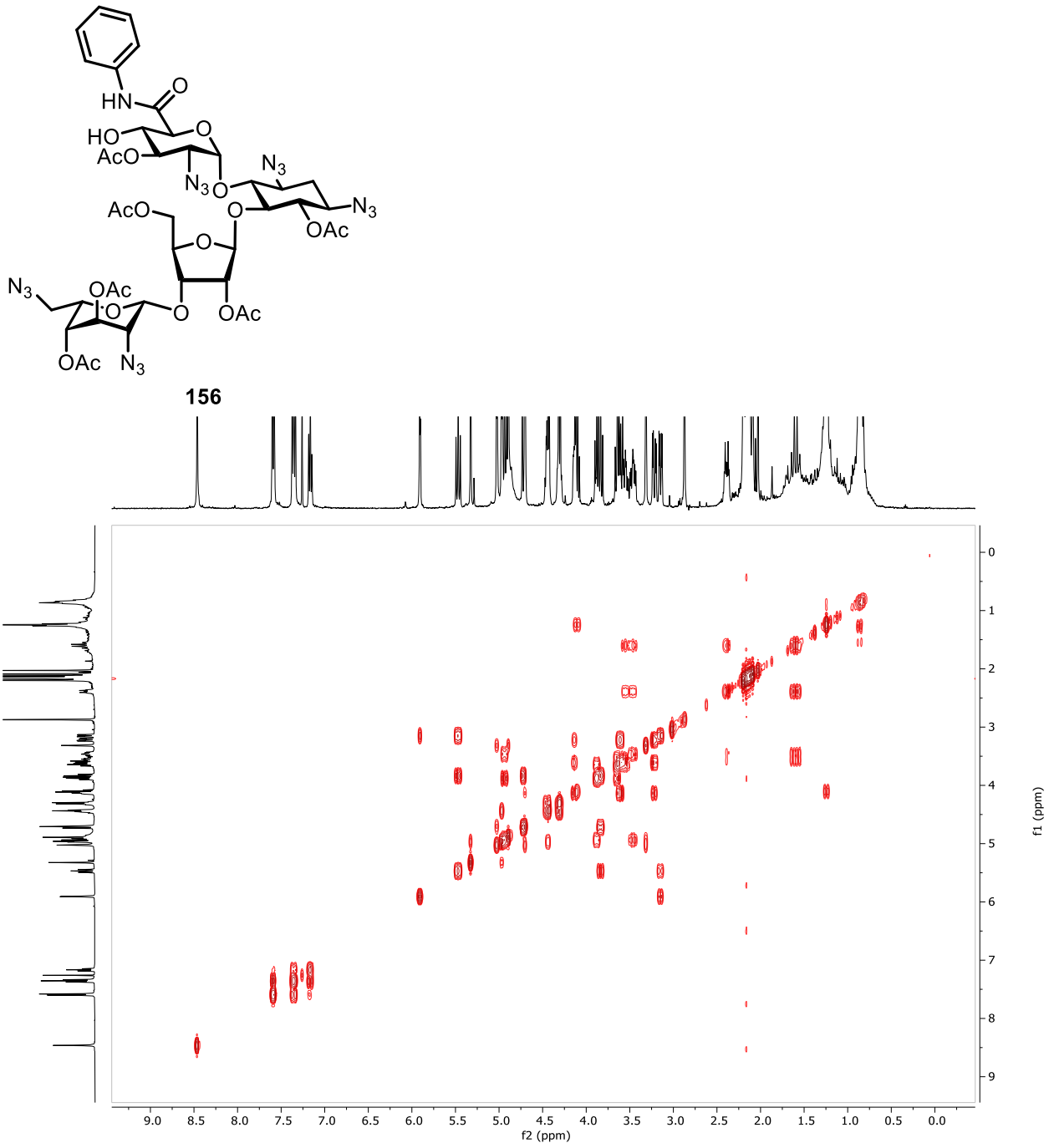
HN
O
HO
AcO
O
N3
N3
O
N3
AcO
O
OAc
O
N3
OAc
O
O
OAc
OAc
N3
156
f2 (ppm)
f1 (ppm)

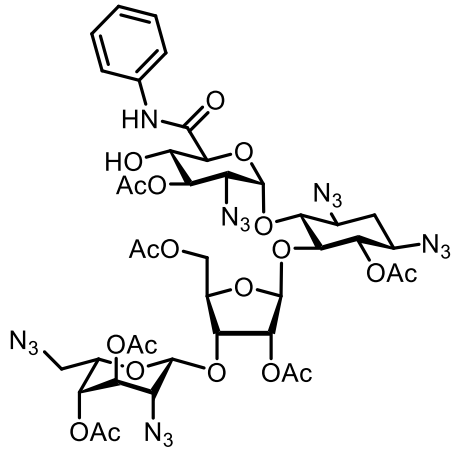
HN
O
HO
AcO
O
N3
N3
O
AcO
O
N3
OAc
O
N3
OAc
O
O
OAc
OAc
N3

156

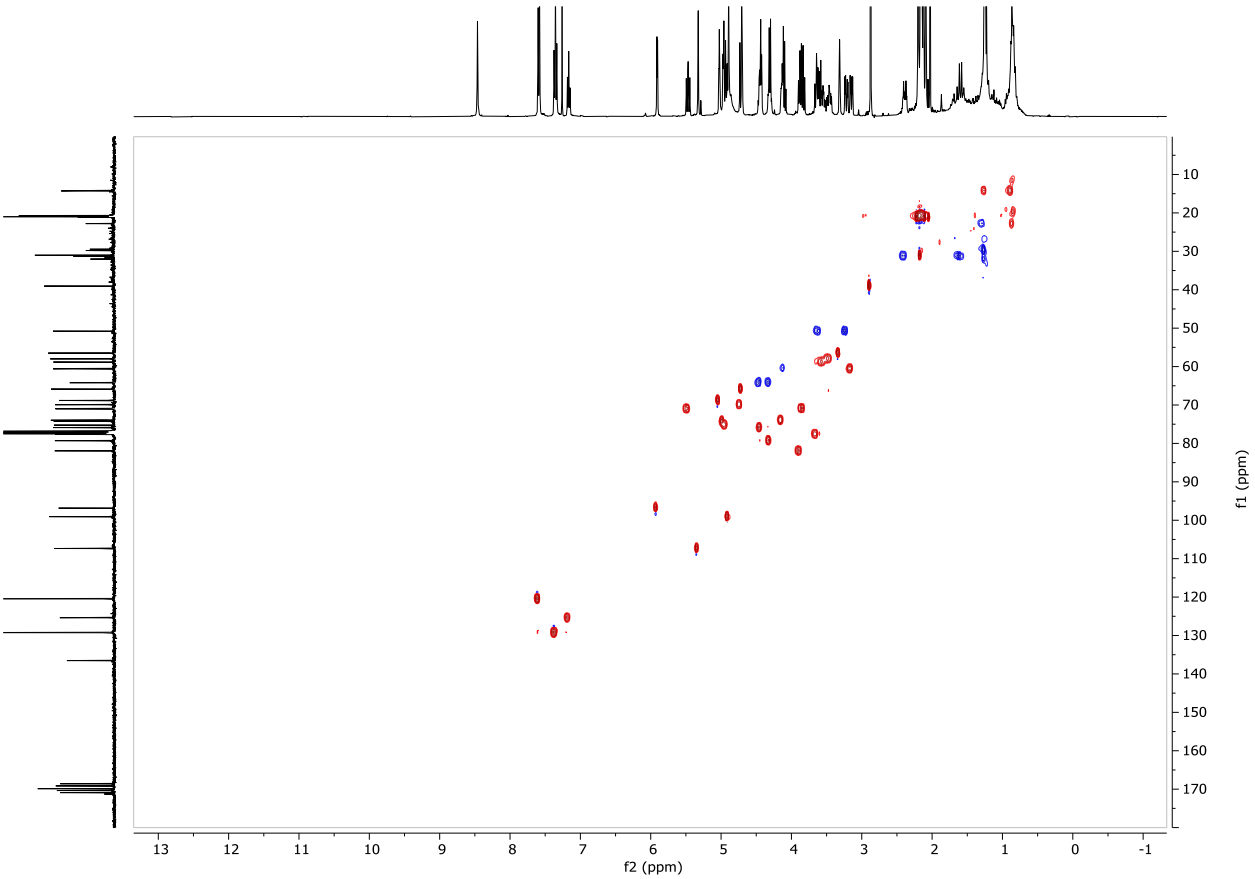
13
12
11
10
9
8
7
6
5
4
3
2
1
0
-1
f2 (ppm)
10
20
30
40
50
60
70
80
90
100
110
120
130
140
150
160
170
f1 (ppm)

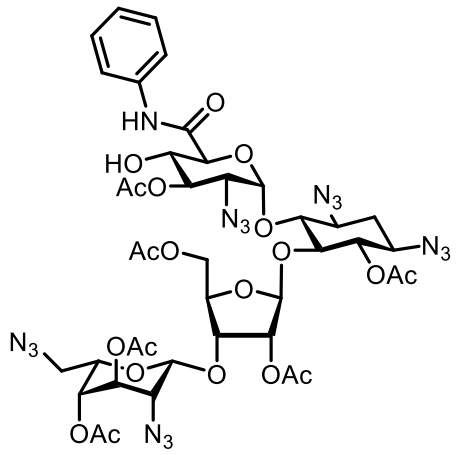
HN
O
HO
AcO
O
N3
N3
O
AcO
O
N3
OAc
O
N3
OAc
O
O
OAc
OAc
N3

156

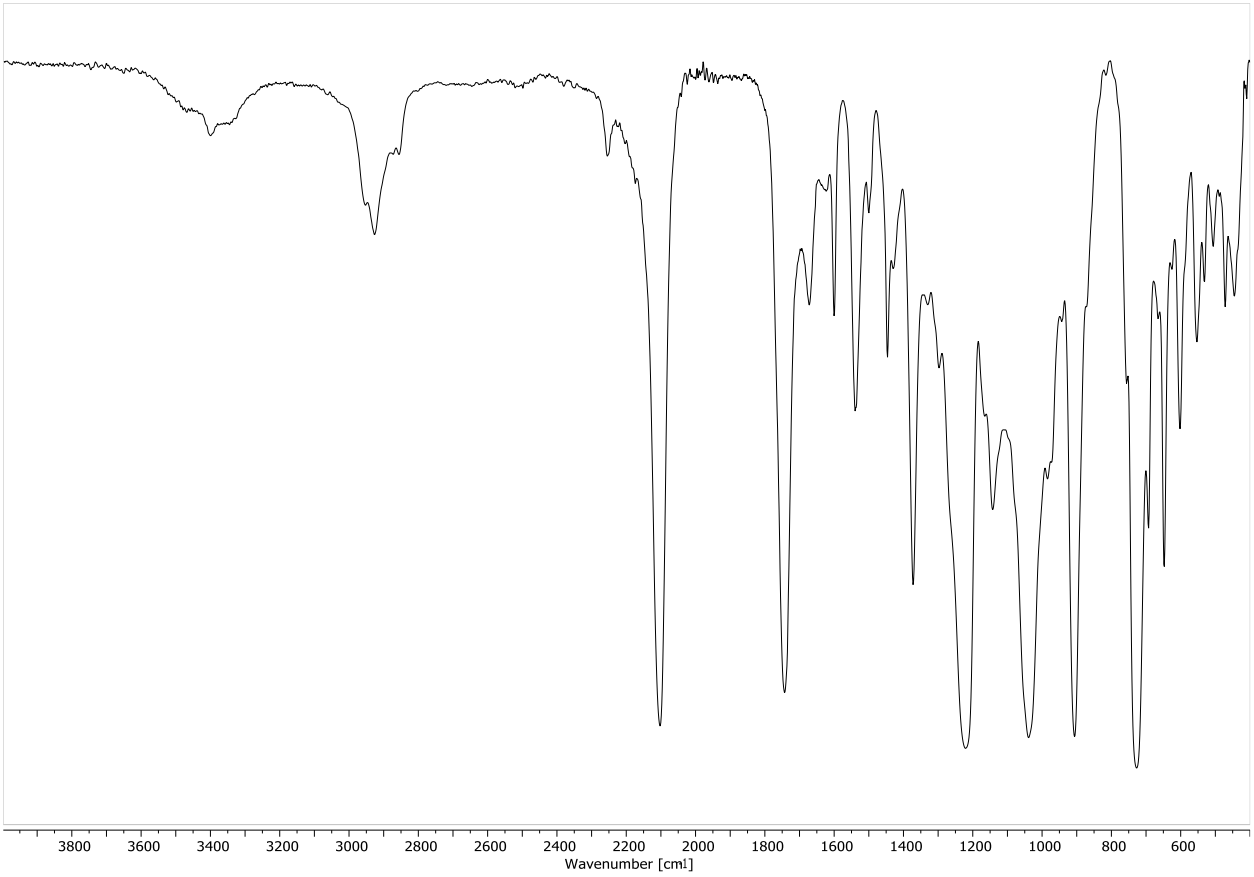
3800
3600
3400
3200
3000
2800
2600
2400
2200
2000
1800
1600
1400
1200
1000
800
600
Wavenumber [cm-1]

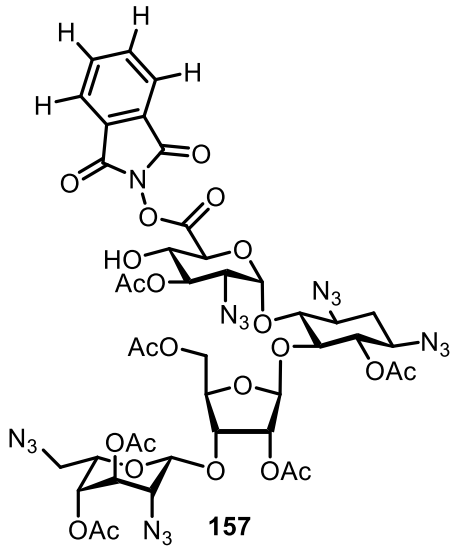
H
H
H
H
O
O
N
O
O
O
HO
AcO
O
N3
N3
O
N3
AcO
O
OAc
O
N3
OAc
O
O
OAc
OAc
N3

157

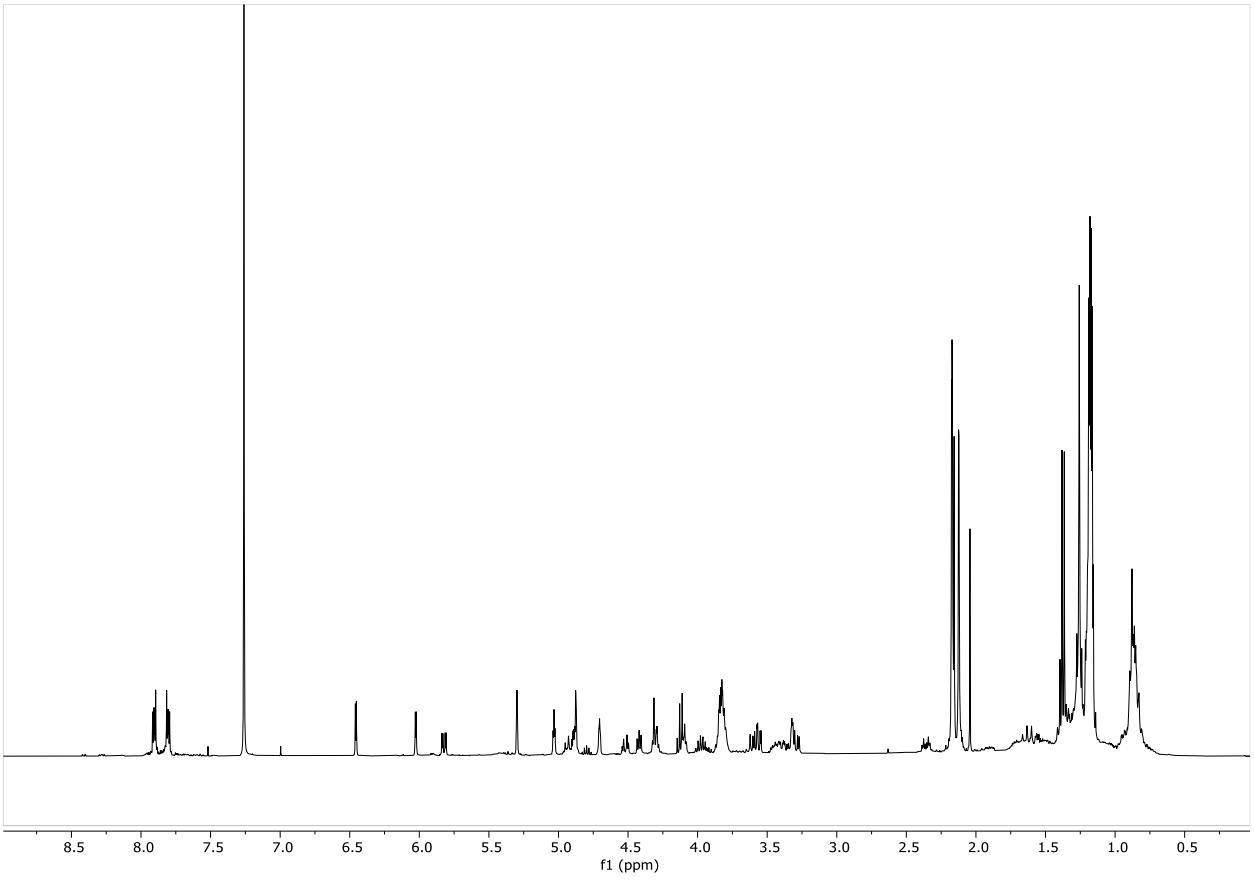
8.5
8.0
7.5
7.0
6.5
6.0
5.5
5.0
4.5
4.0
3.5
3.0
2.5
2.0
1.5
1.0
0.5
f1 (ppm)

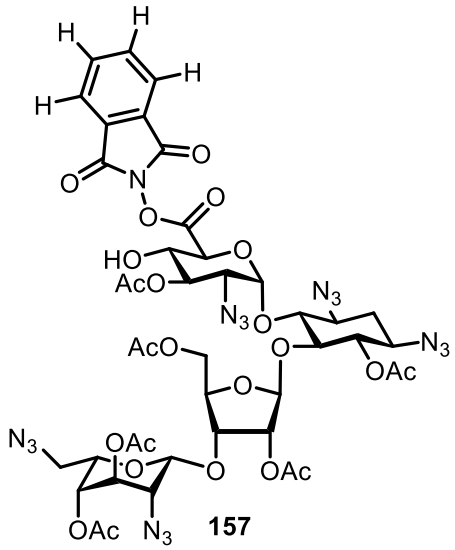
H
H
H
H
O
O
N
O
O
O
HO
AcO
O
N3
N3
O
N3
AcO
O
OAc
O
N3
OAc
O
O
OAc
OAc
N3

157

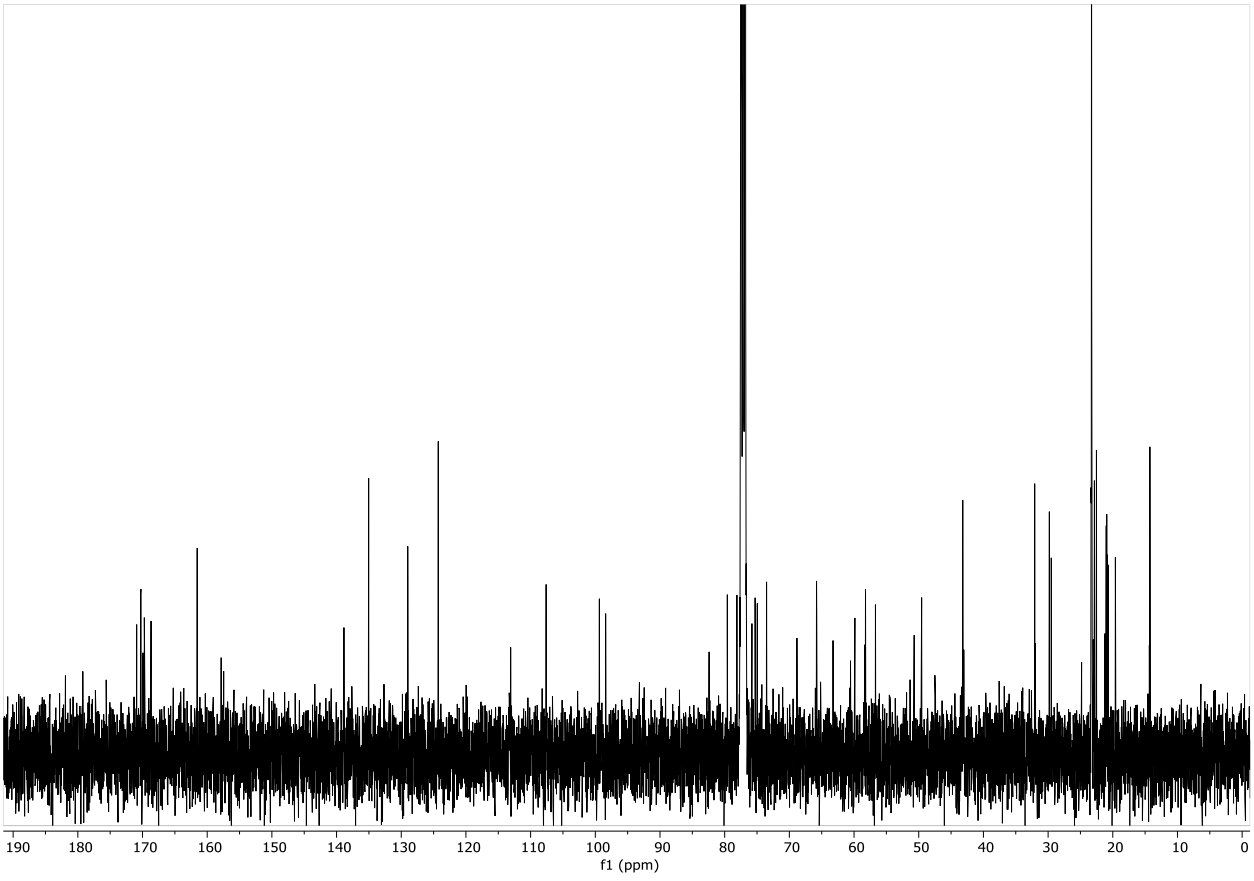
190
180
170
160
150
140
130
120
110
100
90
80
70
60
50
40
30
20
10
0
f1 (ppm)

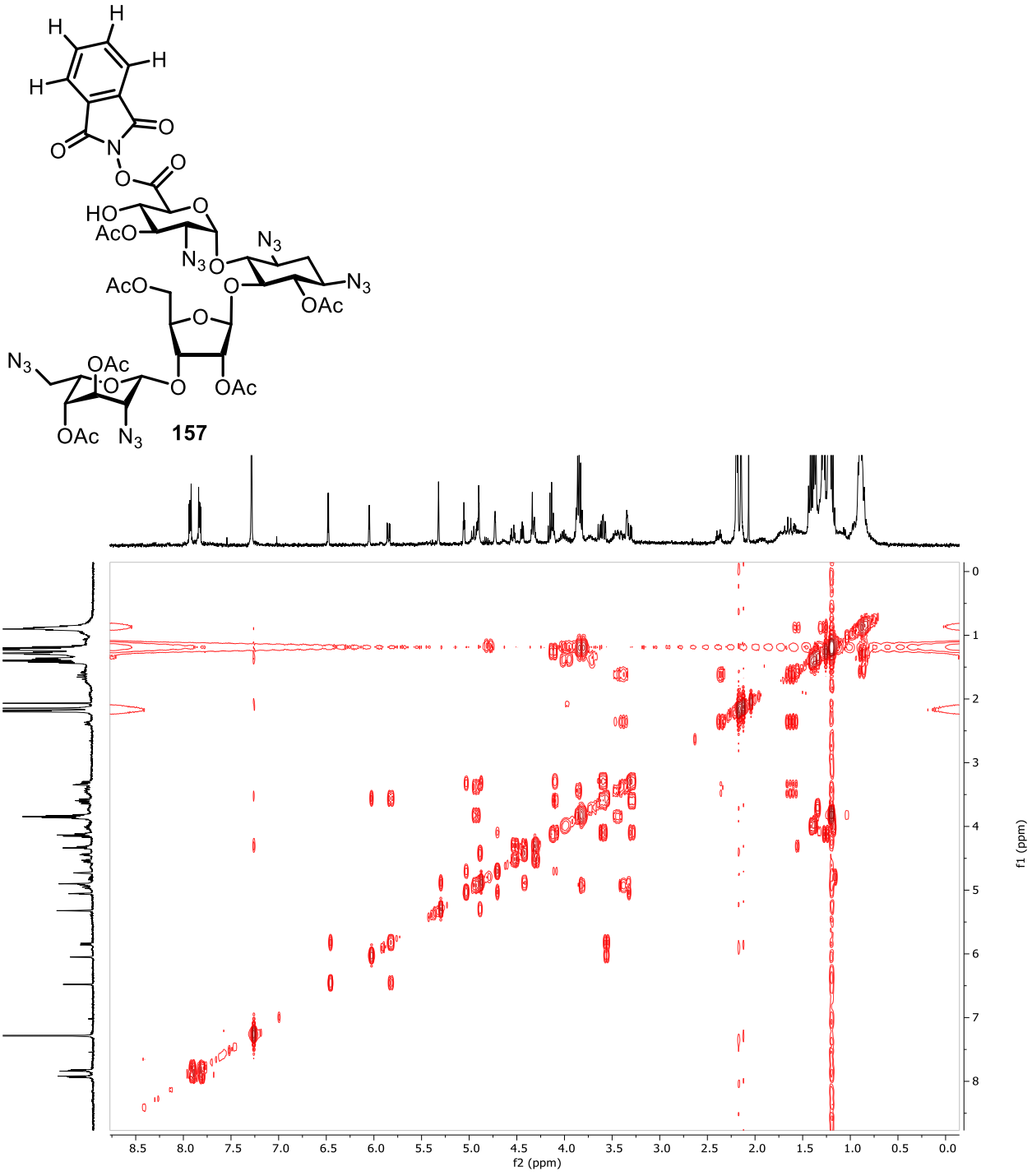
157
f2 (ppm)
f1 (ppm)

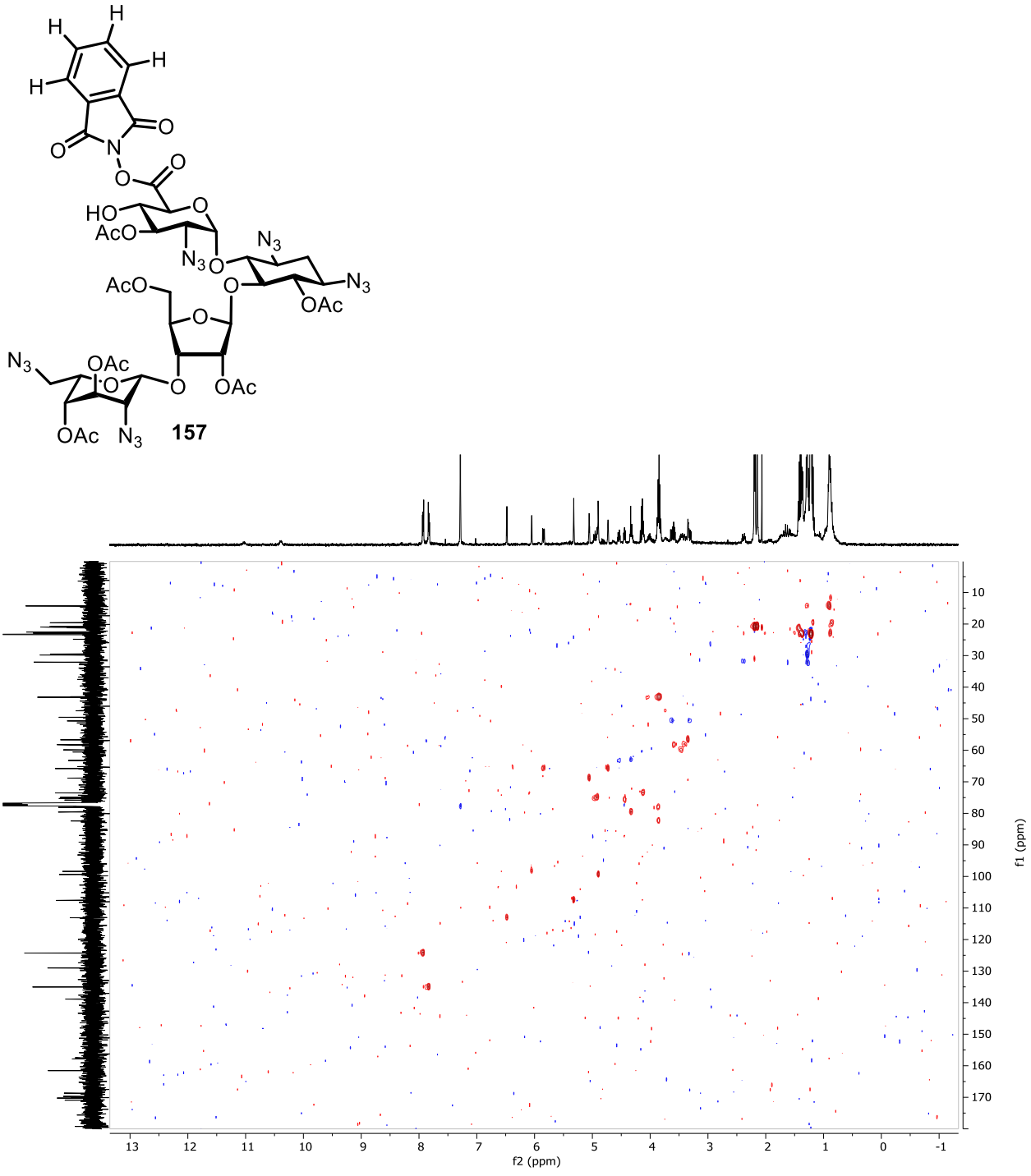
157
f2 (ppm)
f1 (ppm)

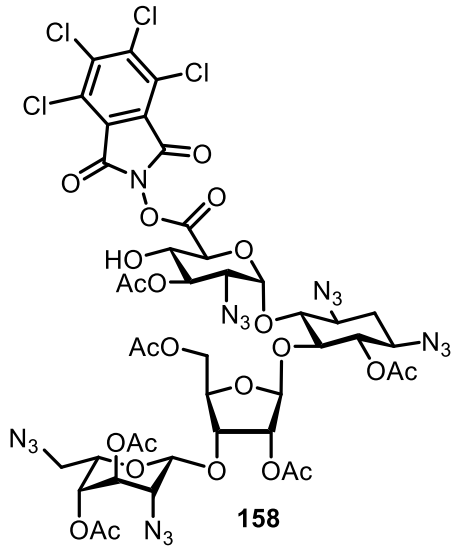
Cl
Cl
Cl
Cl
O
O
N
O
O
O
HO
AcO
O
N3
N3
O
N3
AcO
O
OAc
O
N3
OAc
O
O
OAc
OAc
N3

158

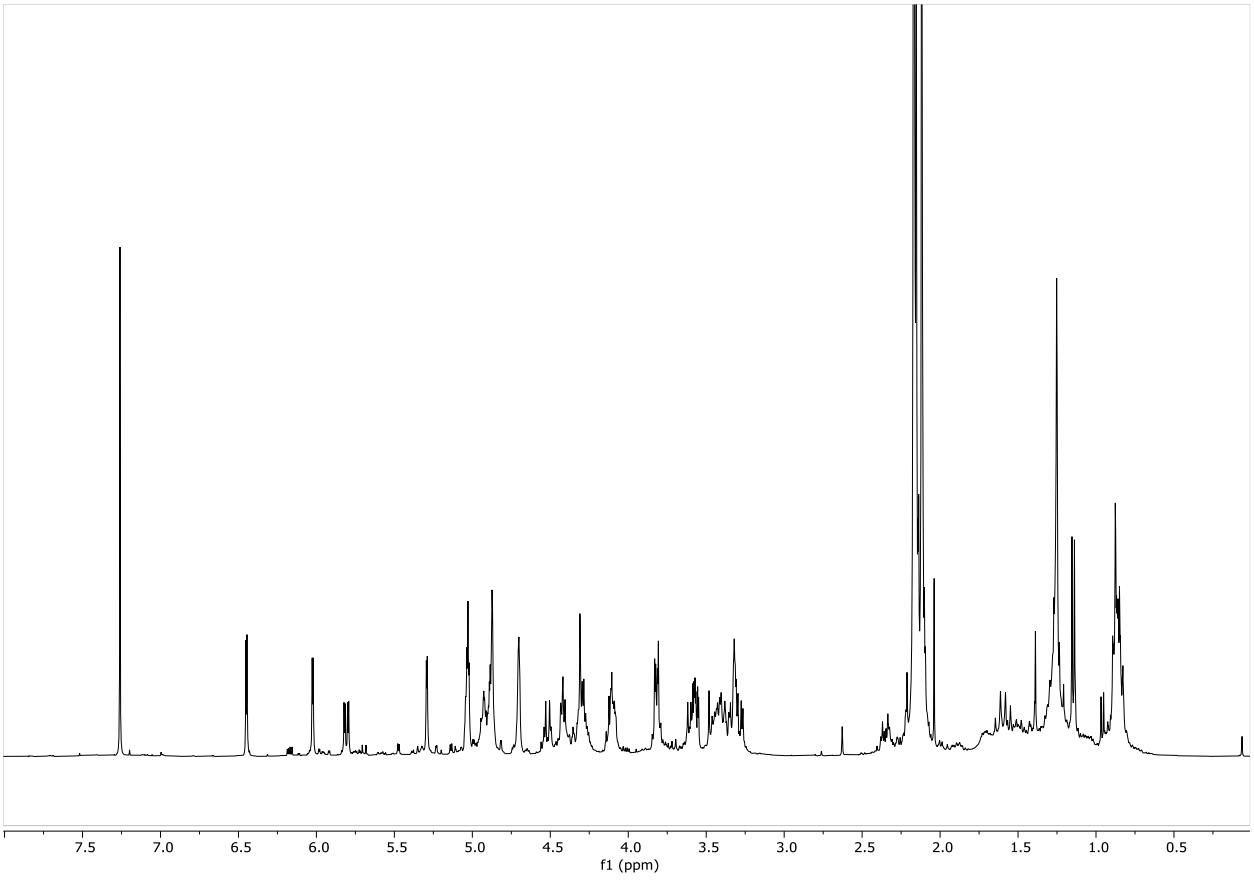
7.5
7.0
6.5
6.0
5.5
5.0
4.5
4.0
3.5
3.0
2.5
2.0
1.5
1.0
0.5
f1 (ppm)

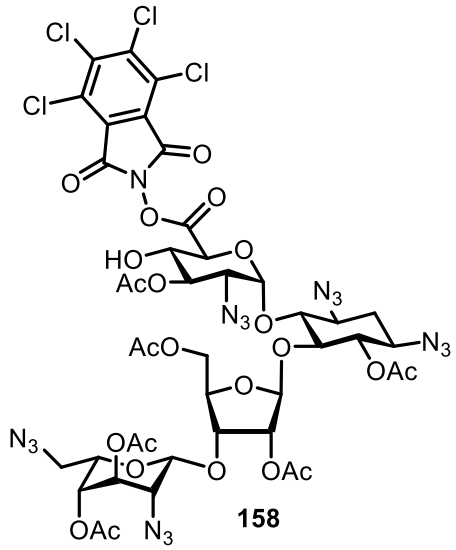
Cl
Cl
Cl
Cl
O
O
N
O
O
HO
AcO
O
N3
N3
O
N3
AcO
O
OAc
O
N3
OAc
O
O
OAc
OAc
N3

158

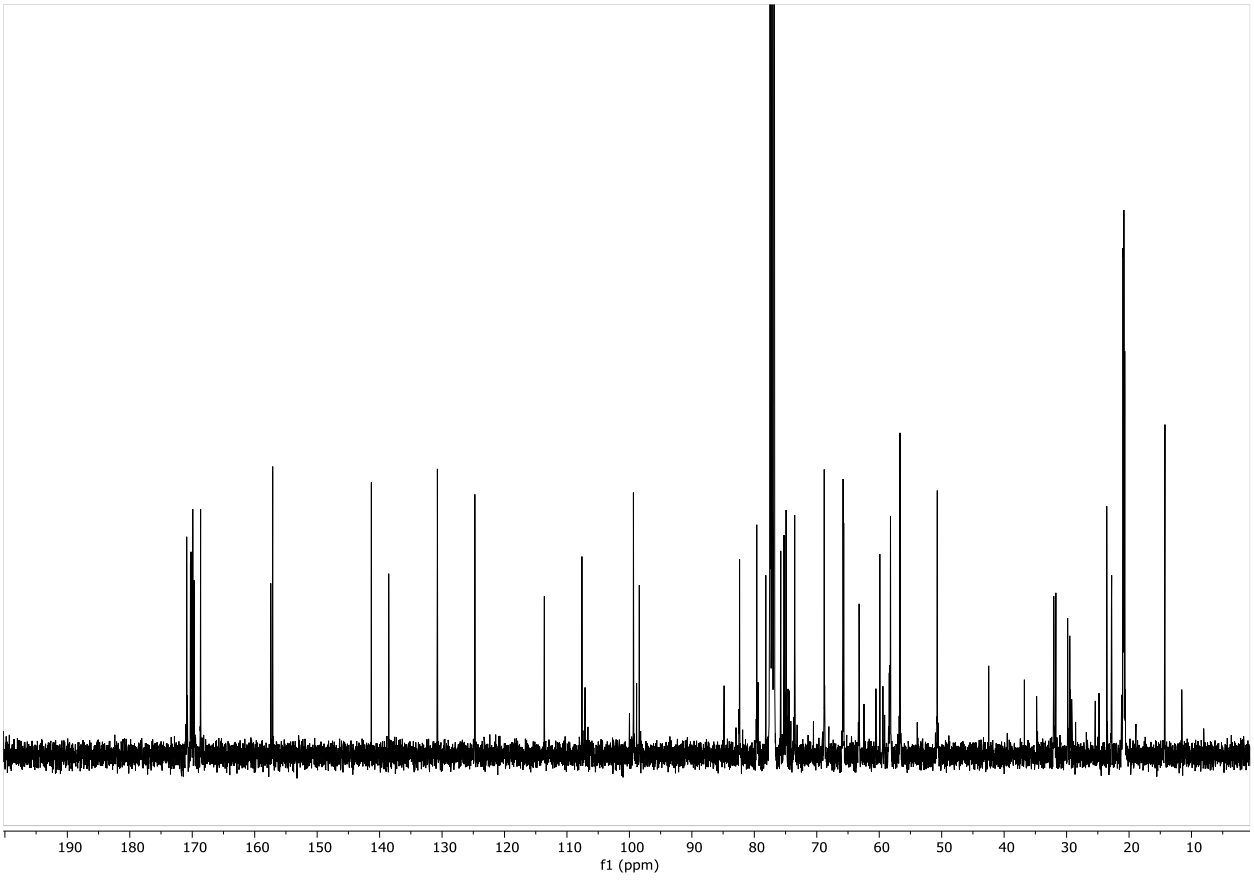
190
180
170
160
150
140
130
120
110
100
90
80
70
60
50
40
30
20
10
f1 (ppm)

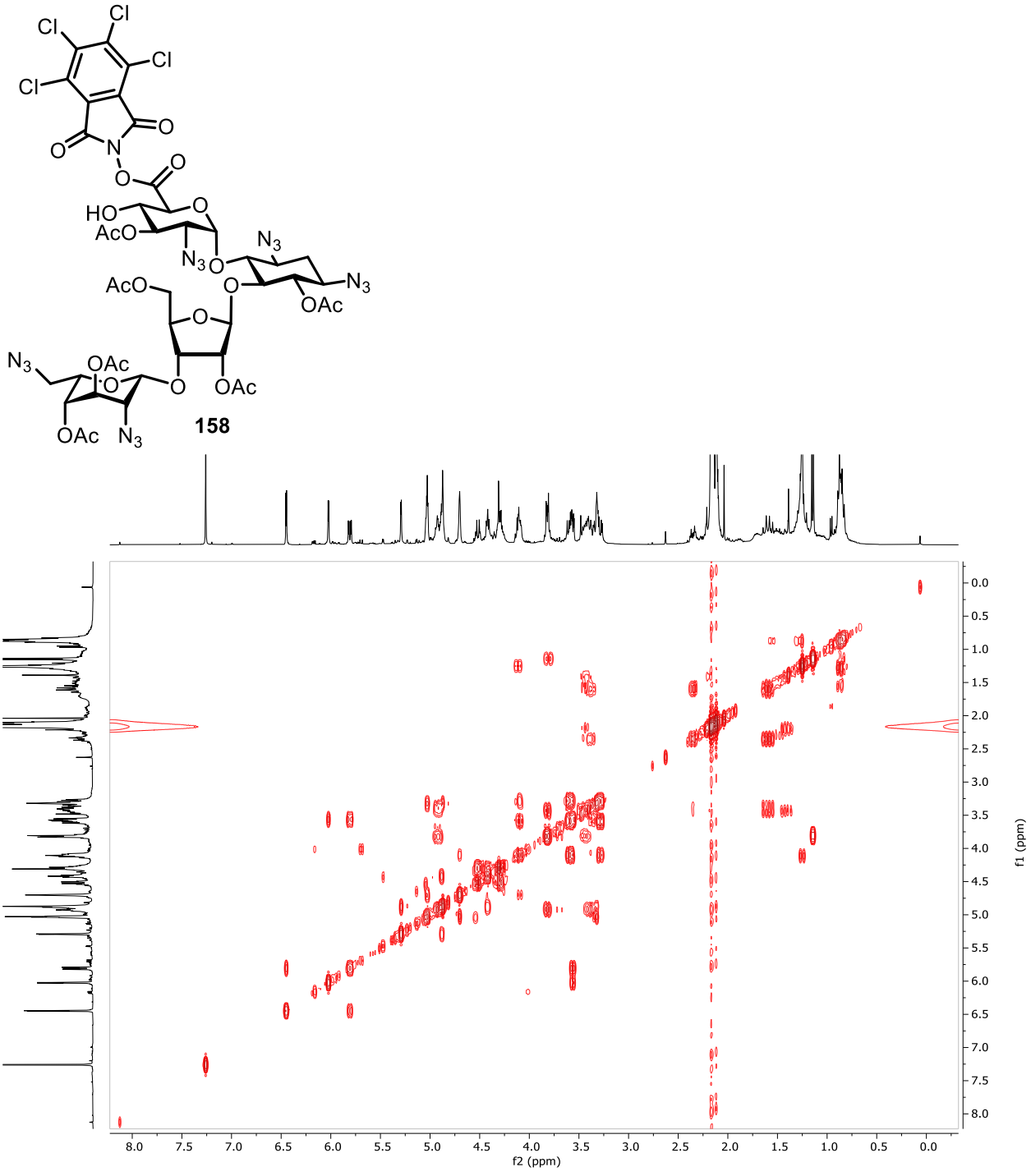
Cl
Cl
Cl
Cl
O
O
N
O
O
HO
AcO
O
N3
N3
O
N3
AcO
O
OAc
O
N3
OAc
O
O
OAc
OAc
N3
158
f2 (ppm)
f1 (ppm)

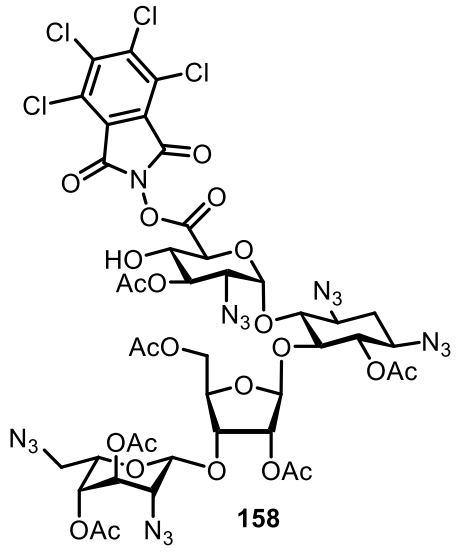
Cl
Cl
Cl
Cl
O
O
N
O
O
HO
AcO
O
N3
N3
O
N3
AcO
O
OAc
O
N3
OAc
O
O
OAc
OAc
N3

158

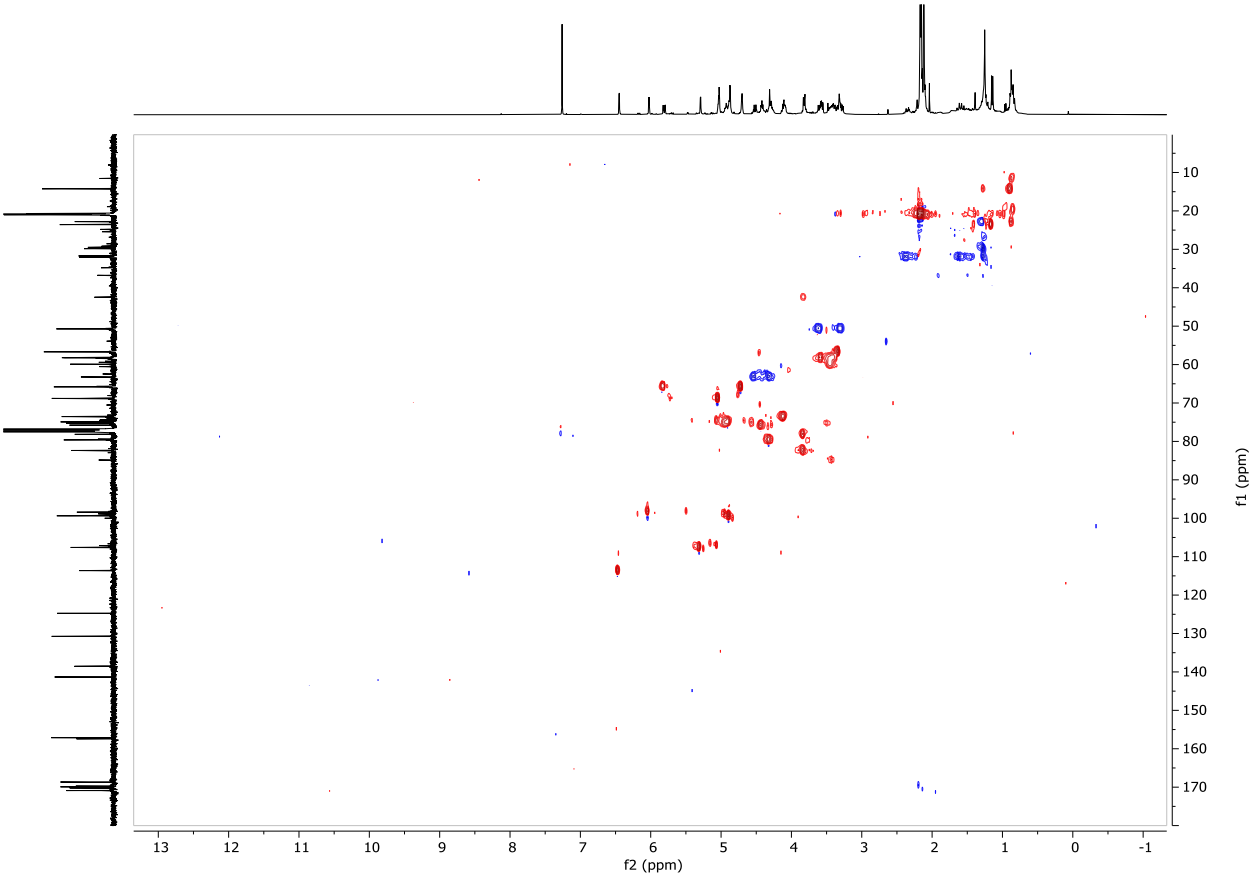
f2 (ppm)
f1 (ppm)

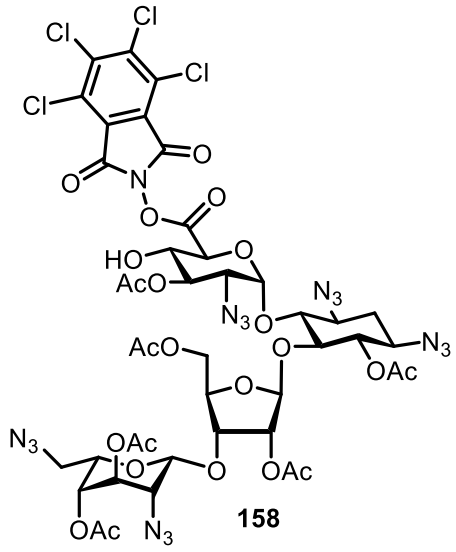
Cl
Cl
Cl
Cl
O
O
N
O
O
HO
AcO
O
N3
N3
O
N3
AcO
O
OAc
O
N3
OAc
O
O
OAc
OAc
N3

158

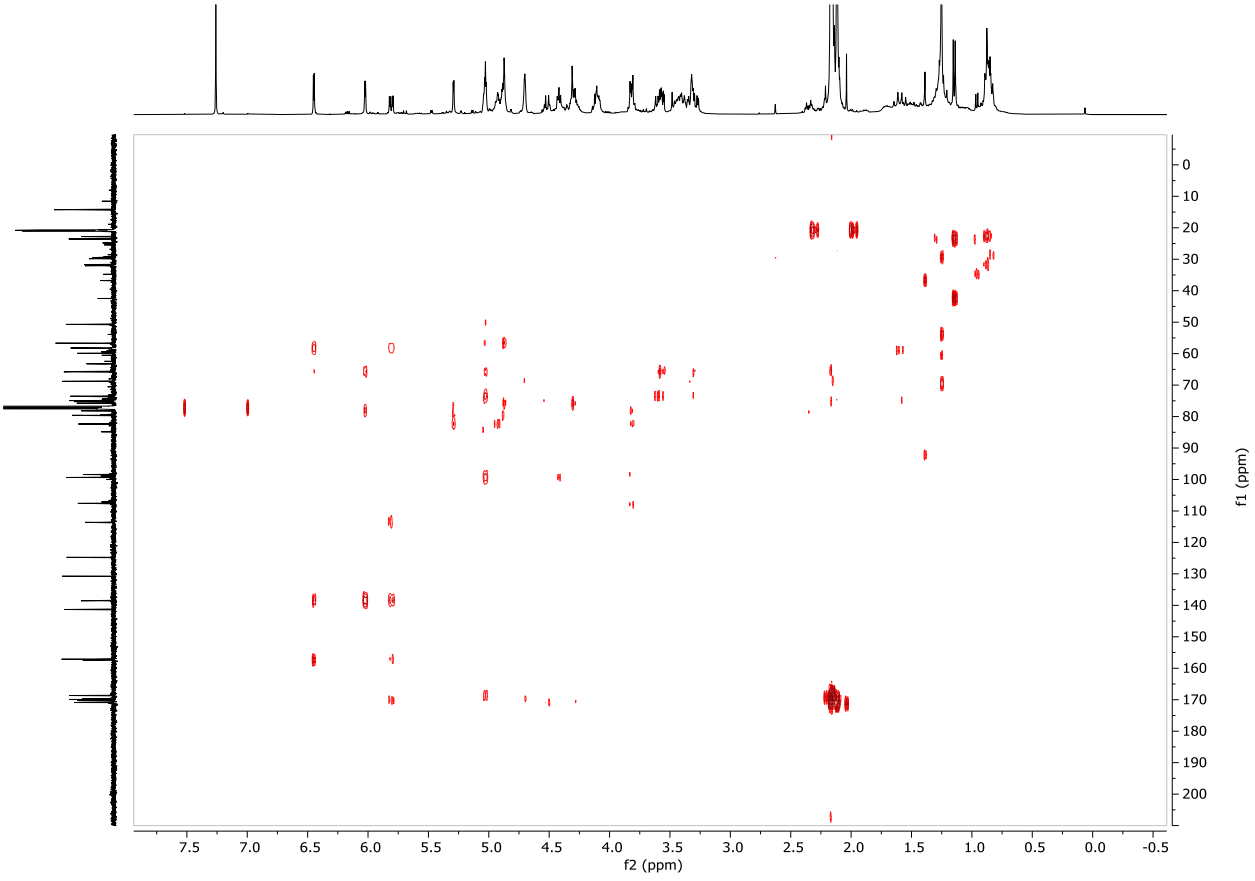
0
10
20
30
40
50
60
70
80
90
100
110
120
130
140
150
160
170
180
190
200
f1 (ppm)
7.5
7.0
6.5
6.0
5.5
5.0
4.5
4.0
3.5
3.0
2.5
2.0
1.5
1.0
0.5
0.0
-0.5
f2 (ppm)

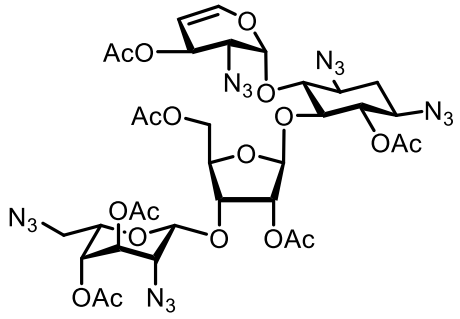

159

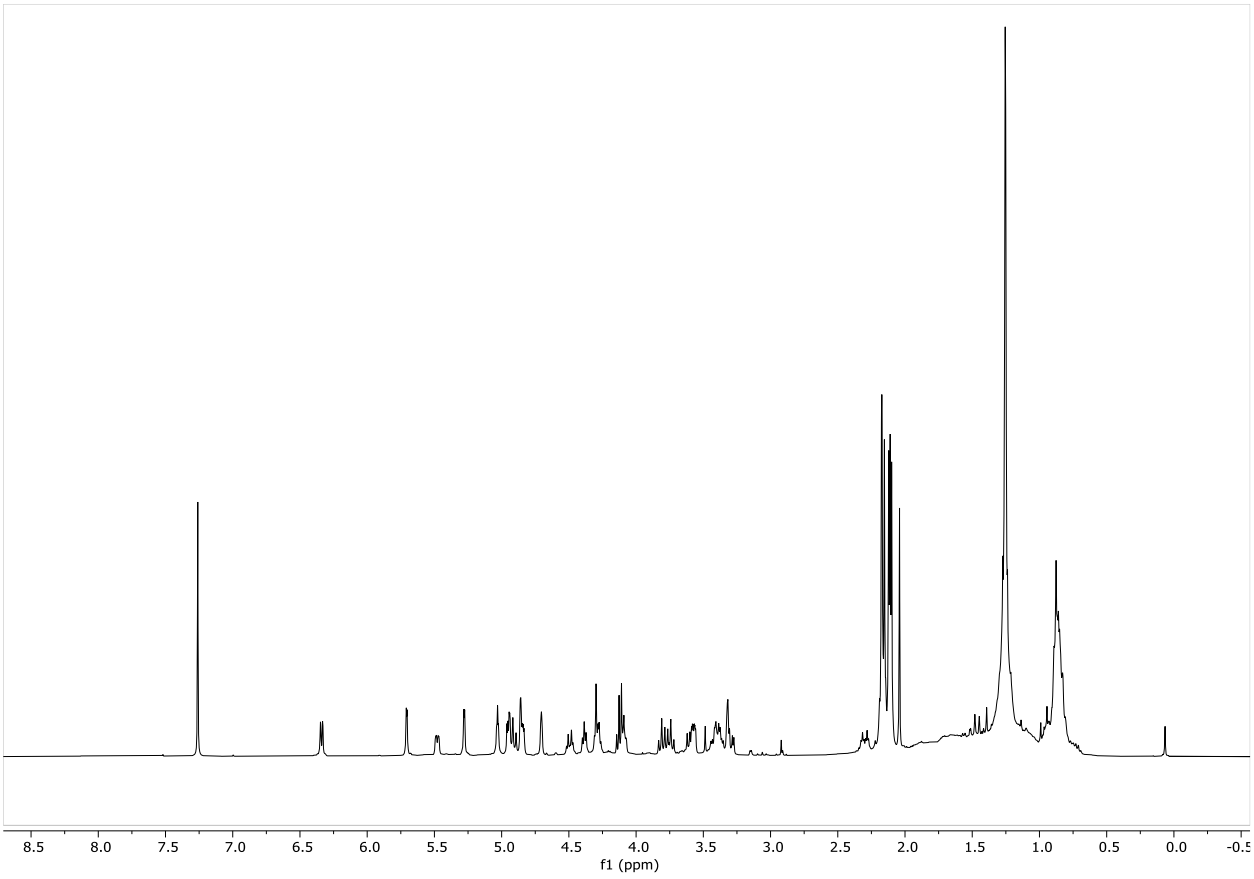

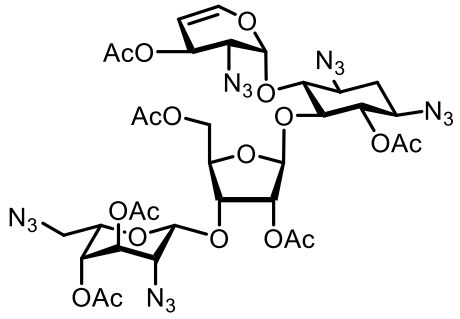
AcO
O
N3
N3
O
N3
AcO
O
OAc
O
N3
OAc
O
O
OAc
OAc
N3

159

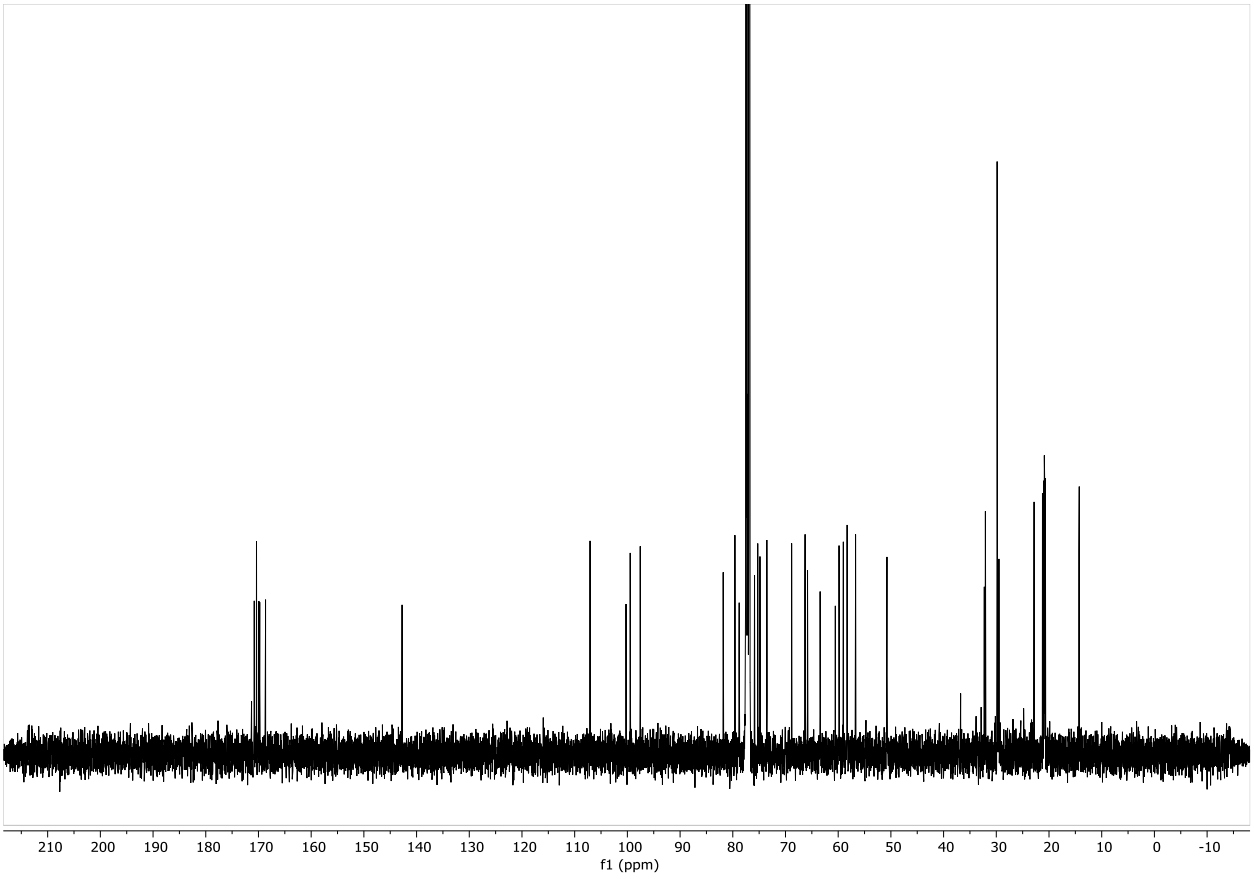
210
200
190
180
170
160
150
140
130
120
110
100
90
80
70
60
50
40
30
20
10
0
-10
f1 (ppm)

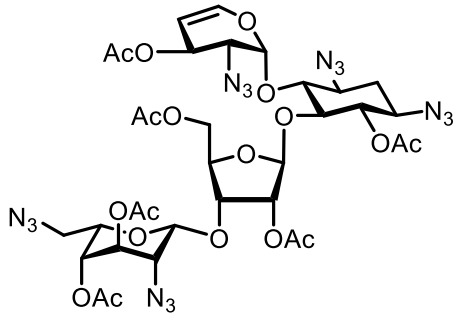
AcO
O
N3
N3
O
N3
AcO
O
OAc
O
N3
OAc
O
O
OAc
OAc
N3

159

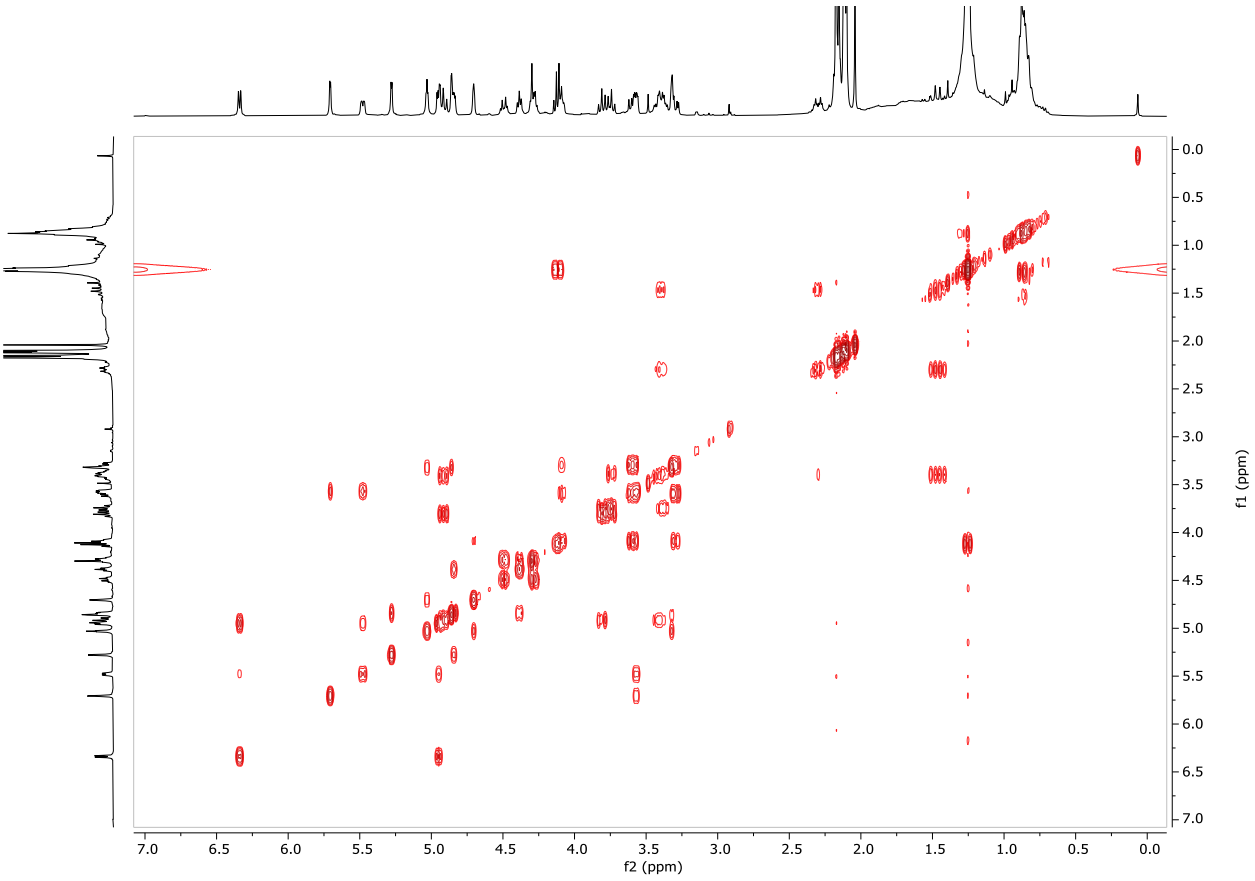
f2 (ppm)
f1 (ppm)
7.0
6.5
6.0
5.5
5.0
4.5
4.0
3.5
3.0
2.5
2.0
1.5
1.0
0.5
0.0

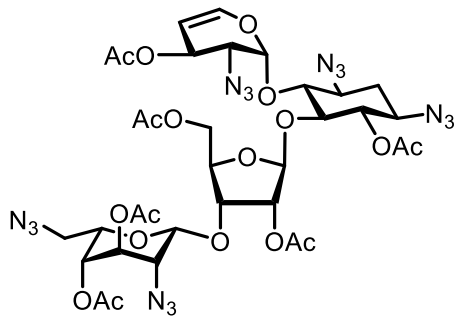

159

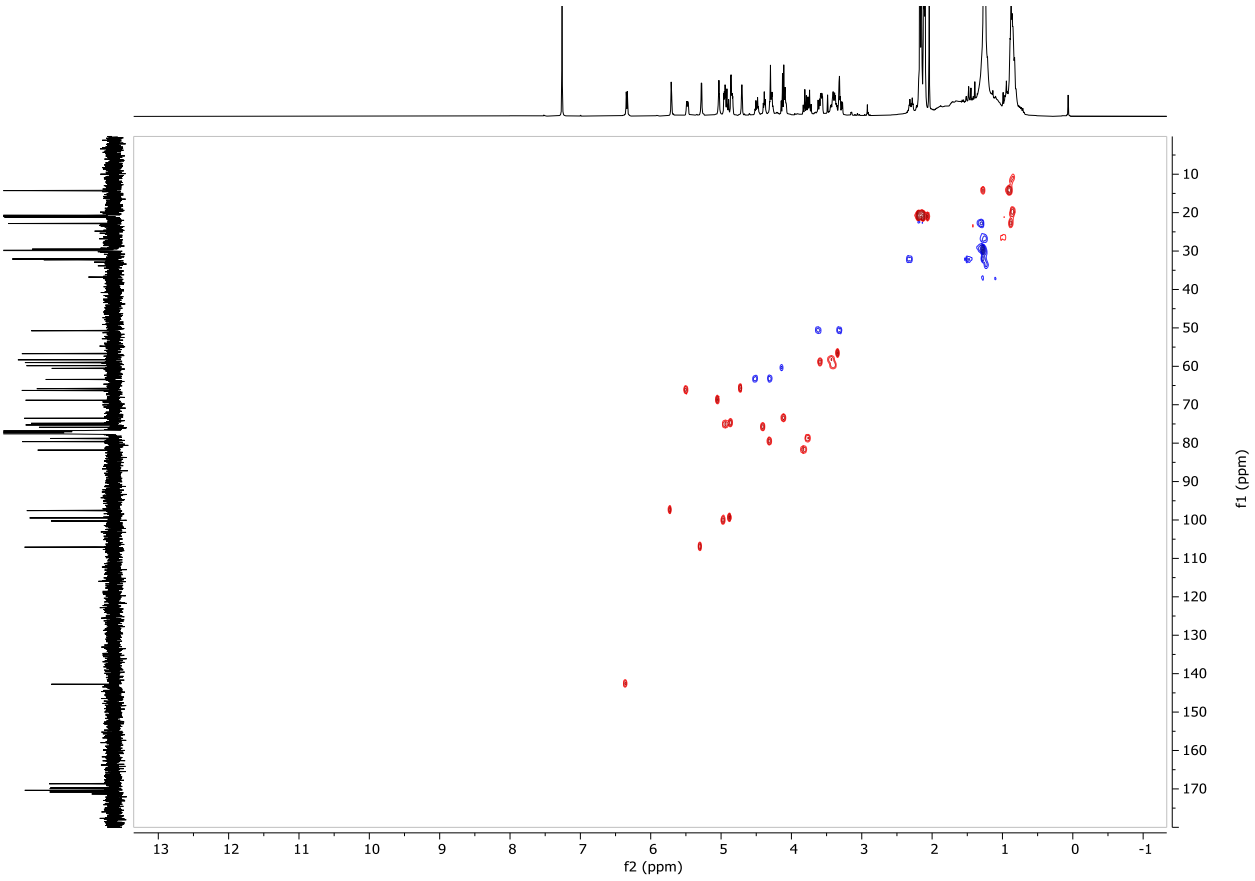

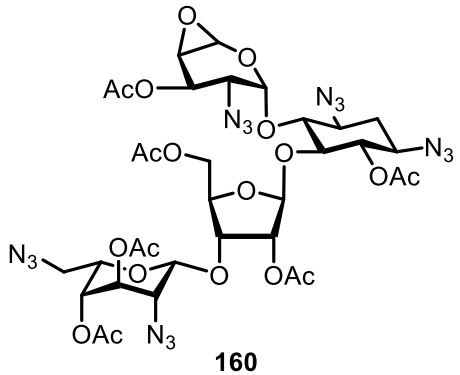
O
O
AcO
N3
N3
O
N3
AcO
O
N3
OAc
O
OAc
N3
O
O
OAc
OAc
N3

160

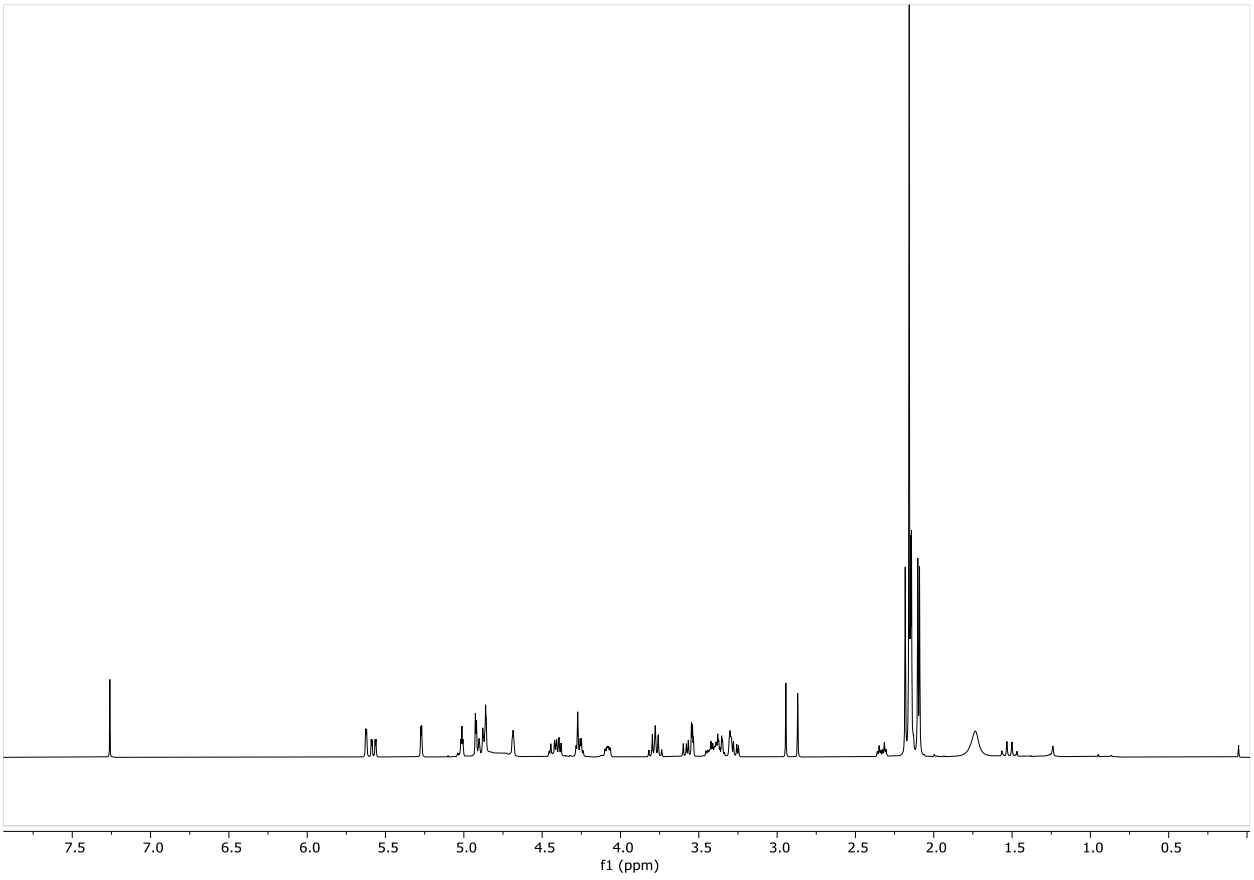
7.5
7.0
6.5
6.0
5.5
5.0
4.5
4.0
3.5
3.0
2.5
2.0
1.5
1.0
0.5
f1 (ppm)

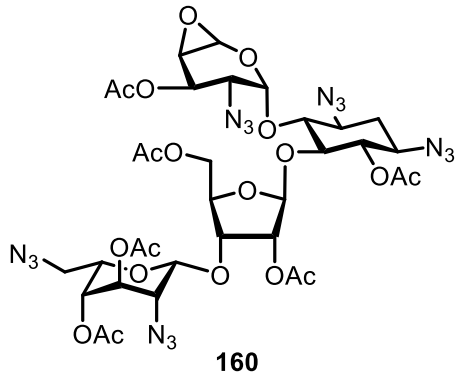

160

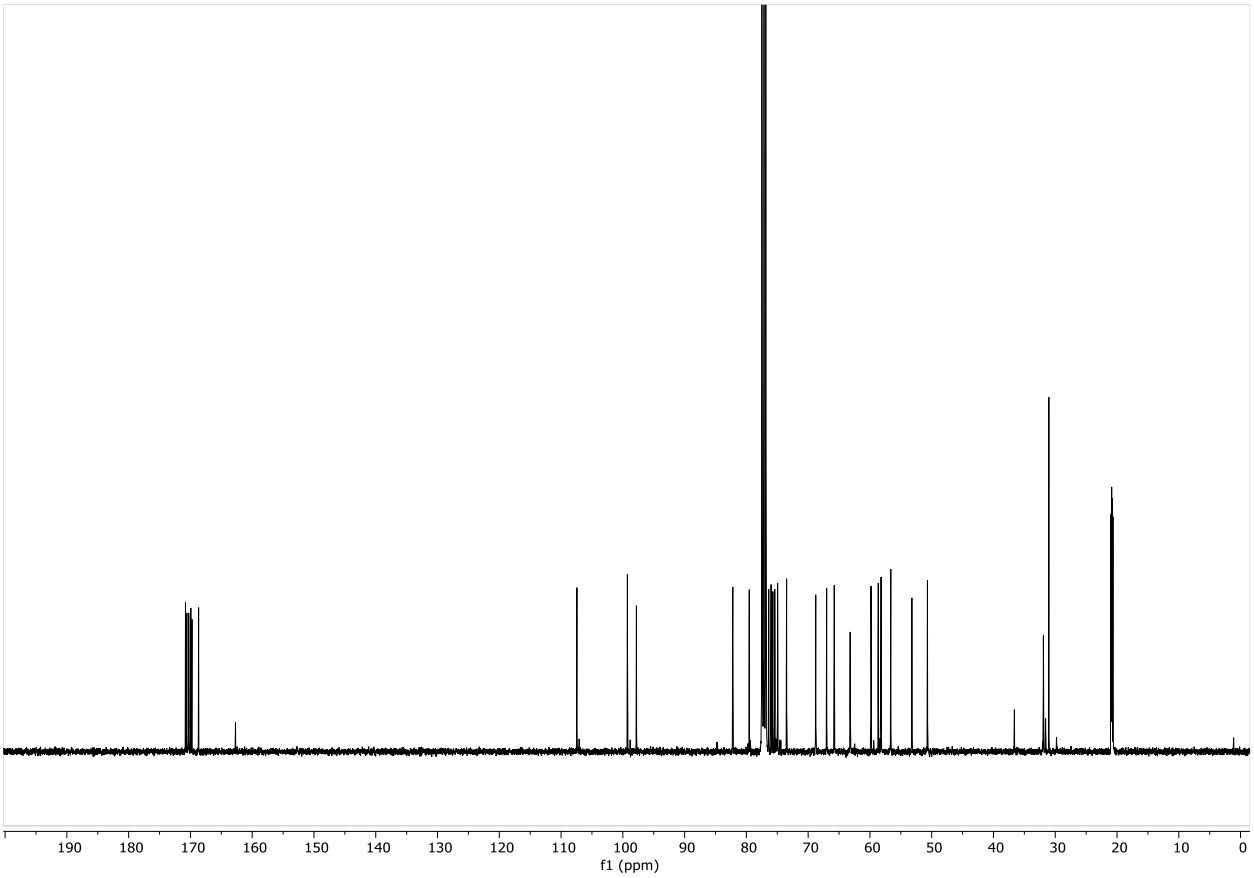
190
180
170
160
150
140
130
120
110
100
90
80
70
60
50
40
30
20
10
0
f1 (ppm)

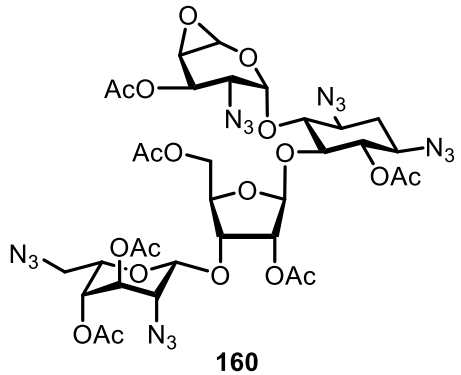
O
AcO
O
N3
N3
O
N3
AcO
O
OAc
O
N3
OAc
O
O
OAc
OAc
N3

160

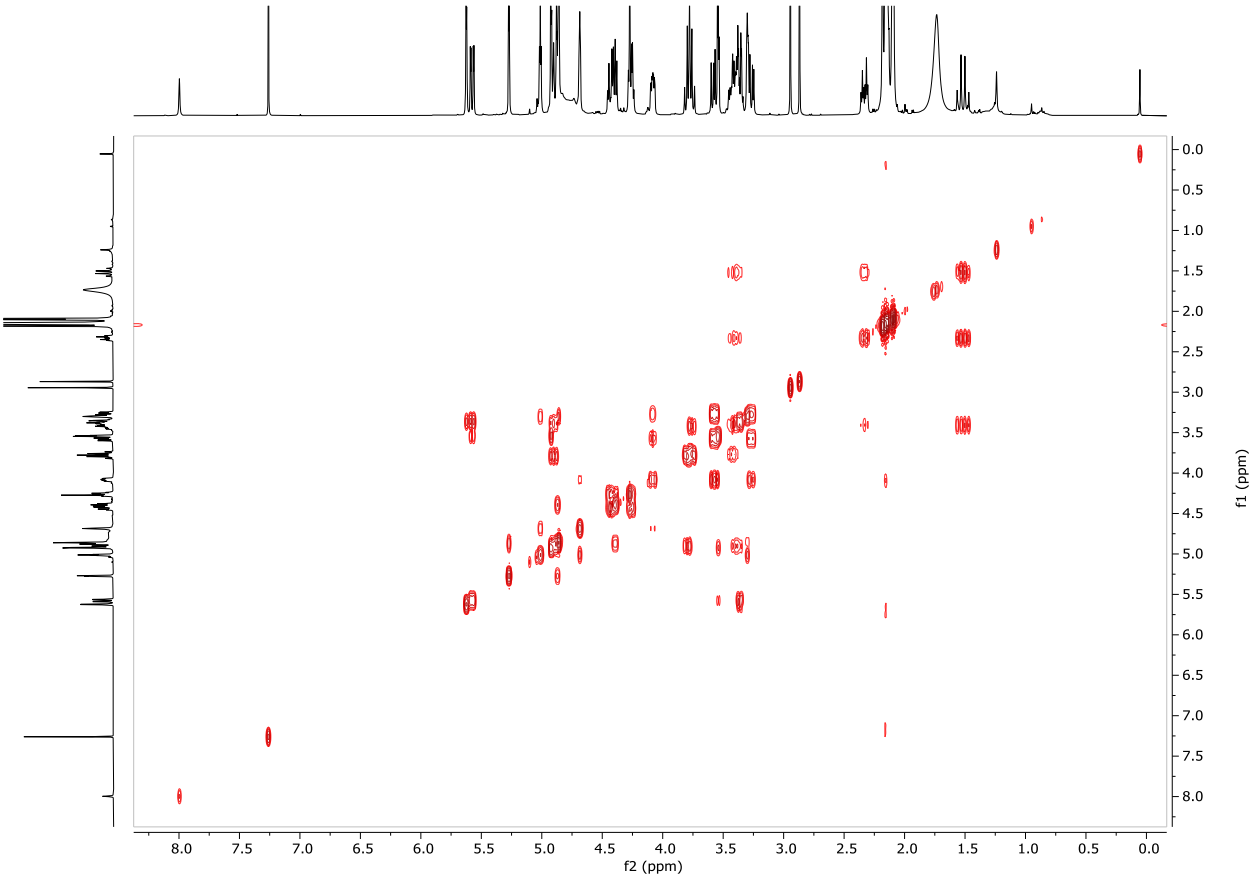
8.0
7.5
7.0
6.5
6.0
5.5
5.0
4.5
4.0
3.5
3.0
2.5
2.0
1.5
1.0
0.5
0.0
f2 (ppm)
f1 (ppm)

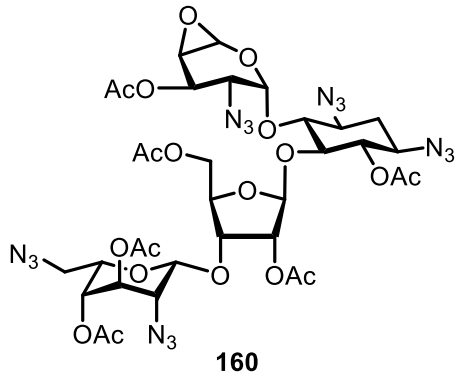
O
AcO
O
N3
N3
O
N3
AcO
O
N3
OAc
O
OAc
N3
O
O
OAc
OAc
N3

160

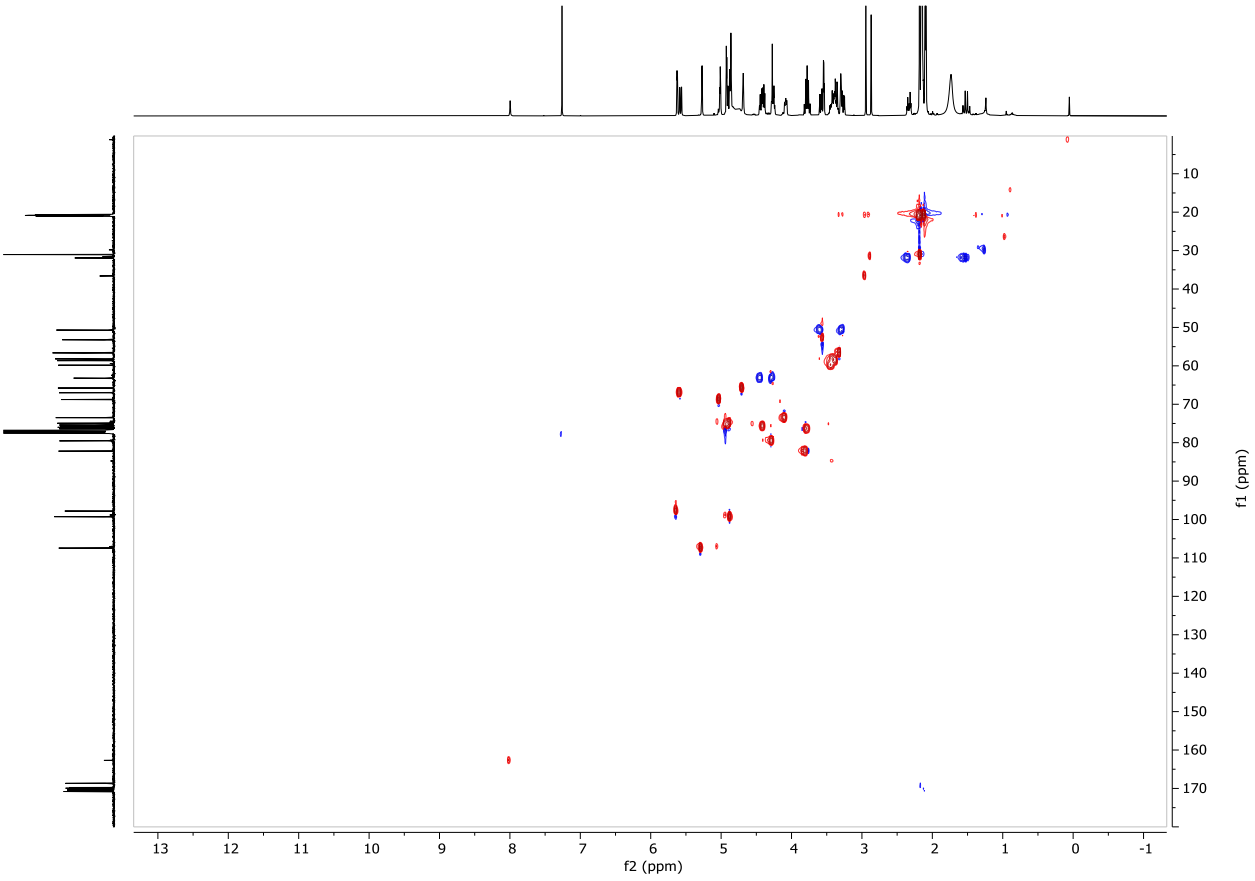
10
20
30
40
50
60
70
80
90
100
110
120
130
140
150
160
170
f1 (ppm)
13
12
11
10
9
8
7
6
5
4
3
2
1
0
-1
f2 (ppm)

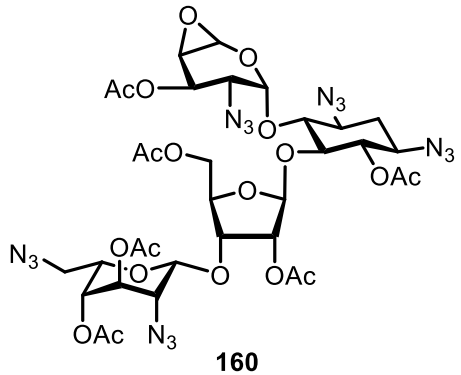
O
AcO
O
N3
N3
O
N3
AcO
O
N3
OAc
O
OAc
N3
OAc
O
O
OAc
OAc
N3

160

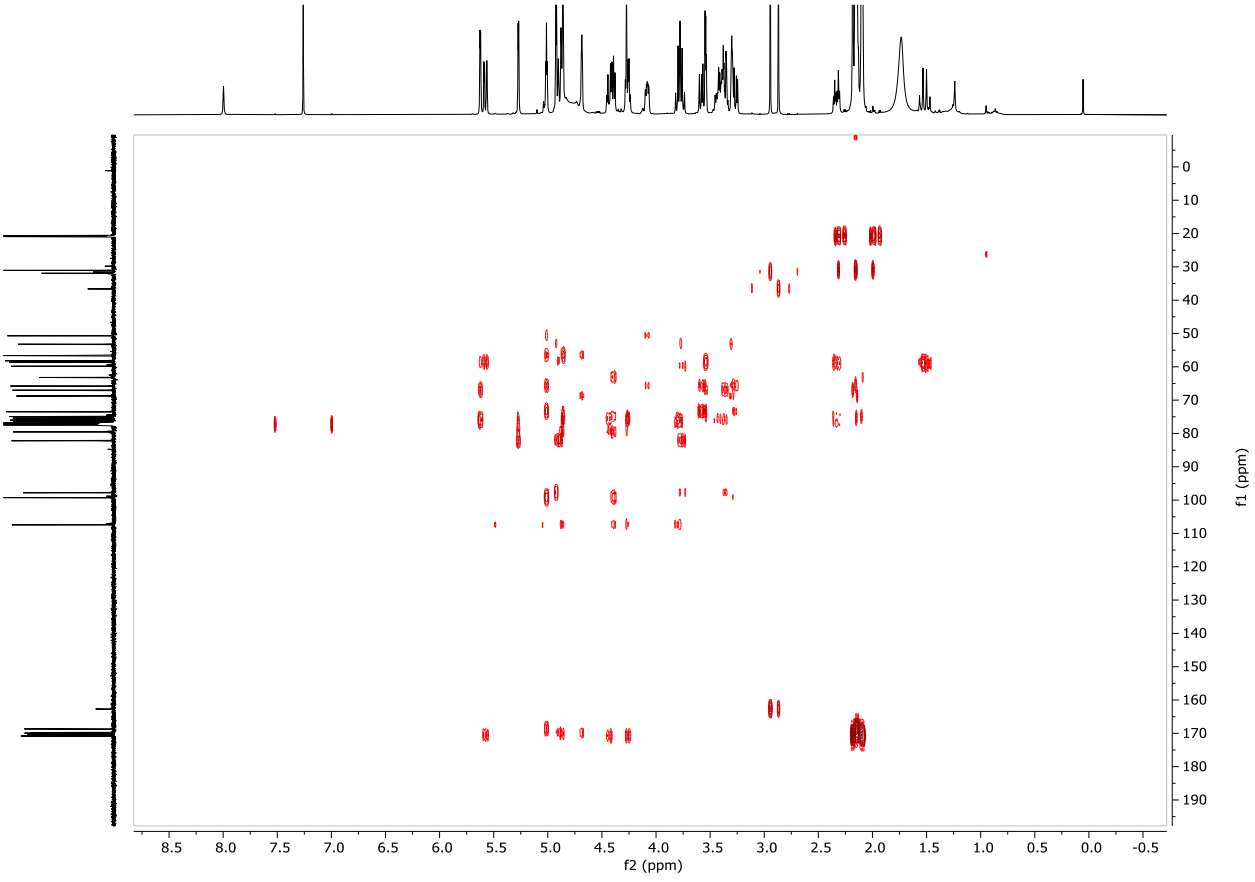
0
10
20
30
40
50
60
70
80
90
100
110
120
130
140
150
160
170
180
190
f1 (ppm)
8.5
8.0
7.5
7.0
6.5
6.0
5.5
5.0
4.5
4.0
3.5
3.0
2.5
2.0
1.5
1.0
0.5
0.0
-0.5
f2 (ppm)

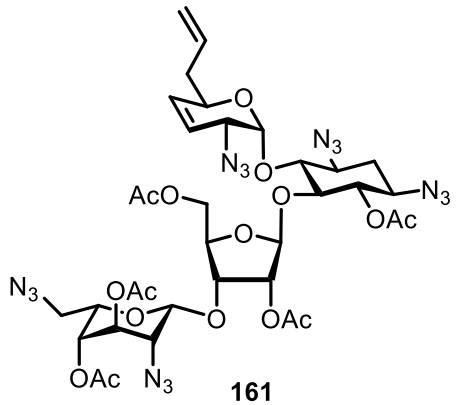
O
N3
N3
O
N3
AcO
O
OAc
O
N3
OAc
O
O
OAc
OAc
N3

161

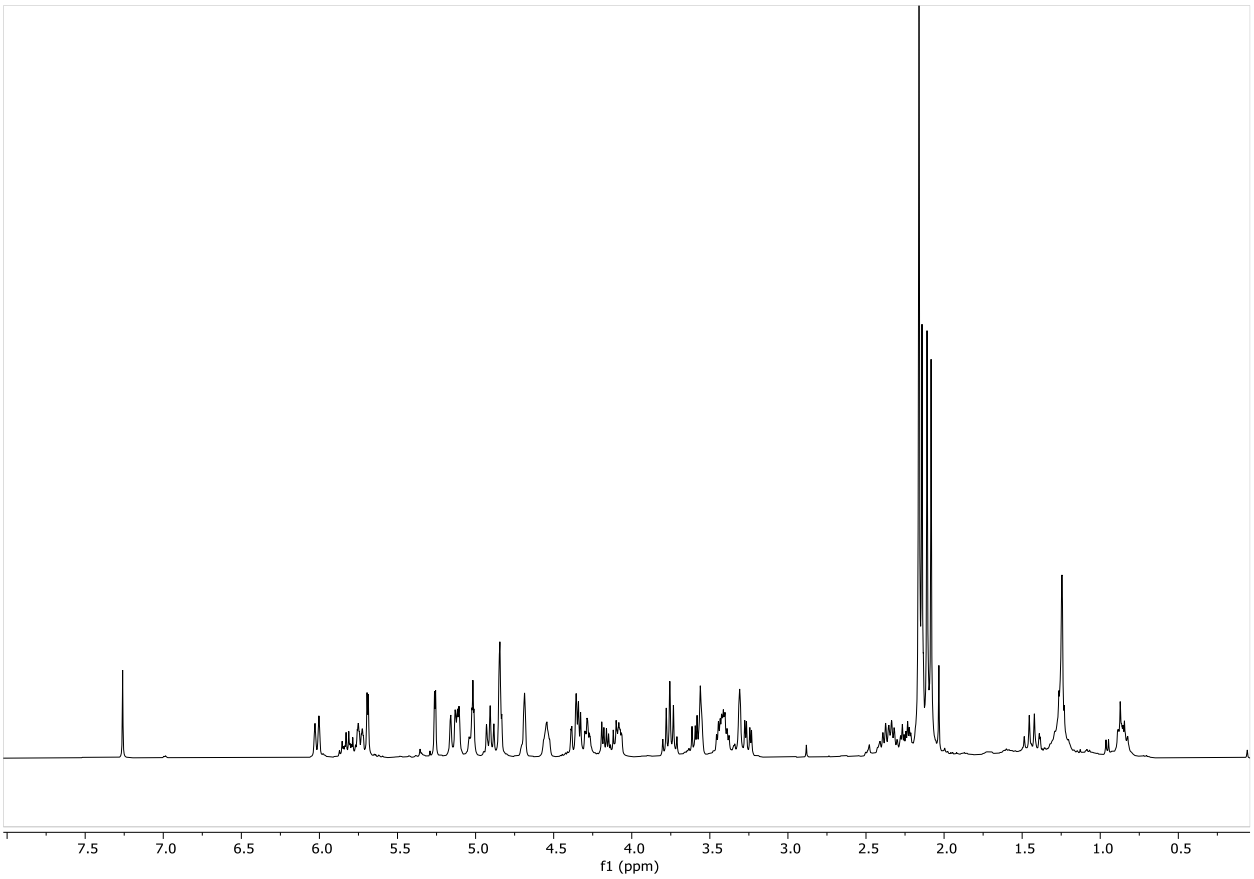
7.5
7.0
6.5
6.0
5.5
5.0
4.5
4.0
3.5
3.0
2.5
2.0
1.5
1.0
0.5
f1 (ppm)

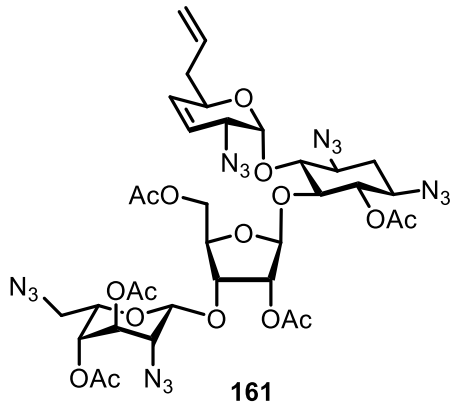
O
N3
N3
O
N3
AcO
O
OAc
O
N3
OAc
O
O
OAc
OAc
N3

161

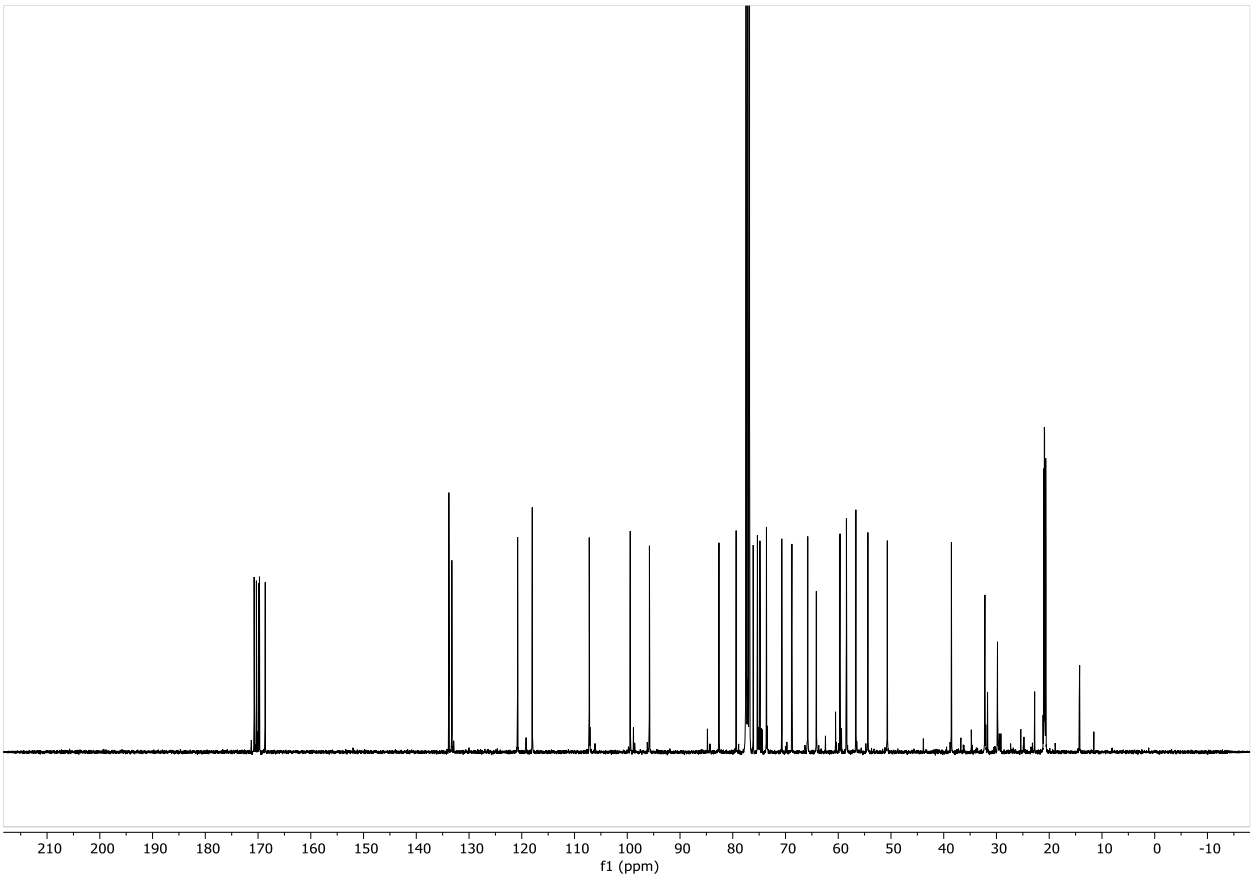
210
200
190
180
170
160
150
140
130
120
110
100
90
80
70
60
50
40
30
20
10
0
-10
f1 (ppm)

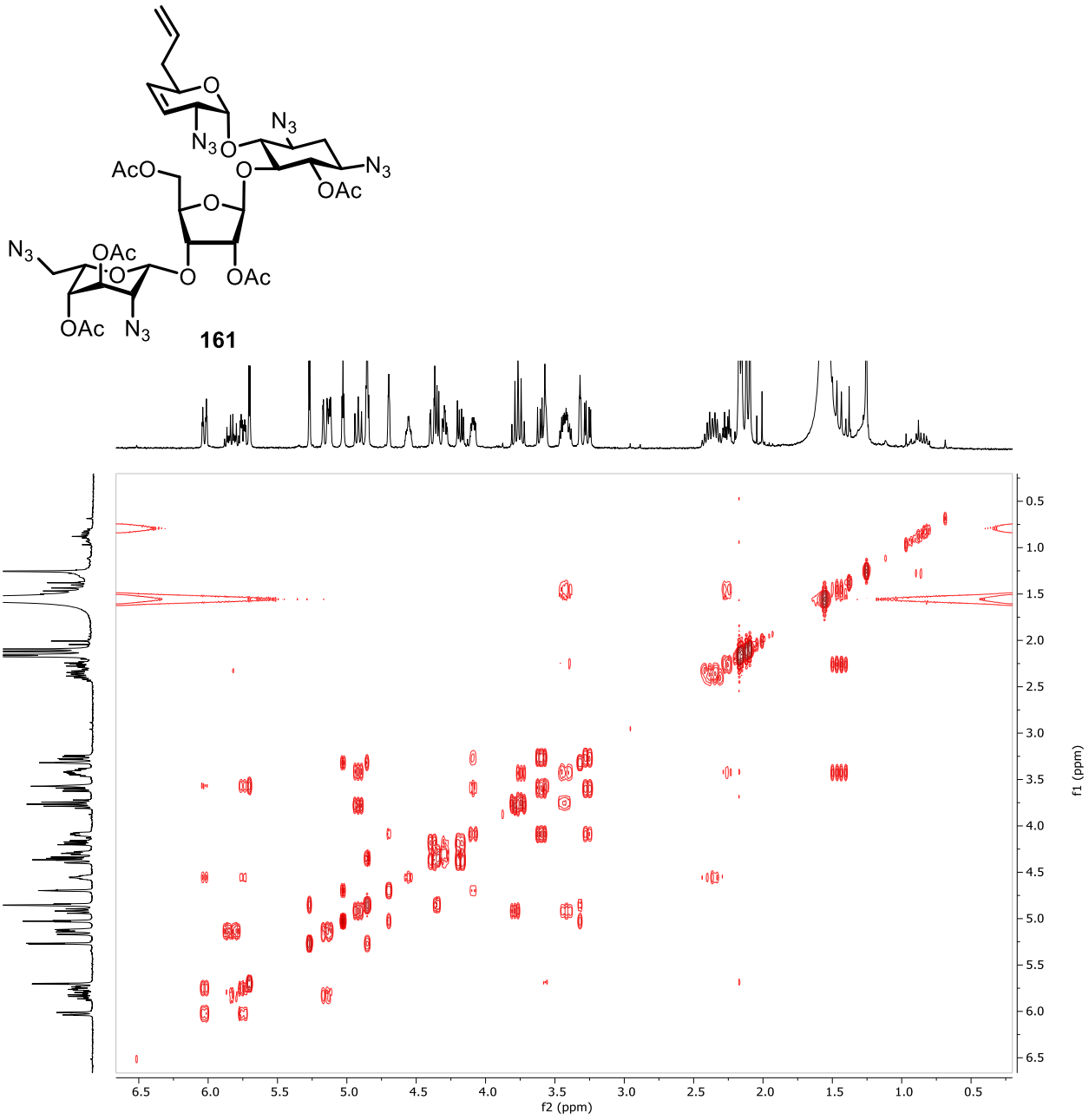
N3
N3
O
N3
AcO
O
N3
OAc
O
N3
OAc
O
O
OAc
OAc
N3
161
f2 (ppm)
f1 (ppm)

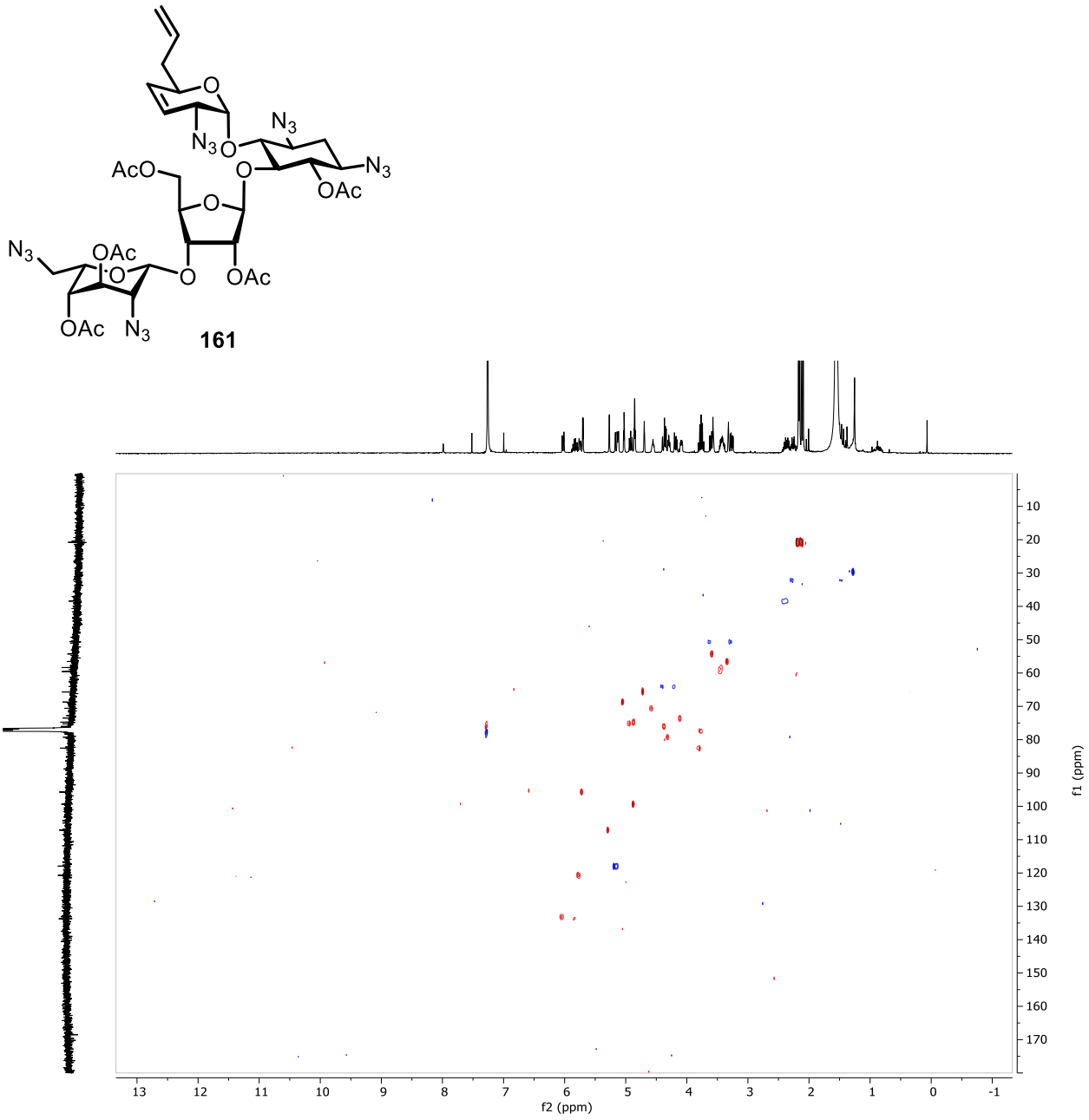
AcO
N3
OAc
OAc
N3
OAc
N3
OAc
N3
161
f2 (ppm)
f1 (ppm)

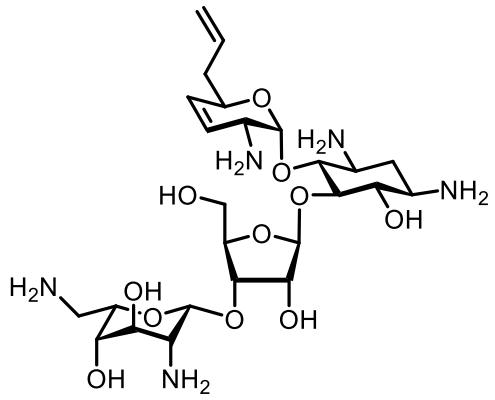

162

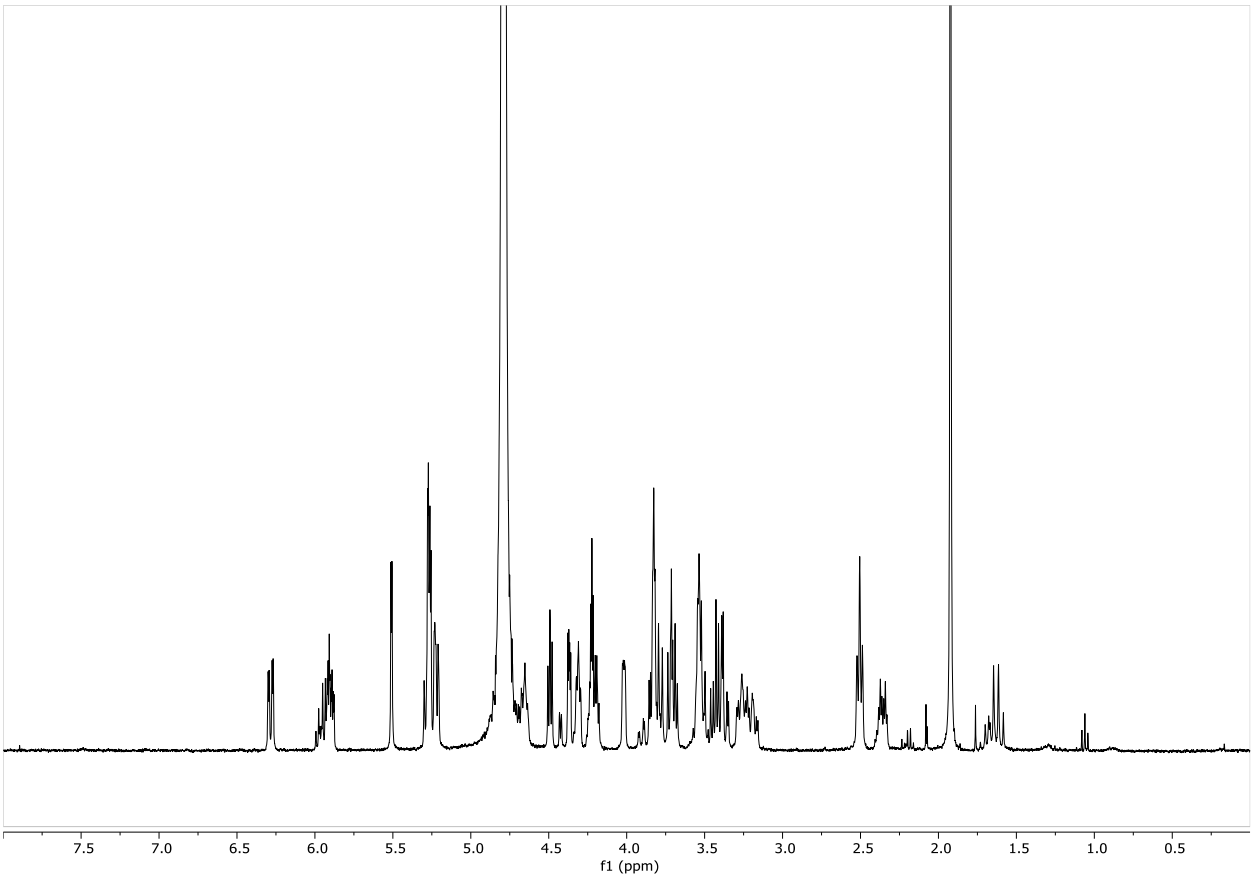

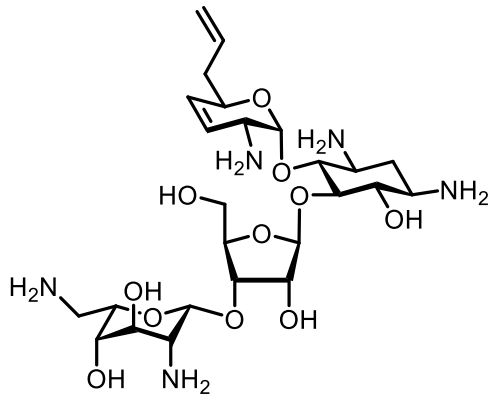
O
H2N
H2N
O
NH2
HO
O
OH
O
H2N
OH
O
O
OH
OH
NH2

162

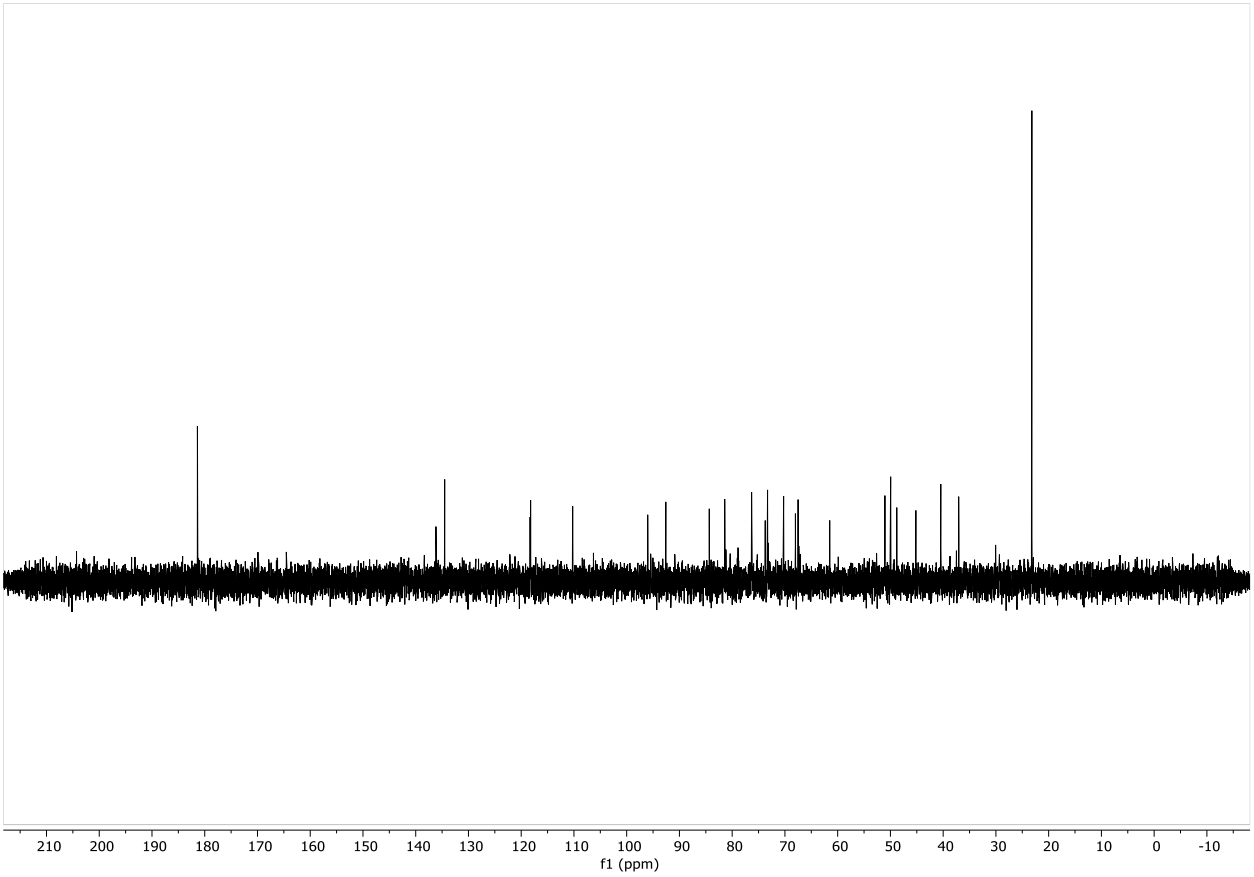
210
200
190
180
170
160
150
140
130
120
110
100
90
80
70
60
50
40
30
20
10
0
-10
f1 (ppm)

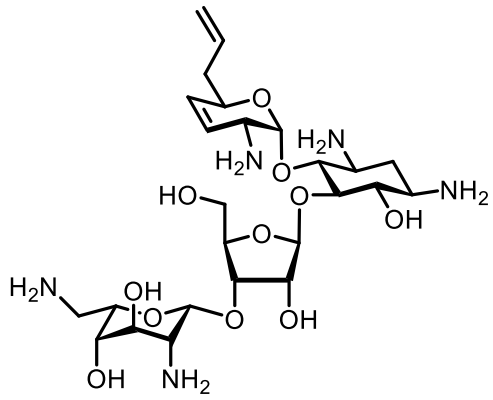
O
H2N
H2N
O
HO
O
NH2
OH
O
H2N
OH
O
O
OH
OH
NH2

162

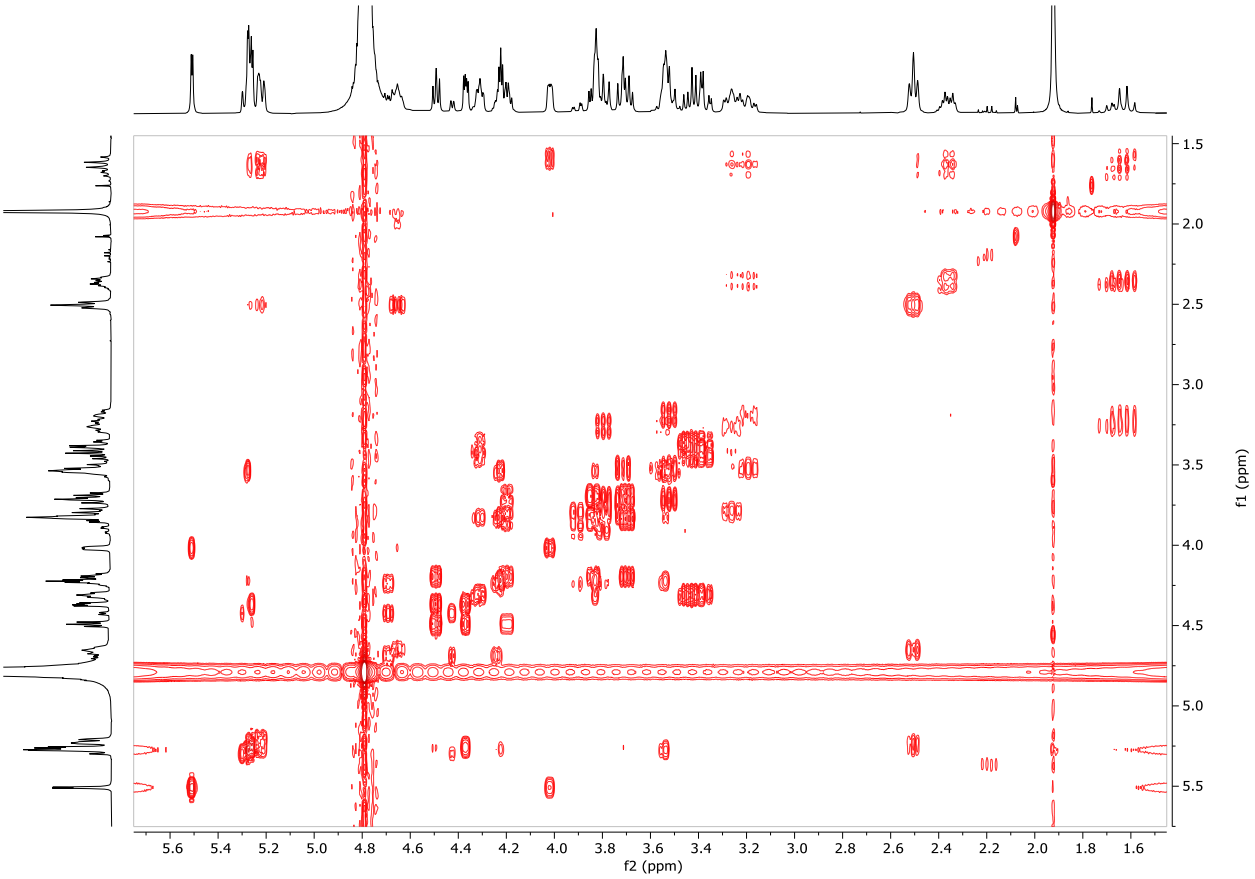
1.5
2.0
2.5
3.0
3.5
4.0
4.5
5.0
5.5
f1 (ppm)
5.6
5.4
5.2
5.0
4.8
4.6
4.4
4.2
4.0
3.8
3.6
3.4
3.2
3.0
2.8
2.6
2.4
2.2
2.0
1.8
1.6
f2 (ppm)

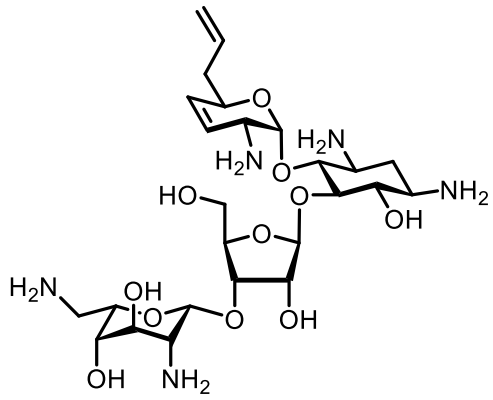
O
H2N
H2N
O
HO
O
NH2
OH
O
H2N
OH
O
O
OH
OH
NH2

162

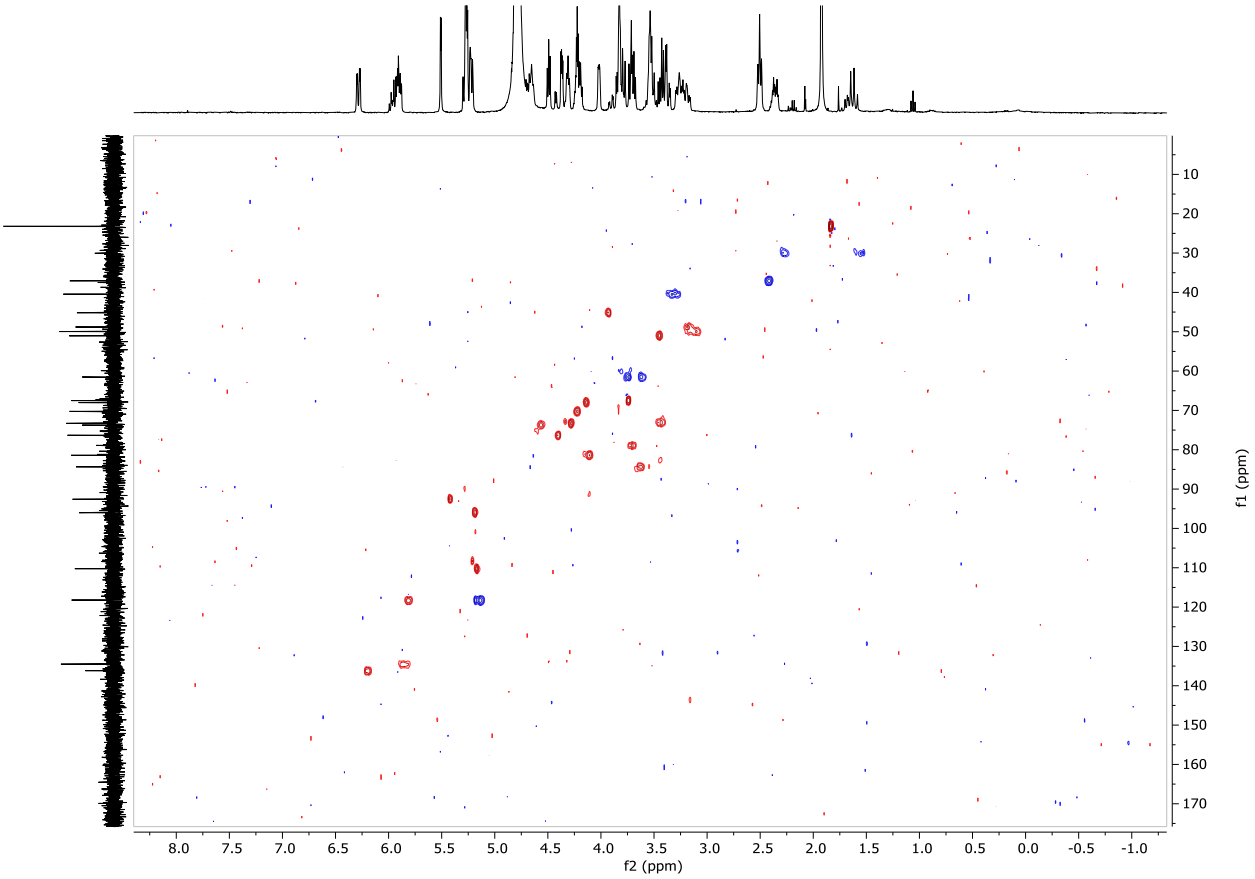
8.0
7.5
7.0
6.5
6.0
5.5
5.0
4.5
4.0
3.5
3.0
2.5
2.0
1.5
1.0
0.5
0.0
-0.5
-1.0
f2 (ppm)
10
20
30
40
50
60
70
80
90
100
110
120
130
140
150
160
170
f1 (ppm)

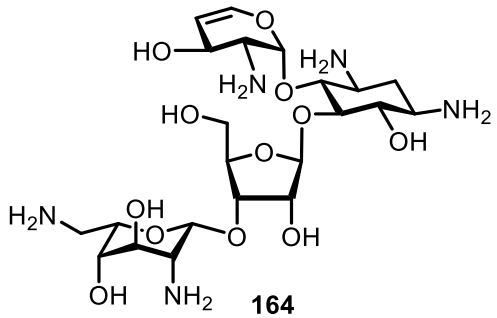

164

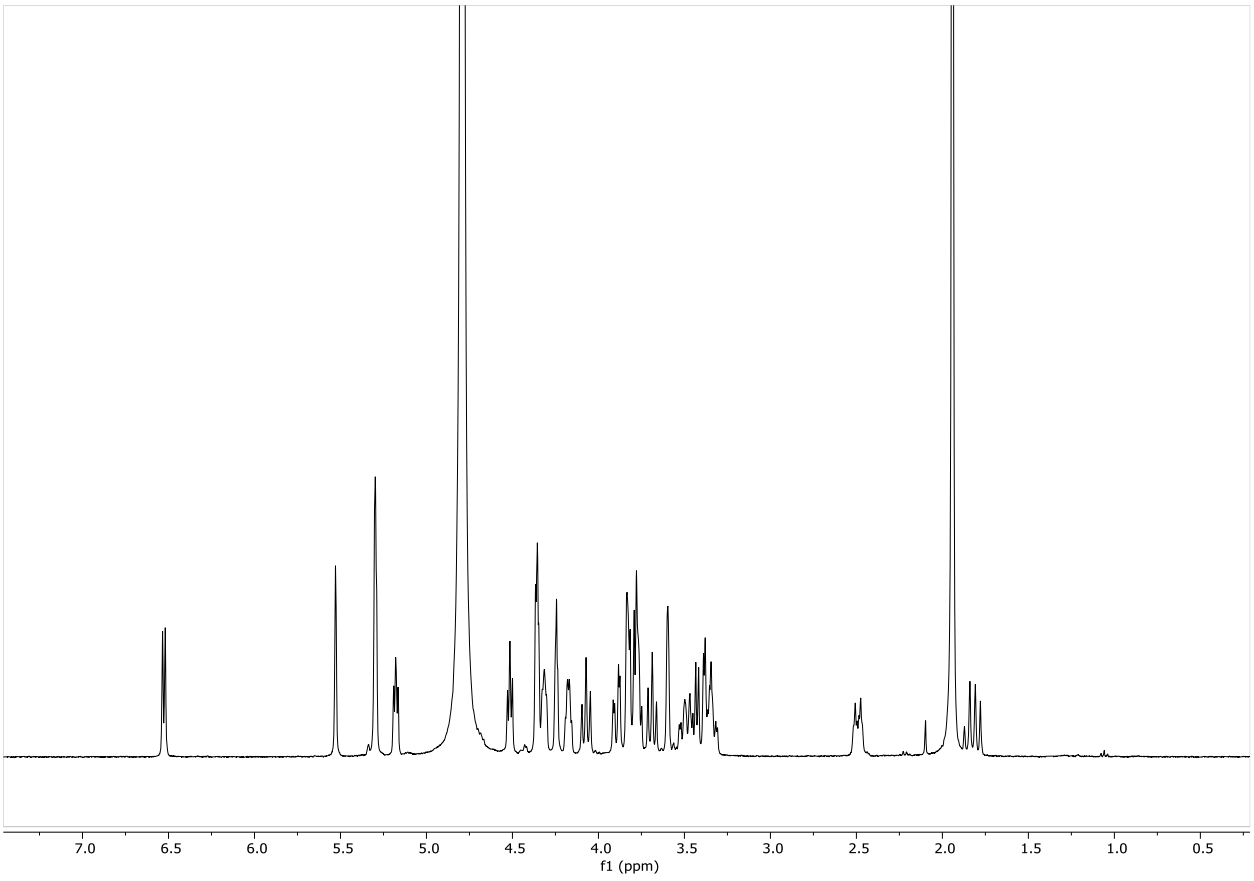

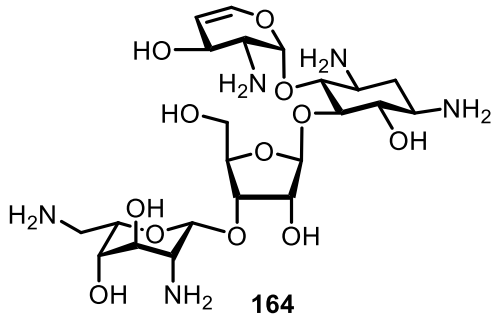
HO
O
H2N
H2N
O
NH2
HO
O
OH
O
H2N
OH
O
O
OH
OH
NH2

164

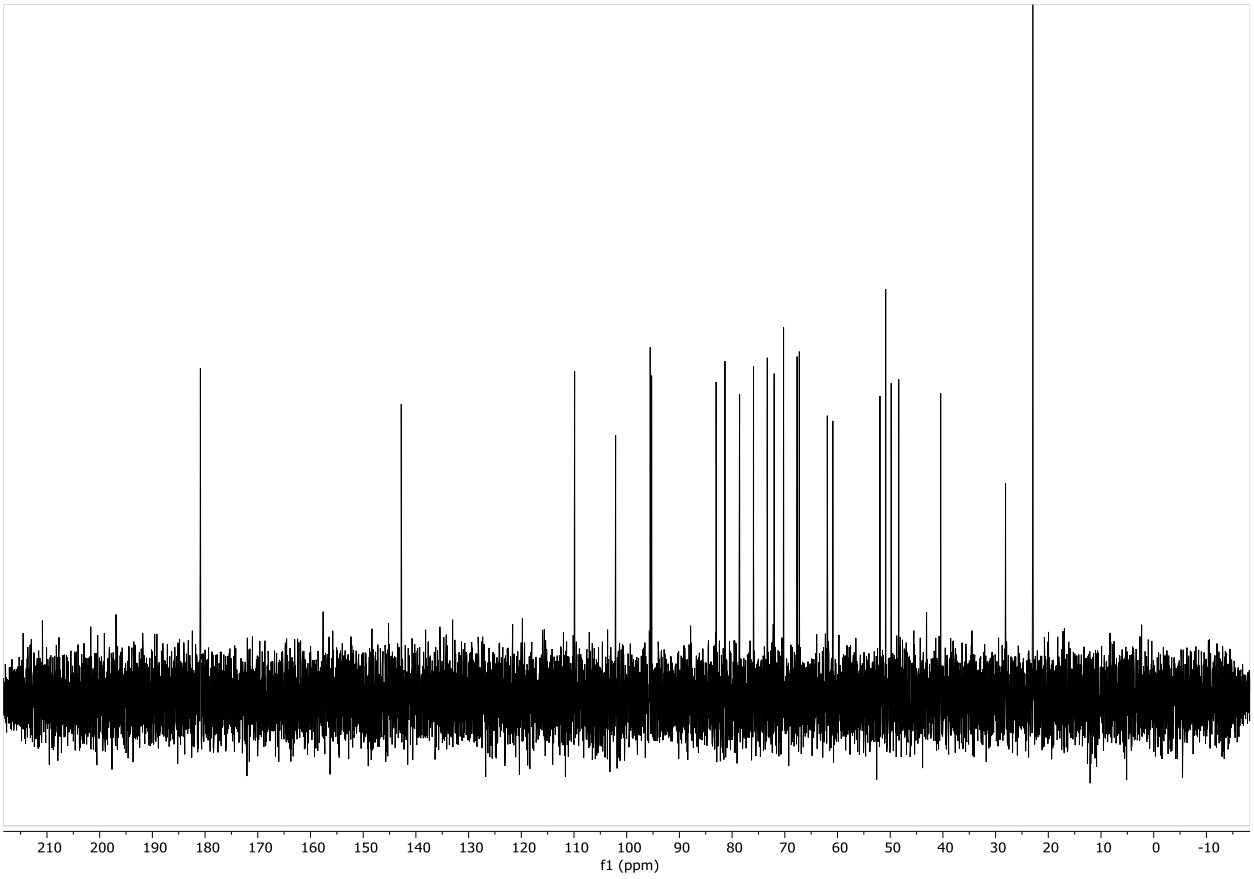
210
200
190
180
170
160
150
140
130
120
110
100
90
80
70
60
50
40
30
20
10
0
-10
f1 (ppm)

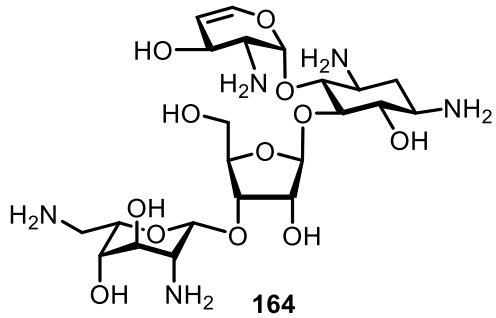
HO
O
H2N
H2N
O
NH2
HO
O
OH
O
H2N
OH
O
O
OH
OH
NH2

164

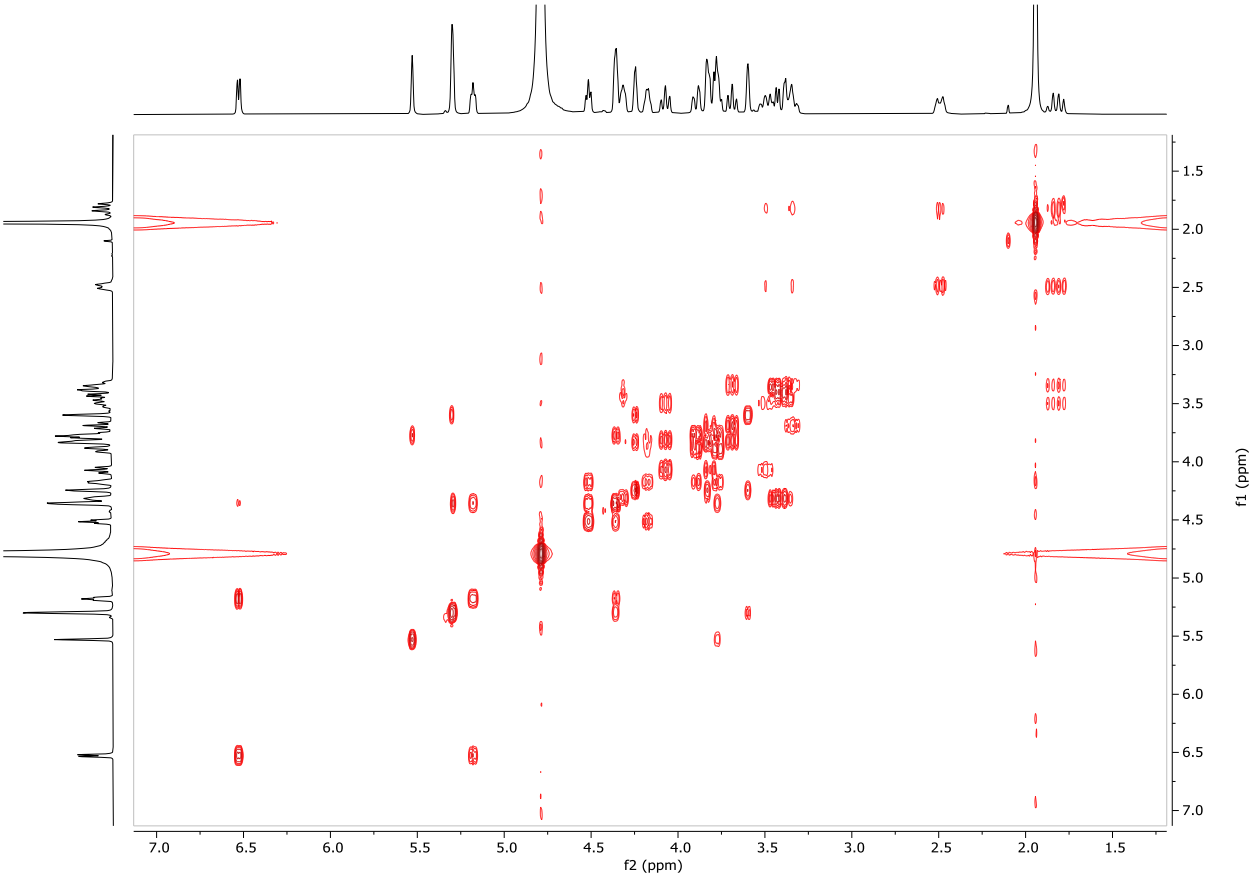
1.5
2.0
2.5
3.0
3.5
4.0
4.5
5.0
5.5
6.0
6.5
7.0
f1 (ppm)
7.0
6.5
6.0
5.5
5.0
4.5
4.0
3.5
3.0
2.5
2.0
1.5
f2 (ppm)

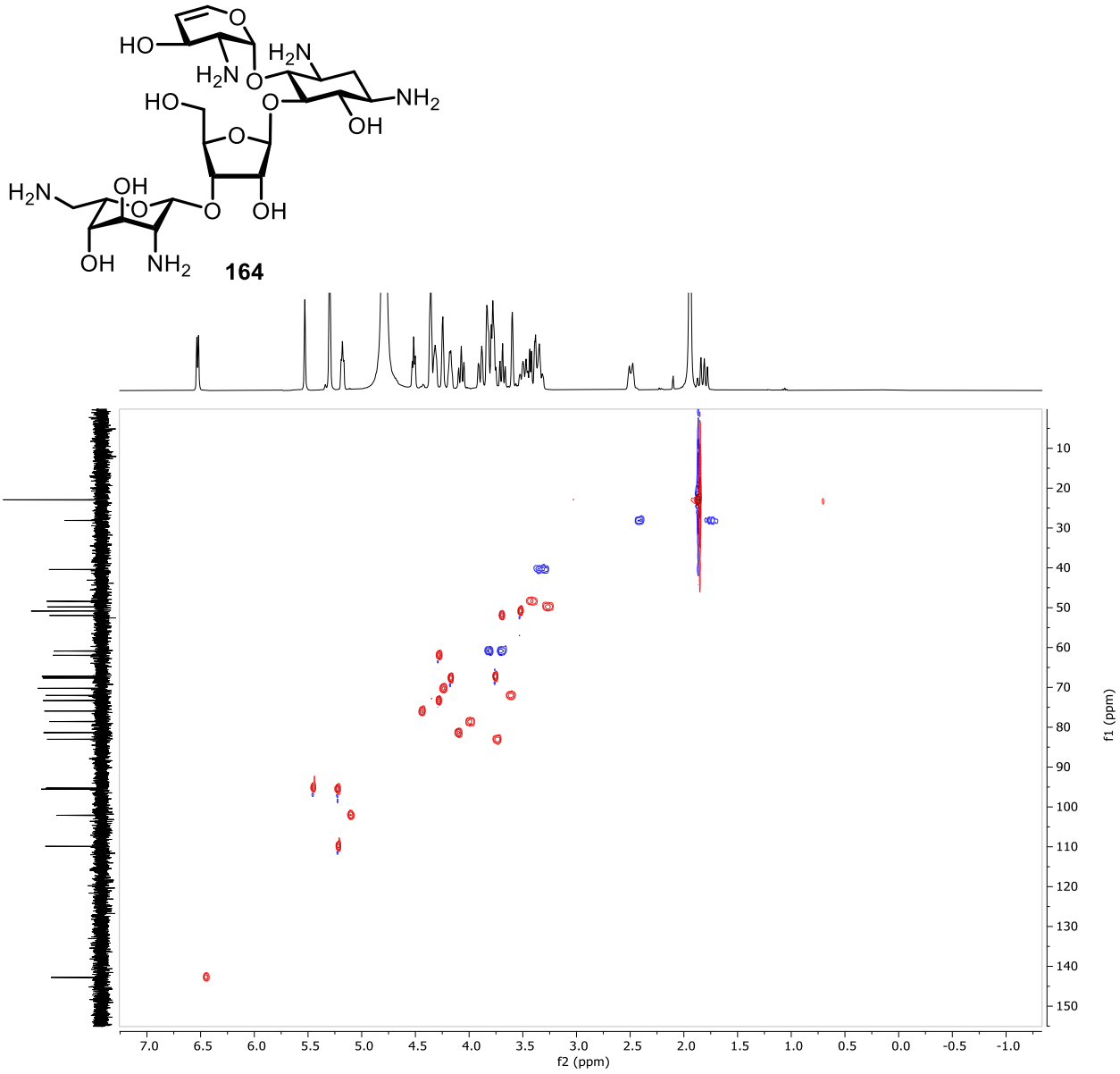
HO
O
H2N
H2N
O
NH2
HO
O
OH
O
H2N
OH
O
O
OH
OH
NH2
164
f2 (ppm)
f1 (ppm)

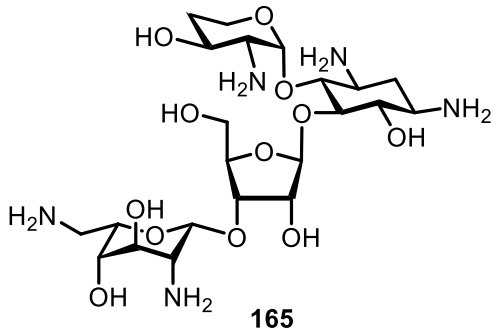
HO
O
H2N
H2N
O
NH2
HO
O
OH
O
H2N
OH
O
O
OH
OH
NH2

165

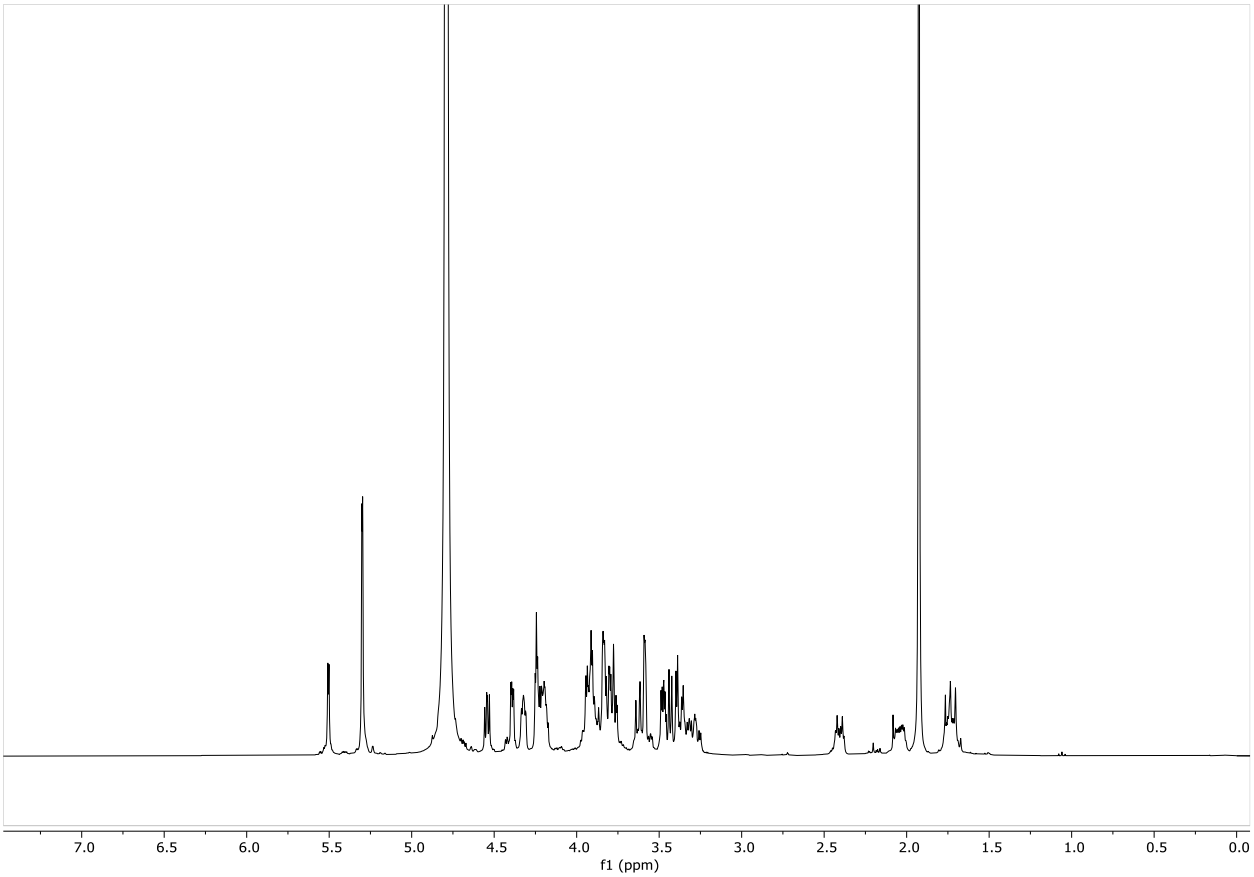
7.0
6.5
6.0
5.5
5.0
4.5
4.0
3.5
3.0
2.5
2.0
1.5
1.0
0.5
0.0
f1 (ppm)

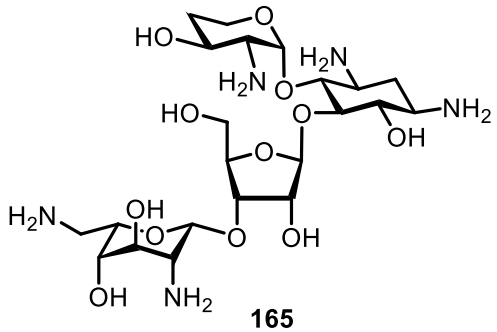
HO
O
H2N
H2N
O
NH2
HO
O
OH
O
H2N
OH
O
O
OH
OH
NH2

165

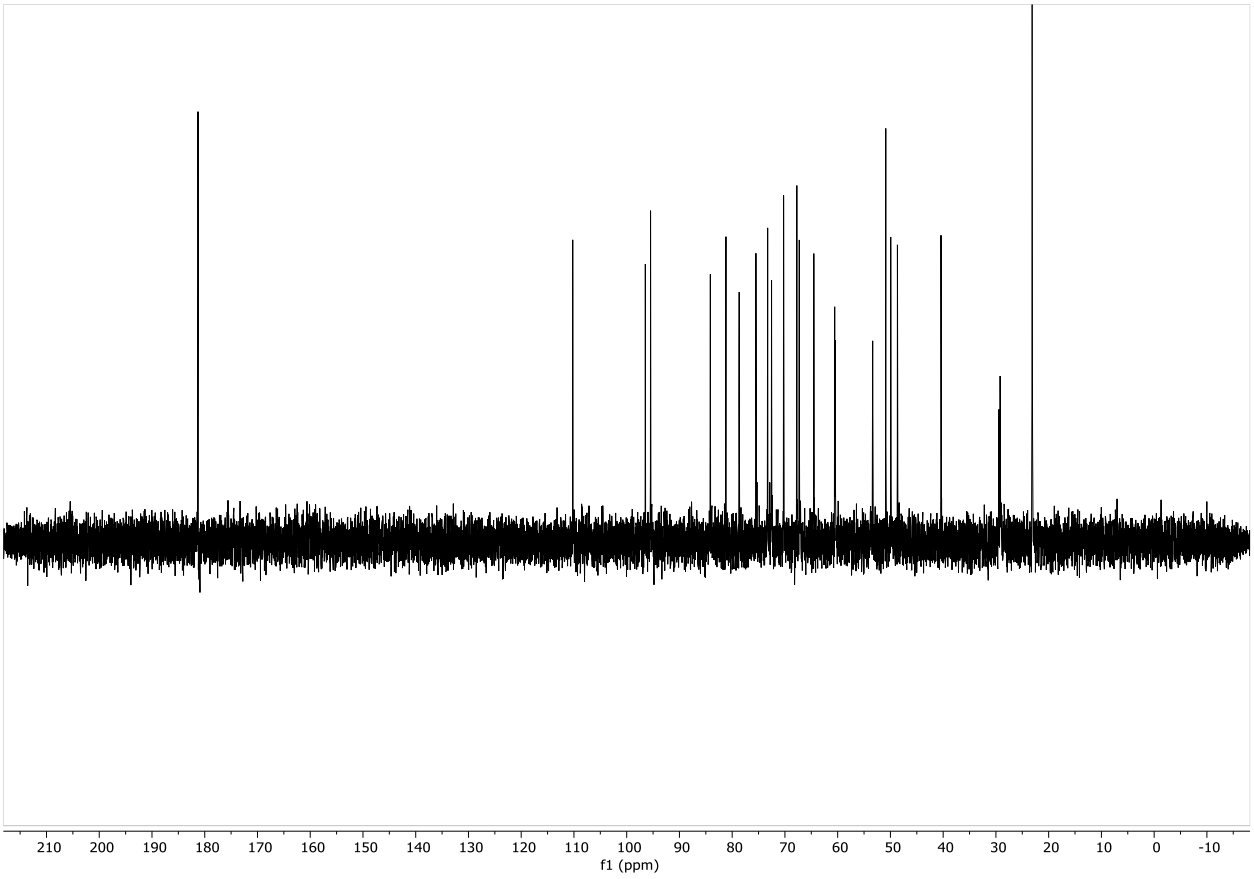
210
200
190
180
170
160
150
140
130
120
110
100
90
80
70
60
50
40
30
20
10
0
-10
f1 (ppm)

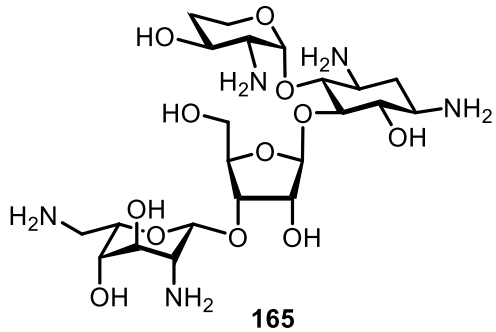
HO
O
H2N
H2N
O
NH2
HO
O
OH
O
H2N
OH
O
O
OH
OH
NH2

165

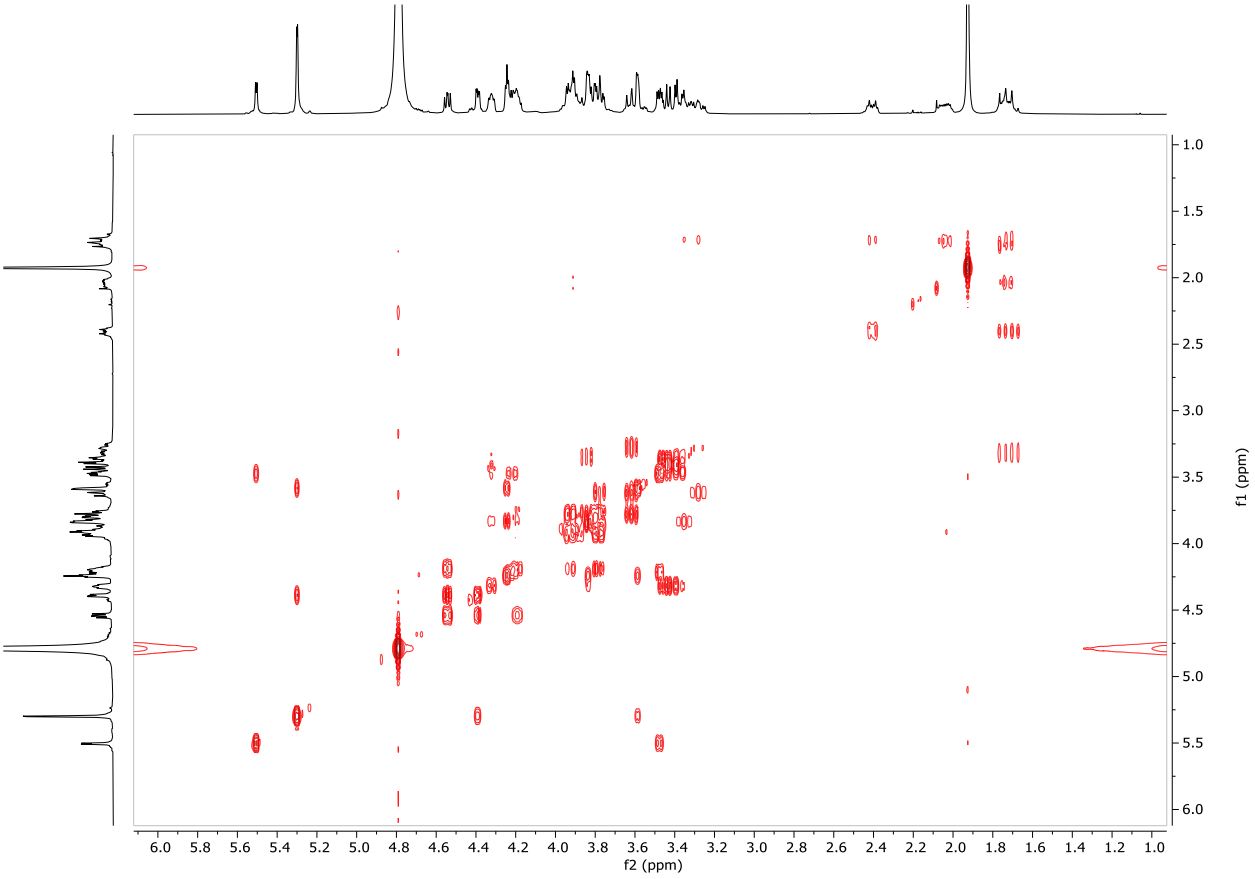
1.0
1.5
2.0
2.5
3.0
3.5
4.0
4.5
5.0
5.5
6.0
f1 (ppm)
6.0 5.8 5.6 5.4 5.2 5.0 4.8 4.6 4.4 4.2 4.0 3.8 3.6 3.4 3.2 3.0 2.8 2.6 2.4 2.2 2.0 1.8 1.6 1.4 1.2 1.0
f2 (ppm)

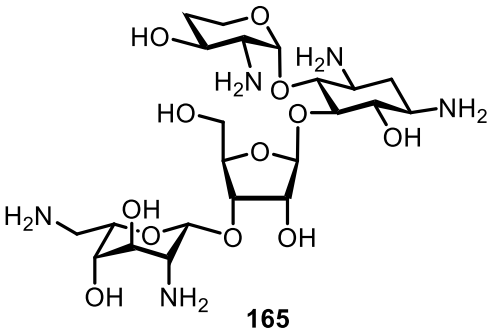
HO
O
H2N
H2N
O
NH2
HO
O
OH
O
H2N
OH
O
O
OH
OH
NH2

165

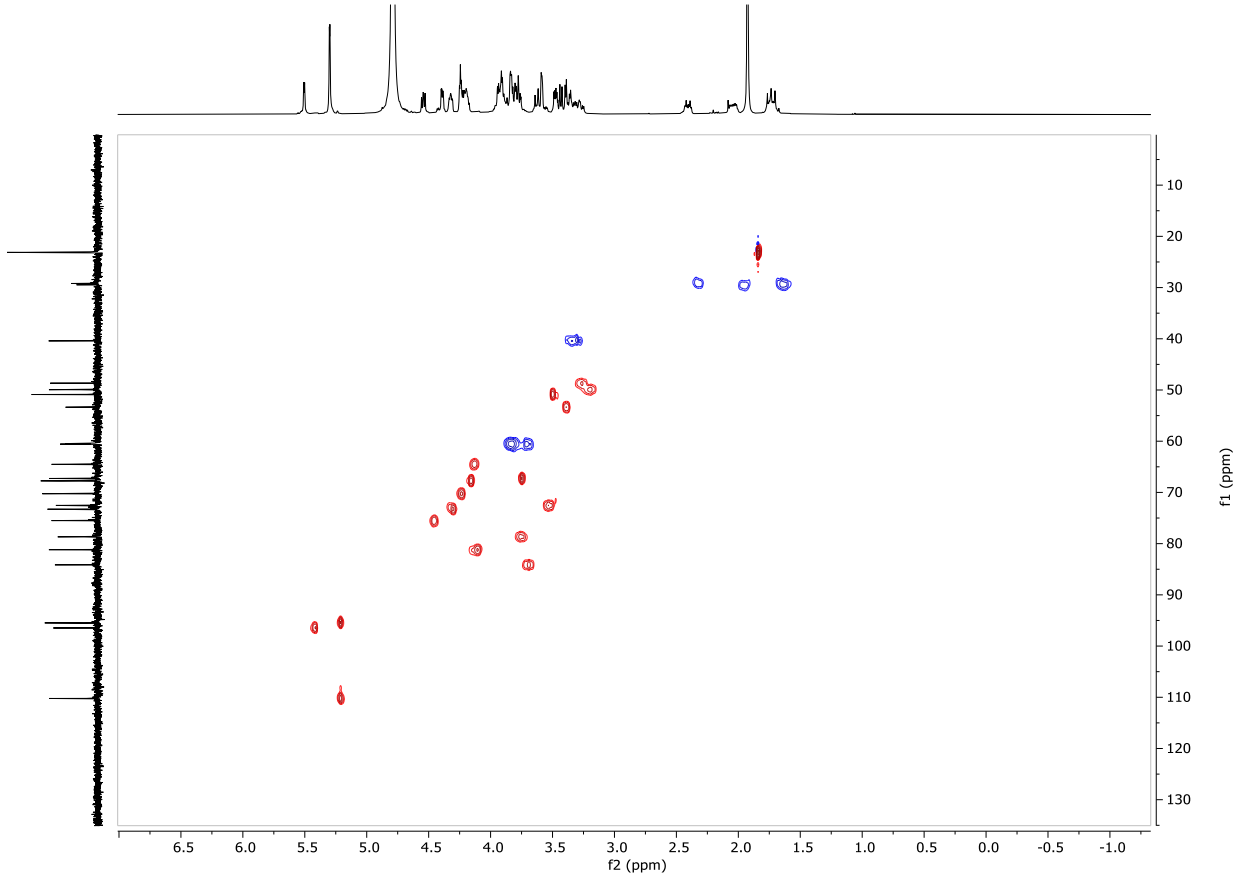
10
20
30
40
50
60
70
80
90
100
110
120
130
f1 (ppm)
6.5
6.0
5.5
5.0
4.5
4.0
3.5
3.0
2.5
2.0
1.5
1.0
0.5
0.0
-0.5
-1.0
f2 (ppm)

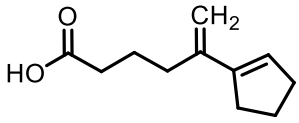

166

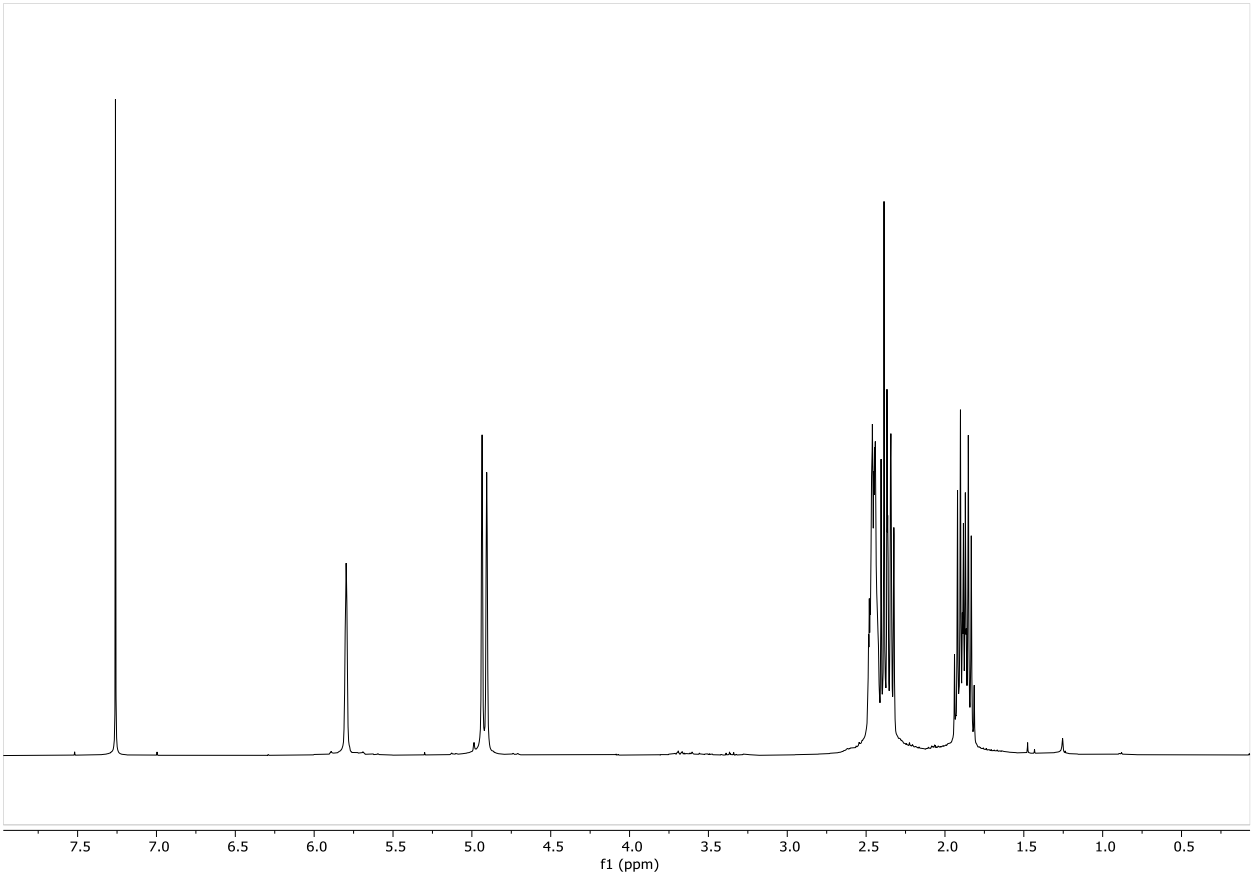

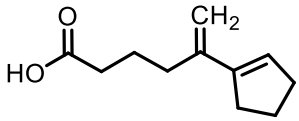
O
CH2
HO

166

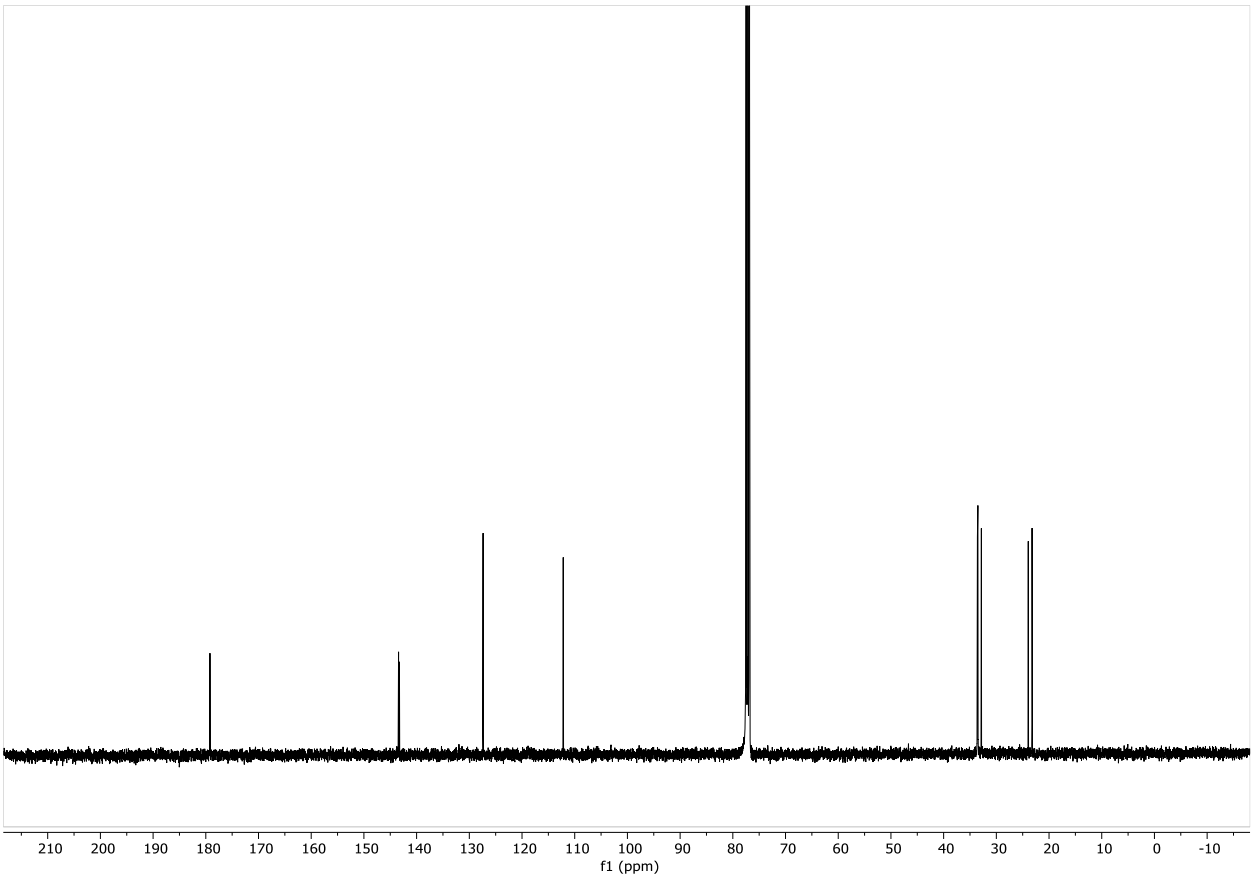
210
200
190
180
170
160
150
140
130
120
110
100
90
80
70
60
50
40
30
20
10
0
-10
f1 (ppm)

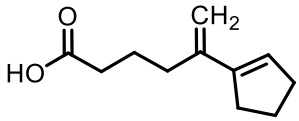
O
CH2
HO

166

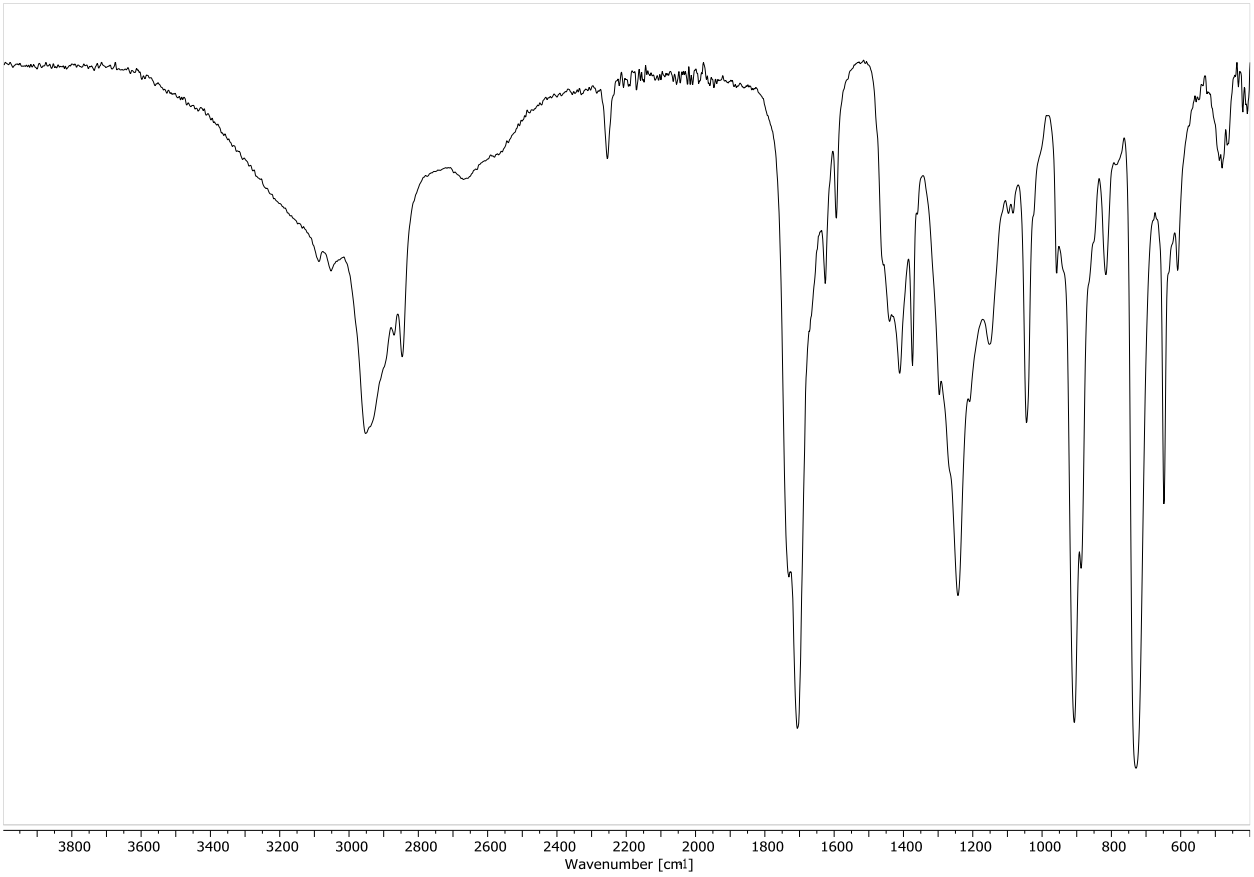
3800
3600
3400
3200
3000
2800
2600
2400
2200
2000
1800
1600
1400
1200
1000
800
600
Wavenumber [cm-1]

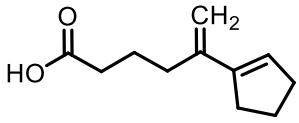

166

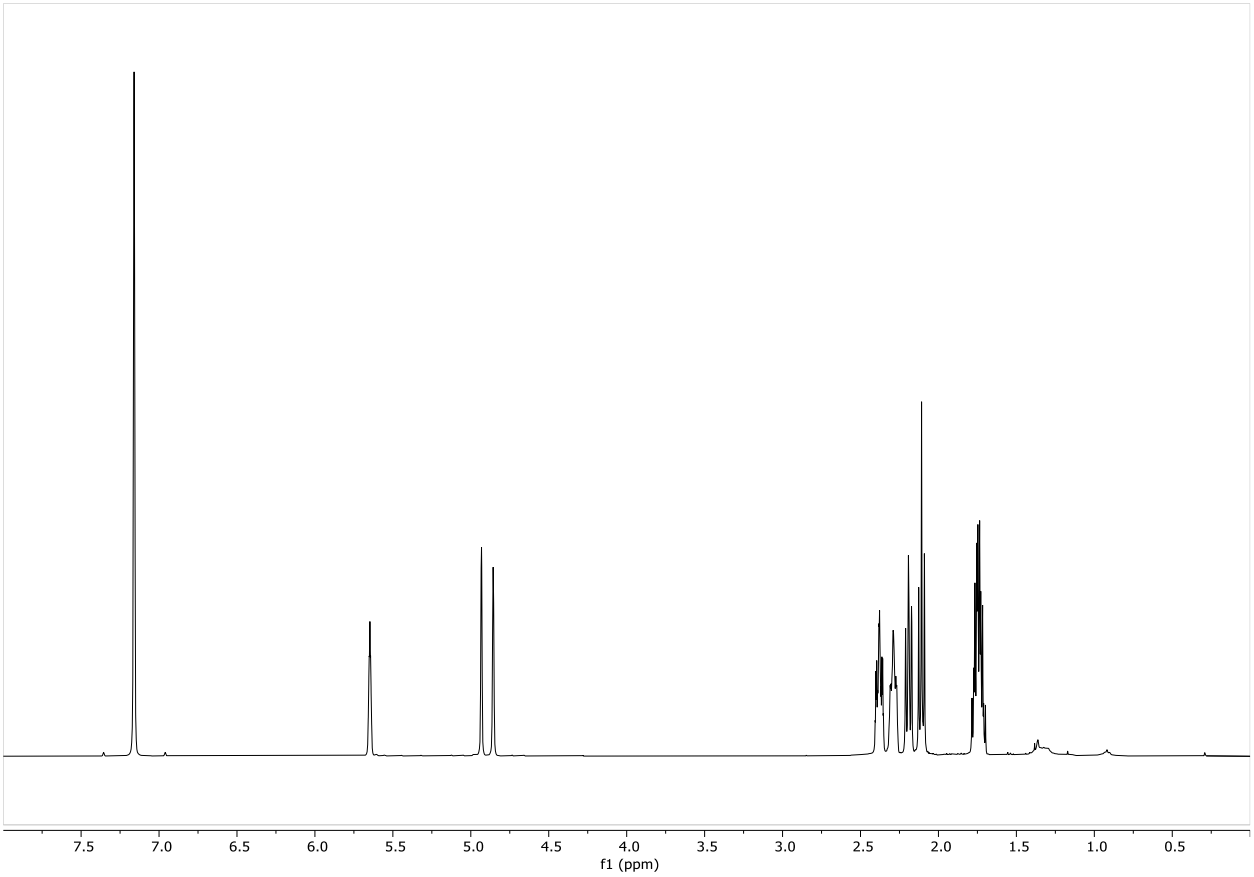

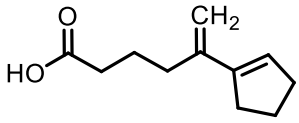
O
CH2
HO

166

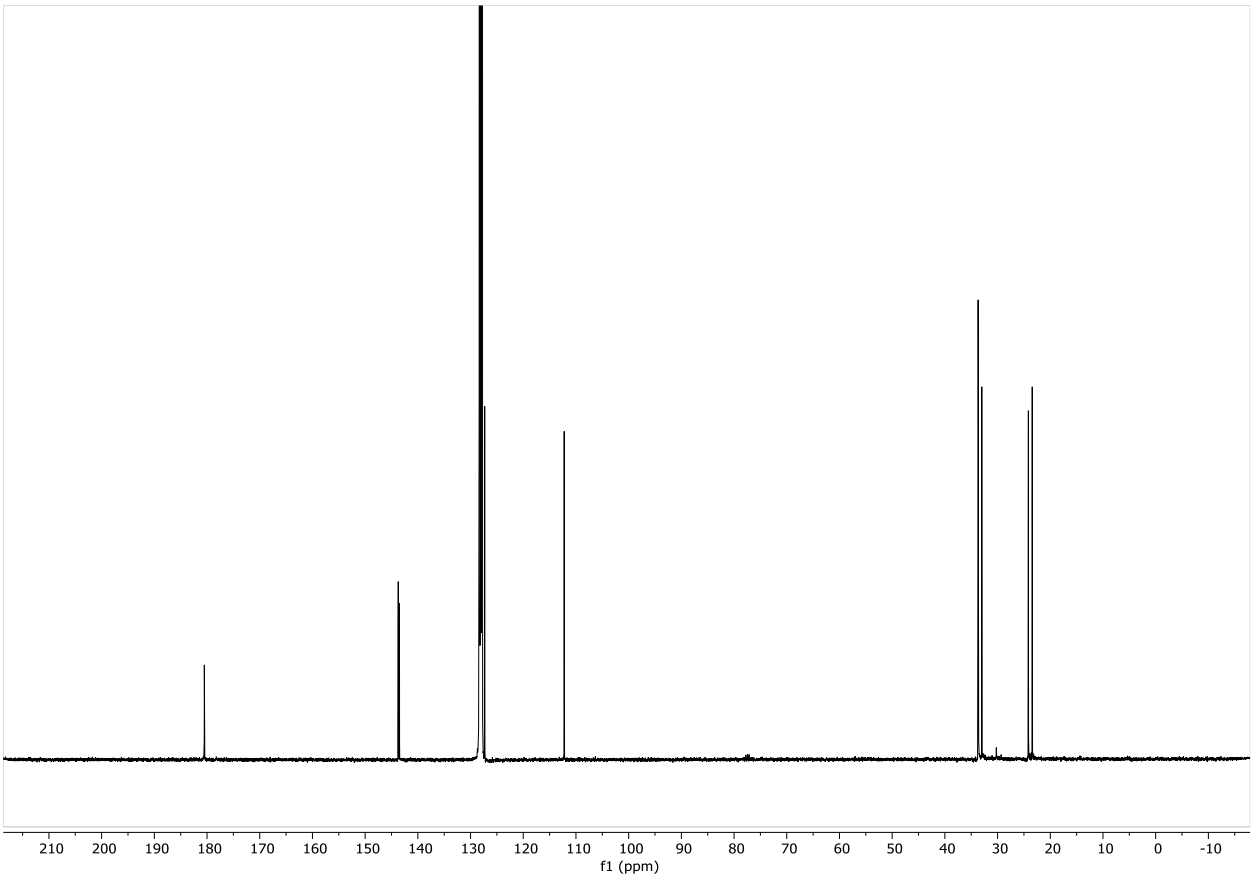
210
200
190
180
170
160
150
140
130
120
110
100
90
80
70
60
50
40
30
20
10
0
-10
f1 (ppm)

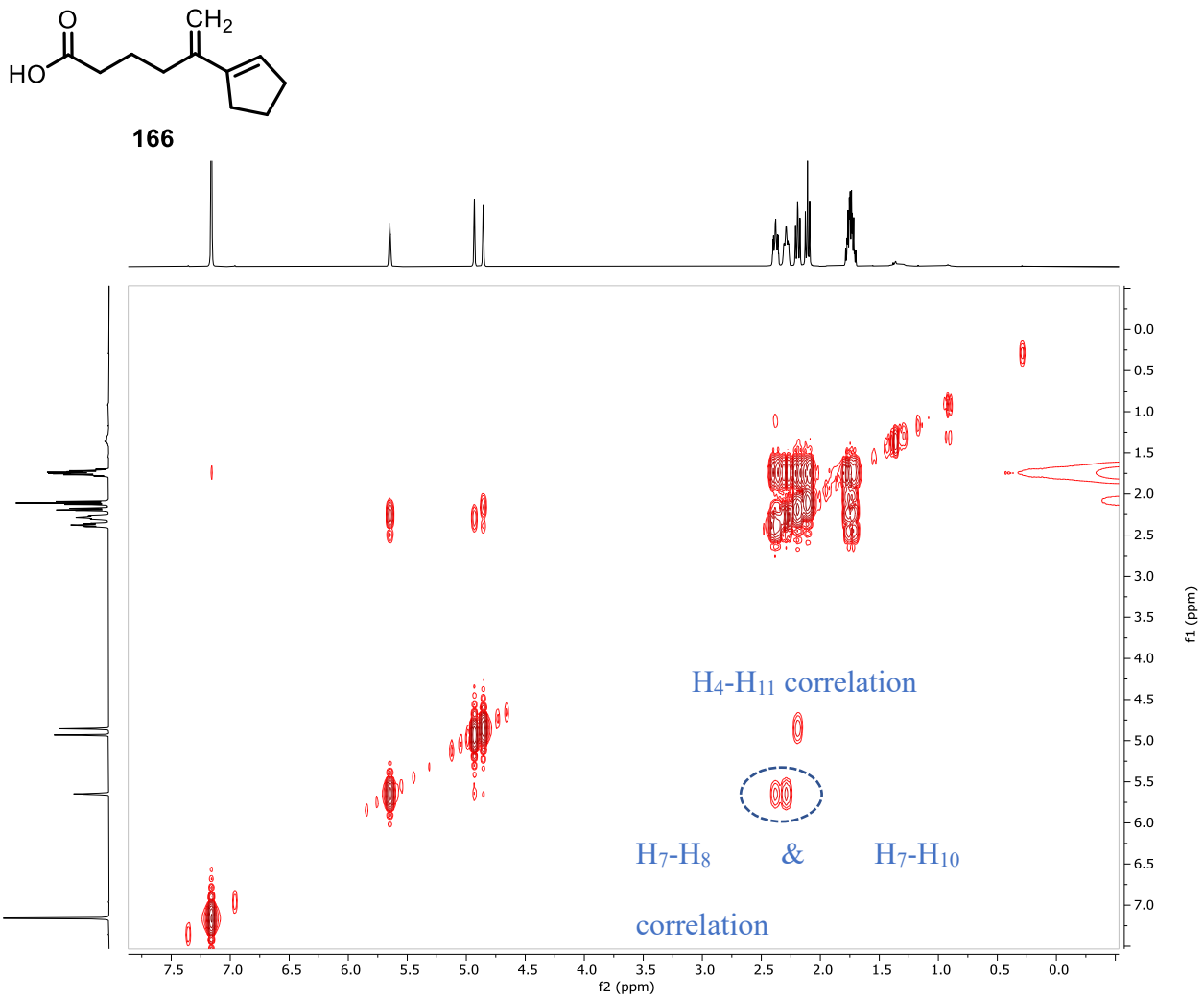
O
CH2
HO
166
H4-H11 correlation
H7-H8 & H7-H10 correlation
f2 (ppm)
f1 (ppm)

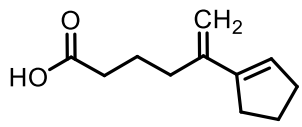
O
HO
CH2

166

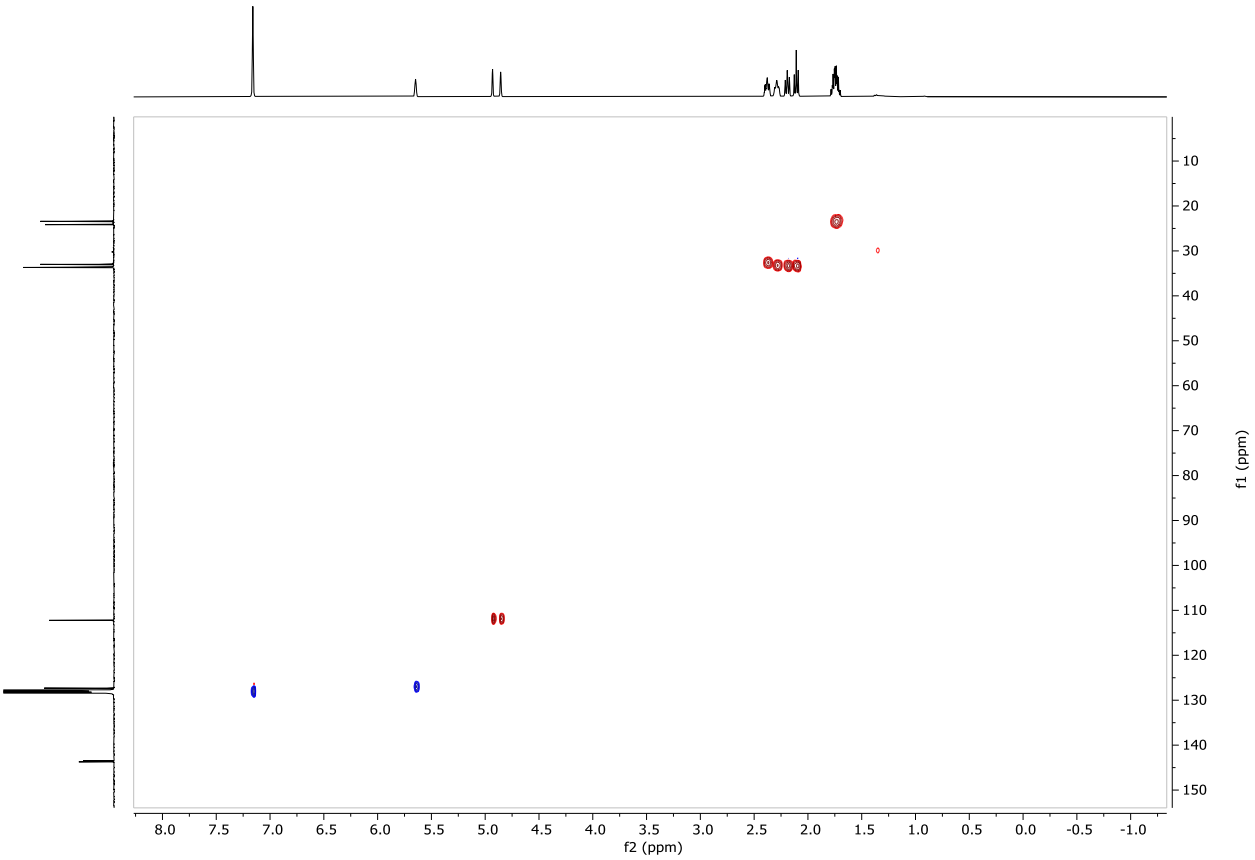
10
20
30
40
50
60
70
80
90
100
110
120
130
140
150
f1 (ppm)
8.0
7.5
7.0
6.5
6.0
5.5
5.0
4.5
4.0
3.5
3.0
2.5
2.0
1.5
1.0
0.5
0.0
-0.5
-1.0
f2 (ppm)

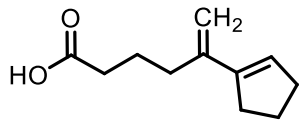
O
CH2
HO

166

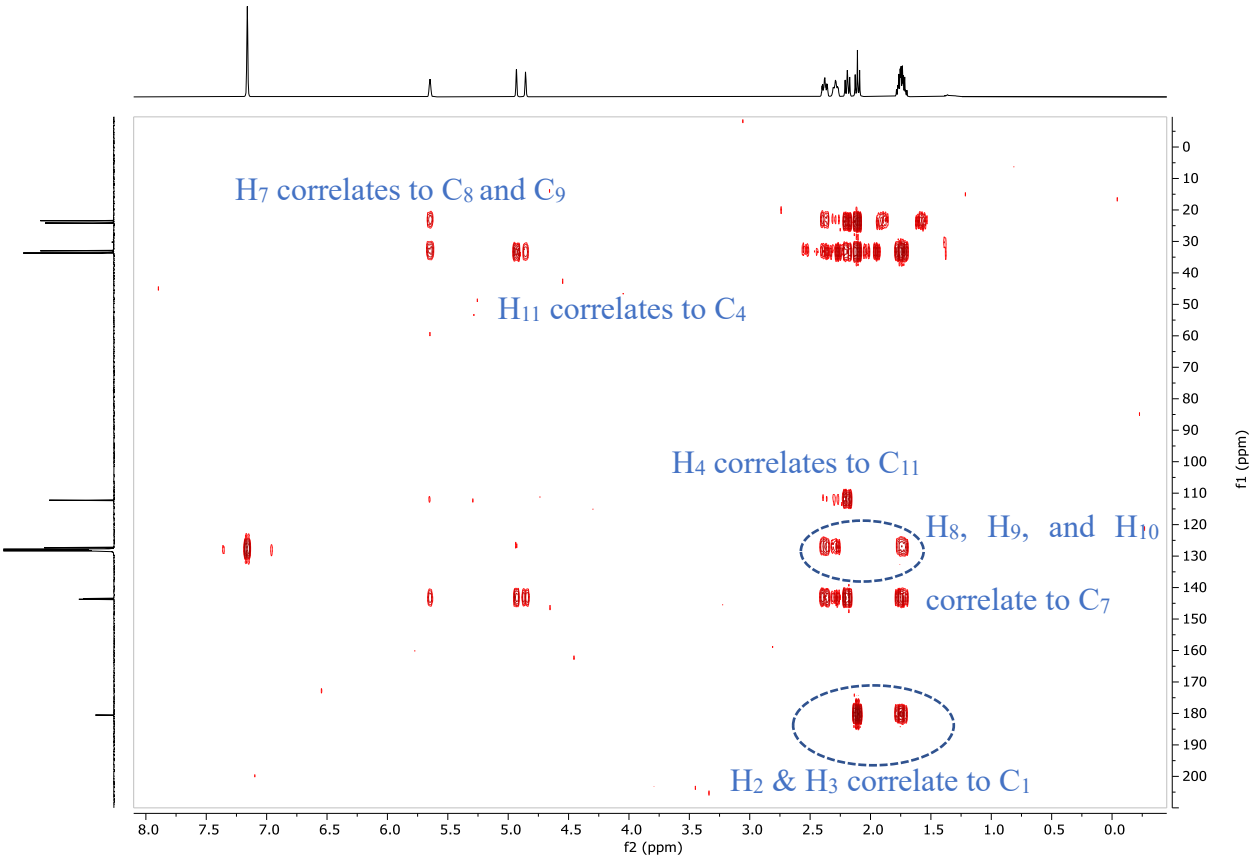
H7 correlates to C8 and C9
H11 correlates to C4
H4 correlates to C11
H8, H9, and H10
correlate to C7
H2 & H3 correlate to C1
f2 (ppm)
f1 (ppm)

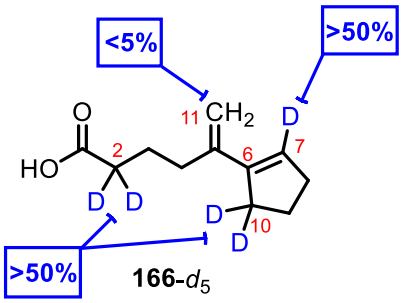
<5%
>50%
O
HO
11
CH2
D
2
6
7
D
D
D
10
D
>50%

166-d_5

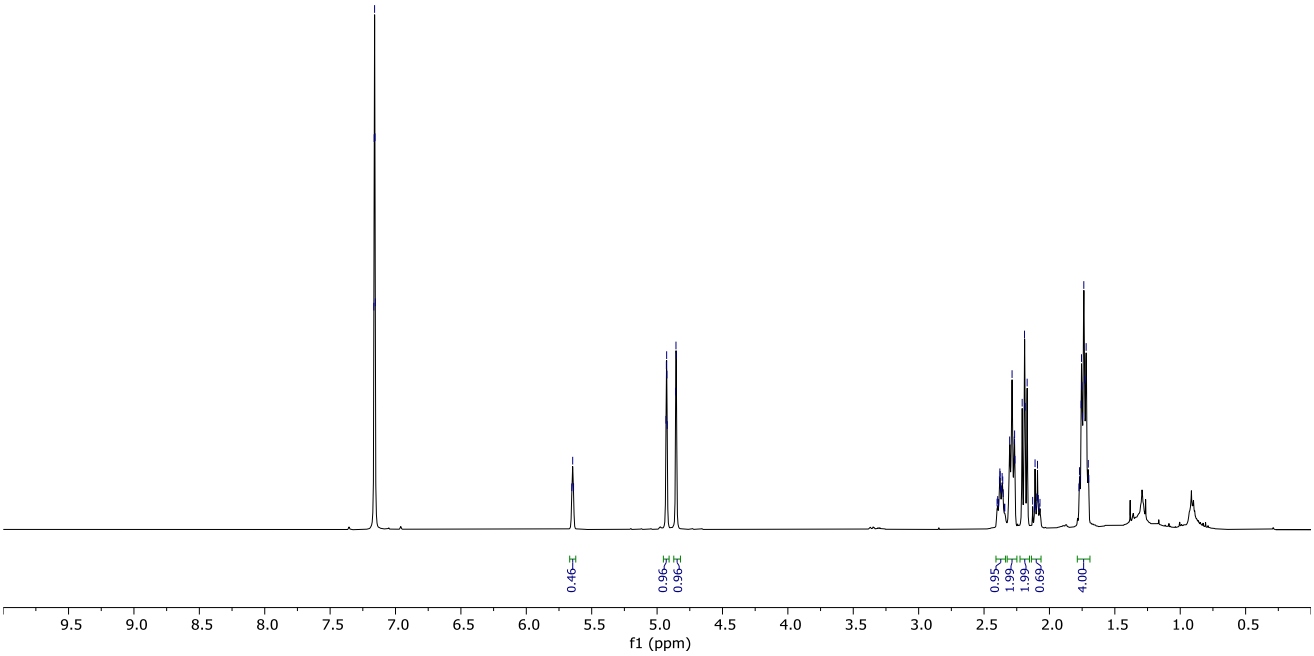
0.46
0.96
0.96
0.95
1.99
1.99
0.69
4.00
9.5
9.0
8.5
8.0
7.5
7.0
6.5
6.0
5.5
5.0
4.5
4.0
3.5
3.0
2.5
2.0
1.5
1.0
0.5
f1 (ppm)

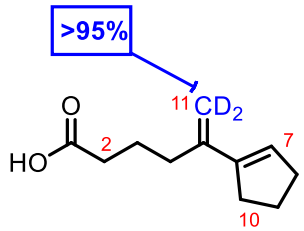
>95%
11
CD2
O
HO
2
7
10

166-d_2

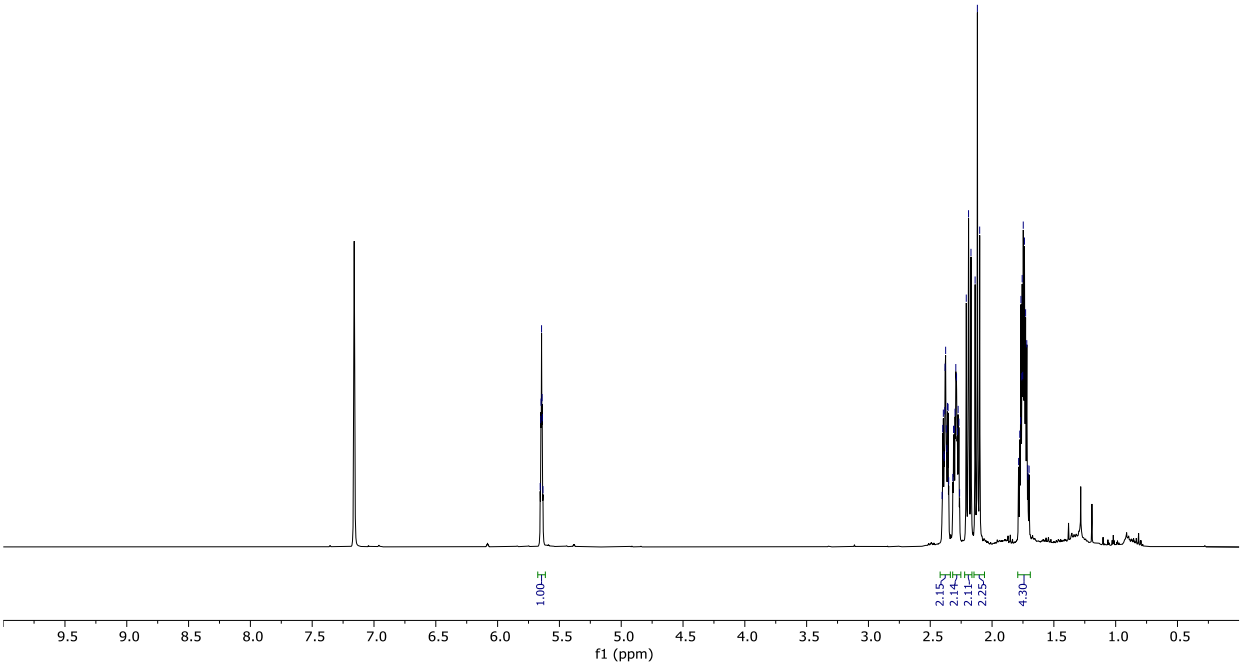
1.00
2.15
2.14
2.11
2.25
4.30
9.5
9.0
8.5
8.0
7.5
7.0
6.5
6.0
5.5
5.0
4.5
4.0
3.5
3.0
2.5
2.0
1.5
1.0
0.5
f1 (ppm)

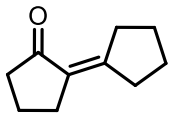

167

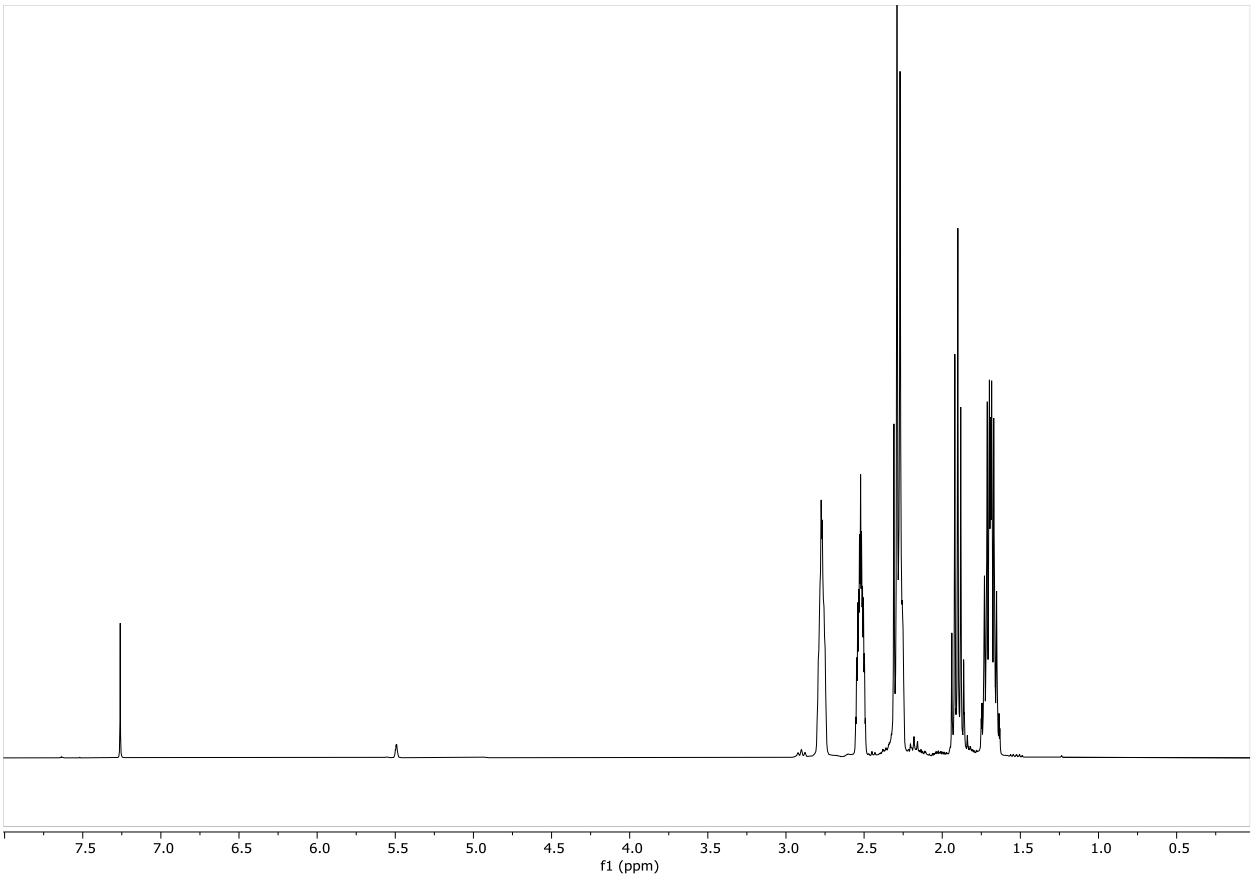

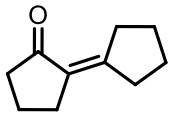

167

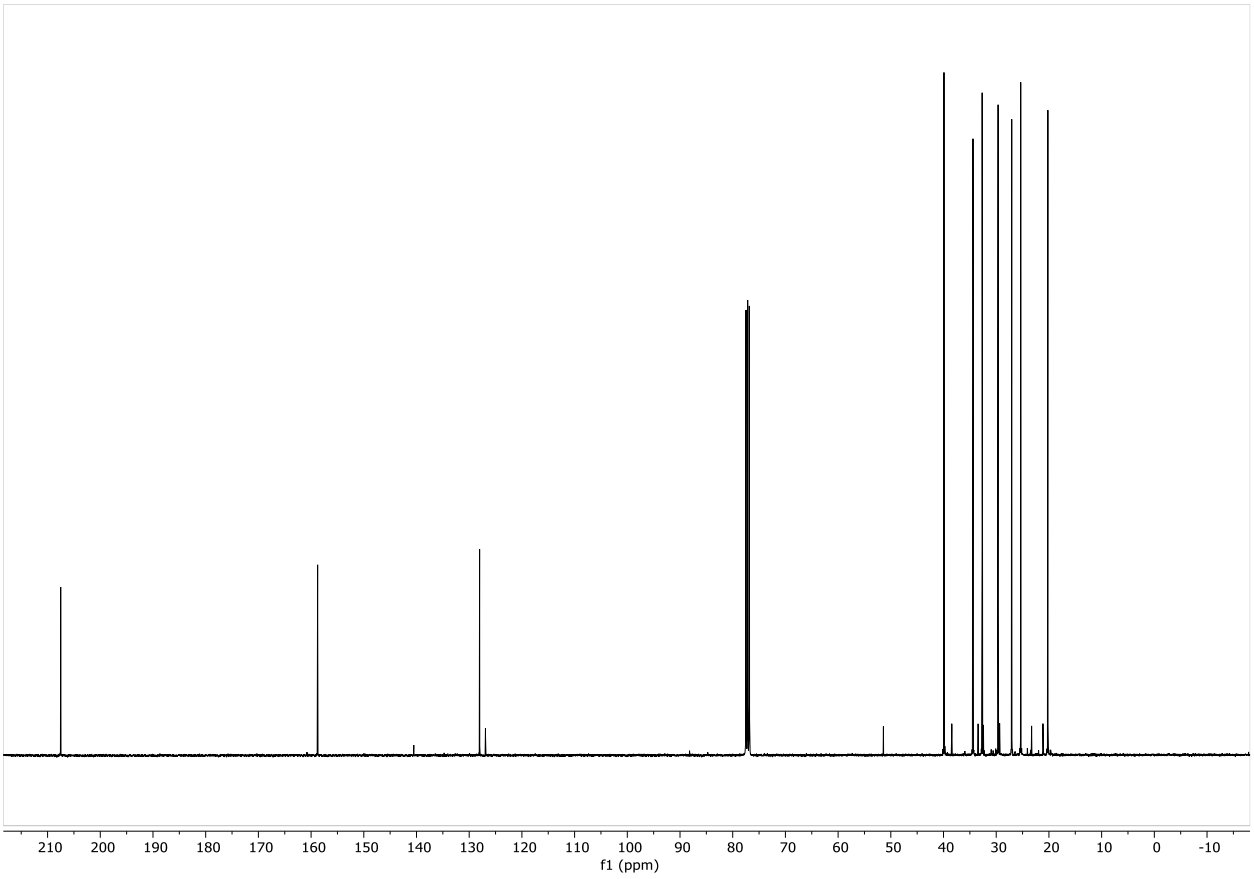
210
200
190
180
170
160
150
140
130
120
110
100
90
80
70
60
50
40
30
20
10
0
-10
f1 (ppm)

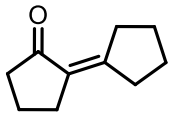

167

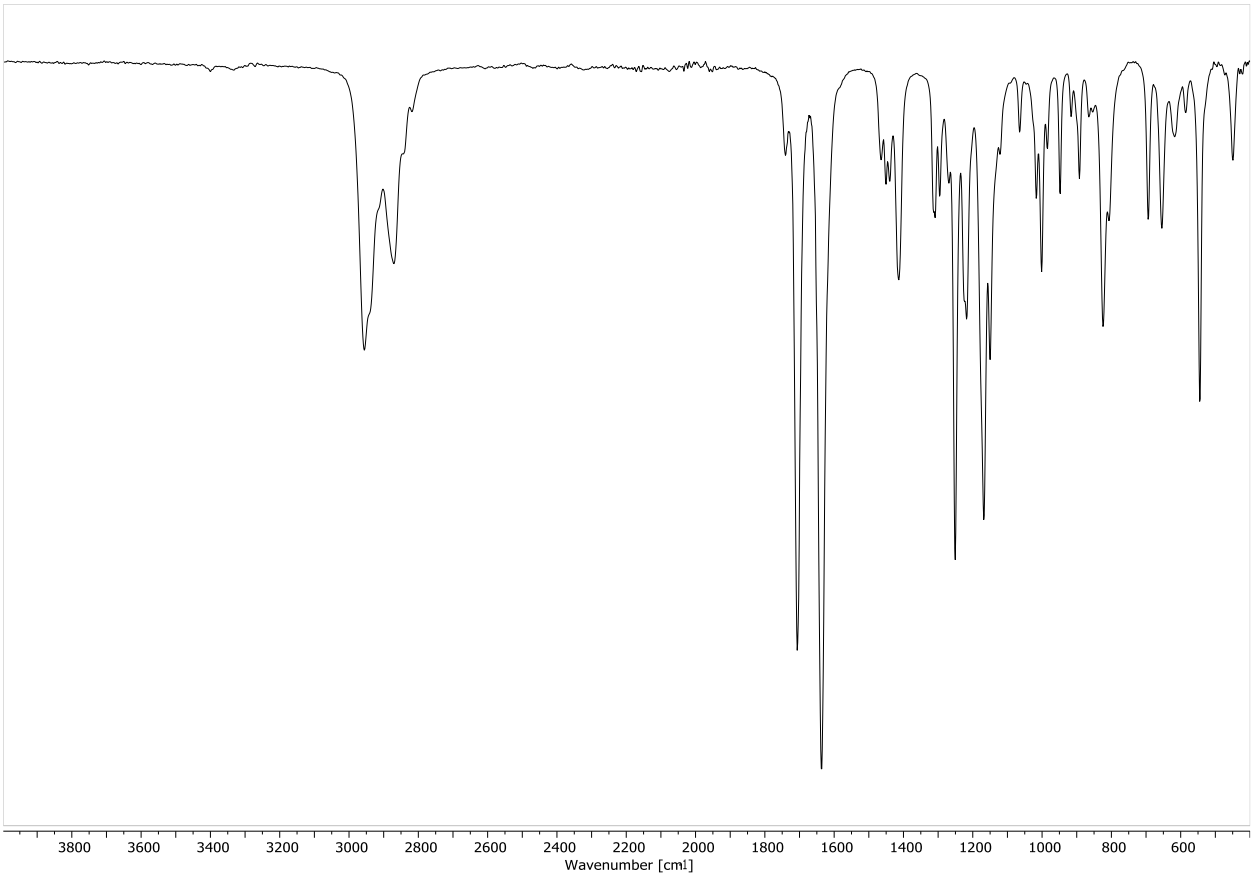
3800
3600
3400
3200
3000
2800
2600
2400
2200
2000
1800
1600
1400
1200
1000
800
600
Wavenumber [cm-1]

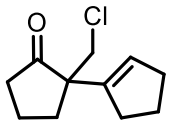

169

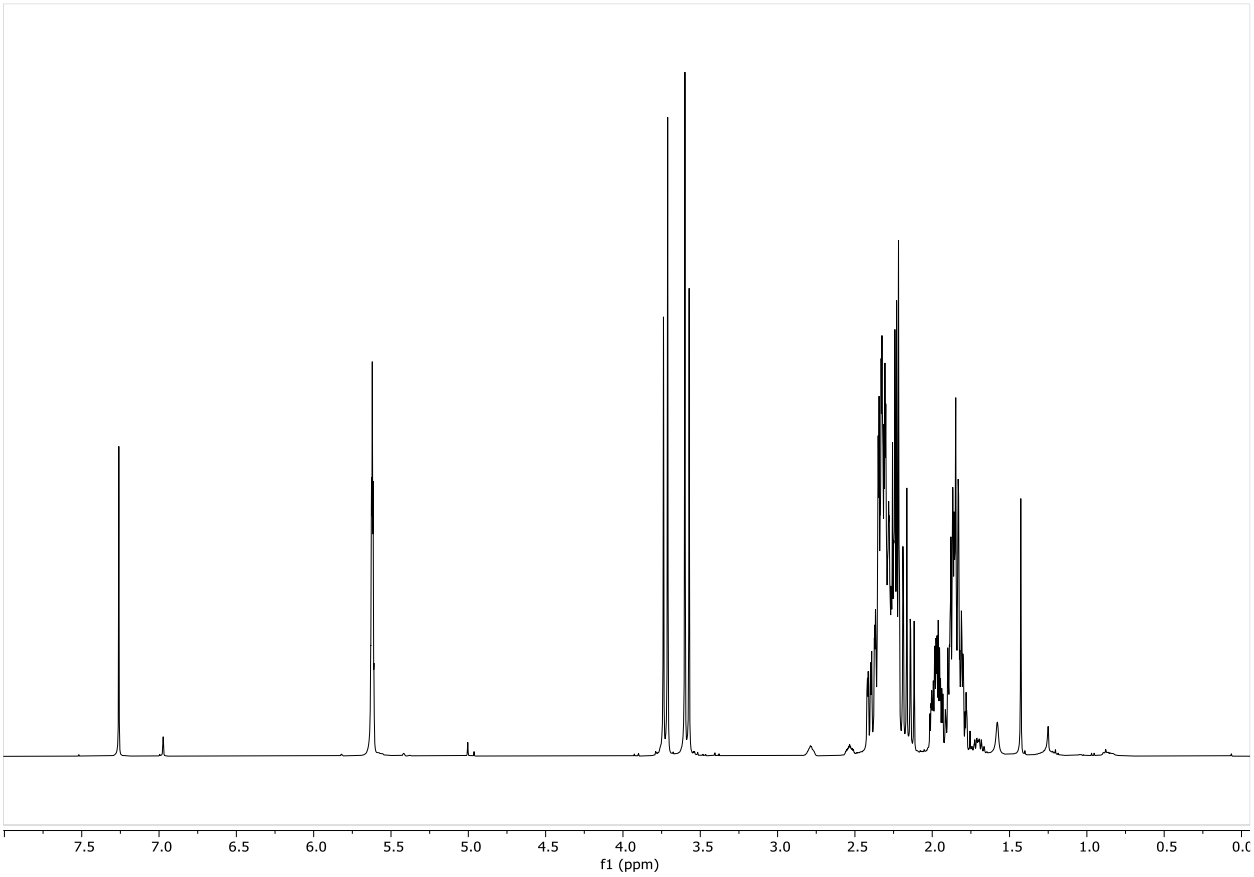

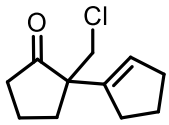
O
Cl

169

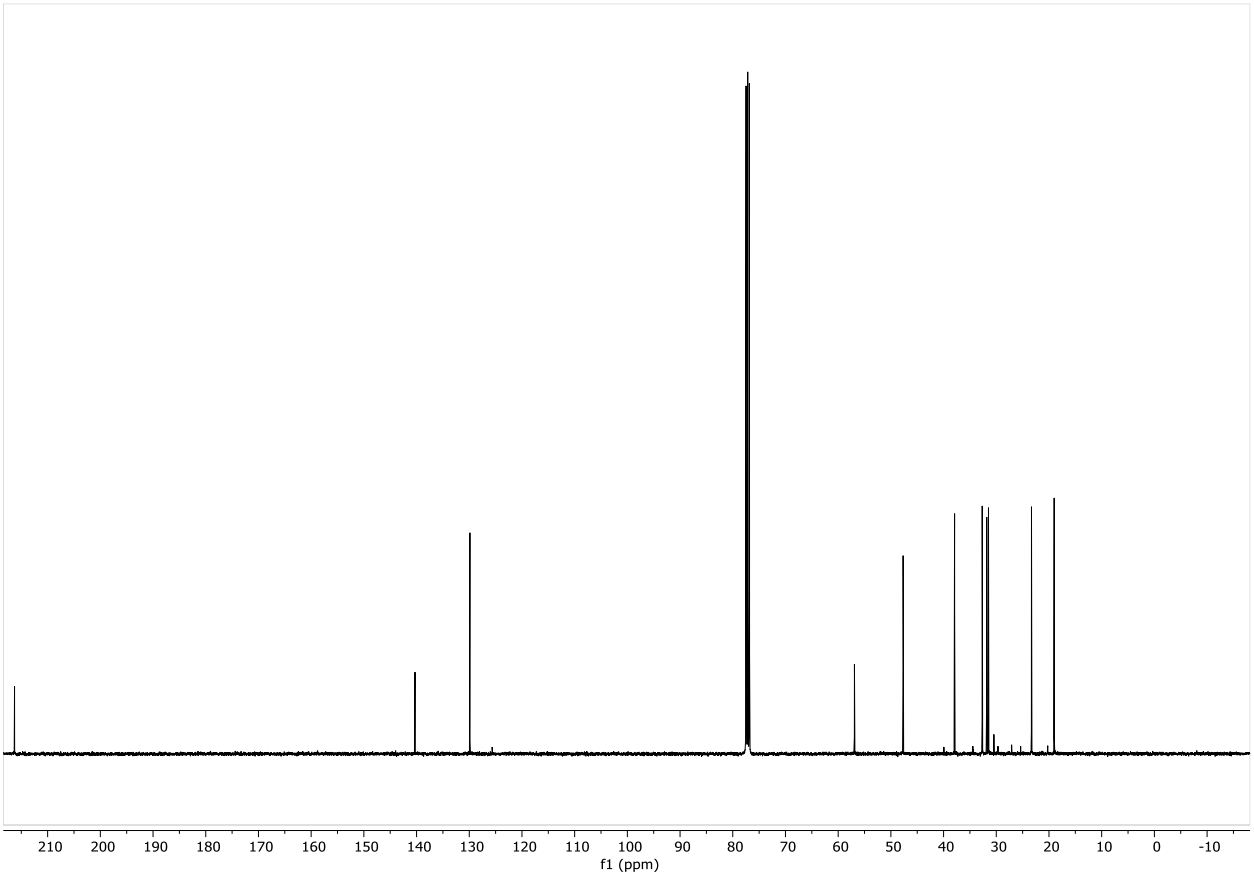
210
200
190
180
170
160
150
140
130
120
110
100
90
80
70
60
50
40
30
20
10
0
-10
f1 (ppm)

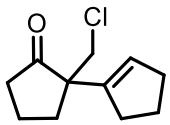
O
Cl

169

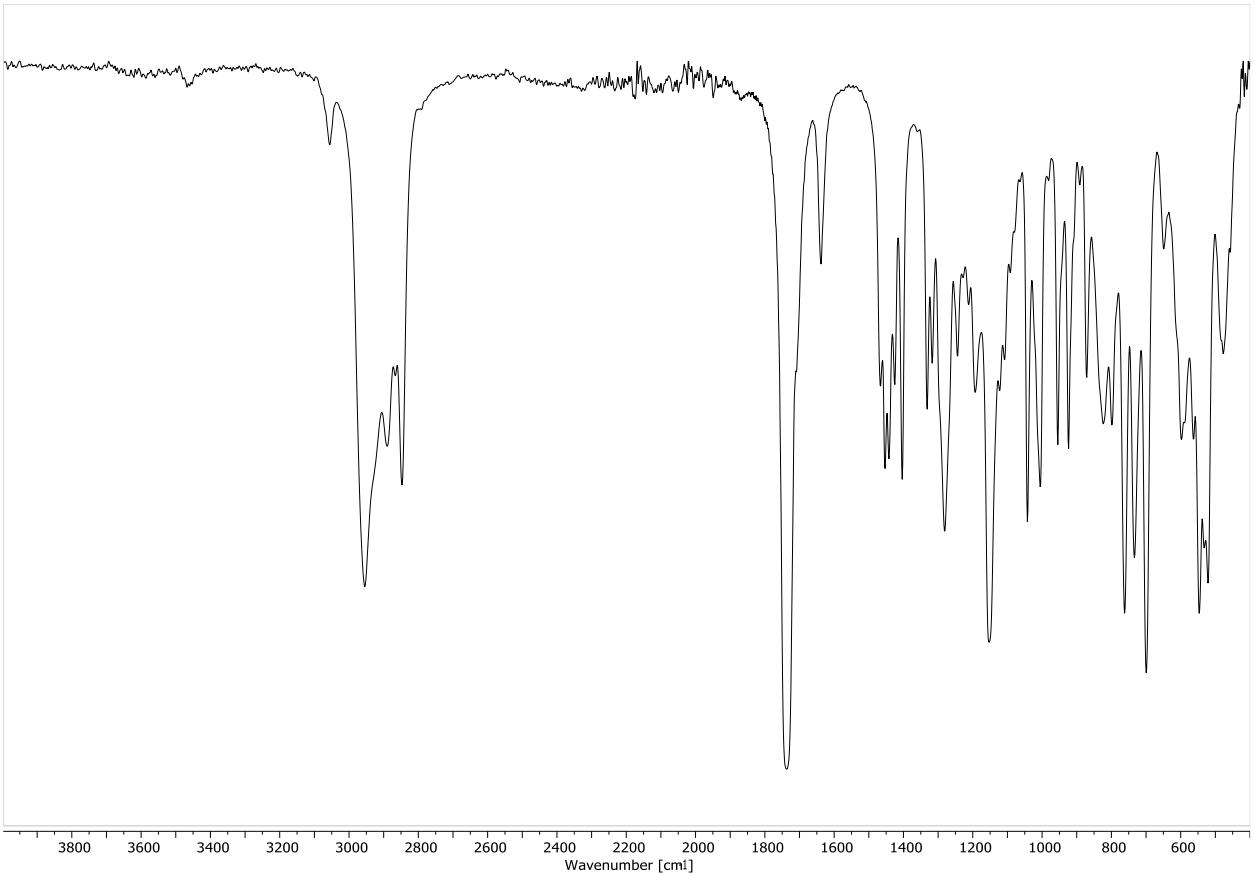
3800
3600
3400
3200
3000
2800
2600
2400
2200
2000
1800
1600
1400
1200
1000
800
600
Wavenumber [cm-1]

Stacked ^{1}H NMR Spectra of **166** collected in $CDCl_3$

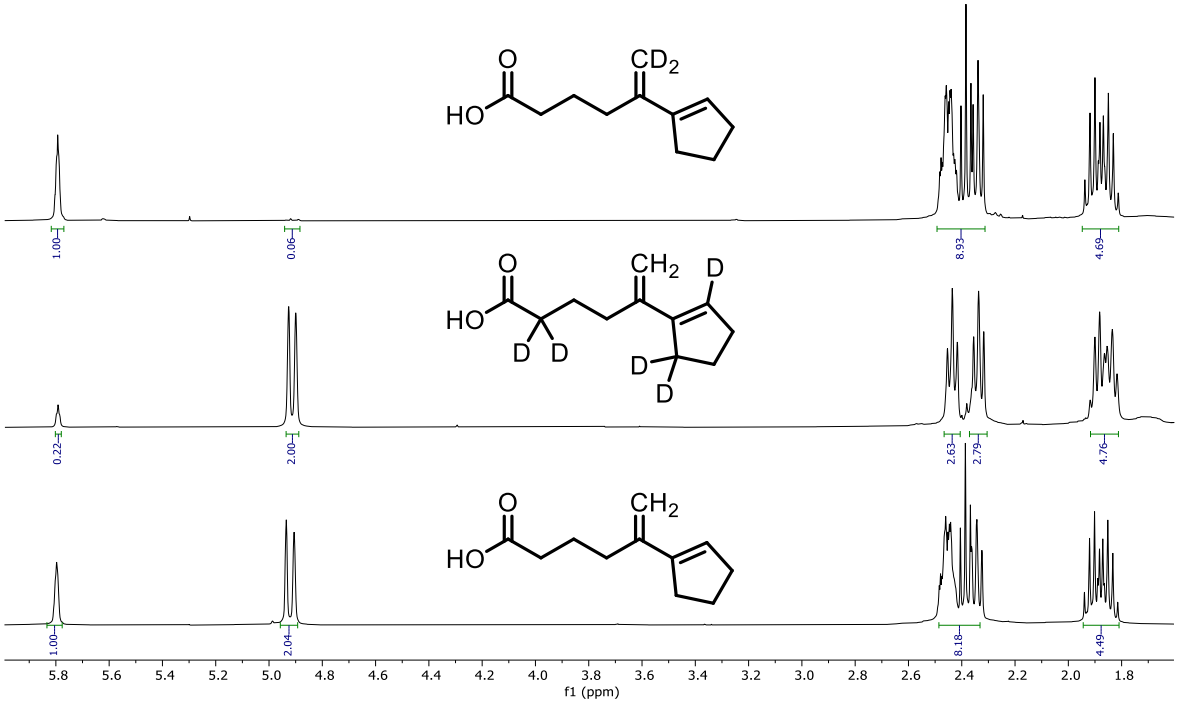

Stacked ^{1}H NMR Spectra of **166** collected in C_6D_6

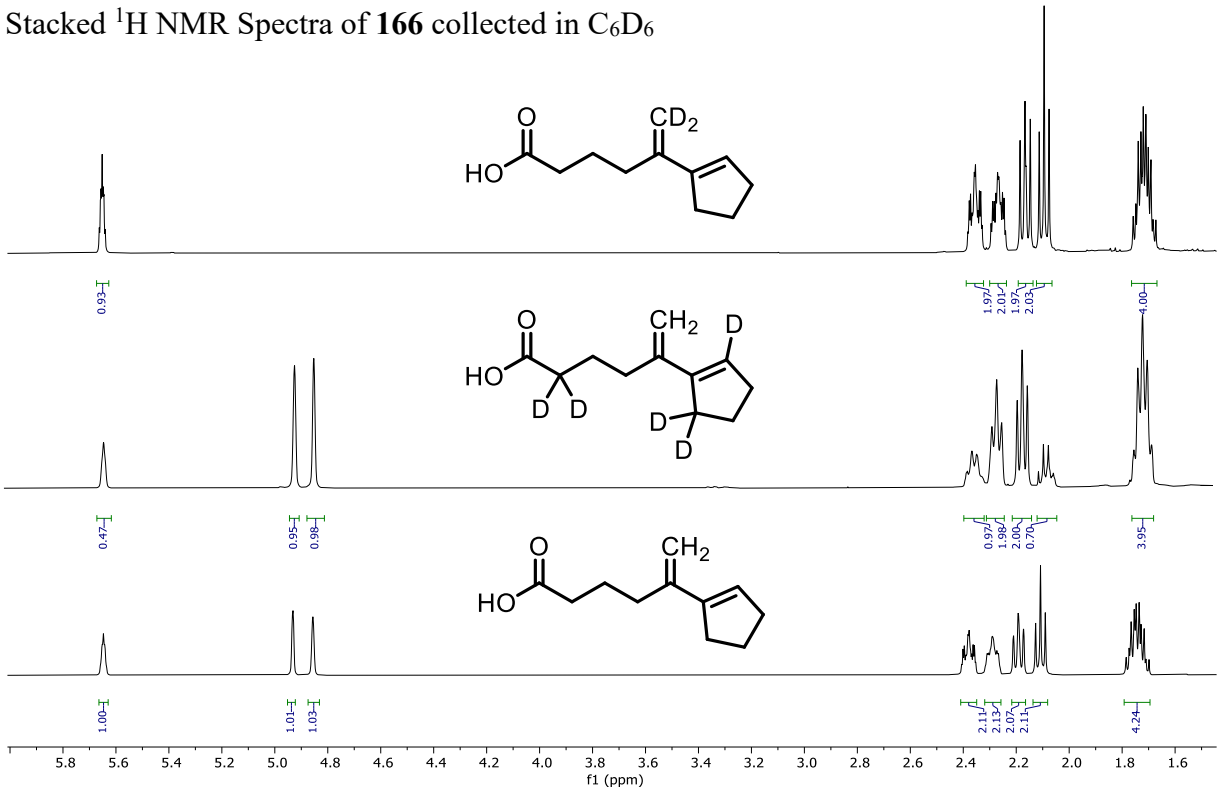

Aliquot of reaction (p.243) quenched with HCl – crude ^{1}H NMR contains **167** and its isomer, not **166**.

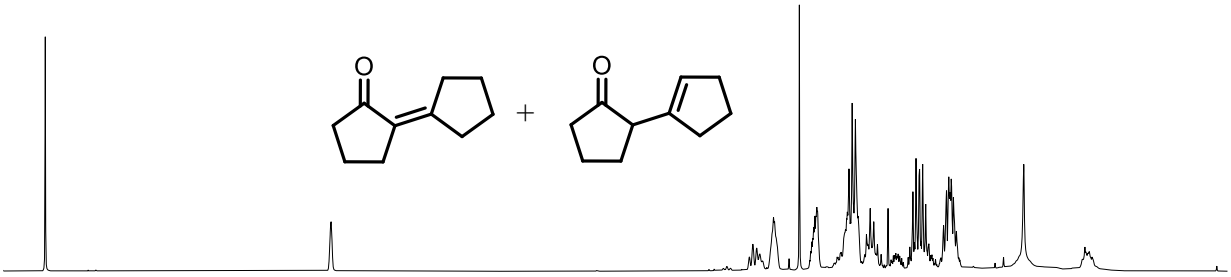

Distilled **167** (trace amounts of isomer)

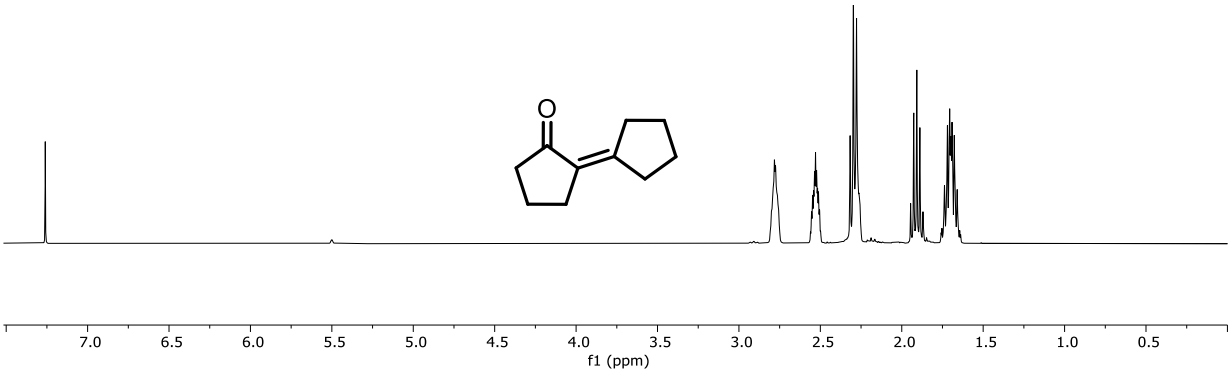

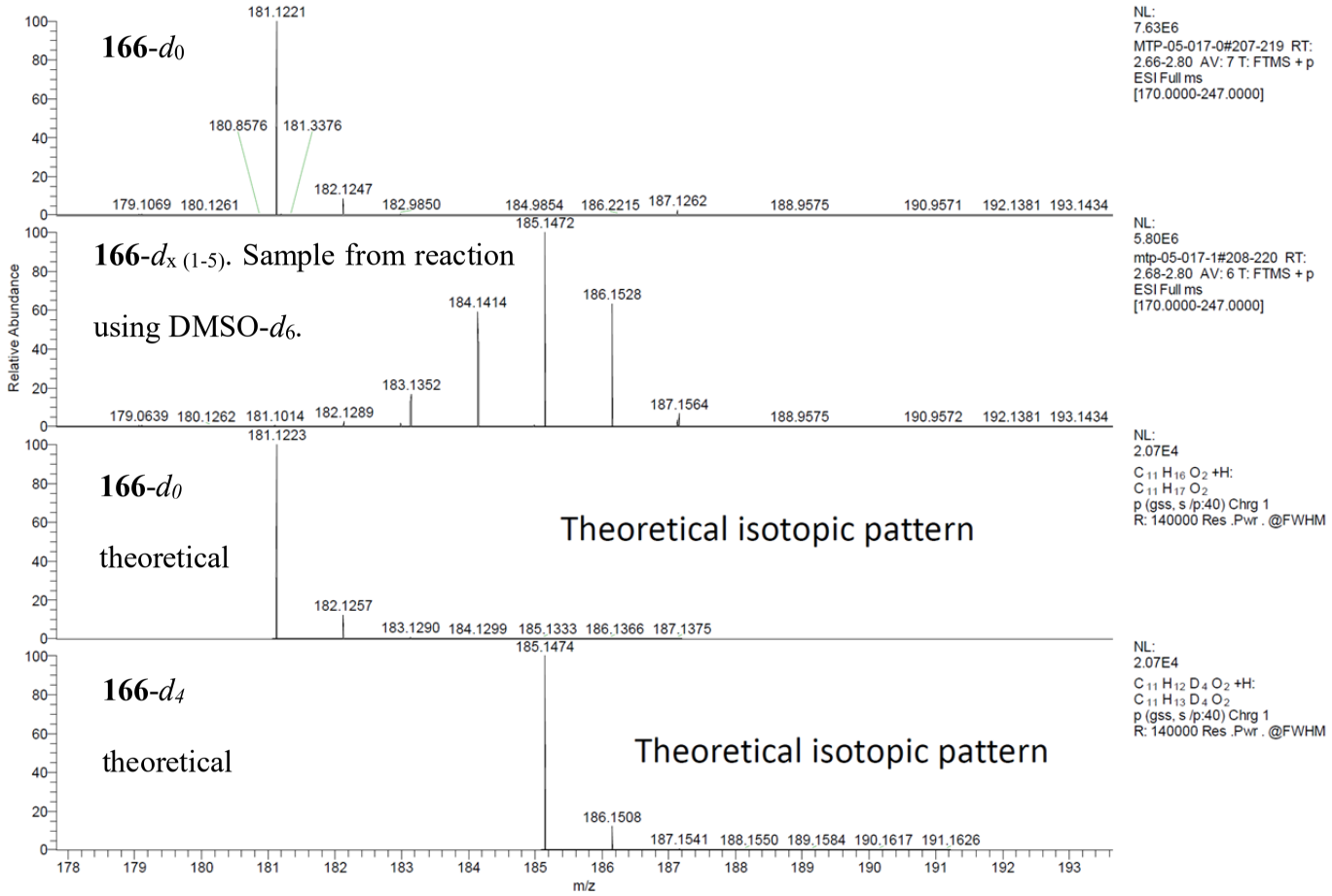

Natural Abundance (%)	D_1 Enrichment (%)	D2 Enrichment (%)	D3 Enrichment (%)	D4 Enrichment (%)	D5 Enrichment (%)	D6 Enrichment (%)	D7 Enrichment (%)
0.1	0.9	6.1	21.8	41.1	30.1	0	0